

**CRANFIELD INSTITUTE OF TECHNOLOGY**

**SCHOOL OF MECHANICAL ENGINEERING  
DEPARTMENT OF FLUID ENGINEERING AND INSTRUMENTATION**

**PhD THESIS**

**Academic Year 1985-1988**

**FLUID FLOW AND HEAT TRANSFER  
AROUND MECHANICAL SEALS**

**N D Barnes**

**Supervisor:**

**Prof M Sanderson**

**Year 1990**

ProQuest Number: 10832131

All rights reserved

INFORMATION TO ALL USERS

The quality of this reproduction is dependent upon the quality of the copy submitted.

In the unlikely event that the author did not send a complete manuscript and there are missing pages, these will be noted. Also, if material had to be removed, a note will indicate the deletion.



ProQuest 10832131

Published by ProQuest LLC (2018). Copyright of the Dissertation is held by Cranfield University.

All rights reserved.

This work is protected against unauthorized copying under Title 17, United States Code  
Microform Edition © ProQuest LLC.

ProQuest LLC.  
789 East Eisenhower Parkway  
P.O. Box 1346  
Ann Arbor, MI 48106 – 1346

## SUMMARY

Mechanical seals are used extensively on rotary applications where the sealed fluid is under pressure. They may rightly be considered to be generally reliable and trouble free, many giving lives of over 3 years. However, a significant number, particularly on arduous and often critical duties, exhibit apparently random mid-life failure characteristics which cannot be easily explained. Of these "random" failures, the largest proportion appear to be attributable to overheating due to loss of the vital interface fluid film. The mechanism of interface film loss depends on a large number of interrelated variables and a substantial amount of work has been carried out over many years to attempt to alleviate the problem. Little work however has been reported on the nature of the fluid flow around the seal; this is determined by seal chamber geometry and affects the removal of potentially deleterious heat, vapour or gases, and solids. At present, many seals are required to run in "stuffing boxes" - cavities designed for soft packing rather than mechanical seals.

The aim of this project has been to study the flow behaviour in these stuffing boxes and a number of novel chamber designs. The techniques involved using transparent housings and direct measurements of convective heat transfer coefficients. Significant improvements over existing designs were achieved using a housing flared at 45° away from the seal and this design forms the basis of recommendations for improved seal systems. This design was tested under simulated field conditions described in a Design Study and Case Study and found to be successful.

The recommendations are backed up by a mathematical model of turbulence viscosity which seeks to explain some of the complex structured flows observed. A corollary to the thesis explains how the results of this work will form a major input to improved international standards.

## TABLE OF CONTENTS

<b>CHAPTER 1 - INTRODUCTION</b>	<b>1</b>
1.1 Introduction to Thesis	2
1.2 Important Factors	6
1.2.1 Sealing Mechanism	6
1.2.2 Sealed Liquid	6
1.2.3 Face Presentation	7
1.2.4 Face Materials	7
1.2.5 Face Cooling	8
1.3 Objectives	10
1.3.1 Seal Geometry	10
1.3.2 Heat Removal	10
1.3.3 Vapour and Gas Control	11
1.3.4 Solids Control	12
1.3.5 Dead-Ended Running	12
1.3.6 Dependence on Other Variables	12
<b>CHAPTER 2 - SEAL UNRELIABILITY - THE COST TO INDUSTRY</b>	<b>14</b>
2.1 The Problem	15
2.2 Reasons for Seal Failure	17
2.3 Cost Benefit Analysis	19
2.3.1 Introduction	19
2.3.2 Model Basis	19
2.3.3 Site Surveys	19
2.3.4 Cost-savings Through Improved Seal Reliability	21
2.3.5 Conclusions	24
2.4 Possible Solutions	25
2.4.1 Selection and Maintenance	25
2.4.2 Seal Face Materials	25
2.4.3 Basic Seal Design	26
2.5 Outstanding Problems	29
<b>CHAPTER 3 - REVIEW OF LITERATURE</b>	<b>31</b>
3.1 Rotating Annular Flows	32
3.1.1 Pre-1950's	33
3.1.2 1950 - 1959	33
3.1.3 1960 - 1969	35
3.1.4 1970 - 1979	37
3.1.5 1980 - 1989	38
3.2 Summary	40

<b>CHAPTER 4 - TEST APPARATUS</b>	<b>41</b>
4.1 Specification	42
4.1.1 Seal Types	42
4.1.2 Seal Housings	43
4.1.3 Piping Plans	44
4.1.4 Test Fluids	44
4.1.5 Flowrates	45
4.1.6 Speeds	46
4.1.7 Experimental Procedure	47
4.2 Design and Manufacture	48
4.2.1 Drive System	48
4.2.2 Test Cell	50
4.2.3 Pumpset	50
4.3 Instrumentation and Measurement Systems	51
4.3.1 Transducers	51
4.3.2 Heat Transfer Measurement	51
4.3.3 Data-logging Systems	56
4.4 Flow Visualisation	57
4.4.1 Visualisation Techniques	57
4.4.2 Exploratory Tests	57
4.4.3 Lighting Techniques	58
4.4.4 Recording Techniques	59
<b>CHAPTER 5 - TEST PROGRAMME</b>	<b>60</b>
5.1 Water/Gas Tests	61
5.1.1 48mm Tests	61
5.1.2 100mm Tests	62
5.2 Glycerol & Water/Gas Tests	63
5.3 Water/Solids Tests	64
<b>CHAPTER 6 - TEST RESULTS</b>	<b>65</b>
6.1 Flow Visualisation Tests	66
6.1.1 Narrow Radial Clearance Housing	67
6.1.2 Wide Radial Clearance Housing	67
6.1.3 12° Positively Flared Housing	68
6.1.4 12° Negatively Flared Housing	68
6.1.5 45° Positively Flared Housing	68
6.2 Heat Transfer Tests	69
6.2.1 Shrouded-spring seal (Seal B)	69
6.2.2 Multiple-spring seal (Seal C)	69
<b>CHAPTER 7 - MATHEMATICAL MODEL</b>	<b>71</b>
7.1 Nature of Rotating Flows	72

7.2	Turbulence Viscosity	73
7.3	Calculation of Turbulence Viscosity	74
7.4	Determination of Wall Shear Stress	76
7.4.1	Bjorklund and Kays (1959):-	76
7.4.2	Cole (1967)	76
7.4.3	Vohr (1968)	76
7.4.4	Castle et al (1971)	77
7.4.5	Floyd (1982)	77
7.4.6	Present Study	77
7.4.7	Summary	78
7.5	Estimation of Boundary Layer Thickness	79
7.6	Results of Analysis	80
<b>CHAPTER 8 - DISCUSSION OF RESULTS</b>		<b>81</b>
8.1	Narrow Radial Clearance Housings	82
8.1.1	Flow Regimes	82
8.1.2	Vapour Control	83
8.1.3	Solids Control	83
8.2	Wide Radial Clearance Housings	84
8.2.1	Flow Regimes	84
8.2.2	Vapour control	84
8.2.3	Solids Control	85
8.3	Flared Housings	86
8.3.1	12° Positively Flared Housing	86
8.3.2	12° Negatively Flared Housing	86
8.3.3	45° Positively Flared Housing	86
<b>CHAPTER 9 - DESIGN STUDY - EFFECT OF CHAMBER DESIGN ON SEAL INSTABILITY</b>		<b>88</b>
9.1	Introduction	89
9.2	Test Apparatus	90
9.3	Test Method	92
9.4	Results	93
9.5	Conclusions	94
<b>CHAPTER 10 - CASE STUDY - SEAL CHAMBER DESIGN FOR A SLURRY SEAL</b>		<b>95</b>
10.1	Introduction	96
10.2	Test Equipment	97
10.2.1	BHRA Large Slurry Pipe Facility	97

10.2.2	Rig Control	97
10.2.3	Instrumentation	97
10.2.4	Data-Logging	98
10.2.5	Test Fluid	98
10.2.6	Inspection Facilities	98
10.3	Experimental Work	99
10.3.1	Test Variables	99
10.3.2	Test Procedure	99
10.4	Results	100
10.4.1	Seal Design	100
10.4.2	Impeller Design	100
10.4.3	Seal Chamber Design	101
10.4.4	Seal Face Materials	101
10.5	Conclusions	103
<b>CHAPTER 11 - CONCLUSIONS</b>		104
11.1	Economic Considerations	105
11.2	Housing Design	106
11.3	Analysis	107
<b>CHAPTER 12 - RECOMMENDATIONS FOR FUTURE WORK</b>		108
12.1	Housing Design	109
12.2	Analysis	110
<b>CHAPTER 13 - COROLLARY THE DEVELOPMENT OF A FUNCTIONAL DESIGN STANDARD FOR MECHANICAL SEAL CHAMBERS</b>		111
13.1	Introduction	112
13.2	Recommended Practice	113
13.2.1	Introduction	113
13.2.2	Heat Transfer	113
13.2.3	Control of Gas and Vapour	116
13.2.4	Control of Solids	116
13.3	Alternative Practice	117
13.3.1	Introduction	117
13.3.2	Heat Transfer	117
13.3.3	Control of Gas and Vapour	117
13.3.4	Control of Solids	117
13.4	Summary	118
<b>ACKNOWLEDGEMENTS</b>		119

<b>REFERENCES</b>	121
<b>APPENDICES</b>	135
Appendix A Extracts from Standards	136
Appendix B Radial Space Requirements for High Duty Seals	148
Appendix C Cost Benefit Analysis - Detailed Calculations	151
Appendix D Viscosity Tables for Water/Glycerol Solutions	158
Appendix E Manufacturers' Recommended Injection Flowrates	161
Appendix F Dantec 56 CTA System	164
Appendix G Turbulence Viscosity Analysis - Sample Spreadsheet	167
Appendix H Mechanical Seal Housing Design Guide	172



## TABLES

- 2.1(a) Seal life variability (Flitney and Nau, 1985)
- 2.1(b) Seal life variability (Flitney and Nau, 1985)
- 2.1(c) Seal life variability (Flitney and Nau, 1985)
- 2.1(d) Seal life variability (Flitney and Nau, 1985)
- 2.1(e) Seal life variability (Flitney and Nau, 1985)
- 2.2 Reasons for outage - Company No 3. (Flitney & Nau, 1989)
  
- 4.1 Test seals - 48 mm
- 4.2 Test housing - 48 mm
  
- 5.1 Seal/housing combinations and variables
  
- 6.1 Heat transfer results - heat transfer coefficient versus peripheral Reynolds No.
  
- 7.1 Predicted flow regimes as a function of speed
  
- 10.1 24-hour start/stop cycle
- 10.2 Seal test data sheet
- 10.3 Seal test log sheet
- 10.4 Typical particle count
  
- 13.1 Recommended Practice - summary of implementation
- 13.2 Duty Specification Table
- 13.3 Alternative Practice - summary of implementation

## FIGURES

- 1.1 Typical mechanical seal installation
  - 1.2 Basic features of a mechanical seal
  - 1.3 Seal instability - low pressure seal design
  - 1.4 Seal instability - high pressure seal design
  - 1.5 Definition of seal balance
  - 1.6 Effect of pressure on the sealing interface
  - 1.7 Effect of temperature on the sealing interface
  - 1.8 Seal flushed from discharge
  - 1.9 Seal flushed by an independent ancillary system
  - 1.10 Stuffing box standard geometries
  - 1.11 Centrifugal pump seal arrangements - BS 6836
  - 1.12 Comparison of radial aspect ratios for DIN and high duty seals
  - 1.13 Thermal stress cracking of a mechanical seal face
  - 1.14 Vapour locking phenomenon in a mechanical seal chamber
- 
- 2.1 Weibull plot - Visbreaker Charge pump
  - 2.2 Weibull plot - bottoms pump
  - 2.3 Transient suction pressures on a boiler feedwater pump (Cranfield, 1988)
  - 2.4 Distribution of seal running life (Flitney & Nau, 1985)
  - 2.5 Distribution of installed seal life (Flitney & Nau, 1985)
  - 2.6 Maintenance costs due to mechanical seal failure
  - 2.7 Reduction in seal failures due to regular record-keeping
  - 2.8 Cost profiles for replacement programmes of between-bearing pumps
  - 2.9 Cumulative costs for replacement programmes of between-bearing pumps
  - 2.10 Example of a pump running well off BEP
  - 2.11 Transient fluctuations of pressure and temperature in a seal chamber
  - 2.12 Prediction of seal life using dimensionless parameters (Buck, 1980)
  - 2.13 Test apparatus for observing interface phenomena (Nau, 1963)
  - 2.14 Effect of air on radial pumping (Nau, 1963)
  - 2.15 Toroidal air bubble around seal faces (Nau, 1963)
  - 2.16 Cavitation in the seal interface (Nau, 1979)
  - 2.17 Conductivity probe measurements at the seal face (Field & Flitney, 1975)
  - 2.18 Non-contacting seal for nuclear reactor primary coolant pump (Morton, 1984)
  - 2.19 Graph for evaluating seal material combinations (Lymer, 1969)
  - 2.20 Instability criterion used for seal evaluation (Dolan, Harrison & Watkins, 1987)
  - 2.21 Hydro-pad design for improved face lubrication (Netzel, 1982)
  - 2.22 Examples of DIN and high-duty seals
  - 2.23 Seal life reduction due to high vibration levels (Flitney & Nau, 1976)
  - 2.24 Sources of vibration (Nau, 1981)
  - 2.25 Flow deflectors to improve seal cooling (Bloch, 1985)
  - 2.26 Slurry seal chamber design (Schopplein, 1986)
  - 2.27 Slurry seal chamber design (Battilana, undated)
  - 2.28 Slurry seal chamber design (Kratzer, 1987)
  - 2.29 Slurry seal chamber design (Bangert, 1986)
  - 2.30 Slurry seal chamber design (Heumann, 1986)
  - 2.31 Slurry seal chamber design (Nolan, 1988)
  - 2.32 Liquid ethylene pump with flared housing (Strazewski, 1985)
  - 2.33 New design of medium duty pump (Standish, 1987)
  - 2.34 Novel seal chamber designs (Davison, 1989)
  - 2.35  $\Delta T$  measurements for seal chambers in Fig 2.34 (Davison, 1989)
  - 2.36 Novel seal chamber design with flow guide (Heald, 1975)

- 3.1 Taylor vortices
- 3.2 Taylor's experimental apparatus (Taylor, 1923)
- 3.3 Super-laminar flow observations (Taylor, 1923)
- 3.4 Turbulent vortices (Pai, 1943)
- 3.5 Skin friction coefficient measurements (Gazely, 1958)
- 3.6 Nusselt number measurements (Gazely, 1958)
- 3.7 Flow regimes in rotating annular flows (Kaye & Elgar, 1958)
- 3.8 Nusselt number measurements (Bjorklund & Kays, 1959)
- 3.9 Vortex regimes (Coles, 1965)
- 3.12 Turbulent Couette flow with structure (Coles, 1965)
- 3.13 Change of torque slope with Taylor number (Castle et al, 1971)
- 3.14 Nusselt number measurements (Kuzay & Scott, 1977)
- 3.15 High speed vortices (Barcilon et al, 1979)
- 3.16 Predicted Nusselt numbers (Simmers & Coney, 1979 (a))
- 3.17 Experimental Nusselt number measurements (Simmers & Coney, 1979 (a))
- 3.18 Typical velocity profiles (Simmers & Coney, 1980)
- 3.19 Vortex development showing re-emergent structure at  $Ta > 10^6$  (Wan & Coney, 1982)
- 3.20 Flow around a circular cylinder rotating in a cone at rest (Wimmer, 1988)
- 3.21 Comparison of Nusselt vs Taylor numbers - empirical expressions

- 4.1 General view of test apparatus
- 4.2 Close-up of test apparatus showing camera position
- 4.3 Heat-transfer probes fitted to Seal B
- 4.4 GA of test apparatus
- 4.5 Axial strake assembly for Housing 2
- 4.6 Axial strake assembly for Housing 7
- 4.7 Helical strake assembly for Housing 2
- 4.8 Housing 1
- 4.9 Housing 2
- 4.10 Housing 3
- 4.11 Housing 4
- 4.12 Housing 5
- 4.13 Housing 6
- 4.14 Housing 7
- 4.15 Cylindrical housing - 100 mm
- 4.16 45° flared housing - 100 mm
- 4.17 Circulation - Plan A
- 4.18 Circulation - Plan B
- 4.19 Circulation - Plan C
- 4.20 Circulation - Plan D
- 4.21 Circulation - Plan E
- 4.22 Reynolds number as a function of flowrate
- 4.23 Power drop-off as a function of time
- 4.24 Power consumption as a function of speed
- 4.25 Diagram of drive system
- 4.26 Pumpset
- 4.27 Instrumentation layout
- 4.28 Set-up arrangement for heat-transfer probe calibration
- 4.29 Results from Probe number 2
- 4.30 Results from Probe number 1
- 4.31 Typical chart record of experiment
- 4.32 Flow visualisation using hollow glass spheres,  $Ta = 1800$
- 4.33 Flow visualisation using hollow glass spheres,  $Ta = 3770$

- 4.34 Flow visualisation using hollow glass spheres,  $Ta = 15450$
  - 4.35 Flow visualisation using high-speed flash photography
  - 4.36 Alternative flash/camera positions
  - 4.37 Flow pictures taken from position A & B
  - 4.38 Alternative lighting/camera positions
  - 4.39 Favoured lighting/camera arrangement
  - 4.40 Typical flow picture obtained using arrangement in Fig 4.39
  - 4.41 Long exposure photographs showing bubble vectors.
- 
- 6.1 Narrow radial clearance housing - Seal B/Plan A/Water
  - 6.2 Narrow radial clearance housing - Seal A/Plan A/Water
  - 6.3 Narrow radial clearance housing - Plan A/Glycerol solution
  - 6.4 Narrow radial clearance housing - Plan B/Water
  - 6.5 Narrow radial clearance housing - Plan B/Water
  - 6.6 Narrow radial clearance housing - Plan A/Solids in suspension
  - 6.7 Wide radial clearance housing - Plan A - formation of vortex
  - 6.8 Wide radial clearance housing - Plan A - high Taylor number flows
  - 6.9 Wide radial clearance housing - Plan A - high Taylor number flows
  - 6.10 Wide radial clearance housing - Plan A/Glycerol solution
  - 6.11 Wide radial clearance housing - Plan A/Solids in suspension
  - 6.12 Wide radial clearance housing - Plan A/Axial strakes
  - 6.13 Wide radial clearance housing - Plan A/Helical strakes
  - 6.14  $12^\circ$  positively flared housing - Plan A/Water
  - 6.15  $12^\circ$  positively flared housing - Plan A/Solids
  - 6.16  $12^\circ$  negatively flared housing - Plan A/Water
  - 6.17  $12^\circ$  negatively flared housing - Plan A/Water
  - 6.18  $12^\circ$  negatively flared housing - Plan D/Water
  - 6.19  $12^\circ$  positively flared housing - Plan A/Water
  - 6.20  $12^\circ$  positively flared housing - Plan A/Glycerol solution
  - 6.21  $45^\circ$  positively flared housing - Plan A - emulsification with glycerol
  - 6.22  $45^\circ$  positively flared housing - Plan A/Solids
  - 6.23  $45^\circ$  positively flared housing - Plan A/Neck-bush/Solids
  - 6.24  $45^\circ$  positively flared housing - Plan A/Axial strakes
  - 6.25 Heat transfer data from Seal B
  - 6.26 Wave form from hot-film probe, speed  $< 600$  rpm
  - 6.27 Wave form from hot-film probe, speed  $> 650$  rpm
  - 6.28 Heat transfer coefficient versus Reynolds number
- 
- 7.1 Flow Regime as a function of Taylor number
  - 7.2 Taylor number plotted against angular velocity
  - 7.3 Experimental churning loss data
  - 7.4 Comparison of reported friction coefficient equation
  - 7.5 Measured velocity profiles (Ho et al, 1964)
  - 7.6 Measured velocity profiles (Simmers & Coney, 1979 (b))
  - 7.7 Measured velocity profiles (Simmers & Coney, 1979 (c))
  - 7.8 Measured velocity profiles (Simmers & Coney, 1980)
  - 7.9 Measured velocity profiles (Abdallah and Coney, 1988)
  - 7.10 Housing 1, Water
  - 7.11 Housing 1,  $v = 15 \text{ mm}^2/\text{s}$
  - 7.12 Housing 1,  $v = 50 \text{ mm}^2/\text{s}$
  - 7.13 Housing 1,  $v = 150 \text{ mm}^2/\text{s}$
  - 7.14 Housing 100-1, Water
  - 7.15 Housing 2, Water
  - 7.16 Housing 2,  $v = 15 \text{ mm}^2/\text{s}$

- 7.17 Housing 2,  $v = 50 \text{ mm}^2/\text{s}$
- 7.18 Housing 1,  $v = 150 \text{ mm}^2/\text{s}$
- 7.19 Housing 100-2, Water
- 7.20 Housing 100-3, Water
- 7.21 Taylor number versus Reynolds number - Housing 1
- 7.22 Taylor number versus Reynolds number - Housing 2
- 7.23 Taylor number versus Reynolds number - Housing 100-1
- 7.24 Taylor number versus Reynolds number - Housing 100-2
- 7.25 Taylor number versus Reynolds number - Housing 100-3
  
- 8.1 Comparison of housings - water/Plan A/Seal B
- 8.2 Comparison of housings - water/Plan A/Seal A
- 8.3 Comparison of housings - water/Plan B/Seal B
- 8.4 Comparison of housings - water/Plan B/Seal A
- 8.5 Housing 100-2 - effect of speed
- 8.6 Housing 100-3 - effect of speed
- 8.7 Taylor number as a function of speed - parallel housings
- 8.8 Effects of the impeller
- 8.9 Effect of axial flow on critical Taylor number (Coney & Simmers, 1979 (a))
  
- 9.1 Typical seal instability curve
- 9.2 General view of instability rig
- 9.3 Test circuit
- 9.4 Leakage measuring system
- 9.5 General arrangement of test chamber
- 9.6 Instability curve - "good" housing
- 9.7 Instability curve - "poor" housing
  
- 10.1 BHRA Large Slurry Pipe facility
- 10.2 Instrumented pump
- 10.3 View of pumpset
- 10.4 Slurry seal fitted with face thermo-couples
- 10.5 Existing seal installation
- 10.6 Modified seal installation
- 10.7 Seal 1
- 10.8 Seal 2
- 10.9 Seal 3
- 10.10 Seal 4
- 10.11 Seal 5
- 10.12 Seal 6
- 10.13 Seal 7
- 10.14 Seal 8
- 10.15 Seal 9
- 10.16 Seal 10
- 10.17 Seal 11
- 10.18 Seal 12 - mid-test inspection
- 10.19 Seal 12 - final inspection
- 10.20 Wear profile - Seal 2
- 10.21 Wear profile - Seal 3
- 10.22 Wear profile - Seal 4
- 10.23 Wear profile - Seal 5
- 10.24 Wear profile - Seal 6
- 10.25 Wear profile - Seal 7
- 10.26 Wear profile - Seal 8

- 10.27 Wear profile - Seal 9
  - 10.28 Wear profile - Seal 10
  - 10.29 Wear profile - Seal 11
  - 10.30 Wear profile - Seal 12
  - 10.31 Chart Trace - Seal 1
  - 10.32 Chart Trace - Seal 2
  - 10.33 Chart Trace - Seal 3
  - 10.34 Chart Trace - Seal 4
  - 10.35 Chart Trace - Seal 5
  - 10.36 Chart Trace - Seal 6
  - 10.37 Chart Trace - Seal 7
  - 10.38 Chart Trace - Seal 8
  - 10.39 Chart Trace - Seal 9
  - 10.40 Seal cover erosion
  - 10.41 Chart Trace - Seal 10
  - 10.42 Chart Trace - Seal 11
  - 10.43 Chart Trace - Seal 12 - starved suction test
- 
- 13.1 Power dissipation results (Nau, 1987)
  - 13.2 Flush arrangement diagram
  - 13.3 Axial strakes for the 45° flared housing
  - 13.4 Helical strake arrangement
  - 13.5 Axial strakes for a wide radial clearance housing

## NOTATION

A	surface area of shaft ( $= \pi dl$ )	[m <sup>2</sup> ]
A <sub>p</sub>	probe area	[m <sup>2</sup> ]
A <sub>+</sub>	constant ( $= 26.0$ ) in equations 7.10 and 7.11	-
b	radial clearance around seal rotor	[m]
b <sub>r</sub>	seal rotor radial depth ( $= r - r_s$ )	[m]
b <sub>s</sub>	strake radial depth	[m]
C <sub>f</sub>	friction coefficient ( $= 2 \tau_w / \rho v^2$ )	-
c <sub>p</sub>	specific heat capacity	[J kg <sup>-1</sup> K <sup>-1</sup> ]
d	diameter of rotating inner cylinder (seal rotor outer diameter)	[m]
d <sub>b</sub>	bearing bore	[m]
d <sub>e</sub>	equivalent diameter ( $= 2r_m$ )	[m]
F <sub>f</sub>	frictional drag on shaft due to churning	[N]
FTR	flushed heat transfer ratio ( $= q/H_s$ )	[-]
H <sub>s</sub>	frictional power generated by seal	[W]
h	convective heat transfer coefficient	[Jm <sup>-2</sup> K <sup>-1</sup> ]
K	constant ( $= 0.4$ ) in equations 7.10 and 7.11	-
k	thermal conductivity	[Jm <sup>-1</sup> K <sup>-1</sup> ]
k <sub>ave</sub>	average thermal conductivity	[Jm <sup>-1</sup> K <sup>-1</sup> ]
L <sub>10</sub>	time elapsed for 10% of seals to fail	[Time]
l	seal chamber length	[m]
M	bearing friction torque	[Nm]
MTBF	mean time between failures	[Time]
N	rotational shaft speed	[rpm]
Nu	Nusselt number ( $= 2 hb/k$ )	-
n	ratio of inner cylinder diameter to housing bore ( $= d/d - 2b$ )	-
P	power dissipated from probe	[W]
P <sub>b</sub>	equivalent bearing load	[N]
P <sub>f</sub>	frictional power loss due to churning	-
Pr	Prandtl number ( $= \rho c_p v/k$ )	-
p <sub>f</sub>	pressure of sealed fluid	[Pa]
Q	flush flowrate	[m <sup>3</sup> s <sup>-1</sup> ]
q	power removed by forced convection	[W]

$q_f$	power removed by external flushing	[W]
$R$	probe resistance	[ $\Omega$ ]
$R_{amb}$	probe ambient resistance	[ $\Omega$ ]
$Re$	Reynolds number ( $= \omega r^2/\nu$ )	-
$Re_a$	axial Reynolds number ( $= v_z b/\nu$ )	-
$R_h$	probe overheat resistance	[ $\Omega$ ]
$r$	radius of inner rotating cylinder (seal rotor outer radius)	[m]
$r_f$	radius of flowmeter orifice	[m]
$r_m$	mean annular radius ( $r + b/2$ )	[m]
$r_s$	shaft radius	[m]
STR	surface transfer ratio ( $= q/H_s$ )	-
SVP	saturated vapour pressure	[Pa]
$Ta$	Taylor number ( $= \omega^2 r b^3/\nu^2$ )	-
$Ta_c$	critical Taylor number	-
$Ta_E$	effective Taylor number ( $= \omega^2 r b^3/\nu_{eff}^2$ )	-
$T_c$	temperature in seal chamber	[ $^{\circ}C$ ]
$T_f$	bulk fluid temperature	[ $^{\circ}C$ ]
$T_p$	probe temperature	[ $^{\circ}C$ ]
$T_s$	seal surface temperature	[ $^{\circ}C$ ]
$V$	probe voltage	[V]
$V_o$	probe offset voltage (voltage when shaft stationary)	[V]
$v$	tangential velocity at seal periphery	[ $ms^{-1}$ ]
$v_f$	velocity at flowmeter orifice	[ $ms^{-1}$ ]
$v_z$	axial velocity in seal chamber	[ $ms^{-1}$ ]
$v_+$	dimensionless velocity ( $= v/v^*$ )	-
$v^*$	friction velocity ( $= (\tau_w/\rho)^{1/2}$ )	[ $ms^{-1}$ ]
$y$	boundary layer thickness	[m]
$y_+$	dimensionless boundary layer thickness ( $= y \tau_w^{1/2} \rho^{1/2}/\nu^{1/2}$ )	-
$\alpha$	constant of proportionality	-
$\alpha_{amb}$	ambient temperature coefficient of resistance	-
$\beta$	Taylor number index	-
$\beta_w$	Weibull index	-
$\Delta T$	Temperature margin ( $= \text{saturated vapour} - T_c$ )	[ $^{\circ}C$ ]



$\mu$	coefficient of sliding friction	-
$\nu$	kinematic viscosity	$[\text{m}^2\text{s}^{-1}]$
$\nu_{\text{eff}}$	effective kinematic viscosity ( $= \nu + \nu_t$ )	$[\text{m}^2\text{s}^{-1}]$
$\nu_t$	turbulence viscosity	$[\text{m}^2\text{s}^{-1}]$
$\nu_+$	dimensionless viscosity ( $= \nu_{\text{eff}}/\nu$ )	-
$\rho$	density	$[\text{kgm}^{-3}]$
$\tau$	shear stress in fluid	$[\text{Nm}^{-2}]$
$\tau_c$	turbulent Couette shear stress factor	-
$\tau_T$	total shear stress	$[\text{Nm}^{-2}]$
$\tau_w$	shear stress at wall of rotatory inner cylinder	$[\text{Nm}^{-2}]$
$\tau_+$	dimensionless shear stress ( $= \tau/\tau_w$ )	-
$\omega$	angular velocity	$[\text{s}^{-1}]$

---

**CHAPTER 1.**

---

**INTRODUCTION**

## 1.1 INTRODUCTION TO THESIS

The main objectives of the thesis are as follows:-

- (i) To assess the way in which a mechanical seal interacts with and is affected by its immediate environment - the envelope governed by the seal chamber.
- (ii) To assess the cost of unplanned and often unexplained failures of mechanical seals, leading to a justification on economic and technical grounds for undertaking a detailed study of the operational environments of mechanical seals.
- (iii) To determine the flow regimes in mechanical seal chambers and their effect on: heat transfer from the seal; the behaviour of gas or vapour bubbles; and solid particles in the vicinity of the seal.

To establish a basis for optimisation of seal chamber geometries.

The contents of each chapter are summarised in the following text.

### Chapter 1 - Introduction

The important factors governing mechanical seal operation are outlined, these being: sealing mechanism, sealed liquid, face presentation, face materials and face cooling. In particular the effects of these factors on the key issue of the stability of the seal interface film and the nature of lubrication are stressed. Following from this, emphasis is placed on the requirement for adequate face cooling and, hence, an understanding of the environment around the seal.

The specific technical objectives of this study are set out. The first of these objectives is to investigate the radial space requirements for a "good" seal design. Radial aspect ratios are assessed for high duty and low duty seals. The main objectives - to study the heat, vapour, gas and solids control mechanisms - all relate to the flow regimes generated within the seal chamber. Their importance for good mechanical seal performance is outlined.

Another objective is to investigate the potential for running seal chambers "dead-ended" ie. they are self-controlling and regulating without the need for external systems which are often expensive and potentially fallible.

### Chapter 2 - Seal Unreliability - the Cost to Industry

The problem and costs of seal unreliability as they confront industry are described by means of a review of published literature and anecdotal evidence. This review goes on to pin-point the major reasons for seal failure. A significant number fail in infancy due to specification faults or damage to the seal on installation and a minority wear out. A large number of seals are shown to fail in mid-life for no obvious reason. The review concludes that an important cause of failure is loss of interface film due to overheating. Whilst reporting some of the important work carried out on other aspects of seal operation, the review highlights the lack of work carried out on studying the nature of the seal environment and how this is affected by seal chamber geometry.

Chapter 2 also includes a cost benefit analysis (CBA) as its basis and thrust for work on improving the environment of seals. The CBA is based on the scarce published data and also on anecdotal evidence. The results are used to propose an approach for reducing random mid-life seal failures thus improving pay-back prospects, safety, and environmental implications.

### Chapter 3 - Review of Literature

This chapter comprises the technical literature review of the thesis. Since the flow regimes around mechanical seals have not been studied in any detail before now, the review concentrates on the nearest approach to this situation. Thus, the most relevant work on rotating annular flow regimes and heat transfer is cited and assessed. The earliest paper reviewed is Taylor's classic paper of 1923 in which the phenomenon of Taylor vortex flow was expounded for the first time. The review then reports the main work, of relevance to this study, reported in each decade up to the present day. Where they are given, formulae for heat transfer as functions of flow governing parameters are noted - these are summarised and compared at the close of the review.

The review also seeks to show where current work simplifies the "real-life" application of a mechanical seal rotating in a seal chamber.

### Chapter 4 - Test Apparatus

The development of the test apparatus and experimental techniques constituted an important and pioneering part of the thesis work; this phase of the work is reported in detail in the chapter. The specification of the apparatus is explained followed by a description of the design and manufacturing phases.

The instrumentation and measurement systems are defined in detail. Hot-film anemometer probes fitted to two mechanical seals were used for measuring convective heat transfer coefficients directly - the first time this has been attempted for mechanical seals.

Finally, the method of flow visualisation and recording of images is described. A number of previously used techniques were tried but none was satisfactory due to the high speed requirements. The most successful solution was to use air bubbles and solid particles filmed with a video camera.

### Chapter 5 - Test Programme

This chapter gives details of the test programme and combinations of variables tested. In particular, the procedure for taking heat transfer measurements is given precisely as good repeatability was only possible by using this approach. The test programme was split into three parts: water/gas tests, water/glycerol/gas tests (for higher viscosities) and water/solids tests.

## Chapter 6 - Test Results

Chapter 6 reports the results of the test work. About 60 hours of video tape was accumulated for the flow visualisation tests from which a 1 hour "Presentation Video" was collated. The first half of this chapter therefore gives a comprehensive summary of the flow visualisation results for each housing type using accompanying diagrams showing bubble and solids patterns.

Certain observed phenomena are highlighted in greater detail; some of these phenomena have no apparent explanation. The heat transfer results are reported in the latter half of the chapter with data being plotted as dimensionless parameters for comparison.

## Chapter 7 - Mathematical Model

In order to explain the phenomena reported in Chapter 6, a turbulence viscosity analysis was set up on a spreadsheet. The model is built on the hypothesis that turbulence viscosity can have a real effect on the ratio of inertial to viscous forces, and hence affect the type of flow regime. This is believed to be the first exposition of such a hypothesis in this application.

The model predicts the turbulence viscosity using a modified Prandtl mixing-length theorem. From this, an explanation for the high-speed vortices is constructed.

## Chapter 8 - Discussion of Results

A discussion of experimental results for each housing is given and distinguishes the gas/vapour, solids and heat transfer controlling characteristics. The implications for each housing design are drawn out and illustrated with comparative diagrams of flow patterns. The poor performance of the narrow radial clearance housing types becomes obvious as is conversely the generally improved performance of the wider housings - in particular the 45° positively flared housing. The results of the mathematical model are discussed, particularly in the light of the experimental results. This produces compelling evidence that the hypothesis outlined in chapter 7 is valid.

## Chapter 9 - Design Study

Some specific work is reported which was carried out on another test rig to investigate the effect of seal housing design on interface film instability. The text describes how a particular seal design was run in two housing configurations - one known to be "poor" from observations and the other known to be "good" (ie. free of gas or vapour). The seal was run on pressurised water at increasing temperature until seal instability was encountered. The results from the study show that instability occurred at lower temperatures (accompanied by some seal failures) for the "poor" housing as opposed to the "good" housing. This supports the test work which formed the mainstream of the study.

## Chapter 10 - Case Study

A parallel test programme provided the opportunity to investigate the effects of seal housing design on a specific duty - clay slurry. Chapter 10 summarises the method of testing using a centrifugal slurry pump and 80m test loop simulating real quarry conditions on full scale equipment. Drawing on experience with water and solids from

the experimental work of the thesis, the seal chamber was redesigned to improve the supply of the lubricating water phase to the seal faces.

The results were dramatic and seal performance significantly enhanced.

### Chapter 11 - Conclusions

The conclusions are split into three sections : economic considerations; housing design; and analysis implications. From an economic viewpoint it is concluded that investment in solving seal failure problems is money well spent. However, it is noted that improvements may be hampered in the short term by difficulties with retro-fitting optimum housing designs to existing pumps and in the long term by restrictive standards currently in use.

A number of conclusions emerge from the experimental work, chief among them being the evident superiority of the 45° flared housing over other designs in many cases. It is also concluded that the technique of heat transfer measurement used in this study was generally successful.

Finally, the analysis is considered to have made an important contribution to explaining the interesting and hitherto unexplained phenomena of structured flows in the turbulent regime.

### Chapter 12 - Recommendations for Future Work

The chapter highlights the main areas of uncertainty raised by the study. In particular, it suggests the need for further and more sophisticated mathematical analysis of the seal chamber flow regimes, probably using a computational fluid dynamics model. Further experimental work is also cited as being necessary to refine the flared housing, improve the compromise when handling large amounts of gas and solids simultaneously, and deal with the problem of retro-fitting through the use of bolt-on seal housing-plus-seal cartridges.

### Chapter 13 - Corollary

The final chapter describes how the results of the thesis can be translated into real benefit through the establishment of functional guidelines and, ultimately, standards. A first step in this direction has been taken by BHR Group Ltd, based on the thesis results and a draft guidelines document (included in the Appendices) has been circulated to sponsor companies for consideration and will shortly be released to a wider audience. It will also form a major input to the UK proposal for the revised ISO 3069 standard.

## 1.2 IMPORTANT FACTORS

### 1.2.1 Sealing Mechanism

The function of a mechanical seal is to prevent the pumped process fluid from leaking out of a pump body at the point where the impeller drive shaft enters. The seal is therefore required to operate under conditions of extreme temperature, and on liquids which are toxic, flammable and corrosive. Moreover, sealed pressures are commonly up to 70 bar and occasionally higher. Naturally, seal users expect virtually zero leakage with such chemicals and at the same time reliable seal operation with lives typically in excess of 3 years. Currently, most mechanical seal installations on centrifugal pumps resemble that shown in Fig 1.1.

Mechanical face seals are, in essence, plain annular thrust bearings and all have the features illustrated in Fig 1.2. The dynamic sealing takes place in the sliding interface between the stator and rotor, other leakage paths being sealed with stationary or pseudo-stationary secondary seals. Unlike a conventional bearing, the mechanical seal runs usually in a mixed-film lubrication regime ie. some boundary and some full-film lubrication with film thickness typically between 1 and 3 $\mu$ m. Consequently, the profiles, surface finish, and materials of the two faces are critically important. Moreover, the mechanical seal cannot usually choose its optimum running fluid but must tolerate the pumped process liquid however poor its lubricating properties.

The stability of the interface fluid film is vital to the successful operation of the seal; should it disappear through vaporisation and the seal run dry then failure will soon occur. Generally this will be caused either by face material distress, secondary seal degradation due to the seal running hot, or by very high face wear. Film stability is influenced by many parameters but the chief ones are sealed liquid, face presentation, material types and face cooling; these are, of course, inter-related thus making analysis difficult.

### 1.2.2 Sealed Liquid

The main liquid properties of importance here are volatility and what is termed "lubricity". In order to keep the interface film in the liquid phase the bulk sealed liquid must be below its saturated vapour point or range. Due to the heating in the interface caused by the very high shear-rate, a "temperature margin" (denoted  $\Delta T$ ) must be allowed if the seal is to run without vaporisation of the interface film. Some very volatile liquids, for example: liquified petroleum gas and light hydrocarbons, must frequently be run at very low  $\Delta T$  values and are prone to instability. For a given seal design,  $\Delta T$  varies with sealed pressure and an instability curve may be drawn. Figures 1.3 and 1.4 illustrate such diagrams -Figure 1.3 is a seal designed for a maximum pressure of 16 bar whereas Figure 1.4 is a high pressure seal.

"Lubricity" is a term used widely in the sealing industry but apparently without an agreed definition. It does, however, convey an impression of the ability of the sealed liquid to allow the face materials to run under boundary conditions and must therefore be influenced by the physics and chemistry of the face surfaces. This latter subject is one which is relatively poorly understood.

### 1.2.3 Face Presentation

A large amount of research work has been concentrated on this subject and it is still on-going. It is generally known that mechanical seal faces need to be very flat, ie. within 2 light bands or of the order of one tenth of a micron. This is achieved usually by diamond lapping and checked using an optical flat. Surface finish is normally in the range 0.05 to 0.20 $\mu$ mRa.

The faces of a mechanical seal are able to move axially and also to cone inwards or outwards. The loading element, usually springs or bellows, provides a nominal closing force on the faces under static or loss-of-suction conditions; it is usually designed to be small compared with the hydraulic loading of the seal in operation. Some seals allow their faces to see full system pressure and are termed "unbalanced" (Fig 1.5). Unbalanced seals are cheap and simple but cannot operate at pressures much in excess of 10 bar owing to vaporisation of the interface film.

Most process mechanical seals are of the balanced type in which the face area over which the sealed pressure acts is reduced by geometry. The ratio of the area over which the pressure acts to the total interface area is known as the "balance ratio". Thus an unbalanced seal will have a balance ratio of 1 or above, and a balanced seal less than 1. Commonly the ratio is around 0.7 or 70% ie. the interface pressure is 0.7 of the sealed pressure. The nearer the balance ratio is to unity, the thinner the film becomes and, the less will be the leakage. However, the shear rate and heat generation increase as a result and a compromise is needed; this varies depending on the application.

The hydraulic force generated by the sealed liquid not only loads the faces axially but also generates a turning moment about the cross-sectional centroid of the seal rings and causing them to cone. Where the sealed liquid is on the outside, as is the case with most seals, the moment tends to cone the faces inwards to cause contact at the outer edges (Fig 1.6). This is denoted "positive" rotation and sets up a face taper which is divergent in the direction of leakage, and cuts off the interface film. On most seals the effect of heat is to distort the seals to rotate negatively, that is, to form a convergent taper (Fig 1.7) which allows the interface film to be maintained.

Ideally, the pressure and thermally-induced rotations are kept in balance so that the faces are as near parallel as possible, or at least with only a very small convergent taper. This can be achieved for steady-state running at a particular design condition, but tolerance to off-design or transient conditions is rather more difficult. Seal "tolerance" is, therefore, an area where there is much current interest.

### 1.2.4 Face Materials

Because most mechanical seals experience boundary conditions during both "steady-state" running and transient conditions, the compatibility of the face materials is of paramount importance. A face pair unable to survive the initial dry running on start-up without damage will probably be the cause of early seal failure.

Tribological compliance is therefore required in one face; in the majority of cases this is satisfied by using a high quality carbon impregnated with resin or metal. Carbon graphite is a good lubricant in its own right providing that it is not starved of oxygen, water or a hydrocarbon in trace amounts; most sealed liquids fulfil this criterion.



Moreover, carbon is a reasonable conductor of heat which is vital to the interface film stability. The main disadvantages of carbon are its low modulus, brittleness, and difficulties with quality assessment and control.

Counterfaces to carbon are always much harder and stiffer and most medium and high duty applications use tungsten or silicon carbides. These materials have proved themselves to be very good in almost all applications and, as a result, their cost is falling as they increasingly become the industry standards. However, that is as far as "standardisation" goes since within each material type there exists a large range of commercial products which have differing grain sizes and shapes, binders and homogeneity. The merits of each grade have yet to be qualified and, like carbon, quality control is an area requiring further work.

### 1.2.5 Face Cooling

Removing heat from the sealing interface is vital to the seal's survival. A 50 mm seal running at 3000 rpm and 30 bar can quite easily generate 1kW due to interface shear. Given the volume of liquid in the interface itself, instant vaporisation would occur were the heat not removed. Although some heat is conducted away through the faces and thence to the sealed fluid, most is convected away by the liquid in the immediate vicinity of the seal faces.

The process of convective heat transfer from the seal faces relies on a good supply of constantly replenished cool liquid. On many applications this can only be achieved by flushing the seal faces with an external line taken either from the discharge side of the pump (Fig 1.8) or an independent ancillary system (Fig 1.9). Usually a neck bush is placed downstream from the seal in the cooling circuit which has the effect of raising the seal chamber pressure and thereby increasing  $\Delta P$ .

External flushing arrangements introduce extra complication to a plant and often need a supply of clean, cool, fresh water for the secondary cooling circuit. They are therefore expensive to install and maintain and subject to operator error; many seal failures can be traced to inadequate cooling systems, poor maintenance and incorrect operation. To be able to dispose of such systems entirely and rely on the intrinsic cooling effect of the flow within the chamber would lead to significant cost savings and enhanced reliability. The nature of this flow is dependent to some extent upon the shape of the chamber.

Most centrifugal pumps allow little room for a mechanical seal and hence the radial clearance around the seal is very small, typically around 2 to 3 millimetres (Fig 1.1). The shape of these chambers, or more correctly "stuffing boxes", is determined by the requirement for fitting soft-packing (Fig 1.10) as defined by the DIN 24960 and ISO 3069 standards - see Appendix A. API 610 states "The seal chamber of overhung pumps shall conform to the minimum dimensions shown in Appendix A. With these dimensions, the minimum radial clearance between the rotating member of the seal and the bore of the seal chamber shall be 1/8 inch (3 millimetres). The bore diameter of the seal chamber shall be a multiple of 1/8 inch or, in the case of metric design, 5 millimetres".

Currently, over 90% of applications are fitted with mechanical seals in preference to soft packing and are likely to remain that way. It would appear sensible, therefore, to design a chamber around the mechanical seal tailored to its needs. The plethora of cooling systems currently required would imply that the very narrow clearance chamber

afforded by the stuffing box is not allowing optimum internal cooling of the seal.

Despite this obvious inadequacy, very little research work in this area has been undertaken.

### 1.3 OBJECTIVES

The objective of the experimental programme presented in this thesis was to generate information which will enable improvements to be made to the operational environments of mechanical face seals in centrifugal pumps.

An optimized seal chamber should provide the following:-

- radial space for an adequately rigid seal
- flow conditions conducive to efficient heat removal
- control of vapour or gas accumulations
- control of suspended solids
- satisfactory performance when running without an external flush
- performance independent or at least unimpaired by seal design, piping plan, injection angle, injection flowrate, and the presence or otherwise of neck bushing.

The experimental programme addressed each of these requirements and sought to provide information which could form the basis of design guidelines for mechanical seal chambers.

#### 1.3.1 Seal Geometry

One of the frequent criticisms of stuffing boxes is that they do not allow the seal designer sufficient radial space to accommodate an optimized seal design. As a result, many mechanical seals are long and slender and are therefore relatively flexible. This tends to make them more prone to large distortions at the faces. An optimized seal chamber must, as a consequence, allow room for an adequately rigid seal as well as sufficient radial clearance around the seal for optimizing the flow of liquid within the chamber. The study of radial clearance ratios was carried out for DIN and high duty seals (Appendix B) and the results are given in Figure 1.12. Quite clearly when seal designers are freed from the constraints of the DIN stuffing box they design seals which require more radial space.

#### 1.3.2 Heat Removal

Removing heat from the sealing interface film is usually the most important function of the liquid in the seal chamber. As mechanical seals are frequently dissipating kilowatts of power, the convective heat transfer coefficient needs to be very high in order to ensure rapid heat removal. If the seal face temperature is allowed to climb, due to poor heat removal or a change in process conditions (higher temperature or pressure), then there is a real danger of seal instability or "puffing". This phenomenon usually occurs in the following way:-

- (i) Interface temperature rises. This often reduces the viscosity of the interface liquid thus reducing the film thickness. The faces come closer, thereby increasing the shear rate and asperity contact and generating more heat.
- (ii) Vaporisation occurs in the film initially at the atmospheric edge where the pressure is lower or at asperity contacts. This reduces hydrostatic support and allows the faces to come even closer together.

- (iii) The whole film vaporises and the seal emits a "puff" of vapour. However, the latent heat of the evaporating film removes heat from the seal faces which cools them to a sub-critical temperature and permits the re-establishment of the liquid film.
- (iv) The liquid film re-heats and the process starts again.

This phenomenon is very common on lighter hydrocarbons and aqueous-based liquids. Typically, complete instability cycles take anything between a few seconds and a few minutes depending on the thermal inertias in the system. The repeated thermal cycling can ultimately cause stress cracking or heat crazing (Fig 1.13) as the surfaces of the faces fail in fatigue.

Clearly, the desirable solution would be to avoid the puffing phenomenon. Since this cannot be effected very easily through process changes then the cooling of the seal faces must be improved by optimising the flow within the seal chamber. This has the same effect as increasing the available  $\Delta T$ .

Improving the seal cooling also has the added benefit of adding thermal damping to the system in case of sudden movements in pressure. Pressure fluctuations are commonplace on most plants due, for example, to valves being opened or shut. Additionally there is a good deal of background "noise" caused by valve and pump cavitation and also by vibrations from rotating or reciprocating machinery which are transmitted, and often amplified, by pipework. All these movements can alter the face presentation, film thickness and wear profile of a mechanical seal.

### 1.3.3 Vapour and Gas Control

There are two sources of vapour in a sealing system. It can originate firstly from the sealing interface film evaporating and, secondly, from vapour in the sealed liquid. The latter emerges as dynamic pressures fall in the high speed rotating flows. In addition, gas in the process may find its way to the seal chamber, whereupon it is centrifuged onto the rotating shaft.

The interface film, as has been noted, is very prone to generating vapour due to its elevated temperature and pressure drop. Some vapour will escape to the atmosphere but the rest is likely to find its way to the product side. Unfortunately, the intrinsic design of most mechanical seals creates a groove at the sealing interface as a result of having one face narrower than the other (Fig 1.2); any vapour appearing at the interface therefore is centrifuged into this groove by the rotating liquid. Ultimately, a continuous toroidal vapour bubble can be formed in the groove (Fig 1.14) which isolates the faces from the cooling liquid causing the seal to run hotter and generating more vapour. The condition is therefore unstable and is known as "vapour-locking". A vapour-locked seal will stand little chance of survival. Vapour-locking can also occur if suspended vapour or gas bubbles are allowed to find their way into the seal environs.

The function of the flow within the seal chamber is (a) to keep potentially harmful vapour and gas bubbles away from the seal and (b) to purge the groove at the sealing interface of any bubbles caused by vaporisation of the interface film.

### 1.3.4 Solids Control

Most processes carry some suspended solids which will find their way to the seal chamber. Commonly these particles are rust, sand or miscellaneous wear debris. In the extremes, where the product is a slurry, solids form the bulk of the sealed fluid. Solids are most harmful when they penetrate the sealing interface; once there they will break up the film and cause extra heating and rapid wear. Only the finest particles can enter the sealing film, but most processes are likely to have a small amount of these particles. Coarser particles could conceivably cause problems if they are allowed to accumulate and "pack-off" the seal, thereby obstructing heat removal processes. Of particular importance in investigating the behaviour of solids in suspension is observing how they are affected by centrifugal forces and turbulence; this will probably also vary with particle size and density.

### 1.3.5 Dead-Ended Running

Running without an external flush is known as running "dead-ended". Some seals are already run dead-ended but these tend to be low duty, non-critical applications. As previously observed, dispensing with an external flush wherever possible is a worthwhile goal. If the environment of the seal could be controlled entirely by the inherent properties of the internal flow then maintenance should be reduced and the human error factor removed. However, to control the environment to the same extent as a properly designed and maintained external cooling system is a very difficult goal to achieve and some compromise in certain situations may be necessary.

### 1.3.6 Dependence on Other Variables

Many variables can influence the seal's environment and these are discussed briefly in the following text:-

#### (i) Seal design

Seals are produced in a number of types, all with different external geometries. As they are rotating at high speeds, often in confined spaces, some influence on flow should be expected. Certain common features are likely to cause local cavitation or additional turbulence; steps in the profile might generate egressing flow, and large springs could generate significant axial flows. In the case of exposed springs, rotational direction may become an additional variable. Ideally, a good seal chamber should perform well irrespective of the type of seal installed.

#### (ii) Piping plan

The operational standards for mechanical seals give a large range of piping plans (Fig 1.8 and 1.9) designed to cater for different applications. However, the assessment of the relative merits of each plan (and the selection of the best one for a given application) is left to the intuition and experience of the seal designer or user. An aim of improving the design of the seal chamber should be to allow the seal to be run with the simpler plans and to evaluate their relative performance.

**(iii) Injection angle**

Most seal flushing systems have radial coolant ports injecting liquid at right angles to the rotating body of liquid in the seal chamber. It is possible that some benefit may result from tangential injection either with or against the swirling flow. Some claims have been made to this effect but, to the author's knowledge, they are not supported by any published experimental data.

**(iv) Injection flowrate**

Although an important variable in the design of a seal cooling system, there are few data published to back up the recommendations made by seal manufacturers. Moreover, few seal users have the facility to measure these flowrates; this, therefore, is something of a grey area.

**(v) Neck bushing**

Neck bushing has two purposes, firstly to act as a pressure raiser in the cooling circuit, and secondly to provide some isolation from the process liquid. It would be reasonable to assume that it also acts to decouple the flow around the impeller from that in seal chamber. The presence or otherwise of a neck bush could, therefore, exert a major influence on the behaviour of vapour and solids in the seal chamber. When running dead-ended it would probably affect the removal of heat from the seal.

---

**CHAPTER 2.**

---

**SEAL UNRELIABILITY -**  
**THE COST TO INDUSTRY**

## 2.1 THE PROBLEM

It has long been recognised that a large part of the maintenance bill for process plant is due to the failures of centrifugal pumps. Will (1982) reported that the annual pump maintenance bill for Exxon's 14,000 pumps amounted to £10 million or £700 per installed pump per year. Similar figures emerge from Ingram's (1984) study of pump performance at Monsanto, namely that on large plants (circa 2000 pumps) the cost was between £2 million and £5 million per year (£1000 to £2500 per installed pump per year). Bloch (1985) states that the cost per pump outage was greater than £3000 and that the mean time between failures (MTBF) was between 6 and 13 months, depending on the duty. In 1986, the cost of seal failure to Exxon was about £4 million according to Bloch (1986). This agrees with Sangerhausen (1981) who suggests £2500 per pump outage. This cost covers spare parts and labour and Sangerhausen is at pains to point out that the real cost of lost production is much greater and more difficult to estimate. He suggests that part of the latter cost manifests itself in the resulting requirement for identical back-up pumps for most duties.

The reasons for the high costs of pump maintenance appear to be numerous, but by far the largest single source of downtime is the failure of the mechanical seals. Bloch (1984) reports that 70% of pump outage is due to mechanical seal breakdown and that 50 pence out of every £1 of the maintenance bill for rotating equipment is spent on seal-induced pump failures. Similarly, Ingram suggests that 55-70% of his pump failures are due to mechanical seals. In similar analyses, other reporters cite 60% (Nau 1985) and 75% (Will 1982) as realistic figures. On one of ICI's petrochemical plants, Summers-Smith (1981) states that in one year one third of all installed pumps required maintenance resulting from seal failure. On another particularly troublesome section of ICI plant, Almond and Passmore (1985) found that the average seal mean time between failures (MTBF) was only 77 days. The BHRA seal reliability survey reported by Flitney and Nau (1982) found that most seals had lives of less than 1500 hours and very few lasted longer than 8000 hours. One seal lasted over four years, but its replacement failed within one month!

Further studies of seal reliability were carried out by BHRA in the period August 1981 to March 1984; the results are reported in Flitney and Nau (1985). The work concluded that 60-70% of pump outage in process plant is associated with seal failures, and in a typical refinery 30% of the pumps required seal replacement within 4-6 months of installation. However, seal lives were still found to be very variable even on a single, nominally identical duty. Some of their examples of seal lives are given in Tables 2.1(a)-(e), reproduced from Appendix II of their report. The data, taken totally, show the widespread nature of seal life variability on a variety of refinery duties. An extreme example is the Desalter Water Pump in Table 2.1(a); the first seal ran for over 3 years before the pump was taken down for repair - its replacement seal lasted only 22 days and the second replacement less than 2 days! Few seals last more than a year (8000 hours) and the majority fail within 6 months. It is the apparent random nature of most of the failures which is particularly irksome.

Two of the pumps reported generated sufficient seal failure data to enable Weibull analysis to be carried out. (Weibull analysis is a statistical technique used to indicate failure modes of a piece of equipment - for a full explanation see Kapur and Lamberson (1977), chapter 11). The two duties are the Visbreaker Charge pump (Table 2.1(c)) and the Bottoms pump, (Table 2.1(e)).



The Weibull plots are shown in Figure 2.1 and 2.2 respectively and both yield Weibull indices of ( $\beta$ ) of 1.3 - this indicates mid-life random failure modes.

Peel (1988) claims that "a major UK chemical manufacturer suffered in an average year 283 breakdowns of the mechanical seals on the 69 pumps in its solvent plant". Unfortunately, no failure data are actually given but his figures suggest an MTBF of about only 3 months and an  $L_{10}$  life of 9 days.

Additional costs are also incurred from the necessarily large inventory of spares required and Nau (1985) reports that Lankro stock three spare seals per installed pump (stock value at least £1000 per installed pump). A senior engineer from ICI estimated that their mechanical seal spare inventory was greater than £2 million. A further cost not generally reported is that of built-in redundancy of back-up pumpsets; these are often necessary solely due to the unpredictability of the mechanical seals. Commonly, the back-up unit stands idle for months or even years and is then expected to work perfectly when the main pump-set is down. Howard (Amoco UK), in a private discussion related a number of instances where the back-up seal had failed under these conditions and part of the plant had to be shut down for several days. The cost to his company in these cases was tens of thousands of pounds per hour in lost profit alone, ie. between one and two millions pounds total downtime cost.

Finally, there is the danger of environmental pollution reported by Nau (1985) from failed seals with unquantifiable economic and political repercussions. Even under normal operating conditions, a walk around a refinery or chemical plant will bring one into contact with many strong and pungent odours! Austin, Flitney and Nau (1980) found that all single seals studied leaked vapour even if no liquid leakage was visible. Measures to prevent vapour leakage require expensive ancillary equipment; Flitney (1977) gives some common examples. Major seal blowouts have been known to cause clouds of dangerous gases or fires. Legislation on this subject is already emerging. For example, the US State of California has issued Rule 1173 which places stringent controls on the amount of volatile organic compounds (VOC's) which can be released into the atmosphere by leaking mechanical seals. On the basis of past experience, this is very likely to be accepted as a requirement for the whole USA and probably Western Europe as well. In the late 1970's BHRA carried out a survey of vapour emissions on behalf of the Dept of Industry and reported in Austin, Flitney and Nau (1980). Little interest followed from this work at the time - things may be set to change, however, in the 1990's.

## 2.2 REASONS FOR SEAL FAILURE

A considerable amount has been written on the causes of seal failures. Failure due to wear-out appears to be uncommon and constitutes less than 10% of all seal failures according to Buck (1980). Using Weibull analysis techniques, Summers-Smith (1981) and Bertele (1984) found that most failures occurred either within a few days or hours (infantile failures) or randomly after periods of months (random mid-life failures). The reasons for infantile failures are explained by a number of authors, and Bloch (1985), Ingram (1984), Bertele (1984) and Summers-Smith (1981) all suggest incorrect seal design, installation errors, damage to the seal on installation, material selection errors and manufacturing errors as plausible reasons.

The reasons for random mid-life failures appear more difficult to explain. Ingram (1984), and Nau (1985) suggest that the pump itself may have a deleterious effect on seal performance if it is operating away from its best efficiency point or if there is excessive shaft deflection or axial vibration. Process operation effects, in particular pressure fluctuations, are also cited as being potentially harmful to the seals by Flitney (1987). Cranfield (1988), in a paper dealing with loss of suction pressure on boiler feed pumps (BFP's), provides indisputable evidence of such effects (Fig 2.3). He states that "under transient operating conditions, difficulties have been experienced with loss of NPSH causing vapour locking of the BFP, pumps overspeeding and an inability to maintain condensate flow". It would be reasonable to assume that, under such conditions, the seal is running with insufficient lubrication and cooling. Flitney and Nau (1984) have found problems with inadequate seal flushing arrangements or complete failure of these ancillary systems due to various causes. Summers-Smith (1981) postulates that many seals are running on an interface which is marginally stable and thus a slight perturbation will result in film evaporation and probably seal failure. Flitney (1977) has found that many failed seal faces show evidence of over-heating which would tend to bear out this theory. In a private discussion, a service engineer for a major seal manufacturer stated that most of the failed seals he changed showed signs of thermal distress at the faces. Sangerhausen (1981), Ingram (1984) and Nau (1985) all question the ability of the flow around seals, however generated, to remove heat, vapour and solids from around the seal faces.

Seal manufacturers have claimed that many seal failures are caused by incorrect specification or poor fitting. Typically, figures of 40-50% failures due to these causes are cited in conversation and sometimes published. Such failures are invariably "infantile" ie. they fail within the first few hundred hours (two weeks) of running. Certainly the manufacturers are often justified in pointing to poor training of both fitters and engineers engaged in seal specification as the cause of a significant proportion of failures. However, Flitney and Nau (1985) suggest that the proportion of infantile failures is nearer 25% as shown in Figures 2.4 and 2.5 taken from their report. Also, from Figure 2 seal wear-out (ie. lives in excess of 2 years (17000 hours)) accounts for less than 10% of failures. The remainder are apparently random mid-life failures although Flitney and Nau explain that, of these failures, about 10% are due to routine maintenance and some 10% are attributable to bearing failure. From their results the following break-down of seal failure causes may be deduced.

Failures due to fitting/incorrect specification	25%
Failures due to wear-out	10%
"Failures" due to bearing replacement	10%
"Failures" due to routine maintenance	10%
Unexplained random mid-life failures	45%

In summary, nearly half of all seal failures occur randomly in the mid-life phase of a seal and are apparently not attributable to any particular cause.

## 2.3 COST BENEFIT ANALYSIS

### 2.3.1 Introduction

Clearly the costs associated with mechanical seal failure can represent a significant drain on resources. To what extent, however, should money be spent to improve the situation? Indeed, what is a reasonable seal life in general sealing applications? The following analysis attempts to address these issues. It notes areas where small investment could result in rapid payback and other areas where a greater understanding of the operation of seals is necessary for significant progress to be made. Unfortunately, there are few published surveys on which to base a model, and the limitations and assumptions inherent in such an approach are set out carefully.

### 2.3.2 Model Basis

In 1985, the cost of rectifying a failed pump was around £3000; this figure includes only the cost of replacement parts and labour. Assuming an annual cost inflation of 10%, the direct cost of overhauling each pump in 1990 is probably approaching £5000.

The model assumes that 70% of pump outages are attributable to seal failures on the basis of published figures. Using the above assumptions, a graph of cost of failure against mean-time-between failures (MTBF) can be plotted for plants of various sizes (Fig 2.6). This simplistic graph suggests that, for a plant with 1000 pumps, "infantile" failures (say plantwide MTBF of less than 1 year) will cost the company nearly 4 million pounds per year in pump outages. Doubling the MTBF to 2 years obviously halves the number of pump outages but will still result in over 2 million pounds worth of maintenance bills. This figure is likely to be on the conservative side as actual seal population generally exceeds pump population due to installations requiring double or tandem seals and between-bearing pumps with a seal either side of the volute.

### 2.3.3 Site Surveys

The following surveys represent the sum total known or available to the author but give some idea of typical MTBF's and  $L_{10}$  lives in industry. The background calculations are given in Appendix C.

Source	MTBF	L <sub>10</sub> Life	Average Cost per installed pump per year/£
Bloch (1985)	13 months (well maintained facility)	6 weeks	1,000
	6 months (industry average)	3 weeks	2,200
Almond and Passmore (1985)	79 days (Vinyl chloride plant)	8 days	23,100
Flitney and Nau (1985) (Company No 1)	17 months (in 1st 21 months of survey)	8 weeks	3,500
	20 months (after full 39 months of survey)	9 weeks	2,900
Flitney and Nau (1985) (Company No 3)	15 months	7 weeks	3,900
Flitney and Nau (1985) (Company No 5)	22 months	10 weeks	2,700

A number of points arise from these surveys:

- (i) Infantile failures reported by Almond and Passmore are very expensive. The pump population of a particular vinyl chloride plant was 49 from which it can be estimated that seal failure on just this one unit was costing his company over £1 million per year! Almond reports that a change of seal design more than doubled the MTBF to 180 days - a saving of about £0.5 million pounds in the first year. Even if the design upgrade had cost £1,000 per pump, then the total cost would have only been £50,000. This represents a pay-back period of just over 1 month.
- (ii) Attention to detail and good practice were largely responsible for the 18% improvement in MTBF reported by Flitney and Nau (Company No 1). Careful records of failures had been kept over the first 2 years of the survey upon which informed troubleshooting was based; the result was a significant fall in the number of seal failures (Fig 2.7). The reduction of £600 per installed pump per year represents a plantwide saving of some £130k per year achieved only at the expense of a small amount of time. If the reliability monitoring required one full-time technician to collect and analyse the data, then the cost per year of his time would be about £40k (assume charge-rate at £20/hr). This amounts to less

than a third of the costs of failure, a saving of £80k net per year and a pay-back period of 4 months. On a recent visit to this plant, the author was impressed to see that the continued use of failure records along with weekly vibration monitoring of every pump on site had reduced seal failures dramatically.

The industry average MTBF appears to be below 2 years ie in 2 years on average a company is replacing one seal on every installed pump. Even on a small plant of 200 pumps, this means that the company is buying and fitting about 100 new seals every year - a cost of some £½ million per year.

Mean  $L_{10}$  lives of seals seem poor when compared with bearings which are typically required to have an  $L_{10}$  life of 4 years. Naturally, on a plant which has a major shutdown every 2 years, an  $L_{10}$  life of about 2 years would probably be acceptable; even this goal seems a long way off if the results of the surveys are to be believed. Indeed at the 12th International Conference on Fluid Sealing in May 1989, a workshop session on mechanical seals was told by some major users that they would like to see  $L_{10}$  lives of 5 years.

Field and Flitney (1975) report that for one diesel engine manufacturer, the  $L_{10}$  life of 100,000 miles for their water pump seals was unacceptably low. They commissioned a study of the seal (described in more detail in sub-sections 2.4.3) to investigate ways of increasing the  $L_{10}$  life significantly in order to extend the warranty period in line with their competitors.

#### 2.3.4 Cost-savings Through Improved Seal Reliability

To gauge the impact of seal failure in cash terms, an imaginary plant was created and analysed based on the information presented in the previous pages. Some conjectural assumptions have to be made in order to simplify normally complex calculations and these will introduce inaccuracies - accordingly the study aims to yield "order-of-magnitude" figures.

The plant is a small oil-refinery with 220 pumps all fitted with mechanical seals. The pumps fall into two groups: overhung pumps (o/h) and between-bearing (b/b) pumps. The plant is running with a pump mean-time-between-failures of 12 months. The rotating machinery engineer is tasked with raising MTBF to 24 months, the interval between routine shutdowns.

- (i) Overhung pumps  
 Population = 200  
 Power range = 50 to 250 kW  
 Fitted with single mechanical seals of unit average cost £500  
 Average cost of pump outage = £5000

Due to the short MTBF, the engineer is forced to keep an average of two spares per installed seal; this inventory of seal spares for the o/h pumps is therefore £200k.

- (ii) Between-bearing pumps  
 Population = 20  
 Power range = 200-500kW

Fitted with double mechanical seals at both the motor and free ends.  
Average cost of pump outage = £6000

These 20 pumps handle the high-power duties on the refinery. They are running on very arduous duties with high pressures and temperatures - hence the need for double seals. Again, the engineer has to stock two spares for every installed seal, making a total of 160 seals (of value £80k) for just 20 pumps. Due to the added costs of the seals and the increased man-hours associated with overhauling and installing these pumps the cost of a pump outage is higher than for the overhung pumps.

Taking the refinery globally, the cost of seal failures per year is:-

o/h pumps, 200 failures @ £5000	= £1.0M
b/b pumps, 80 failures @ £6000	= £0.5M
Total	= <u>£1.5M</u>

Of that £1.5 million the costs associated with different causes of seal failures are likely to be as follows:-

<u>Failure</u>	<u>Cost [fk]</u>
Infantile (25%)	375
Routine maintenance (10%)	150
Bearing failures (10%)	150
Wear-out (10%)	150
Random mid-life (45%)	675

The infantile failures are probably due to poor specification or fitting. These can often be prevented by attention to detail of the installation design and operation, liaison with seal manufacturers and proper training for everyone involved in handling the seals. The best discipline for carrying this out is good record-keeping. Within 2 to 3 years of instigating this discipline the imaginary plant could expect to reduce its annual maintenance bill by £375k by this means.

However, random mid-life failures are also costing a large amount of money. Drawing on the fact that the commonest type of mid-life failure is thermal distress it would seem reasonable to assume that improving the environment of these seals would significantly reduce the incidence of failure in half of these cases. In other words, improved seal environments could save about £340k per year - money which could either be spent on new plant or be added to the profitability of the plant.

One problem facing the engineer is how to improve the environment of the seal - can he retro-fit a better chamber or is it a case of buying a brand new state-of-the-art pump with all the latest technology built in?

The engineer considers the two different types of pump separately:-

(i) Over-hung pumps

The average cost of a new replacement pump is £10k making the cost of a total upgrade of the population £2.0 million. Clearly this is not likely to be acceptable to the refinery director! However, half of the pumps can be retro-fitted with an improved chamber

design - this involves boring out the stuffing box when the pump is in the workshop as the result of a seal failure. The extra cost is negligible - a few man hours. Of these 100 pumps, only a half actually benefitted from the modification by having their MTBF raised to 24 months. However, this represents a saving in maintenance bills of £25k per year for very little extra cost. The engineer had to recruit one extra man in the workshop to bore out the stuffing boxes - his annual cost to the company amounted to £25k, making a net saving of £100k per year. This £100k can now be re-invested in replacing 10 pumps in the second year, another 10 the third year and so on. The first pumps to be replaced would obviously be the "problem" pumps ie. where MTBF is of the order of a few months. A seal failing more than twice in one year buys a replacement pump with double the life in only two years.

(ii) Between-bearing pumps

Due to the high costs associated with these 20 pumps, the engineer managed to persuade the refinery director that a phased replacement of the whole population over a period of time was justified. But how fast should they be replaced?

The following costs are involved:-

Annual cost of maintenance of "old" design pumps	= £6k
Annual cost of maintenance of "new" design pump (assuming a doubling of seal life).	= £3k
Cost of replacement "new" design pump	= £20k

The options are to replace the pumps at the rate of 2, 4, 10 or 20 pumps in a year. The new pumps will start saving money as soon as they are running but the initial capital outlay is high. The options are given in the table below. It is assumed that investment begins in Year 1.

	YEAR	COST [£k] (inflation adjusted)			
		2/yr	4/yr	10/yr	20/yr
	0	120	120	120	120 - baseline cost
	1	148	176	260	400
	2	142	164	230	60
	3	136	152	60	60
	4	130	140	60	60
	5	124	128	60	60
	6	118	60	60	60
	7	112	60	60	60
	8	106	60	60	60
	9	100	60	60	60
	10	94	60	60	60
	11	60	60	60	60
Cum. cost	=	1390	1240	1150	1120
		(1440)	(1440)	(1440)	(1440)
Payback time (yrs)	=	10	7½	6	5½

The figures in brackets denote the cumulative costs after 12 years if no remedial action is taken. The cost profiles are illustrated graphically in Figure 2.8 and the cumulative costs in Figure 2.9. To replace 20 or even 10 pumps a year requires very high capital



investment and a pay-back time of 5 to 6 years. To replace only 2 pumps per year would double the pay-back time. However, a replacement rate of 4 pumps per year represents a manageable amount of capital investment whilst still giving a pay-back time of 7 years.

In summary, the engineer can expect to see good cost savings as a result of his upgrade programme. This consists of:-

- (a) Reduction in seal spares inventory of £140k per year.
- (b) Reduction in seal failures on overhung pumps of 25% giving a saving of £100k per year. If he chooses, this money can be used to replace "problem" pumps.
- (c) Replacement of between bearings pumps at the rate of 4 per year. Payback in 7 years - thereafter an annual saving of £60k per year on these 20 pumps.
- (d) A total reduction in maintenance bill of over £300k per year through improvements to the environments of the mechanical seals - a saving of £15k per installed pump per year.

### 2.3.5 Conclusions

Remedying infantile mortality cannot of itself bring about  $L_{10}$  lives in excess of 2 years; this can only come about if the random mid-life failures can be explained and avoided and seals made more tolerant to running in off-design conditions. A recent BHRA site investigation (Barnes, Flitney and Nau (1989)) found that most pumps were running a long way off best-efficiency point with flowrates typically between 25% and 50% of values specified in the plant design manual (Fig 2.10). This is bound to result in cavitation and high vibration levels. Instrumentation on seal chambers detected cases where seal chamber pressure fell below suction pressure or became very close to saturated vapour pressure. In other words, the actual  $\Delta T$  was considerably less than the  $\Delta T$  recommended by the seal manufacturer. Furthermore, even on "constant head" duties quite significant pressure transients were measured (Fig 2.11), (greater than 10% of seal chamber pressure). These effects, which the plant instrumentation could not detect, could conceivably cause seal failure under marginal circumstances.

It is difficult to quantify the amount of money which should be spent on implementing improvements but it can be safely asserted that payback periods on most options are likely to be short. For example, a bold attempt to cure a problem by replacing a complete pump and seal with a brand new design might cost £5000. However, that improved unit would only need to save a couple of outages to pay for itself. On many plants that could mean payback in less than a year. On the imaginary plant of 220 pumps in sub-section 2.3.4 cost savings due to improved seal chamber design amounted to £300k per year.

## 2.4 POSSIBLE SOLUTIONS

Reports dealing with solutions to mechanical seal unreliability are numerous and range from basic operational "handbooks", such as that produced by Dahlheimer (1970) based on plant experience, through to complex mathematical seal models.

### 2.4.1 Selection and Maintenance

It would appear that a marked improvement in seal performance can be obtained simply by attention to fundamental areas such as appropriate selection and careful fitting. Eeds, Ingram and Moses (1977) estimate that engineering contractors engaged in pump selection spend only 10% to 35% of the allotted time on the mechanical seal system. Furthermore, they suggest that there is little consultation with the seal manufacturer which leads inevitably to some mis-matches of seal to duty. These thoughts are echoed by Bloch (1984) who goes on to call for a reduction in the number of seals available in order to simplify the selection process. The paper puts forward a number of "standard" seals based on categories of operation which cover most duties. Phillips (1973), representing a seal manufacturer, agrees with Bloch and suggests a number of standard duties and seal systems. According to Michaelis (1985), who gives detailed advice, his company's attention to selection has resulted in marked improvement in safety and reliability.

Closely linked to correct seal selection is careful fitting and appropriate maintenance. Bertele (1984) and Brown (1978) agree that many infantile seal failures could have been avoided if seals had been fitted by specially trained personnel. Bertele (1984) favours the removal of the pump into a workshop or "clean" area for seal fitting and postulates that the extra cost involved is soon offset by the improvement in seal life. Pump maintenance is a subject tackled by Lock (1971) who found that bearing wear, leading to excessive axial play and run-out, caused many seals to fail. The benefits of attention to this kind of detail are reflected in the results of BHRA survey reported by Flitney and Nau (1987). One company participating in the survey reported that, in the first year, seal failure accounted for 78% of pump outage but in the second year this figure had reduced to 63% (Table 2.2). The author spent a fortnight with the maintenance personnel of the company in August 1988 and found that, in the two months preceding his visit, there had been only one pump outage due to a seal failure. Three years previously the company would have expected between 10 and 15 failures per month. This improvement was largely due to improved maintenance practice, including weekly vibration monitoring of all pumps.

### 2.4.2 Seal Face Materials

Another area where improvements have been made is in developments of seal face materials. Wakely (1986) explains the recent advances in carbon types and quality. Flitney and Nau (1986) reinforce the need for closer definition of carbon quality by presenting results of identical tests carried out on seals with nominally identical carbons. The difference between "good" running and catastrophic failure correlated precisely with carbon microstructure. Adams (1987) relates that his company pays particular attention to this aspect. In specialist high-duty applications, Tribe and Green (1986) have found carbon-fibre reinforced carbons to be particularly good. They attribute this to improved strength and thermal conductivity. Advantages resulting from using carbons reinforced with a shrink-fit stainless-steel ring are claimed by Li and Liu (1987). By reducing carbon distortion in this way they found that frictional torque and leakage were reduced.

As a suitable counterface to carbon, silicon carbide emerges frequently in the literature as the best material in many high-duty applications, for example in reports of Wakely(1986), Bloch (1984), Martel (1987) and Giles (1972). Its success is generally attributed to high hardness, good wear resistance, and high thermal conductivity. Anon (1988) presents data which show that running with silicon carbide counterfaces permits hotter running of seals before the interface film is lost and therefore increases the effective  $\Delta T$ . Adams (1987) has found that similar benefits result from using titanium carbide and puts forward the advantages of running seals much hotter with such advanced materials. The performance of titanium carbide under very arduous conditions is also reported by Marr, Phelps and Katz (1983). In this application, on a PWR cooling water pump, the carbon/titanium carbide seals were able to withstand a half-hour loss of cooling water in a laboratory test during which the seal temperature rose to 250°C. That the seal survived the re-introduction of cooling water and sudden temperature drop would indicate its good thermal shock properties. One problem which does beset the carbides is quality control. Klimek (1988) explains the complexities involved in that area and calls for specific material standards.

The introduction of carbide face materials appears to have brought about a dramatic improvement in the reliability of pumps handling abrasives or slurries. Cameron (1987) reports success on abrasive bio-reactor duties using tungsten carbide against silicon carbide. Silicon carbide running against itself is a popular choice for many, particularly on flue gas desulphurisation process slurry duties; Kratzer (1987) claims seal lives of 6000 to 7000 hours on these demanding applications. Similar results are reported by Bangert (1986) and Battilana (undated).

### 2.4.3 Basic Seal Design

In addition to extensive work on new face materials, a good deal of work on basic seal design is reported. The advent of finite-element analysis (FEA) has brought about many mathematical models of seals. Using FEA, the complex effects of pressure and thermally-induced face distortions have been studied by Salant and Key (1984), Robinson and Burton (1969), Basu, Hughes and Beeler (1986), Doust and Parmar (1987) and Adams (1987) to list but a few. In each case the aim has been to investigate the interface film behaviour for a specific seal under varying conditions. The researchers report that seal geometry can easily be modified by conducting "what-if" studies until the best compromise is reached. The Doust and Parmar (1987) model has the added sophistication of dealing with transient seal behaviour, for example on start-up. Their results suggest that steady-state models may be unduly optimistic and are using the model to design more transient-tolerant seals.

Certainly, FEA is a powerful tool in the hands of experienced seal designers. However, most authors admit that their models are only first approximations and it is important to read their lists of assumptions. Unfortunately, the difference between a successful and failed mechanical seal can be a few microns change in interface geometry which is difficult to model reliably. Furthermore, all models assume that the seal face geometry is constant, although experience indicates that most seals wear to some degree.

A different approach to modelling is to use dimensional analysis. Buck (1980) has carried out such an analysis and derived three dimensionless parameters: stability factor, liquid design factor and strength design factor. He then calculated these parameters for a large number of refinery applications for which he had operational data. By comparing parameter values of successful and failed seals he formulated a range of

criteria by which to evaluate new seal designs without actually placing them in the field. In particular, he found that his three parameters gave a more accurate prediction of seal life than did the commonly used pressure-velocity factor. However, the results of the three factors, when plotted against seal life, were still subject to a large amount of scatter (Fig 2.12).

A number of researchers have attempted to improve seal performance using an experimental approach. Summers-Smith (1961) was one of the first to study the lubrication regimes of seals by measuring interface friction. Nau (1963) showed visually that seals usually run with an incomplete interface fluid film and that a successfully operating seal usually runs in a mixed lubrication regime using a glass-faced mechanical seal (Fig 2.13). By running the seal with liquid both on the inside and outside of the face, he was able to measure the inward radial flow by monitoring the pressure rise in the trapped inner volume. Of special interest to this study, however, is the effect of radial flow of adding air to the outer oil reservoir as shown in Figure 2.14. Up to about  $t=260$  minutes with liquid on both sides ("homogeneous" system) the pressure of the inner reservoir rises steadily. As soon as a small amount of air is introduced into the outer reservoir, the pressure rise stops, indicating a cessation of inward radial pumping. Nau observed that the air was centrifuged into a continuous toroidal bubble in the groove at the seal face (Fig 2.15) which blocks the passage of liquid to the interface. At this point he also noted the onset of cavitation streaks in the interface (Fig 2.16). It would also be reasonable to assume that the presence of the toroidal bubble would have a dramatic effect on interface film temperatures - not only does it cause the film to collapse through cavitation but it also must hinder the removal of heat from the interface into the surrounding liquid. So the smallest trace of vapour or gas at the seal faces could lead to film vaporisation, thermal distress of the faces and possible seal failure. This has important implications for the design of seal chambers to prevent vapour or gas from forming in the seal face groove. Some later work at BHRa carried out by Field and Flitney (1975) studied the flow around a water pump seal on a six-cylinder in-line diesel engine following problems with thermal stress cracking of the ceramic seal faces. It was suspected that intermittent loss of thermal contact with the coolant was to blame. Field and Flitney carried out tests on an actual pump mounted on a cylinder block at various temperatures, pressures and pumping rates. The flow was observed through a transparent window made of perspex. Additionally, a conductivity probe was located near the seal interface to indicate the presence of water or vapour. At low speeds there was no evidence of cavitation, but at medium to high speeds a large number of air bubbles were noted around the seal. At the highest speed the seal was completely obliterated by vapour. The conductivity probe showed that vapour was present at the interface after only a few revolutions (Fig 2.17). Field and Flitney suggest that these bubbles may exist for 50 to 80 percent of the time and recommend design changes to improve the circulation of water around the seal.

Studies on interface lubrication mechanics have also been carried out by Orcutt (1964), Barnard and Weir (1978), Morton (1984), Silvaggio, Lipski and Bramar (1987) and Fujita (1987). The aim of these studies was to obtain the best compromise between reducing leakage and protecting the seal face. Morton (1984) specifically aimed to design a non-contacting seal for a nuclear reactor primary coolant pump (Fig 2.18). The extra leakage was collected by secondary and tertiary seals. Due to its "thick film running", it was less sensitive to transients.

Most seal systems are single stage and are required to operate on a thin film in order

to minimise leakage. The stability of this film has been studied by Lymer (1969) in an attempt to explain the well-known "puffing" or "ringing" phenomenon exhibited particularly by seals on light hydrocarbon duties. The onset of "puffing" was known to be an indication that the seal was distressed and might fail. Lymer found that the "puffing" was due to momentary film vaporisation and led to face contact. Immediately, extra heat was generated thus leading to prolonged loss of lubrication and either seal face damage or unacceptably high wear rates. Laboratory experiments simulated these effects and enabled him to determine operational parameter values at which instability would occur. He also found that instability onset varied with seal design and material combinations. So repeatable were the results that Lymer suggested using the phenomenon for evaluating seal design and new materials (Fig 2.19). Some years later this was adopted by Dolan, Harrison and Watkins (1987) for selecting seals for the critical main oil line pumps in the Forties field (Fig 2.20). As a result, seal life has been greatly improved.

Other workers have attempted to improve interface film stability. Bloch (1985) has reduced the face width and claims that the reduced heat generation leads to better seal life. Summers-Smith (1981), Young and Lebeck (1986) and Lebeck (1988) all suggest imposing waviness on the seal face to give added face separation through hydrodynamic effects. Netzel (1982) proposes lubrication recesses or "hydro-pads" (Fig 2.21) in the seal face to reduce the local intense heating.

One interesting feature of seal design is the ratio of radial space occupied by the seal to the shaft radius - termed the "clearance ratio". As noted in 1.3.1 seal designers are usually limited for radial space by the constraints of existing stuffing boxes; consequentially most seals tend to be long and slender with small clearance ratios. However, where seal design is not so constrained, for example in some high-duty or externally mounted seals, the clearance ratio is much higher. Dimensional information from a number of seal catalogues was used to generate a graph of corresponding ratios for DIN 24960 seals and high duty seals. The difference is quite dramatic (Figs 2.22 and 1.12) and implies that the constraints of stuffing boxes force the seal designer to adopt poor compromises.

In the final analysis, the best seal design could still be ruined if quality control in manufacturing is inadequate. This point is strongly put by Phillips and Johnson (1978).

The seal must also be designed to accommodate external factors - chief among these is vibration. Flitney and Nau (1976) report that high vibration levels can reduce seal life dramatically (Fig 2.23) - indeed this could be a plausible cause of some apparently "random" mid-life failures. Nau (1981) tabulates the vibration sources which affect mechanical seals (Fig 2.24) and goes on to construct a mathematical model to analyse seal behaviour under these conditions. He concludes that a greater understanding of the factors involved is required if more vibration-tolerant seals are to be designed.

## 2.5 OUTSTANDING PROBLEMS

The last three decades have seen activity by many people attempting to understand and then improve the design of mechanical seals; many advances have been made. It is clear, however, that seal performance is not fully understood as inexplicable unreliability still causes many problems, particularly on more arduous duties. Eeds, Ingram and Moses (1977) give a list of common seal failures and at the top is the phenomenon known as "heat checking" of the faces caused by thermal shocks which occur as a result of momentary losses of interface film or instability. Once surfaces are damaged in this way, the seal usually fails. Clearly, reducing the seal face temperature would reduce the risk of heat checking. Eeds, Ingram and Moses (1977) suggest using materials with a higher thermal conductivity and shock resistance, such as silicon carbide and flushing the faces with a cool external fluid. Summers-Smith (1961), Plumridge and Floyd (1986) and Hirabayashi, Oka and Ishiwata (1969) also stress the need for a good flush when the process fluid is close to its saturated vapour pressure. Bloch and Schuebl (1985) suggest fitting flow deflectors to direct coolant precisely onto the seal faces (Fig 2.25).

There are problems associated with flushing: firstly the flow rate cannot be excessively high, otherwise carbon erosion may occur and, secondly, it is very expensive. Hershey (1967) showed that the cost of supplying suitable coolant water had risen sharply, a trend which has probably continued. He wrote two subsequent reports (1969, 1971) proposing cheaper methods of cooling such water. The ideal solution would be to dispense with the expensive ancillary cooling equipment altogether.

There appears to be little information in the published literature pertaining to the real effectiveness of flushing systems - Hummer (1973) is one of the few examples. Indeed, the whole area of fluid flow around mechanical seals is a vague one despite its importance in affecting the operational environment of the seal. Complaints about the restrictiveness of stuffing boxes were voiced by Philips in 1973 and have been echoed more recently by Bloch (1986), Ingram (1984) and Netzel (1984). Principally, the wish is for more space to enable the easier fitting of more rigid and reliable seals. Ingram is particularly resentful of the compromise necessary in seal design and suggests that the "stuffing box" should be custom-designed as a "seal housing" since the facility for soft-packing retro-fit is rarely required. However, there is resistance to these views from some pump manufacturers. Grohmann (1984) presents a list of "ideal seal requirements" including: conformance of all seals to DIN/24960, greater tolerance to dry running and operation with little, if any, coolant flush provided. This is a very hard, if not impossible, target for manufacturers to achieve.

On some duties, however, the pump manufacturers have departed from traditional stuffing boxes. Some slurry pumps now have flared seal cavities, presumably with the aim of encouraging solid particles away from the seal faces by centrifugal action. These cavities are open to the impeller and it is claimed that the liquid phase of the slurry is an effective lubricator and heat remover at the faces. Typical examples of such systems are described by Schöpplein (1986) (Fig 2.26), Battilana (undated) (Fig 2.27), Kratzer (1987) (Fig 2.28) and Bangert (1986) (Fig 2.29), Heumann (1986) (Fig 2.30) and Nolan (1988) (Fig 2.31).

Unfortunately, none of these authors indicates the types of experimental work employed to arrive at these conclusions. Straszewski (1985) describes a liquid ethylene pump which features a conical housing (Fig 2.32). Again, no mention is made of the reasons

for this feature. Standish (1987) describes the development of a new type of general medium-duty pump (Fig 2.33) which involved the re-design of the seal chamber to allow for better access and improved cooling. Unfortunately, no experimental performance data are presented.

Davison (1989) concluded from his study of seal chambers that more space around the seal gave enhanced heat removal - the geometries he tested are shown in Figure 2.34. The paper contains some useful data, although there are a few inconsistencies. Unfortunately, Davison did not test a housing with a large taper angle - in reality his "Enlarged Tapered" and "Enlarged Cylindrical I" seal chambers are not vastly different - this was borne out by his  $\Delta T$  measurements Figure 2.35. It would also have been interesting to have seen some analysis of likely flow regimes, either theoretically or from visual observations. This would have enabled Davison to attempt to optimise the radial clearance and predict the behaviour of vapour gas and solids within the seal chamber.

Some flow experiments using transparent housings are given by Heald (1975) who adopted a wider seal chamber, slightly flaring away from the seal and with circulation guides (Fig 2.36). This design was patented by his company but further use or development of his design has not been found. Flitney and Nau (1985) report a few tests carried out with a transparent housing in which it was noted that gas bubbles in the chamber "lodged" in the seal face area, presumably due to centrifugal forces, thus impairing the flow of heat away from the faces. Nau (1963), some years earlier, had noted a similar toroidal air bubble around the nose of a carbon running against a glass face - the phenomenon of "vapour locking". He found that the seal face temperature rose in such a condition thus leading ultimately to vaporisation of the interface film and seal failure. Flitney, Nau and Reddy (1984) found that removal of this toroidal air bubble was not an easy matter and required further and more comprehensive study, including changing the seal chamber geometry. Schmidthals (1986) is very concerned about de-gassing of fluids on high speed seals. He suggests that friction and whirl losses in the seal chamber could, in themselves, raise the temperature above boiling point in many applications.

In 1984, Nau presented an assessment of the "state of the art" for mechanical seals in process duties. In a wide-ranging paper he summed up the current knowledge base and the extent to which seals performed to the users' satisfaction. In particular he addressed the area of mechanical seal standards and found it badly wanting in a number of respects. One of the major complaints was the use of DIN 24960 for defining the chamber into which a seal was expected to fit and work perfectly. He criticised the specification for in no way taking account of the requirements of efficient cooling as well as removal of gas, vapour or solids which are present around many seal faces. He therefore suggests that "the optimisation of housings is an area requiring experimental investigation prior to the definition of an improved standard".

---

**CHAPTER 3.**

---

**REVIEW OF LITERATURE**

---



### 3.1 ROTATING ANNULAR FLOWS

In order to predict the movements of heat, vapour bubbles and solids within a seal chamber it is necessary to know something about the likely types of flow regimes which are generated. The rotation of a complex component, with steps, springs and other geometric vagaries, will probably develop flows which defy even the most sophisticated mathematical analysis. However, as a first approximation a number of types of seal may be considered as smooth circular cylinders rotating concentrically inside a cylindrical housing. A considerable amount has been written about the nature of rotating annular flows due to their relevance for the cooling of rotating machinery. The conclusions from these workers are of value in this study.

Several distinct flow regimes occur in annular clearances with a rotating inner member. The behaviour of gas, vapour and solids within the seal chamber is governed to a great extent by the nature of the flow regime.

A rotating annular flow of the type created in mechanical seal chambers is inherently unstable and attempts, given the right conditions, to resolve itself into a system of toroidal counter-rotating vortices (Figure 3.1).

The existence, or otherwise, of these vortex structures depends on the ratio of inertial to viscous forces expressed as a Taylor number  $Ta$ :-

$$Ta = \frac{\omega^2 r b^3}{\nu^2} \quad (3.1)$$

Consequently, at low Taylor numbers, viscous forces dominate and the flow is laminar. At a Taylor number of 1708 the flow enters the vortex regime.

This has been shown to result in :-

- Improved heat transfer.
- Gas/vapour removed from the shaft and safely 'locked' in vortex cores.
- Solids drawn into vortex peripheries.

At higher Taylor numbers ( $> 10^5$ ) (where most mechanical seals operate) the vortices tend to be broken down by turbulent eddies, but under certain conditions a turbulent vortex structure exists.

Given the fluid viscosity, seal geometry and speed, the only variable available for influencing the Taylor number (and thereby the flow regime) is the radial clearance. In other words, the design of the seal chamber could directly, and possibly crucially, effect the flow regime around the seal.

This review of the main developments in work on heat transfer in rotating annular flows gives an indication of the types of flow regimes likely to be encountered around mechanical seals. The implications of any structure within the flow are certain to exert an important influence over the movement of heat, gas and solids around the seal.

However, it should be borne in mind that a typical mechanical seal involves a number of additional complications so far un-quantified in this area:-

- (a) Irregular exterior
- (b) Finite length with low length-to-gap ratio
- (c) Operation at very high Taylor numbers
- (d) Real fluids often multi-phase and non-Newtonian

### 3.1.1 Pre-1950's

The first major investigation was reported by Taylor (1923). He derived the equations of motion for a viscous fluid between two infinitely long rotating cylinders (Fig 3.2) and studied the stability of the flow when an infinitesimally small perturbation was introduced. Using Bessel functions, he expanded the equations and then found the solution for the resulting infinite determinant for the lowest speed at which these perturbations would grow. He found that, with the inner cylinder rotating and outer stationary, the flow would be made unstable at a critical ratio of angular velocity to kinematic viscosity. At this point the laminar Couette flow was re-organised into a series of counter rotating toroidal vortices evenly spaced along the length of the shaft. Based on his theoretical predictions, he built an experimental apparatus accordingly with a facility for injecting dye from strategic points along the inner cylinder. The experimental results and theoretical predictions matched to within a few percent and are borne out by his photographs (Fig 3.3). Taylor showed that for a given liquid and configuration the vortex flow (later named "Taylor Vortices" by subsequent researchers) was present over a particular range of speeds; increasing speed resulted in increasing vorticity. At a sufficiently high speed, however, the vortices began to break up and the dye dispersed. He concluded that turbulent motion was beginning to predominate at this point.

Pai (1943) carried out extensive experiments in the turbulent regime and found that structured flow was still present and resembled the super-laminar Taylor vortex flow (Fig 3.4). He concluded that he was observing vortices with super-imposed turbulence but offered no explanation for the phenomenon.

### 3.1.2 1950 - 1959

Thirty-five years after Taylor's initial work, Gazley (1958) postulated that the Taylor-vortex flow should have an effect on heat transfer between rotating cylinders. His principal interest was in the cooling of electric motor rotors with air as the working fluid. Gazley suspected that the efficient transfer of momentum from one cylinder to the other (inherent in the vortex flow) would give enhanced heat transfer capability over laminar flow; this he found to be the case. Of particular interest were the tests conducted at speeds well in excess of the critical speed for vortex formation. He noted that the flow became increasingly turbulent with speed but that the convective heat transfer coefficient (or Nusselt number in non-dimensional form) reduced as the turbulent regime was encountered. Gazley's work was not confined to smooth cylinders but also addressed the effects of slotted rotors. He found that the vortex flow was not prevented by the slots - hence the heat transfer coefficient was not measurably affected. At high peripheral Reynold's number, in the turbulent regime, heat transfer was improved appreciably. In addition to his experimental work, Gazley formulated predictive equations for Nusselt number in each flow regime. In the turbulent regime, he used the heat and momentum analogy to evaluate Nusselt number as a function of

Reynolds number, Prandtl number, friction coefficient and geometry.

The equation he derived is based on an expression for heat transfer to a flow between two parallel plates where only one plate is a heat source.

$$Nu = \frac{f \cdot Pr \cdot Re (C_f / 2)^{0.5}}{10 [Pr + \ln (1 - 5 Pr) + \frac{1}{2} \ln \frac{Re}{120} (C_f / 2)^{0.5}]} \quad (3.2)$$

where  $f$  is the correction factor for asymmetric heating which for air:-

$$f = 0.715 \text{ at } Re = 10^4$$

$$f = 0.785 \text{ at } Re = 10^6$$

For calculating skin friction coefficient ( $C_f$ ) he took the expression:

$$\frac{1}{\sqrt{C_f}} = 2.04 + 1.768 \ln Re \sqrt{C_f} \quad (3.3)$$

Although the effects of curvature and Taylor vortex flow were neglected, this expression showed reasonable correlation with the friction measurements of Taylor (1936) as shown in Figure 3.5. His results for heat transfer from the rotor to the air are given in Figure 3.6. The relationship for Nusselt number is:

$$Nu = 0.04 Re^{0.8} \quad (3.4)$$

Concurrent with Gazley's work, Kaye and Elgar (1958) were also investigating methods of cooling rotating electrical machinery utilising the effect of Taylor vortices and studying their behaviour in the presence of axial flow. Using smoke tracing and hot-wire anemometry, they isolated four distinct flow regimes as a result of changing Taylor number and axial Reynolds number, as shown diagrammatically in Figure 3.7. It is noteworthy that at low axial flow velocities fully turbulent flow is not achieved; on the contrary some form of structured vortex flow persists even at high Taylor numbers. A third dimension was added to Figure 3.7 in the form of Nusselt number. In the laminar and turbulent regimes there was a weak dependency with speed of rotation, but in the vortex regime Nusselt number rose steadily with increasing speed. Under some conditions it was possible to decrease the heat transfer coefficient by increasing the axial flow velocity.

Bjorklund and Kays (1959) furthered the field by supplying numerous heat transfer results with air as the test fluid for various radial clearance ratios although they did not investigate axial flow effects. By correlating their results they established an empirical formula relating Nusselt number to Taylor number:

$$Nu = 0.175 Ta^{0.25} Nu_{cond} \quad (3.5)$$

where

$$Nu_{cond} = \frac{(b/r)}{\ln(1 + b/r)} \quad (3.6)$$

in the range  $10^4 < Ta < 10^8$

The analogy model of Gazley was modified to take account of curvature and the vortex flow phenomenon. The analysis also utilized experimental friction data and optical visualisation of velocity profiles. The relationship between Taylor and Nusselt numbers agreed well with the experimental results as far as trend was concerned, which indicated that the mechanisms and flow regions postulated were valid. Above Taylor numbers of  $10^8$ , however, the model consistently predicted Nusselt numbers about 20% above the data points. Both their experimental results and analyses predict Nusselt numbers well below those recorded by Gazley (Fig 3.8).

### 3.1.3 1960 - 1969

Tachibana, Fukui and Mitsumura (1960) extended the heat transfer work by carrying out experiments with liquids (spindle and mobile oils) as well as air. They derived the following expression for Nusselt number based upon Reynolds number, clearance ratio and Prandtl number:

$$\begin{aligned} Nu &= 0.21 (b/r)^{0.25} Pr^{0.25} Re^{0.5} \\ &= 0.21 Pr^{0.25} Ta^{0.25} \end{aligned} \quad (3.7)$$

The work of Kaye and Elgar (1958) on adiabatic flows was then extended to diabatic flows by Becker and Kaye (1962). Their heat transfer data accord well with Bjorklund and Kays (1959) but not with Gazley (1958). They form the basis for empirical formulae for Nusselt number in terms of a modified Taylor number incorporating a geometrical factor to compensate for gap width:

$$Nu = 0.128 (Ta/Fg)^{0.367} \quad (3.8)$$

in the range  $17.6 \times 10^3 < (Ta/Fg) < 10^4$

and 
$$Nu = 0.409 (Ta/Fg)^{0.241} \quad (3.9)$$

in the range  $10^4 < (Ta/Fg) < 10^7$

where 
$$Fg = (\pi^4/1697)(1 - b/2r_m)^{-2} P^{-1} \quad (3.10)$$

and 
$$P = 0.0571 \left[ 1 - 0.652 \frac{b/r_m}{1 - b/2r_m} \right] + 0.00056 \left[ 1 - 0.652 \frac{b/r_m}{1 - b/2r_m} \right]^{-1} \quad (3.11)$$

Becker and Kaye (1962) also managed to fit a single curve to their data by least squares, namely:

$$Nu = 0.409 (Ta/Fg)^{0.241} - 137 (Ta/Fg)^{-0.75} \quad (3.12)$$

in the range  $1.7 \times 10^3 < (Ta/Fg) < 10^7$

Their report also includes dimensionless radial temperature profiles for various Taylor and axial Reynolds number as measured, and from theoretical calculations. The four-regime system of flow proposed by Kaye and Elgar (1958) for rotating cylinders with axial flow was confirmed by the heat transfer data for laminar, laminar-and-vortices and turbulent regimes. However, the turbulence-plus-vortices regime was only detectable at certain axial Reynolds numbers on their apparatus.

Although the transition from laminar to vortex flow was well documented and understood by this time, the transition from vortex into turbulent or chaotic vortex flows was little understood. Nissan, Nardicci and Ho (1963) set out to explain this phenomenon. They used two methods of flow visualisation:

- (i) dispersion of ethyl alcohol and water droplets in mineral oil
- (ii) aluminium powder in oil

Tests were carried out with both horizontal and vertical apparatus. They noted that at a certain value of Taylor number (about  $12 \times 10^3$ ) the steady Taylor vortices became wavy but without any apparent change in cross section (Fig 3.9). Increasing the Taylor number further to about  $5 \times 10^5$  caused alternate vortices to expand and the intermediate ones to contract. They called these "high speed wavy vortices". Even at the highest Taylor number achievable by their apparatus (about  $10^7$ ) they report some structure to the flow, thus indicating that full turbulence had not been attained. However, they stop short of proposing an explanation of these phenomena.

In 1964, Ho, Nardicci and Nissan built upon the earlier work on the heat transfer characteristics of vortex systems. Using theoretical and experimental techniques they derived a relationship for Nusselt number versus Taylor number. The exponent of the

Taylor number itself was governed by the ratio of Prandtl number to Grashoff number:

$$\text{Nu} = (\text{Ta}^{0.5} / 41.2 \text{ Fg})^m \quad (3.13)$$

where  $\text{Fg}$  is defined in the same way as equation 3.6 and 3.7. For water,  $m$  is 0.23.

Ho et al also made measurements of radial temperature profiles across the annulus. They found that across most of the annulus the temperature gradient was zero. At the cylinder walls, and particularly at the inside, the gradient was steep (Fig 3.10). They suggested that the point of transition from the flat to steep curve was the outer edge of the thermal boundary layer. In a series of experiments in which viscosity and Taylor number were varied they built up a number of curves for thermal boundary layer. At criticality the boundary layer at the inner cylinder occupied about 10% of the annulus for low viscosity fluids. This decreased to about 6% at Taylor numbers of the order of  $10^6$ .

Coles (1965) gives a comprehensive explanation of the Taylor vortex phenomenon and a brief summary of the work carried out previously. His paper is particularly noteworthy for the excellent photographs of different vortex regimes (Fig 3.11); again aluminium paint pigment suspended in oil was the visualisation technique employed. Of special interest are his pictures of turbulent Couette flows (Fig 18) showing the existence of high speed vortices at elevated Taylor numbers ( $> 10^7$ ).

#### 3.1.4 1970 - 1979

Castle, Mobbs and Markho (1971) studied the effects of eccentricity on flow regimes and torque. Their results contain useful data for friction coefficient versus Taylor number over the range  $200 > \text{Ta} > 25000$  and show definite discontinuity and change of slope at and above the critical Taylor number (Fig 3.13). Further data for torque versus speed were added by Younes, Mobbs and Coney (1972), incorporating axial flow.

Kuzay and Scott (1977) verified the turbulent heat transfer results of previous workers and added their own for a wide gap case. Using radial temperature measurements they built up profiles by which thermal boundary layers could be detected. Comparison of their own and previous results (Fig 3.14) led them to the following relationship:

$$\text{Nu} = 0.022 \text{ Re}^{0.8} \text{ Pr}^{0.5} \quad (3.14)$$

In a significant addition to work on rotating annular flows, Barcion, Brindley, Lessen and Mobbs (1979) studied the complex vortex flows observed at Taylor numbers between  $10^6$  and  $10^8$ . Their report contains fascinating pictures of high speed vortices made visible by "herring-bone" streaks around their periphery (Fig 3.15). They felt that these features were similar to those observed by Pai (1943) and postulated that the streaks were Görtler vortices due to instabilities in the wall boundary layers. They did not speculate on what effect these instabilities would have on heat transfer at the walls.

Simmers and Coney (1979)(a) constructed a heat and momentum analogy solution incorporating Taylor vortex and axial flow. They assumed that the flow consisted of three layers: a laminar sub-layer adjacent to the wall (viscosity dominated), a buffer layer (in which viscosity and turbulence held influence) and a central regime (in which turbulence dominated). Built into the model was the observed fact that the velocity across the central region of the annulus (presumably where the vortices are effective) was nearly constant and of value one third of the peripheral rotor velocity. The result of the analogy was a relationship for Nusselt number as a function of Taylor, Axial Reynolds and Prandtl numbers:

$$Nu = \frac{4 Pr Re_a^{0.5} Ta^{0.3675}}{B \frac{A^{0.5}}{1-n} \frac{n^{0.25}}{1-n} Ta_c^{0.617}} \quad (3.15)$$

where

$$A = \frac{[1 + n^2 + (1 - n^2)/\ln n]}{[2 + (1 - n^2)/\ln n]} \quad (3.16)$$

and  $B = Pr + \ln \left\{ 1 + Pr \times \exp \left[ \frac{2}{3} \frac{1-n}{n} \right]^{0.25} \frac{nA}{(1-n)^2} \right\}^{0.5}$

$$\times Re_a^{-0.5} Ta^{0.1325} Ta_c^{0.1175} - 1] - Pr \} \quad (3.17)$$

The plots for equation 3.15 show the expected increase in Nusselt number slope above critical Taylor number (Fig 3.16). For low axial Reynolds numbers a second transition point, at which the slope again increased, was predicted. Experimental results appeared to trend with the predictions but usually with some offset (Fig 3.17). Evidently the mechanisms assumed in the model were valid. In another paper, Coney and Simmers (1979)(a) refined their analogy model further by direct measurement of wall shear stress on the outer wall using flush-mounted hot film anemometer probes. Again a tertiary regime was detected at low axial Reynolds numbers but no explanation was volunteered.

Using their established techniques, Simmers and Coney (1979)(b) went on to measure the effects of development length on velocity profiles. A wealth of similar data exist in subsequent publications, viz Simmers and Coney (1980). Studies of these data show that the boundary layer thickness at the inner cylinder is generally 10-15% of the gap width (Fig 3.18). This accords well with previous results for radial temperature profiles.

### 3.1.5 1980 - 1989

The work of Wan and Coney (1982)(a) and (b) shed more light on the nature of the tertiary regime. In (a) it was found that Nusselt number fell or levelled off in this regime (depending on axial Reynolds number). The second study (b) involved flow

visualisation using oil and aluminium paint pigment in suspension. At Taylor numbers in excess of  $10^6$  a re-emergent turbulent vortex flow was clearly evident (Fig 3.19) with the characteristic vortex length twice that of classical Taylor vortices. No explanation for this phenomenon was given. Unfortunately, rig limitations did not permit running at Taylor numbers much in excess of  $10^6$ .

Until recently, all the work on rotating annular flows dealt with cylindrical annuli. Wimmer (1988) made a major contribution to the literature in his wide-ranging report on instabilities in other geometries. Of particular interest are his experiments with a circular cylinder rotating inside a cone at rest (Fig 3.20). He found that the formation of vortices was still dependent upon the critical Taylor number at a given point, ie the first vortex starting at the point of widest radial clearance, with others following towards the apex of the cone as the speed increased. The size of the vortices varied depending on the gap size at a given axial position.

Of special interest to the study of fluid flow regimes in mechanical seal chambers is the recently published work of Koga and Koschmieder (1989), describing Taylor vortex flow in short fluid columns. The aim of their work was to study the influences of end effects (from stationary plates) and column length. They found that, in all their experiments;

- the column was always filled with an even number of vortices
- the number of vortices depended on the column aspect ratio, and rate of start-up from rest
- flow at the stationary boundaries was always inwards
- vortices start at each end of the chamber at a sub-critical Reynold number. Increasing Reynolds number results in additional, adjacent, vortices being formed throughout the chamber.

The work of Koga and Koschmieder provides a tantalizing glimpse into a whole new branch of Taylor vortex flow. It will be interesting to see if their work will encompass turbulent vortices flows in future years.



### 3.2 SUMMARY

Heat transfer in rotating annular flow has been the subject of a large body of literature and many empirical or semi-empirical expressions for Nusselt number have been derived through analysis and experimentation. It should be remembered that these expressions are all for long smooth circular cylinders (ie neglecting end effects) with relatively small clearance ratios and up to Taylor numbers typically of  $10^8$ . Furthermore, some of the expressions were derived using air as a test fluid and do not include Prandtl number as a factor. To effect a comparison, the expressions for Nusselt number were computed for a DIN standard housing geometry running on water and plotted against Taylor number.

The following expressions result:-

$$\text{Gazley (1958)} \quad \text{Nu} = 0.16 \text{ Ta}^{0.4} \quad (3.18)$$

$$\text{Bjorklund and Kays (1959)} \quad \text{Nu} = 0.18 \text{ Ta}^{0.25} \quad (3.19)$$

$$\text{Tachibana, Fukui and Mitsumura (1960)} \quad \text{Nu} = 0.34 \text{ Ta}^{0.25} \quad (3.20)$$

$$\text{Becker and Kaye (1962)} \quad \text{Nu} = 0.40 \text{ Ta}^{0.241} \quad (3.21)$$

$$\text{Ho, Nardicci and Nissan (1964)} \quad \text{Nu} = 0.42 \text{ Ta}^{0.12} \quad (3.22)$$

$$\text{Kuzay and Scott (1977)} \quad \text{Nu} = 0.18 \text{ Ta}^{0.4} \quad (3.23)$$

Plotted on log/log scales, these are shown in Figure 3.21. A large amount of spread is notable - perhaps attributable in part to the effect of Prandtl number - although the results do fall into distinct families of curves. Why the results of Gazley and Kuzay and Scott should be almost coincidental and yet predicting Nusselt numbers nearly an order of magnitude greater than most of the other curves is not clear. However, Figure 3.21 does give a basis for comparing the results of the current work with those obtained by previous workers.

Of special interest to this study is the apparent existence of turbulent vortex flows, hitherto unexplained under certain conditions at high Taylor numbers - most mechanical seals will operate in turbulent flows. If this high-speed structured flow has similar effects to laminar Taylor vortices than it should be beneficial for heat transfer and controlling gas and vapour. To be of real use in designing seal chambers, this phenomenon and the mechanisms involved need to be better understood and its effect quantified.

-----  
**CHAPTER 4.**  
-----

**TEST APPARATUS**

## 4.1 SPECIFICATION

The test apparatus was designed to run typical centrifugal process pump-seals in a range of traditional and novel seal chamber geometries. General views of the rig are shown in Figs 4.1 and 4.2.

### 4.1.1 Seal Types

Two sizes of seals were tested, 48mm and 100mm; the dimension refers to the shaft diameter.

#### (i) 48mm seals (seal outside diameter = 66mm)

The five seals tested are shown in Table 4.1; all are commonly used and fit into a DIN 24960/ISO 5199 stuffing box (see Appendix A), but possess widely varying external profiles. Two of the seals were fitted with heat transfer probes.

The characteristics of each seal are as follows:-

- |        |   |
|--------|---|
| Seal A | exposed single spring:- may be considered as a pair of rotating discs separated by a large spring rather than a rotating cylinder. The spring might be expected to cause axial flow when rotated; rotational direction could be important. Lack of space on the seal rotor precluded the fitting of heat transfer probes. |
| Seal B | shrouded single spring:- a fair approximation to a smooth circular cylinder, although there are four rectangular cut-outs at the rear of the rotor. Heat transfer probes were fitted at the front of the shroud (see Fig 4.3 ).   |
| Seal C | multiple spring:- a smooth shroud covers most of the rotor but punctuated by four circular cut-outs at the mid-point. At the rear of the seal part of the multiple spring assembly is exposed. Heat transfer probes were fitted at the front of the shroud as for Seal B.   |
| Seal D | rotating metal bellows:- effectively a pair of rotating discs connected by an edge-welded set of bellows. When under normal compression the whole rotor looks not unlike a solid cylinder. Space did not permit the fitting of heat transfer probes.  |
| Seal E | stationary metal bellows:- an exact reflection of Seal D. The only rotating component is a short disc; again this did not allow space for the fitting of heat transfer probes.  |

#### (ii) 100mm seals (outside diameter = 124mm)

Seal B-100:- exposed single spring:- similar to its 48mm counterpart but exposing rather more of its drive spring at the rear of the rotor.

Seal D-100:- rotating metal bellows:- an exact scale-up of the 48mm seal.

All of the seven seals tested are alike in having a nose on their carbon face and, hence, a significant groove at the sealing interface (Fig 1.2).

#### 4.1.2 Seal Housings

Two sets of housings were manufactured in perspex for the two seal sizes. All housings were polished inside and outside to give good optical clarity.

##### (i) 48mm seal housings

Five housing geometries were investigated (Table 4.2). All were equipped with two sets of four tapped holes, one in the plane of the seal face, the other at the lantern ring position (Fig 4.4); This configuration permitted single or multi-port injection of liquid or air and the insertion of temperature and pressure transducers. On five of the housings, the ports were aligned radially whilst two additional housings were equipped with tangential ports. All housings could be run with or without a stationary neck bush. A few tests were run with a rotating neck bush. Two of the housing geometries could be fitted with strake assemblies designed to act as vortex modifiers. The strake assemblies consisted of four strips of brass equispaced circumferentially around the seal. The strips ran both axially (Figs 4.5 and 4.6) and helically (Fig 4.7).

The principal features of each housing are listed below:-

- Housing 1 : Cylindrical. Constructed to conform to DIN 24960 ie radial clearance around the seal of 2mm. Radial ports (Fig 4.8)
- Housing 2 : Cylindrical. Radial clearance around the seal of 12mm. Radial ports. Optional axial and helical strake inserts. (Fig 4.9)
- Housing 3 : As housing 1 but with tangential ports. (Fig 4.10)
- Housing 4 : As housing 2 but with tangential ports. (Fig 4.11)
- Housing 5 : 12° positive flare. Continuous flare from seal plate to backing plate. Radial ports. (Fig 4.12)
- Housing 6 : 12° negative flare. Continuous flare from backing plate to seal plate. Radial ports. (Fig 4.13)
- Housing 7 : 45° positive flare. Flared over the seal rotor, wide cylindrical section between rear of seal and backing plate. Radial ports, at seal face position only. Optional axial and helical strake assemblies. (Fig 4.14)

**(ii) 100mm seal housings**

Four housing geometries were tested. All had four equispaced radial ports in the plane of the seal face and could be run with or without a stationary neck bush. The geometries were as follows:-

Housing 1-100: (Fig 4.15)	Cylindrical. Constructed to conform to DIN 24960, ie radial clearance around the seal of 2.5mm.
Housing 2-100: (Fig 4.15)	Cylindrical. Radial clearance around the seal of 7.5mm.
Housing 3-100: (Fig 4.15)	Cylindrical. Radial clearance around the seal of 20mm.
Housing 4-100: (Fig 4.16)	45° positive flare. Continuous flare from seal plate to backing plate.

**4.1.3 Piping Plans**

The port configuration of the houses permitted great flexibility in the arrangement of piping plans. However, to maintain a reasonable number of variables, five were selected:-

Plan A: (Fig 4.17)	No injection to seal cavity (dead-ended).
Plan B: (Fig 4.18)	Single point injection at seal face. Exhaustion past impeller.
Plan C: (Fig 4.19)	Multiple point injection at seal face. Exhaustion past impeller.
Plan D: (Fig 4.20)	Single point injection at lantern ring position. Exhaustion past impeller.
Plan E: (Fig 4.21)	Single point injection at lantern ring position. Exhaustion at seal face position.

At all times, fluid was continuously and independently circulated through the impeller housing.

**4.1.4 Test Fluids**

The test fluids covered a range of viscosities from 1 to 140 mPa.s (1 to 140 cP) and included gaseous and solid contaminants. Generally, the fluid temperature was maintained at  $15^{\circ}\text{C} \pm 2^{\circ}\text{C}$ .

**(i) Tap water:-**

Most test work was carried out on water, including the heat transfer measurements.

**(ii) Water + air:-**

Air was injected continuously through a fine hypodermic underneath the seal face (Fig 4.4). Flowrate was about six bubbles per second.

**(iii) Water + glycerol solutions:-**

Three solution strengths were tested giving viscosity ranges of 10-15 mPa.s, 50-60 mPa.s and 100-140 mPa.s. Glycerol being hygroscopic, the viscosity could not be accurately maintained over a period of more than a day, particularly at the higher viscosities. Viscosity was therefore checked before and after each test using a cylinder-in-bucket type viscometer. The viscosity tables for glycerol solutions are given in Appendix D.

**(iv) Water + carbon dust:-**

relative density = 2.3  
average particle size = 10  $\mu\text{m}$ .  
concentration < 10% by volume

**(v) Water + silica dust:-**

relative density = 2.2  
average particle size = 10  $\mu\text{m}$ .  
concentration < 10% by volume

**(vi) Water + sand particles:-**

relative density = 2.2  
average particle size = 100  $\mu\text{m}$   
concentration < 10% by volume

**(vii) Water + iron oxide dust:-**

relative density = 5.1  
average particle size = 10  $\mu\text{m}$ .  
concentration < 10% by volume

**4.1.5 Flowrates**

Flowrates could be set in the range 0 to 4 litres/minute by varying the drive-speed of a rubber-impeller type pump. In general, experiments were carried out with set flowrates.

The choice of flowrates was based initially upon recommended values listed in manufacturers' catalogues which are given in Appendix E. Additionally, a lower flowrate was used to simulate the effect of an inefficient or partially blocked flushing system. The target values were 2 and 4 litres/minute, although the highest flowrate was not achievable with the more viscous water/glycerol solutions.

The flowrates were computed in terms of axial flow velocity past the seal body ( $v_z$ ) and axial Reynold's Number ( $Re_a$ ) (Fig 4.22) and indicated that:-

Flowrate = 2 l/min gave:  $v_z = 0.062$  m/s

$$Re_a = 320$$

Flowrate = 4 l/min gave:  $v_z = 0.125$  m/s

$$Re_a = 625$$

These  $Re_a$  values fall within the ranges of validity (typically 0 to 1500) of the Nusselt number equations in Chapter 3 - an important consideration for the heat transfer experiments.

#### 4.1.6 Speeds

The speed range was 0-6000 rpm continuously variable. In practice, set speeds of 500, 1000, 3000 and 5000 rpm were used for most experiments. Speeds in excess of 5000 rpm on 48 mm seals and 2300 rpm on 100 mm seals were unattainable due to lack of power owing to turbulent churning losses. In addition, significant radial spring growth was noted with one seal design which caused contact with the narrowest housing at 6000 rpm.

Prior to flow studies, the power consumption of the bearings plus the seal was measured throughout the speed range. For a given speed the power consumption was noted immediately, and after a period of 10 minutes. Two things were noteworthy: (i) there was a significant drop in consumption with time, particularly at higher speeds (Fig 4.23), and (ii) the relationship between power consumption and speed was approximately linear (Fig 4.24). These data were used in the experimental determination of churning friction for validating the turbulence viscosity model (Chapter 7).

#### 4.1.7 Experimental Procedure

The standard experimental procedure followed for most of the test work is given below:-

Stage	Flowrate (l/min)	Speed (rpm)
1	0	0-5000 (continuous)
2	0	5000
3	2	5000
4	4	5000
5	2	5000
6	0	5000
7	0	3000
8	2	3000
9	4	3000
10	2	3000
11	0	3000
12	0	1000
13	2	1000
14	4	1000
15	2	1000
16	0	1000
17	0	500
18	2	500
19	4	500
20	2	500
21	0	500
22	0	500 -0

Each complete test lasted between 20 to 30 minutes, depending on observed phenomena. The criterion for progressing to the next stage was an apparent "steady state" condition at the current stage. The experiment was filmed throughout, each run prefaced by a title block entered using the camera, and archived. The film was accompanied by a sound-track in real time onto which were dictated values of flowrate, speed, pressures and temperatures at each stage.



## 4.2 DESIGN AND MANUFACTURE

The test apparatus superficially resembles a typical process pump-set, both in the drive and ancillary systems. Figures 4.1 and 4.2 show views of the apparatus and Figure 4.25 gives a diagrammatic representation. The individual parts of the rig are dealt with separately below.

### 4.2.1 Drive System

The motor is a 0-6000 rpm, 7kW thyristor-controlled DC drive. This was chosen to give a smooth, continuously variable speed capability, considered to be important to the detection of flow developments and transitional phenomena. Calculations of power requirement were made on the basis of assumed bearing friction, seal friction and turbulence losses.

#### (i) Bearing friction

Calculated using a formula for friction torque (M) in the SKF general catalogue, where:-

$$M = 0.058 \mu P_b d_b \quad [\text{Nm}] \quad (4.1)$$

From the catalogue,  $\mu$ , the coefficient of friction for a single row deep groove ball bearing, is 0.0015.

P is the equivalent bearing load and  $d_b$  is the bearing bore in metres.

#### (ii) Seal friction

This was estimated from an empirical formula derived by Nau from the results of seal friction tests carried out at BHRA.

The frictional power generated ( $H_s$ ) is given by:

$$H_s = 6.1 \times 10^{-4} p_f^{0.67} d^{1.8} N^{0.8} \quad [\text{W}] \quad (4.2)$$

where

$p_f$  = sealed pressure [MPa]

$d$  = seal diameter [mm]

$N$  = speed [rpm]

**(iii) Churning friction**

The empirical formula employed was derived by Mobbs (Leeds University) from extensive work on super-laminar and turbulent flow in journal bearings and quoted in his final year lecture notes on Turbulence.

The basis of the calculation is an empirical expression for the turbulent Couette shear stress factor:

$$\tau_c = 1 + 0.0012 Re^{0.94} \quad (4.3)$$

The total shear stress (where there is no axial pressure gradient) is given by:

$$\tau_t = \frac{\mu v}{b} \tau_c \quad (4.4)$$

and hence frictional drag of the rotating shaft:-

$$F_f = \int \tau_t dA \quad (4.5)$$

where A is the surface area of the shaft, and frictional power due to churning:-

$$P_f = F_f v \quad (4.6)$$

It was calculated that 7kW would be sufficient to drive the system to 6000 rpm. In the event, it was often found that the full motor power was required at a lower speed of about 5200 rpm. Since most of the test seals were not normally rated above 4000 rpm, this was not considered a serious limitation.

By modifications to the power circuitry, a switch was fitted enabling clockwise and counter-clockwise rotation. The motor and control gear incorporated a tachometer and a power meter giving overall power consumption based on motor current.

The main test shaft was supported on two deep-groove roller bearings. The bearings were lubricated by a drip-feed system driven by a peristaltic pump, and the bearing chamber sealed with lip seals.

The test and motor shafts were coupled using a precision geared coupling and aligned up to give 0.02 mm total indicated run-out at the test seal. Vibration levels were thus very low, even at 6000 rpm.

Two stainless steel sleeves were manufactured for the 48 and 100mm seals respectively, these requiring a total indicated run-out of less than 0.04mm at the test seal location; this was comfortably achieved. A disc keyed onto the end of the test shaft represented a pump impeller.

### 4.2.2 Test Cell

A general arrangement drawing of the test cell for the 48mm seal is shown in Fig 4.4, although the 100mm set-up was very similar.

The seal plate was manufactured to DIN 24960 dimensions and screwed into the adaptor plate mounted on the bearing unit. This permitted the substitution of alternative seal plates in the event of testing non-DIN seals. For the 100mm arrangement, the adaptor and seal plates were one component. Studs protruding from the adaptor plate supported the backing plate and impeller housing which, in turn, were loaded by retaining nuts to hold the test housing in position.

The test seal was mounted in the normal way and any leakage was caught by a secondary lip seal and drained off. Tests could be run with or without the neck bush bolted to the backing plate. When running with strakes, the strake assemblies were bolted to the backing plate in place of the neck bush.

### 4.2.3 Pumpset

The test fluid was supplied and conditioned by the pumpset adjacent to the test cell (Fig 4.26). The fluid was held in a stainless steel reservoir of 25 litres capacity having a conical bottom to allow for running with solids in suspension. Fluid was pumped from the reservoir by a rubber-impeller type pump driven by a 0-700 rpm DC motor. As the pump was of a moving cavity type, an accumulator was required to smooth the output flow. The flow was split to supply the impeller housing at all times and, optionally, the test housing through a stainless-steel manifold. Fluid supplied to the test housing was metered using an electro-magnetic flowmeter fitted with a low flow range facility.

Returning fluid was re-combined and passed through a heat exchanger and 10  $\mu$ m polypropylene filter (except when testing with solid contaminants) and then back to the reservoir.

### 4.3 INSTRUMENTATION AND MEASUREMENT SYSTEMS

The layout of the instrumentation and data-logging systems is shown diagrammatically in Figure 4.27 and described in the following sections.

#### 4.3.1 Transducers

Speed:	0-6000 rpm tachometer fitted to the DC drive motor.
Power:	total input power to the system calculated electronically using the motor current
Flowrate:	electromagnetic flowmeter flanked by bespoke expander and reducer sections
Pressure:	Two 0-2 bar absolute diaphragm transducers
Temperature:	Two platinum-resistance probes sheathed in stainless steel
Heat transfer:	Two mutually orthogonal, flush-mounted hot-film anemometer probes of the glue-on type (Fig 4.3) (DANTEC Type 55R47). The signals from these probes were carried via wires in the centre of the test shaft (see Fig 4.4) and through precision silver-graphite slip-rings designed for milli-volt signals. They were then processed, filtered and time-averaged using a Dantec 56 system (see Appendix F)

#### 4.3.2 Heat Transfer Measurement

##### (i) Probe set-up

The heat transfer probes required balancing before each test and checking afterwards, as drift was found to be a common occurrence. The procedure for each test was as follows:

- (a) Seal chamber and piping systems thoroughly purged of air.
- (b) Test fluid circulated around system until temperature equilibrium attained.
- (c) Probes balanced.
- (d) Offset voltage and temperature measured.
- (e) Rig started and speed gradually stepped up. At each speed, time-averaged voltage and temperature measurements were taken. Waveforms were monitored on a dual-beam cathode-ray oscilloscope.
- (f) Rig stopped. Offset voltage and temperature measured.
- (g) Calculation of Nusselt number

The values of probe voltage were converted into power dissipation into the water from:

$$P = \frac{V^2}{R} \quad (4.7)$$

where  $R$  = probe resistance =  $10.7 \times$  (manufacturer's measurement)

$$\text{Now } P = hA(T_p - T_c) \text{ (per unit time)} \quad (4.8)$$

where  $h$  = convective heat transfer coefficient

$$A_p = \text{probe area}$$

$$T_p = \text{probe temperature}$$

$$T_c = \text{seal chamber temperature}$$

From the manufacturer's literature (Appendix F):

$$A_p = 9 \times 10^{-8} \text{ m}^2$$

$$\text{and } T_p = \frac{(R_h/R_{amb}) - 1}{\alpha_{amb}} + T_c \quad (4.9)$$

where  $R_h$  = overheat resistance =  $12.8 \Omega$

$R_{amb}$  = ambient probe resistance =  $10.7 \Omega$

$T_c$  = seal chamber temperature =  $16^\circ\text{C}$

$\alpha_{amb}$  = ambient temperature coefficient of resistance =  $0.0040$

Hence  $T_p = 65^\circ\text{C}$  and  $\Delta T = 49^\circ\text{C}$

Therefore  $h$  can be calculated:

$$h = \frac{V^2}{R_{amb} A (T_p - T_c)} \quad (4.10)$$

$$\text{or } h = \frac{P - P_o}{A_p (T_p - T_c)} \quad (4.11)$$

$$= 227 \times 10^3 (P - P_o)$$

where  $P_o$  = probe power output at zero flow velocity

The offset power output,  $P_o$ , was probably attributable to conduction, radiation and natural convection losses and tended to fluctuate from day to day. The net power output was largely dependent upon the forced convection due to fluid in relative motion to the probe.

## (ii) Probe calibration

An attempt was made to calibrate the probes by passing a purely axial laminar flow over the seal and matching the results to the expression for wall shear stress in laminar Poiseuille flow in an annulus. This result was, however, treated with some caution as the flow was not perfectly laminar or axial, owing to the complex geometry of the seal and the end effects caused by the seal plate. It did give some indication of the order of magnitude of convective heat transfer coefficient to be expected.

Theoretical predictions of heat transfer from the probes in purely axial laminar flow were made for the shrouded spring seal (Seal B) in the narrow radial clearance housing with water as the liquid.

The formula for shear stress ( $\tau_w$ ) for such a flow is:

$$\tau_w = \frac{\rho v^2 Re_a}{r_m \left(1 + n^2 + \frac{1-n^2}{\ln n}\right)} \cdot \frac{1}{r_2} \left(2 + \left(1 - \frac{n^2}{\ln n}\right)\right) \quad (4.12)$$

where

$$\mu = \text{dynamic viscosity} = 10^{-3} \text{ Pa.s}$$

$$Re_a = \text{axial Reynolds number}$$

$$= 2 \frac{v_{ave} r_m}{\nu} \quad (4.13)$$

$$v_{ave} = \text{average velocity in annulus.}$$

$$n = \text{ratio of inner to outer radius} = \frac{r}{(r+b)} = 0.94$$

$$\rho = \text{density} = 1000 \text{ kg/m}^3$$

$$r_m = \text{equivalent radius of annulus}$$

$$r_2 = \text{outer radius} = r+b = 0.035$$

$$\text{also: } h = \frac{c_p \tau_w}{v_{ave}} \quad (4.14)$$

where  $c_p$  = specific heat capacity =  $4.18 \times 10^3 \text{ J/kgK}$

$$\text{Let } A = 1 + n^2 + \frac{1-n^2}{\ln n} = 2.40 \times 10^{-3} \quad (4.15)$$

$$B = 2 + \frac{1-n^2}{\ln n} = 0.119 \quad (4.16)$$

equation 4.12 simplifies to:

$$\tau_w = \frac{B}{A} \cdot \frac{\rho v^2 Re_a}{r_m r_2} \quad (4.17)$$

Substituting for  $Re_a$  gives

$$\tau_w = \frac{2B}{A} \cdot \frac{\rho v v_{ave}}{r + b} \quad (4.18)$$

Substituting for  $\tau_w$  in equation 4.14 yields:

$$\begin{aligned} h &= \frac{2B}{A} \cdot \frac{c_p \rho v v_{ave}}{(r + b) v_{ave}} \\ &= \frac{2B}{A} \cdot \frac{c_p \rho v}{r + b} \end{aligned} \quad (4.19)$$

Inputting parameter values:

$$h = 11.8 \times 10^3 \text{ W/m}^2 \text{ K}$$

Note that  $h$  is independent of the axial flow velocity.

The experimental arrangement for the probe calibration tests is shown in Figure 4.28; water was injected at the two ports in the impeller housing and exhausted at the four ports around the seal face. This was the nearest approximation to laminar Poiseuille flow obtainable on the test apparatus.

The results for both probes are given in the tables below; Probe 1 was mounted across the direction of the flow and Probe 2 in the direction of the flow.

## Probe 1

Flow velocity (through meter) [m/s]	Voltage [V]	P [W]	P - P <sub>0</sub> [W]	h [kW/m <sup>2</sup> K]
0.00	2.32	0.50	0.00	0.00
0.28	2.46	0.57	0.07	15.9
0.90	2.67	0.67	0.17	38.5
1.43	2.80	0.73	0.23	52.2
1.72	2.88	0.78	0.28	63.5
1.98	2.94	0.81	0.31	70.3
2.16	2.98	0.83	0.33	74.8
2.35	3.02	0.85	0.35	79.4
2.51	3.06	0.88	0.38	86.2
2.65	3.09	0.89	0.39	88.4
2.72	3.10	0.90	0.40	90.7

## Probe 2

Flow velocity (through meter) [m/s]	Voltage absolute [V]	P [W]	P - P <sub>0</sub> [W]	h [kW/m <sup>2</sup> K]
0.00	0.88	0.07	0.00	0.00
0.33	0.98	0.09	0.02	4.54
0.94	1.04	0.10	0.03	6.81
1.49	1.10	0.11	0.04	9.08
1.78	1.15	0.12	0.05	11.4
2.03	1.18	0.13	0.06	13.6
2.21	1.20	0.13	0.06	13.6
2.42	1.22	0.14	0.07	15.9
2.56	1.24	0.14	0.07	15.9
2.69	1.26	0.15	0.08	18.2
2.76	1.26	0.15	0.08	18.2

Theoretically, the measured values of  $h$  should be constant with increasing flow velocity and  $h$  should be of the order of  $10\text{kW/m}^2\text{K}$  given the result of equation 4.19. Clearly this was not the case for Probe 1, although the measured values at very low flow velocities accorded reasonably well. The results from Probe 2 were in better agreement with equation 4.19. The reasons for the differences between the probes was not obvious - orientation to the flow may have been a factor. In all probability, the flow over the probes was not perfectly laminar Poiseuille at higher flow velocities owing to the seal and chamber geometries.

Despite the uncertainties over the data from the probes, they were used in two valuable ways:

- (a) In indicating a first approximation for  $h$ . Most of the measured values lie within an order of magnitude of the predicted value.



- (b) As a tool for comparison between different housing shapes providing that the same probe was used. Whilst the absolute numbers should be treated with caution, their consistency for relative measurements was good.

#### 4.3.3 Data-logging Systems

All transducer signals were fed into a 32-channel Molytek 2702 chart recorder which gave a continuous read-out throughout testing. Where desired, the signals were manipulated mathematically within the recorder to give, for example, flowrate instead of flow velocity. Pressure and temperature differences were calculated from pairs of incoming signals and printed out on a separate channel. A typical trace is shown in Fig. 4.31.

#### 4.4 FLOW VISUALISATION

##### 4.4.1 Visualisation Techniques

Prior to experiments commencing a survey of literature on flow visualisation techniques in annular flows was carried out; this revealed three main techniques which had been successfully used with liquids.

###### (i) Dye injection:-

Dye injection was used by Taylor (1923) in his pioneering work on annular flows. Having predicted the positions of the vortices mathematically, Taylor arranged to inject dye at strategic locations to show the flow patterns. He achieved considerable success at (or just above) the critical, but notes that dye dispersion became a problem when the flow became turbulent.

###### (ii) Aluminium paint pigment in oil:-

This technique has been used by many workers: Nissan, Nardicci and Ho (1963); Coles (1965); Barcion, Brindley, Lessen and Mobbs (1979); and Coney and Summers (1979 (b)); to name but four groups. The paint pigment consists of tiny platelettes which align themselves in the flow; edge-on they reflect no light, but flat-on they are very lustrous. Hence areas of ingressing or egressing flow appear dark, but where the vortex flow runs parallel to the outer cylinder the area appears highly illuminated. The pictures obtained by the cited authors are consequently very clear, even at high Taylor numbers. The only drawback to this method is that water cannot be used as a carrier fluid as this results in adhesion of the pigment to the walls of the vessel. This was amply confirmed by the author who conducted a simple replication using a plastic shaft driven by an electric drill rotating in a glass measuring cylinder.

###### (iii) Hollow glass micro-spheres in water

Hollow glass micro-spheres have been used for flow tracing for some years at Leeds University. Being of lower density than water, the spheres are drawn to the centres of the vortices thus enabling studies of vortex core behaviour to be made especially in wavy modes.

##### 4.4.2 Exploratory Tests

For the present study, it had been decided by the sponsors that water was to be used as the principal test fluid; hence suspended aluminium paint pigment was not an option. Furthermore, flow studies would generally be at elevated Taylor numbers, thus ruling out the use of injected dye.

To begin with, using the hollow glass micro-spheres showed promise, especially for picking out super-laminar flows. The bubbles used were in the size range 30-50  $\mu\text{m}$  and had a relative density of 0.32; they therefore readily migrated to stagnation regions. Unfortunately, their buoyancy also caused accumulations at the top of the seal chamber, thus obscuring the vortex patterns.

Preliminary tests using the spheres were carried using the shrouded-spring 48 mm seal in the narrow radial clearance housing. For water, the relationship between Taylor number and speed in revolutions per minute for this geometry was:-

$$Ta = 2.9 N^2 \quad (4.20)$$

The test rig was run dead-ended (Fig 4.17) with the micro-spheres circulating in the flow through the impeller cavity; some micro-spheres accumulated at the top of the seal chamber. The seal was started and run up to a speed of 25 rpm ( $Ta = 1800$ ) (Fig 4.32); no flow structure was apparent. At 37 rpm ( $Ta = 3970$ ) (Fig 4.33) the vortex action was well established and by the time speed had reached 73 rpm ( $Ta = 15450$ ) (Fig 4.34) some very thin lines of micro-spheres picked out vortex flows; frequently these lines bifurcated and rejoined as a result of turbulent perturbations.

All trace of flow structure had disappeared by the time the speed had reached 130 rpm ( $Ta = 49 \times 10^3$ ); it was considered that the flow was now highly turbulent and chaotic. On reducing the speed the vortex flow re-asserted itself. Above 130 rpm the micro-spheres were invisible and apparently unable to pick out any structure which might have been present. This was considered a serious draw-back as most mechanical seals operate well in excess of these speeds and Taylor numbers.

Whilst carrying out tests with the micro-spheres it was noticed that any air bubbles present in the seal chamber congregated in the same places on the micro-spheres. Moreover these did not disappear when the speed exceeded 130 rpm and were capable of picking out flow patterns even at the highest speeds.

The technique finally adopted for flow visualisation was therefore simply to add small amounts of air to the seal chamber bubbled in through a hypodermic under the seal faces. As well as picking out the vortex cores and stagnation regions at all but the lowest speeds, this represented a valid test of the gas-handling capability of the seal chamber on test.

#### 4.4.3 Lighting Techniques

Satisfactory illumination of the tracer bubbles was not particularly easy and much time was spent in developing the best arrangement. Fig 4.35 shows an early attempt at photographing bubble patterns using a high-speed flash placed on top of the camera; troublesome reflections from the perspex housing and glare from the seal rotor impair its quality.

Four flash positions were tried in an attempt to improve matters (Fig 4.36). Positions A and B produced the type of picture shown in Fig 4.37, C and D generated deep shadows on the camera side of the chamber and poor focusing. A modification tried was to put the flash behind a slitted piece of black card thereby reducing glare and reflections. Unfortunately this did not allow sufficient light onto the subject.

The next option tried was to use a 1000W video light to illuminate the seal chamber. Although shutter speeds would be slower and unable to freeze the subject it was envisaged that flow vectors could be determined from bubble streaks. Again a number of lighting and camera positions were tried (Fig 4.38).

To avoid the problems of glare and reflection, the first two arrangements used light bounced from a low white false ceiling over the test apparatus, but insufficient light was available. Plan C produced deep shadows as before, and plans D and E predictably caused unwanted reflections, although some improvement was brought about by spraying the seal and shaft matt black.

Finally, it was found necessary to employ a second weaker light source of 100W. This allowed the shadows caused by plan C to be filled in by the second lamp from underneath the camera, as shown in Fig 4.39. The quality of picture obtainable by this means is illustrated in Fig 4.40. Some reflection was inevitable, but most of the seal was visible and the patterns generated by the bubbles can be clearly seen.

#### 4.4.4 Recording Techniques

Traditionally, stills photography has been the principal technique for recording flow patterns. It has the advantage of allowing the detailed flow structure at a given time and can be used to determine the vectors of flow tracers by judicious adjustment of exposure time. However, many pictures are required if a time-dependent phenomenon is being studied, one example being vortex behaviour on the introduction of axial flow or vortex modifiers.

In the current study, stills photography was found useful for studying "steady-state" events where perturbing mechanisms were not effective. Flash-photography was used to "freeze" air bubbles and hence determine their distribution, as in Fig 4.35 and 4.37. Long-exposure photography was also used with the aim of determining the vectors of individual bubbles. Fig 4.41 shows typical examples of this type of photograph and it is noteworthy that bubble traces show up clearly against the black seal.

Owing to the nature of flow types found in the seal chambers, it soon became clear early in the programme that the video camera was the best instrument for recording the flow patterns and their evolution. The camera was fitted with a macro-lens which enabled very close-up study of the area around the seal. Once illumination techniques had been developed (Fig 4.2) the video camera was used for all visualisation experiments. Some film of flow patterns was taken using a stroboscope as a light-source, but insufficient light gave somewhat indistinct pictures. Real time commentary was added as experiments took place using a roving microphone, and title pages created using the camera's own titling facility. An in-house editing suite was extensively used to produce an edited "highlights" tape, complete with descriptive voice-over.

---

**CHAPTER 5.**

---

**TEST PROGRAMME**

## 5.1 WATER/GAS TESTS

The water/gas tests comprised the major component of the experimental programme and were used to investigate the effect of geometric and other variables. Two seal sizes, 48mm and 100mm were tested. A summary of tests is given in Table 5.1.

### 5.1.1 48mm Tests

#### (i) Flow Visualisation

For a given seal and housing a series of test runs were carried out with the appropriate piping plan and neck bush arrangement. Clockwise or counter-clockwise rotation was selected in the case of Seal A. The test was run according to the plan given in Section 4.1.6. Throughout the test, air was injected through a hypodermic under the seal faces. The test run was filmed throughout and information such as speed, flowrate, pressures, and temperatures and descriptive comments were dictated directly onto the tape.

#### (ii) Heat Transfer

Heat transfer measurements were confined to the shrouded single spring and multi-spring seals, since these were the only seals offering sufficient space to mount the heat transfer probes.

Five housings: 1, 2, 3, 5 and 7, were tested and were run with/without neck bushing, dead-ended and with injection at the seal face.

Following the set-up procedure set out in Section 4.3.2. the pattern of each test followed precisely the form given below:-

- (a) Speed = 0
- plan : seal face injection
  - flowrate = 4 l/min
  - temperature and probe voltage recorded

A chamber with injection at the seal face was the base-line condition as it enabled the seal chamber temperature to be kept reasonably constant.

- (b) Speed = 100 rpm
- plan : seal face injection
  - flowrate = 4 l/min
  - temperature logged
  - probe voltage time-averaged over 10 seconds and recorded
  - temperature logged

- (c) Speed = 100 rpm
- plan : dead-ended
  - flowrate = 0 l/min
  - temperature logged
  - probe voltage time-averaged over 10 seconds and recorded
  - temperature logged

- (d) Speed = 100 rpm
  - plan : seal face injection
  - flowrate = 4 l/min
  - temperature logged
  - speed slowly increased to next setting
- (e) Steps (i) to (iv) repeated for speeds of 200, 300, 400, 500, 600, 800, 1000, 1250, 1500, 1750, 2000, 2250, 2500, 2750, 3000, 3500, 4000, 4500 and 5000 rpm.
- (f) Speed = 0
  - plan : seal face injection
  - flowrate = 4 l/min
  - temperature logged
  - offset probe voltage recorded

By adhering to an identical procedure for every test, systematic errors were minimised. However, keeping the seal chamber temperature constant during test runs was very difficult, particularly at the higher speeds and when running dead-ended. The effect of heating was to decrease the signal from the probes. Such sensitivity precluded using the probes in the water/glycerol tests where heat generation was even more significant.

### 5.1.2 100mm Tests

The procedure given in 5.1.1 was adopted for a more restricted set of variables.

Two seal types, single-spring and rotating metal bellows, were run in four housings. The housings were selected on the basis of the 48mm tests with the narrow radial clearance housing as the baseline geometry. Two piping plans, dead-ended and seal-face injection, were investigated as was the effect of a neck bush. The set speeds were 500, 1000 and 2000 rpm; there was insufficient rig power to run above 2300 rpm.

## 5.2 GLYCEROL & WATER/GAS TESTS

The glycerol/water tests were confined to four housings, narrow and wide radial clearances and the two positively flared - all with radial injection.

All five seals ran with fluids of viscosity 10 mPa.s (10cP) and 100 mPa.s (100cP) and one seal with an extra set of tests at 50 mPa.s (50cP). These viscosity values were target figures as actual values varied over a period of time due to water take-up. The actual viscosity was therefore checked regularly using a cylinder-in-bucket type viscometer. The test procedure was identical to the water/gas tests. A summary of tests is given in Table 5.1.



### 5.3 WATER/SOLIDS TESTS

These tests were run with two seal designs, shrouded and exposed single springs, in the same four housings used for the glycerol/water test. Tests could only be run dead-ended since injection of clean flush would lead to dilution in the closed loop system. The standard procedure was used and incorporated axial strakes as an additional variable for two of the housings.

Four solids were tested in suspension, giving a range of size and density:

- (a) carbon dust
- (b) silicon dioxide powder
- (c) sand
- (d) iron oxide

A few tests were run for a water/sand/air mixture with housings fitted with helical strakes.

A summary of tests is given in Table 5.1.

---

**CHAPTER 6.**

---

**TEST RESULTS**

## 6.1 FLOW VISUALISATION TESTS

### 6.1.1 Narrow Radial Clearance Housing (Nos 1,3 and 1-100)

Figures 6.1 to 6.6 give an impression of the performance of the housing. When run dead-ended (Fig 6.1), air was seen to linger in the vicinity of the seal, usually trapped in well defined discrete bands along the length of the seal rotor. No such bands were visible around the exposed single spring seal however (Fig 6.2). This seal encouraged vapour removal when run counter-clockwise, ie. pumping away from the seal faces. Running with glycerol/water solutions resulted in a large void being opened up over the seal face (Fig 6.3).

The best operating mode for the narrow radial housing was achieved by fitting a neck bush and adding a good flush to the seal face (Fig 6.4). Generally this was sufficient to remove air from the immediate environs of the seal faces, but not from around the seal rotor (Fig 6.5). These pictures also show how air bubbles collecting in cut-outs on the seal rotor body were allowed to remain there, apparently unaffected by the flush. At speeds in excess of 3000 rpm, the effectiveness of the flush diminished. Flushing was essential with the glycerol/water solution to maintain any fluid at all around the seal faces.

Tangential injection did not appear to provide any marked benefit; indeed, injection in the direction of rotation lead to reduced air purging. Multi-port injection was found to be of some benefit in many of the cases in which it was tested and certainly never worsened performance.

The narrow radial clearance housing was a poor performer when solids were present. Fig 6.6 shows the extent to which the seal faces could not be seen due to the dense cluster of orbiting sand particles.

### 6.1.2 Wide Radial Clearance Housing (Nos. 2, 4, 2-100 and 3-100)

The water/gas experiments demonstrated the ability of this housing to prevent gas accumulation at the seal faces by drawing air into a large vortex-like feature located usually halfway down the seal rotor (Fig 6.7). This vortex formed at a distinct speed which was different for each particular housing geometry but, once formed, remained a feature of the flow, even at the highest speed (Fig 6.8). Above 2500 rpm the seal chamber took on an increasingly misty appearance, which, under a stroboscope, was seen to be caused by very fine air bubbles held in suspension (Fig 6.9).

It was notable that, although gas was purged from the seal faces, it accumulated in large quantities at the impeller end of the seal chamber when a neck bush was in place. Removal of the neck bush allowed the excess air to vent into the impeller housing.

Flushing by any piping plan did not visibly improve the gas-purging ability of the housing, and there was no perceived advantage gained from tangential or multi-port injection.

Seal design did not appear to affect the flow patterns. The wide radial clearance housing experienced difficulties with the more viscous liquids however. Consistently it managed to maintain cooling fluid at the seal face, unlike the narrow radial clearance housing, but allowed large amounts of air to remain over the seal rotor (Fig 6.10). At speeds in excess of 2000 rpm the glycerol/water solution emulsified, rendering the seal invisible. When running dead-ended on 100 mPa.s solution it was found that the liquid temperature in the seal chamber rose dramatically, typically increasing by 30°C in 3 minutes, at 3000 rpm. At this speed the motor was delivering its maximum 7 kW.

When solid contaminants, particularly the sand, were introduced the strong vortex feature noted on the water/gas experiments was again evident. This time it drew particles into itself in high speed orbit (Fig 6.11), a phenomenon which could potentially cause rapid erosion in a small area. The addition of axial strakes diffused the concentrated solids (Fig 6.12) but also caused some cavitation. The air removed from solution was drawn into a circumferential "corkscrew", suggesting that a modified vortex was still extant but perhaps too weak to hold dense solids. This housing appeared to be unable to deal with fine solids in suspension, even at high speeds. The attempt to improve the gas handling ability of the strake arrangement by using helical strakes (Fig 6.13) was inconclusive owing to time-limitations curtailing its development.

### 6.1.3 12° Positively Flared Housing

Like the wide radial clearance housing, a strong vortex situated over the seal rotor was a feature of the 12° positively flared housing with all seal types (Fig 6.14); it behaved in the same way as described in 6.1.2. This housing performed best with gas when running without a neck bush. Mistiness of the seal chamber was observed at speeds above 3000 rpm although this was alleviated over the seal by a seal-face injection flowrate in excess of 2 litres/minute. A flush was essential for the water/glycerol solution in order to keep liquid at the seal face continuously.

The flared housing had no observable effect on the fine solids but was effective with all seal types when run on coarse solids (Fig 6.15). Very little solid contaminant found its way down the seal chamber to the seal faces.

#### 6.1.4 12° Negatively Flared Housing

Figure 6.16 gives an impression of the performance of this housing at various speeds. At speeds above 1000 rpm, it was poor. Strong vortex action over the seal was seen to create dense white clusters of bubbles over the faces, and at high speeds the whole seal chamber was "flooded" with air. Strong injection at the seal face helped to move the main vortex away from the seal plate slightly but not sufficiently (Fig 6.17). It might be expected that lantern ring injection and seal face exhaustion would bring out the best from this housing but this was not the case (Fig 6.16).

Owing to its inadequacies with water/gas mixtures this housing was dropped from subsequent experiments.

#### 6.1.5 45° Positively Flared Housing

The 45° positively flared housing was impressive in all the water/gas tests irrespective of the seal design, piping plan or speed, and in many cases seemed impervious to the presence or otherwise of a neck bush. In general, most traces of gas could be removed from the seal chamber using this housing design (Fig 19). The only exception was, when running with a neck bush at speeds of less than 1000 rpm, gas lingered in the region behind the seal rotor.

Running with the glycerol/water solution was not quite as good although gas was kept well away from the vicinity of the seal faces (Fig 6.20). Injection to the seal faces in these cases made sure of efficient gas purging, however. As with previous experiments, emulsification of the solution occurred at speeds above 2000 rpm (Fig 6.21).

Like the other housings tested, the 45° flare did nothing to modify the behaviour of fine solids. Coarse solids were affected however. A dense build-up of solids was formed around the seal faces and not centrifuged out as might be expected (Fig 6.22). Insertion of a neck bush helped to alleviate the position by moving the dense cluster of particles behind the seal rotor and adjacent to the bush (Fig 6.23). The only way of keeping the particles away from the seal environs completely was to insert axial strakes (Fig 6.24). However, this was at the expense of some cavitation and poorer gas handling ability.

## 6.2 HEAT TRANSFER TESTS

### 6.2.1 Shrouded-spring seal (Seal B)

Setting-up of the hot-film anemometer probes proved to be time-consuming and many hours of run-time were spent trying to optimise the gain and filter setting on the signal processing equipment. As expected, there was a good deal of electrical noise generated by the rotating shaft, especially at higher speeds, and this was filtered out using the Dantec signal processing equipment. A dual beam cathode-ray oscilloscope was used to view the time-averaged signals.

Unfortunately, having set up the probes, only one set of data was obtained before both probes went open circuit; these data are plotted out in Figure 6.25 and show gradually increasing voltage and scatter with speed. Of interest were the waveforms observed during the experiment; at speeds below 600 rpm the waveform was apparently random (Fig 6.26) but above 650 rpm there was a definite structure (Fig 6.27) which remained thereafter.

It had been observed that the temperature in the seal chamber had fluctuated during the experiment, which affected the voltage output from the probes. Consequently, all subsequent experiments were carried out with the procedure given in Section 5.1.1 (ii).

### 6.2.2 Multiple-spring seal (Seal C)

The results of tests, using the radial-ported housing are given in Table 6.1 and shown graphically in Fig 6.28. A relationship between the heat transfer coefficient and peripheral Reynolds number is apparent, albeit with some deviations at the extremities. The fall-off in readings at the highest Reynolds number was probably due to the slight, and unavoidable, rise in chamber temperature due to turbulent churning. The line of best fit from Fig 6.28 was used to derive a relationship for the heat transfer coefficient to Reynolds number:

$$h = 141 \text{ Re}^{0.5} \quad (6.1)$$

The results for heat transfer coefficient within the laminar flow regimes ( $\text{Re} < 2000$ ) agree reasonably well with the theoretically predicted value for  $h$  of  $11.8 \text{ kW/m}^2\text{K}$ . The effect of highly turbulent flow at the highest Reynolds numbers is generally to increase  $h$  by an order of magnitude.

Given that:

$$\text{Ta} = (\text{Re})^2(b/r)^3 \quad (6.2)$$

then the agreement between equation 6.1 and the equations of earlier workers, listed in equations 3.18 to 3.23, is good for the index of Reynolds number. The constant of proportionality measured in the current work is somewhat higher. This may be due to effects associated with the seal and chamber geometries but may present a more accurate reflection of the actual environment of the seal.

The results shown in Fig 6.28 suggest that radial clearance around the seal has no direct influence on the heat transfer coefficient. Given that the latter depends chiefly on the behaviour of the turbulent boundary layer, then this is probably a correct conclusion.

However, if the effective heat transfer area was to be reduced by poor housing design allowing vapour or gas accumulations, the actual power dissipation potential could be seriously impaired.

---

**CHAPTER 7.**

---

**MATHEMATICAL MODEL**



## 7.1 NATURE OF ROTATING FLOWS

The work on rotating annular flows summarised in Chapter 3 has demonstrated that the flow regime present for a given set of fluid and geometric conditions is governed by the Taylor number. The flow regimes reported occur in the following sequence, with increasing Taylor number: Laminar, Taylor-vortex, turbulent, turbulent-vortex as shown in Fig 7.1. No explanation for the turbulent-vortex regime has been proposed in the technical literature and little work has been undertaken to investigate the flow characteristics at very high Taylor numbers ( $> 10^8$ ). Since many mechanical seals operate at these very elevated Taylor numbers, an understanding of the mechanisms involved is desirable.

The flow between a rotating inner cylinder and a stationary outer cylinder is inherently unstable. In an unbounded non-viscous curved flow an element of fluid moving at a circumferential velocity  $v_1$  around a circle of radius  $r_1$  will be subjected to a centrifugal force per unit mass of  $v_1^2/r_1$ . If the element is displaced outwards to an orbit of radius  $r_2$  whilst retaining its angular momentum, its new velocity will be  $v_1 r_1/r_2$  and the centrifugal force per unit mass will be  $v_1^2 r_1^2/r_2^3$ . However, the surrounding fluid at radius  $r_2$ , moving at velocity  $v_2$ , is subjected to a centrifugal force of  $v_2^2/r_2$ . For equilibrium to be satisfied this force must be balanced by an equal and opposite force due to a radial pressure gradient - the same condition applies to the displaced fluid. If  $v_1^2 r_1^2/r_2^3 < v_2^2/r_2$ , then the fluid returns to its original orbit and flow stability is maintained. If, as is the case of current interest,  $v_1^2 r_1^2/r_2^3 > v_2^2/r_2$ , the displaced fluid continues to move outwards and the flow is unstable. Put another way, if  $v_1^2 r_1^2 > v_2^2 r_2^2$ , the so-called "Rayleigh criterion"), instability is an inherent feature of the system. The system resolves its instability in a bounded flow by adopting the Taylor-vortex type of flow regime. Given that the vortex regime is the preferred flow system it is necessary to understand why this structure is not present at all times.

In a real liquid, viscous forces are present. At low speeds, where forces are sufficient to overcome the de-stabilising inertial forces, outward movement of fluid is prevented. The flow is laminar because the vortices are suppressed. As the speed increases a point is reached where the inertial forces overcome the viscous forces and the classical Taylor-vortex flow is established. This transition has been widely studied and is well understood. A further increase in speed causes the Taylor-vortices to become wavy and to bifurcate in a complex fashion - the flow is not turbulent at this stage.

The breakdown into turbulent flow at higher speeds is not so well understood and it is probable that turbulent transition occurs in some parts of the flow system earlier than in others. It is likely that the scale of turbulent eddies is also of importance. The first eddies would be of similar scale to the Taylor-vortices which would enable them to disrupt the vortices with great effectiveness. This accomplished, the decay of ordered flow into apparently random turbulence is understandable. Why structured flow should re-appear as the speed is increased still higher is as yet unexplained. On a classical basis vortex flow should only be dominant at Taylor numbers in the range  $10^3$  to  $10^4$ .

## 7.2 TURBULENCE VISCOSITY

The Taylor number is the ratio of inertial to viscous forces. For a given geometry the inertial forces increase as the speed increases and the viscous forces are assumed to be constant. In a turbulent flow additional stresses are present in the fluid. These "Reynolds" or "turbulence" stresses are not a consequence of the fluid but of the turbulence. Their effects, though, are real and result in additional frictional drag on the rotating shaft. Given their physical effects it is reasonable to propose that the associated turbulence viscosity can influence the flow regime.

The classical Taylor number can be redefined as an "effective Taylor number",  $Ta_E$ :

$$Ta_E = \frac{\omega^2 r b^3}{(v_{eff})^2} \quad (7.1)$$

where  $v_{eff}$  is the effective fluid viscosity:

$$\text{and } v_{eff} = v + v_t \quad (7.2)$$

where  $v_t$  is the turbulence viscosity.

The effect of adding in  $v_t$  as the flow becomes turbulent will be to reduce the effective Taylor number. Conceivably, if the effective Taylor number is sufficiently depressed it may return to a value of between  $10^3$  and  $10^4$  - the vortex flow condition. The shape of the curve might resemble that shown in Figure 7.2 which gives the corresponding flow regimes expected at each speed.

### 7.3 CALCULATION OF TURBULENCE VISCOSITY

Validation of the hypothesis outlined in 7.2 relies crucially on the prediction of turbulence viscosity.

Effective viscosity can be estimated in a number of ways; see Launder and Spalding (1972) for a good summary. The simplest analysis is based upon the Prandtl mixing-length theorem which is analogous to the laws governing gas kinetics. The theorem may be used here because the flow is bounded and the area of principal interest is close to this boundary, namely the inner cylinder where heat transfer occurs. In addition, the shear in the turbulent boundary layer on the inner cylinder is responsible both for generating the turbulent energy in the flow and for driving the toroidal vortices.

The basis for the calculation of effective viscosity is, in a partially turbulent Couette flow, as set forth by Patankar and Spalding (1970). In essence it uses the Prandtl theorem but incorporates the Van Driest modification.

For ease, certain parameters are non-dimensionalized:-

$$v_+ = \frac{v_{eff}}{v} \quad (7.3)$$

$$\tau_+ = \frac{\tau}{\tau_w} \quad (7.4)$$

$$y_+ = y \frac{\tau_w^{1/2}}{\rho^{1/2} v} \quad (7.5)$$

$$v = v/v^* = v/(\tau_w^{1/2}/\rho) \quad (7.6)$$

(where  $v^*$  is the "friction velocity")

From the theorem (equations 1.4-47 and 48, in Patankar and Spalding (1970))

$$v_+ = 1 + K^2 y_+^2 + \left[ 1 - \exp \frac{-y_+ \tau_+^{1/2}}{A_+} \right]^2 \frac{dv_+}{dy_+} \quad (7.7)$$

$$\begin{aligned} \frac{dv_+}{dy_+} &= \text{dimensionless velocity gradient} \\ &= \frac{2 \tau_+}{1 + [1 + 4K^2 y_+^2 \tau_+ \{ 1 - \exp\left(\frac{-y_+ \tau_+^{1/2}}{A_+}\right)\} ]^{1/2}} \end{aligned} \quad (7.8)$$

It may be assumed:-

$K = 0.4$  (from Nikuradse formula for the region near a wall)

$A_+ = 26.0$  (see Launder & Spalding (1972) p.40)

$\tau_+ = 1$  (for high Reynolds numbers, see Launder and Spalding (1972) p.43)

The last assumption is intended as a first approximation and is based on the assertion that flows in seal chambers are typically at high Reynolds numbers, compared with open channel or pipe flows.

To solve equation 7.7 and determine the dimensionless effective viscosity requires a prediction of the dimensionless boundary layer thickness,  $y_+$  (equation 7.5). The density and molecular viscosity are properties of the fluid but the wall shear stress and boundary layer thickness must be calculated on the basis of existing experimental data.

#### 7.4 DETERMINATION OF WALL SHEAR STRESS

In order to calculate  $y_+$ , the wall shear stress in the turbulent regime must be known.

$$\text{Now } \tau_w = \frac{1}{2} C_f \rho v^2 \quad (7.9)$$

The coefficient of friction ( $C_f$ ) at the wall for turbulent Couette flow can be based upon the results of one of the empirical relationships developed in the past and reported in the literature. In each case the published expression has been converted into a consistent style using the peripheral Reynolds number. This enabled the curves to be plotted onto log/log graph paper and a typical expression derived. The equations used are described in the following text.

##### 7.4.1 Bjorklund and Kays (1959):-

In the course of their investigations, they combined experimental friction data of Taylor (1935) and Wagner (1932) to derive the relationship between  $C_f$  and  $Re$ :

$$C_f = 3.74 Re^{-0.48} \quad (7.10)$$

$$6.8 \times 10^3 < Re < 6.8 \times 10^5$$

for a clearance ratio,  $b/r$ , of 0.16

##### 7.4.2 Cole (1967)

From the friction factor, the following relationship for the turbulent regime was derived:-

$$C_f = 0.88 Re^{-0.52} \quad (7.11)$$

$$2 \times 10^3 < Re < 5 \times 10^3$$

##### 7.4.3 Vohr (1968)

Vohr's experimental data for concentric cylinders fall into three distinct regimes:-

$$(a) C_f = 0.18 Re^{-0.34}$$

$$10_3 < Re = 3.16 \times 10^3 \quad (7.12)$$

$$(b) C_f = 0.63 Re^{-0.48}$$

$$3.16 \times 10^3 < Re < 10^5 \quad (7.13)$$

$$(c) C_f = 0.063 Re^{-0.14}$$

$$10^5 < Re < 3.16 \times 10^5 \quad (7.14)$$

#### 7.4.4 Castle et al (1971)

For concentric cylinders the data reported can be approximated to:-

$$C_f = 0.33 \text{ Re}^{-0.38}$$

$$1.1 \times 10^3 < \text{Re} < 3.4 \times 10^3 \quad (7.15)$$

#### 7.4.5 Floyd (1982)

Floyd gives three expressions for friction coefficient for different clearance ratios at very high Reynolds numbers:-

(a)  $\frac{b}{r} = 0.046$

$$C_f = 0.056 \text{ Re}^{-0.237} \quad (7.16)$$

$$2 \times 10^6 < \text{Re} < 2 \times 10^7$$

(b)  $\frac{b}{r} = 0.093$

$$C_f = 0.0212 \text{ Re}^{-0.184} \quad (7.17)$$

$$2 \times 10^6 < \text{Re} < 2 \times 10^7$$

(c)  $\frac{b}{r} = 0.19$

$$C_f = 0.023 \text{ Re}^{-0.190} \quad (7.18)$$

$$2 \times 10^6 < \text{Re} > 2 \times 10^7$$

#### 7.4.6 Present Study

Data from the experiments carried out as part of the housing investigation were used to calculate a relationship between friction coefficient and peripheral Reynolds number.

Power consumption measurements were measured of the 100 mm rotating metal bellows seal running in three different parallel housings dead-ended and with a neck bush. The seals were run with the dummy impeller.

The results of total power consumption versus speed are given in Figure 7.3, together with the curve for the power consumption of the bearings and seals alone, as given in Section 4.1.6. The pressure in the seal chamber was less than 1 bar gauge and thus it is reasonable to assume that the mechanical friction would not greatly increase due to the additional hydraulic loads. The total power consumption for the three housing was similar.

The bulk of the power not accounted for mechanically may be attributable to the turbulent churning losses. The churning losses and speeds were non-dimensionalized into wall friction coefficient and Reynolds number which yielded the following relationship:-

$$C_f = 10.0 \text{ Re}^{-0.54} \quad (7.19)$$

#### 7.4.7 Summary

Fig 7.4 summarises the friction curves; the agreement is reasonable. As a first approximation, a universal relationship for friction coefficient versus Reynolds number can be derived. An acceptable fit is obtained by the equation:-

$$C_f = 0.14 \text{ Re}^{-0.3} \quad (7.20)$$

and hence

$$\tau_w = 0.07 \rho v^2 (\text{Re})^{-0.3} \quad (7.21)$$

The expression for friction coefficient derived by the author from data collected during the current study predicts values of  $C_f$  of an order of magnitude greater than other expressions. The reason for the discrepancy of the constant of proportionality probably is due to the geometry of the rotating cylinder and the impeller. For the other studies listed the rotor was a long smooth circular cylinder.

## 7.5 ESTIMATION OF BOUNDARY LAYER THICKNESS

The selection of a correct value for the boundary layer thickness may be estimated from radial temperature and velocity profiles across the annulus.

Dorfman (1963) examined the velocity profile data of Taylor (1935) and Reichardt (1956). Two things are evident from these results:

- (i) the boundary layer on the inner cylinder occupies about 10% of the annulus width.
- (ii) the velocity at the edge of the boundary layer is between half and two-thirds that of the peripheral velocity of the rotating cylinder.

Analysis of velocity and temperature profiles measured by Ho, Nardicci and Nissan (1964), Simmers and Coney (1979)(b) and (c), Simmers and Coney (1980) and Abdallah and Coney (1988) lends support to these assertions.

This is evident from Figures 7.5 - 7.9 which are taken from the above reports. For each graph the edge of the turbulent boundary layer was estimated as a proportion of the annulus width. Although there is, inevitably, some variability, assertion (i) seems a reasonable first approximation for the purposes of the model.

The velocity at the edge of the turbulent boundary layer was also estimated as a proportion of peripheral velocity from Figures 7.6 - 7.8.

Dorfman suggests that the velocity profile in the absence of axial flow may be expressed as follows:

$$\frac{v}{v^*} = \frac{1}{2} \frac{v_w}{v^*} - 5.75 \log \frac{(y/b)}{1 - (y/b)} \quad (7.25)$$

Equation 7.25 may be re-arranged to make  $y$  the subject, thus:

$$y = \frac{\frac{b}{1}}{\exp(0.174 \frac{v_w}{2v^*} - \frac{v}{v^*})} + 1 \quad (7.26)$$

It will be assumed that

$$v = 0.6 v_w \text{ (from assertion (ii))} \quad (7.27)$$

Dorfman's profile agrees well with the measurements of Figs 7.5-7.9.



## 7.6 RESULTS OF ANALYSIS

Using a spreadsheet (see for example, Appendix G) the turbulence viscosity and effective Taylor numbers were calculated for a range of different molecular viscosities and chamber geometries. The latter corresponded to particular conditions investigated in the experimental studies.

On the basis of the graphs produced (Figs 7.10-7.20) and the hypothesis put forward in Section 7.2, predictions of expected flow regimes throughout the speed range were made. Necessarily these predictions were a first approximation and were intended to give an indication of the existence of a regime rather than pin-pointing exact speeds at which the regime would change. Table 7.1 summarises the predictions of the graphs; these are compared with the experimental observations in Chapter 8.

An interesting feature of the results is the almost ubiquitous nature of the vortex structure, either in its classical or turbulent forms. Given that the vortex structure is the preferred resolution of the instability of the flow system, this is not too surprising. The major exceptions are the three wide radial clearance housings where the effective Taylor number exceeds  $10^4$  at speeds varying from 300 to 1300 rpm, depending on the radial clearance. At this point the model predicts a breakdown of high-speed vortices into a more "homogeneous" turbulent regime.

An alternative presentation of the results is to plot the Taylor numbers against the peripheral Reynolds number. This takes out the effect of changing the molecular viscosity and allows all of the predictions for a given seal chamber geometry to be displayed on one graph as shown in Figures 7.21 to 7.25. It is interesting to note that the predicted effective Taylor number curves are relatively flat; a change in Reynolds number in the turbulent-dominated regime, due to a viscosity change for example, has a generally small effect on the flow regime.

---

**CHAPTER 8.**

---

**DISCUSSION OF RESULTS**

## 8.1 NARROW RADIAL CLEARANCE HOUSINGS

### 8.1.1 Flow Regimes

#### (i) Water

Comparison of the results for the two seal sizes (Figs 7.10 and 7.14) showed that the predicted effective Taylor number was similar in both cases. Classical Taylor vortices existed only at very low speeds. It can safely be assumed that the flow around seals handling low viscosity liquids, eg. water and light hydrocarbons, is turbulent. However, the experimental results for these housings showed quite clearly that the turbulence was not truly random but was structured - this structure bore a striking resemblance to that of Taylor vortices.

For the 48 mm seals, it had been observed that Taylor vortex flow had deteriorated into apparently random flow at about 100 rpm but by the time the speed had reached about 600 rpm the flow structure was certainly evident once again. Moreover, the flow regime was highly structured even at 5000 rpm.

Comparing these observations with Figure 7.10 leads to some interesting observations. At the onset of turbulence and break-up of Taylor vortex flow (about 100 rpm) the predicted effective Taylor number is about 1000 - in other words, it is sub-critical. Table 7.1 would indicate a regime in which vortices were suppressed - in this case by the turbulent eddies. However, when the speed is 1000 rpm the model predicts that the effective Taylor number is critical and the flow is structured once again into turbulent toroidal vortices. Within the bounds of inaccuracy in the model, this could quite plausibly be the same point at which re-emergent for structure was observed (600 rpm). In addition, it is noteworthy that even at 5000 rpm the effective Taylor number is still only about 4500 - well within the vortex regime. This could well explain the existence of structure at such high Taylor numbers - a feature also observed by Wan and Coney (1982 (b)).

#### (ii) Higher viscosities

A slight increase in viscosity has a dramatic effect on the speeds at which the different flow regimes are predicted as shown in Table 7.1. Interestingly, truly homogenous turbulent flow is not predicted at all - the transition out of the Taylor-vortex regime is immediately into a vortex regime (Figs 7.11 and 7.12).

Strong vortex flow was indeed a feature of the water/glycerol tests but, unfortunately, accurate corroboration of the predictions was made impossible by the emulsification which repeatedly occurred at a speed of about 2000 rpm.

It is interesting to note the sensitivity of flow regime to changes in viscosity due to, for example, shear-thinning or heating within the seal chamber. Although not apparently of great importance for the lower viscosities, at higher viscosities the effects are more dramatic. As an example consider a 48 mm seal rotating at 1000 rpm in a liquid of viscosity 150 cS (Fig 7.13) where the regime is comfortably laminar. A reduction of viscosity by an order of magnitude (not a large amount in real terms) would, from Fig 7.11, cause the regime to become Taylor-vortex dominated.

### 8.1.2 Vapour Control

The test programme showed that the narrow radial clearance housing performed poorly compared with other housing types (Figs 8.1 and 8.2) and an independent flush to the seal face was required for satisfactory removal of gas or vapour from around the seal (Figs 8.3 and 8.4). This was particularly obvious with more viscous fluids (water/glycerol mixtures). As noted in Section 6.2.2, this has potentially serious consequences for the amount of frictional heat which can be dissipated. Furthermore, the choice of seal influenced the effectiveness of gas purging of the stuffing box and in this respect the two single-spring seals emerged as marginally better than the multi-spring or bellows seals. However, the best performance from the exposed single spring seal was only achieved by rotating it counter-clockwise so that it pumped fluid away from the seal face, enhancing the flush.

The performance of the narrow radial clearance housing was also sensitive to tangential flushing and the presence of a neck bush. In the case of the former, flushing against the direction of rotation was usually effective, although not noticeably better than radial injection. However, injection in the direction of rotation was generally ineffective. The presence of a neck bush, from the perspective of heat and gas removal, usually made matters worse.

Multi-port injection was helpful at higher speeds and certainly never resulted in any worsening of performance.

### 8.1.3 Solids Control

The narrow radial clearance housing was consistently unable to deal with solids suspended in water irrespective of size or density (Fig 6.6). Tests with sand resulted in such dense accumulations around the seal faces as to obscure them completely from view. Flushing would be essential for this housing if solids were present.

## 8.2 WIDE RADIAL CLEARANCE HOUSINGS

### 8.2.1 Flow Regimes

#### (i) Water

All housings are influenced by turbulence throughout the experimental speed range (10-5000 rpm). An interesting observation of all these housing was the apparent randomness of flow at low speeds which was replaced by a definite flow structure at a certain speed for each housing. Evidence of this was striking - air bubbles in the seal face groove were suddenly drawn out into orbit around the seal body. The same phenomenon had been noted on the narrow radial clearance housing, 48 mm seal on water at 600 rpm - a Taylor number of about  $10^6$  and effective Taylor number of about 2000 - the onset of turbulent vortices. Apparently, this phenomenon was also occurring at much higher Taylor numbers - when computed for the three housings, the Taylor numbers were in the range  $5 \times 10^8$  to  $5 \times 10^9$  (Fig 8.7).

Comparison of the observed results with the predictions in Table 7.1 appear to show a contradiction in each case. The model suggests high-speed vortex flow at the lower speeds which breaks down into homogenous turbulence at higher speeds typically  $> 1000$  rpm. The predicted transitional speeds give Taylor numbers in the range  $5 \times 10$  to  $5 \times 10^9$ . Moreover, the point at which transition is reached also corresponds in each case to a predicted effective Taylor number of between  $10^4$  and  $5 \times 10^4$  (see Figs 7.15, 7.19 and 7.20). It is tempting to draw an analogy with the breakdown of Taylor vortices at classical Taylor numbers of the same values. This is the point at which the turbulence viscosity analysis predicted an effective viscosity changes which dropped the effective Taylor number back into the vortex regime and predicts the high-speed or turbulent vortices. Could this flow system be the subject of a repeating vortex phenomenon or is it simply a quirk of seal geometry?

#### (ii) Higher Viscosities

Even at the highest viscosities tested, turbulence was a key influence at realistic mechanical seal operational speeds. As with the narrow radial clearance housing, a vortex-type of structure was a particular feature of the flow, although the same emulsification problem prevented close observation of the flow patterns at speeds in excess of 2000 rpm. Note especially the column for "High-Speed Vortices" and "Taylor Vortices" which encompass wide speed ranges for liquids of viscosity 15 to 150 mm<sup>2</sup>/s. The pre-dominance of vortex flow is predicted by the model, as shown in Table 7.1, which suggests that structured flow should be a dominant feature even at 5000 rpm. Unlike the narrow radial clearance housing, a significant change in viscosity is therefore unlikely to bring about a change in flow regime; this is potentially a desirable design advantage.

### 8.2.2 Vapour control

Generally, this housing performed better than the narrow radial clearance housing but not as well as the 45° housing (Figs 8.1 and 8.2). Within the speed range of 600-3000 rpm it appeared capable of running dead-ended (Fig 6.7 and 6.8) but was weak outside this range. When tests were carried out with 100mm seals running in the two wider

clearance housings, there appeared to be definite speed ranges within which the housings were successful at removing gas from the seal faces (Figs 8.5 and 8.6). For water, these ranges are shown in Figure 8.7. The lower ends of the ranges consistently corresponded to Taylor numbers in the region of  $5 \times 10^8$  to  $5 \times 10^9$ . Initially this obvious and repeatable regime change was unexplained. The analysis offers an explanation for this phenomenon; this is dealt with in sub-section 8.2.2.

Seal face injection was necessary at higher speeds ( $> 3000$  rpm) on water and for any speed when running with the glycerol/water solution. Injection was less effective for this housing than the narrow radial clearance housing, presumably due to increased radial clearance. This also would account for the complete ineffectiveness of tangential injection, either with or against the direction of rotation. Clearly, higher injection velocities would be needed to penetrate the radial clearance should this housing be used on a pump.

### 8.2.3 Solids Control

Fine solids could not be influenced by any means attempted. It was concluded that the turbulent mixing of the flow was generating a pseudo-homogeneous slurry. Presumably, the only way to keep the solids from the seal faces would be to use an external clean flush to the seal face.

When running with coarse solids it was necessary to include axial vortex modifiers for satisfactory dead-ended running (Fig 6.12) - although this compromised the vapour control ability of the housing. Without strakes in position, dense accumulations of solids were seen in the environs of the seal faces and just inside of the neck bush if fitted.

The reason for the unexpected accumulation of solids around the seal faces in the absence of a neck bush may be due to factors other than the toroidal vortex flow structure.

It is conceivable that the flow field around the rotating impeller could cause a large axial vortex in the seal chamber, as shown simplistically in Figure 8.8. Outward flow from the impeller might proceed along the chamber bore and return along the rotating seal. It has been widely reported that axial flows delay the onset of Taylor vortices although the precise reasoning is not fully understood. Coney and Summers (1979 (a)) review the work done on this effect, including their own, and their summary graph is reproduced in Figure 8.9.

If axial flow can have this effect on laminar vortices, it might be reasonable to presume that it could suppress turbulent vortex action. Clearly this is an area warranting further investigation. Moreover, the wider the radial clearance the stronger this effect is likely to be.

### 8.3 FLARED HOUSINGS

#### 8.3.1 12° Positively Flared Housing Housing 5

##### (i) Vapour control

The 12° positively flared housing was an improvement over the narrow radial clearance housing due to its ability to draw air from the seal faces into strong toroidal vortices over the seal rotor (Figs 6.14 and 6.15). It did not, however, offer enhanced gas handling performance over the wide radial clearance housing (Figs 8.1 to 8.4).

##### (ii) Solids control

With coarse solids the housing managed to cope reasonably well since the strong vortex located at the front part of the rotor appeared able to drag the particles into its orbit. This left the seal faces relatively clear. Such a strong vortex action could potentially be undesirable if, in the long run, it caused severe chamber erosion and perhaps cutting through the chamber wall completely - this has been reported by one company known to the author! With fine solids it did appear to be clearer at the seal face than in the rest of the chamber - this may simply have been due to the reduced radial clearance creating an illusion of clarity.

#### 8.3.2 12° Negatively Flared Housing (Housing 6)

This housing is not recommended as a potential design for a seal chamber owing to its poor gas handling ability.

Although its heat transfer abilities might have been acceptable in the absence of air due to the strong vortex flows, it was considered that its effective ability would be seriously limited by the presence of so much vapour.

As with the other 12° flared housing, the wide radial clearance housing would always be recommended in preference to this one.

#### 8.3.3 45° Positively Flared Housing (Housings 7 and 4-100)

The 45° positively flared housing emerged as the best of the designs tested in most situations and gave satisfactory dead-ended operation.

##### (i) Vapour control

Gas purging around the seal was very good at all speeds when running dead-ended on water and performance was independent of seal design (Fig 6.19). Gas removal with higher viscosities (glycerol/water mixtures) was less effective and a flush to the seal face was required. Although the fitting of a neck bush impaired the gas purging capabilities of this housing, performance was still superior to narrow radial clearance housing. A recommended improvement would be to vent the housing behind the seal either through a port or into the pump volute.

**(ii) Solids control**

When running with solids in suspension, it was necessary to use axial vortex modifiers in the seal chamber (Fig 6.24). The highly structured vortex flow, which was probably the reason for the efficient air removal, unfortunately concentrated solids around the seal faces (Fig 6.22); hence the need for disrupting this process. Although effective for coarse solids, it was not possible to remove fine particles from the seal chamber without a flush to the seal face. The centrifugal forces acting on the small particles were apparently outweighed by turbulent mixing.



---

**CHAPTER 9.**

---

**DESIGN STUDY -**

**EFFECT OF CHAMBER DESIGN ON SEAL INSTABILITY**

## 9.1 INTRODUCTION

It is well known that, at sufficiently high temperatures, a mechanical seal can become 'unstable' and leak intermittent "puffs" of vapour. This phenomenon has been applied by various workers, including Lymer (1969), to define a temperature-margin ( $\Delta T$ ). More recently a technique has been developed for establishing the of seals required for Main Oil Line Pumps where water in the crude oil was causing vaporisation damage to the seals, as reported by Dolan, Morrison & Watkins (1987).

The parameter is the difference between the temperature at SVP and the bulk fluid temperature at which vaporisation or instability occurs at the seal face. A seal operating with a required  $\Delta T$  of zero would be able to run stably up to the SVP curve for the product; this never happens in practice owing to the heat generated at the sealing interface. For most seals,  $\Delta T$  required is quite large and tends to rise with increasing pressure (Fig 9.1). Past workers have used  $\Delta T$  as a test of seal design -a good design will tend to run with a minimum amount of heat generation and, therefore, a small  $\Delta T$  is required. However,  $\Delta T$  is also affected indirectly by the effectiveness with which heat is removed from the seal.

The experimental work reported in the previous chapters has shown that housing design has an important bearing upon the existence or otherwise of gas and vapour in the seal chamber, thereby reducing, sometimes drastically, the seal area available for heat transfer. Given this, it would seem reasonable to suggest that a "poor" housing with large accumulations of gas will require a larger  $\Delta T$  than a "good" housing which keeps gas away from the seal.

Therefore, to assess the findings of the seal housing study, temperature-margin tests were run for two different housing geometries. Should the variations in heat transfer efficiency due to the gas handling abilities of the two housing designs be of practical significance, these would translate into an improved temperature-margin performance for the seal.

## 9.2 TEST APPARATUS

A general view of the test apparatus is shown in Figure 9.2. The layout is given in Figure 9.3, and details of the rig circuit and instability measurement facilities in Figure 9.4. Detailed discussions were held with the authors of Dolan, Harrison & Watkins, and the test rig design was based on their experience.

Key details of the rig were as follows:

Drive:-

Variable speed drive, 500-3000 rev/min, AC motor with TASC unit, Torque meter in drive line to test housing

Fluid circuit:-

Closed circuit, rated for 30 bar operation with:

positive displacement circulating pump - 5 litres/min  
static pressure control from air-hydropump  
heater and cooling  
pressure gauge  
thermocouple

Instability monitoring:

A 'leakage collection chamber' was fitted outboard of each seal. This comprised a top hat enclosing the shaft at the non-drive end and a chamber closed by a dry-running lip seal on the drive end of the rig.

Each chamber had two outlets. The leakage outlet had a 3mm orifice venting to a measuring cylinder for leakage collection. The upper port fed to a sensitive pressure transducer (0.1 bar fsd). A pressure limiter was fitted between the chamber and transducer to protect the transducer in the event of sudden seal failure. Similarly, a pressure switch to stop and depressurise the rig was connected to the seal leakage chamber.

Additional thermocouples were fitted:-

- (a) in the seal chamber as close as practicable to the seal faces, to measure fluid temperature in the immediate locality of the seal.
- (b) in contact with the rear face of seal stator
- (c) near the "impeller", providing a measure of pumped product temperature.

The housing geometry was varied by provision of alternative insert arrangements. Housings were selected for the tests on the basis of representing the "best" and "worst" in light of the results of flow visualisation studies. They were:

- (i) 45° flare with parallel section without neck bush, believed to be a "good" design.

- (ii) Parallel housing with narrow clearance, radial clearance approximately 2mm, corresponding to the current DIN/ISO housing, in this case with a neck bush fitted. This was believed to be a "poor" design.

The two housing arrangements are shown schematically in Figure 9.5. Both arrangements were run dead-ended.

The seal selected was a metal bellows design, with rotating bellows and carbon-v-Ni-resist faces (Seal D). This seal was chosen as it was the only balanced seal available from the housing tests and would fit directly to the shaft without a step.

### 9.3 TEST METHOD

The procedure for each test was as follows:-

- (i) Set the circuit pressure at one of 5, 8 or 16 bars absolute
- (ii) Set the water temperature at about 80°C
- (iii) Run the motor to set speed
- (iv) Allow the rig to stabilise for 15 minutes
- (v) Increase water temperature slowly, 1 to 2°C per minute
- (vi) Note the onset of intermittent instability
- (vii) Note the onset of continuous instability
- (viii) Switch off heaters and allow water to cool slowly
- (ix) After cooling back to 80°C allow rig to run for 15 minutes before commencing next test.

It was noted that any rapid variations in speed, pressure or temperature could cause erratic seal behaviour; hence the need for a carefully controlled procedure.

#### 9.4 RESULTS

The results for the 45° flared housing are shown in Figure 9.6, and for the parallel housing with neck bush in Figure 9.7.

For the 45° housing the housing temperature and product temperature are coincident, indicating effective circulation of fluid around the seal and into the product. But for the parallel housing the housing fluid temperature was significantly higher than the product, 20°C differential at 16 bar, adversely affecting the available temperature-margin. Thus, the parallel housing is significantly worse than the 45° housing.

It is interesting that two seal failures occurred during the tests on the parallel housing, and it may be significant that the main housing study showed that this housing had a distinct tendency to retain vapour.

## 9.5 CONCLUSIONS

This design study has demonstrated that the temperature-margin of the seal can be significantly affected by housing design. It also provides support for the findings of the seal housing study and emphasises that a good design of seal chamber can make the difference between seal failure and survival. In the longer term, the temperature-margin test could be used to carry out further investigations of the efficiency of seal housings under conditions more representative of actual practice than are possible on the flow visualisation rig.

---

**CHAPTER 10.**

---

**CASE STUDY -**

**SEAL CHAMBER DESIGN FOR A SLURRY SEAL.**



## 10.1 INTRODUCTION

A slurry seal test programme provided the opportunity to investigate the effects of housing design and seal performance with clay and chalk slurries. The programme reproduced typical slurry handling pump operating conditions.

In the past, clay slurries pumps have been sealed with gland packing which required an external clean flush. The impellers were often fitted with back-vanes which create a low pressure region at the throat of the stuffing box. This tends to draw clean flush liquid through the packed gland and thereby providing lubrication, reducing heat build-up and removing solid particles. However, packed glands have two major drawbacks on this duty: firstly they wear out very quickly and, secondly, the obligatory flush dilutes the slurry. On one plant known to the author, these effects were serious: packed glands had to be changed once a week (this was always in overtime) and the water content of the clay slurry, which had to be maintained to within one per cent, was difficult to control.

An unflushed mechanical seal lasting about a year would return major cost savings in the long run even though the seal itself would be fairly costly. However, the duty is very severe as the seal must (among other requirements):

- (i) Have a hard/hard face combination for wear resistance. As has been noted, two highly intolerant face materials require very careful face presentation and lubrication for effective sealing without destroying each other.
- (ii) Be lubricated by water containing fine solids which will inevitably penetrate the seal interface. A copious intrinsic supply of the water phase to the seal is essential. Slurry de-watering in or near the interface is probably likely to result in rapid failure.

The aim of the programme was to find ways to control the environment to ensure that both the above conditions were met.

## 10.2 TEST EQUIPMENT

### 10.2.1 BHRA Large Slurry Pipe Facility

The tests were carried out at BHRA using the large slurry pumping test facility. The facility comprised an 80 m long closed pipe loop of pipe inside diameter 200 mm (Fig 10.1). The reservoir of 4500 litres gave a maximum static head to the loop of 4.5 metres. The pump was a Warman 6x4-EAH slurry pump (Fig 10.2) driven by a 250 kW AC motor through Fluidrive fluid coupling (Fig 10.3).

In the course of the experiments it was necessary to install a water spray cooling system on the pipework to control slurry temperature. Additional slurry transfer tanks were built adjacent to the pump-house.

### 10.2.2 Rig Control

The motor starter was fitted with a programmable automatic timer to permit 24-hour running including start/stop cycle comprising 2-hour runs interspersed with 10, 20 and 30 min stops as per the timetable given in Table 10.1.

The rig was designed to trip in the event of:

- (a) gross loss of slurry - low level switch in tank
- (b) excessive seal face temperature - relays from chart recorder
- (c) chart recorder/face thermocouple mal-function

### 10.2.3 Instrumentation

The test facility was equipped with the following instrumentation:

- (a) Electronic transducers to indicate:
  - shaft rotational speed
  - suction pressure
  - seal cavity pressure
  - discharge pressure
  - bulk slurry temperature (in tank)
  - suction temperature
  - discharge temperature
  - seal cavity temperature (x 2)
  - seal face temperature (x 2)
  - ambient temperature
  - outboard bearing temperature
  - inboard bearing temperature
  - liquid flowrate
- (b) Mechanical transducers to indicate:
  - suction pressure
  - seal cavity pressure
  - discharge pressure
  - return-line pressure
  - motor current

- power consumption
- leakage

Seal face thermocouples were installed (Fig 10.4) and overlaid with heavy duty tape to protect them from damage.

Outputs from electronic transducers were logged continuously during tests.

#### 10.2.4 Data-Logging

A 32-channel programmable chart recorder was used for monitoring all tests and controlling the seal face over-temperature relays. The maximum scan rate was 2 seconds. A UV recorder was employed on selected tests to analyse transients generated by starts and stops.

Set-up parameters, eg seal reference number, installation and adjustment, suction pressure, impeller type, etc were recorded on the "Seal test data sheet" (Table 10.2) and manual checks of test readings recorded on the "Seal test log sheet" (Table 10.3).

#### 10.2.5 Test Fluid

The test fluid was clay slurry taken directly from the quarry process line and transported by tanker to BHRA.

In production, the water content of the slurry was controlled 30-31% by volume. The slurry was highly non-Newtonian and contained a high proportion of very fine solids, shown by the particle counts listed in Table 10.4. Some degradation was noticed after 100 hours testing although this was not considered to be serious. The slurry in the pipe-loop was replaced after each 100 hour test.

#### 10.2.6 Inspection Facilities

The seal inspection facilities employed were as follows:

- Optical microscope
  - Up to 40x magnification. Photomicrography
- Optical flat
  - Pre and post test flatness checks
- Talyrond
  - Measurements of circumferential waviness
- Cranfield Precision Engineering Ltd: Ultra Precision Laboratory
  - Radial wear profiles

### 10.3 EXPERIMENTAL WORK

#### 10.3.1 Test Variables

A schematic drawing of the standard seal installation is shown in Fig 10.5. The following versions of impeller and seal housing were tested.

##### (i) Impellers

- (a) as new, 100% back-vanes
- (b) 50% back-vanes
- (c) no back-vanes

##### (ii) Housings

- (a) standard seal cover
- (b) modified seal cover, flare angle 45°, four axial strakes (Fig 10.6). This housing was based directly on the recommendations of the experimental work which forms the basis of this thesis.

##### (iii) Seal Face Materials

The following face materials were investigated:

- (a) reaction-bonded silicon carbide
- (b) tungsten carbide (nickel bound)
- (c) carbonised silicon carbide
- (d) siliconised carbon
- (e) alpha-sintered silicon carbide

#### 10.3.2 Test Procedure

The standard test procedure was as follows:

- (i) Pre-test checks made of face condition, flatness and waviness
- (ii) Seal installed in carrier and instrumented
- (iii) Seal installed
- (iv) Instrumentation checked
- (v) Suction valve opened
- (vi) Static pressure readings checked
- (vii) Set-up data recorded
- (viii) Test started
- (ix) Seal run in
- (x) Test run as timetable (Table 10.1) unless seal failed (ie over temperature or excessive leakage)
- (xi) 1st suction pressure reduction after 24 hours to -0.12 bar g
- (xii) 2nd suction pressure reduction after 48 hours to -0.25 bar g
- (xiii) 3rd suction pressure reduction after 72 hours to -0.37 bar g
- (xiv) Test stopped after 96 hours
- (xv) Seal removed
- (xvi) Post-test inspection of face condition, flatness, waviness radial wear and general seal condition

## 10.4 RESULTS

Post-test photographs of the seals are shown in Figs 10.7 to 10.21, and radial wear profiles in Figs 10.22 to 10.33.

### 10.4.1 Seal Design

Tests on the existing standard installation produced failures characterized by severe cracking and scuffing of the faces, and face temperatures in excess of 220°C (Fig 10.31). This was indicative of poor housing heat transfer. Observation of seal performance highlighted the critical dependence of housing design on efficient heat transfer. Seal 1 was run through the high temperature period to near total destruction (Fig 10.7) and its post-test condition was similar to field failures on the same duty. Despite the poor condition of the seal, leakage was only evident at start-up and shut-down and amounted to a few gallons on each occasion. There was no static or steady-state dynamic leakage; this was attributed to the highly non-Newtonian nature of the slurry!

Although Seal 2 was set at zero axial face load, the test had to be stopped after 20 hours due to very high face temperatures (Fig 10.32). This phenomenon was quite commonly observed on site. The most plausible explanation attributed it to vacuum conditions at the seal generated by the impeller back-vanes. The radial micro-cracking evident on both faces (Fig 10.8) was the first sign of material distress, ultimately developing into the type of failure seen in Seal 1.

Changing to tungsten carbide faces (Seal 6) appeared at first to have helped matters by reducing the steady-state seal temperature rise  $\Delta T$ . However, the negative cavity pressures and consequent loss of interface lubrication caused the test to be terminated due to overheating, (Fig 10.33). Again, thermal stress cracking and scuffing were evident (Fig 10.12).

### 10.4.2 Impeller Design

Tests with the standard seal installation suggested that the negative pressures seen at the seal were caused by the impeller back-vanes; since these back-vanes were designed originally to draw flushing water through a packed gland, this was to be expected. Two experimental impellers were therefore tested, with 50% and 100% of the back-vanes removed respectively.

#### (i) 50% Back-Vanes Removed

Seal 5, running with the 50% back-vane impeller, performed similarly to the normal impeller, that is negative cavity pressures and zero axial loading. The test ran for 50 hours at a low steady-state  $\Delta T$  but then overheated suddenly for no apparent reason (Fig 10.34). Heat checking and scuffing were evident (Fig 10.11). Post-test face waviness was between 8 and 9.5  $\mu\text{m}$  peak-to-peak for the rotor and stator respectively.

For both impellers with back-vanes it was probable that axial impeller setting, and hence clearance between the back-vanes and the liner, would influence cavity pressure and recirculation.

## (ii) 100% Back-Vanes Removed

The common features with this impeller, which became the standard for all subsequent tests, were the high cavity pressures and increased hydraulic face loading.

Seals 3 and 4 ran at noticeably higher steady-state  $\Delta T$  values than previously noted. In the case of Seal 3, this resulted in heavy face wear and scuffing (Fig 10.9) but Seal 4, by contrast, experienced light scuffing (Fig 10.10) and completed the four-day test. However, high temperature unstable running was a feature of these tests (Figs 10.35 and 10.36).

As before, substituting tungsten carbide (Seal 7) for silicon carbide faces resulted in unsatisfactory running and failure due to over-temperature (Fig 10.37) of the faces causing severe heat checking. The appearance of these faces and their wear profiles indicated that the faces were running convergently, ie. contacting on the inner half of the interface (Fig 10.13). The outer halves of the interface appeared to have suffered abrasive 3-body wear. This pattern was typical of most of the test seals.

### 10.4.3 Seal Chamber Design

It was considered that the existing seal chamber design might impair an adequate supply of cool liquid from reaching the faces to remove heat and provide interface lubrication. The experimental work described in the preceding chapters concluded that heat transfer from mechanical seals is better with an open, 45° flared chamber. When running with solids it was also found beneficial to run with axial vortex modifiers or strakes, as these prevented accumulation of solids around the seal faces and helped to avoid localised erosion due to vortex action. Tests were therefore run with a modified seal chamber design.

The first tests were run with a 45° housing and tungsten carbide faces (Seal 8) providing a direct comparison with the runs on Seal 7. The cavity pressures were found to be very much higher. Owing to high slurry temperature, the seal ran hot (80-90°C at the face thermocouple position) (Fig 10.38) but without perceivable distress, and completed a run of 105 hours. However, the inner halves of the seal faces were found to be very highly polished and heat checked (Fig 10.14).

Seal 9 ran stably with low  $\Delta T$  (Fig 10.39), and completed the full 4-day test (despite problems with impeller blockages). Moreover, the faces were in good condition and there was no heat-checking (Fig 10.15). As a result the 45° cavity was accepted as the standard for the remaining tests.

As expected, some increased erosion of the seal cover was noted, more especially around the strakes (Fig 10.40) but this was not considered to be too serious.

### 10.4.4 Seal Face Materials

Seal 11, running with siliconized carbon faces, failed in infancy owing to material incompatibility (Fig 10.17). Seal 10, fitted with carbon-impregnated silicon carbide faces, ran well with very low  $\Delta T$  and stable face temperatures (Fig 10.41). Post-test inspection revealed that all the surface carbon particles had been stripped out from the SiC matrix.

Seal 12 was run with alpha-sintered silicon carbide faces. The seal faces ran hot, though stably, (Fig 10.42); this may be a feature of the tribology of the material. After an extended reduced suction test, the faces appeared to be in good condition apart from some inner edge chipping. Neither the 100 hr endurance test, run at high discharge and cavity pressure, nor the two starved suction tests caused the seal distress. This is quite surprising when, for much of the endurance test, the face temperatures were around 100°C. During the starved suction tests, the face temperature rose to 150°C, with severe thermal shock occurring on re-opening of the suction valve (Fig 10.43). It was also encouraging that the post-test flatness of the two faces was good (2.0 and 3.2  $\mu\text{m}$  ptp stator and rotor respectively). A concern was the chipping on the inner edge of both faces. Between the mid-test inspection (Fig 10.18), after the reducing-suction procedure, and the final inspection, following the endurance and starved-suction tests (Fig 10.19), this chipping had grown where it was already present and established itself in new areas. This had no discernible effect on seal performance but it was undesirable, threatening the long-term integrity of the sealing interface.

## 10.5 CONCLUSIONS

- (i) The standard sealing configuration suffered infant mortality owing to overheating and poor lubrication at the sealing interface.
- (ii) The impeller back-vanes subjected the seal to vacuum conditions. Removal of the back-vanes allowed positive seal cavity pressures to be maintained under all but starved-suction conditions.
- (iii) The 45° flared housing gave higher cavity pressures and noticeably better heat transfer and interface lubrication. This was evident from the much improved face temperature stability under even the most arduous conditions. Some increased erosion was noted but was not considered to be serious. This adds considerable credence to the results of the experimental work on which it was based.
- (iv) The alpha sintered silicon carbide faces were capable of running under arduous conditions without distress, apart from edge chipping at the inner diameter.
- (v) The revised sealing arrangement incorporating the features outlined in (ii) to (iv), ran well. It exhibited good stability with zero leakage even under arduous and adverse conditions.



-----

**CHAPTER 11.**

-----

**CONCLUSIONS**

## 11.1 ECONOMIC CONSIDERATIONS

Mechanical seal failure is by far the commonest cause of pump down-time and hence the largest single source of maintenance cost on rotating machinery in the process industry. Although some failures are infantile and may be explained relatively easily, a significant proportion are random mid-life failures. Random mid-life failures are difficult to explain but many appear to have suffered thermal distress.

The cost benefit analysis carried out on seal failure data suggested that the pay-back time for reducing the incidence of mid-life mechanical seal failures would be short, typically 12 months or less. Even the most drastic solution to the problem, total pump replacement, was shown often to be a viable option, even for moderately troublesome pumps.

The problem of retro-fitting new housing design to pumps where radial space was a problem could be overcome in many cases by adopting a system of bolt-on cartridges comprising a seal assembled by the manufacturer in an optimized housing. Despite the extra initial cost to the user the payback period would probably be short on pumps where the mean time between seal failures was less than two years.

The current standards covering the design of seal chambers are shown to be inadequate and probably contribute directly or indirectly to unnecessary seal failures. Evidence of this has come from the results of the Design Study, Chapter 9. However, the drawing up of realistic seal chamber standards has been severely hampered by a lack of reliable experimental data. One important product of the work reported in this thesis has been a set of housing design guidelines - these are described in Chapter 13 as a corollary to the research. It is planned that these guidelines will eventually form a major input to the revised ISO 3069 standard.

## 11.2 HOUSING DESIGN

The method of measuring heat transfer direct by flush-mounting hot-film anemometer probes on mechanical seals was an innovation. Although the probes were difficult to operate and calibrate, they nevertheless yielded data which represented a considerable leap forward in the science of seal design. Previous expressions for heat transfer were based on experiments carried out with smooth, long cylinders - no account had been taken of the vagaries of seal geometry and end effects.

The narrow radial clearance housing, as defined or admitted by all the current standards, was consistently a poor performer. In particular it was prone to gas or solids choking and exhibited poor heat removal ability. The lack of radial space obviously can force seal designers into unsatisfactory compromises. Dead-ended running with these housings is not advised - a flush is considered essential to ensure satisfactory performance. The design study showed that the narrow radial clearance housing could fail to prevent seal failures under marginal conditions.

Enlarging the radial clearance is of great benefit in some cases - especially with water and air at lower speeds. At higher speeds good running can only be ensured under carefully controlled conditions where turbulent vortices dominate the flow regime; simply giving the seal more space is not a universal panacea. Where coarse solids are present in reasonable quantities, then axial strakes are an effective means of keeping them away from the seal interface. Strakes do not destroy the vortices but move them axially - hence seal chamber erosion is spread over a larger area and not concentrated in one place.

The 45° flared housing creates flow conditions in which heat transfer and removal of gas, vapour and solids are considerably enhanced over the other housing designs tested. Of the housing designs tested, this one was by far the most appropriate as a mechanical seal chamber. In many cases, the 45° housing can operate dead-ended where other chambers would require flushing. The performance of the 45° housing is independent of seal design, unlike the narrow clearance housing. Further confirmation of the suitability of this housing was obtained in the Case Study, Chapter 10, where the design was successfully employed on a very difficult application.

### 11.3 ANALYSIS

The observations of fluid flow within the seal chambers produced some surprising results - in particular, the discovery of highly structured flow under conditions where homogeneous turbulence might be expected. The formation of vortices was known to be confined to a fairly well defined range of Taylor number. In the turbulent vortex regime where inertial forces are dominant, it was proposed that turbulence viscosity was increasing the effective viscosity sufficiently to reduce the Taylor number into the prescribed vortex range. An analysis of turbulence viscosity for a rotating annular flow was constructed using a modified Prandtl-mixing length theorem and "effective Taylor numbers" were calculated.

For all the housing geometries tested the effective Taylor numbers for the conditions of turbulent vortices were invariably in the range  $10^2$  to  $10^4$ . Conversely, no structure was detectable when the effective Taylor number fell below this range. These observations lend support to the hypothesis.

At very high Taylor numbers (about  $10^9$ ) a definite flow transition was observed - at this point the effective Taylor number was invariably in excess of the  $10^4$  limit of the vortex regime. Whilst it is tempting to speculate upon the reasons for this repeating flow phenomenon, the level of analysis possible within the constraints of the current work did not permit a more detailed study.

---

**CHAPTER 12.**

---

**RECOMMENDATIONS FOR FUTURE WORK**

## 12.1 HOUSING DESIGN

- (i) It is not known whether a 45° straight flare is, in fact, the optimum solution, although it was clearly better than the 12° straight flare. Further refinement may be possible, for example by adopting different flare angles, or shapes.
- (ii) Only one port size has been used during this study. It is not known whether effective seal flushing depends on volumetric flowrate or injection velocity.
- (iii) There is a conflict between effective gas and solids removal; gas purging is possible through strong vortex action, but solids removal is better in the absence of strong vortices. Where both gas and solids are present in a system, the study has not been able to suggest a satisfactory compromise for dead-ended running.
- (iv) Glycerol/water mixtures emulsify in the housing at about 2000 rpm, making visualisation difficult thereafter. Above 2000 rpm the seal chamber temperature rose quite sharply due to an increase in churning losses. It is unclear whether this is due to the physical nature of the emulsion or an increase in the effective viscosity.
- (v) The optimum housing designs require extra space around the seal. Where the casing around the seal chamber is already thin or water-jacketed, then one solution may be to opt for complete bolt-on seal/housing cartridges. The design of these merits investigation.
- (vi) Increasing the turbulence intensity within the seal chamber promotes increased churning losses and heat generation of itself, particularly in more viscous liquids. There must, therefore, be some compromise whereby low heat generation may be obtained without sacrificing good convective heat transfer from the seal.
- (vii) Efficient gas removal and good heat transfer ability appear to coincide well despite the difficulties associated with quantifying the latter. With the added expense of measuring heat transfer using the hot-film probes in mind, it seems inadvisable to recommend this technique to subsequent researchers. A more realistic and practical solution to the problem is to infer the heat transfer ability of a housing design using thermal stability tests of the type described in the Design Study (Chapter 9).
- (viii) The "impeller" used in the experimental work was a plain disc. The interaction between the flow around the disc and flow in the seal chamber are evidently coupled for the more open housings in ways which are not fully understood. Moreover, in a real pump the impeller would generate a rather more complex flow. A study of these would be a logical development.

## 12.2 ANALYSIS

The constraints imposed by the test requirements for the reported work did not permit the undertaking of a complex and sophisticated analysis of the observed flow phenomena. The Prandtl mixing-length analysis was justifiably used to give a first approximation but is limited in application. It did, however, prove a very useful pointer to further developments and allowed the potential effects of turbulence viscosity on flow regime to be investigated. A more sophisticated analysis is warranted, based probably on a two-equation model using a good computational fluid dynamics package.

A good and validated model of the flow in a seal chamber would be of benefit to the mechanical seal designer and would provide good quality boundary conditions for finite element models of the actual seal.

---

**CHAPTER 13.**

---

**COROLLARY**

**THE DEVELOPMENT OF A FUNCTIONAL DESIGN STANDARD FOR  
MECHANICAL SEAL CHAMBERS**



### 13.1 INTRODUCTION

The existing standards reviewed in Chapter 2 give very little guidance on the design of the chamber for a mechanical seal. It was noted that many seal users, seal manufacturers and pump manufacturers are looking for purpose-designed seal chambers, and an end to the restrictiveness of the current standards.

The area of mechanical seal-related standards is increasingly coming under scrutiny, as highlighted by Barnes, Flitney and Nau (1990). The British Standards Institution (BSI) has recently established The Mechanical Seals Standards Committee (MCE 6/4) with the task of updating and upgrading relevant standards. A working group (MCE 6/4/2), which includes representatives from BHRA, has also been set up by the Committee to look specifically at ISO 3069. ISO 3069 is overdue for revision and the UK has been invited to table a revised proposal incorporating the best available current knowledge. The working group has completed its draft revision which is to be submitted to the Committee in November 1990.

The best available current knowledge has been gathered from several sources but a major input stems from the results of the work described in this thesis. As a first step towards the creation of a new standard, the salient design information from the thesis has been collated as a "Mechanical Seal Housing Design Guide" (Appendix H). This has been written to be directly applicable to people in industry needing to optimise seal chamber design. It attempts to be easy-to-use without being over-compromising and, therefore, presents in its main text the minimum information required to gain the optimum solution for a given duty.

An explanation of the origins of the document is given in the following text.

## 13.2 RECOMMENDED PRACTICE

### 13.2.1 Introduction

From results of the work reported in this thesis there is little doubt that the 45° positively flared housing is the best available technology. However, as has been noted, there are occasions when modifications to the basic design are required for optimum performance. Although the chamber design allows dead-ended running under many conditions, it is also necessary to know when modifications are advisable. The exact configuration for a given situation depends on heat transfer, gas or vapour purging, and solids handling requirements. These are considered in turn below and summarised in Table 13.1.

### 13.2.2 Heat Transfer

The user of the Guide is asked to fill in the Duty Specification Table shown in Table 13.2; this contains all the information necessary for ascertaining the optimum housing geometry. In all cases fluid properties refer to the bulk conditions, as local conditions are unlikely to be known.

The analysis of heat transfer within the seal chamber may be treated as a heat balance system. A finite amount of heat is generated by the seal at the interface due to high film shear and asperity contact. This heat must be shed at a rate in excess of the rate of generation if the chamber temperature is to remain at its desired level. As shown in Chapter 9, increasing the chamber temperature reduced  $\Delta T$  (which is often quite small on many volatile liquids) may lead to seal instability and possibly failure.

In a well-designed seal chamber the work reported in this thesis has demonstrated that heat generated at the seal can often be carried away to the pump casing, due purely to the forced convection caused by the flow-type intrinsic to that chamber design. In a poorly designed chamber - where gas choking is a problem - this intrinsic cooling, due to forced convection, is insufficient to keep pace with the generated heat. Additional cooling is required from an external cool flush applied at the seal face, to carry the heat down the seal chamber into the bulk fluid.

#### (i) Frictional power generation at seal

Seal interface friction is notoriously difficult to measure reliably and even more difficult to predict. Flitney & Nau (1989) report large amounts of scatter on their friction data even under well controlled laboratory conditions. Other workers have also published similar friction data. When plotted against a dimensionless number, the duty parameter (G), Nau (1987) illustrated the scatter graphically as shown in Figure 13.1. The average line of best fit yields the following expression for frictional power generation:

$$H_s = 6.1 \times 10^{-4} p_f^{0.67} d^{1.8} N^{0.8} \quad (13.1)$$

For the purposes of the Design Guide, it was necessary to be more conservative for circumstances where the actual frictional power was not known and choose an expression below which most friction data fell. The line chosen is shown in Figure 13.1 and is described by the following expression.

$$H_s = 2.44 \times 10^{-3} p_f^{0.67} d^{1.8} N^{0.8} \quad (13.2)$$

**(ii) Power dissipation due to forced convection**

From the heat transfer measurements reported and discussed in the foregoing chapters it was possible to extract a general expression for heat transfer coefficient as a function of peripheral Reynold's number, (equation 6.1):

$$h = 141 \text{ Re}^{0.5}$$

Now the heat flowrate ( $\dot{q}$ ) from the seal to the bulk liquid due to forced convection is given by:-

$$\dot{q} = hA (T_s - T_c) \quad (13.3)$$

where  $(T_s - T_c)$  is the temperature difference between the seal surface and the seal chamber.

From experience, this temperature differential may be taken to be  $5^\circ\text{C}$  as a starting value. Evidence of this may be found in the site measurements reported by Barnes, Flitney and Nau (1989) and Flitney & Nau (1989) in their laboratory tests on seal instability.

By substituting in equation 13.3 for  $h$ ,  $A$  and  $(T_s - T_c)$  yields:-

$$\dot{q} = 1.1 \times 10^3 d^2 l^{1.0} \omega^{-0.5} v^{-0.5} \quad (13.4)$$

For ease of use, equation 13.4 may be converted into the units given in Table 13.2:-

$$\dot{q} = 3.56 \times 10^{-7} d^2 l^{1.0} N^{0.5} v^{-0.5} \quad (13.5)$$

[ $d$ ,  $l$  and  $l$  in mm,  $N$  in rpm,  $v$  in  $\text{mm}^2/\text{s}$ ]

**(iii) Power dissipation due to external flushing**

Consider the diagrammatic representation of a seal chamber shown in Figure 13.2. From the Second Law of Thermodynamics, the rate of heat removal due to the external flush ( $q_f$ ) is given by:-

$$\dot{q}_f = \rho Q c_p (T_c - T_f) \quad (13.6)$$

Typically, the temperature difference between the seal chamber and bulk fluid is taken as  $25^\circ\text{C}$  (see for example "Mechanical Seal Practice for Improved Performance",

Chapter 1 (ed. Summers-Smith)). This seems rather high - a more sensible design objective should be 5°C to encourage good running. Moreover, a high value of  $(T_c - T_f)$  might create an over - optimistic impression of available heat removal due to the flush.

Substituting for  $(T_c - T_f)$  in equation 13.6 and also putting the flowrate,  $Q$ , in litres/minute gives:-

$$\dot{q} = 8.33 \times 10^{-5} \rho Q c_p \quad (13.7)$$

#### (iv) Heat transfer ratios

To determine the heat balance for the system, two ratios can be formed:-

Surface Transfer Ratio (STR) =  $\frac{\text{Heat removal due to forced convection}}{\text{Heat generated by seal}}$

$$= \frac{\dot{q}}{H_s} \quad (13.8)$$

and

Flushed Transfer Ratio (FTR) =  $\frac{\text{Heat removal due to external flush}}{\text{Heat generated by seal}}$

$$= \frac{\dot{q}_f}{H_c} \quad (13.9)$$

It is interesting to note that the radial clearance,  $b$ , does not exert a strong influence over  $q$  and, hence, STR. This is probably a correct inference since the heat transfer at the surface of the rotating inner cylinder is a function of shear in the turbulent boundary layer. However, the choice of radial clearance may be an important variable in determining the behaviour of gas or vapour in the chamber. Large amounts of gas in the critical heat transfer region at the seal could dramatically reduce the effective seal chamber length,  $l$ .

#### (v) Use of heat transfer ratios.

To avoid the temperature of the seal chamber rising, the value of the initial Surface Transfer Ratio should be greater than unity. If STR is less than or equal to one, then additional cooling from an external flush is advisable.

If the flowrate is not known, then its minimum value ( $Q_{\min}$ ) can be computed by re-arrangement of equation 13.7.

### 13.2.3 Control of Gas and Vapour

The Duty Specification Table (Table 13.3) asks whether gas or vapour are likely to be present in the seal chamber. In practice, it is wise to assume that they will be present at some point even in duties where the temperature margin is quite large. Gas may well be trapped in the chamber due to poor venting at start-up, or a process upset could cause momentary de-priming of the pump.

The Recommended Practice is to use the 45° flared housing without a neck bush in all cases. This housing has shown itself to be consistently superior to the other designs tested, particularly when handling gas or vapour. The ability to remove gas or vapour from the seal environs into the bulk fluid is intrinsic to the housing design - no external flush is usually required to accomplish this task. A flush is, however, advised for high viscosity fluids. If a neck bush must be used (ie. required by company practice), then care should be taken to vent the chamber properly on start-up.

### 13.2.4 Control of Solids

The recommendations made are based on the best available information set forth in the thesis. It has been shown that a plain 45° flared housing requires modification in the form of axial strakes (Fig 13.3) to keep coarse solids from accumulating at the throat of the housing. Strong vortex flow, beneficial in handling gas or vapour, may present a problem with coarse solids by concentrating erosive wear in a particular part (or parts) of the chamber wall. Strakes are beneficial as they disrupt the vortices, causing them to "corkscrew", and spreading the erosion over a wider area.

Where gas or vapour is likely to be a real problem, helical strakes should be used - the suggested arrangement is shown in Figure 13.4.

Fine solids present a difficult problem if present in large quantities (> 10% by volume) as they appear to form a pseudo-homogeneous slurry due to the intense turbulent agitation. Vortex flows and centrifugal force have no visible effects on these fluids. The only solution for guaranteeing their absence of the seal face is to use a clean external flush.

### **13.3 ALTERNATIVE PRACTICE**

#### **13.3.1 Introduction**

The Recommended Practice is mainly targeted at new pump designs. Retro-fitting to existing pumps may be possible, but many pumps will not have sufficient radial wall thickness around the stuffing box to fit a recommended 45° flared seal chamber. Where this chamber cannot be used, the next best (but less effective) alternative is to use a cylindrical housing with a radial clearance tailored to give strong vortex flow (laminar or turbulent).

The suggested ranges of Taylor number for strong vortex flow are based directly on the results reported and discussed in the thesis. The modes of operating these housings are summarised in Table 13.3.

#### **13.3.2 Heat Transfer**

Heat transfer considerations may be approached in the same way as for the 45° flared housing. Hence, the Heat Transfer Ratios should be computed and used in exactly the same way as outlined in section 13.2.2. The choice of radial clearance does not greatly affect the heat balance but will become more important when considering gas and vapour handling.

#### **13.3.3 Control of Gas and Vapour**

Narrow radial clearance housings have been shown to be very poor handlers of gas in many of the tests carried out; this is particularly noticeable with more viscous liquids. The problem of "gas choking" is certain to place the seal under severe distress and must be avoided. Obviously, an external flush could be used, but under quite a number of tests with the wide radial clearance housings it was found that dead-ended running without a neck-bush gave satisfactory performance, providing the speed was not too high. The Guide therefore suggests that a cylindrical housing with a wide radial clearance around the seal (> 10 mm) can be run dead-ended, subject to adequate heat transfer, under the constraints of Table 13.3. If radial space restricts the radial clearance then the seal should be flushed.

#### **13.3.4 Control of Solids**

Generally, the same rules apply to the wide radial clearance housing as to the 45° flared housing, as described in section 13.2.4. When running with coarse solids, axial strokes of the type shown in Figure 13.5 should be used.

As before, fine solids can only be removed using an external clean flush.

The guidelines are summarised in Table 13.3.

#### **13.4 SUMMARY**

The work presented in the thesis is being successfully translated into documents which are of direct relevance to industry. The industrial sponsors of the work have been closely involved, and are very supportive, of this initiative. Already, two major documents have emerged from the work: a comprehensive Housing Design Guide and input to a draft UK proposal for the revised ISO 3069.

Both documents should gain widespread visibility in the next few years and stand a real chance of improving mechanical seal reliability.

---

**ACKNOWLEDGEMENTS**

---



My thanks are due to BHRA for giving me permission and support for the Total Technology Ph-D. In addition, use was granted for computing and library facilities essential for production of the thesis, analysis and literature reviews.

The project was sponsored by the following consortium of companies to whom I am indebted:-

Amoco (UK) Ltd  
 BP International Ltd  
 B-W/IP - Seals Division  
 Britoil  
 Caltex (UK)  
 Department of Trade and Industry  
 EG & G - Seals Division  
 ICI  
 John Crane Ltd  
 Lucas Aerospace  
 Morganite Special Carbons Ltd  
 Shell Expro  
 T & N Technology

My special thanks are due to Mr Noel Howard of Amoco (UK) Ltd for enabling me to spend a fortnight on a refinery and also for our valuable discussions on mechanical seal performance.

I acknowledge the vital role of my support panel comprising:-

Professor Michael Sanderson	- Cranfield Institute of Technology
Mr Graham Clarke	- Cranfield School of Management
Dr Bernard Nau	- BHRA, Manager, Fluid Sealing
Mr Robert Flitney	- BHRA, Manager, Industrial Applications, Fluid Sealing
Mr Colin Armstrong	- BHRA

I have benefitted considerably from their valuable comments, criticisms and suggestions throughout the period of the work.

The thesis was typed by a number of BHRA typists but, in particular, I wish to thank Mrs June Wells for her efficient and accurate typing of the bulk of the manuscript. My grateful thanks also to Mrs Marion Goddard for her painstaking proof-reading of my thesis.

---

**REFERENCES**

---

ABDALLAH, Y A G, CONEY, J E R  
Adiabatic and diabatic flow studies by shear stress measurements in  
annuli with inner cylinder rotation  
Unpublished, 1988

ADAMS, W V  
Better high temperature sealing  
Hydrocarbon Processing, 1987, Jan, pp 53-59

ALMOND, C, PASSMORE, W J  
Pump mechanical seal failure analysis - VC3  
ICI internal report, Aug 1985

ANON  
Ceramics for better mechanical seals  
Process Engg, 1988, May, pp 77-78

AUSTIN, R M, FLITNEY, R K, NAU, B S  
Rotary seal vapour emission  
BHRA Report RR 1616, 1980

BANGERT, P  
Slurry transport  
Industrie-Anzeiger, 1986 Vol 91, p 50

BARCILON, A, BRINDLEY, J, LESSEN, M, MOBBS, F R  
Marginal instability in Taylor-Couette flows at a very high Taylor number  
J Fluid Mech, 1979, Vol 94, part 3, pp 453-463

BARNARD, P C, WEIR, R S L  
A theory for mechanical seal face thermodynamics  
8th ICFS, BHRA, 1978, Paper H1, pp 1-8

BARNES, N D  
Heat transfer in an annulus with a heated rotating inner-cylinder and  
axial flow  
Private communication, 1985

BARNES, N D, FLITNEY, R K, NAU, B S  
Mechanical seal housing optimisation study  
BHRA Report CR 3005, 1988

BARNES, N D, FLITNEY, R K, NAU, B S  
Mechanical seal housing design guide  
BHRA Report CR 3006, 1989 (a)

BARNES, N D, FLITNEY, R K, NAU, B S  
Effect of housing on mechanical seal temperature margin  
BHRA Report CR 3008, 1989 (b)

BARNES, N D, FLITNEY, R K, NAU, B S  
Mechanical seal performance: site investigations  
BHRA Report CR 3027, 1989 (c)

BARNES, N D, FLITNEY R K, NAU BS  
Designing chambers for mechanical seals  
World Pumps, 1990, April, pp 22-25

BASU, P, HUGHES, W F, BEELER, R M  
Centrifugal Inertia Effects in Two-phase Face Seal Films  
Trans ASLE, 1986, Vol 30.2, pp 177-186

BATTILANA, R E  
Seal housing design affects seal life in pumping slurries  
Pump technical library, McGraw Edison Co, 20RP-2013

BECKER, K M, KAYE, J  
Measurements of diabatic flow in an annulus with an inner rotating  
cylinder  
Trans ASME, Jnl Ht Transfer, 1962, Vol 84, pp 97-105

BERTELE, O V  
Why do seals fail unpredictably?  
10th ICFS, BHRA, 1984, Paper L4, pp 523-532

BJORKLUND, I S, KAYS, W M  
Heat transfer between concentric rotating cylinders  
Trans ASME, 1959, Series C, Vol 81, pp 175-186

BLOCH, H P  
Downtime prompts upgrading of centrifugal pumps  
Chem Engg, 1985 Nov 25, pp 35-49

BLOCH, H P  
Selection strategy for mechanical shaft seals in petrochemical plants  
Proc 1st International Pump Symp 1984, pp 115-121

BLOCH, H P  
Mechanical seals for upgraded medium duty pumps  
International Sealing Conf, 1986, pp 1-13

BLOCH, H P, SCHUEBL, W  
Reliability improvement in mechanical seals, analysis of design considerations  
Proc 2nd Int Pump Symp 1985, pp 115-126

BROWN, M  
Correct fitting of mechanical seals prevents failure  
Processing, 1978, Oct, pp 89-91

BUCK, G S  
A methodology for design and application of mechanical seals  
Trans ASLE (1980) Vol 23, 3, pp 244-252

CAMERON, W  
Mechanical seals for bio-reactors  
Chem Engr, 1987, Nov, pp 41-42

CASTLE, P, MOBBS, F R, MARKHO, P H  
Visual observations and torque measurements in the Taylor vortex regime between eccentric rotating cylinders  
Trans ASME, Jnl Lub Tech, 1971, Jan, pp 121-129

COLE, J A  
Taylor vortices with eccentric rotating cylinders  
Nature, 1967, Dec 23, Vol 216, pp 1200-1202

COLES, D  
Transition in circular Couette flow  
J Fluid Mech, 1965, Vol 21, part 3, pp 385-425

CONEY, J E R, SIMMERS, D A  
A study of fully developed, laminar, axial flow and Taylor vortex flow by means of shear stress measurements  
J Mech Eng Sci, 1979(a), Vol 21, No 1, pp 19-24

CONEY, J E R, SIMMERS, D A  
The determination of shear stress in fully developed laminar axial flow and Taylor vortex flow using a flush-mounted hot-film probe  
DISA Info, 1979(b), May, No 24, pp 9-14

CRANFIELD, R R  
Studies of power station feed pump loss of suction pressure incidents  
Trans ASME, Jnl of Fluids Engg, 1988, Dec, Vol 110, pp 453-461

DAHLHEIMER, J C

Stretching the life of face seals

Machine Design, 1970, Nov 12, pp 170-173

DAVISON, M P

The effects of seal chamber design on seal performance

Proc Sixth Inst Pump Users Symp, 1989, pp 3-8

DOLAN, P J, HARRISON, D, WATKINS R

Mechanical seal selection and testing

11th ICFS, BHRA, 1987, Paper A1, pp 1-16

DORFMAN, L A

Hydrodynamic resistance and the heat loss of rotating solids

Oliver & Boyd, 1963, pp 163 et seq

DOUST, T G, PARMAR, A

Transient thermoelastic effects in a mechanical face seal

Design Engg, 1987, Aug, pp 29-32

EEDS, J M, INGRAM, J H, MOSES, S T

Mechanical seal application - a user's viewpoint

Proc 6th Turbomachinery Symp, 1977, pp 171-185

FIELD, G J, FLITNEY, R K

Tests on a diesel engine water pump

BHRA Report CR 1273, 1975

FLITNEY, R K

Factors affecting mechanical seal design and application

Trib International 1977, Oct, pp 267-272

FLITNEY, R K

Reliability of seals in centrifugal process pumps

Process Engg, 1987, July, pp 39-42

FLITNEY, R K, NAU, BS

Seals Survey: Part 1

BHRA Report, 1976

FLITNEY, R K, NAU, B S

Mechanical seal reliability study

BHRA Report No CR 1886, 1982

FLITNEY, R K and NAU, B S

A study of factors affecting mechanical seal performance  
Proc I Mech E, 1984, Vol 200, No 107, pp 1-12

FLITNEY, R K, NAU, B S

Mechanical seal reliability study: part 2  
BHRA Report No DCR 2543, 1985

FLITNEY, R K and NAU, B S

Reliability of mechanical seals in centrifugal process pumps  
11th ICFS, BHRA, 1987, Paper A2, pp 17-45

FLITNEY, R K, NAU, B S, REDDY, M D

Mechanical seal reliability study: part 1  
BHRA Report No CR 2165, 1984

FLITNEY, R K, NAU, B S

Mechanical Seal Performance Determination : Background Research  
BHRA Report No CR 3007, 1989

FLOYD, C G

A study of frictional losses of enclosed rotors at high Reynolds numbers  
PhD Thesis, 1982, Bristol University

FUJITA, T, MATSUMOTO, S, KOGA, T

Design and performance of mechanical seals for liquified gas application  
Lubr Engg, 1987, June, Vol 43, No 6, pp 440-446

GAZLEY, C

Heat-transfer characteristics of the rotational and axial flow between  
concentric cylinders  
Trans ASME, 1958, Vol 80, pp 79-89

GILES, O

New design concepts and materials for mechanical shaft seals  
Mech Engg, 1972, Apr, pp 18-22

GROHMANN, M

The requirements of a pump manufacturer: present and future  
World Pumps, 1984, Sept, pp 334-335

HEALD, J M

The seal's environment - its housing  
7th ICFS, BHRA, 1975, Paper B4, pp 17-24

HERSHEY, L E

Comparison of water-cooling methods for mechanical seals  
3rd ICFS, BHRA, 1967, Paper 132, pp 17-28

HERSHEY, L E

Evaporative cooling applied to mechanical seals  
4th ICFS, BHRA, 1969, pp 104-108

HERSHEY, L E

Evaluation of an air-cooled heat exchanger for mechanical seals  
5th ICFS, BHRA, 1971, Paper A3, pp 17-24

HEUMANN, A

Shaft seals or centrifugal pumps handling media with suspended solids,  
under special consideration of the problems associated with flue-gas  
desulphurisation  
International Sealing Conf, 1986, Paper 10, pp 1-15

HINZE, J O

Turbulence (2nd edition)  
McGraw Hill, 1975

HIRABAYASHI, H, OKA, K, ISHIWATA, H

The relationship between ringing, heat transfer and sealing condition  
4th ICFS, BHRA, 1969, pp 115-123

HO, C Y, NARDACCI, J L, NISSAN, A H

Heat transfer characteristics of fluids moving in a Taylor system of  
vortices  
A I Ch E Jnl, 1964, Mar, Vol 10, No 2, pp 194-202

HUMMER, H B

Requirements for sealing liquified petroleum gas  
Lubr Engg, 1973, July, Vol 29, pp 308-314

INGRAM, J H

Pump specifications that improve mechanical seal performance  
Proc 1st Int Pump Symp 1984 pp 123-129

KAPUR, K C, LAMBERSON, L R

Reliability in engineering design  
Wiley, 1977



KAYE, J, ELGAR, E C

Modes of adiabatic and diabatic fluid flow in an annulus with an inner rotating cylinder

Trans ASME, 1958, Vol 80, pp 753-764

KLIMEK, E J

Selection, properties and quality assurance of face materials for rotating mechanical seals

Lubr Engg, 1988, Aug, Vol 44, No 8 pp 719-726

KOGA, J K, KOSCHMIEDER, E L

Taylor Vortices in short fluid columns

Phys. Fluids, 1989, A 1, (9), pp 1475-1478

KRATZER, A

Centrifugal pumps for flue-gas desulphurisation plants using the lime-washing process

World Pumps, 1987, Nov, pp 363-367

KUZAY, T M, SCOTT, C J

Turbulent heat transfer studies in annulus with inner cylinder rotation

Trans ASME, Jrnl Ht Transfer, 1977, Feb, pp 12-19

LAUNDER, B E, SPALDING, D B

Mathematical models of turbulence

Academic Press, 1972

LEBECK, A O

Contacting mechanical seal design using a simplified hydrostatic model

Trib International, 1988, Feb, Vol 21, No 1, pp 2-14

LI, X, LIU, Z

Experimental investigation on face friction of mechanical seal

Private communication 1987

LOCK, K R U

Cut capital lock-up and downtime with good seal practice

Process Engg, 1971, Aug, pp 51-55

LYMER, A

An engineering approach to the selection and application of mechanical seals

4th ICFS, BHRA, 1969, pp 239-246

MARR, A H C, PHELPS, R L, KATZ, B  
Loss of component cooling water capability  
ASME Preprint, 1980, No 80-C2/PVP-28

MARTEL, Y, BOTTE, J M, REGAZZICCI, P  
Reduce costs with metal bellows shaft seals  
Hydrocarbon Processing, 1987, Oct, pp 39-40

MICHAELIS, P M M  
Sealing of hazardous fluids and light hydrocarbons  
World Pumps, 1985, Jan, pp 7-15

MORTON, T R  
Seal performance from the manufacturer's viewpoint  
ASME Preprint, 1984, No 84-PVP-115

NAU, B S  
An investigation into the nature of the interface film, the pressure  
generating mechanism and centrifugal pumping in mechanical seals.  
BHRA Report, RR 754, 1963

NAU, B S,  
Observation and analysis of mechanical seal film characteristics  
ASME Pre-print 79-Lub-36, 1979

NAU, B S  
Vibration and rotary mechanical seals  
Trib International, 1981, Feb, pp 55-59

NAU, B S  
Heat transfer from rotating cylinders  
BHRA International Communication, 1982

NAU, B S  
Power Dissipation Results  
BHRA International Communication, 1987

NAU, B S  
Rotary mechanical seals in process duties, an assessment of the state of  
the art  
Proc I Mech I (1985), Vol 199, No A, pp 17-31

NETZEL, J P

The effect of interface cooling in controlling surface disturbances in mechanical face seals

Wear, 1982, No 79, pp 119-127

NETZEL, J P

Symmetrical seal design: a sealing concept for today

Proc. First Int Pump Symp, 1984, pp 109-112

NISSAN, A H, NARDACCI, J L, HO, C Y

The onset of different modes of instability of flow between rotating cylinders

A I Ch E Jnl, 1963, Sept, pp 620-624

NOLAN, D

Sorting out slurry pump seals

Coal, 1988, Mar, pp 86-90

ORCUTT, F K

An investigation of the operation and failure of mechanical face seals

4th ICFS, BHRA, 1969, pp 155-167

PAI, S I

Turbulent flow between rotating cylinders

N A C A Tech Note no 892, 1943

PATANKAR, S V, SPALDING, D B

Heat and mass transfer in boundary layers (2nd edition)

Intertext Books, 1970

PEEL, I

Magnetic drives give more reliable pumps

Drives & Controls, 1988, Sept, pp 69-71

PHILLIPS, J

Standardisation of mechanical seals

Pumps, 1973, Vol 81, pp 261-263

PHILLIPS, J, JOHNSON, C M

Quality control and its place in shaft sealing

8th ICFS, BHRA, 1978, Paper E1, pp 1-12

PLUMRIDGE, J M, FLOYD, C G

Tolerant seal design for difficult applications

CME, 1986, Dec, pp 28-29

REICHARDT, H

Über die Geschwindigkeitsverteilung in einer geradlinigen Couetteströmung  
Z Angew Math Mech, 1956, Vol 36, pp 26-29

ROBINSON, R P, BURTON, R

Temperature gradients in seal rings : a method of analysis  
4th ICFS, BHRA, 1969, pp 109-114

SALANT, R F, KEY, W E

Improved mechanical seal design through mathematical modelling  
Proc 1st Int Pump Sym, 1984, pp 37-46

SANGERHAUSEN, C R

Proper design is first step in reducing failures  
Oil & Gas Journal, 1981, Mar 23, pp 138-144 and Mar 30, pp 169-178

SCHMIDTHALS, W

Mechanical seals in the high speed range for gas-containing liquids  
Internatioanl Sealing Conf, 1986, paper 14, pp 1-10

SCHOPPLEIN, W

Application of mechanical seals to slurries with particular reference to  
pumps and agitators on flue gas desulphurisation plants  
Trib International, 1986, Aug, Vol 19, No 4, pp 187-192

SILVAGGIO, J A, LIPSKI, M J, BRAMER, K G

Successful field operation through seal development and testing  
Lubr Engg, 1987, June, Vol 43, No 6, pp 433-439

SIMMERS, D A, CONEY, J E R

A Reynolds analogy solution for the heat transfer characteristics of  
combined Taylor vortex and axial flows  
Int Jnl, Ht Mass Transfer, 1979(a), Vol 22, pp 679-689

SIMMERS, D A, CONEY, J E R

The effect of Taylor vortex flow on the development length in concentric  
annuli

Jnl Mech Eng Sci, 1979(b), Vol 21, No 2, pp 54-64

SIMMERS, D A, CONEY, J E R

The experimental determination of velocity distribution in annular flow  
Int J Ht & Fluid Flow, 1979(c), Vol 1, No 4, pp 177-184

SIMMERS, D A , CONEY, J E R

Velocity distributions in Taylor vortex flow with imposed laminar axial flow and isothermal surface heat transfer

Int Jnl, Heat & Fluid Flow, 1980, Vol 2, No 2, pp 85-91

SOROUR, M M, CONEY, J E R

The effect of temperature gradient on the stability of flow between vertical, concentric, rotating cylinders

J Mech Eng Sci, 1979, Vol 21, No 6, pp 403-409

STANDISH, D

Planning a pump evolution

CME, 1987, Mar, pp 39-40

STRASZEWSKI, C J

Mossmoran - a new peak in mechanical sealing

World Pumps, 1985, Jan, pp 18-19

SUMMERS-SMITH, J D

Laboratory investigation of the performance of a radial face seal

1st ICFS, BHRA, 1961, Paper D1

SUMMERS-SMITH, J D

Performance of mechanical seals in centrifugal process pumps

9th ICFS, BHRA, 1981, Paper H1 pp 323-331

TACHIBANA, F, FUKUI, S, MITSUMURA, H

Heat transfer in an annulus with an inner rotating cylinder

Bulletin JSME, 1960, Vol 3, No 9, pp 119-123

TAYLOR, G I

Stability of a viscous liquid contained between two rotating cylinders

Phil Trans Royal Soc, 1923, A233, pp 289-343

TAYLOR, G I

Distribution of velocity and temperature between concentric rotating cylinders

Proc Royal Soc, 1935, Series A, Vol 151, pp 494-512

TAYLOR, G I

Friction between rotating cylinders

Proc. Royal Soc, 1936, A, Vol 157, pp 546-578

TRIBE, F J, GREEN, G A

Assessment of mechanical seal face materials under controlled interface Torque

Trans ASLE, 1986, Vol 42, No 11, pp 686-693

VOHR, J H

An experimental study of Taylor vortices and turbulence in flow between eccentric rotating cylinders

Trans ASME, Jnl Lub Tech, 1968, Jan, pp 285-296

WAGNER, E M

Frictional resistance of a cylinder rotating in a viscous fluid within a co-axial cylinder.

Thesis for the degree of engineer, Stanford University, 1932

WAKELY, K

Mechanical seals: some developments in face materials

Trib International, 1986, Aug, Vol 19, No 4, pp 198-203

WAN, C C, CONEY, J E R

An experimental study of diabatic spiral vortex flow

Int Jnl Ht & Fluid Flow, 1982(a), Vol 3, No 1, pp 31-38

WAN, C C, CONEY, J E R

An investigation of adiabatic spiral vortex flow in wide annular gaps by visualisation and digital analysis

Int Jnl Ht & Fluid Flow, 1982(b), Vol 3, No 1, pp 39-44

WILL, T P

Experimental observation of a face-contact mechanical shaft seal operating on water

Lubr Eng (1982), Vol 38, 12, pp 767-772

WIMMER, M

Viscous flows and instabilities near rotating bodies

Progress in Aerospace Sci, 1988, Vol 25, pp 43-103

YOUNES, M A M A, MOBBS, F R, CONEY, J E R

Hydrodynamic stability of the flow between eccentric rotating cylinders with axial flow : torque measurements

Proc I Mech E, 1972, Tribology Convention

YOUNES, M A M A, MOBBS, F R, CONEY, J E R

Power losses due to secondary flow between rotating eccentric cylinders

Trans ASME, Jnl Lubr Tech, 1974, June, pp 141-144

YOUNG, L A, LEBECK, A O

The design and testing of moving-wave mechanical face seals under variable operating conditions in water

Lubr Engg, 1986, Vol 42, No 11, pp 677-685

-----  
**APPENDICES**  
-----



APPENDIX A

EXTRACTS FROM STANDARDS

---

A1

DIN 24960 : 1989

---

**Gleitringdichtungen**  
Wellendichtungsraum  
Hauptmaße, Bezeichnung und Werkstoffschlüssel



Vorlage November 1989

Mechanical seals; cavities; principal dimensions, designation and material codes  
Garnitures mécaniques d'étanchéités; logement; dimensions principales, signification et code de matériel

Ersatz für  
DIN 24 960 06.80  
Anwendungswarnvermerk :  
siehe

Zusammenhang mit der von der International Organization for Standardization (ISO) herausgegebenen Norm ISO 3069 siehe Erläuterungen.

Maße in mm

**1 Geltungsbereich**

Diese Norm enthält die Hauptmaße für den Einbau von innenliegenden Einzel- und Doppel-Gleitringdichtungen mit unlaufenden Federteil oder mit stationärem Federteil als vormontierte Baueinheiten in den Wellendichtungsraum und legt deren Bezeichnung und Werkstoffschlüssel fest.

**2 Mitgeltende Normen**

DIN 7168 Teil 1 Allgemeintoleranzen; Freimaßtoleranzen; Winkel und Längenmaße

**3 Maße**

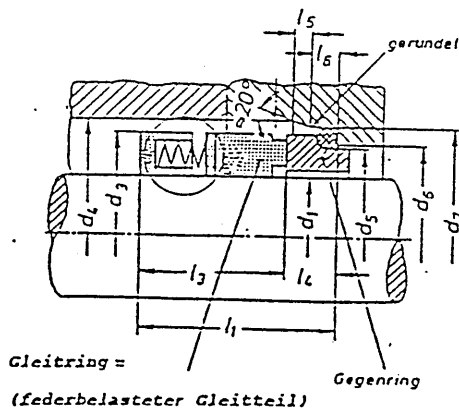
Die Gleitringdichtungen und Wellendichtungsräume brauchen der bildlichen Darstellung nicht zu entsprechen; nur die angegebenen Maße sind einzuhalten. Die Darstellungen zeigen Runddichtringe (O-Ringe) als Nebendichtungen; andere Profildichtungen können ebenfalls als Nebendichtungen verwendet werden.

Allgemeintoleranzen: DIN 7168 – mittel

**3.1 Gleitringdichtung mit unlaufenden Federteil, Ausführung N und K 12)****3.1.1 Einzel-Gleitringdichtung 13)**

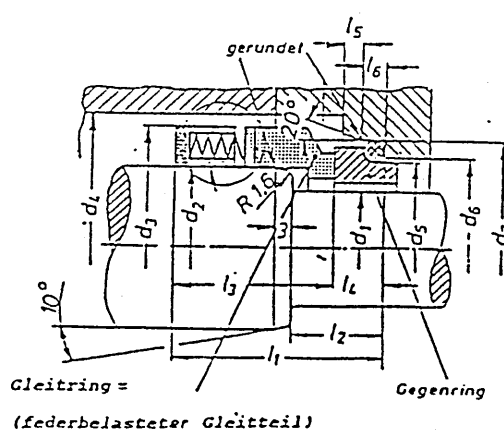
Form U

ohne Wellenabsatz



Form B

mit Wellenabsatz



12) Erklärung siehe Seite 4, Tabelle 2

13) Kurzzeichen nach DIN ISO 5199 "5"

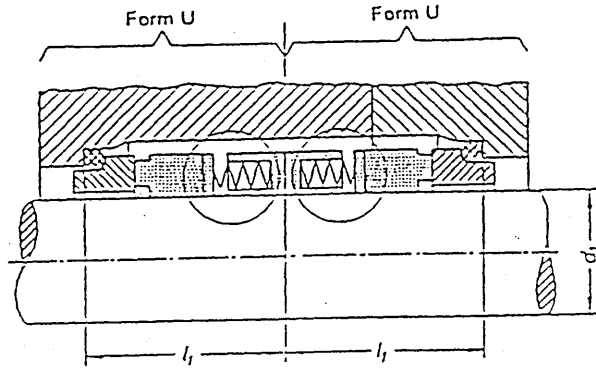
Fortsetzung Seite 2 bis  
Erläuterungen Seite

Normenausschuß Maschinenbau (NAM) im DIN Deutsches Institut für Normung e. V.

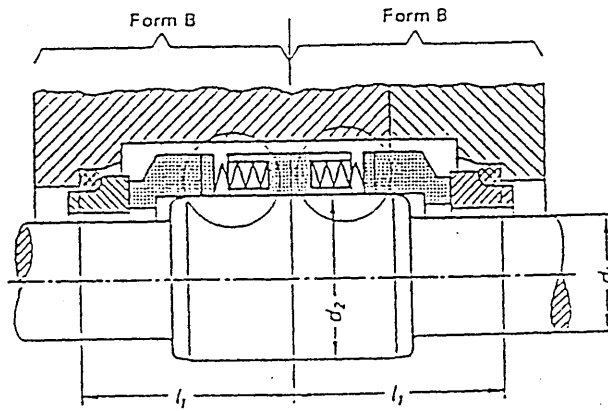
- Seite 2 DIN 24 960

3.1.2 Doppel-Gleitringdichtung (bestehend aus zwei Einzel-GLRD der Ausführung K1 14)

Form UU



Form BB



Form UB

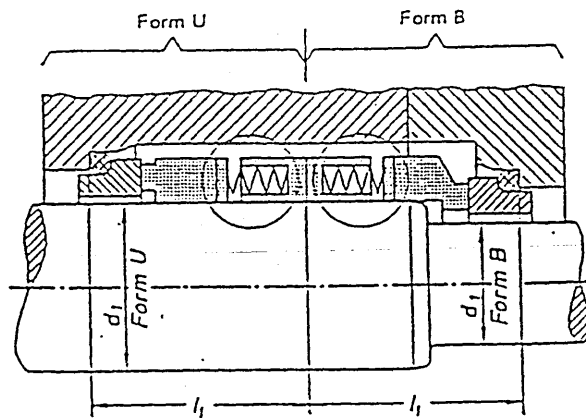


Tabelle 1. Zuordnung der Nenndurchmesser bei der Form U B

$d_1$	Form B	15)	10	12	14	16	18	20	24	25	28	30	32	33	35	38	40	43	45	48	50	53	55	58	60	63	65	70	75	80	85	90	95
	Form U		14	16	18	20	22	24	28	30	33	35	38	38	40	43	45	48	50	53	55	58	60	63	65	58	70	75	80	85	90	95	100

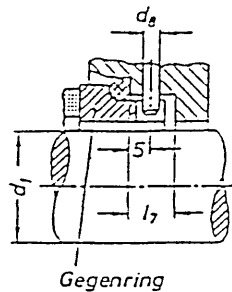
14) Kurzzeichen nach DIN ISO 5199 "D" 15) Nenn-Ø bei der Form UB

3.1.3 Sicherung des Gegenrings  
 3.1.3.1 Gegen Verdrehen

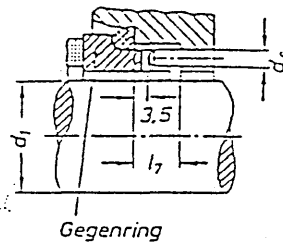
Gestaltung nach Wahl des Herstellers oder nach Vereinbarung

Beispiele für atmosphärenseitigen Gegenring

mit radialer Anordnung eines Stiftes



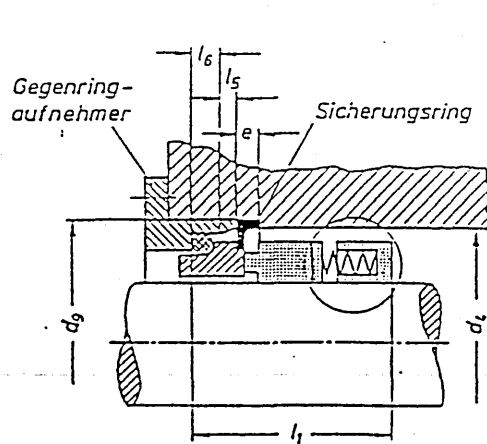
mit axialer Anordnung eines Stiftes



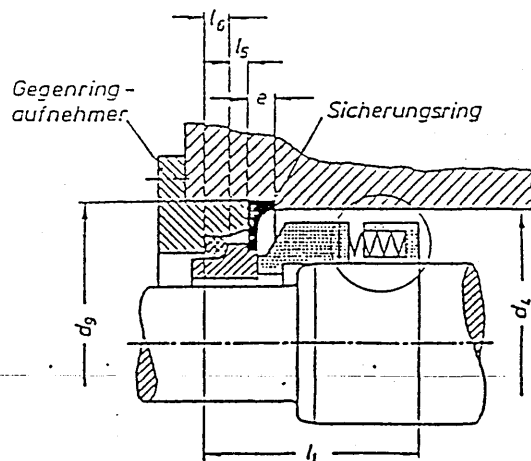
Die Anordnung gilt für Form U und B

3.1.3.2 Mit Gegenringaufnahme und Sicherungsring gegen axiales Verschieben  
 (gilt nur für produktseitige GLRD der Form UJ, EE und UB)

Beispiel für Form U



Beispiel für Form B



Um eine ausreichende Anlage des Sicherungsringes zu gewährleisten, ist bei axialer Sicherung des produktseitigen Gegenrings darauf zu achten, daß das Maß  $d_4$  das Maß  $d_9$  um mindestens 2 mm unterschreitet. Für eine axiale Sicherung des produktseitigen Gegenrings ist vom Gleitringdichtungs-Hersteller der Sicherungsring für den Einbauraum  $e$  auf Anforderung beizustellen.  $d_8$  ist der Durchmesser für den Einbauraum des Sicherungsringes.

Teil 4 DIN 24 950

3.1.4 Mastabelle für Ausführung N und K



Tabelle 2.

d <sub>1</sub> Nenn- Durchmesser	d <sub>2</sub>	d <sub>3</sub> 1)		d <sub>4</sub> 1)		d <sub>5</sub>	d <sub>6</sub>	d <sub>7</sub>	d <sub>8</sub>	d <sub>9</sub>	e	l <sub>1</sub>				l <sub>2</sub>	l <sub>3</sub>	l <sub>5</sub>	l <sub>6</sub>	l <sub>7</sub>	
		Größtmaß		Kleinstmaß								Ausführung N 2)		Ausführung K							
		Form U	Form B	Form U	Form B							Form U	Form B	Form U	Form B						± 0.5
10	14	20	24	22	26	h8	H11	H8	Form U	Form B	Form U	Form B	Form U	Form B	± 0.5	± 0.5	± 0.5	± 0.5	± 0.5	± 0.5	± 0.5
12	16	22	26	24	28	h8	H11	H8	Form U	Form B	Form U	Form B	Form U	Form B	± 0.5	± 0.5	± 0.5	± 0.5	± 0.5	± 0.5	± 0.5
14	18	24	32	26	34	h8	H11	H8	Form U	Form B	Form U	Form B	Form U	Form B	± 0.5	± 0.5	± 0.5	± 0.5	± 0.5	± 0.5	± 0.5
16	20	26	34	28	36	h8	H11	H8	Form U	Form B	Form U	Form B	Form U	Form B	± 0.5	± 0.5	± 0.5	± 0.5	± 0.5	± 0.5	± 0.5
18	22	32	36	34	38	h8	H11	H8	Form U	Form B	Form U	Form B	Form U	Form B	± 0.5	± 0.5	± 0.5	± 0.5	± 0.5	± 0.5	± 0.5
20	24	34	38	36	40	h8	H11	H8	Form U	Form B	Form U	Form B	Form U	Form B	± 0.5	± 0.5	± 0.5	± 0.5	± 0.5	± 0.5	± 0.5
22	26	36	40	38	42	h8	H11	H8	Form U	Form B	Form U	Form B	Form U	Form B	± 0.5	± 0.5	± 0.5	± 0.5	± 0.5	± 0.5	± 0.5
24	28	38	42	40	44	h8	H11	H8	Form U	Form B	Form U	Form B	Form U	Form B	± 0.5	± 0.5	± 0.5	± 0.5	± 0.5	± 0.5	± 0.5
(25)	30	39	44	41	46	h8	H11	H8	Form U	Form B	Form U	Form B	Form U	Form B	± 0.5	± 0.5	± 0.5	± 0.5	± 0.5	± 0.5	± 0.5
28	33	42	47	44	49	h8	H11	H8	Form U	Form B	Form U	Form B	Form U	Form B	± 0.5	± 0.5	± 0.5	± 0.5	± 0.5	± 0.5	± 0.5
(30)	35	44	49	46	51	h8	H11	H8	Form U	Form B	Form U	Form B	Form U	Form B	± 0.5	± 0.5	± 0.5	± 0.5	± 0.5	± 0.5	± 0.5
(32)	38	46	54	48	58	h8	H11	H8	Form U	Form B	Form U	Form B	Form U	Form B	± 0.5	± 0.5	± 0.5	± 0.5	± 0.5	± 0.5	± 0.5
33	38	47	54	49	58	h8	H11	H8	Form U	Form B	Form U	Form B	Form U	Form B	± 0.5	± 0.5	± 0.5	± 0.5	± 0.5	± 0.5	± 0.5
(35)	40	49	56	51	60	h8	H11	H8	Form U	Form B	Form U	Form B	Form U	Form B	± 0.5	± 0.5	± 0.5	± 0.5	± 0.5	± 0.5	± 0.5
38	43	54	59	58	63	h8	H11	H8	Form U	Form B	Form U	Form B	Form U	Form B	± 0.5	± 0.5	± 0.5	± 0.5	± 0.5	± 0.5	± 0.5
(40)	45	55	61	60	65	h8	H11	H8	Form U	Form B	Form U	Form B	Form U	Form B	± 0.5	± 0.5	± 0.5	± 0.5	± 0.5	± 0.5	± 0.5
43	48	59	64	63	68	h8	H11	H8	Form U	Form B	Form U	Form B	Form U	Form B	± 0.5	± 0.5	± 0.5	± 0.5	± 0.5	± 0.5	± 0.5
(45)	50	61	66	65	70	h8	H11	H8	Form U	Form B	Form U	Form B	Form U	Form B	± 0.5	± 0.5	± 0.5	± 0.5	± 0.5	± 0.5	± 0.5
48	53	64	69	68	73	h8	H11	H8	Form U	Form B	Form U	Form B	Form U	Form B	± 0.5	± 0.5	± 0.5	± 0.5	± 0.5	± 0.5	± 0.5
(50)	55	66	71	70	75	h8	H11	H8	Form U	Form B	Form U	Form B	Form U	Form B	± 0.5	± 0.5	± 0.5	± 0.5	± 0.5	± 0.5	± 0.5
53	58	69	78	73	83	h8	H11	H8	Form U	Form B	Form U	Form B	Form U	Form B	± 0.5	± 0.5	± 0.5	± 0.5	± 0.5	± 0.5	± 0.5
55	60	71	80	75	85	h8	H11	H8	Form U	Form B	Form U	Form B	Form U	Form B	± 0.5	± 0.5	± 0.5	± 0.5	± 0.5	± 0.5	± 0.5
(58)	63	78	83	83	88	h8	H11	H8	Form U	Form B	Form U	Form B	Form U	Form B	± 0.5	± 0.5	± 0.5	± 0.5	± 0.5	± 0.5	± 0.5
60	65	80	85	85	90	h8	H11	H8	Form U	Form B	Form U	Form B	Form U	Form B	± 0.5	± 0.5	± 0.5	± 0.5	± 0.5	± 0.5	± 0.5
(63)	68	83	88	88	93	h8	H11	H8	Form U	Form B	Form U	Form B	Form U	Form B	± 0.5	± 0.5	± 0.5	± 0.5	± 0.5	± 0.5	± 0.5
65	70	85	90	90	95	h8	H11	H8	Form U	Form B	Form U	Form B	Form U	Form B	± 0.5	± 0.5	± 0.5	± 0.5	± 0.5	± 0.5	± 0.5
(68)	-	88	-	93	-	h8	H11	H8	Form U	Form B	Form U	Form B	Form U	Form B	± 0.5	± 0.5	± 0.5	± 0.5	± 0.5	± 0.5	± 0.5
70	75	90	99	95	104	h8	H11	H8	Form U	Form B	Form U	Form B	Form U	Form B	± 0.5	± 0.5	± 0.5	± 0.5	± 0.5	± 0.5	± 0.5
75	80	99	104	104	109	h8	H11	H8	Form U	Form B	Form U	Form B	Form U	Form B	± 0.5	± 0.5	± 0.5	± 0.5	± 0.5	± 0.5	± 0.5
80	85	104	109	109	114	h8	H11	H8	Form U	Form B	Form U	Form B	Form U	Form B	± 0.5	± 0.5	± 0.5	± 0.5	± 0.5	± 0.5	± 0.5
85	90	109	114	114	119	h8	H11	H8	Form U	Form B	Form U	Form B	Form U	Form B	± 0.5	± 0.5	± 0.5	± 0.5	± 0.5	± 0.5	± 0.5
90	95	114	119	119	124	h8	H11	H8	Form U	Form B	Form U	Form B	Form U	Form B	± 0.5	± 0.5	± 0.5	± 0.5	± 0.5	± 0.5	± 0.5
95	100	119	124	124	129	h8	H11	H8	Form U	Form B	Form U	Form B	Form U	Form B	± 0.5	± 0.5	± 0.5	± 0.5	± 0.5	± 0.5	± 0.5
100	105	124	129	129	134	h8	H11	H8	Form U	Form B	Form U	Form B	Form U	Form B	± 0.5	± 0.5	± 0.5	± 0.5	± 0.5	± 0.5	± 0.5

Eingeklammerte Nenndurchmesser sind bei Neukonstruktion zu vermeiden.

1) Zur Festlegung eines Sicherheitsabstandes zwischen Gleitringdichtung und Gehäuse werden die Maße d<sub>3</sub> als Größtmaße und die Maße d<sub>4</sub> als Kleinstmaße empfohlen.

2) Der Gleitringdichtung-Hersteller kann eine kürzere Gleitringdichtung (Ausführung N) als dem Maß l<sub>1</sub> entspricht, liefern. Dabei ist der Längenunterschied durch ein Distanzstück auszugleichen. Dieses ist vom Gleitringdichtung-Hersteller mitzuliefern.

A2

ISO 3069 - 1974

---

## End suction centrifugal pumps – Dimensions of cavities for mechanical seals and for soft packing

### 1 SCOPE AND FIELD OF APPLICATION

This International Standard specifies the dimensions of the cavity for balanced and unbalanced mechanical seals and for soft packing for use with end suction centrifugal pumps, rating 16 bar, in accordance with ISO 2858. It can, however, apply to other rotating machinery.

### 2 REFERENCE

ISO 2858, *End-suction centrifugal pumps for chemical liquids (rating 16 bar) – Designation, nominal duty point and dimensions.*

### 3 SPECIFICATION OF DIAMETERS OF SHAFTS AND CAVITIES

The diameters shown in figures 1, 2 and 3 shall have the values given in the table.

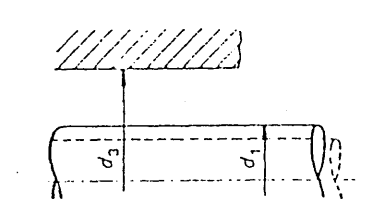


FIGURE 1 – Unbalanced mechanical seal or soft packing with or without sleeve

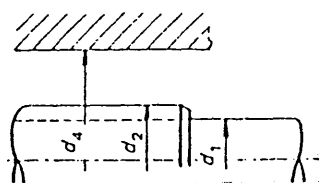


FIGURE 2 – Balanced mechanical seal with or without short sleeve

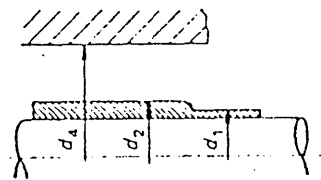


FIGURE 3 – Balanced mechanical seal with sleeve

Dimensions in millimetres

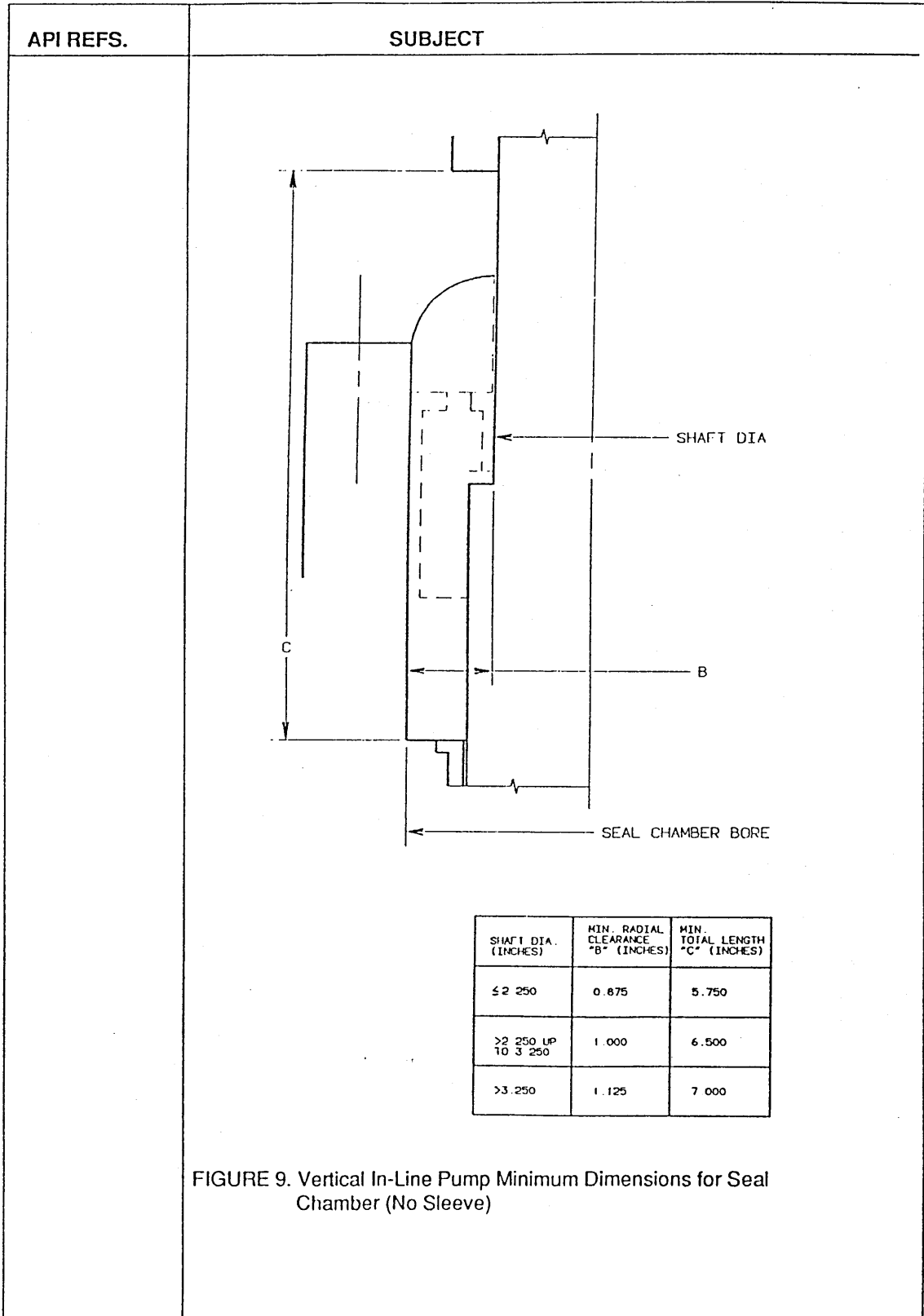
$d_1$	$d_2$	$d_3$	$d_4$
18	22	34	38
20	24	36	40
22	26	38	42
24	28	40	44
25	30	41	46
28	33	44	49
30	35	46	51
32	38	48	58
33	38	49	58
35	40	51	60
38	43	58	63
40	45	60	65
43	48	63	68
45	50	65	70
48	53	68	73
50	55	70	75
53	58	73	83
55	60	75	85
58	63	83	88
60	65	85	90
63	68	88	93
65	70	90	95
68	—	93	—
70	—	95	—

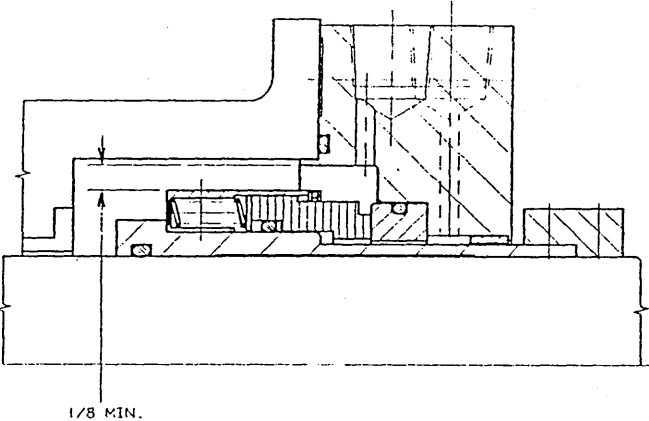


A3

API 610 7th Edition

API REFS	SUBJECT																								
<p>2.1.1.8</p> <p>2.7.1.4</p>	<p><b>SEAL CHAMBER</b></p> <p>The term "seal chamber" is used to identify the cavity between a bore and a shaft into which a mechanical seal is installed. (This includes the bore on the gland as well as the bore of the pump.) "Stuffing box" refers to the cavity designed to accept packing and enclosing the stationary parts surrounding a shaft. The seal chamber must have either an internal or external vent to allow the complete venting of the chamber before equipment start-up.</p> <p>One of the most significant additions to the API 610 Standard was the specification of minimum dimensions for seal chambers on overhung pumps. Figures 7 through 9 show the minimum dimensions for seal chambers. The "B" dimension in all cases will be larger. "C" dimensions could be less than on previous models. <b>Therefore, two full size balanced seals may not fit into some new seal chamber designs due to limited axial space.</b></p> <div style="display: flex; justify-content: space-around; align-items: flex-start;"> <div data-bbox="458 1037 916 1299" style="text-align: center;"> </div> <div data-bbox="977 1081 1285 1277"> <table border="1"> <thead> <tr> <th>SHAFT DIA (INCHES)</th> <th>MIN RADIAL CLEARANCE "B" (INCHES)</th> <th>MIN TOTAL LENGTH "C" (INCHES)</th> </tr> </thead> <tbody> <tr> <td>≤ 2.000</td> <td>1.000</td> <td>5.750</td> </tr> <tr> <td>2.001<sup>1</sup> TO 3.000</td> <td>1.125</td> <td>6.500</td> </tr> <tr> <td>&gt; 3.000</td> <td>1.250</td> <td>7.000</td> </tr> </tbody> </table> </div> </div> <p style="text-align: center;"><b>FIGURE 7. Minimum Dimensions for Seal Chamber With Sleeve</b></p> <div style="display: flex; justify-content: space-around; align-items: flex-start;"> <div data-bbox="443 1474 931 1736" style="text-align: center;"> </div> <div data-bbox="962 1517 1270 1714"> <table border="1"> <thead> <tr> <th>SHAFT DIA (INCHES)</th> <th>MIN RADIAL CLEARANCE "B" (INCHES)</th> <th>MIN TOTAL LENGTH "C" (INCHES)</th> </tr> </thead> <tbody> <tr> <td>≤ 2.250</td> <td>0.875</td> <td>5.750</td> </tr> <tr> <td>2.250 UP TO 3.250</td> <td>1.000</td> <td>6.500</td> </tr> <tr> <td>&gt; 3.250</td> <td>1.125</td> <td>7.000</td> </tr> </tbody> </table> </div> </div> <p style="text-align: center;"><b>FIGURE 8. Minimum Dimensions for Seal Chamber Without Sleeve</b></p>	SHAFT DIA (INCHES)	MIN RADIAL CLEARANCE "B" (INCHES)	MIN TOTAL LENGTH "C" (INCHES)	≤ 2.000	1.000	5.750	2.001 <sup>1</sup> TO 3.000	1.125	6.500	> 3.000	1.250	7.000	SHAFT DIA (INCHES)	MIN RADIAL CLEARANCE "B" (INCHES)	MIN TOTAL LENGTH "C" (INCHES)	≤ 2.250	0.875	5.750	2.250 UP TO 3.250	1.000	6.500	> 3.250	1.125	7.000
	SHAFT DIA (INCHES)	MIN RADIAL CLEARANCE "B" (INCHES)	MIN TOTAL LENGTH "C" (INCHES)																						
≤ 2.000	1.000	5.750																							
2.001 <sup>1</sup> TO 3.000	1.125	6.500																							
> 3.000	1.250	7.000																							
SHAFT DIA (INCHES)	MIN RADIAL CLEARANCE "B" (INCHES)	MIN TOTAL LENGTH "C" (INCHES)																							
≤ 2.250	0.875	5.750																							
2.250 UP TO 3.250	1.000	6.500																							
> 3.250	1.125	7.000																							



API REFS	SUBJECT
<p>2.7.1.4</p>	<p>In addition, the minimum radial clearance between the rotating member of the seal and the bore of the seal chamber is to be 1/8" (3mm). The bore diameter of the seal chamber (or gland bore) is to be in increments of 1/8" (3 mm), or in the case of metric designs, 5mm.</p> <p>The intent of the standard is to allow for increased circulation around the seal. This would not apply to the clearance between the pumping ring OD and the chamber bore.</p>  <p>1/8 MIN.</p> <p>FIGURE 10. Minimum Clearance Seal OD to Bore</p>
2.5.11.2	Refer to pg. 6 for seal chamber face run-out tolerance.
2.7.1.12	Refer to pg. 13 for seal chamber pressure.

APPENDIX B

RADIAL SPACE REQUIREMENTS  
FOR HIGH DUTY SEALS

A comparison of radial aspect ratio for 2 DIN seals and 3 high duty seals was carried out.

$$\text{Radial aspect ratio} = \frac{\text{seal radial depth}}{\text{shaft radius}}$$

$$= h/r$$

The dimensional data was taken from manufacturers' catalogues; all dimensions are in millimetres.

## B1 DIN SEALS

### B1.1 Flexibox

r	h	h/r
5	5	1.00
10	7	0.70
15	7	0.70
20	8	0.40
25	8	0.32
30	8	0.33
35	10	0.29
40	12	0.30
45	12	0.27
50	12	0.24

### B1.2 Sealol

r	h	h/r
5	5	1.00
10	6	0.60
15	6.5	0.43
20	8	0.40
25	8	0.32
30	10	0.33
35	9.5	0.27
40	10.5	0.26
45	10	0.22
50	11	0.22

B2 HIGH DUTY SEALSB2.1 BW/IP Seals - Type UHT

r	h	h/r
27	26	0.96
33	26.5	0.80
40	26.0	0.65
46	26.0	0.57
52	26.5	0.51
57	28.0	0.49
64	30.0	0.47
70	30.0	0.43
76	30.0	0.39
83	30.0	0.36

B2.2 Flexibox - Type RREP

r	h	h/r
20	16.5	0.83
25	18.5	0.74
30	19.0	0.63
35	23.0	0.66
40	23.0	0.58
45	23.5	0.52
50	24.5	0.49
60	24.5	0.41
70	29.0	0.41
80	32.0	0.40

B2.3 Sealol - Type 652 (externally mounted)

r	h	h/r
14	16	1.14
19	17	0.89
25	18	0.72
30	23	0.77
35	23	0.66
38	23	0.61

APPENDIX C

COST BENEFIT ANALYSIS  
DETAILED CALCULATIONS

---



## C1 BLOCH (1985)

### C1.1 Well maintained facility

Bloch asserts that the pump MTBF for a well maintained plant is 13 months or 56 weeks.

Consider a medium sized plant with a pump population of 1000. After 56 months, on average, every pump will have had one mechanical seal replaced.

In other words, the seals are being replaced at a rate of about 18 per week, ie. 1.8% of the installed seal population is failing every week. This equates to an  $L_{10}$  life (or 10% population failure time) of about 5-6 weeks.

Bloch also reports that in 1985 the estimated cost to his company worldwide (6000 pumps) due to mechanical seal failure alone was \$6,272,000. Inflated to 1990 costs, this figure amounts to about £6m, or an average cost per installed pump per year of £1000.

### C1.2 Industry average

Bloch claims that the industry average for pump MTBF is nearer 6 months, or 26 weeks.

By analogy with the scenario considered in sub-section C1.1, this yields an  $L_{10}$  life of only 2-6 weeks.

If Bloch's figures given in C1.1 are taken pro-rata for the industry average, then the cost per installed pump per year is about £2,200.

## C2 ALMOND AND PASSMORE (1985)

The preparation of the study carried out by Almond and Passmore are as follows:-

Number of pumps = 49

Length of study = 950 days (31 months).

For the purposes of this analysis, it has been assumed that the seals which did not fail in the 950 days study period would have worn out and been replaced after 4 years, or 1461 days. Hence, in the table below, 3 of the pumps with no failures after 950 days are adjusted to having  $950/1461 = 0.65$  failures in the study period.

The total number of failures was calculated from the data given in the report which is contained in the table shown overleaf.

FAILURES PER PUMP (f)	NUMBER OF PUMPS (x)	fx
0.65	3	1.95
1	3	3
2	3	6
3	4	12
4	2	8
5	1	5
6	1	6
7	2	14
8	1	8
9	3	27
11	1	11
12	3	36
14	2	28
15	2	30
16	3	48
19	2	38
20	1	20
21	5	105
22	2	44
23	1	23
25	1	25
26	1	26
29	1	29
32	1	32
	<u>49</u>	<u>585.95</u>

$\Sigma fx$  = Total number of failures

The results are as follows:-

- Average number of seal failures per day =  $\frac{586}{950} = 0.62$
- Mean-time-between-failures =  $49/0.62 = 79$  days
- $L_{10}$  life (ie. time for 4.9 failures to occur) =  $4.9/0.62 = 8$  days
- Cost of pump failures per day  $\pounds 5000 \times 0.62 = \pounds 3100$
- Cost of pump failures per year =  $\pounds 3100 \times 365 = \pounds 1.13m$
- Average cost per installed pump per year =  $\frac{\pounds 1.13m}{49} = \pounds 23,100$

C3 FLITNEY AND NAU (1985)C3.1 Company No. 1

Number of pumps surveyed = 221

Assume that the maximum seal life is 4 years

## (i) First 21 months

NUMBER OF FAILURES (f)	NUMBER OF PUMPS (x)	fx
0.44	111	48.8
1	57	57
2	26	52
3	16	48
4	3	12
5	2	10
6	3	18
7	3	21
	<u>221</u>	<u>266.8</u>

$\Sigma fx$  = Total number of failures

The results are as follows:-

- Average number of seal failures per month =  $\frac{266.8}{21} = 12.7$
- Mean-time-between-failures =  $\frac{221}{12.7} = 17.4$  months (75 weeks)
- $L_{10}$  life = 7.5 weeks
- Cost of pump failures per month = £63,500
- Cost of pump failures per year = £762,000
- Average cost per installed pump per year = £3,448

(ii) Full 39 months of survey

NUMBER OF FAILURES (f)	NUMBER OF PUMPS (x)	fx
0.81	113	92
1	42	42
2	24	48
3	14	42
4	7	28
5	5	25
6	3	18
7	5	35
8	3	24
9	1	9
10	0	0
11	2	22
12	1	12
25	1	25
	<u>221</u>	<u>422</u>

Σfx = Total number of failures

The results are as follows:-

- Average number of seal failures per month =  $\frac{422}{39} = 10.8$
- Mean-time-between-failures =  $\frac{221}{10.8} = 20.4$  months  
(88.5 weeks)
- $L_{10}$  life = 9 weeks
- Cost of pump failures per month = £54,000
- Cost of pump failures per year = £648,000
- Average cost per installed pump per year = £2,900

C3.2 Company No 3

Number of pumps = 322

Length of survey = 24 months

Assume that maximum seal life is 4 years

NUMBER OF FAILURES (f)	NUMBER OF PUMPS (x)	fx
0.5	167	83.5
1	55	55
2	41	82
3	14	42
4	19	76
5	7	35
6	6	36
7	6	42
8	2	16
9	3	27
12	2	24
	<u>322</u>	<u>518.5</u>

 $\Sigma fx$  = Total number of failures

The results are as follows:-

- Average number of seal failures per month = 21.6
- Mean-time-between-failures = 15.4 months  
(66.6 weeks)
- $L_{10}$  life = 6.7 weeks
- Cost of pump failures per month = £108,000
- Cost of pump failures per year = £1.3m
- Average cost per installed pump per year = £3,900

C3.3 Company No 5

Number of pumps = 77

Length of survey = 16 months

Assume that maximum seal life is 4 years

NUMBER OF FAILURES (f)	NUMBER OF PUMPS (x)	fx
0.33	52	17.3
1	18	18
2	5	10
4	1	4
7	1	7
	-----	-----
	77	56.3
	-----	-----

$\Sigma fx$  = Total number of failures

The results are as follows:-

- Average number of seal failures per month = 3.5
- Mean-time-between-failures = 21.9 months (94.8 weeks)
- $L_{10}$  life = 9.5 weeks
- Cost of pump failures per month = £17,500
- Cost of pump failures per year = £210,000
- Average cost per installed pump per year = £2,700

APPENDIX D

VISCOSITY TABLES

FOR WATER/GLYCEROL SOLUTIONS

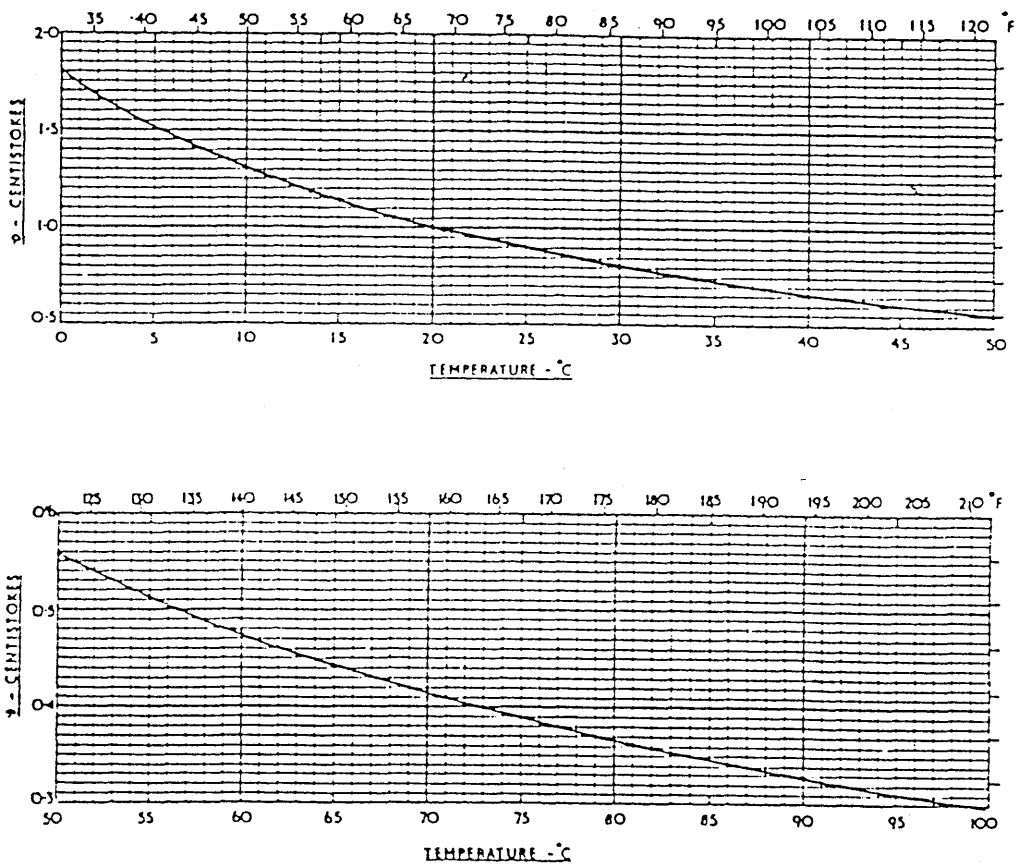


FIG. 6. VISCOSITY-TEMPERATURE DATA FOR WATER.

38

## MECHANICAL PROPERTIES OF MATERIALS

[1.4

## (iii) Viscosity of aqueous glycerol solutions

Data from Sheely, *Industr. Engng. Chem.*, 1932, 24, 1060, corrected to recent value for the viscosity of water (p. 36).

Relative density 25°/25 °C	% weight glycerol	$\eta$ /(N s m <sup>-2</sup> )		
		20 °C	25 °C	30 °C
1.262 01	100	1.495	0.942	0.622
1.259 45	99	1.194	0.772	0.509
1.256 85	98	0.971	0.627	0.423
1.254 25	97	0.802	0.521 5	0.353
1.251 65	96	0.659	0.434	0.295 8
1.249 10	95	0.543 5	0.365	0.248
1.209 25	80	0.001 8	0.045 72	0.034 81
1.127 20	50	0.006 032	0.005 024	0.004 233
1.061 15	25	0.002 089	0.001 805	0.001 586
1.023 70	10	0.001 307	0.001 149	0.001 021



## (iii) Viscosity of aqueous glycerol solutions

Data from Sheely, *Industr. Engng. Chem.*, 1932, 24, 1060, corrected to recent value for the viscosity of water (p. 36).

Relative density 25°/25 °C	% weight glycerol	$\eta/(N s m^{-2})$		
		20 °C	25 °C	30 °C
1.262 01	100	1.495	0.942	0.622
1.259 45	99	1.194	0.772	0.509
1.256 85	98	0.971	0.627	0.423
1.254 25	97	0.802	0.521 5	0.353
1.251 65	96	0.659	0.434	0.295 8
1.249 10	95	0.543 5	0.365	0.248
1.209 25	80	0.061 8	0.045 72	0.034 81
1.127 20	50	0.006 032	0.005 024	0.004 233
1.061 15	25	0.002 089	0.001 805	0.001 586
1.023 70	10	0.001 307	0.001 149	0.001 021

## (iv) Viscosity of aqueous sucrose solutions

Data from Bingham and Jackson, *National Bureau of Standards, Bulletin*, 1918, 14, 59, corrected to recent value for the viscosity of water (p. 36).

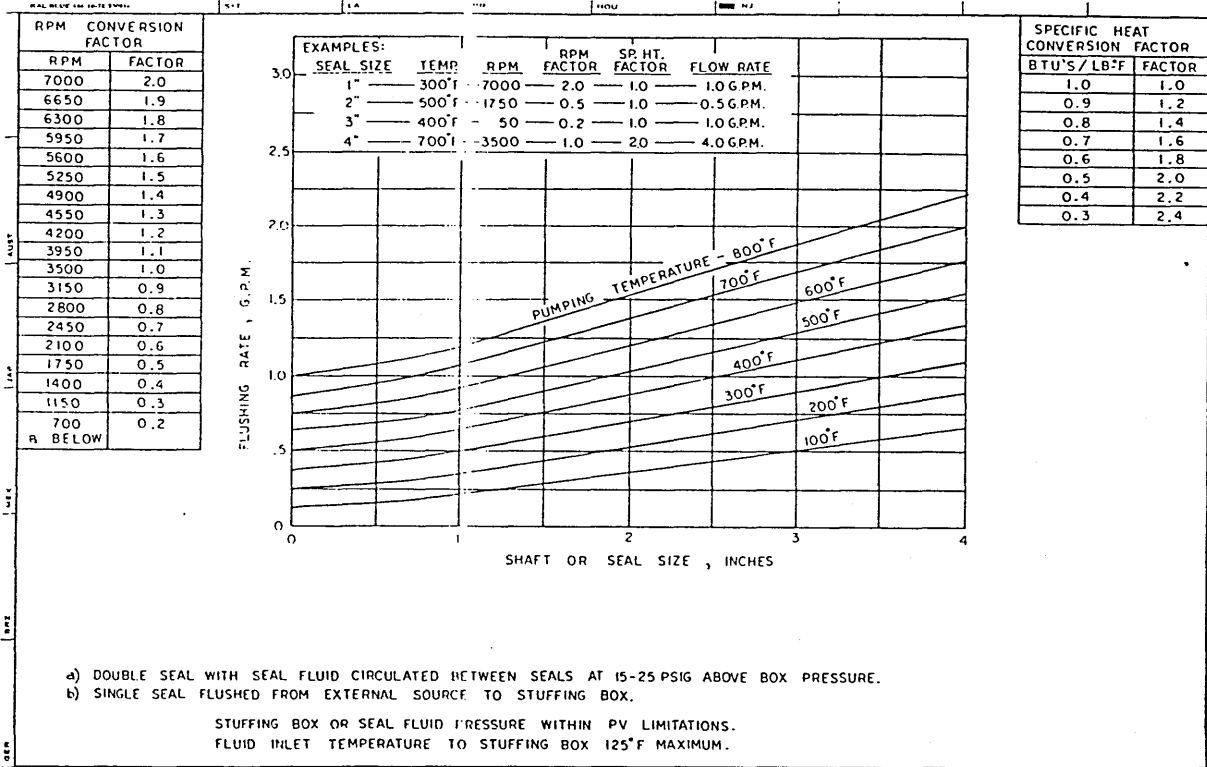
Relative density 20°/4 °C	% weight sucrose	$\eta/(N s m^{-2})$		
		15 °C	20 °C	25 °C
1.3790	75	4.039	2.328	1.405
1.3472	70	0.746 9	0.481 6	0.321 6
1.3163	65	0.211 3	0.147 2	0.105 4
1.2865	60	0.079 49	0.058 49	0.040 03
1.2296	50	0.019 53	0.015 43	0.012 40
1.1764	40	0.007 463	0.006 167	0.005 164
1.1270	30	0.003 757	0.003 187	0.002 735

## Viscosities of glasses and minerals

$\log_{10} \eta$  in  $N s m^{-2}$

Material	900 °C	1000 °C	1100 °C	1200 °C	1300 °C	1400 °C	1600 °C	1800 °C	2000 °C
Plate glass . . . . .	4.00	3.03	2.41	1.87	1.46	1.07	—	—	—
Medium flint glass . . .	3.9	2.8	1.9	1.4	0.9	0.7	—	—	—
Silica . . . . .	—	—	14.6	12.7	11.8	9.7	8.2	4.7	3.4
Olivine . . . . .	—	—	—	2.5	1.5	1.2	—	—	—
Diorite . . . . .	—	—	—	3.1	2.3	1.8	—	—	—
Diopside. . . . .	—	—	—	—	0.52	0.43	—	—	—

APPENDIX E  
MANUFACTURERS' RECOMMENDED  
INJECTION FLOWRATES



**FIG. IV-U SEALING AND FLUSHING LIQUID REQUIREMENTS**

**MINIMUM FLUSHING LIQUID FLOW RATES**

Regardless of which throat restriction device is to be used, a minimum flushing flow rate is required for proper cooling and lubrication of the mechanical seal. Figure IV-U "Sealing and Flushing Fluid Requirements for Dura Seals to Operate in Proper Temperature Environment" is a guide to the minimum flushing flow rates that are required for proper operation of the mechanical seal.

## Calculation of circulation requirements

There are two aspects to be considered in calculating the circulation flow rate. First, the flow rate must be sufficient to prevent sediment settlement in the stuffing box; secondly, the temperature rise of the flow should not affect the thermal characteristics of the seal.

1 The minimum flow rate to avoid settlement of sediment, is calculated from the number of fluid change in the stuffing box per unit time. Table 1 gives the minimum quantities required for RR, RM, RR and RRN seals using the stuffing box bore dimensions shown in the respective sections of the catalogue. Where stuffing box bores exceed the normal dimension by more than 5 mm these quantities should be increased by 5% for every millimetre increase in box bore.

FF-S seals, in general, require the same minimum flow rates as RR and RRN seals, but RR-SM seals should have the minimum quantity shown for RR seals raised by a factor of 1.5.

2 To calculate the amount of flow required to satisfy the thermal aspects of circulation, the following formula is used:

$$Q = X \times K \times \frac{t_2 - t_1}{5}$$

Where

Q = Heat generated per unit time by the seal

X = Quantity of flow in weight per unit time

K = Specific heat of product

t<sub>1</sub> = Product temperature

t<sub>2</sub> = Vapour temperature at sealed pressure

Note

An upper limiting value of 50°F (25°C) should be applied for

$$\frac{t_2 - t_1}{5}$$

to avoid deterioration of seal components which could occur under certain conditions.

### Example

Seal Size	RRN90
Pressure	400 psig
Speed	3000 rpm
Product	Pentane (Group 2 product)
Product temp.	300°F
Specific gravity	0.61
Specific heat	0.5
Vapour temperature	370°F at 400 psig (from vapour pressure curves in "Seal Selection")

Power absorbed by RRN 90 seal  
(from "Seal Selection Catalogue").

$$= 0.32 \text{ HP} \text{ per } 1000 \text{ rpm} = 0.96 \text{ HP}$$

Expressed as heat generation

$$= 41 \text{ BTU/min}$$

Satisfying the equation

$$41 = X \times 0.5 \times \left( \frac{370 - 300}{5} \right)$$

$$X = \frac{41}{0.5 \times 14} = 5.8 \text{ lb/min}$$

With a specific gravity of 0.61, this quantity is equivalent to 0.95 gals/min required to satisfy the thermal aspects of circulation. It is however less than the 1.05 gpm required for sediments disposal (From Table 1). Thus, the figure of 1.05 gpm is the minimum recommended circulation figure for this duty.

It is appreciated that the above method of calculating circulation flow rates may seem complex, and it is not designed to supersede practice built up by years of experience. When, however, an accurately calculated rate is required, for instance to keep cooler or other auxiliary equipment requirements to a minimum cost level, it can be used to determine the minimum required circulation flow rate for a given seal and duty.

Table 1 Minimum circulation flow requirements for RR, RRN, RM and RA seals

Shaft or Sleeve Size (mm)	Min circulation quantity for RR and RRN seals		Min circulation quantity for RM/RA seals	
	Gallons/min	Litres/min	Gallons/min	Litres/min
20	0.1	0.45	0.08	0.35
25	0.1	0.45	0.12	0.5
30	0.17	0.75	0.15	0.7
35	0.19	0.85	0.17	0.8
40	0.22	1.00	0.20	0.9
45	0.30	1.4	0.25	1.2
50	0.35	1.6	0.30	1.4
55	0.45	2.0	0.35	1.6
60	0.55	2.5	0.45	2.0
65	0.65	3.0	0.47	2.1
70	0.75	3.5	0.50	2.5
75	0.80	4.0	0.60	2.7
80	0.85	4.2	0.75	3.5
85	0.95	4.5	0.80	4.0
90	1.05	5.0	0.90	4.2
95	1.20	5.5	0.95	4.5
100	1.40	6.5	1.00	5.0

APPENDIX F

DANTEC 56 CTA SYSTEM

### 3.3.5 TYPICAL EXAMPLE OF SETTING

As choice of measuring medium, probe, required overheat, cable length etc. influences adjustment, it is impossible to cover all possibilities, for which reason only one example is shown. Measurement in air, overheat 0.8 and bridge supply 8 V with a standard 5  $\mu$ m wire probe (Table 5).

SWITCH	5 m Cable	20 m Cable	100 m Cable
BRIDGE ADJ.	33	28	14
CABLE LENGTH	1000	0100	0111
GAIN	0110	0010	0000
FILTER	10	00	11
SHAPE	11	11	11

Table 5

### 3.4 CALIBRATION OF THE ANEMOMETER

#### 3.4.1 GENERAL CONSIDERATIONS

Heat transfer from a heated sensor positioned in a fluid medium depends on a great number of physical processes, such as fluid velocity, thermal buoyancy, compressibility, thermal and viscous diffusivity, molecular free path etc., as well as on specific probe-related characteristics, such as sensor geometry, length-to-diameter ratio and overheating ratio. However, a satisfactory mathematical description based on physical theory does not exist.

Traditionally, the shape of CTA calibration curves for velocity measurements in incompressible, isothermal flows has been based on the early works of L.V. King on the heat transfer of infinite, circular cylinders in a uniform flow normal to the cylinder axis. This work resulted in the so-called King's Law, which affords a reasonable approximation to the overall shape of a hot-wire calibration curve:

$$Q = RI^2 = A + B \cdot \sqrt{u}$$

where  $Q$  is the heat loss (by convection) from the sensor,  $RI^2$  is the electric power dissipated in the sensor while  $A$  and  $B$  are constants derived by King.

An often used and more accurate, but purely empirical expression for the calibration curve of a hot-wire (or hot-film) anemometer, is the so-called generalized King's Law:

$$V^2 = A' + B' \cdot (U_e)^{n'}$$

where  $V$  is the output voltage of the anemometer,  $A'$ ,  $B'$  and  $n'$  are empirical constants and  $U_e$  is the so-called effective cooling velocity. For most hot-wire probes,  $n'$  is approximately 0.45 (for a velocity range in air between 0.3 and 80 m/s), but the optimum value of  $n$  depends on probe geometry and velocity range. Effective cooling velocity can in most cases be taken as the velocity component normal to the wire, but for more accurate measurements the directional sensitivity of the wire must be taken into account.

On the assumption that the basic heat transfer mechanism from the sensor is convection, the temperature dependence on the calibration curve can be shown explicitly:

$$V^2 = [A'' + B'' \cdot (U_e)^{n''}] \cdot a$$

where  $a$  is the overheating ratio and  $A''$ ,  $B''$  and  $n''$  are empirical constants nearly independent of temperature. However, it must be noted that the above assumption only holds in very special cases, e.g. for wires with a very large  $l/d$  ratio.

Many other analytical expressions have been used to model the calibration curve, even though in most cases the generalized King's Law yields remarkably good results with only 3 adjustable parameters.

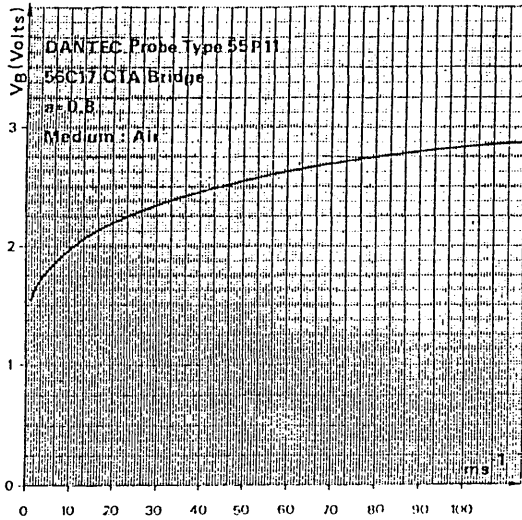


Fig. 11. Typical Calibration Curve.

### 3.4.2 TYPICAL CALIBRATION CURVE

Fig. 11 shows a typical calibration curve for the 56C17 CTA Bridge with a 5  $\mu$ m wire probe (55P11).

During calibration, the probe should be positioned in a flow with a known variable velocity, e.g. mounted on the Type 55D90 Calibration Equipment.

#### NOTE

A calibration curve for a probe connected to a 56C01/C17 CTA Bridge, is not necessarily valid if 56C17 CTA Bridge is moved to another 56C01 CTA.

## 4. MAINTENANCE AND SERVICE

Fig. 12 shows the 56C17 CTA Bridge circuit diagram. It is normally used together with the diagram in the Service Manual for the CTA system. Here it substitutes the standard plug-in. The 56C17 CTA Bridge contains few active elements. Troubleshooting on the unit alone is normally limited to a visual control or resistance measurement for locating the fault or the defective component.

## 5. TECHNICAL DATA

Top Resistance

20  $\Omega$

Bridge Ratio

1 : 20

Sensor Resistance Range

3 - 30  $\Omega$

( $R_{\text{probe}} + R_{\text{cable}}$ )

Resistance Measuring Sensitivity

0.1 V/ $\Omega$

Resistance Measurement Accuracy

Better than 5%

Overheat Setting

Any value between 3 and 30  $\Omega$

Accuracy better than 1%

(voltmeter as indicator)

Probe Cable Length

1) 5 m (4 m + 1 m probe support)

$\pm 0.5$  m

2) 20 m + 1 m probe support  $\pm 2$  m

3) 100 m + 1 m probe support  $\pm 2$  m

Amplifier Shape

Wire, Film or Flat

Probe Current

1) Bridge Supply 8 Volt:

0.21 A

( $R_{\text{probe}} + R_{\text{cable}} + R_{\text{lead}} = 7.8 \Omega$ )

2) Bridge Supply 16 Volt:

0.315 A max.

3) Resistance Measuring

approx. 0.5 mA

Maximum Bandwidth

150 kHz (with 5 m cable)

Temperature Dependent Drift

of Bridge Resistors

$\leq 100$  ppm/ $^{\circ}$ C

Temperature Range

+5 to +40 $^{\circ}$ C

## Manufacturer's Responsibility

DANTEC is responsible for the safety, reliability and performance of the equipment only if:

1. Assembly operations, extensions, readjustments, modification or repair are carried out by persons authorized by DANTEC.
2. The specific environmental conditions correspond to the requirements in the IEC 359 Group 1.
3. The equipment is used in accordance with the instructions for use.

APPENDIX G

TURBULENCE VISCOSITY ANALYSIS -

SAMPLE SPREADSHEET



A sample spreadsheet for the turbulence viscosity analysis is given in the following pages; the spreadsheet, as shown, has values appropriate to a 48 mm seal running in a narrow radial clearance housing on water.

The derivations of each column are given in Table G1.

COLUMN	PARAMETER	EQUATION NO
A	Speed [rpm]	
B	Speed [rps]	
C	Angular velocity	
D	Rotating cylinder radius	
E	Tangential velocity	
F	Kinematic viscosity	
G	Friction coefficient	7.20
H	Density	
I	Wall shear stress	7.21
J	Friction velocity	7.6
K	( ) in equation 7.26	
L	Boundary layer thickness	7.26
M	Dimensionless b.l.t.	7.5
N	Dimensionless shear stress	7.4
O	{ } in equation 7.8	
P	[ ] in equation 7.8	
Q	Dimensionless velocity gradient	7.8
R	EXP. value in equation 7.7	
S	Dimensionless viscosity	7.7
T	Effective viscosity	7.3
U	Radial clearance	
V	Effective Taylor number	7.1
W	Classical Taylor number	3.1

TABLE G1

A	B	C	D	E	F	G	
Speed [rpm]	Speed [revs/sec]	Ang. Vel [rads/sec]	Rot. Cyl. Rad. [m]	Tang. Vel. [m/s]	Kin. Visc. [m <sup>2</sup> /s]	Reynolds No.	Fric. coeff
1	0.02	0.13	0.033	0.004	0.000001	132	0.07414842
10	0.17	1.07	0.033	0.035	0.000001	1155	0.03190992
20	0.33	2.07	0.033	0.068	0.000001	2244	0.02450705
30	0.5	3.14	0.033	0.104	0.000001	3432	0.02074471
40	0.67	4.21	0.033	0.139	0.000001	4587	0.01844873
50	0.83	5.21	0.033	0.172	0.000001	5676	0.0169412
60	1	6.28	0.033	0.207	0.000001	6831	0.01572155
70	1.17	7.35	0.033	0.243	0.000001	8019	0.01476265
80	1.33	8.35	0.033	0.276	0.000001	9108	0.01402829
90	1.5	9.42	0.033	0.311	0.000001	10263	0.01336777
100	1.67	10.49	0.033	0.35	0.000001	11550	0.01280469
200	3.33	20.91	0.033	0.69	0.000001	22770	0.00971712
300	5	31.4	0.033	1.04	0.000001	34320	0.00825862
400	6.67	41.89	0.033	1.38	0.000001	45540	0.00735928
500	8.33	52.31	0.033	1.73	0.000001	57090	0.00673357
600	10	62.8	0.033	2.07	0.000001	68310	0.00625886
700	11.67	73.29	0.033	2.42	0.000001	79860	0.00588385
800	13.33	83.71	0.033	2.76	0.000001	91080	0.00557915
900	15	94.2	0.033	3.11	0.000001	102630	0.0053218
1000	16.67	104.69	0.033	3.45	0.000001	113850	0.00510173
1100	18.33	115.11	0.033	3.8	0.000001	125400	0.00491172
1200	20	125.6	0.033	4.14	0.000001	136620	0.00474333
1300	21.67	136.09	0.033	4.49	0.000001	148170	0.00459355
1400	23.33	146.51	0.033	4.83	0.000001	159390	0.00445997
1500	25	157	0.033	5.18	0.000001	170940	0.0043383
1600	26.67	167.49	0.033	5.53	0.000001	182490	0.0042275
1700	28.33	177.91	0.033	5.87	0.000001	193710	0.00412666
1800	30	188.4	0.033	6.22	0.000001	205260	0.00403317
1900	31.67	198.89	0.033	6.56	0.000001	216480	0.0039467
2000	33.33	209.31	0.033	6.91	0.000001	228030	0.0038669
2100	35	219.8	0.033	7.25	0.000001	239250	0.003792
2200	36.67	230.29	0.033	7.6	0.000001	250800	0.00372194
2300	38.33	240.71	0.033	7.94	0.000001	262020	0.00365663
2400	40	251.2	0.033	8.29	0.000001	273570	0.00359477
2500	41.67	261.69	0.033	8.64	0.000001	285120	0.00353642
2600	43.33	272.11	0.033	8.98	0.000001	296340	0.00348162
2700	45	282.6	0.033	9.33	0.000001	307890	0.00342934
2800	46.67	293.09	0.033	9.67	0.000001	319110	0.00337971
2900	48.33	303.51	0.033	10.02	0.000001	330660	0.00333281
3000	50	314	0.033	10.36	0.000001	341880	0.00328781
3100	51.67	324.49	0.033	10.71	0.000001	353430	0.00324488
3200	53.33	334.91	0.033	11.05	0.000001	364650	0.00320411
3300	55	345.4	0.033	11.4	0.000001	376200	0.00316483
3400	56.67	355.89	0.033	11.74	0.000001	387420	0.00312718
3500	58.33	366.31	0.033	12.09	0.000001	398970	0.00309129
3600	60	376.8	0.033	12.43	0.000001	410190	0.00305657
3700	61.67	387.29	0.033	12.78	0.000001	421740	0.00302318
3800	63.33	397.71	0.033	13.12	0.000001	432960	0.00299125
3900	65	408.2	0.033	13.47	0.000001	444510	0.00296026
4000	66.67	418.69	0.033	13.82	0.000001	456060	0.00293037
4100	68.33	429.11	0.033	14.16	0.000001	467280	0.00290169
4200	70	439.6	0.033	14.51	0.000001	478830	0.0028738
4300	71.67	450.09	0.033	14.85	0.000001	490050	0.00284682
4400	73.33	460.51	0.033	15.2	0.000001	501600	0.00282087
4500	75	471	0.033	15.54	0.000001	512820	0.00279557
4600	76.67	481.49	0.033	15.89	0.000001	524370	0.00277105
4700	78.33	491.91	0.033	16.23	0.000001	535590	0.00274742
4800	80	502.4	0.033	16.58	0.000001	547140	0.00272433
4900	81.67	512.89	0.033	16.93	0.000001	558690	0.0027019
5000	83.33	523.31	0.033	17.27	0.000001	569910	0.00268025

H	I	J	K	L	M	N	O
Density [kg.m <sup>3</sup> ]	Wall shr. strs.	Friction Vel.	{}	y [m]	y+	Dimless. Sh.St.	A
1000	0.00059319	0.00077019	-0.0903677	0.00089633	0.69034446	1	0.00069
1000	0.01954483	0.00442095	-0.1377531	0.00084272	3.72563565	1	0.0178
1000	0.05666603	0.0075273	-0.1571878	0.00082098	6.17977305	1	0.0448
1000	0.11218739	0.01059185	-0.1708483	0.0008058	8.53493469	1	0.0783
1000	0.17822392	0.01335005	-0.1811678	0.0007944	10.6052259	1	0.1122
1000	0.2505942	0.01583017	-0.1890567	0.00078571	12.4379799	1	0.1446
1000	0.33682634	0.01835283	-0.1962531	0.00077782	14.2752569	1	0.1785
1000	0.43535982	0.02087726	-0.2025266	0.00077097	16.0957013	1	0.213
1000	0.53430937	0.02311513	-0.20776	0.00076527	17.6892503	1	0.2436
1000	0.64647188	0.02542581	-0.212831	0.00075976	19.3174686	1	0.2749
1000	0.78428717	0.02800513	-0.2174602	0.00075474	21.1366656	1	0.3096
1000	2.31316061	0.04809533	-0.2496292	0.00072026	34.6413052	1	0.542
1000	4.46626038	0.06683009	-0.2707762	0.00069798	46.6459534	1	0.695
1000	7.00750228	0.08371083	-0.2868446	0.00068126	57.0289813	1	0.789
1000	10.0764496	0.10038152	-0.2998759	0.00066785	67.0396221	1	0.854
1000	13.4092983	0.11579852	-0.3110402	0.00065646	76.0173464	1	0.895
1000	17.229079	0.13125959	-0.3207994	0.00064659	84.8712643	1	0.925
1000	21.2498783	0.14577338	-0.3294429	0.00063791	92.9908112	1	0.945
1000	25.7365089	0.16042602	-0.3373144	0.00063007	101.078863	1	0.959
1000	30.3616472	0.17424594	-0.3445131	0.00062293	108.543663	1	0.969
1000	35.4626504	0.1883153	-0.3511133	0.00061643	116.083955	1	0.977
1000	40.6493912	0.20161694	-0.3572914	0.00061038	123.063807	1	0.982
1000	46.3032436	0.21518189	-0.3630696	0.00060476	130.132616	1	0.987
1000	52.0231414	0.22808582	-0.3684666	0.00059953	136.74348	1	0.99
1000	58.20347	0.24125395	-0.373598	0.00059458	143.444267	1	0.992
1000	64.6403841	0.25424473	-0.3784621	0.00058991	149.981256	1	0.994
1000	71.0960181	0.26663837	-0.3830582	0.00058552	156.121314	1	0.995
1000	78.0185059	0.27931793	-0.3874724	0.00058132	162.372235	1	0.996
1000	84.9203389	0.29141095	-0.3916943	0.00057732	168.236359	1	0.997
1000	92.318624	0.3038398	-0.3957151	0.00057352	174.258777	1	0.998
1000	99.6584566	0.31568728	-0.3996043	0.00056987	179.899346	1	0.998
1000	107.489581	0.32785604	-0.4033478	0.00056636	185.684475	1	0.998
1000	115.263704	0.33950509	-0.4069335	0.00056301	191.146061	1	0.999
1000	123.523738	0.35145944	-0.41042	0.00055977	196.737164	1	0.999
1000	131.996329	0.36331299	-0.413792	0.00055665	202.237325	1	0.999
1000	140.379629	0.3746727	-0.417036	0.00055365	207.438265	1	0.999
1000	149.260071	0.38634191	-0.4202029	0.00055074	212.772793	1	0.999
1000	158.016256	0.39751259	-0.4232772	0.00054792	217.803722	1	1
1000	167.307519	0.40903242	-0.4262449	0.0005452	223.005409	1	1
1000	176.439927	0.42004753	-0.4291514	0.00054255	227.897729	1	1
1000	186.10054	0.43139372	-0.4319813	0.00053998	232.943931	1	1
1000	195.615169	0.44228404	-0.4347206	0.0005375	237.726375	1	1
1000	205.650604	0.45348716	-0.4374104	0.00053507	242.645684	1	1
1000	215.505867	0.4642261	-0.4400356	0.0005327	247.293508	1	1
1000	225.92397	0.4753146	-0.4425827	0.00053041	252.112396	1	1
1000	236.127799	0.48592983	-0.445089	0.00052817	256.651368	1	1
1000	246.885971	0.49687621	-0.44754	0.00052597	261.344337	1	1
1000	257.448452	0.50739378	-0.4499227	0.00052385	265.798598	1	1
1000	268.556217	0.5182241	-0.4522715	0.00052176	270.389825	1	1
1000	279.839019	0.52899813	-0.4545725	0.00051972	274.931818	1	1
1000	290.903048	0.53935429	-0.4568129	0.00051774	279.245176	1	1
1000	302.524792	0.55002254	-0.4590248	0.00051579	283.694965	1	1
1000	313.893542	0.56026203	-0.4611949	0.00051388	287.906096	1	1
1000	325.86729	0.57084787	-0.4633108	0.00051202	292.285195	1	1
1000	337.55371	0.58099373	-0.4654026	0.00051019	296.415322	1	1
1000	349.834072	0.59146773	-0.4674575	0.00050839	300.696705	1	1
1000	361.85285	0.60154206	-0.4694634	0.00050664	304.766112	1	1
1000	374.453953	0.61192643	-0.4714488	0.00050491	308.970182	1	1
1000	387.216132	0.62226693	-0.4734013	0.00050322	313.136482	1	1
1000	399.69644	0.6322155	-0.4753094	0.00050157	317.097846	1	1

P	Q	R	S	T	U	V	W
B	du+/dy+	C	Dimless. Visc.	Eff. Visc. [ $\mu\text{m}^2/\text{s}$ ]	Rad. Clr. [ $\mu\text{m}$ ]	Turb. Ta. No.	Lam. Taylor No.
1	1	0.973798	1	0.000001	0.002	4.4616	4.4616
1.076	0.96339114	0.8665	1.04	0.00000104	0.002	279.450444	302.2536
1.447	0.81732734	0.788452	1.22	0.00000122	0.002	760.019887	1131.2136
2.156	0.63371356	0.720171	1.58	0.00000158	0.002	1042.67521	2602.9344
3.013	0.49838026	0.66505	2.01	0.00000201	0.002	1158.17985	4679.1624
3.914	0.40700041	0.619784	2.46	0.00000246	0.002	1184.15665	7166.0424
4.927	0.33743884	0.577499	2.96	0.00000296	0.002	1188.33747	10411.7376
6.026	0.28465699	0.538447	3.51	0.00000351	0.002	1157.6156	14261.94
7.056	0.24826216	0.506437	4.03	0.00000403	0.002	1133.35714	18406.74
8.164	0.21824531	0.475694	4.58	0.00000458	0.002	1116.79838	23426.4096
9.462	0.19116804	0.443548	5.23	0.00000523	0.002	1062.06605	29050.5864
20.427	0.09334018	0.263854	10.71	0.00001071	0.002	1006.31293	115428.2184
31.126	0.06225487	0.166281	16.06	0.00001606	0.002	1009.18815	260293.44
40.537	0.04814984	0.111534	20.78	0.00002078	0.002	1072.83655	463259.8344
49.572	0.03954758	0.075892	25.29	0.00002529	0.002	1129.47262	722392.7304
57.541	0.03416409	0.053732	29.28	0.00002928	0.002	1214.454	1041173.76
65.309	0.03016182	0.038224	33.15	0.00003315	0.002	1290.4058	1418055.962
72.325	0.02727583	0.027971	36.66	0.00003666	0.002	1376.49199	1849944.122
79.194	0.02493952	0.020493	40.12	0.00004012	0.002	1455.40507	2342640.96
85.484	0.02312566	0.015379	43.26	0.00004326	0.002	1546.11323	2893438.97
91.798	0.02155219	0.011507	46.4	0.0000464	0.002	1624.77816	3498082.394
97.566	0.02029097	0.008798	49.31	0.00004931	0.002	1712.82582	4164695.04
103.432	0.01915122	0.006704	52.2	0.0000522	0.002	1794.38384	4889408.858
108.851	0.01820648	0.005199	54.91	0.00005491	0.002	1879.47077	5666807.546
114.3	0.01734605	0.004018	57.65	0.00005765	0.002	1957.96358	6507336
119.629	0.01657976	0.003124	60.3	0.0000603	0.002	2036.79382	7405965.626
124.588	0.01592509	0.002467	62.8	0.0000628	0.002	2118.77753	8356119.578
129.642	0.01530901	0.00194	65.33	0.00006533	0.002	2195.53522	9370563.84
134.391	0.01477203	0.001548	67.69	0.00006769	0.002	2279.19138	10443109.27
139.271	0.01425811	0.001228	70.1	0.0000701	0.002	2353.68233	11566018.49
143.779	0.01381416	0.000989	72.39	0.00007239	0.002	2433.89674	12754378.56
148.402	0.0133867	0.000791	74.73	0.00007473	0.002	2507.0565	14000839.8
152.844	0.01300018	0.000641	76.9	0.0000769	0.002	2586.66099	15296504.28
157.314	0.01263312	0.000517	79.15	0.00007915	0.002	2659.14095	16658780.16
161.712	0.01229166	0.000419	81.37	0.00008137	0.002	2730.54633	18079157.21
165.871	0.01198531	0.000343	83.46	0.00008346	0.002	2806.3134	19547576.95
170.136	0.01168661	0.000279	85.61	0.00008561	0.002	2876.73096	21083768.64
174.246	0.01141253	0.00023	87.58	0.00008758	0.002	2956.62365	22678061.5
178.407	0.01114784	0.000188	89.67	0.00008967	0.002	3024.51398	24319236.51
182.321	0.01090982	0.000156	91.63	0.00009163	0.002	3100.18671	26029344
186.358	0.01067475	0.000129	93.65	0.00009365	0.002	3169.50177	27797552.67
190.184	0.01046113	0.000107	95.57	0.00009557	0.002	3242.02967	29611482.94
194.119	0.01025016	0.000088	97.54	0.00009754	0.002	3310.41995	31495506.24
197.837	0.01005849	0.000074	99.4	0.0000994	0.002	3384.25227	33437630.71
201.692	0.00986719	0.000061	101.33	0.00010133	0.002	3450.05002	35424316.25
205.324	0.00969349	0.000052	103.15	0.00010315	0.002	3522.79402	37482255.36
209.078	0.00952027	0.000043	105.03	0.00010503	0.002	3589.63063	39598295.64
212.641	0.0093615	0.000036	106.81	0.00010681	0.002	3660.26997	41757736.44
216.314	0.00920327	0.00003	108.65	0.00010865	0.002	3726.40854	43989591.36
219.948	0.0090519	0.000026	110.47	0.00011047	0.002	3792.28	46279547.45
223.398	0.00891274	0.000022	112.19	0.00011219	0.002	3862.18348	48611743.51
226.958	0.00877355	0.000018	113.98	0.00011398	0.002	3927.00984	51017514.24
230.327	0.00864577	0.000016	115.66	0.00011566	0.002	3997.94006	53481386.14
233.83	0.0085168	0.000013	117.41	0.00011741	0.002	4061.36369	55986337.47
237.134	0.00839863	0.000011	119.06	0.00011906	0.002	4131.55924	58566024
240.559	0.00827955	0.000009	120.78	0.00012078	0.002	4195.54535	61203811.71
243.815	0.00816943	0.000008	122.41	0.00012241	0.002	4263.25621	63881518.3
247.178	0.00805873	0.000007	124.09	0.00012409	0.002	4327.42569	66635120.64
250.511	0.00795194	0.000006	125.75	0.00012575	0.002	4391.73779	69446824.15
253.68	0.00785299	0.000005	127.34	0.00012734	0.002	4458.53626	72297286.01

APPENDIX H  
MECHANICAL SEAL  
HOUSING DESIGN GUIDE

**NON CONFIDENTIAL**

**August 1990**

**MECHANICAL SEAL  
HOUSING DESIGN GUIDE**

**N D Barnes  
R K Flitney  
B S Nau**

**BHR Group Project No 51057**

**Report prepared on behalf of:  
Mechanical Seal Group**

**Amoco (UK)  
BP International  
F Burgmann & Sons  
BW/IP International, Seals Division  
Caltex (UK)  
John Crane UK  
Durametalllic Corporation  
EG & G Ltd Sealol Division  
ICI  
Lucas Aerospace  
Morganite Special Carbons  
Shell Expro  
Turner & Newall Technology  
Weir Pumps Ltd  
with the support of:-  
Dept of Trade & Industry**

## 1. INTRODUCTION

Existing standards give little guidance on designing chambers for mechanical seals.

API 610 - 7th Edition, requires that the minimum radial clearance between the rotating member of a mechanical seal and the bore of the seal chamber shall be 3 millimetres; no further guidance for designing the seal chamber is given. DIN 24960 and ISO 3069 dimensions are currently based solely on requirements for soft packing and are widely regarded as unsatisfactory as they impose severe design constraints on mechanical seals.

None of the above takes into account the flow regimes around the seal and, consequently, the ability of the seal chamber to control the seal's environment for optimum performance.

This document provides design guidance for mechanical seal chambers, in particular, for: improved heat transfer, and vapour and solids control in the seal environs. The recommendations are based on tests with a representative range of seal-plus-housing configurations, the test conditions are summarised in Appendix B. Care is necessary when extrapolating to other configurations as flow conditions may differ.

## 2. RELATED DOCUMENTS

- (i) API 610 - "Centrifugal pumps for general refinery services". 7th Edition.
- (ii) DIN 24960: 1980 - "Mechanical seals; cavities; principal dimensions, designation and material codes."
- (iii) ISO 3069: 1974 - "End suction centrifugal pumps - Dimensions of cavities for mechanical seals and for soft packing."
- (iv) "Mechanical Seal Practice for Improved Performance", J D Summers-Smith, MEP. 1989.
- (v) "Mechanical Seal Housing Optimisation Study". BHRA Report No CR3005 1988.

### 3. SUMMARY OF METHODS

The recommendations in this Guide are based on extensive tests carried out using various flow visualisation techniques with transparent housings and seals fitted with heat transfer probes. The range of design and test parameters covered is given in Appendix B.

### 4. DEFINITION OF TERMS

#### Chamber Clearance

- the radial distance between the outside periphery of the seal and the inside of the seal chamber (Fig 1). (This is different from the API definition of "radial clearance" which refers to the distance between the shaft and the inside of the seal chamber)

#### Clearance Ratio

- the ratio of chamber clearance to seal average outside radius (Fig 1)

#### Neck Bush

- close clearance bushing fitted between seal chamber and rear of pump impeller (Fig 1)

#### Solids

- sizes refer to characteristic dimensions of granular particles.
- "fine":- particle size less than 100  $\mu$  m
- "coarse":- particle size greater than or equal to 100  $\mu$  m

#### Strake

- a rigid vane to modify the fluid flow in the seal chamber.



$\Delta T$

- temperature difference between seal surface and surrounding bulk liquid.

Seal Surface Heat Transfer Ratio (STR)

- ratio of theoretical amount of heat removed from the seal surface by forced convection to theoretical amount of heat generated at seal interface, for the required  $\Delta T$ . These are not necessarily equal for a non-optimised design.

Flush Transfer Ratio (FTR)

- ratio of predicted amount of heat removed from the seal chamber by external flushing to heat generated at seal interface, for the required  $\Delta T$ .

## 5. TECHNICAL BACKGROUND

Effective removal of heat, vapour, gas and solids from around the faces of a mechanical seal is essential for successful operation. These transfer processes rely on the detail of the flow fluid flow within the seal chamber, which in turn is influenced by chamber geometry, seal geometry and external injection or circulation. Frequently, the requirements are conflicting and the final design will be a compromise.

A 'good' general purpose chamber geometry will create beneficial flow conditions with a wide range of seal designs.

In this Guide, two alternative approaches to chamber design are presented:

- (i) Recommended Practice : this is the best available technology.
- (ii) Alternative Practice : this is for use when practical constraints prevent application of the Recommended Practice.

To understand the basis of the above it is necessary to appreciate certain aspects of the technical background.

### 5.1 Fluid Flow Behaviour in Seal Chamber

Flow in seal chambers is highly structured due to a combination of circumferential rotation, driven by the rotating seal and shaft, and axial recirculation which may be influenced by one or more of the following:

- (i) rotating radial planes of the seal assembly.
- (ii) stationary end walls of the chamber.
- (iii) rotating rear face of the pump impeller (in absence of a neck bush).
- (iv) Taylor vortices.

The flow pattern is further modified if fluid is injected into (or recirculated through) the chamber, as for flushing, cooling etc.

Pumping rings will also have a major effect on chamber flows but are not considered here, being a specialised topic.

More detail of Taylor vortex flow is given in Appendix A.

## 5.2 Injection Flow Behaviour

Injected flow has three modes of action:

- (i) Exchange of the fluid in the chamber; removing hot fluid, solids or gas and replacing with cool or clean fluid.
- (ii) Highly localised modification of the flow, and state of the fluid, in the immediate vicinity of the edge of the sealing interface.
- (iii) Global modification of the seal chamber flow pattern.

Mode (i) is a 'neutral' fluid exchange process which does not materially affect the chamber flow. Although usually of secondary importance in practice, it is often assumed as a basis for calculation of flow requirements for removal of heat from the chamber.

When a jet of injected flow is directed at the edge of the sealing interface mode (ii) results. In the case of heat transfer this has two effects, it increases the local shear rate so enhancing the local heat transfer coefficient; secondly, cool fluid gains close proximity to the hottest part of the seal, this raises the temperature differential enhancing the local heat transfer from the seal. Erosion of the seal is a potential problem with mode (ii). Thermal distortions will also be affected.

Mode (iii) will normally occur in some degree but the state of the art does not yet permit its use as a means of controlling chamber flow patterns.

### 5.3 Heat Flow

Frictional heat generated at the sealing interface is dispersed by a complex of processes, generally in the following sequence:

- (i) Conduction through the body of the seal to exposed wetted surfaces.
- (ii) Transfer from exposed wetted surfaces to an adjacent fluid boundary layer.
- (iii) Forced convection from boundary layers to the bulk chamber fluid.
- (iv) Transfer from the fluid to wetted walls of the seal chamber.
- (v) Conduction through the chamber walls to the main pump body, with radiation and convection to the surroundings.
- (vi) Transport to an external heat sink, such as a heat exchanger; or drain, if external cooling facilities are provided; or into the pumped fluid if there is fluid flow to the pump volute from the seal chamber.

All the above, except (i) and (v), depend on details of the fluid flow in the seal chamber.

The sealing interface must be maintained below a prescribed temperature to prevent interface fluid boiling, which is likely to cause loss of lubrication and consequent seal failure. It is therefore necessary to maintain the bulk fluid at or below a certain temperature determined by (a) the temperature at which interface boiling would occur and (b) the Required Temperature Margin,  $\Delta T_{\text{required}}$ , necessary to drive the frictional heat from the sealing interface to the chamber fluid.

It is possible that the predicted heat transfer at the seal surface (step ii) is insufficient to permit the seal to operate within this Required Temperature Margin. A design parameter,  $S_{TR}$ , is therefore introduced which indicates the ratio of the theoretical heat transfer at the seal

surface  $\dot{q}$  to that required; the latter is equal to the interface heat generation  $H_s$ , thus:

$$\text{STR} = \frac{\text{(theoretical heat transfer at seal surface)}}{\text{(interface heat generated)}} = \dot{q}/H_s \quad (1)$$

**[Note:** STR is not  $(\Delta T_{\text{available}})/(\Delta T_{\text{required}})$ , in fact:

$$\text{STR} = \frac{(\Delta T_{\text{required}} - \Delta T_{\text{cond}})}{(\Delta T_{\text{available}} - \Delta T_{\text{cond}})}$$

where  $\Delta T_{\text{cond}}$  is the temperature differential within the body of the seal, due to conduction alone]

A similar ratio can be defined to represent the heat transported from the seal chamber by flow leaving the seal chamber,  $\dot{q}_f$ , (to an external cooling loop for example).

$$\begin{aligned} \text{FTR} &= \frac{\text{(Heat transported from seal chamber)}}{\text{(interface heat generated)}} \\ &= \dot{q}_f/H_s \quad (2) \end{aligned}$$

## 6. RECOMMENDED PRACTICE

An optimum housing should be designed to remove heat efficiently from the seal and control gas or vapour and solids if they are present.

Of the seal chamber geometries tested, the 45° flare (Fig 2) is consistently superior to other designs.

The main advantages of this housing are:-

- (i) Efficient removal of vapour and gas from around the seal.
- (ii) Enhanced and more uniform cooling of the seal, due to good gas/vapour purging, thereby increasing the available temperature margin.
- (iii) Ancillary flushing equipment may be dispensed with in certain conditions, thereby reducing costs and avoiding seal ring erosion due to a flush.
- (iv) Equally effective with all seal designs.

The 'Procedure' for the Recommended Practice deals lists the steps produce a housing for a specific duty. The Procedure is supported by explanatory text in sections 6.1 to 6.3. Some worked examples are given in Appendix C.

**PROCEDURE FOR RECOMMENDED PRACTICE**

- (i) Assemble the required data using the Duty Specification Table shown in Table 1. Calculate  $\dot{q}$ ,  $\dot{q}_f$ ,  $H_s$  (equations 3-5 respectively). (If the chamber is dead-ended then  $\dot{q}_f$  is not applicable.) If the flush flowrate is not known, assume a design value of 5 litres/minute as a starting value.
- (ii) Outline the seal housing using the dimensions shown in Fig 2.
- (iii) Assess the heat transfer requirements of the seal for :-
- option of running dead-ended.
  - necessity for flush.
  - minimum flush flowrate (if required).

The procedure for this is:-

- (a) Calculate the Heat Transfer Ratio (STR) using equation 1.
  - (b) If  $STR > 1$ , the housing can be run dead-ended if desired.
  - (c) If  $STR \leq 1$ , an external flush is advised. Compute FTR using equation 2. If  $TR > 1$ , the flushing system is adequate. If  $FTR < 1$ , compute the minimum flush flowrate using equation 6.
- (iv) If there is a likelihood of gas or vapour being present at the seal then an external flush is advised in some cases irrespective of the heat transfer requirements. Guidance on this is given in Table 2.
- (v) If solids are present in the chamber fluid in high concentrations (>10% w/w) flushing and strakes may be needed - consult Table 2 for the best arrangement.

## 6.1 HEAT TRANSFER

Quantitative design is possible using formulae for  $\dot{q}$ , the theoretical seal surface heat transfer, at the exposed surface of the seal;  $\dot{q}_f$ , the heat transported from the chamber when injection is applied; and  $H_s$ , the heat generation at the sealing interface.

The expressions for  $\dot{q}$ ,  $\dot{q}_f$  and  $H_s$  are as follows:-

$$\dot{q} = 3.65 \times 10^{-7} k^{0.6} c_p^{0.4} \rho^{0.4} \nu^{-0.3} b^{0.05} d^{1.65} l N^{0.7}, \text{ Watts} \quad (3)$$

$$\dot{q}_f = 8.33 \times 10^{-5} \rho c_p Q, \text{ Watts} \quad (4)$$

$$H_s = 2.44 \times 10^{-3} p_f^{0.67} d^{1.8} N^{0.8}, \text{ Watts} \quad (5)$$

where:  $k$  - thermal conductivity of process liquid (W/mK)

$c_p$  - specific heat capacity of process liquid (J/kgK)

$\rho$  - density of process liquid (kg/m<sup>3</sup>)

$\nu$  - kinematic viscosity of process liquid (mm<sup>2</sup>/s)

$b$  - chamber clearance (mm)

$d$  - seal outside diameter (mm)

$l$  - chamber length (mm)

$N$  - speed (rpm)

$Q$  - flush flowrate (l/min)

$p_f$  - sealed pressure differential (MPa)



Equations 3 and 5 are empirical (see Appendix E), Equation 4 is a simple physical expression and assumes a temperature rise, inlet to outlet, of 5°C (higher values are sometimes proposed but may not be achievable).

Evaluating  $\dot{q}$ ,  $\dot{q}_f$  and  $H_s$  and substituting in equations (1) and (2) yields HTR and TR.

For satisfactory dead-ended running, STR should be greater than unity. If STR is less than unity the chamber will be unable to maintain thermal equilibrium and an external flush is necessary. Note that the expression for STR assumes that there is no gas or vapour which might impair the convective heat transfer process.

For a flushed seal chamber, from thermal considerations, TR should be greater than unity. The minimum flowrate ( $Q_{\min}$ ) for  $TR > 1$  is calculated using the following equation.

$$Q_{\min} = 29.4 p_f^{0.67} d^{1.8} N^{0.8} / \rho c_p \quad (\text{see Appendix E}) \quad (6)$$

Check for parity with the actual flowrate (if known).

Appendix C contains some worked examples illustrating the application of these equations.

## 6.2 Control of Gas and Vapour

Quantitative design is not yet possible for the handling of gas and vapour in the sealed fluid. The Recommended Practice is explained below.

The 45° flared housing without a neck bush is intrinsically self-purging and self-venting. Under most conditions any gas or vapour in the area around the seal is rapidly removed; flushing is generally not necessary.

An exception to this rule, when flushing is advised is when the pumped fluid has a kinematic viscosity in excess of 10 mm<sup>2</sup>/s (10cS).

For control of gas and vapour it is important to vent the chamber at start-up. This is not necessary for a flared housing where there is an obvious vent flow path from the seal chamber into the process stream.

### 6.3 Control of Solids

Quantitative design is not yet possible for the handling of solids in the sealed fluid. The Recommended Practice is set out below.

Where abrasive solids are present in large quantities (>10% w/w), strong vortex action may be a disadvantage, due to the possibility of concentrating erosive wear. In this case, vortex modifiers or strakes can be used particularly with coarser particles. Strakes may be axial (Fig 3) or helical (Fig 4); the latter to be used if gas and/or vapour are present in addition to the solids. The helical strakes are to be handed so that a screw turned in the direction of shaft rotation would advance towards the seal faces and away from the impeller end of the seal chamber. The strake angle should be 30° to the shaft axis.

If fine solids are present in relatively high concentrations (> 10% by volume) then a clean external flush is recommended for satisfactory operation.

## 7. ALTERNATIVE PRACTICE

Where a 45° flared chamber cannot be implemented the next best, but less effective, alternative is a cylindrical housing with a radial clearance tailored to give beneficial flow conditions.

Several distinct flow regimes occur in cylindrical annular clearances with a rotating inner member. The behaviour of gas, vapour and solids within the seal chamber is governed by the nature of these flow regimes.

The flow regimes are in turn dictated by a dimensionless parameter known as the Taylor number,  $Ta$ , the significance of which is outlined in Appendix A. Sections 7.1, 7.2 and 7.3 explain the Alternative Practice for heat transfer, control of gas and vapour, and control of solids respectively.

The 'Procedure' for Alternative Practice lists the requirements to produce a housing for the duty in question which represents the best alternative solution - in some cases this is a near-optimum solution. Some worked examples are given in Appendix C.

## PROCEDURE FOR ALTERNATIVE PRACTICE

- (i) Assemble the required data using the Duty Specification Table shown in Table 1. Calculate  $\dot{q}$ ,  $\dot{q}_f$ ,  $H_s$  (equations 3-5 respectively). (If the chamber is dead-ended then  $\dot{q}_f$  is not applicable). Where the flush flowrate is not known, assume a starting value of 5 litres/minute.
- (ii) Determine the chamber clearance to give a strong vortex flow. This may be achieved by using selected ranges of Taylor number. (Refer to Appendix A for further details).

The chamber clearance,  $b$  is determined from the formula given below:-

$$b = 5.67 \left\{ \frac{v^2 Ta}{d N^2} \right\}^{1/3} \quad (7)$$

[Units as shown in the Duty Parameters Table (Table 1)]

The preferred ranges of Taylor number, where vortex flows are strongest and most influential, are as follows:-

$$\text{Range 1} \quad 2 \times 10^3 < Ta < 10^4$$

$$\text{Range 2} \quad 10^6 < Ta < 10^7$$

$$\text{Range 3} \quad Ta > 10^9$$

Substitute extreme values of Taylor number for each range into equation 7. This yields the maximum and minimum chamber clearances for ranges 1 and 2 and the minimum chamber clearance for range 3. The chosen chamber clearance should fall into one of these ranges subject to the following constraints.

- (a) The chamber clearance should be greater than 10mm to avoid gas choking of the seal (see step vi).
- (b) The chamber clearance should be less than 80mm. Chamber clearances in excess of 80mm have not been evaluated in the

background work to the Guide and flow behaviour might be unpredictable.

(iii) Assess the heat transfer requirements of the seal for:

- running dead-ended
- requirement for flush
- minimum flush flowrate (if required).

The procedure for this is:

- (a) Calculate the Heat Transfer Ratio (STR) using equation 2.
  - (b) If  $STR > 1$ , the housing can be run dead-ended if desired.
  - (c) If  $STR \leq 1$ , an external flush is advised. Compute the FTR equation 2. If  $FTR > 1$ , the flushing system is adequate. If  $FTR < 1$ , compute the minimum flush flowrate using equation 6.
- (iv) If there is a likelihood of gas or vapour being present at the seal then an external flush is advised in some cases irrespective of the heat transfer requirements. Guidance on this is given in Table 3.
- (v) If solids are present in the pumped fluid in high concentrations ( $> 10\%$  w/w) flushing and strakes may be needed - consult Table 3 for the best arrangement.
- (vi) If the chamber clearance is constrained, by considerations outside the scope of this document, to be less than 10 mm, a flush of more than 5 litres/min is strongly advised. This is to avoid gas choking of the chamber which can seriously degrade seal performance.

### 7.1 Heat Transfer

The procedure for designing for optimum heat transfer with the Alternative Practice is the same as given in section 6.1, using the empirical ratios STR and FTR. It should be remembered, however, that the equations given in 6.1 assume that gas and/or vapour, which may impair heat transfer, are absent from the seal chamber. This condition is more difficult to ensure with a cylindrical housing (see Section 7.2).

### 7.2 Control of Gas and Vapour

Quantitative design is not yet possible for the handling of gas and vapour in the sealed fluid. The Alternative Practice is set out below. Vortex flows are known to be good at handling gas or vapour by "locking" bubbles in the vortex cores away from the seal faces. Control of gas and vapour can be best effected by designing for vortex flows. However there are limits to the extent of this control; in these cases an external flush should be used.

- (i) As a rule, chambers with clearances of less than 10 mm are prone to gas build-up which ultimately destroys the vortex flow.
- (ii) If the pumped fluid has a kinematic viscosity in excess of  $10 \text{ mm}^2/\text{s}$  (cS), emulsification may be a problem at higher speeds. The heat transfer properties of emulsions are not well understood and it is wise to flush the seal face with liquid.
- (iii) If the pumped fluid contains a large amount of solids (> 10% w/w) consult Section 7.3 for guidance.

Control of gas and vapour will also be helped by venting the chamber at start-up.

### 7.3 Control of Solids

Quantitative design is not yet possible for the handling of solids in the sealed fluid. The Alternative Practice is as follows.

Where solids are present in large quantities ( $> 10\%$  w/w), strong vortex action may be a disadvantage, due to the possibility of concentrating erosive wear. In this case, vortex modifiers or strakes can be used particularly with coarser particles.

Strakes may be axial (Fig 8) or helical (Fig 9) the latter to be used if gas and/or vapour are present in addition to the solids.

If fine solids are present in relatively high concentrations ( $>10\%$  by volume) then a clean external flush is recommended for satisfactory operation.

NDB/gmh/51057-R/jmw

3.7.90

List of Figures

- Table 1. Duty Parameters Table.
- Table 2. Operation table for 45° flared housing (Recommended Practice).
- Table 3. Operation table for parallel housings (Alternative Practice).
- Fig. 1. Definition of geometric parameters.
- Fig. 2. 45° flared housing.
- Fig. 3. Axial strakes - 45° flared housing.
- Fig. 4. Helical strakes - 45° flared housing.
- Fig. 5. Chamber clearance versus seal diameter,  $10^3 < Ta < 10^4$
- Fig. 6. Chamber clearance versus seal diameter,  $10^6 < Ta < 10^7$
- Fig. 7. Chamber clearance versus seal diameter,  $Ta > 10^9$
- Fig. 8. Axial strakes - parallel housing.
- Fig. 9. Helical strakes - parallel housing.
- 
- Fig. A1. Taylor vortex flow.
- Fig. A2. Turbulent vortex flow.
- Fig. A3. Flow regime versus Taylor number.
- Fig. A4. Flow regime structures.
- Fig. A5. Probable flow regimes in mechanical seal chambers.



Table B1. Seal/housing test combinations.

Table C1. Duty parameters Table Example 1.

Table C2. Duty Parameters Table Example 2.

Table C3. Duty Parameters Table Example 3.

\* Plant = WSR Naptha Splitter/Stabiliser : Duty = Naptha Splitter Reheater  
Furnace

Motor or Free End	Installed Life	Running Life	Reason
(HE)	8280	1665	leakage
(HE)	3816	2952	inspection
(HE)	1944	720	leakage
(HE)	6312	5352	leakage
(HE)	11712	10800	leakage
(FE)	8280	1665	leakage
(FE)	3816	2952	inspection
(FE)	4992	3096	leakage
(FE)	1296	432	leakage
(FE)	11712	10800	leakage
(FE)	168	168	leakage

seal components reused

\* Plant = Crude Unit + Sour Water Shipping : Duty = Desalter Water Pump

Motor or Free End	Installed Life	Running Life	Reason
(HE)	29448	27600	pump repair
(HE)	3288	528	leakage
(HE)	744	42	leakage
(HE)	5424	408	leakage
(HE)	480	432	leakage
(FE)	12096	10800	pump repair
(FE)	4032	576	pump repair

seal components reused

\* Plant = WSR Naptha Splitter/Stabiliser : Duty = HCAD Slop Oil

Installed Life	Running Life	Reason
33960	28392	leakage
10704	9288	leakage
6840	3624	leakage
792	744	leakage
840	840	leakage

seal components reused

\* Plant = Boiler Utilities : Duty = Vacuum Residue

Installed Life	Running Life	Reason
3000	1968	bearing failure
5112	3816	leakage
1464	48	bearing failure
No information		
984	912	leakage
2736	1872	leakage
No information		
72	48	seal and bearing failure

Seal components reused

Table 2.1 (a) Seal life variability (Flitney and Nau, 1985)

\* Plant = Gas Treating/Sulphur Recovery : Duty = Amine Stripper Reflux

Installed Life	Running Life	Reason
2590	576	pump failure
3552	0	pump report
3760	3528	leakage
2928	1944	leakage mods to seal to be lined
312	312	leakage
312	312	leakage
11184	5184	leakage

\* Plant = Vacuum Distillation Unit : Duty = Vacuum Bottoms

Motor or Free End	Installed Life	Running Life	Reason
(ME)	4180	4180	leakage
(ME)	4584	2688	inspection
(ME)	720	216	leakage
(ME)	13488	4224	inspection plant off in 1983
(ME)	4584	2688	inspection
(ME)	720	216	leakage
(ME)	13488	4224	inspection plant off in 1983
(FE)	8760	5616	inspection
(FE)	13488	4224	inspection
No information			
(FE)	384	384	leakage

\* Plant = Vacuum Distillation Unit : Duty = Vacuum Bottoms

Installed Life	Running Life	Reason
7510	4560	bearing change
4320	1392	leakage
4728	3192	bearing failure
9912	2976	bearing failure
2640	504	leakage

\* Plant = FCCU/GCH : Duty = Debutaniser Reflux + Overhead Product

Installed Life	Running Life	Reason
720	720	leakage
240	216	leakage plant stopped 2-3 hours
1248	888	leakage
192	20	pump vibrating
9720	696	inspection plant off for 1982
1632	216	leakage
336	168	leakage
144	24	leakage

\* Plant = FCCU/GCU : Duty = Reactor Recycle Overhead

Installed Life	Running Life	Reason
2930	2930	plant shutdown
3720 or	1944	leakage
155	81	
1128	1128	leakage
1800	120	leakage
792	576	leakage

Table 2.1 (b) Seal life variability (Flitney and Nau, 1985)

\* Plant = Distillate Hydrotreating Unit : Duty = Debutanizer Reflux + Overhead Product

Motor or Free End	Installed Life	Running Life	Reason
(NE)	2210	2210	leakage
No information			
(NE)	6480	6336	pump vibration
(NE)	1920	1920	leakage
(FE)	16870	16870	leakage
(FE)	6480	6336	pump vibration
(FE)	264	264	leakage
(FE)	1440	1440	leakage

\* Plant = Vacuum Distillation Unit : Duty = Visbreaker Charge

Motor or Free End	Installed Life	Running Life	Reason
(FE)	8784	6000	leakage
(FE)	172	86	leakage
(FE)	576	504	leakage
(FE)	624	624	leakage
(FE)	720	696	leakage
(FE)	1032	984	leakage
(FE)	3528	2736	leakage
(FE)	864	672	leakage
(FE)	1200	1056	leakage
(FE)	5112	5112	leakage
(FE)	1728	1440	leakage
(FE)	1296	312	leakage
(FE)	408	408	leakage
(FE)	1008	600	leakage
(ME)	3576	2856	leakage
(NE)	3696	3000	leakage
(ME)	3000	2832	leakage
(ME)	3504	2736	leakage
(NE)	456	384	leakage
(NE)	1200	984	leakage
(NE)	288	288	bearing failure
(NE)	5112	5112	inspection
(NE)	1728	1440	leakage
(NE)	1296	312	inspection
(ME)	1104	960	leakage
			reconditioned seal
			seal components reused

Table 2.1 (c) Seal life variability (Flitney and Nau, 1985)

\* Plant = Naptha Hydrotreater : Duty = Reactor Lead

Motor or Free End	Installed Life	Running Life	Reason
(ME)	16580	15600	leakage
(NE)	1824	1464	leakage
(NE)	1680	1056	plant shut-down seal components re-used
(ME)	2760	1416	leakage
(ME)	3360	3360	leakage
(NE)	11688	11376	plant shut-down
(ME)	3096	2040	leakage
(FE)	18720	16800	plant shut-down seal components re-used
No information			
(FE)	2688	1260	leakage
(FE)	8976	8688	plant shut-down
(FE)	1632	624	leakage

\* Plant = Platformer and LFC : Duty = Platformer Charge

Motor or Free End	Installed Life	Running Life	Reason
(NE)	18648	16000	bearing failure
(NE)	135	135	pump repair
(NE)	8880	7512	seal over-haul
(ME)	10560	9744	plant shut-down
(ME)	6660	6456	leakage
(FE)	18816	16000	pump repair
(FE)	8712	7344	bearing failure
No information			
(FE)	4152	4152	plant shut-down
(FE)	6660	6456	leakage

\* Plant = Vacuum Distillation Unit : Duty = Furnace Recycle

Installed Life	Running Life	Reason
8712	6720	leakage
1704	1392	plant shut-down seal components re-used
3024	1224	pump repair
0	0	leakage failed on start up
24	2	leakage
24	0	leakage
0	0	leakage modifications to pump
No information		
5904	1128	leakage

\* Plant = Vacuum Distillation Unit : Duty = Top Pump Around

Installed Life	Running Life	Reason
6936	4152	leakage
960	960	plant shut down } seal components re-used
2640	792	leakage } seal components re-used
696	696	leakage
2592	2616	leakage
No information		
2040	720	inspection
744	240	leakage

Table 2.1 (d) Seal life variability (Flitney and Nau, 1985)

\* Plant = Crude Tapping Unit : Duty = Intermediate Reflux

Installed Life	Running Life	Reason
5832	3600	pump repair
4440	1896	leakage
3624	3288	pump repair
14112	1224	leakage
1776	528	leakage

Plant Ref. No. 2C-12 Seal Type R3200M-OR

Installed Life	Running Life	Reason
33216	17520	leakage
2904	1368	leakage
12552	576	leakage

\* Plant = Visbreaker : Duty = Bottoms Pump

Installed Life	Running Life	Reason
5280	4800	leakage
7560	1152	leakage
528	384	leakage
840	312	pump repair
240	216	pump repair
No information		
312	48	leakage
1200	1080	leakage
240	240	leakage
5016	4776	leakage
2520	1392	leakage
1992	696	leakage
2112	1896	leakage

\* Plant = Platformer and LPC : Duty = Splitter Column Reflux

Installed Life	Running Life	Reason
2280	2280	bearing failure
1560	1560	bearing failure
4536	2040	leakage
8280	8280	leakage
384	360	bearing failure
8040	7536	leakage

\* Plant = Crude Tapping Unit : Duty = Reduced Crude

Motor or Free End	Installed Life	Running Life	Reason
(ME)	2540	2540	plant shutdown
(ME)	7248	5184	leakage
(ME)	11304	1944	inspection
(FE)	2540	2540	plant shutdown
(FE)	5016	2472	leakage
(FE)	984	984	leakage
(FE)	106	104	leakage
(FE)	11304	1944	inspection

Table 2.1 (e) Seal life variability (Flitney and Nau, 1985)

### REASONS FOR REMOVAL - Company 3

	Phase 1 %	Phase 2 %
Leakage	78	63
Seal failure	1	0
Other seal failed	1	1
Seal and bearing failure	2	3
Bearing replacement	6	15
Unscheduled pump maintenance	9	11
Routine Maintenance	3	5
Plant Shutdown	-	1
Other	-	0

Table 2.2 Reasons for outage - Company No.3. (Flitney & Nau, 1989)




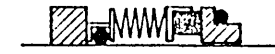

Seal Type	Designation	Sectional View
Exposed single spring	A	
Shrouded single spring	B	
Multiple spring	C	
Rotating metal bellows	D	
Stationary metal bellows	E	

Table 4.1 Test seals - 48 mm

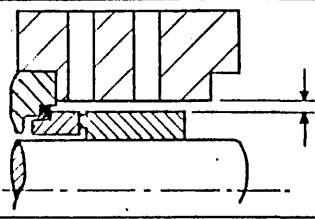
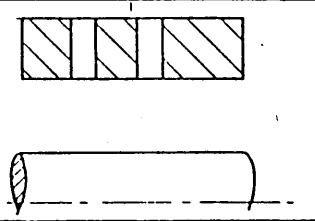
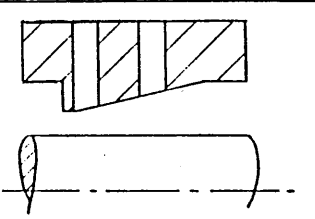
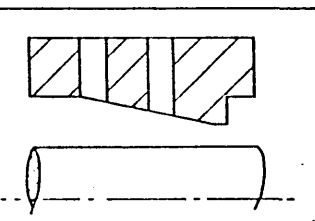
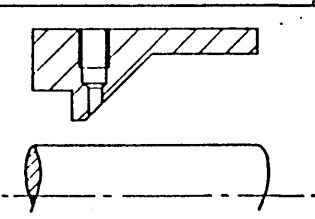
Housing name	Housing No.	
Narrow radial clearance	1 - radial ports 3 - tangential ports	
Wide radial clearance	2 - radial ports 4 - tangential ports	
Positive shallow flare	5	
Negative shallow flare	6	
Positive wide flare	7	

Table 4.2 Test housing - 48 mm



SEAL TYPE	SHAFT DIAM. [mm]	HOUSING							
		Cylindrical - radial clearance [mm]			Flared - flare angle				
		2	2.5	7.5	12	20	+12°	-12°	+45°
A	48	W: abcdefg G: abcdeg S: agjklm	W: abcdefg G: abcdeg S: agjklm	W: abcdefg G: abcdeg S: agjklm	W: abcdefg G: abcdeg S: agjklm	W: abcdefg G: abcdeg S: agjklm	W: abcdeg G: abcdeg S: agjklm	W: abcdeg G: abcdeg S: agjklm	W: abcg G: abcg S: aghjklm
B	48	W: abcdefgi G: abcdeg S: agjklm	W: abcdefgi G: abcdeg S: agjklm	W: abcdefgi G: abcdeg S: agjklm	W: abcdefgi G: abcdeg S: agjklm	W: abcdefgi G: abcdeg S: agjklm	W: abcdegi G: abcdeg S: agjklm	W: abcdegi G: abcdeg S: agjklm	W: abcgi G: abcg S: aghjklm
B	100	W: abcg	W: abcg	W: abcg	W: abcg	W: abcg	W: abcg	W: abcg	W: abcg
C	48	W: abcdefgi G: abcdeg S: agjklm	W: abcdefgi G: abcdeg S: agjklm	W: abcdefgi G: abcdeg S: agjklm	W: abcdefgi G: abcdeg S: agjklm	W: abcdefgi G: abcdeg S: agjklm	W: abcdegi G: abcdeg S: agjklm	W: abcdegi G: abcdeg S: agjklm	W: abcgi G: abcg S: aghjklm
D	48	W: abcdefg G: abcdeg S: agjklm	W: abcdefg G: abcdeg S: agjklm	W: abcdefg G: abcdeg S: agjklm	W: abcdefg G: abcdeg S: agjklm	W: abcdefg G: abcdeg S: agjklm	W: abcdeg G: abcdeg S: agjklm	W: abcdeg G: abcdeg S: agjklm	W: abcg G: abcg S: aghjklm
D	100	W: abcg	W: abcg	W: abcg	W: abcg	W: abcg	W: abcg	W: abcg	W: abcg
E	48	W: abcdefg G: abcdeg S: agjklm	W: abcdefg G: abcdeg S: agjklm	W: abcdefg G: abcdeg S: agjklm	W: abcdefg G: abcdeg S: agjklm	W: abcdefg G: abcdeg S: agjklm	W: abcdeg G: abcdeg S: agjklm	W: abcdeg G: abcdeg S: agjklm	W: abcg G: abcg S: aghjklm

KEY:

T: test fluid  
W: water  
G: glycerol  
S: solids

Variables

a - Plan A  
b - Plan B  
c - Plan C  
d - Plan D  
e - Plan E  
f - tangential injection  
g - with/without neck-bush  
h - strokes  
i - heat transfer measurement  
j - carbon dust  
k - silica dust  
l - sand particles  
m - iron oxide dust

Table 5.1 Seal/housing combinations and variables

Reynolds No.	1/ntb/B	1/ntb/D	1/tb/B	1/tb/D	2/ntb/B	2/ntb/D	2/tb/B	2/tb/D
0	0	0	0	0	0	0	0	0
1710	3178	5902	1362	5448	4540	4540	9080	9080
5700	7264	8172	4994	3178	9080	9080	13620	13620
11400	10442	11350	6810	6810	13620	13620	18160	18160
22800	15890	15890	10442	11350	18160	18160	24970	24970
45600	24516	24970	16798	16798	27240	24970	31780	31780
68400	31326	32688	19976	21338	34050	31780	38590	38590
91200	38136	39952	23608	25424	38590	38590	43130	43130
114000	44492	46308	26332	27694	45400	43130	47670	47670
142500	51756	53118	30872	32234	49940	47670	52210	52210
171000	57658	60382	32234	34504	54480	52210	56750	56750
199500	63560	65376	35412	37682	56750	56750	59020	61290
228000	68566	61744	35866	37682	61290	59020	61290	63560
256500	65376	74456	36320	40406	61290	61290	63560	65830
285000	69462	74910	34958	39498	63560	63560	63560	65830
313500	59928	79450	37682	42222	65830	65830	63560	68100
342000	71732	82628	33596	41768	65830	65830	61290	68100
399000	61744	89892	33596	45400	65830	68100	61290	68100
456000	83082	90800	28148	44038	61290	63560	56750	63560
513000	80358	93070	0	42222	52210	59020	52210	61290
570000	73548	93070	0	0	45400	56750	38590	49940

3/ntb/B	3/ntb/B/ccw	3/ntb/D	3/ntb/D/ccw	3/tb/B	3/tb/B/ccw	3/tb/D	3/tb/D/ccw	5/ntb/B
0	0	0	0	0	0	0	0	0
6810	11350	11350	13620	9080	11350	11350	9080	11350
15890	15890	13620	18160	18160	15890	15890	15890	15890
20430	20430	18160	22700	24970	24970	22700	22700	22700
27240	27240	27240	31780	34050	34050	34050	34050	29510
34050	38590	38590	43130	38590	52210	47670	52210	40860
38590	47670	43130	54480	45400	65830	54480	65830	52210
40860	54480	47670	61290	49940	74910	63560	79450	61290
45400	61290	52210	70370	59020	83990	68100	88530	68100
49940	70370	59020	77180	79450	90800	88530	99880	77180
52210	72640	63560	81720	93070	97610	104420	108960	83990
54480	77180	68100	88530	97610	99880	113500	113500	88530
61290	77180	74910	93070	104420	95340	120310	115770	95340
65830	77180	81720	95340	111230	95340	131660	122580	99880
65830	68100	83990	93070	111230	90800	136200	124850	102150
65830	68100	83990	93070	111230	90800	140740	129390	104420
65830	45400	88530	90800	111230	79450	147550	136200	106690
61290	47670	90800	95340	120310	56750	158900	131660	108960
54480	29510	95340	81720	111230	56750	165710	131660	118040
49940	27240	95340	68100	102150	52210	165710	124850	111230
40860	11350	95340	59020	97610	27240	165710	102150	115770

5/ntb/D	5/tb/B	5/tb/D	7/ntb/B	7/ntb/D	7/tb/B	7/tb/D
0	0	0	0	0	0	0
2270	6810	0	9080	18160	2724	7718
9080	11350	2270	13620	22700	5902	9534
15890	13620	6810	22700	31780	9534	13166
27240	18160	13620	36320	43130	14982	16798
38590	24970	20430	52210	56750	23154	23608
34050	29510	24970	18160	70370	30418	29964
40860	34050	27240	24970	79450	37228	37682
47670	38590	31780	29510	88530	43130	44038
54480	40860	36320	36320	97610	51756	51756
61290	45400	38590	43130	108960	58112	58566
65830	47670	40860	45400	115770	64468	64014
70370	49940	43130	49940	122580	69916	68554
74910	49940	45400	54480	129390	73548	74456
77180	52210	47670	56750	133930	79450	78088
81720	54480	47670	59020	140740	83082	82628
86260	52210	49940	59020	143010	87168	87168
88530	49940	49940	61290	147550	91254	93070
90800	45400	45400	61290	147550	93524	96248
99880	38590	45400	52210	138470	96702	99426
99880	31780	40860	47670	127120	99880	101696

Table 6.1 Heat Transfer Coefficient versus Reynolds Number

HOUSING TYPE	HOUSING NUMBER	LIQUID VISCOSITY [mm <sup>2</sup> /s]	SPEED [rpm]				FIGURE NUMBER	DISCUSSION SECTION NO. [CHAPTER 8]
			LAMINAR FLOW	TAYLOR-VORTEXES	TURBULENT FLOW	HIGH-SPEED VORTEXES		
<i>Narrow radial clearance</i>	1	1	10 to 25	25 to 200	200 to 600	600 to 5000	7.10	8.1.1(i)
	1	15	10 to 350	350 to 800	-	800 to 5000	7.11	8.1.1(ii)
	1	50	10 to 1100	1100 to 3000	-	3000 to 5000	7.12	8.1.1(ii)
	1	150	10 to 3500	3500 to 5000	-	-	7.13	8.1.1(ii)
	100-1	1	-	10 to 30	30 to 500	500 to 5000	-	7.14
<i>Wide radial clearance</i>	2	1	-	-	-	10 to 700	7.15	8.2.1(i)
	2	15	10 to 25	25 to 60	-	60 to 5000	7.16	8.2.1(ii)
	2	50	10 to 80	80 to 200	-	200 to 5000	7.17	8.2.1(ii)
	2	150	10 to 250	250 to 600	-	600 to 5000	7.18	8.2.1(ii)
	100-2 100-3	1 1	- -	- -	- -	- -	10 to 1300 10 to 300	7.19 7.20

Table 7.1 Predicted Flow Regimes as a function of Speed



## SIZE ANALYSES BY ANDREASEN PIPETTE TECHNIQUE

Size [Microns]	Initial Sample [Cumulative %]	After 100 hours [Cumulative %]
150	91.56	93.75
75	86.00	89.43
45	82.40	87.04
32	79.63	85.18
16	71.94	79.80
8	62.21	73.40
4	50.10	61.93
2	38.89	45.79

Table 10.4 Typical particle count

PUMPED FLUID CONDITION		FLUSH	STRAKES
No gas/vapour likely at seal Solids concentration < 10% by volume		Not required if: HTR >1 Recommended if: HTR <1	Not required
Gas or vapour likely at seal		Not required if: HTR >1 Viscosity < 10 cS Recommended if: HTR <1 Viscosity >10cS	Not required
Solids concentration >10% by volume	Predominantly fine	Clean flush to seal face recommended unless hard faces fitted	Not required
	Predominantly coarse	Not required if HTR >1	Axial
	Mixed	Clean flush to seal face recommended unless hard faces fitted	Axial
Gas or vapour likely at seal Solids concentration > 10% by volume		Clean flush to seal face recommended unless hard faces fitted Recommended if: HTR <1 Viscosity >10cS	Helical

Table 13.1 Recommended Practice - summary of implementation

INSTALLATION NUMBER  
PUMPED FLUID

Parameter	Units	Symbol	Value
Temperature	°C	T <sub>f</sub>	
Thermal Conductivity	W/mK	k	
Specific Heat Capacity	J/kgK	c <sub>p</sub>	
Density	kg/m <sup>3</sup>	ρ	
Kinematic Viscosity	mm <sup>2</sup> /s (cS)	ν	
Pressure	MPa	P <sub>f</sub>	
Radial Clearance	mm	b	
Seal Rotor Outside Diameter	mm	d	
Seal Chamber Length	mm	l	
Speed	rpm	N	
Flush Flowrate	l/min	Q	
Taylor Number (cylindrical housings) [Ta = 5.5 x 10 <sup>-3</sup> d b <sup>3</sup> N <sup>2</sup> / ν <sup>2</sup> ]		Ta	
Gas or Vapour			Yes/No
Solids :- concentration > 10% w/w size			Yes/No Coarse/Fine

Table 13.2 Duty Specification Table

PUMPED FLUID CONDITION		FLUSH	STRAKES
No gas/vapour likely at seal Solids concentration < 10% by volume		Not required if: HTR >1 Speed < 3000rpm Recommended if: HTR <1 Speed > 3000rpm	Not required
Gas or vapour likely at seal		Not required if: HTR >1 Viscosity < 10 cS Speed < 3000rpm Recommended if: HTR <1 Viscosity >10cS Speed > 3000rpm	Not required
Solids concentration >10% by volume	Predominantly fine	Clean flush to seal face recommended unless hard faces fitted	Not required
	Predominantly coarse	Not required if HTR >1	Axial
	Mixed	Clean flush to seal face recommended unless hard faces fitted	Axial
Gas or vapour likely at seal Solids concentration > 10% by volume		Clean flush to seal face recommended unless hard faces fitted Recommended if: HTR <1 Viscosity >10cS Speed > 3000rpm	Helical

Table 13.3 Alternative Practice - summary of implementation

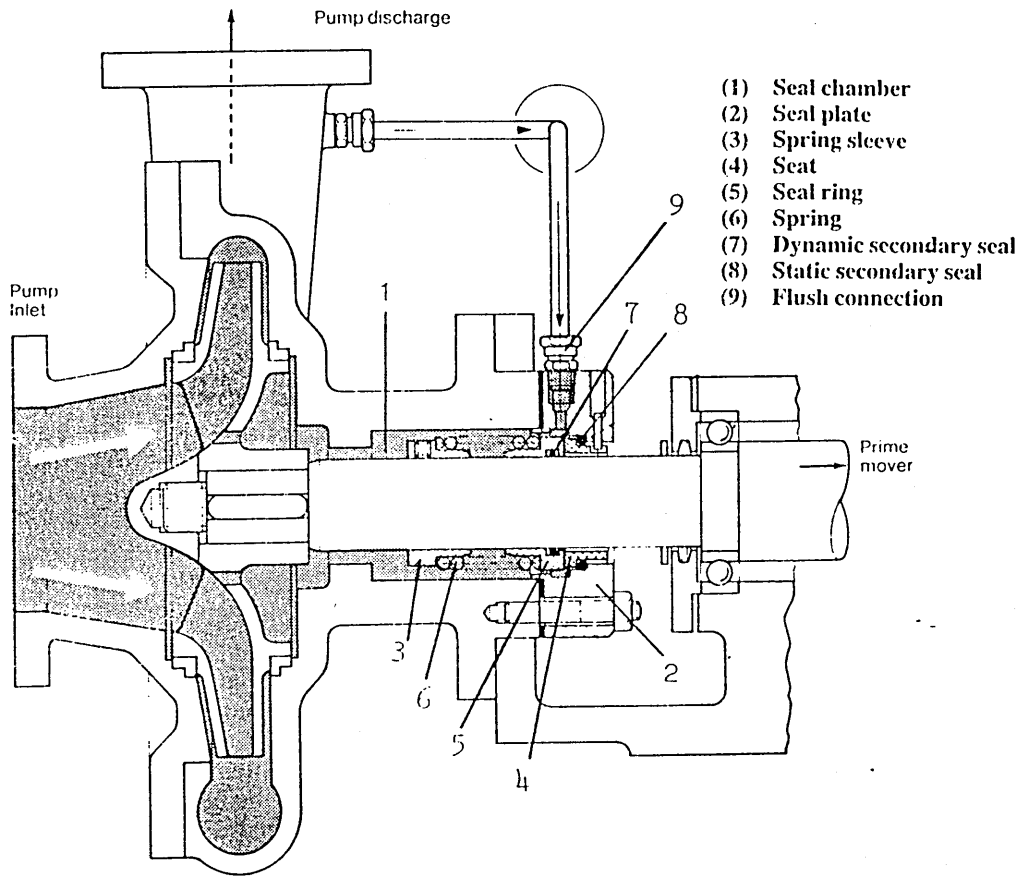


Figure 1.1 Typical mechanical seal installation

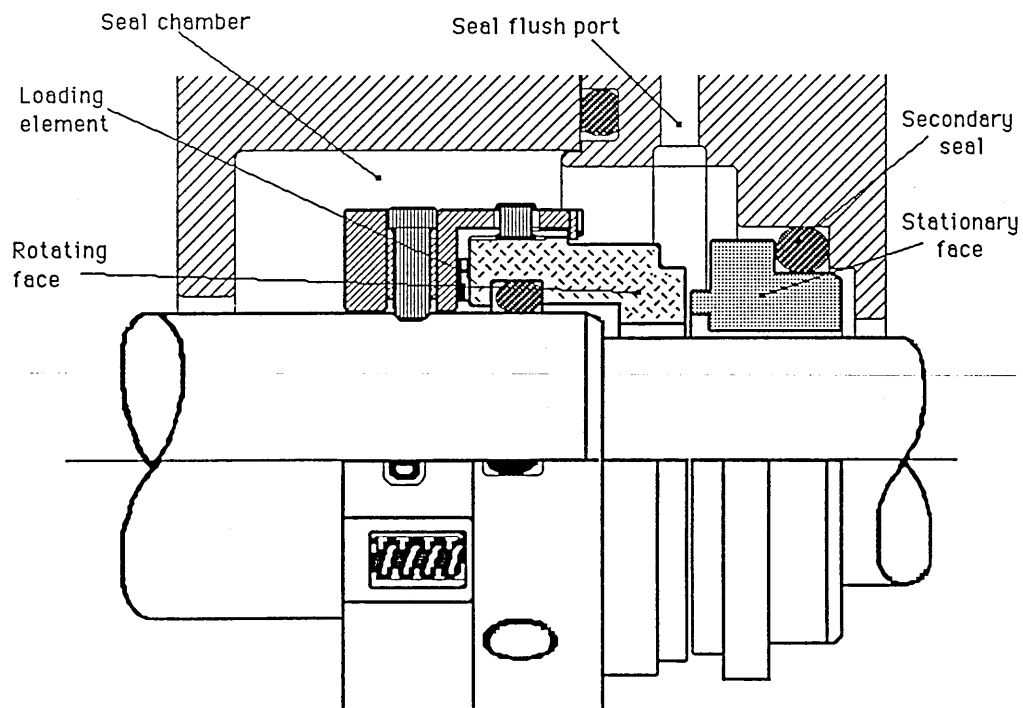


Figure 1.2 Basic features of a mechanical seal

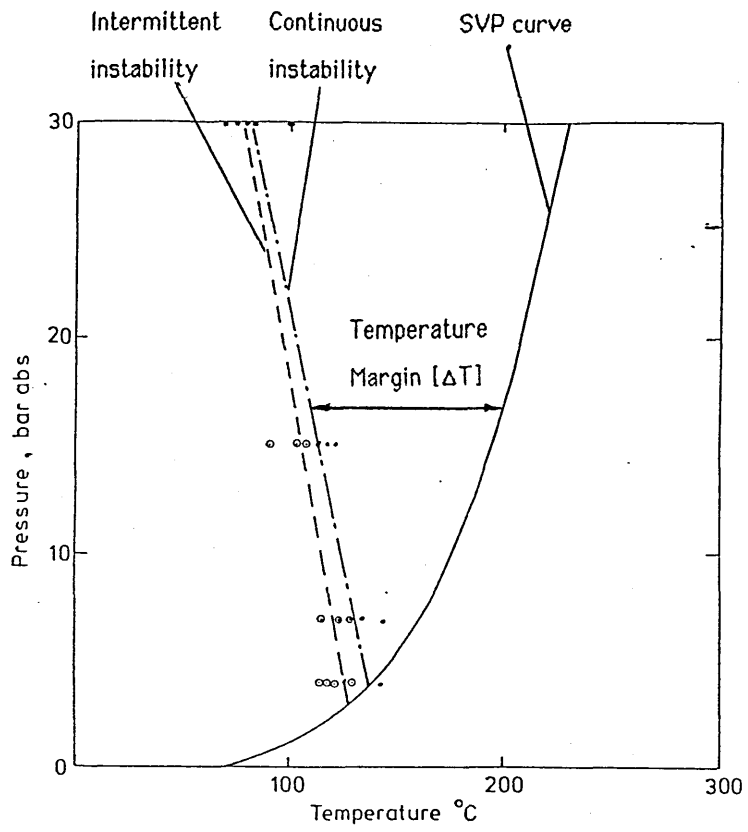


Figure 1.3 Seal instability - low pressure seal design  
 [Source: Flitney & Nau (1989)]

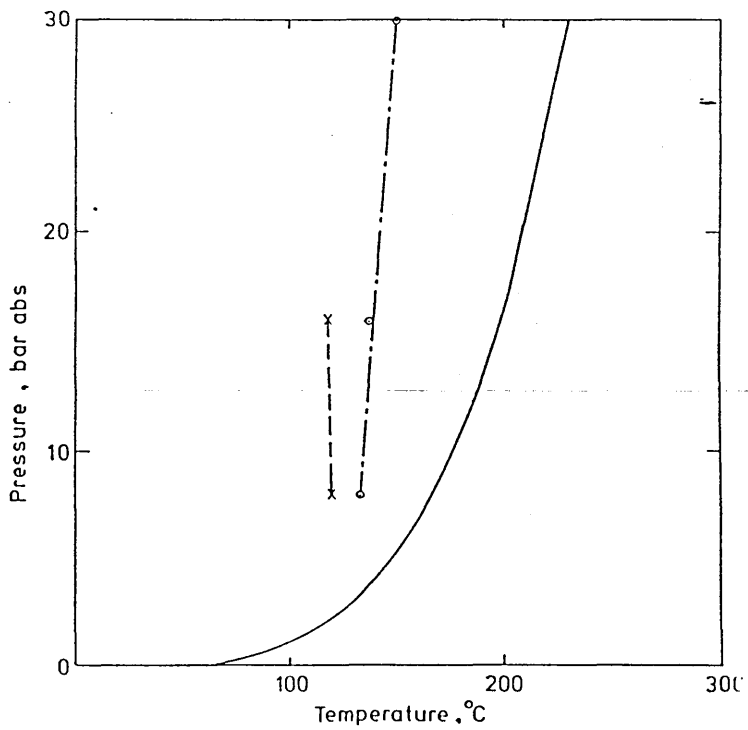
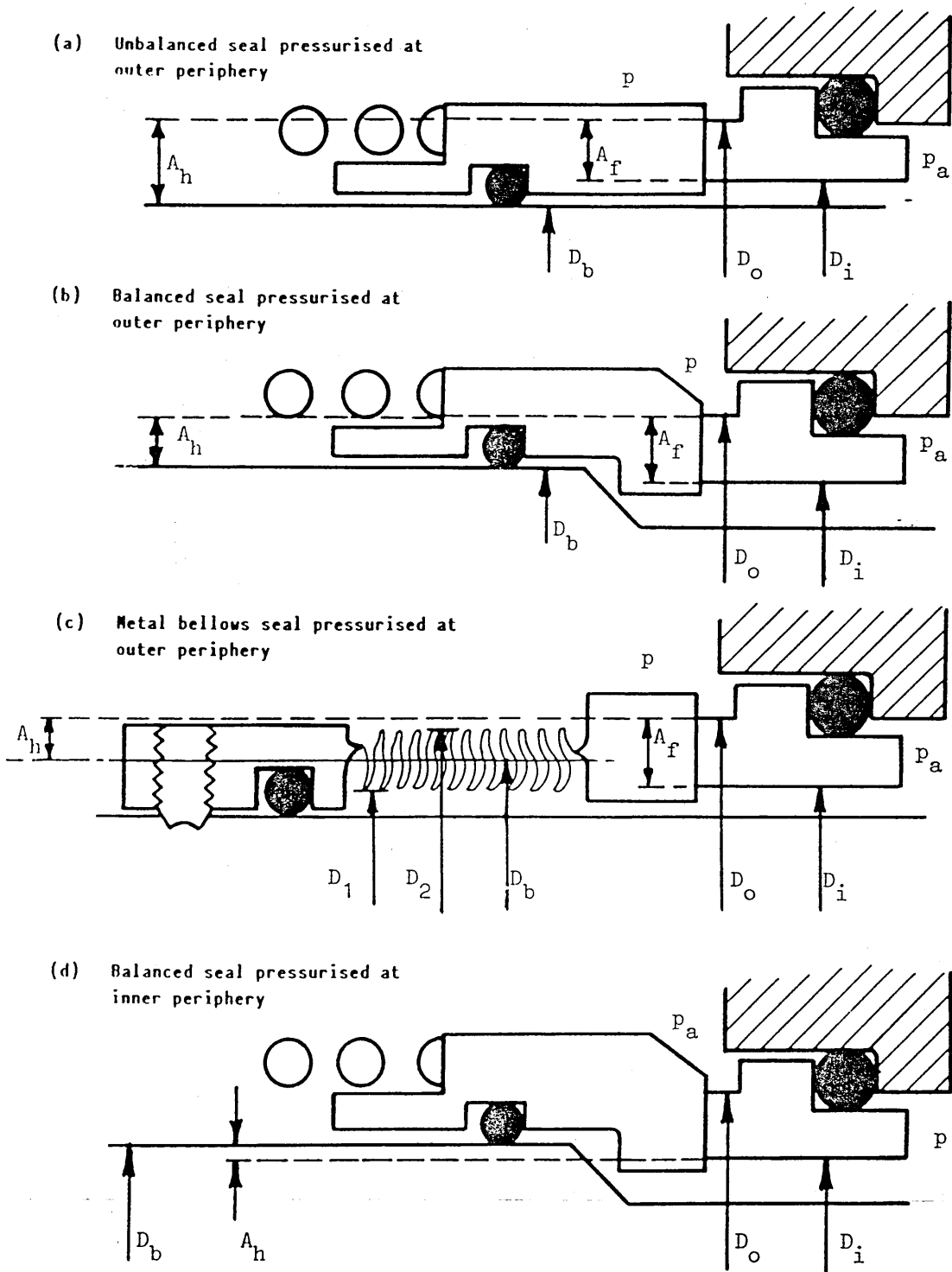


Figure 1.4 Seal instability - high pressure seal design  
 [Source: Flitney & Nau (1989)]





$A_f$  = area of sealing interface  
 $A_h$  = hydraulic loading area  
 $D_2$  = outside diameter of bellows  
 $D_1$  = inside diameter of bellows  
 $D_o$  = outside diameter of sealing interface  
 $D_i$  = inside diameter of sealing interface  
 $D_b$  = balance diameter

Figure 1.5 Definition of seal balance

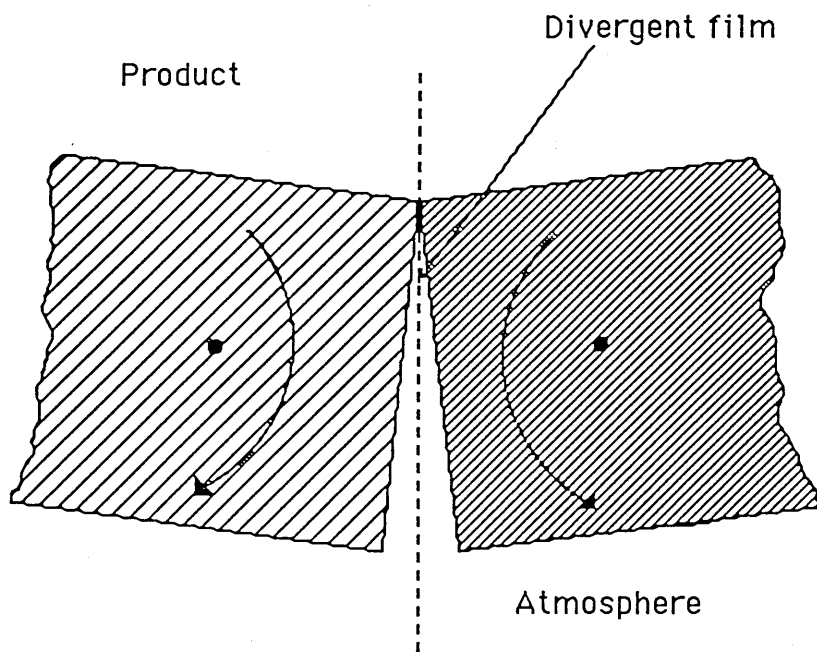


Figure 1.6 Effect of pressure on the sealing interface

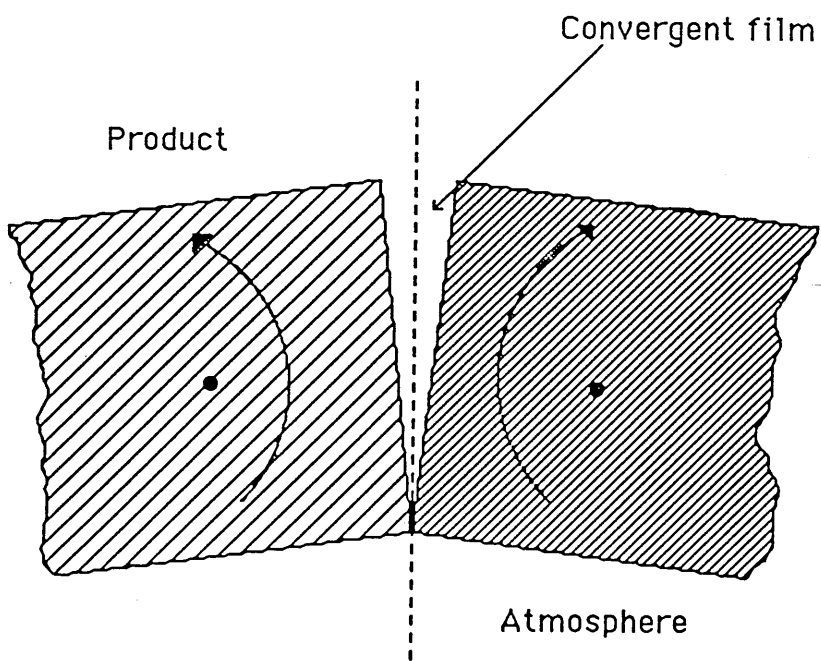


Figure 1.7 Effect of temperature on the sealing interface

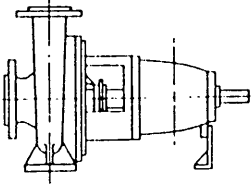
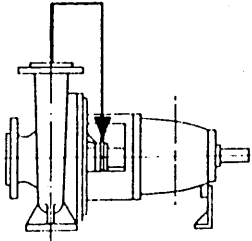
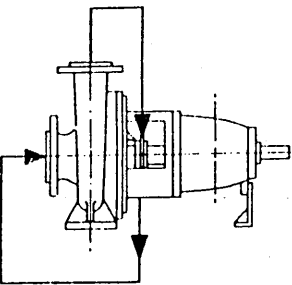
Basic arrangement			Applied to			
Designation code	Figure	Description	Soft packing	Single mechanical seal	Double mechanical seal	Quench
			P	S	D	Q
00		No piping, no circulation	x	x		
01		No piping, internal circulation	x	x		
02		Circulated fluid from pump outlet to seal cavity (with internal return)	x	x		
03		Circulation fluid from pump outlet to seal cavity and return to pump inlet	x	x		

Figure 1.8 Seal flushed from discharge

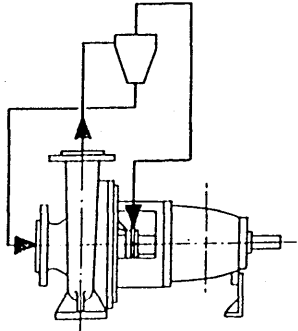
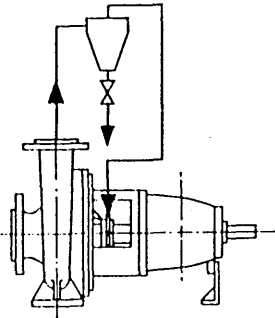
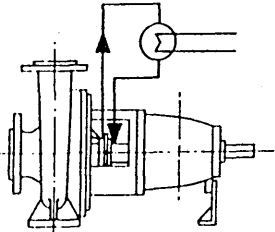
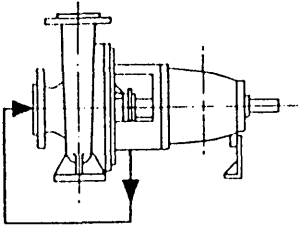
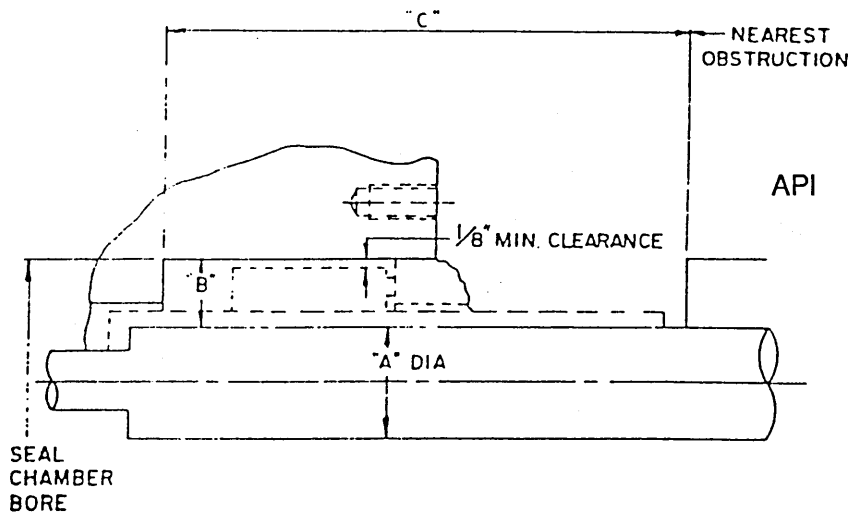
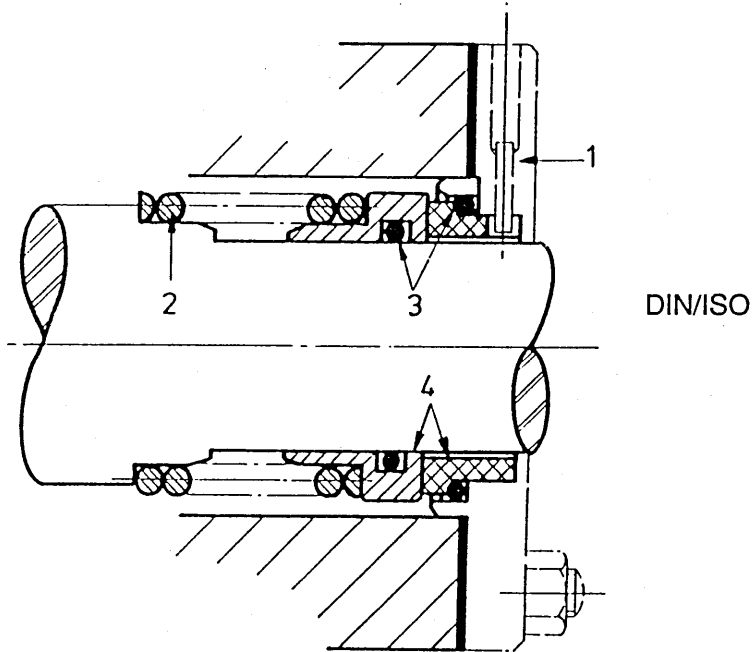
Basic arrangement			Applied to			
Designation code	Figure	Description	Soft packing	Single mechanical seal	Double mechanical seal	Quench
			P	S	D	Q
04		Circulation fluid via cyclone (with internal return) dirty line to pump inlet	x	x		
05		Circulation fluid via cyclone; dirty line to drain	x	x		
06		Circulation fluid by pumping device from seal cavity via heat exchanger back to seal cavity		x		
07		Internal circulation fluid to seal and return to pump inlet	x	x		

Figure 1.9 Seal flushed by an independent ancillary system



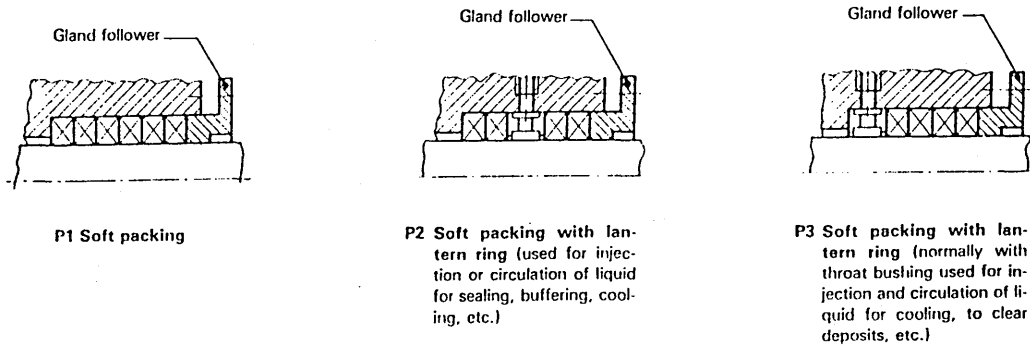
Shaft Diameter (A), inches	Minimum Radial Dimension (B), inches	Minimum Total Length (C), inches
<2.000	1.000	5.750
2.125-3.000	1.125	6.500
>3.125	1.250	7.000

Figure 1.10 Stuffing box standard geometries

Annex D

Typical seal arrangements

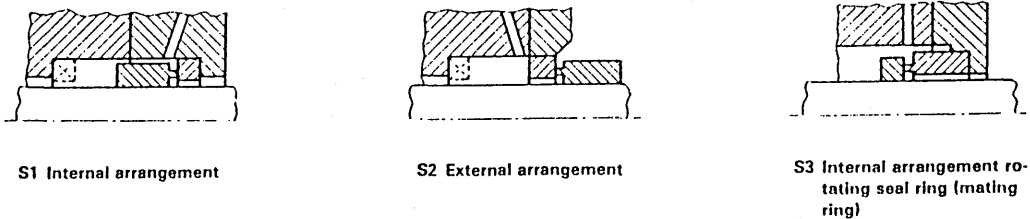
D.1 Soft packing<sup>1)</sup> (P)



D.2 Single mechanical seal<sup>1)</sup> (S)

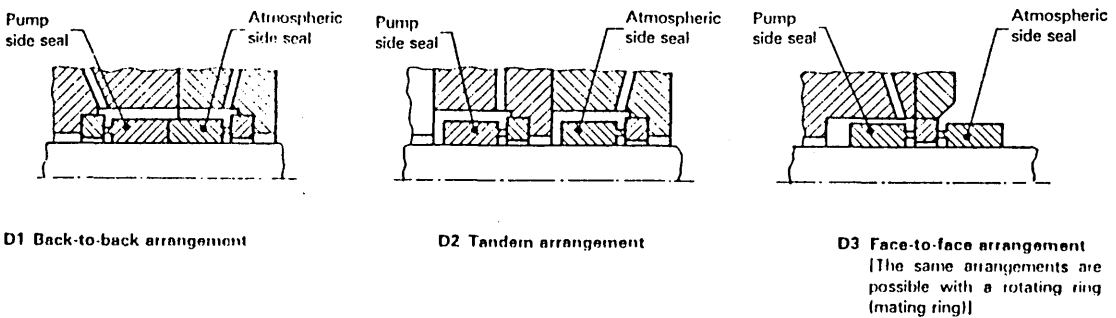
These seals can be

- a) unbalanced (as in the figure) or balanced normally;
- b) with or without circulation or injection to the sealed faces;
- c) with or without throat bushing.



D.3 Double mechanical seal<sup>1)</sup> (D)

Either or both of these seals may be unbalanced (as in the figure) or balanced.



1) Left-hand side of figures shows the pump side.

Figure 1.11 Centrifugal pump seal arrangements - BS 6836

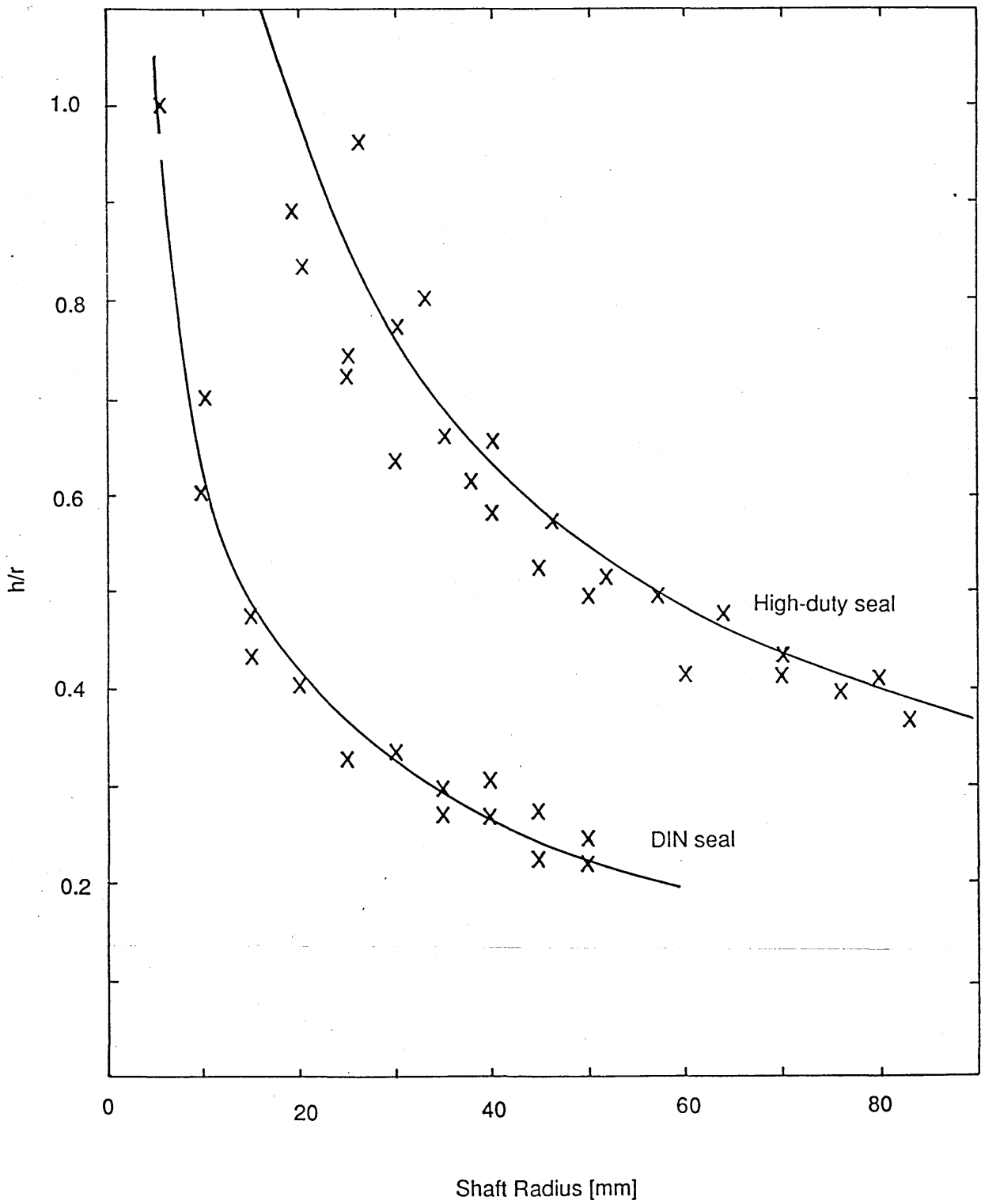


Figure 1.12 Comparison of radial clearance ratios for DIN and high duty seals

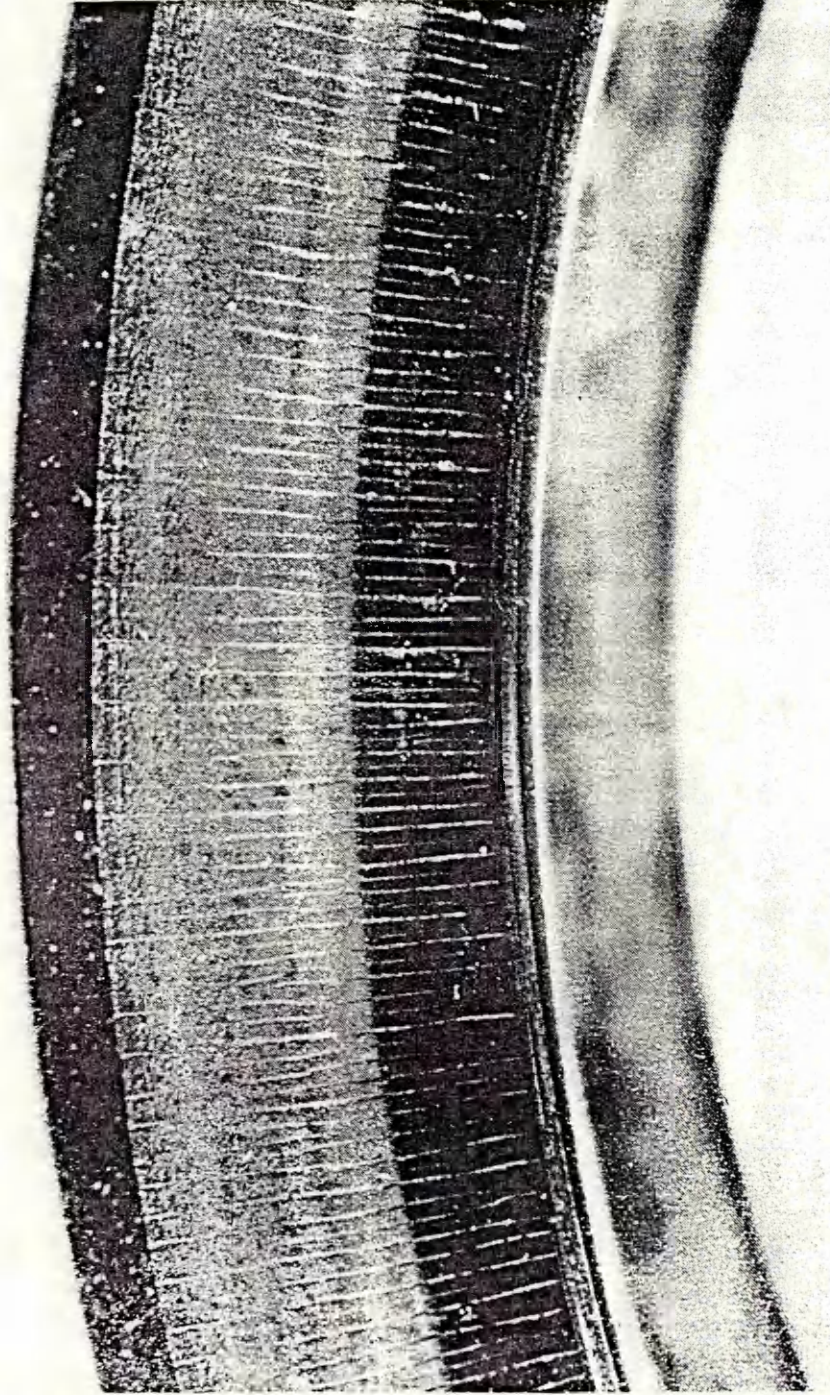


Figure 1.13 Thermal stress cracking of a mechanical seal face



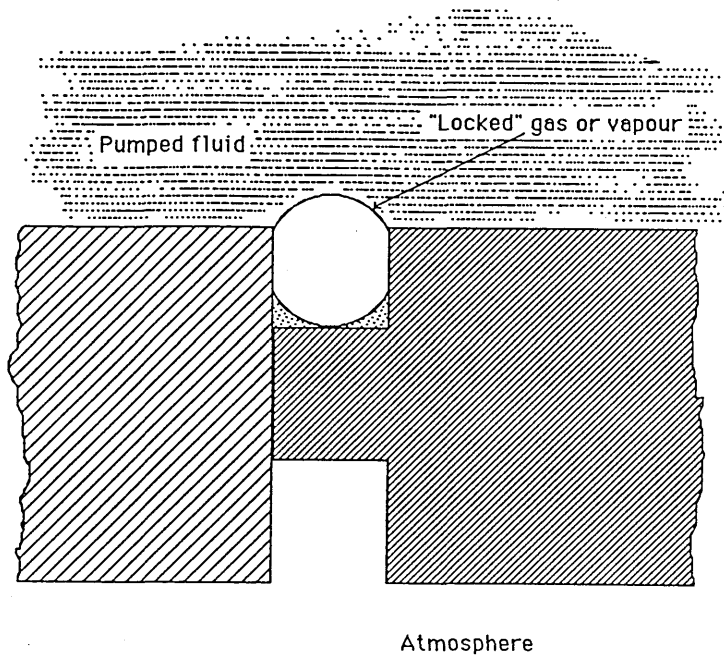


Figure 1.14 Vapour locking phenomenon in a mechanical seal chamber

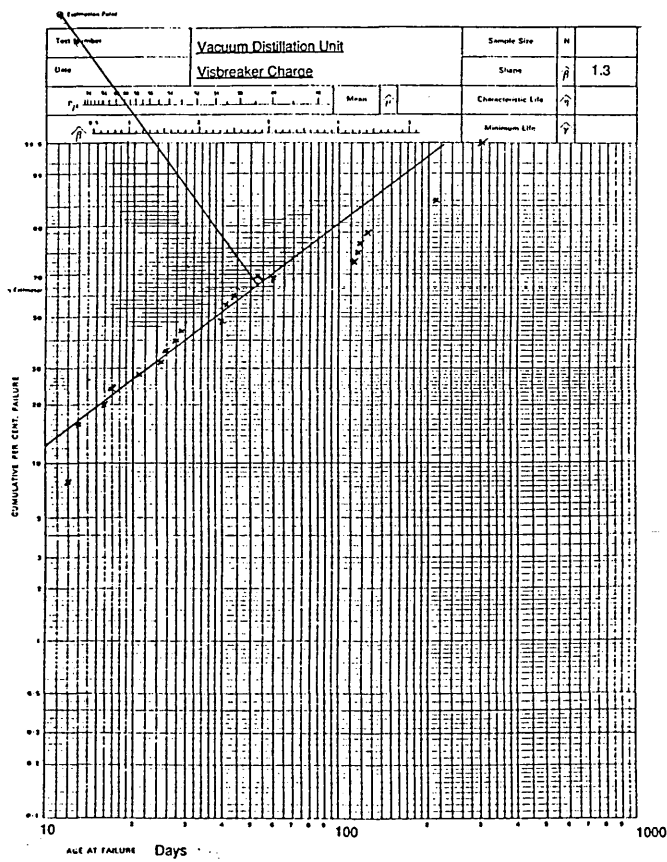


Figure 2.1 Weibull plot - Visbreaker Charge pump

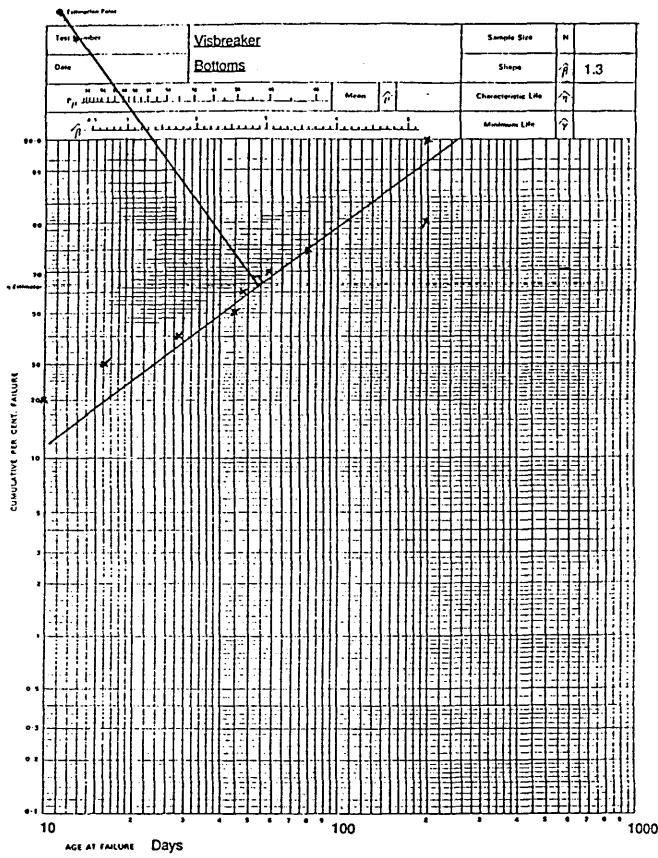
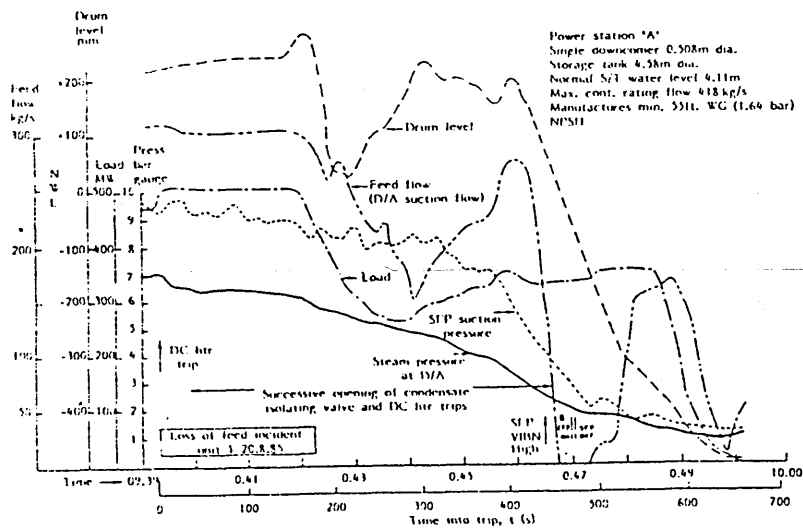


Figure 2.2 Weibull plot - Bottoms pump



Power Station "A." Recorded data during a loss of boiler feed pump net positive suction head incident.

Figure 2.3 Transient suction pressures on a boiler feedwater pump (Cranfield, 1988)

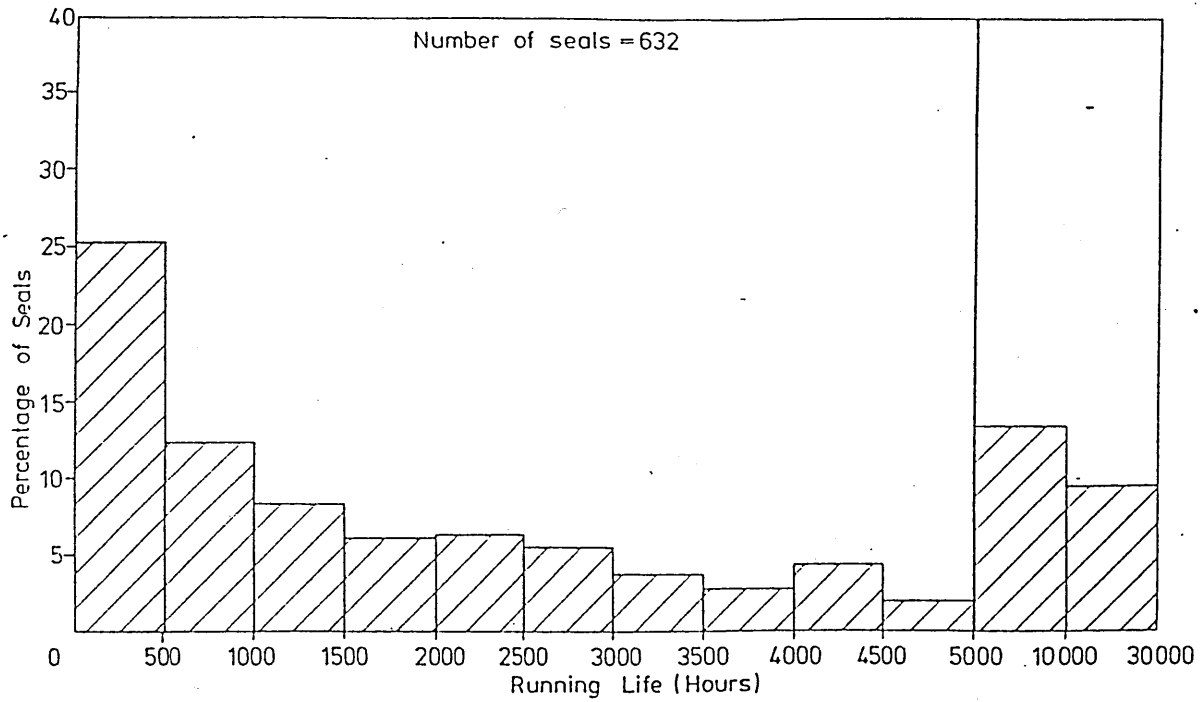


Figure 2.4 Distribution of seal running life (Flitney & Nau, 1985)

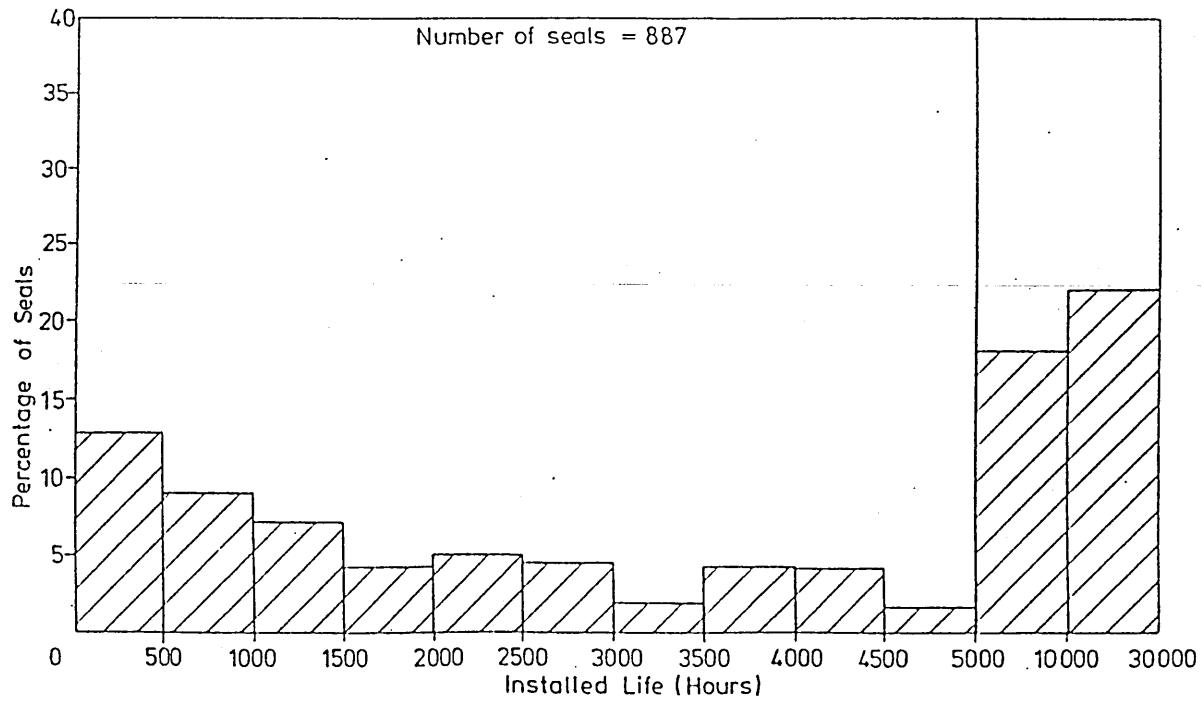


Figure 2.5 Distribution of installed seal life (Flitney & Nau, 1985)

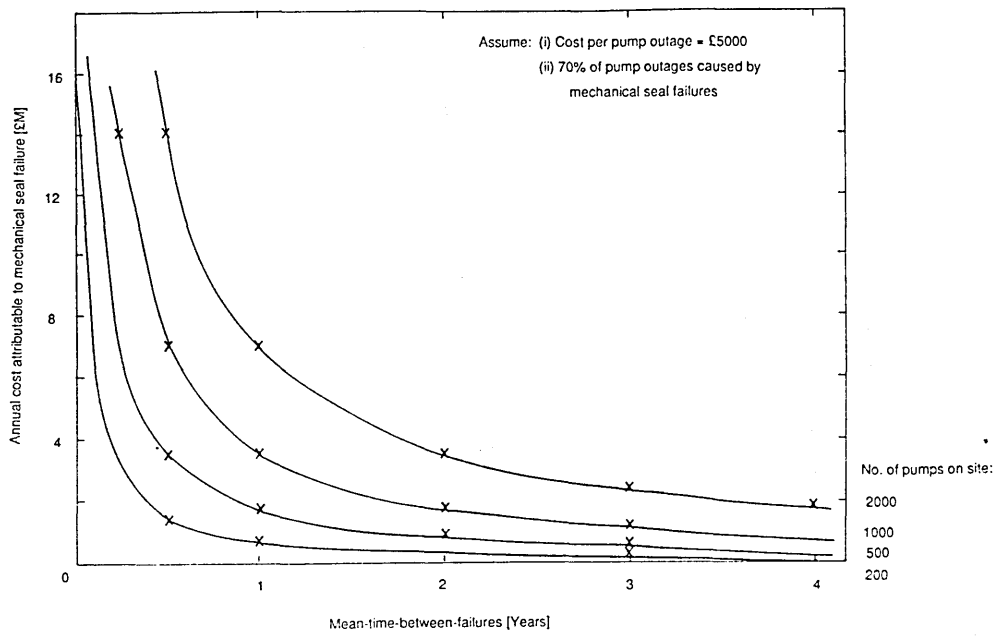


Figure 2.6 Maintenance costs due to mechanical seal failure

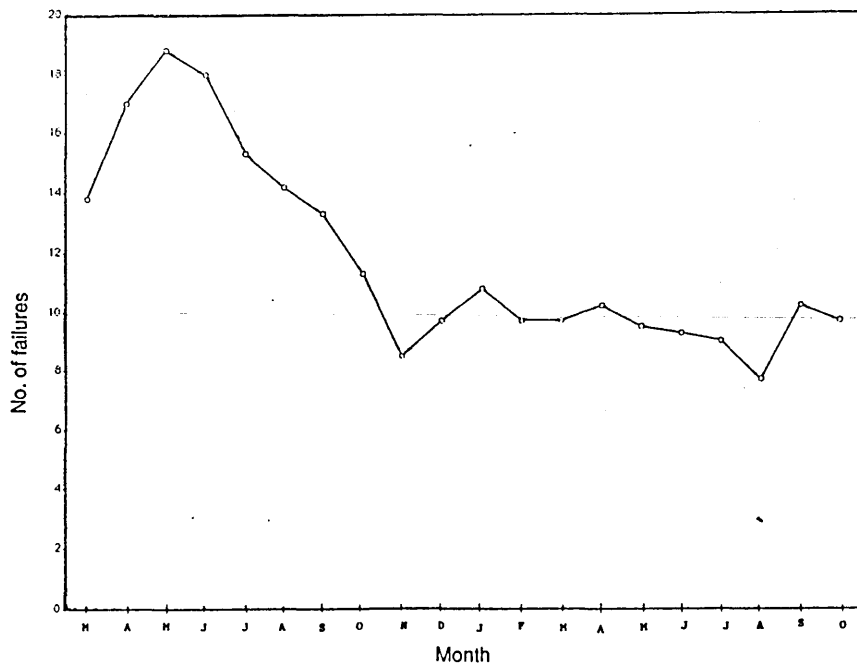


Figure 2.7 Reduction in seal failures due to regular record-keeping

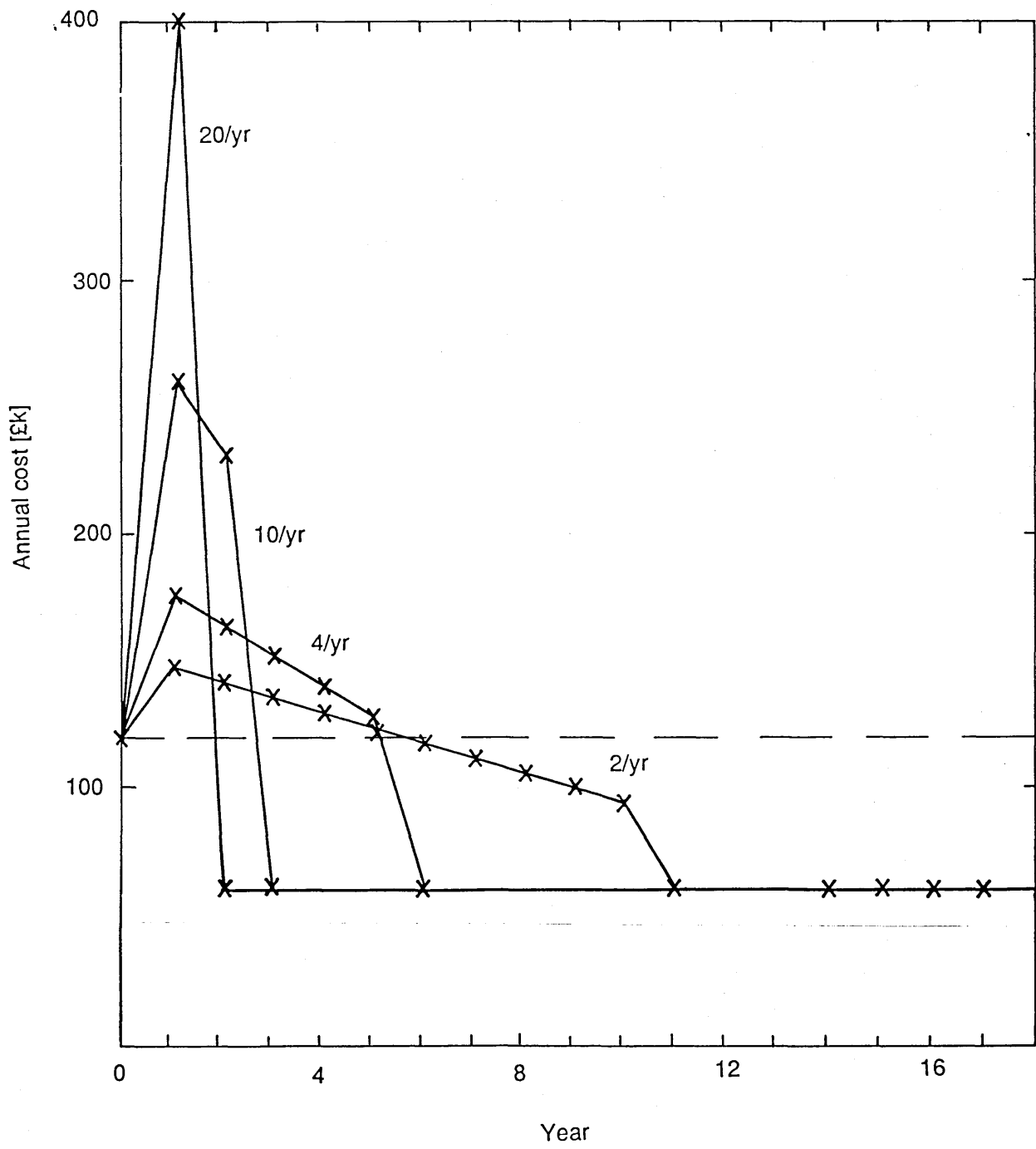


Figure 2.8 Cost profiles for replacement programmes of between-bearing pumps

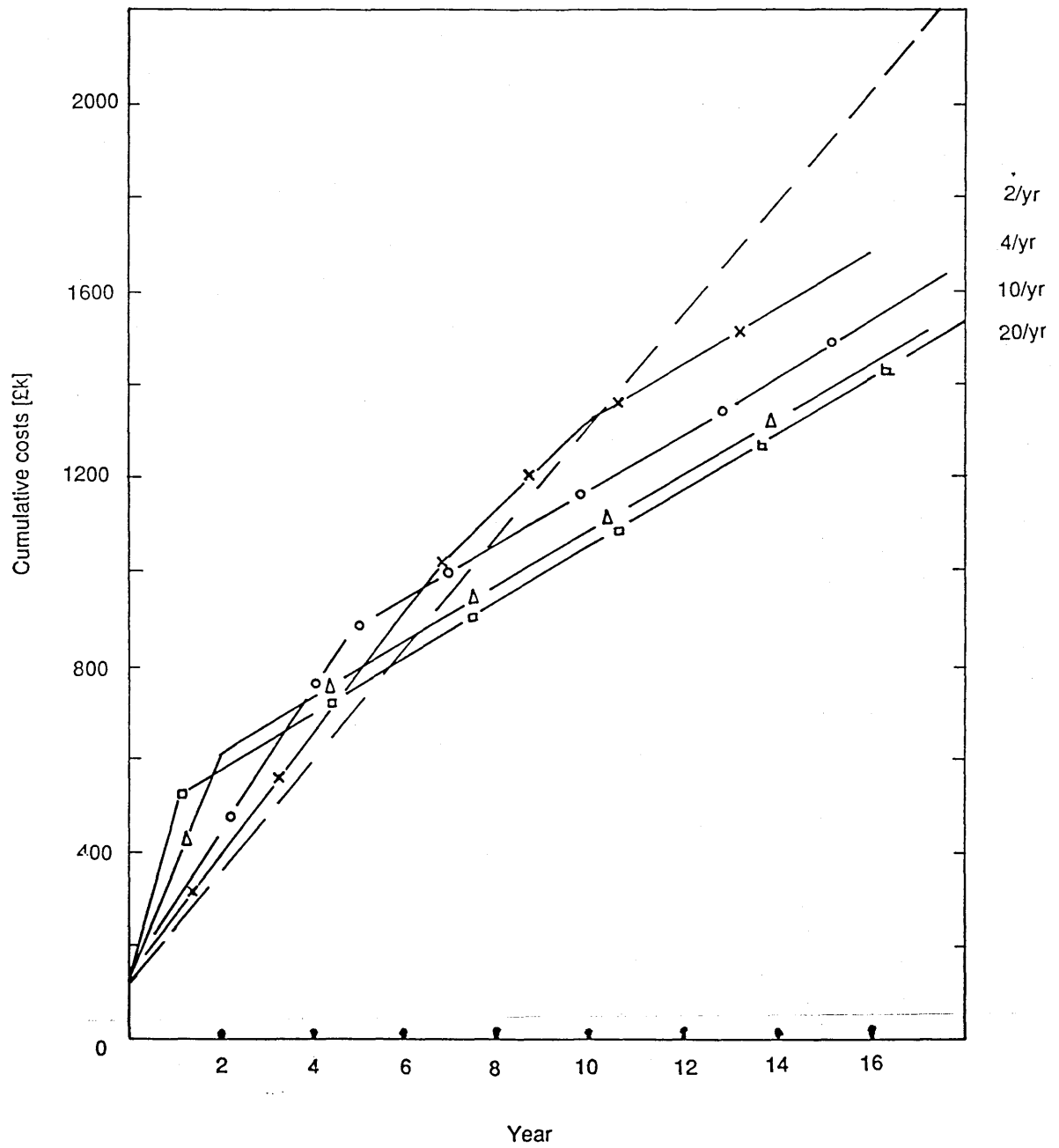


Figure 2.9 Cumulative costs for replacement programmes of between-bearing pumps

SERVICE SPEED[rpm]	HEAVY DIESEL PUMP AROUND PUMP 1480
SUCTION PRESSURE [kPa]	469
DISCHARGE PRESSURE [kPa]	750
FLOW TEMPERATURE [ C]	332
VAPOUR PRESSURE [kPa]	356
CAPACITY [m <sup>3</sup> /h]	352

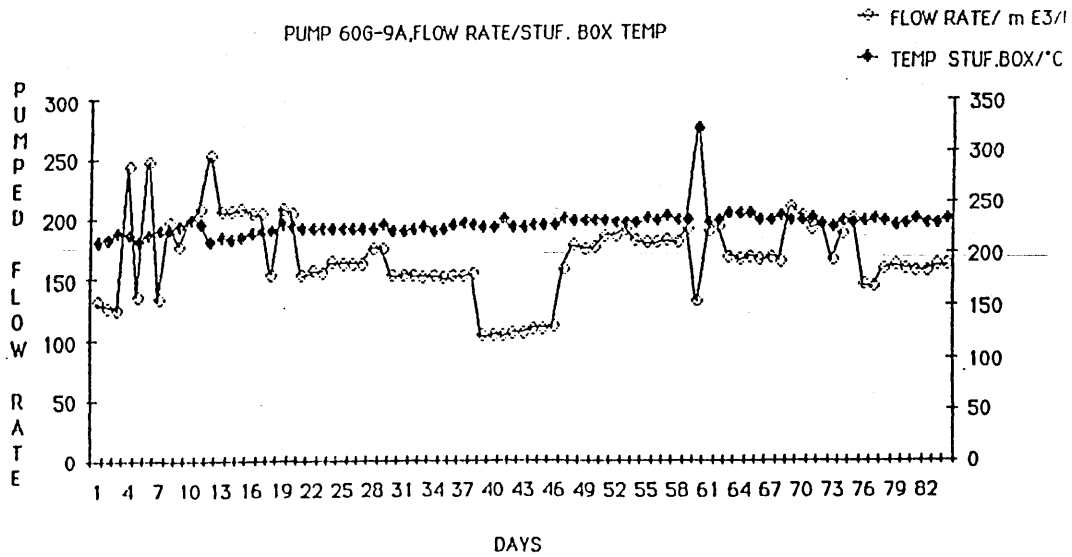
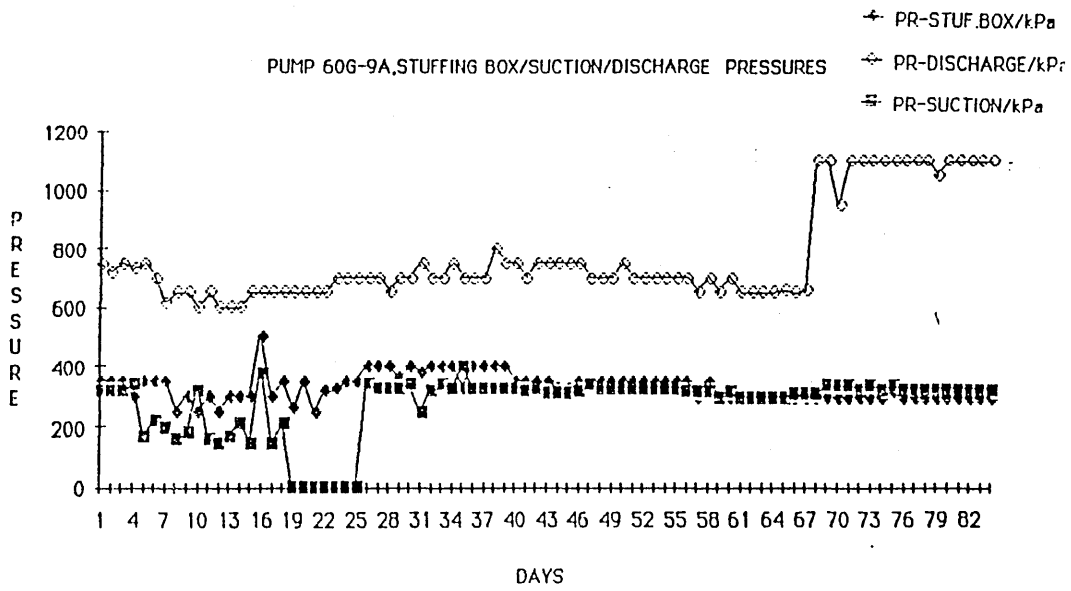


Figure 2.10 Example of a pump running well off BEP

Duty : Hot Water, 24 bar

Site : Amoco Refinery, Milford Haven

Source : Barnes, Flitney & Nau (1989)(c)

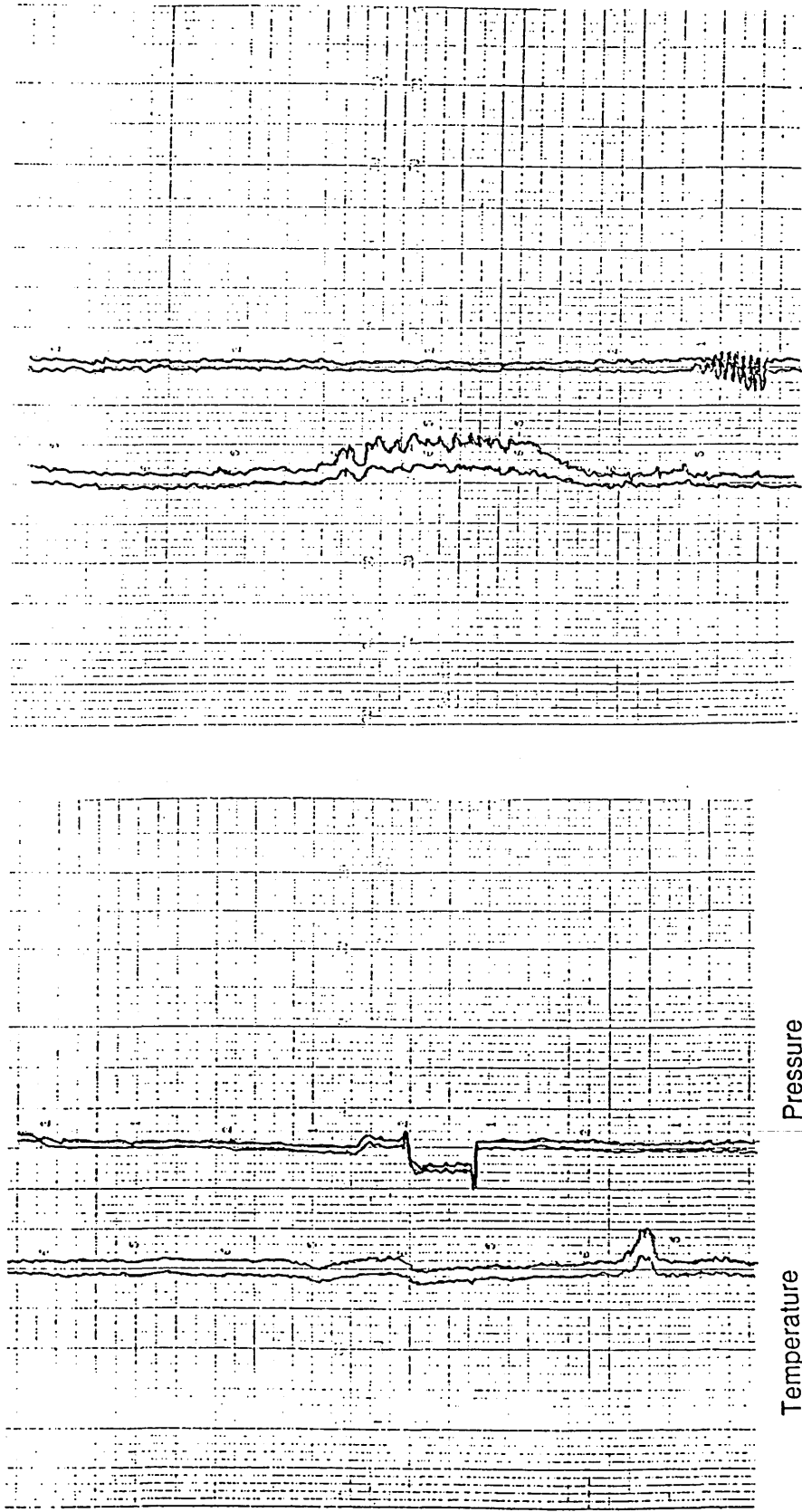


Figure 2.11 Transient fluctuations of pressure and temperature in seal chamber



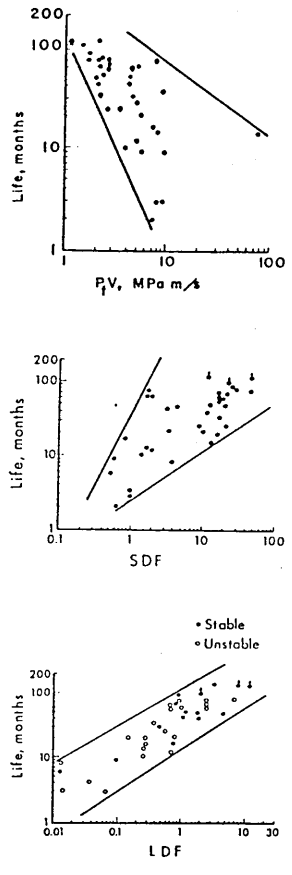


Figure 2.12 Prediction of seal life using dimensionless parameters (Buck, 1980)

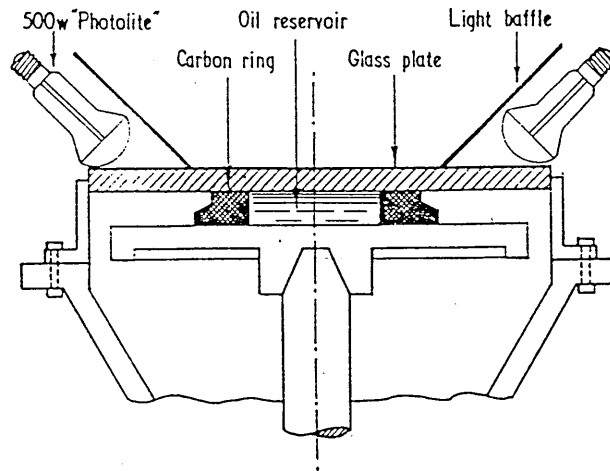


Figure 2.13 Test apparatus for observing interface phenomenon (Nau, 1963)

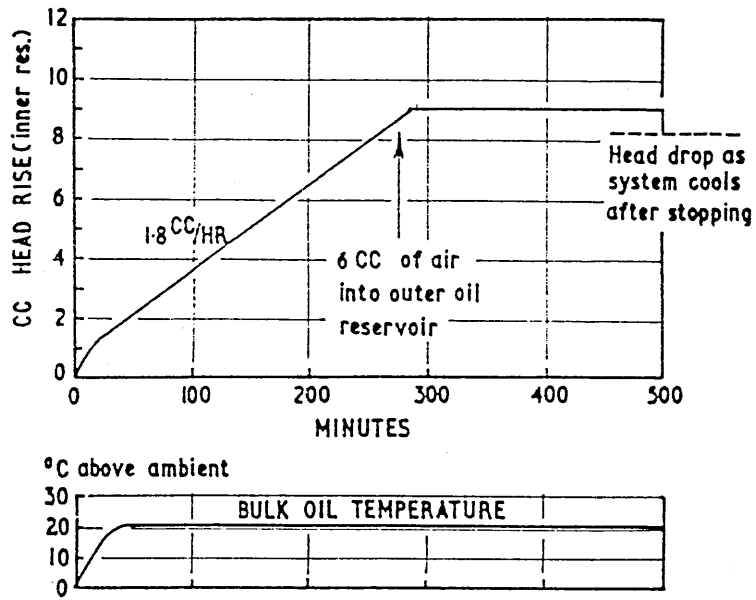


Figure 2.14 Effect of air on radial pumping (Nau, 1963)

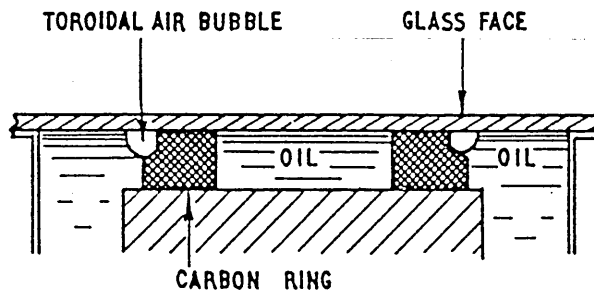
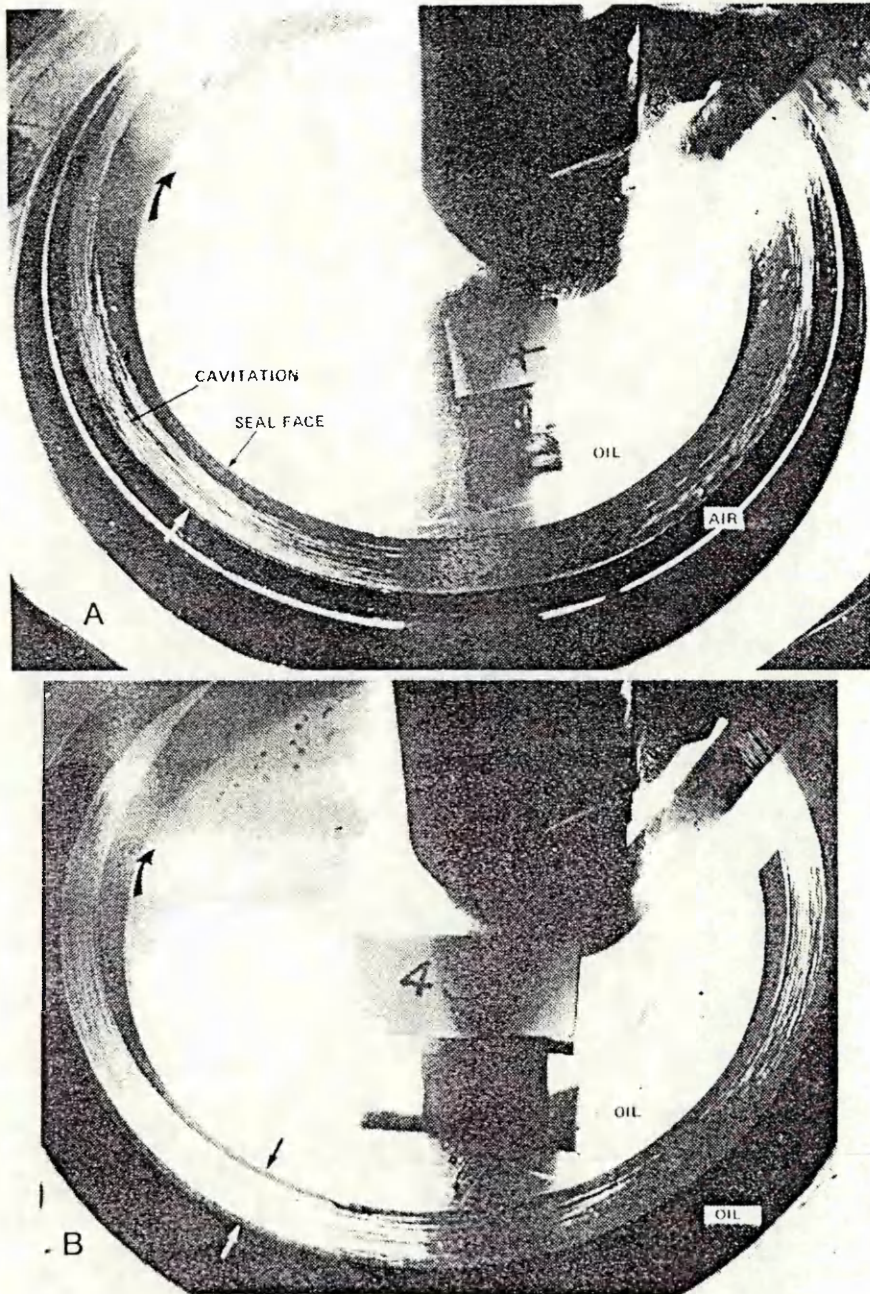


Figure 2.15 Toroidal air bubble around seal faces (Nau, 1963)



Mechanical seal interface conditions with oil: (a) oil inside, air outside, (b) oil both sides

Figure 2.16 Cavitation in the seal interface (Nau, 1979)

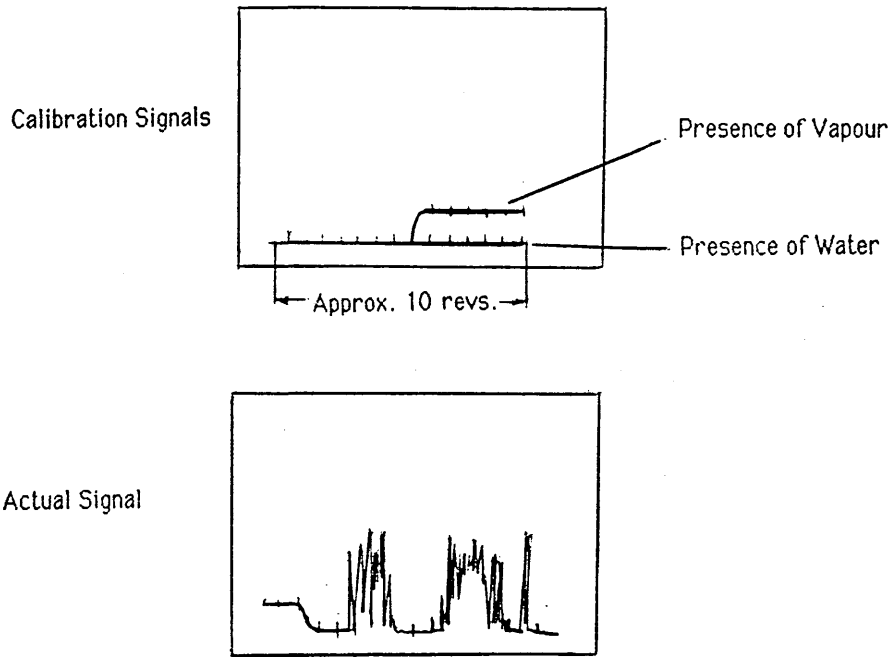


Figure 2.17 Conductivity probe measurements at the seal face (Field & Flitney, 1975)

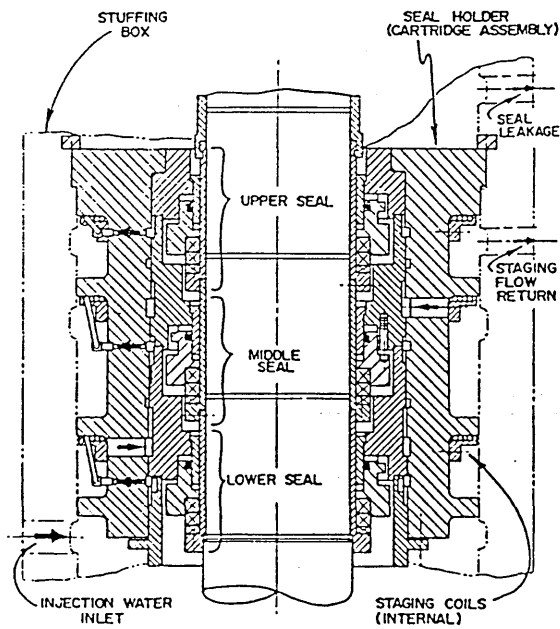
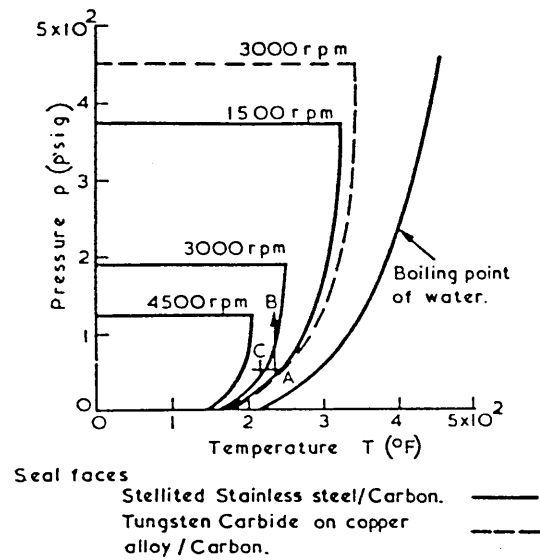


Figure 2.18 Non-contacting seal for nuclear reactor primary coolant pump (Morton, 1984)



PRESSURE, TEMPERATURE LIMITATIONS FOR  
 1 1/4 INCH BALANCED SEAL IN WATER.

Figure 2.19 Graph for evaluating seal material combinations (Lymer, 1969)

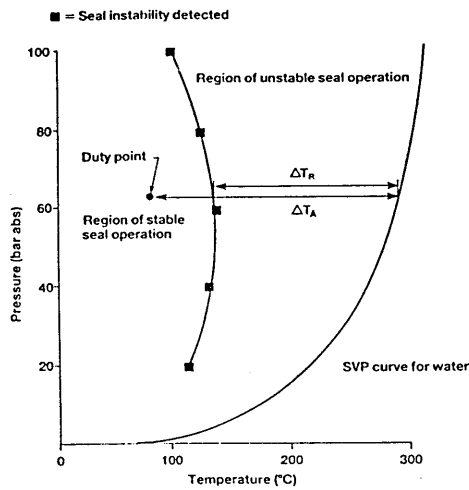


Figure 2.20 Instability criterion used for seal evaluation (Dolan, Harrison & Watkins, 1987)

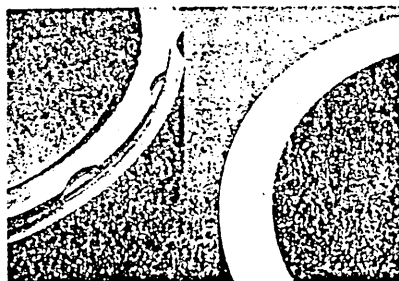


Figure 2.21 Hydro-pad design for improved face lubrication (Netzel, 1982)

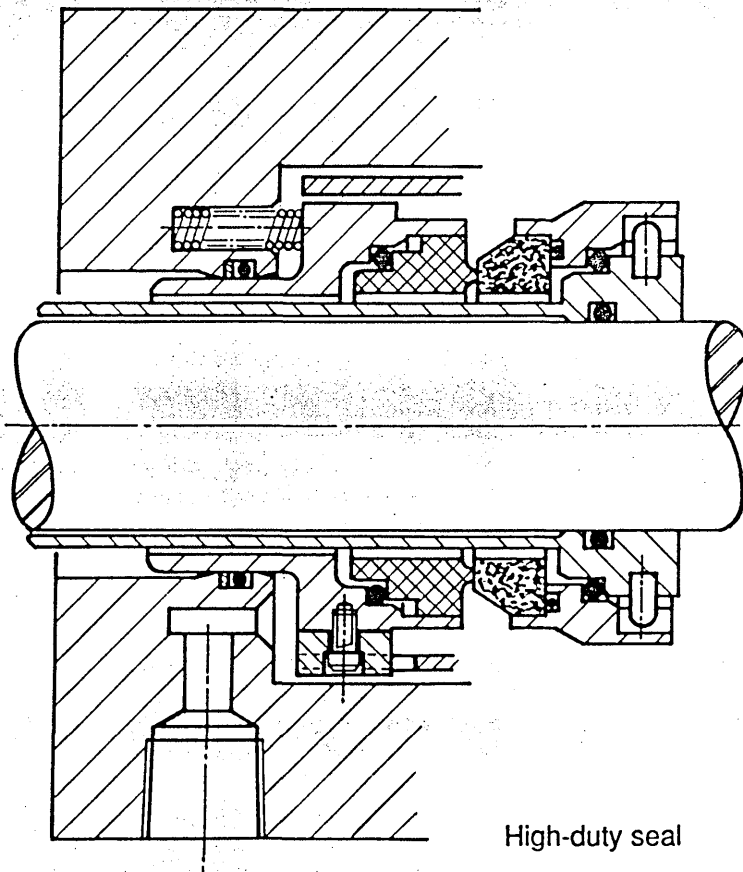
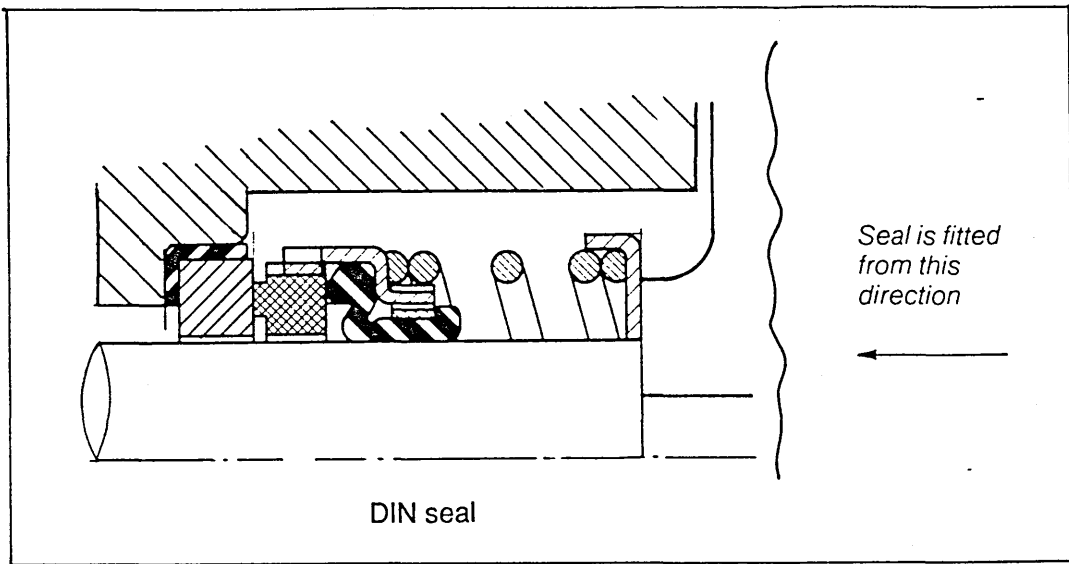


Figure 2.22 Examples of DIN and high-duty seals

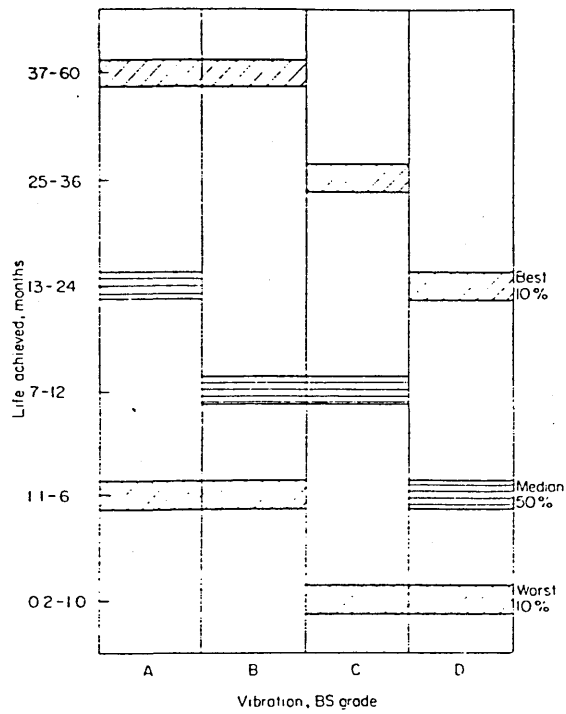


Figure 2.23 Seal life reduction due to high vibration levels ( Flitney & Nau, 1976)

Vibration sources affecting mechanical seals		
Origin	Type	Possible source
Self-induced	Angular misalignment of faces to axis of rotation	Manufacturing tolerances
	- both faces misaligned	
	- one face misaligned, one way	
	Both faces wavy	Manufacturing tolerances
	Dynamic out-of-balance of seal rotor	Non-axisymmetric design features eg, drive slots
External	Shaft vibration	
	- axial	Pump flow mismatch
	- radial	Pump flow mismatch
	- angular	Diesel drive, warped shaft etc.
	- torsional	
	Housing vibration	
	- locally excited	as above via pipework or foundations
	- remote excitation	

Figure 2.24 Sources of vibration (Nau, 1981)

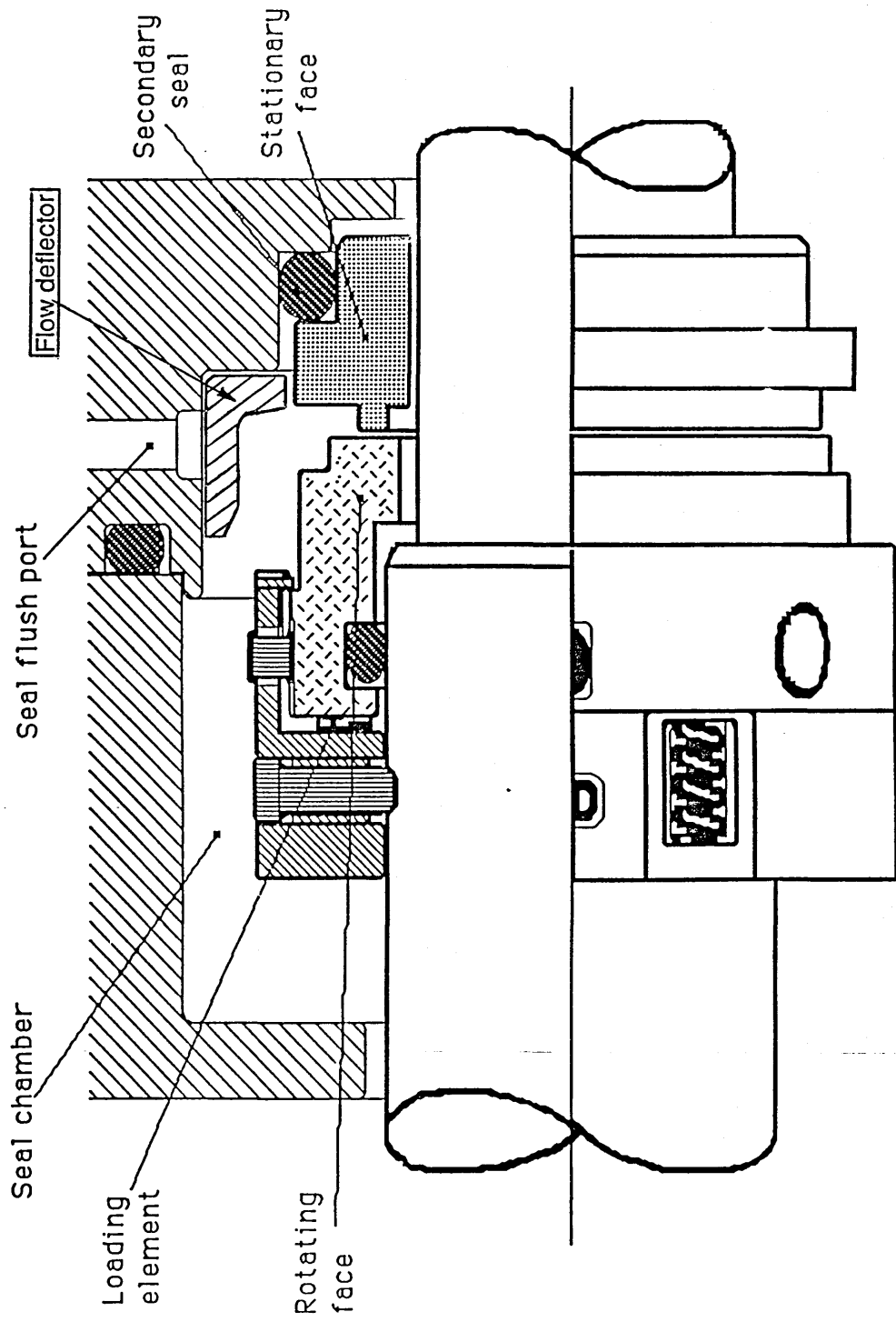


Figure 2.25 Flow deflector to improve seal cooling (Bloch, 1985)



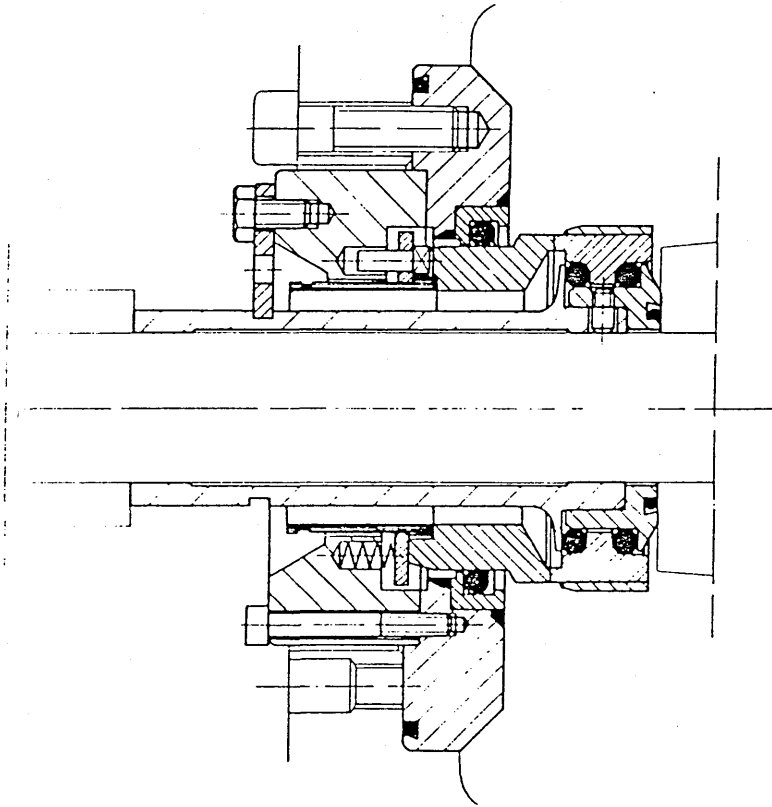


Figure 2.26 Slurry seal chamber design (Schopplein, 1986)

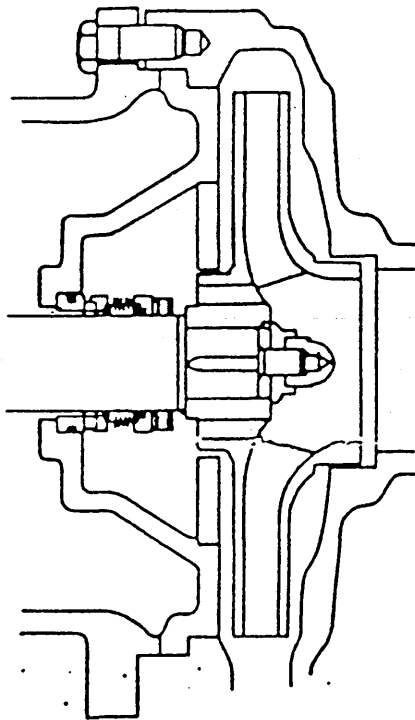


Figure 2.27 Slurry seal chamber design (Battilana, undated)

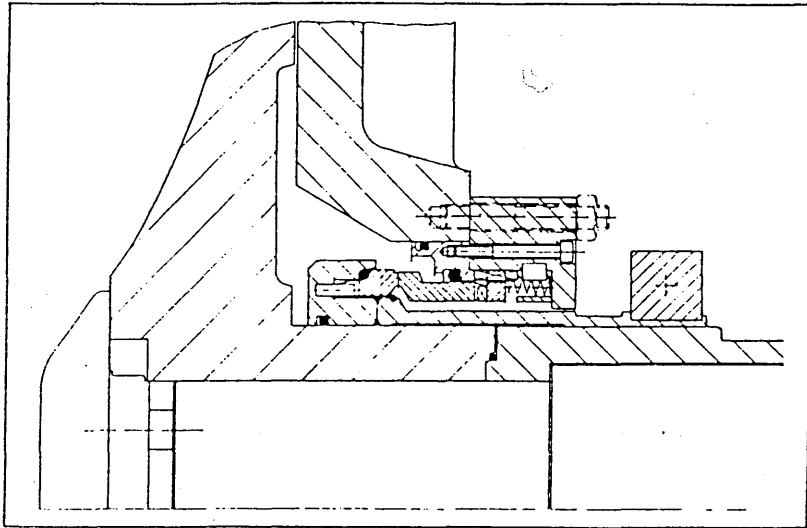


Figure 2.28 Slurry seal chamber design (Kratzer, 1987)

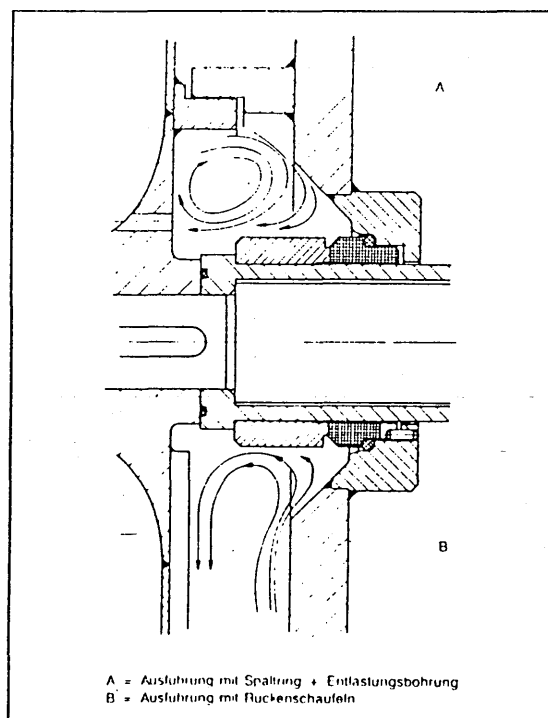


Figure 2.29 Slurry seal chamber design (Bangert, 1986)

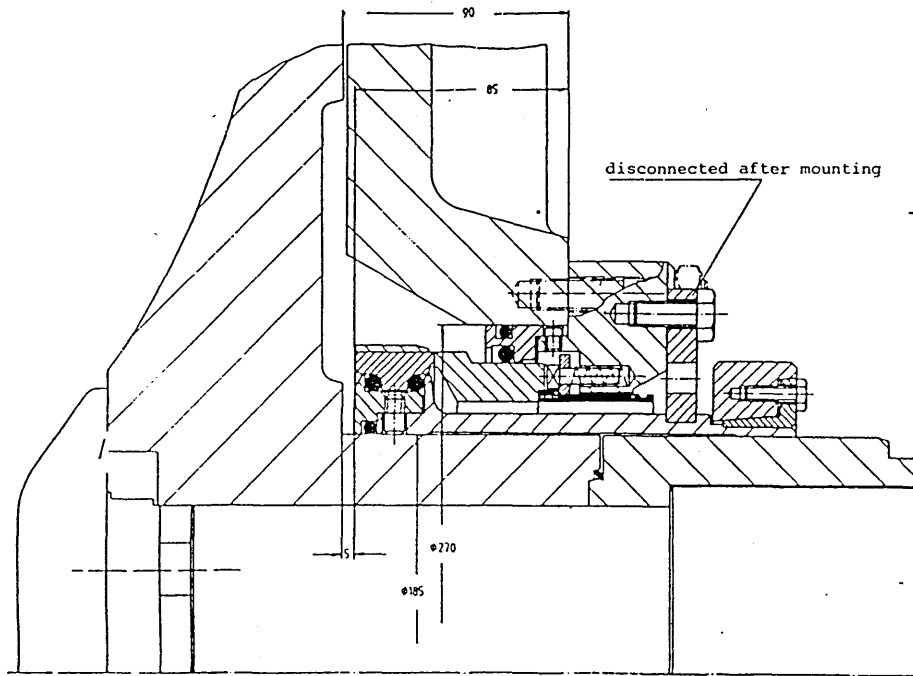


Figure 2.30 Slurry seal chamber design (Heumann, 1986)

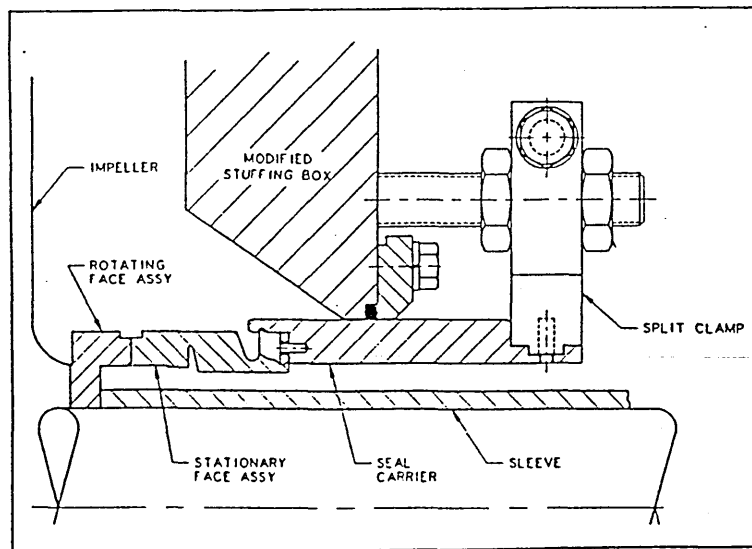


Figure 2.31 Slurry seal chamber design (Nolan, 1988)

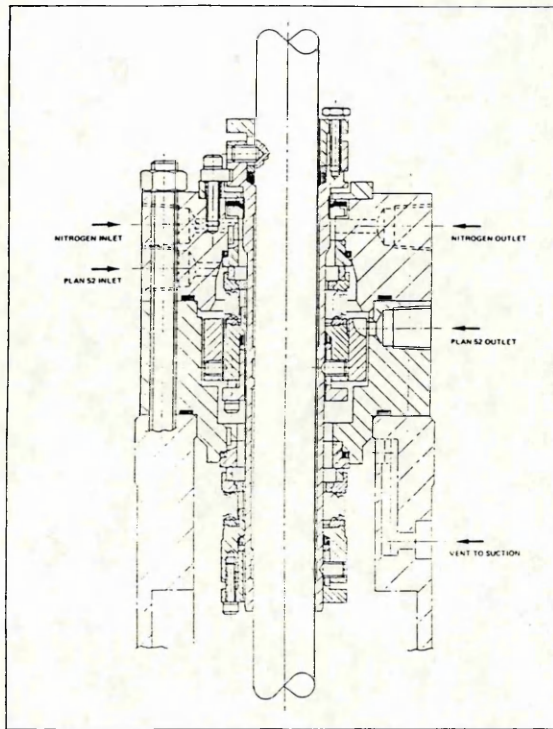


Figure 2.32 Liquid ethylene pump with flared housing (Strazewski, 1985)

Features to make the new pump range the backbone of the company's business for 15 years or more:

- Volute casings designed to increase efficiency and decrease wear
- Enclosed joints with metal-to-metal fits on all ranges
- High tensile stainless steel studs on all major fixings
- Back pull out construction
- Removable suction cover allowing front access to the impeller and mechanical seal
- Interchangeability of parts—only four bearing brackets covering 21 volute casings
- Good access to the seal area and a seal housing unique in design, both aimed at a longer seal life with less likelihood of problems
- Shaft manufactured from high strength duplex stainless steel
- Reasonably priced, high quality pump range

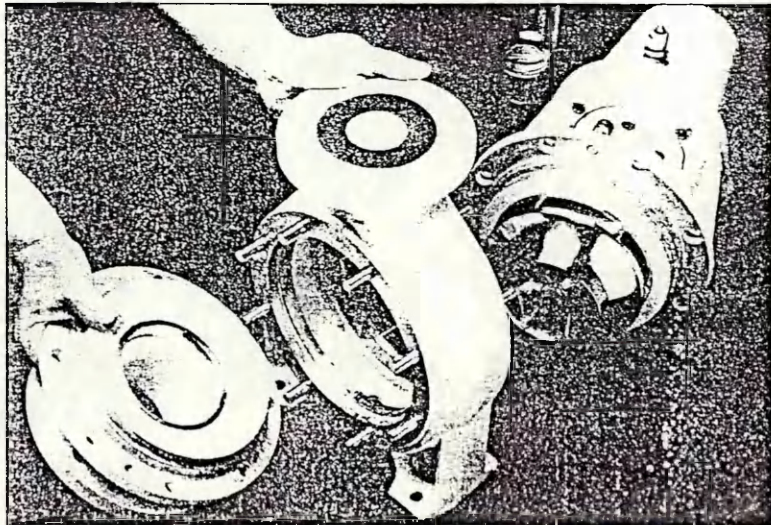
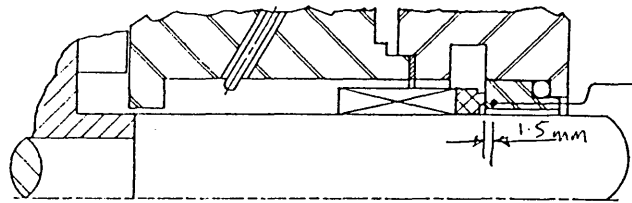
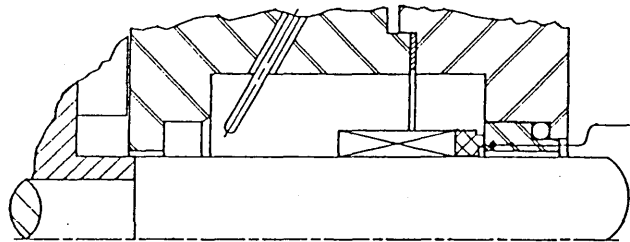


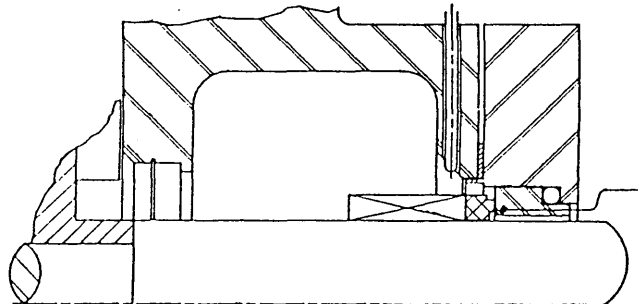
Figure 2.33 New design of medium duty pump (Standish, 1987)



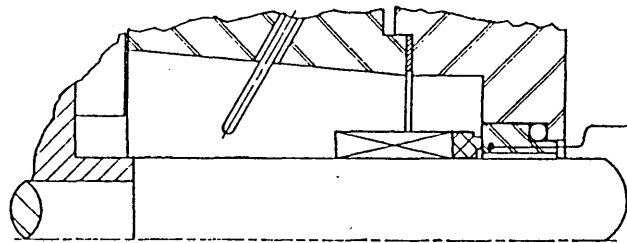
*Standard Stuffing Box, Pump A.*



*Enlarged Cylindrical I Seal Chamber, Pump A.*

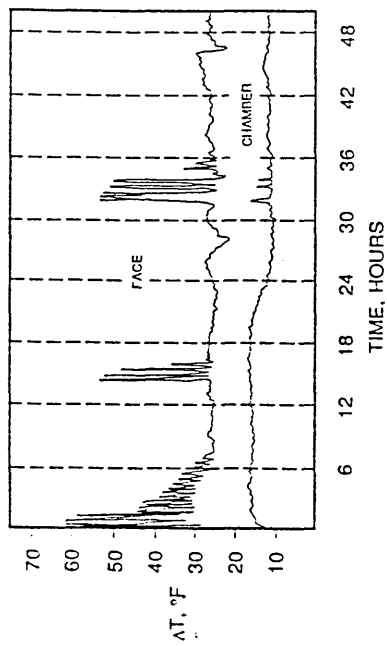


*Enlarged Cylindrical II Seal Chamber, Pump A.*

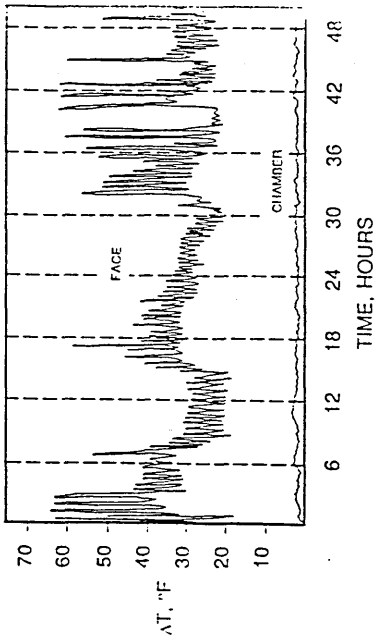


*Enlarged Tapered Seal Chamber, Pump A.*

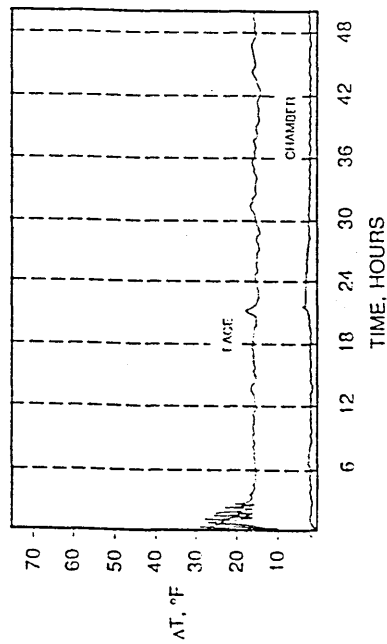
**Figure 2.34** Novel seal chamber designs (Davison, 1989)



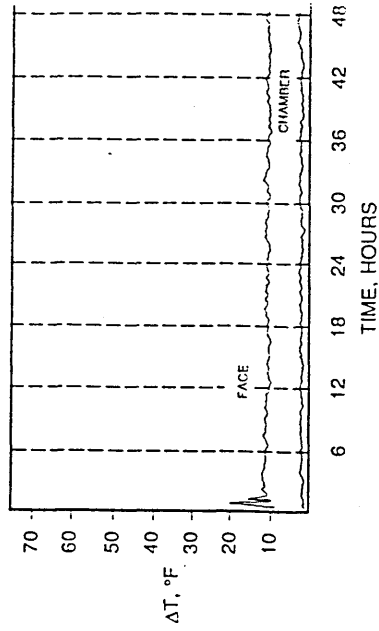
*Seal Face and Seal Chamber Temperatures for the Standard Stuffing Box in Pump A.*



*Seal Face and Seal Chamber Temperatures for the Enlarged Cylindrical II Seal Chamber in Pump A*



*Seal Face and Seal Chamber Temperatures for the Enlarged Cylindrical I Seal Chamber in Pump A.*



*Seal Face and Seal Chamber Temperatures for the Enlarged Tapered Seal Chamber in Pump A.*

**Figure 2.35**  $\Delta T$  measurements for seal chambers in Fig 2.34 (Davison, 1989)

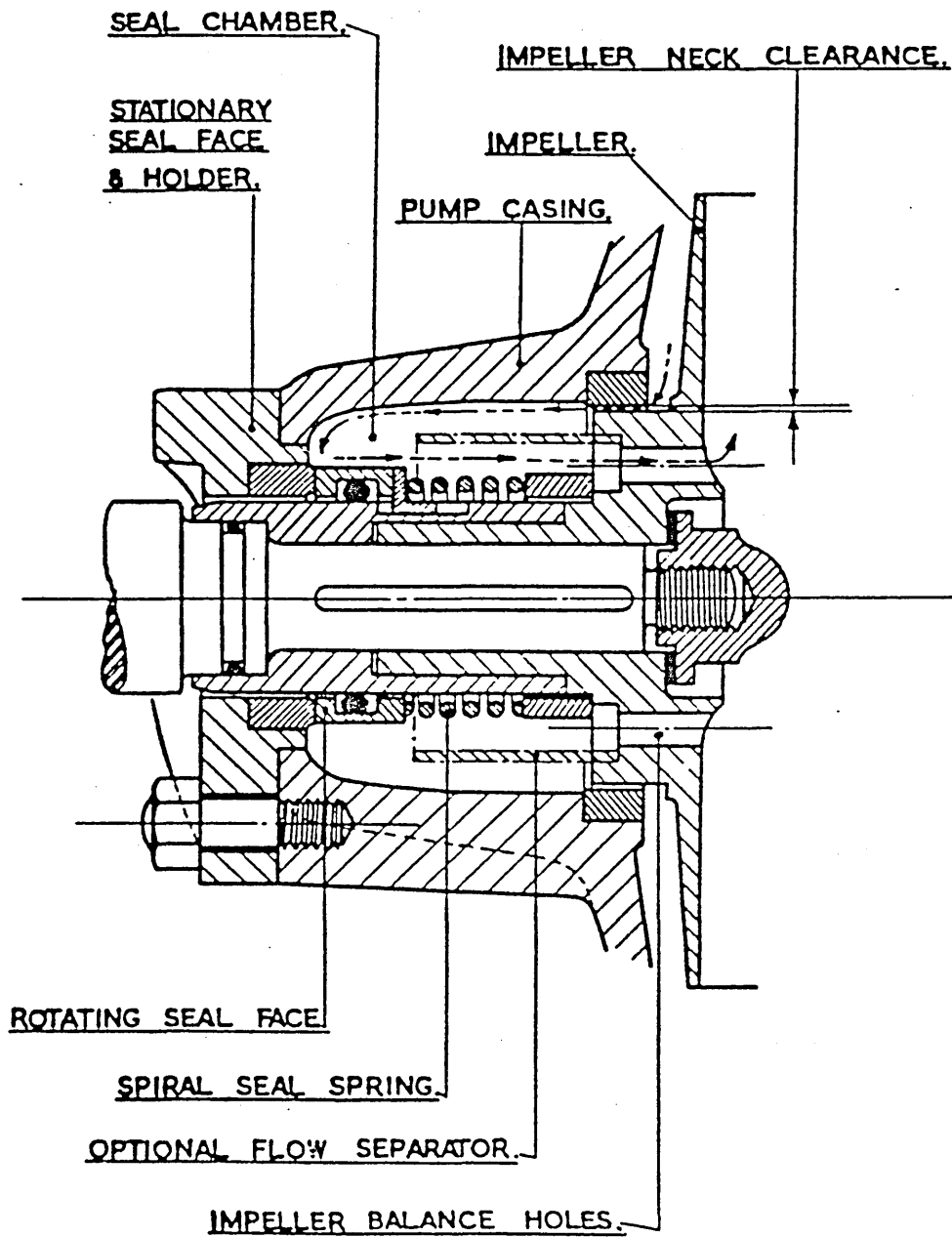


Figure 2.36 Novel seal chamber design with flow guide (Heald, 1975)

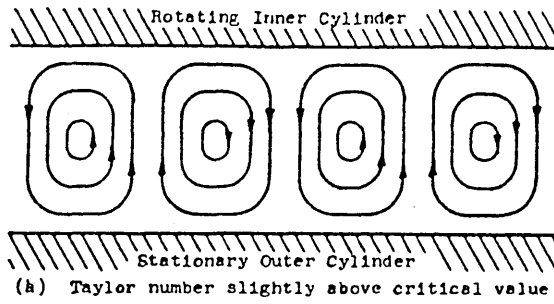


Figure 3.1 Taylor vortices

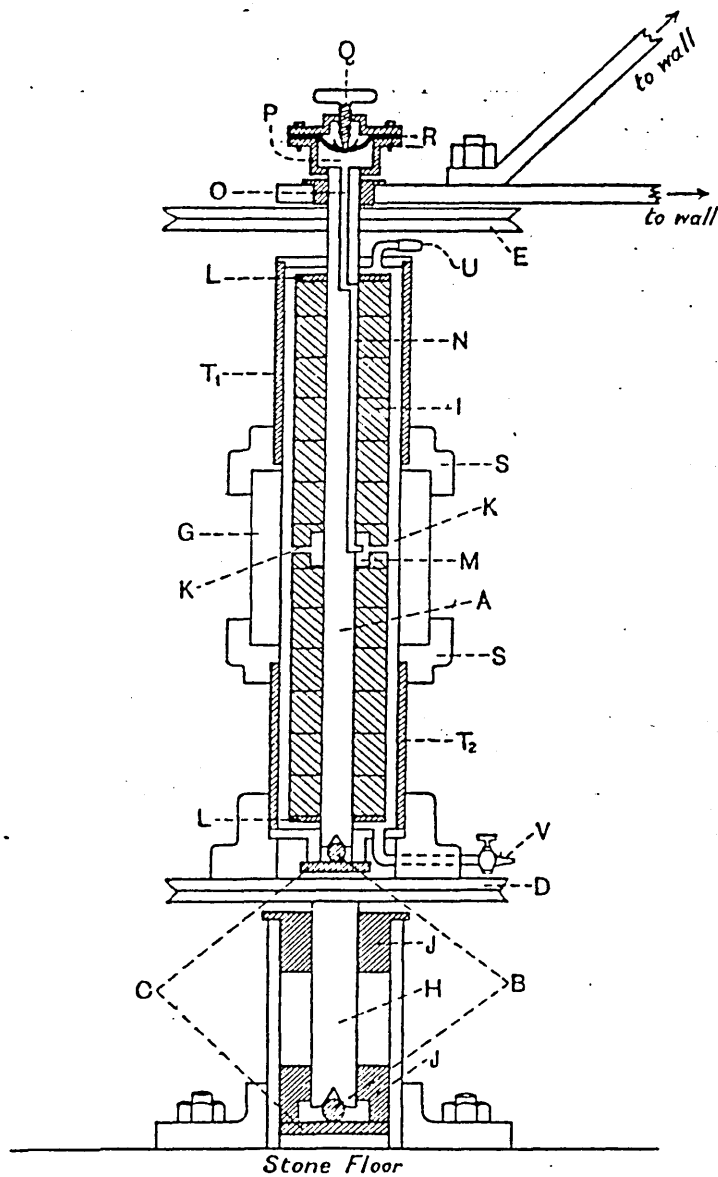


Figure 3.2 Taylor's experimental apparatus (Taylor, 1923)



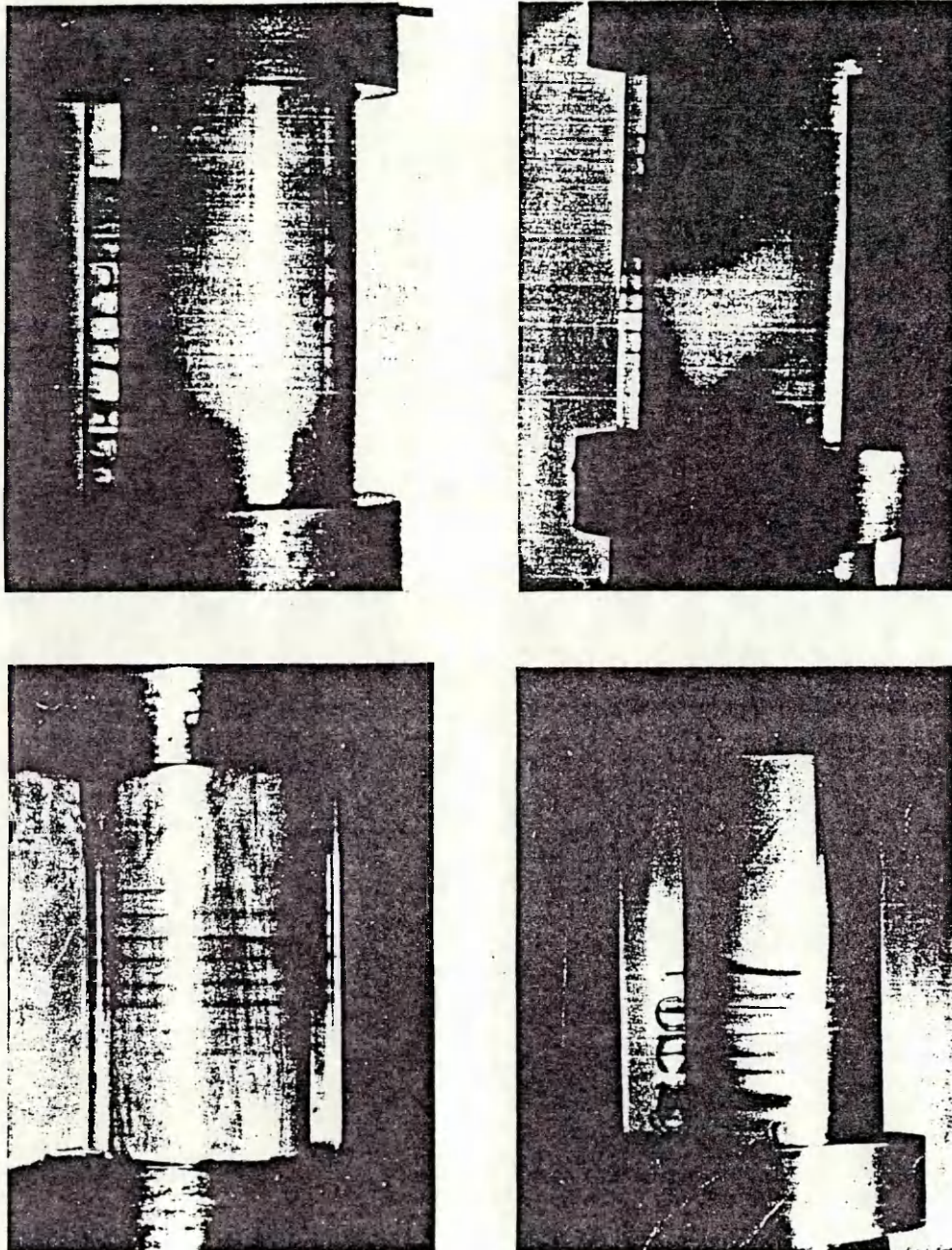
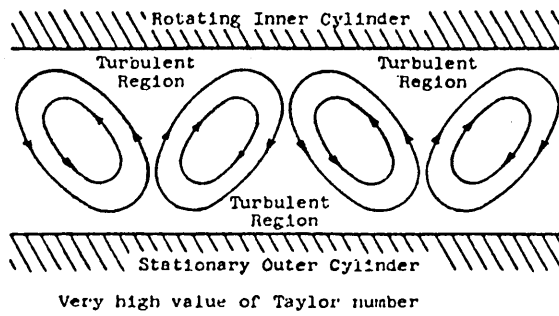
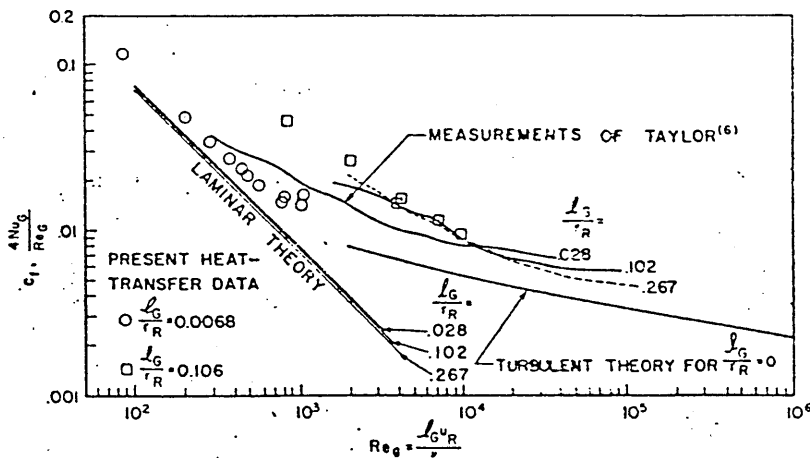


Figure 3.3 Super-laminar flow observations (Taylor, 1923)



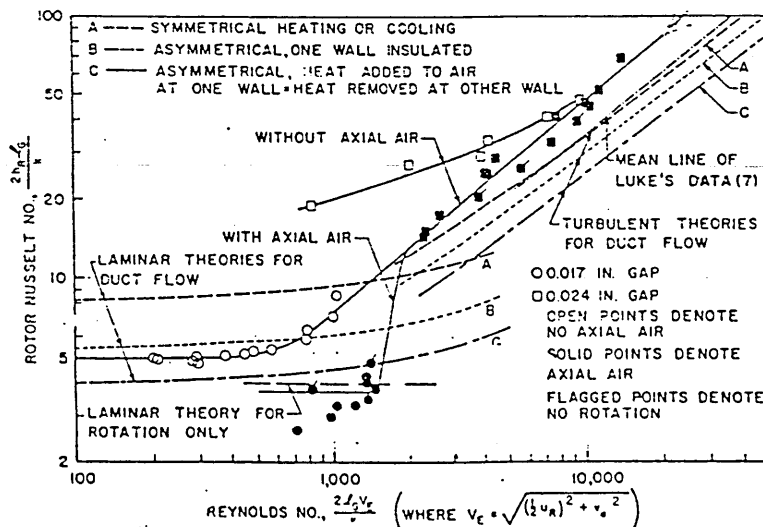
Probable vortex patterns between concentric rotating cylinders

Figure 3.4 Turbulent vortices (Pai, 1943)



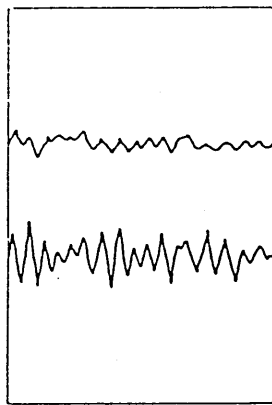
SKIN FRICTION ON OUTER CYLINDER FOR ROTATION OF INNER CYLINDER AND NO AXIAL FLOW. COMPARISON OF THEORIES FOR LAMINAR AND TURBULENT FLOW WITH EXPERIMENTS OF TAYLOR

Figure 3.5 Skin friction coefficient measurements (Gazley, 1958)



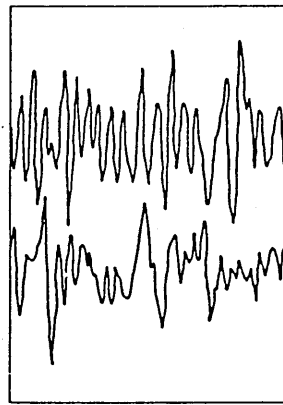
AIR-GAP HEAT TRANSFER (SMOOTH SURFACES). HEAT TRANSFER BETWEEN ROTOR SURFACE AND AIR

Figure 3.6 Nusselt number measurements (Gazley, 1958)



(CAPACITANCE = 50 mfd.)

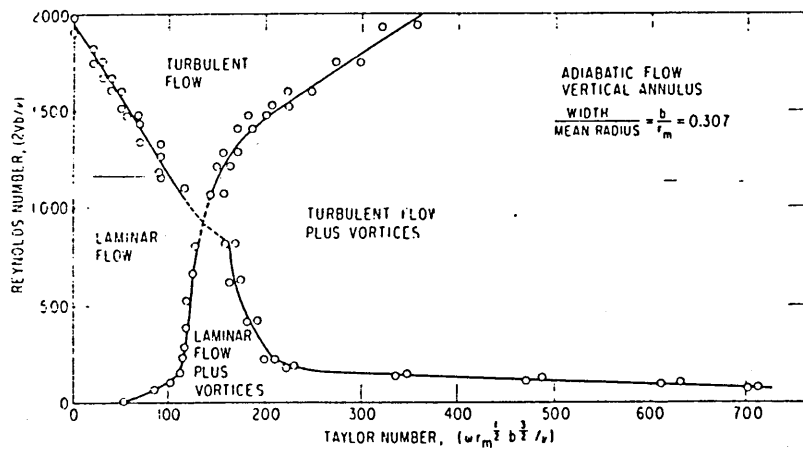
FIG. 12a TURBULENT FLOW



(CAPACITANCE = 50 mfd.)

FIG. 12b TURBULENT-PLUS-VORTICES FLOW

TRANSITION FROM TURBULENT TO TURBULENT-PLUS-VORTEXES FLOW



FOUR FLOW REGIONS FOR WIDE ANNULUS

Figure 3.7 Flow regimes in rotating annular flows (Kaye & Elgar, 1958)

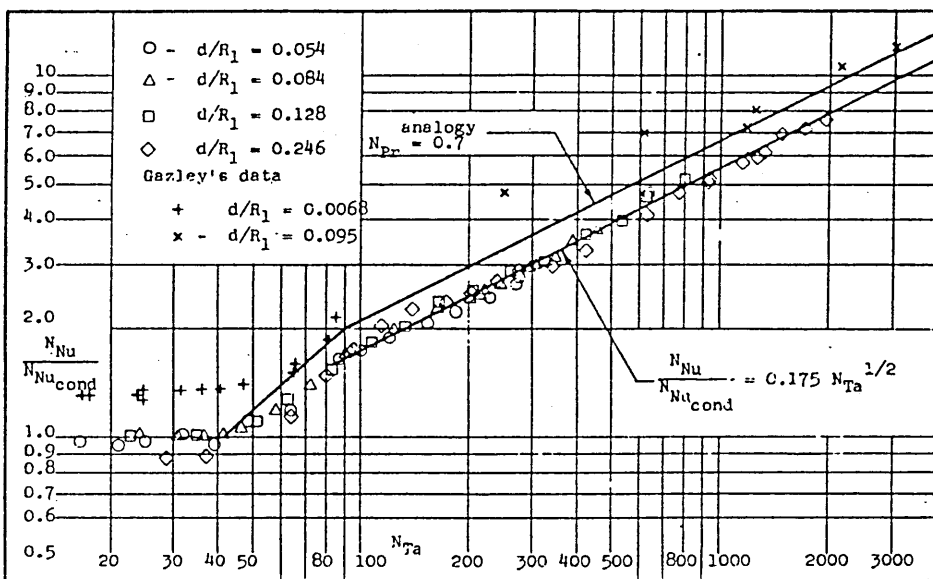
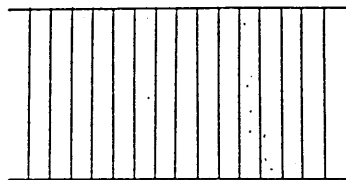
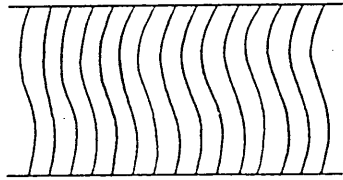


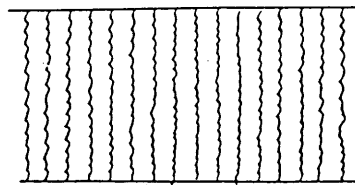
Figure 3.8 Nusselt number measurements (Bjorklund & Kays, 1959)



(a) Steady Vortices



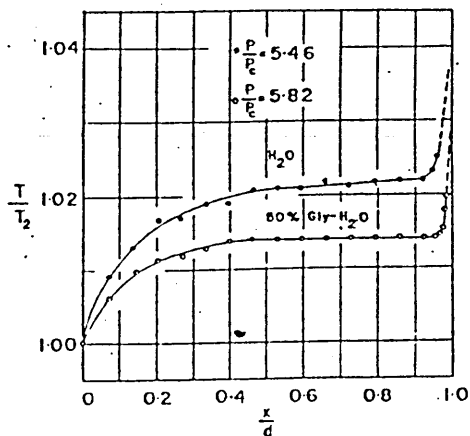
(b) Wavy Vortices



(c) High Speed Wavy Vortices

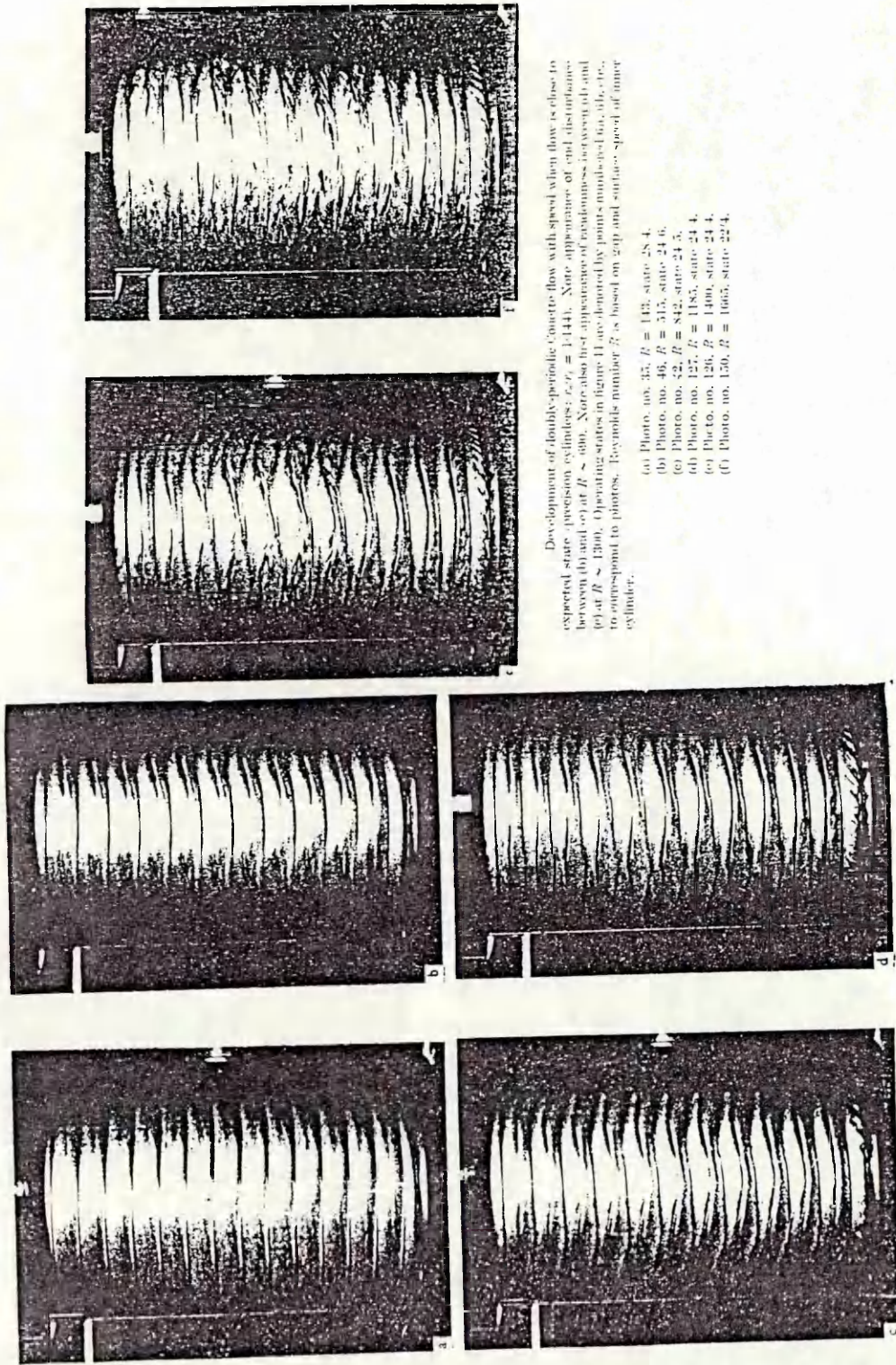
(a) Vortex pattern for  $1 < \frac{P}{P_c} < 1.21$ ;  
 (b) vortex pattern for  $1.21 < \frac{P}{P_c} < 7$ ; (c)  
 vortex pattern for  $\frac{P}{P_c} > 7$ . All views are in elevation;  
 that is, as they appear to external observer. Outer cylinder stationary.

Figure 3.9 Vortex development with increasing Taylor number ( Nissan, 1963)



Radial temperature profiles for water and a 50% water-glycerine solution.

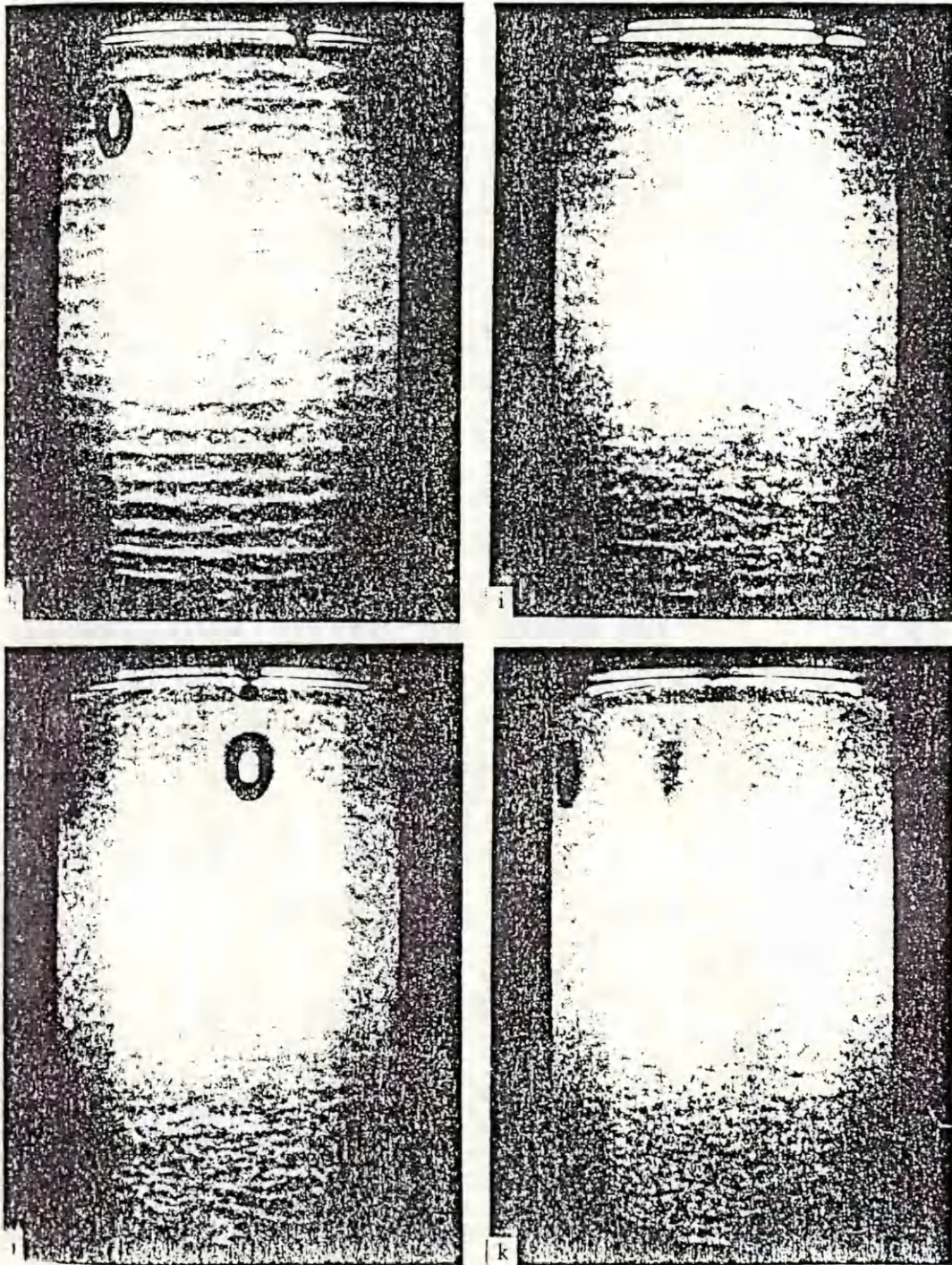
Figure 3.10 Radial velocity profile across the annulus (Ho, 1964)



Development of doubly-periodic Couette flow with speed when flow is close to expected state (precision cylinders;  $\epsilon = 1/44$ ). Note appearance of end disturbance between (b) and (c) at  $R \approx 400$ . Note also first appearance of randomness between (d) and (e) at  $R \approx 1300$ . Operating states in figure 11 are denoted by points numbered (a), (b), (c), (d), (e), (f) in figure 11. Reynolds number  $R$  is based on gap and surface speed of inner cylinder.

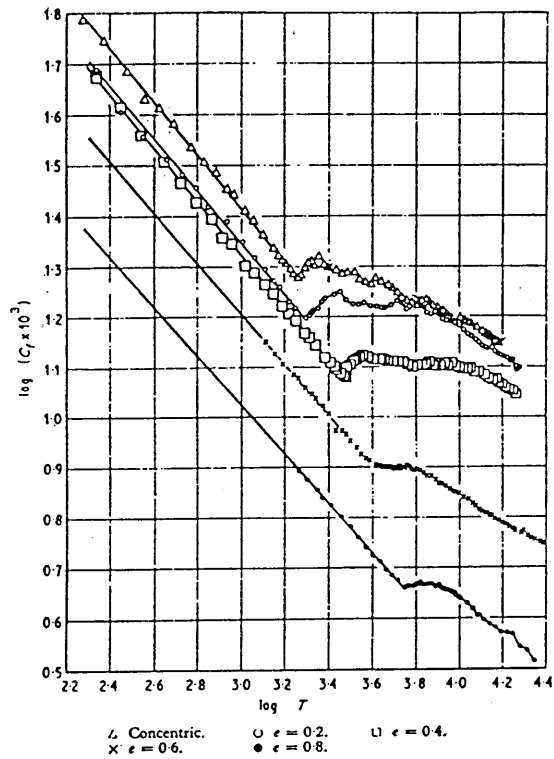
- (a) Photo. no. 35,  $R = 143$ , state 28.4.
- (b) Photo. no. 46,  $R = 315$ , state 24.6.
- (c) Photo. no. 52,  $R = 842$ , state 24.5.
- (d) Photo. no. 127,  $R = 1185$ , state 24.4.
- (e) Photo. no. 130,  $R = 1400$ , state 24.4.
- (f) Photo. no. 150,  $R = 1065$ , state 22.4.

Figure 3.11 Vortex regimes (Coles, 1965)



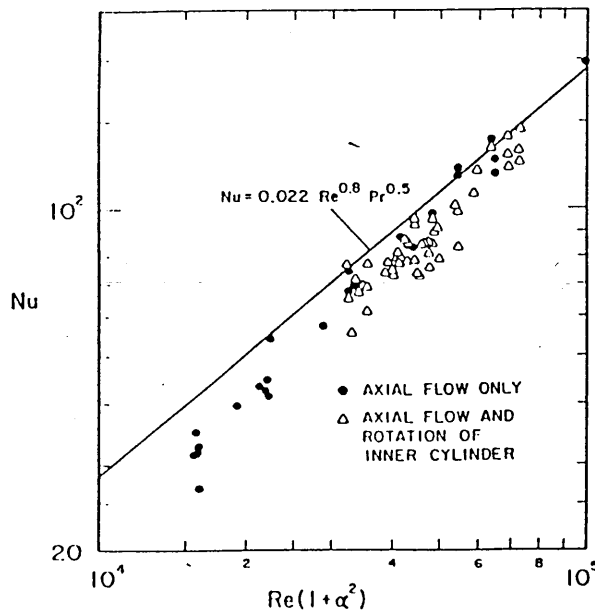
Turbulent Couette flows showing disappearance of residual periodicity when outer cylinder rotates opposite to inner one (rough cylinders;  $r_o/r_i = 1.135$ ). All scenes are taken from motion picture. (h) Flow at H in figure 2(a);  $R_i = 18,800$ ,  $R_o = 0$ . (i) Flow at I in figure 2(a);  $R_i = 18,800$ ,  $R_o = -10,850$ . (j) Flow at J in figures 2(a) and (b);  $R_i = 8350$ ,  $R_o = -10,850$ . (k) Flow at K in figure 2(a);  $R_i = 18,900$ ,  $R_o = -27,700$ .

Figure 3.12 Turbulent Couette flow with structure (Coles, 1965)



Friction coefficient—Taylor number characteristics for different eccentricities covering a wider range of Taylor numbers.

Figure 3.13 Change of torque slope with Taylor number (Castle et al, 1971)



Correlation of the fully developed Nusselt number with rotation parameter

Figure 3.14 Nusselt number measurements (Kuzay & Scott, 1977)



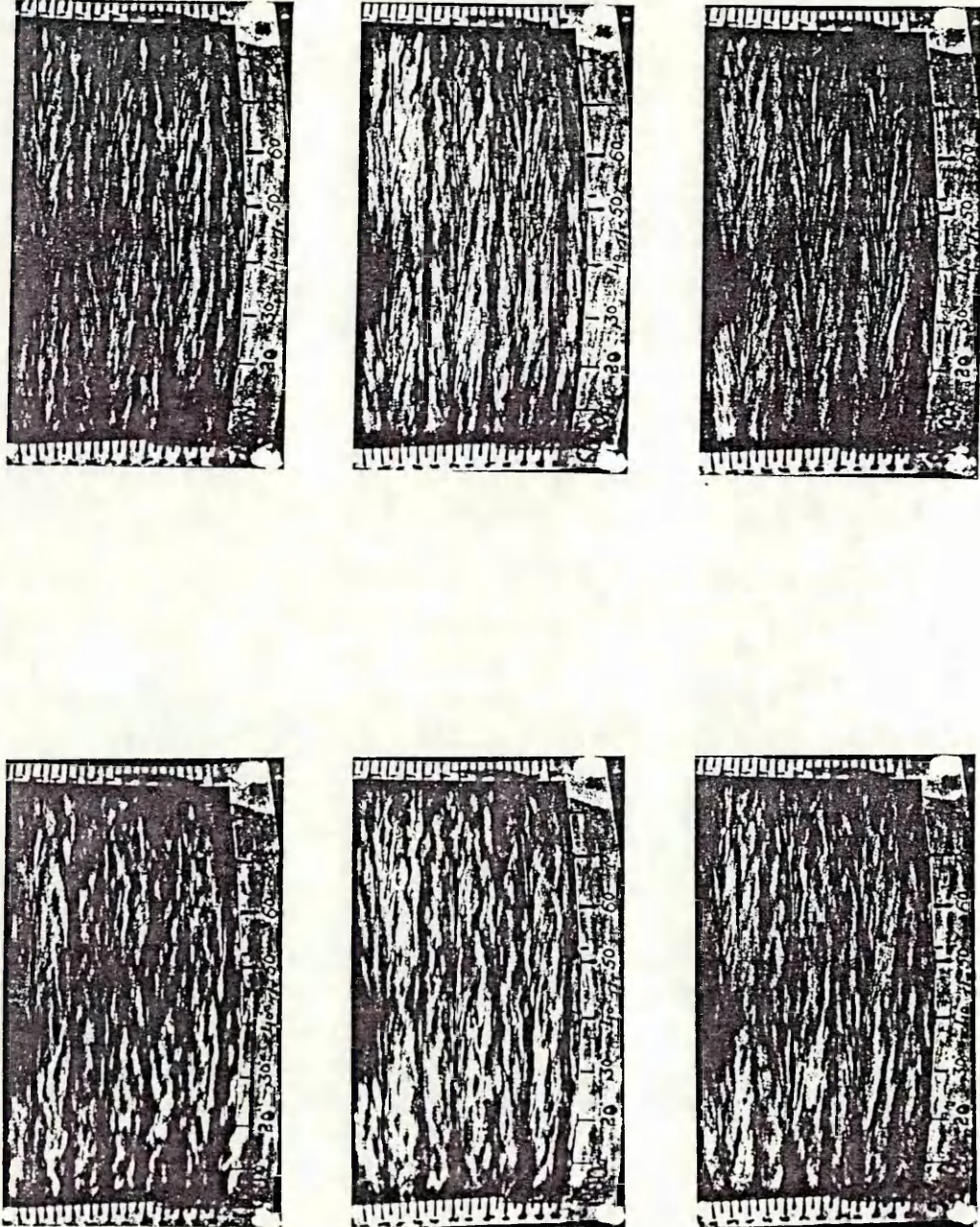
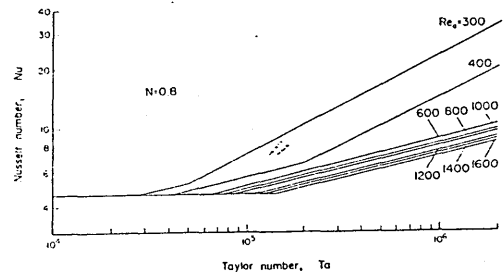
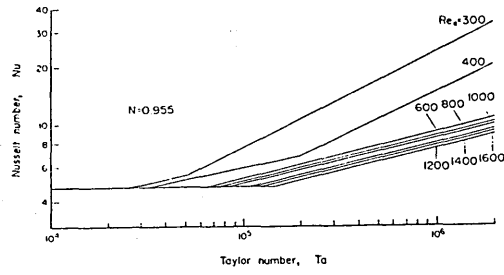
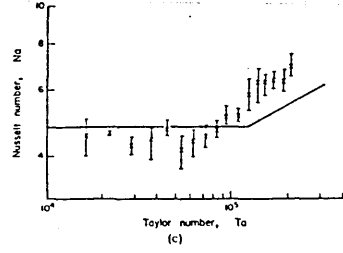
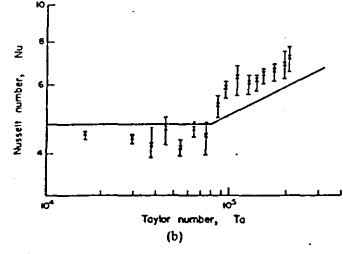
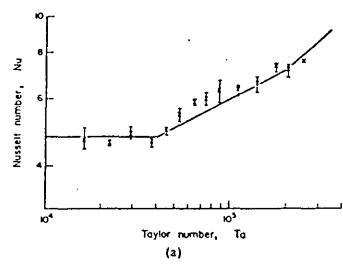


Figure 3.15 High speed vortices (Barcilon et al, 1979)



Results of Reynolds analogy solution.

Figure 3.16 Predicted Nusselt numbers (Simmers & Coney, 1979 (a))



- (a) Nusselt number vs Taylor number,  
 $N = 0.955, Re_e = 400.$
- (b) Nusselt number vs Taylor number,  
 $N = 0.955, Re_e = 800.$
- (c) Nusselt number vs Taylor number,  
 $N = 0.955, Re_e = 1200.$

Figure 3.17 Experimental Nusselt number measurements (Simmers & Coney, 1979 (a))

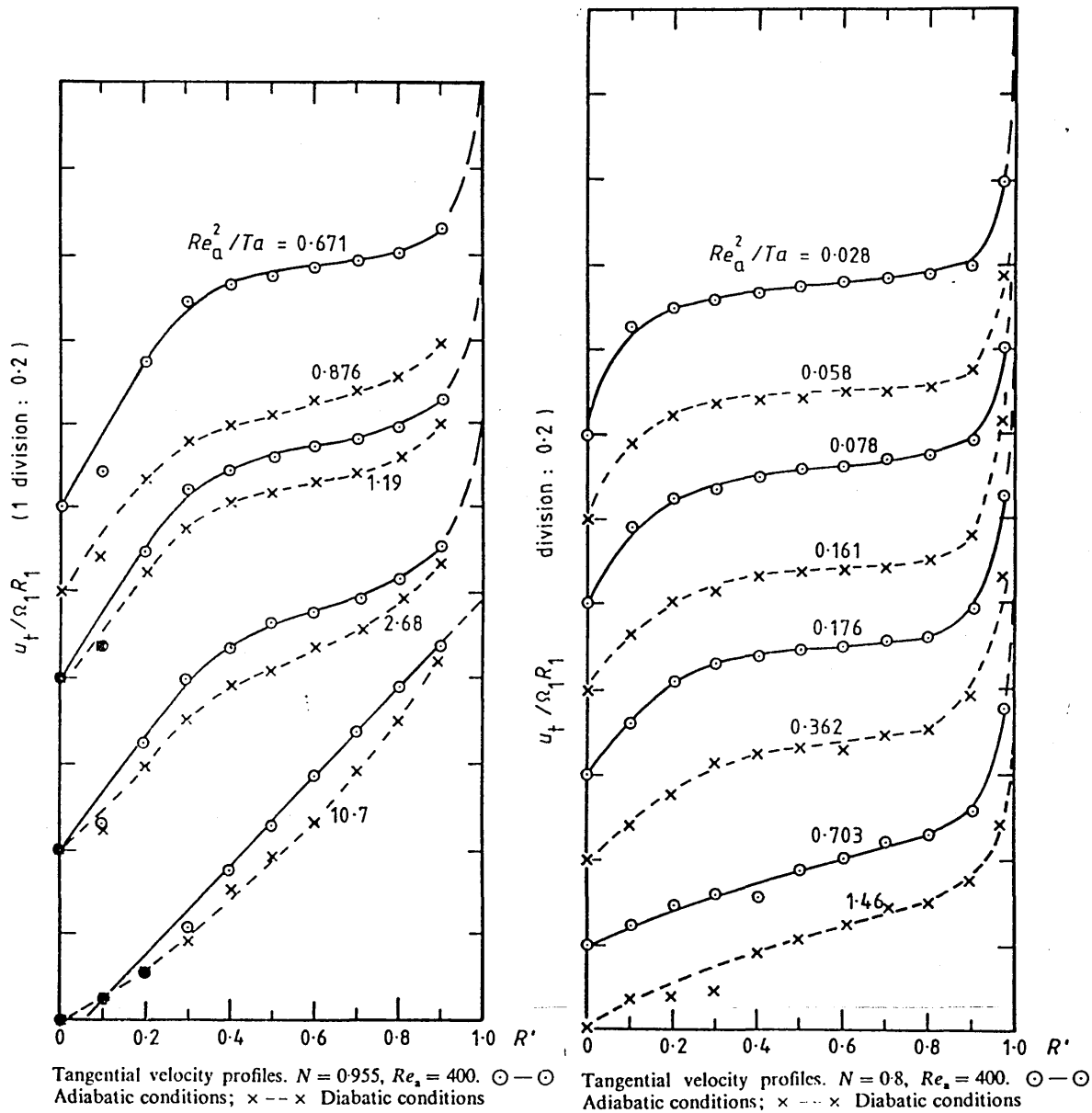


Figure 3.18 Typical velocity profiles (Simmers & Coney, 1980)

*Visual results for oil,*  
 $Re_a = 250$ ,  $N = 0.848$ : (a)  $Ta = 14\ 700$  (b)  $Ta = 20\ 700$  (c)  $Ta = 28\ 000$  (d)  $Ta = 260\ 000$  (e)  $Ta = 1.05 \times 10^6$

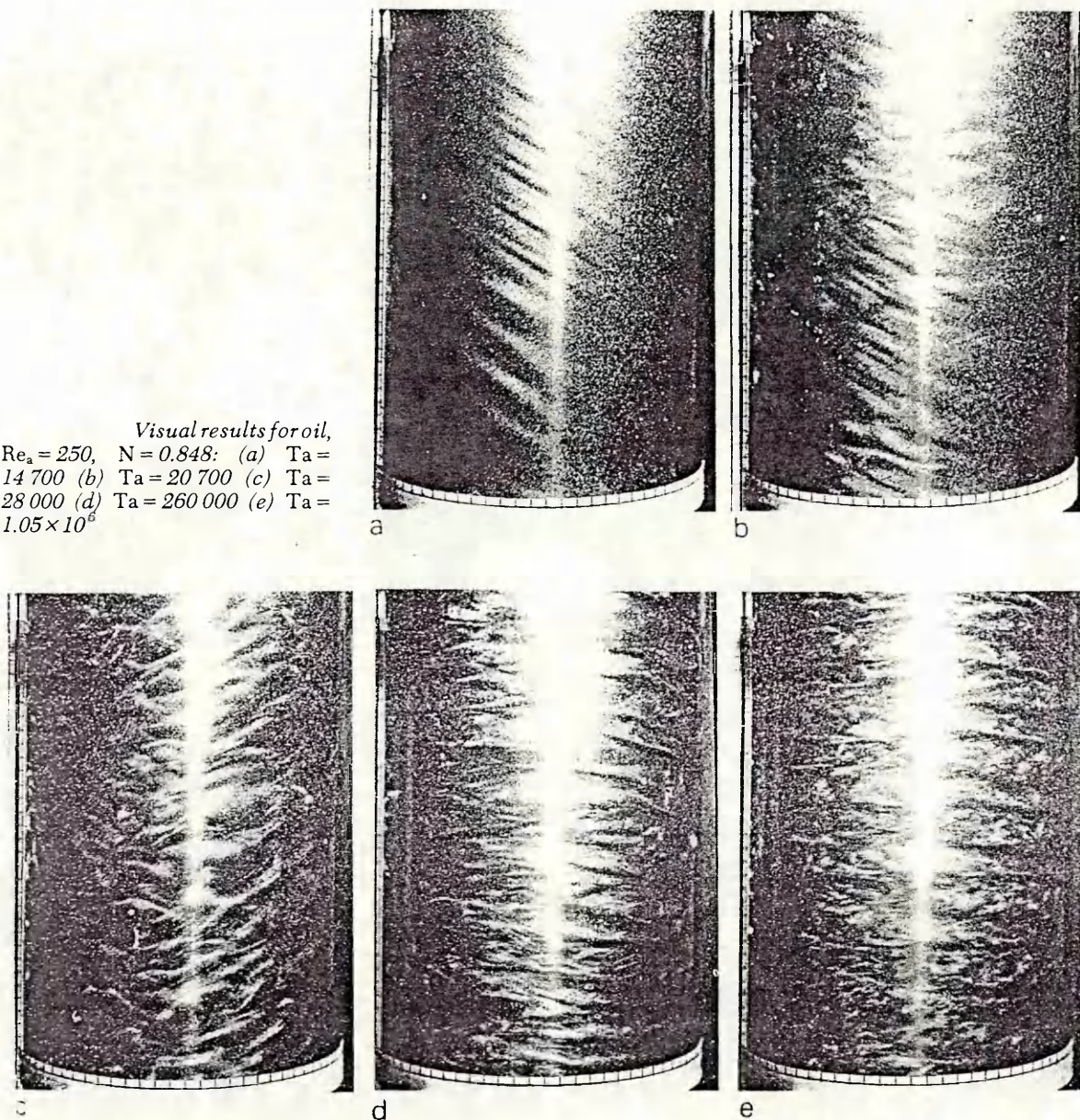
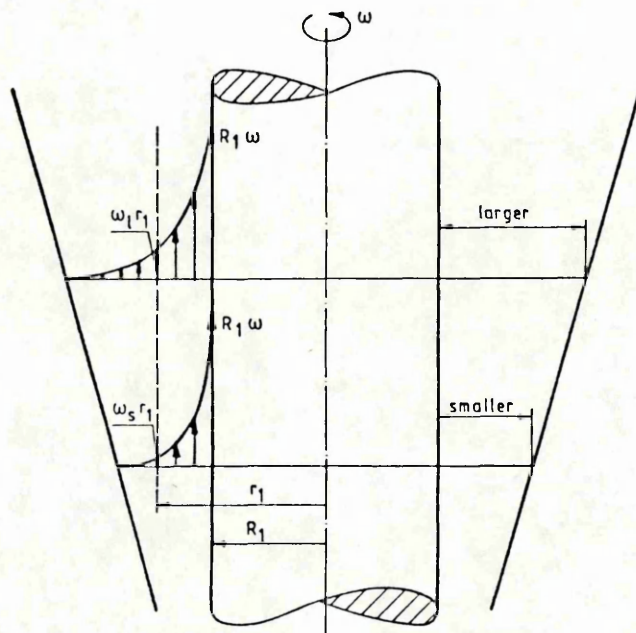
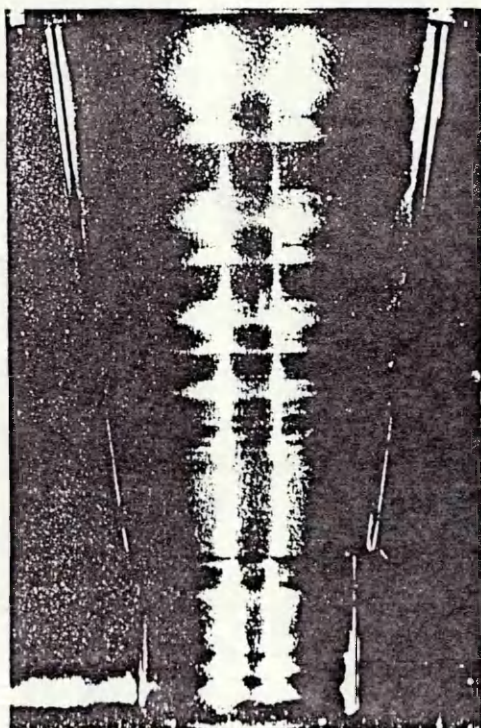


Figure 3.19 Vortex development showing re-emergent structure at  $Ta > 10^6$  (Wan & Coney, 1982)



velocity profiles  
turned about 90°

Different velocity profiles in a gap between a rotating cylinder and a cone.



Verticals in the gap between a rotating cylinder and a cone.

Figure 3.20 Flow around a circular cylinder rotating in a cone at rest (Wimmer, 1988)

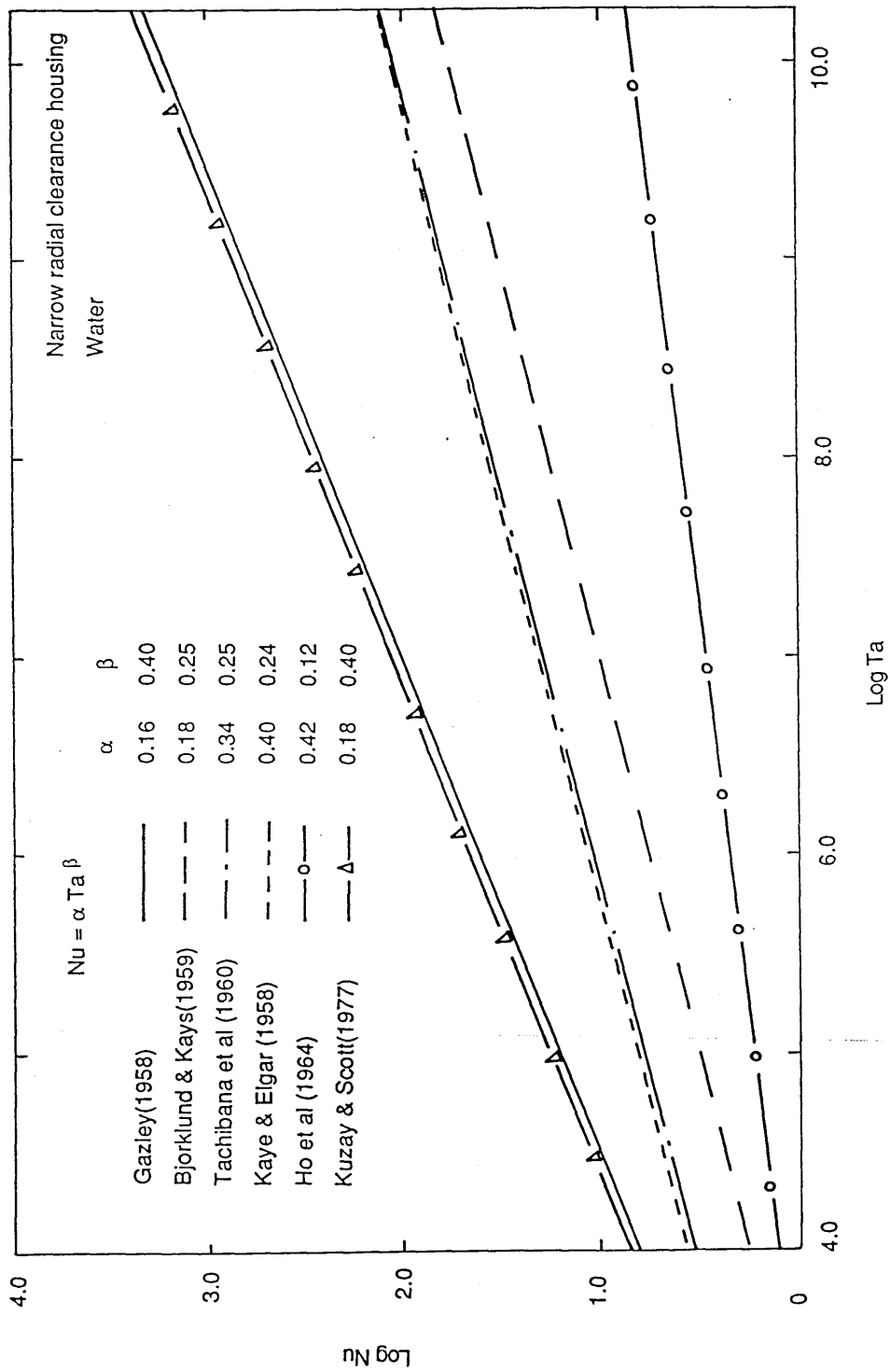


Figure 3.21 Comparison of Nusselt vs Taylor numbers - empirical expressions

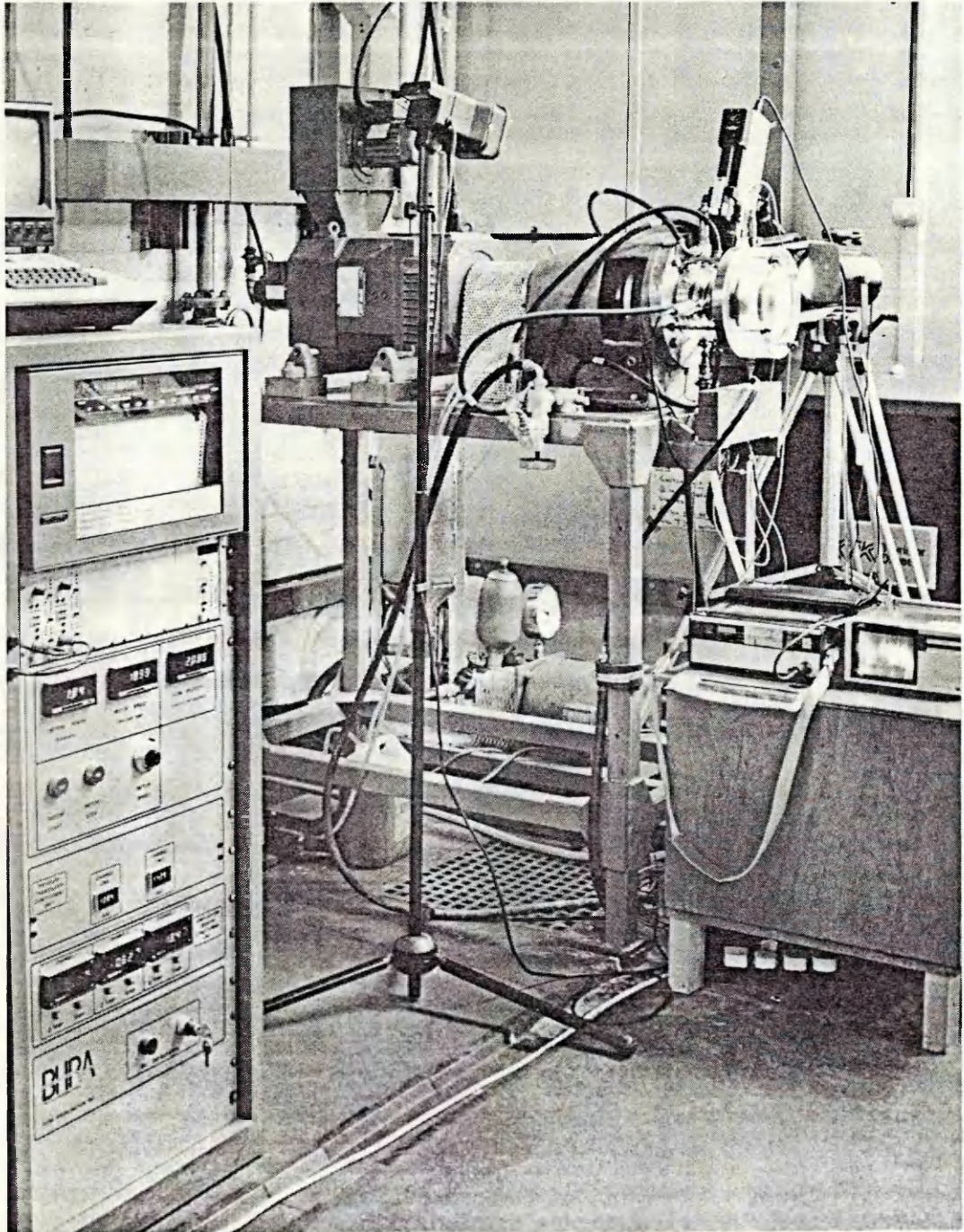


Figure 4.1 General view of test apparatus

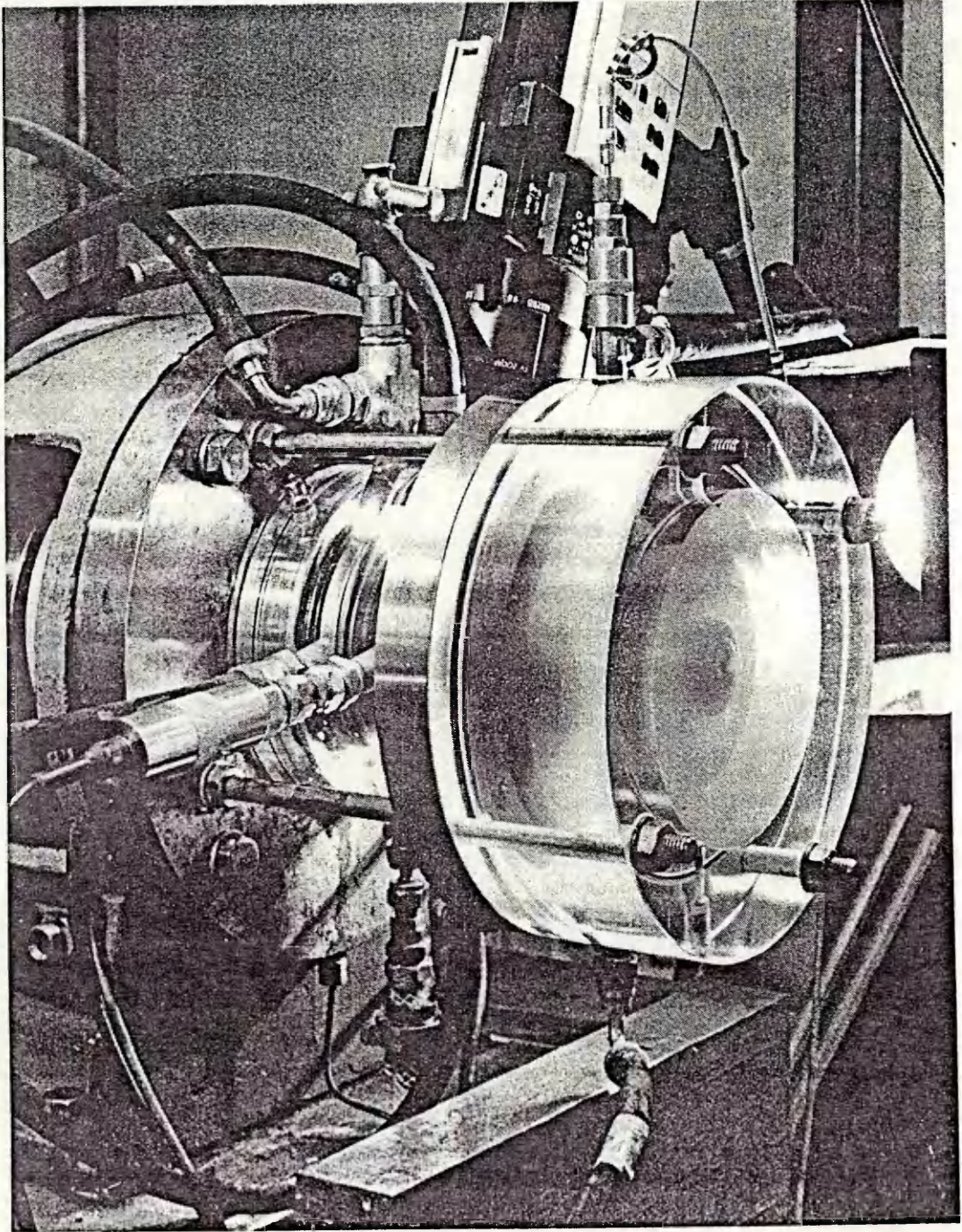


Figure 4.2 Close-up of test apparatus showing camera position



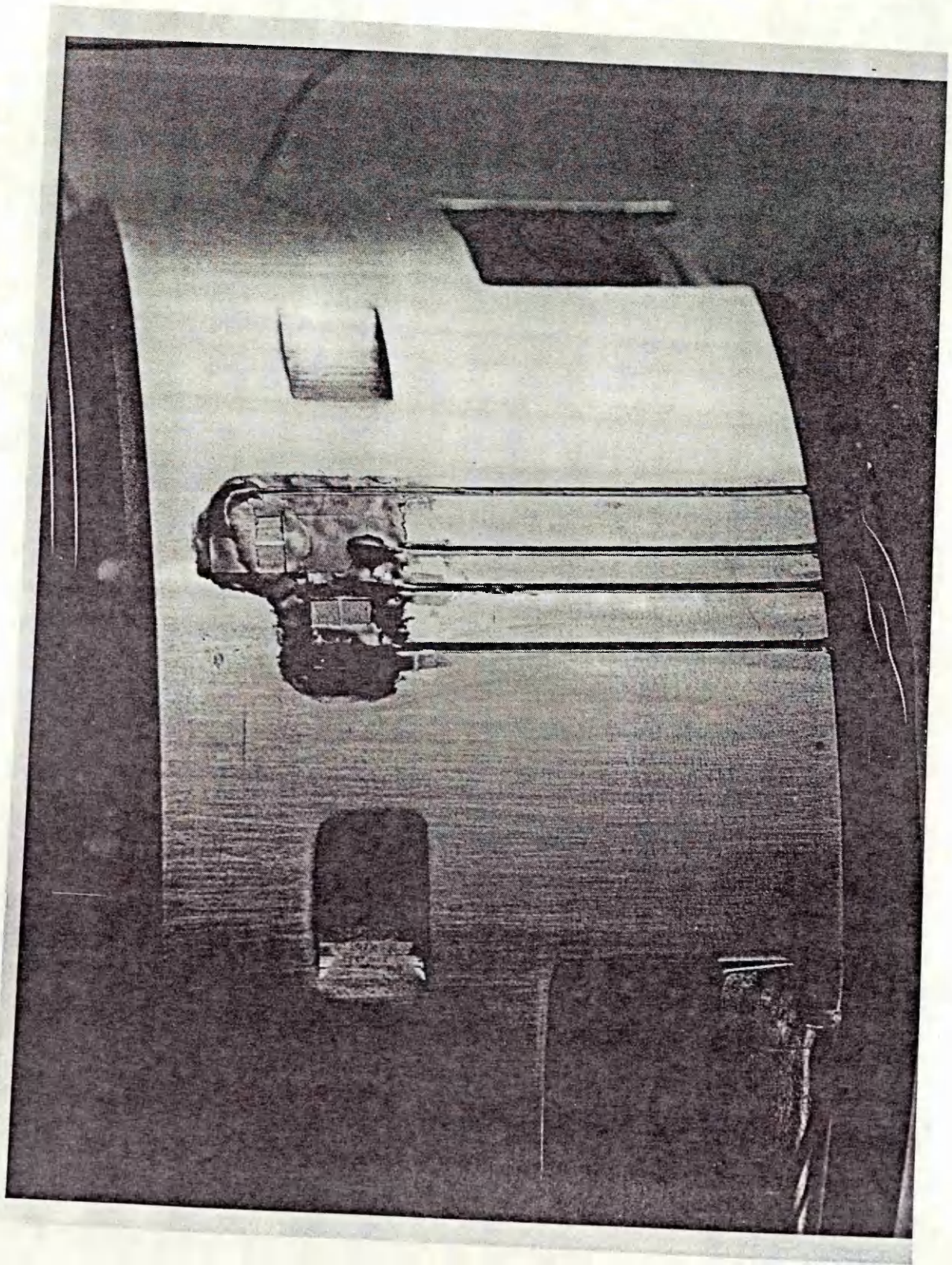


Figure 4.3 Heat-transfer probes fitted to Seal B

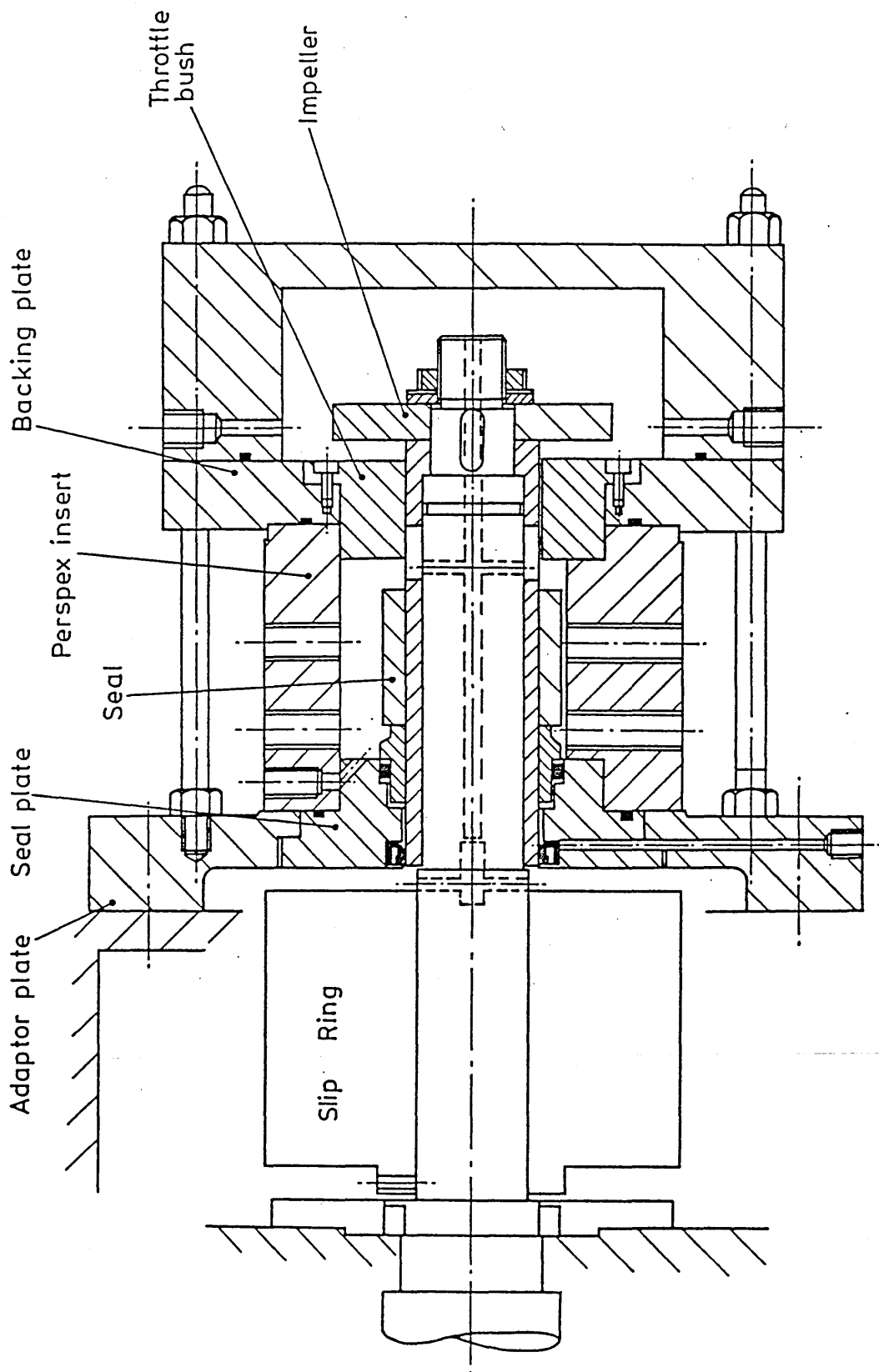


Figure 4.4 GA of test apparatus

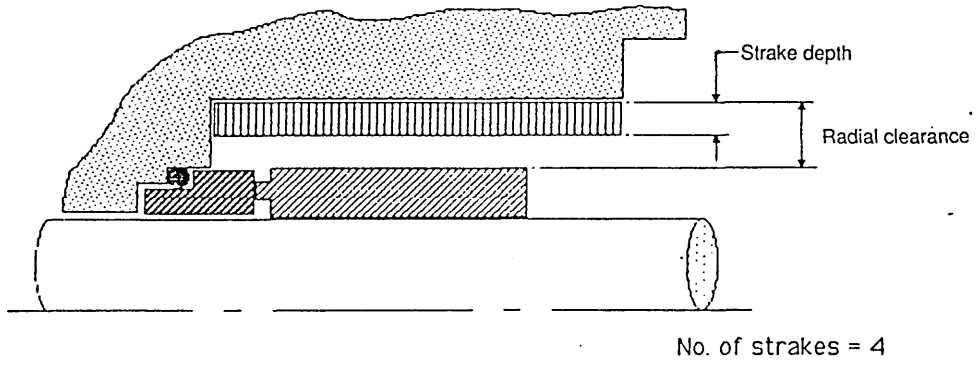


Figure 4.5 Axial strake assembly for Housing 2

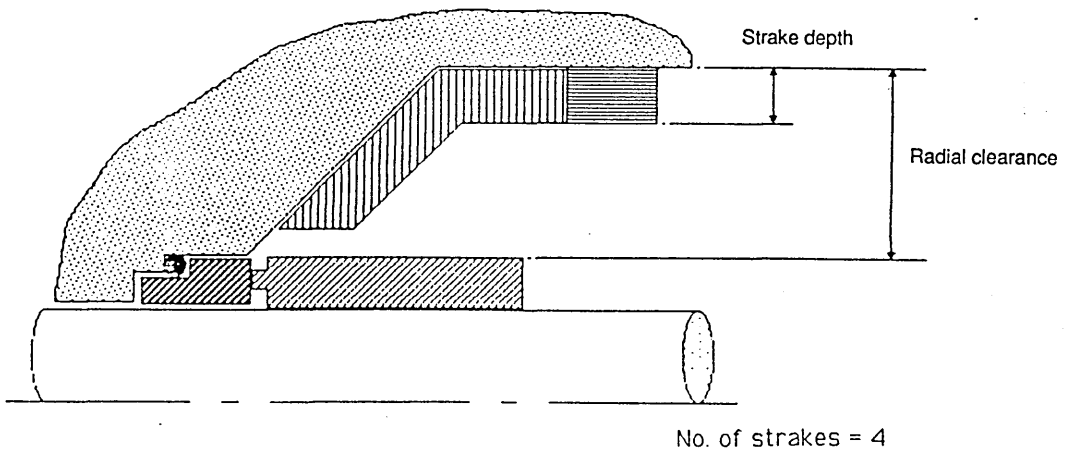


Figure 4.6 Axial strake assembly for Housing 7

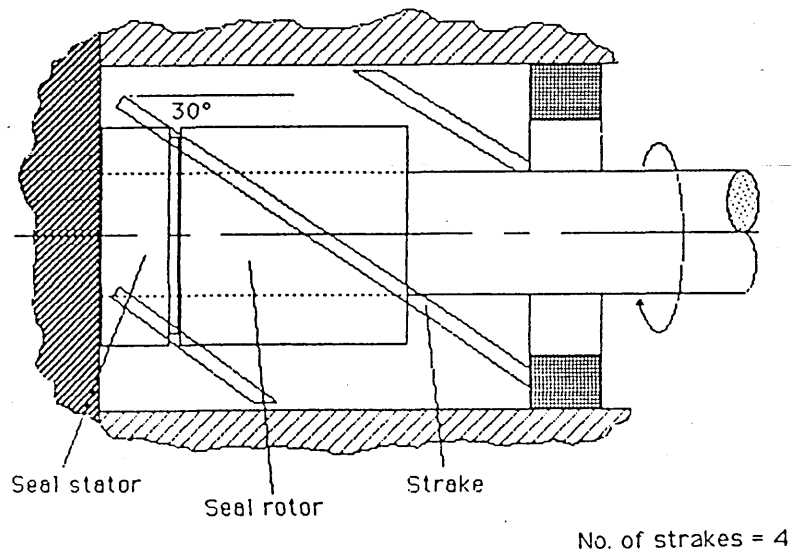


Figure 4.7 Helical strake assembly for Housing 2

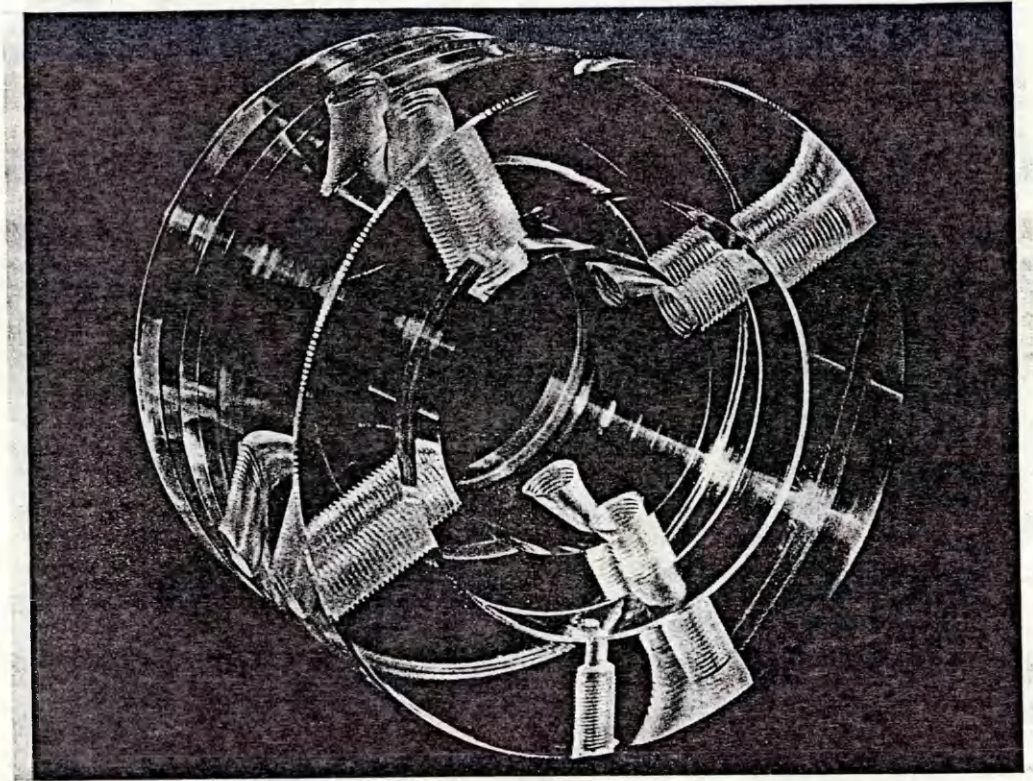


Figure 4.8 Housing 1

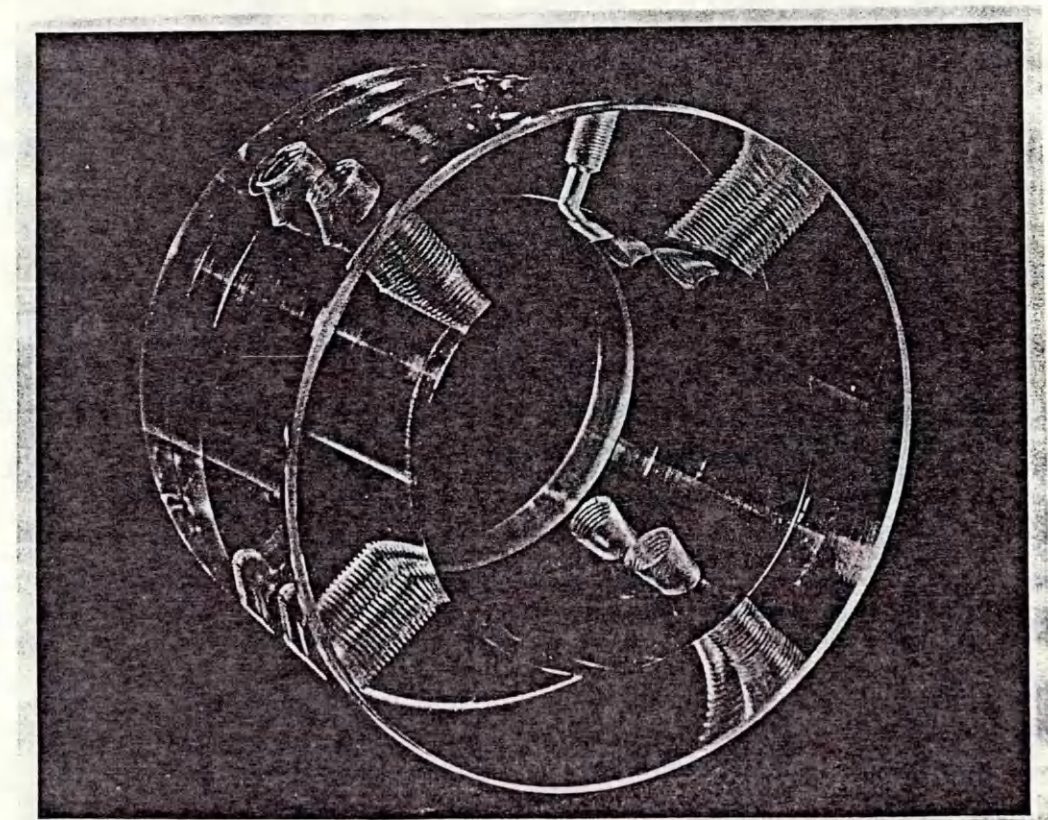


Figure 4.9 Housing 2

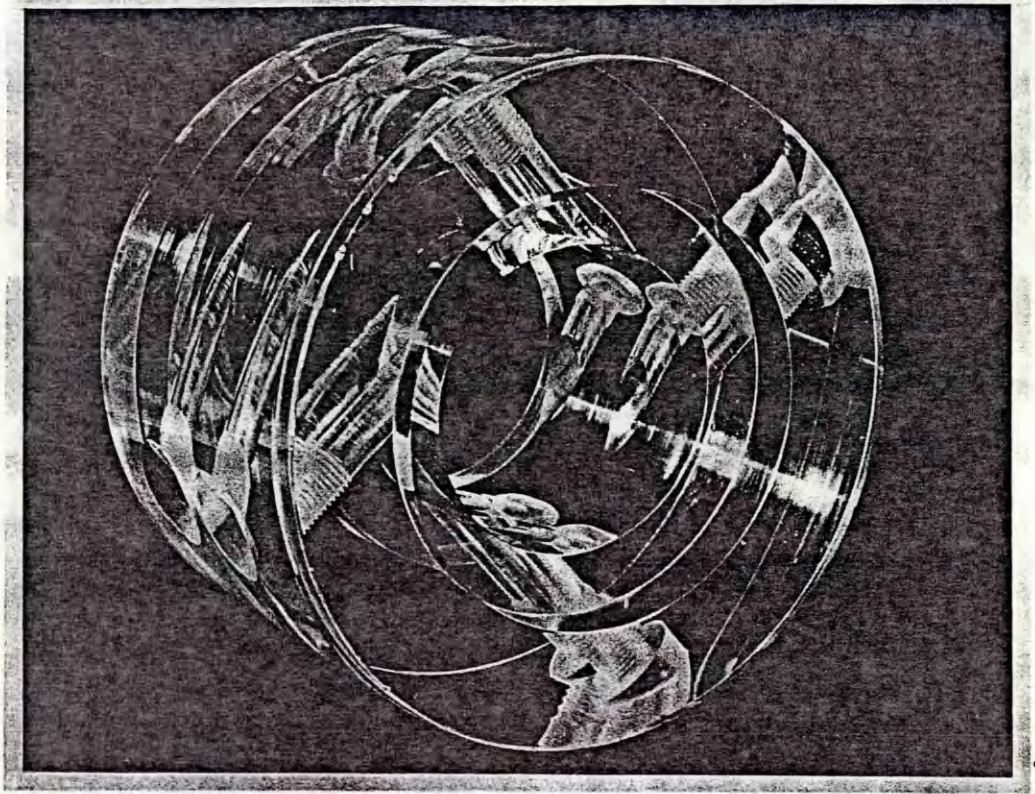


Figure 4.10 Housing 3



Figure 4.11 Housing 4

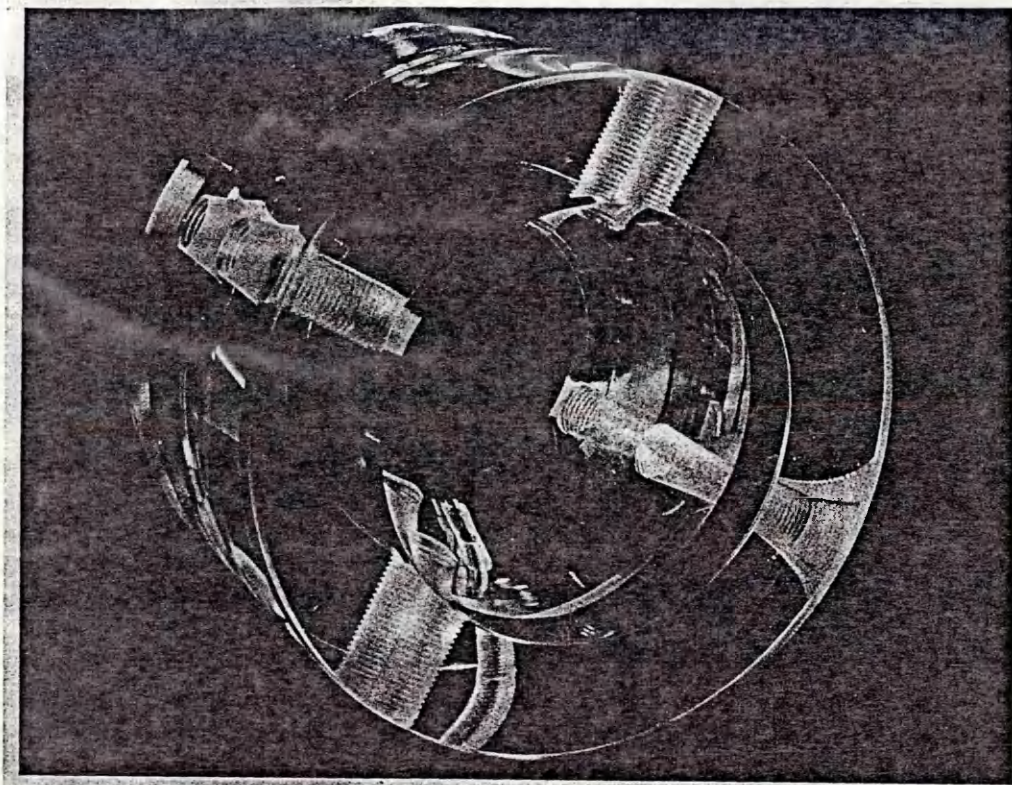


Figure 4.12 Housing 5

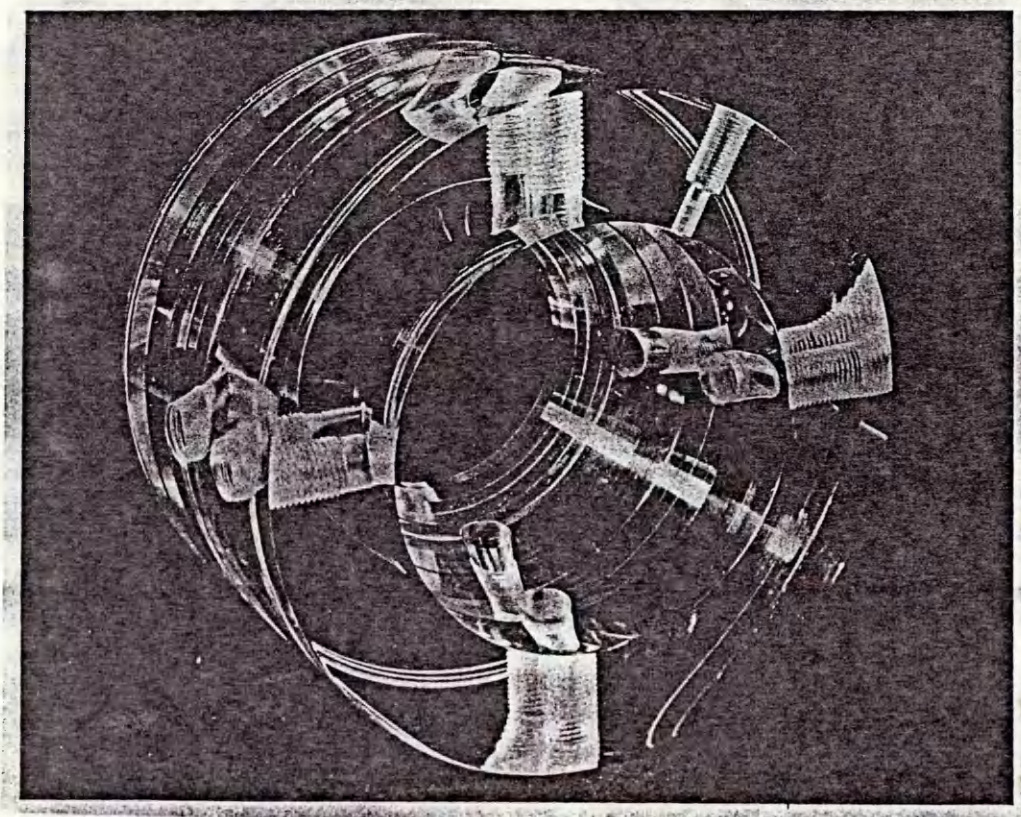
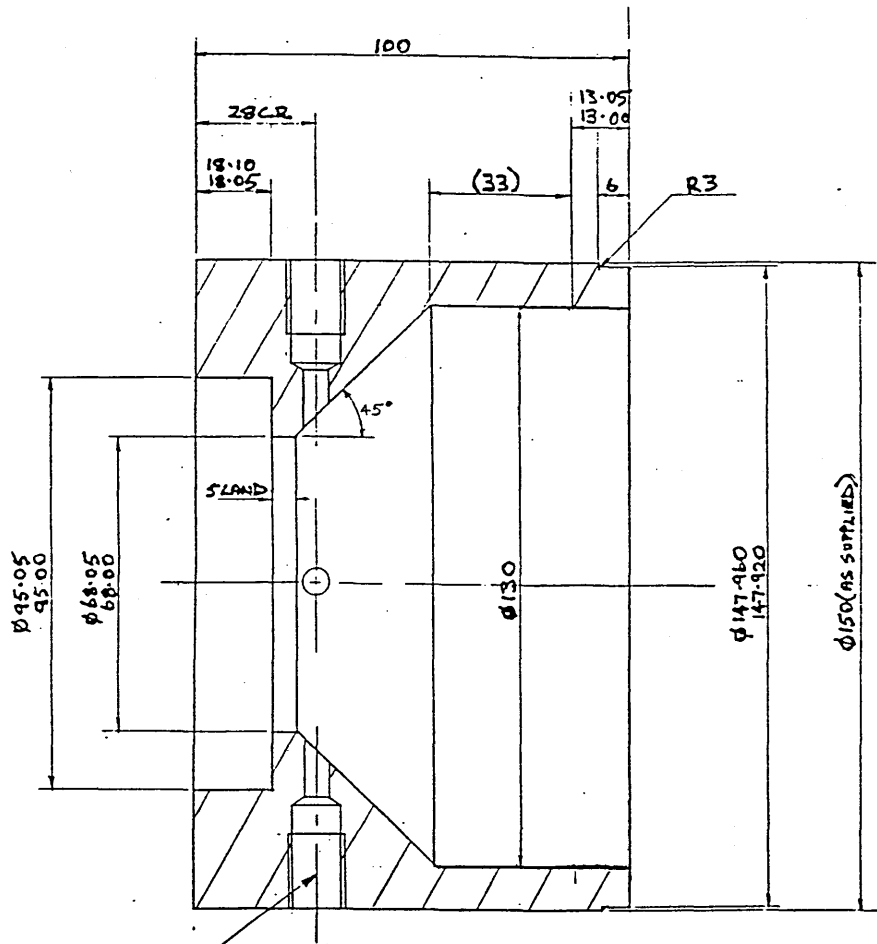


Figure 4.13 Housing 6



4 HOLES DRILL  $\phi 6$  THRO',  
 DRILL  $\phi 11.8 \times 24$  DEEP,  
 AND TAP  $\frac{1}{4}$ " BSP  $\times 17$  DEEP

Figure 4.14 Housing 7

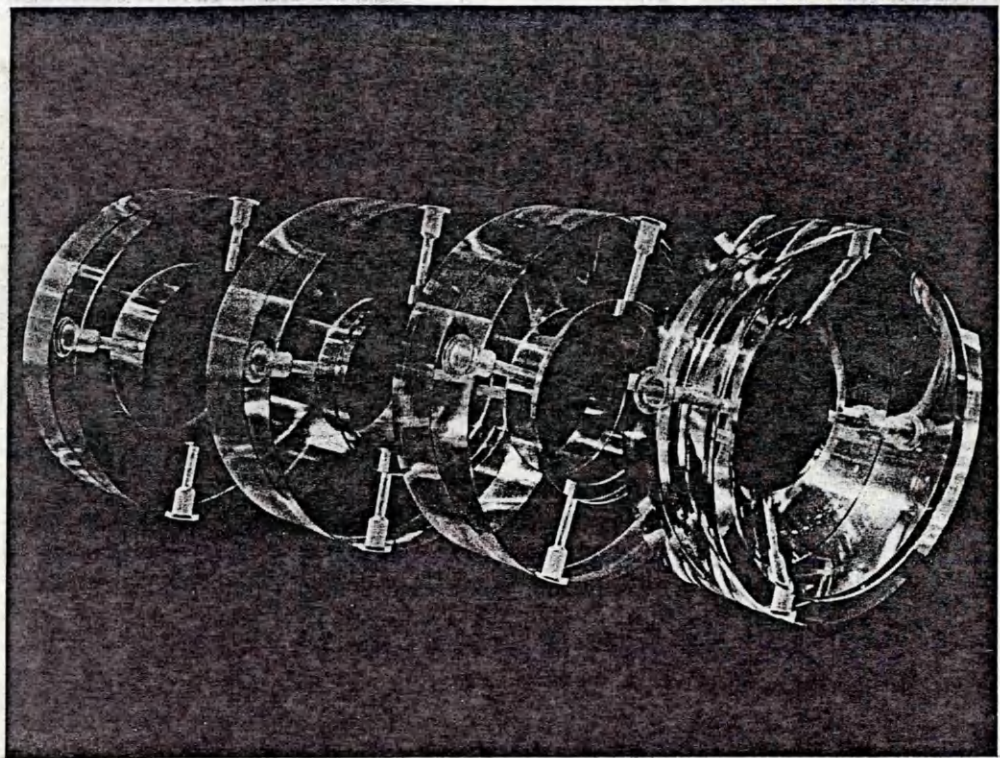


Figure 4.15 Cylindrical housings - 100 mm

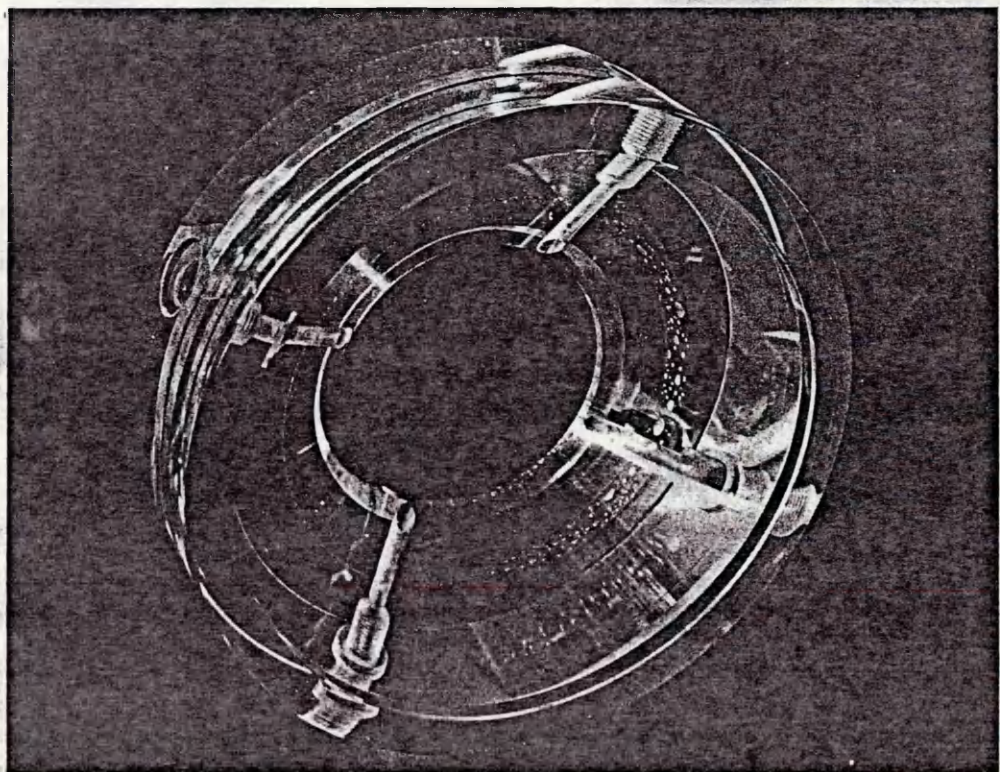


Figure 4.16 45° flared housing - 100 mm



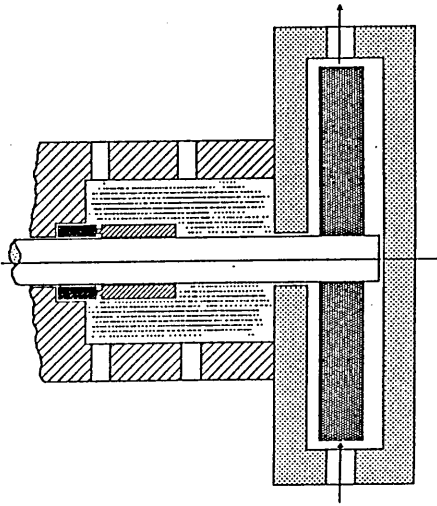


Figure 4.17 Circulation - Plan A

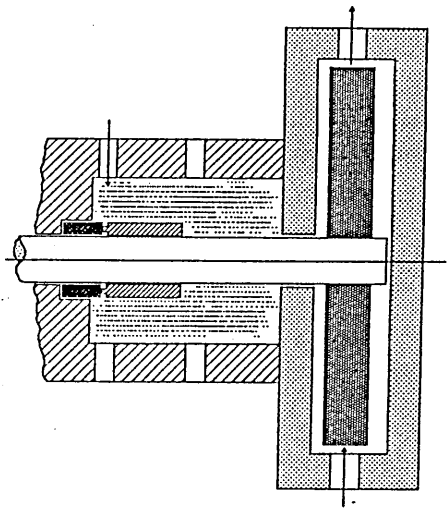


Figure 4.18 Circulation - Plan B

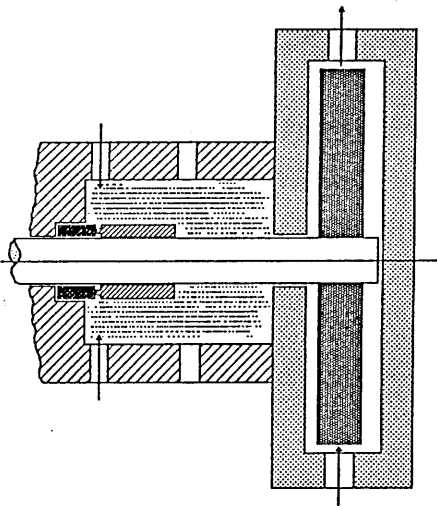


Figure 4.19 Circulation - Plan C

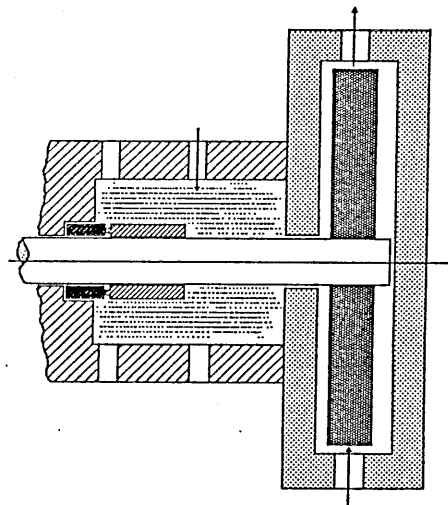


Figure 4.20 Circulation - Plan D

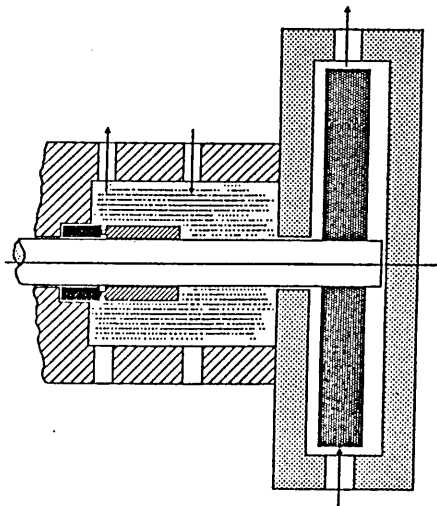


Figure 4.21 Circulation - Plan E

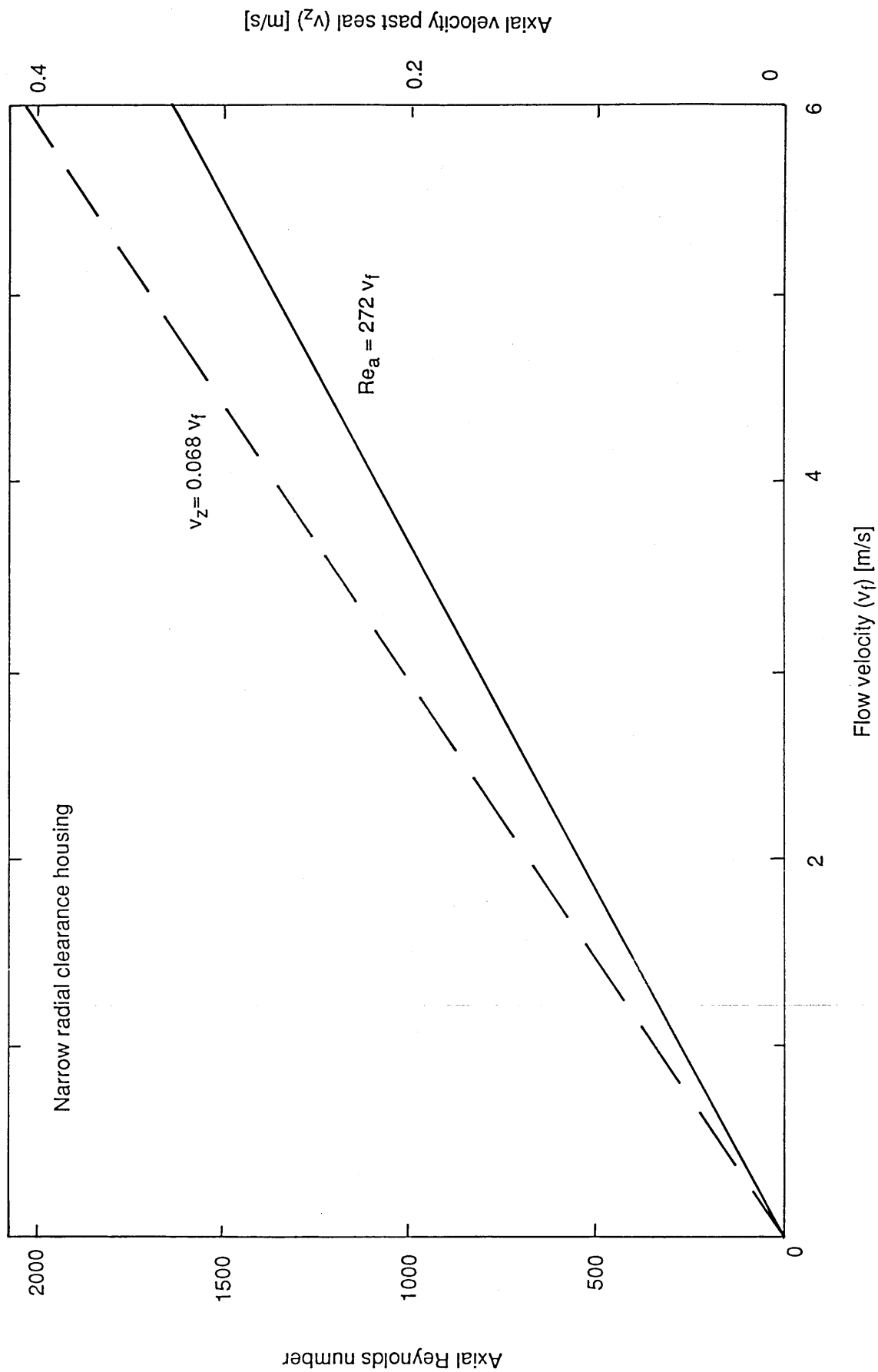


Figure 4.22 Reynolds number as a function of flowrate

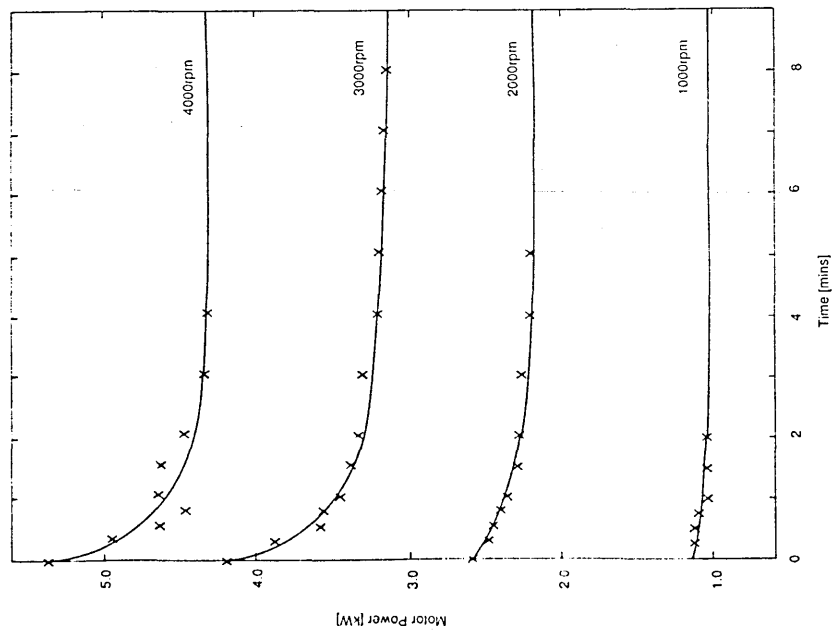


Figure 4.23 Power drop-off as a function of time

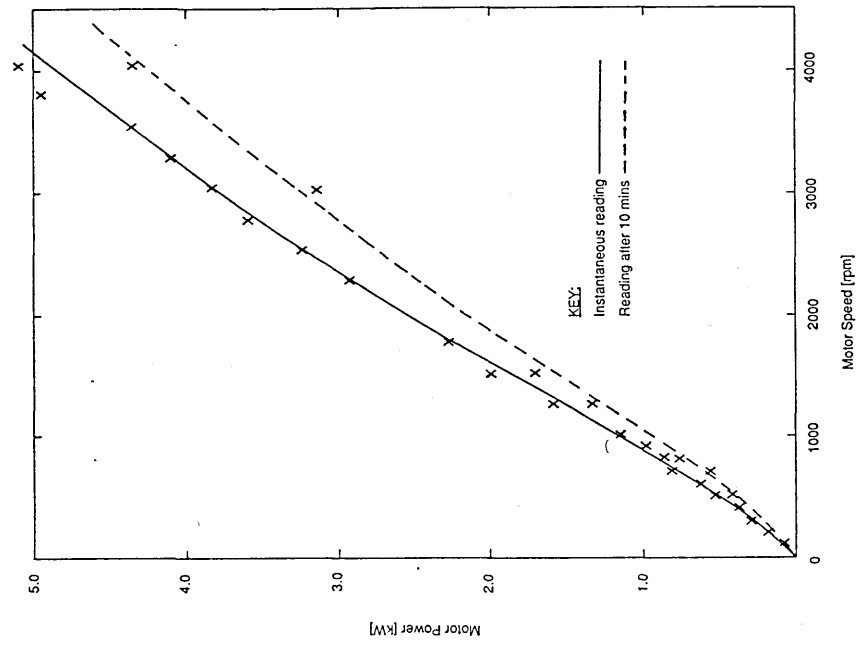


Figure 4.24 Power consumption as a function of speed

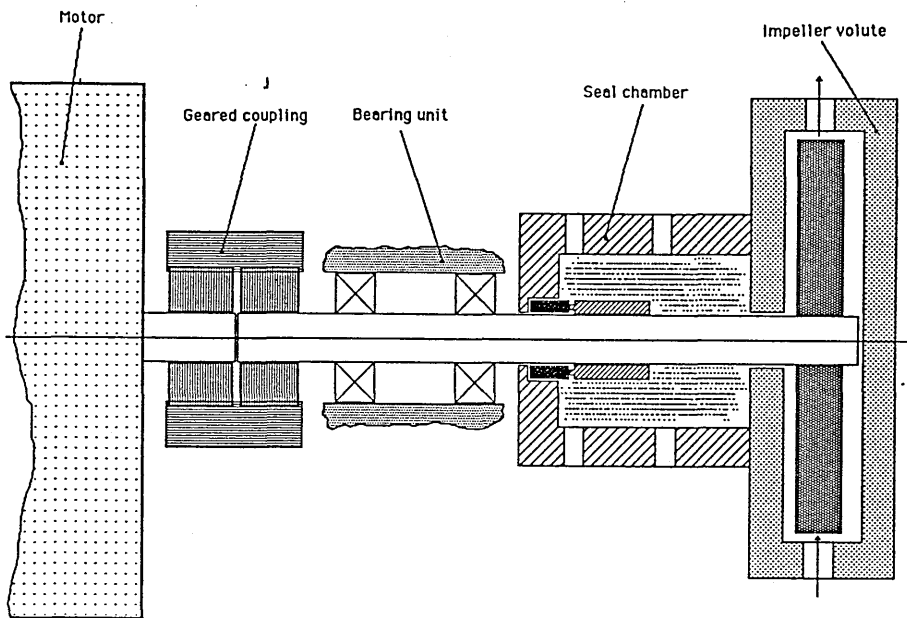


Figure 4.25 Diagram of drive system

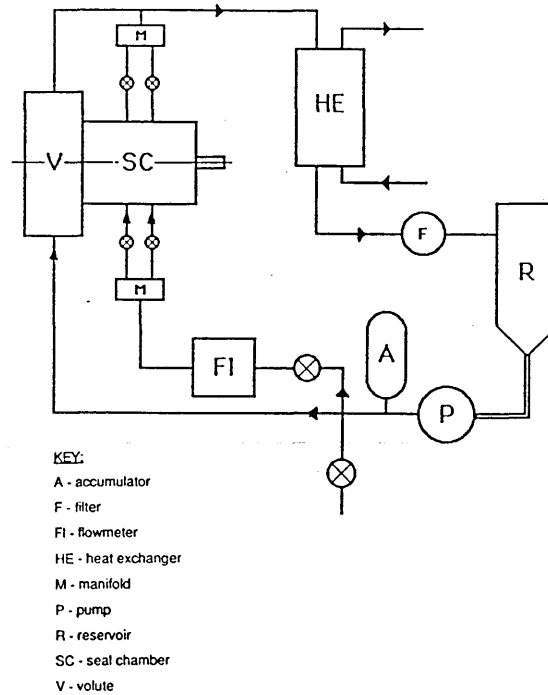


Figure 4.26 Pumpset

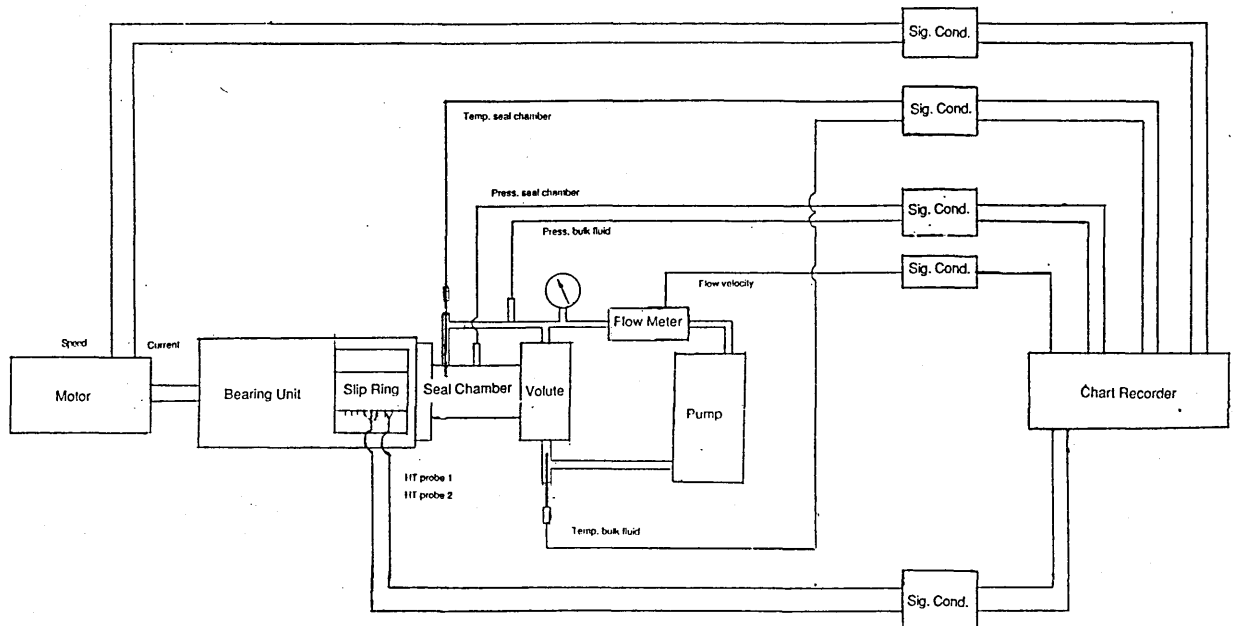


Figure 4.27 Instrumentation layout

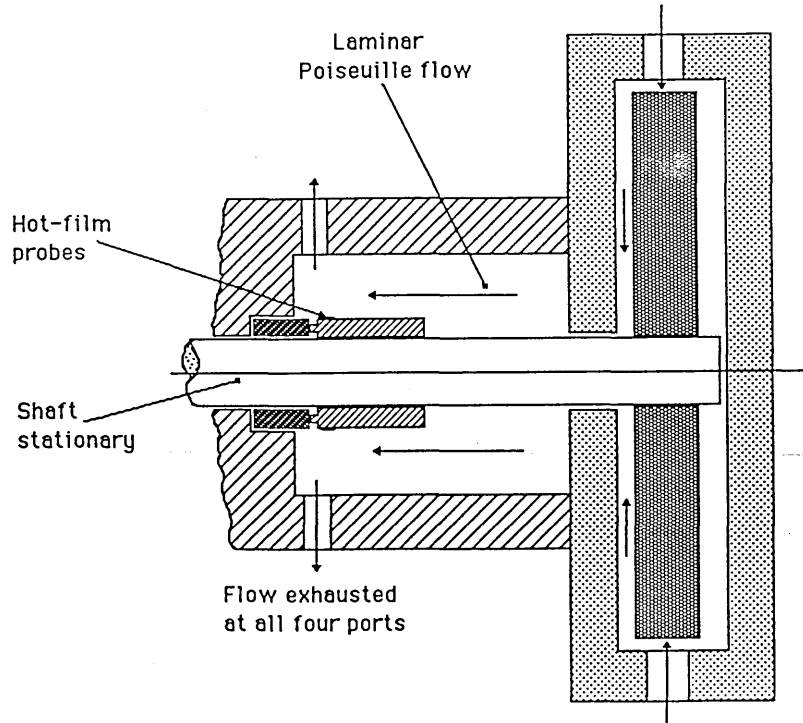


Figure 4.28 Set-up arrangement for heat-transfer probe calibration

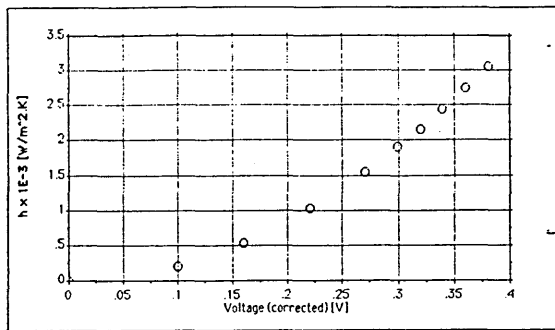


Figure 4.29 Results from Probe number 2

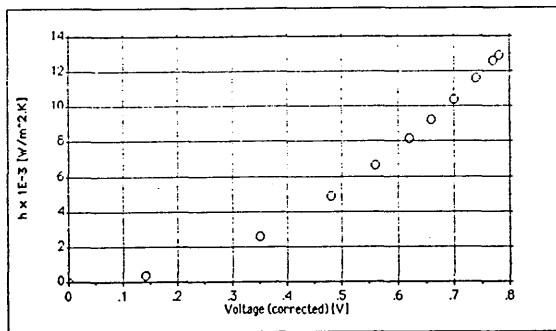


Figure 4.30 Results from Probe number 1

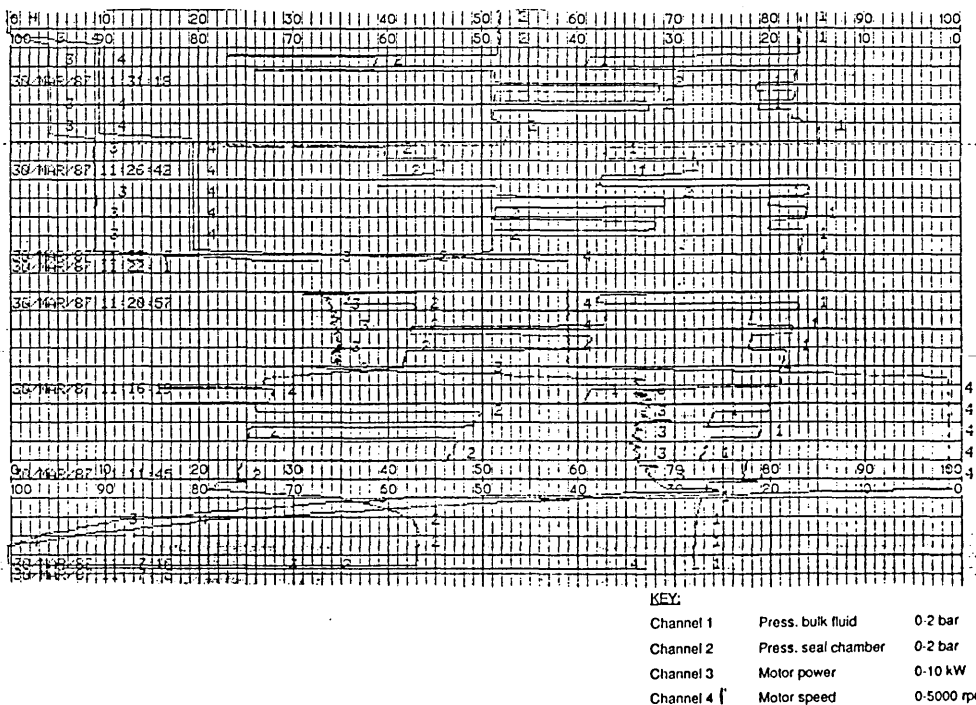


Figure 4.31 Typical chart record of experiment

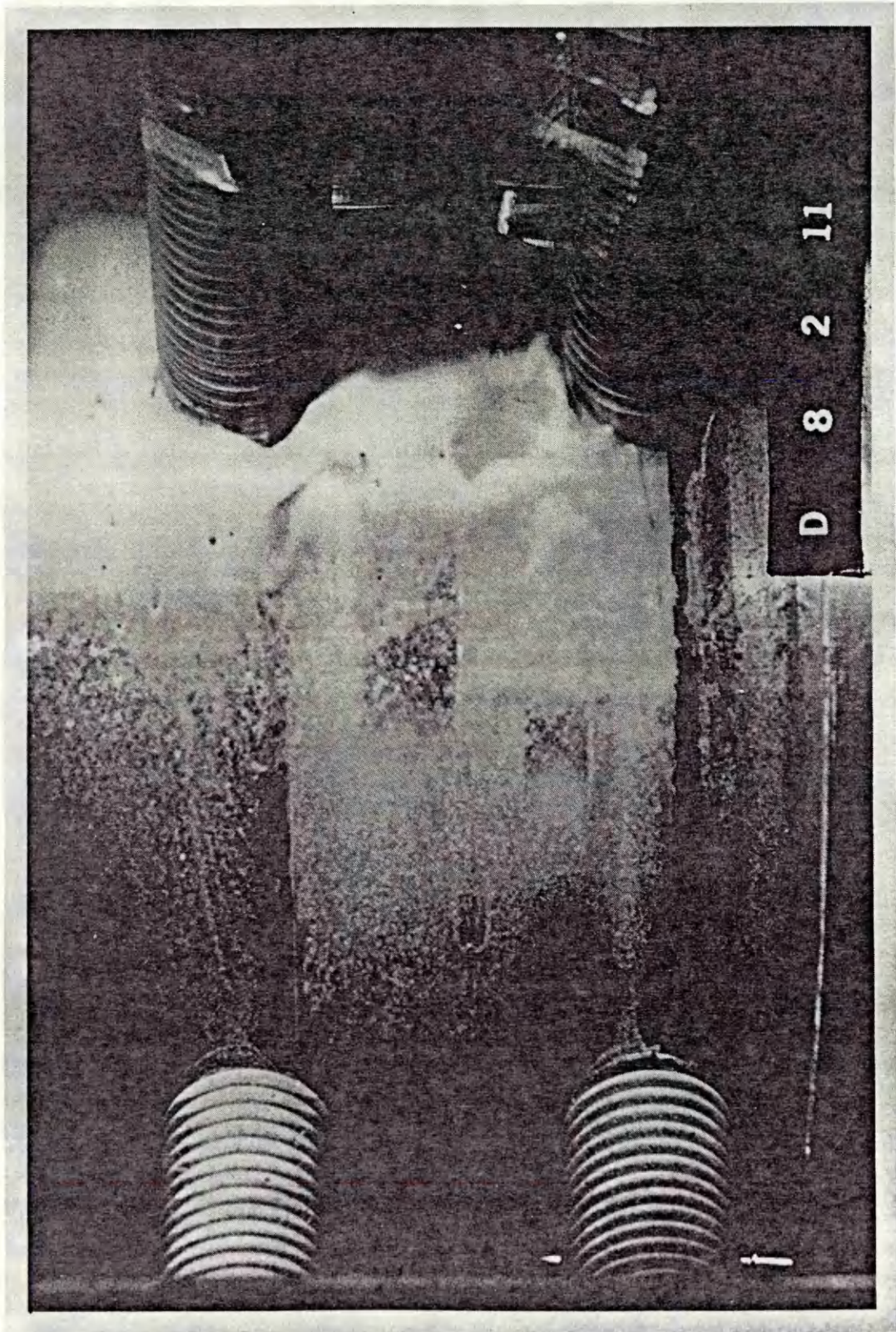


Figure 4.32 Flow visualisation using hollow glass spheres,  $Ta = 1800$

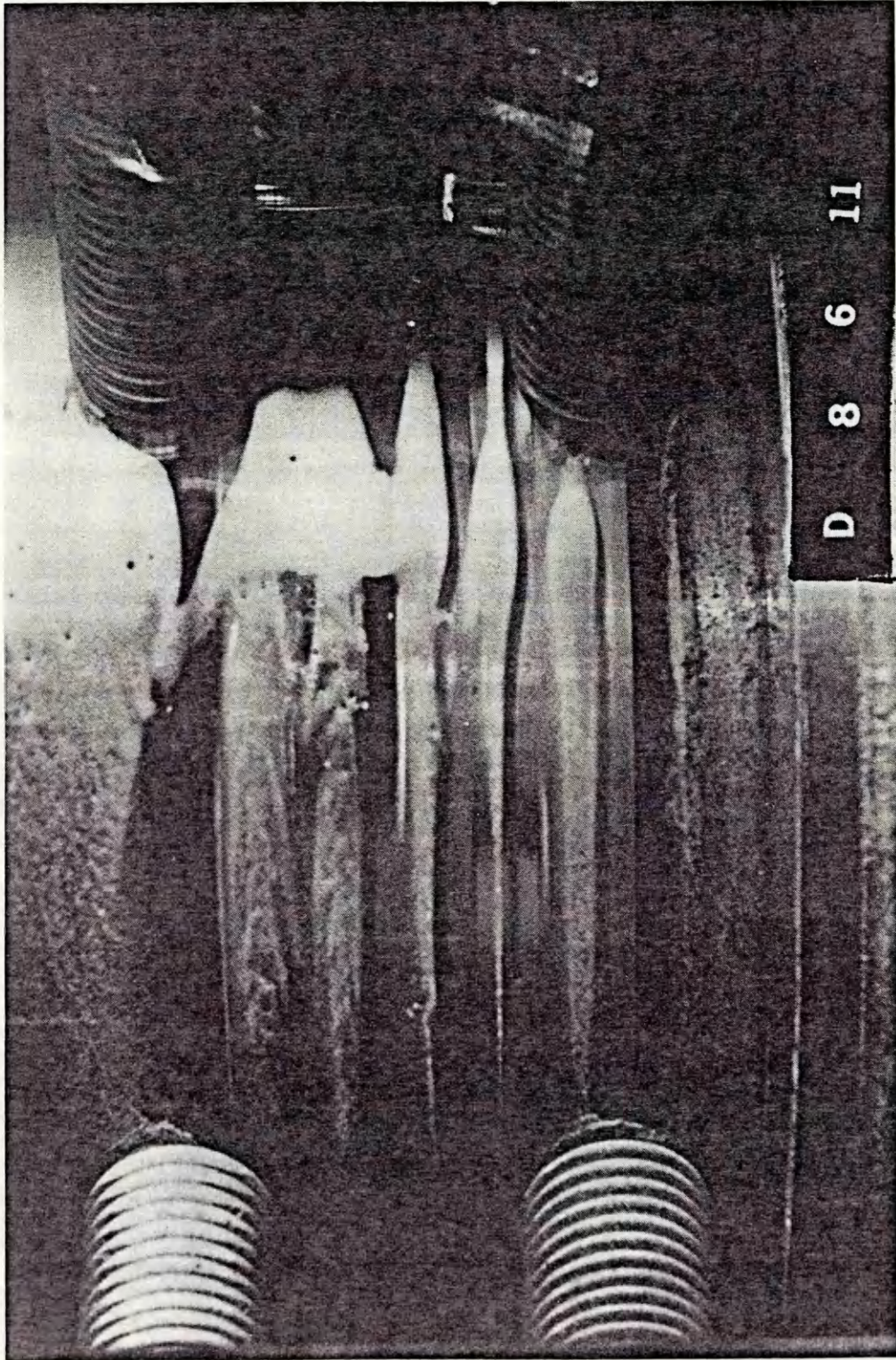


Figure 4.33 Flow visualisation using hollow glass spheres,  $Ta = 3970$



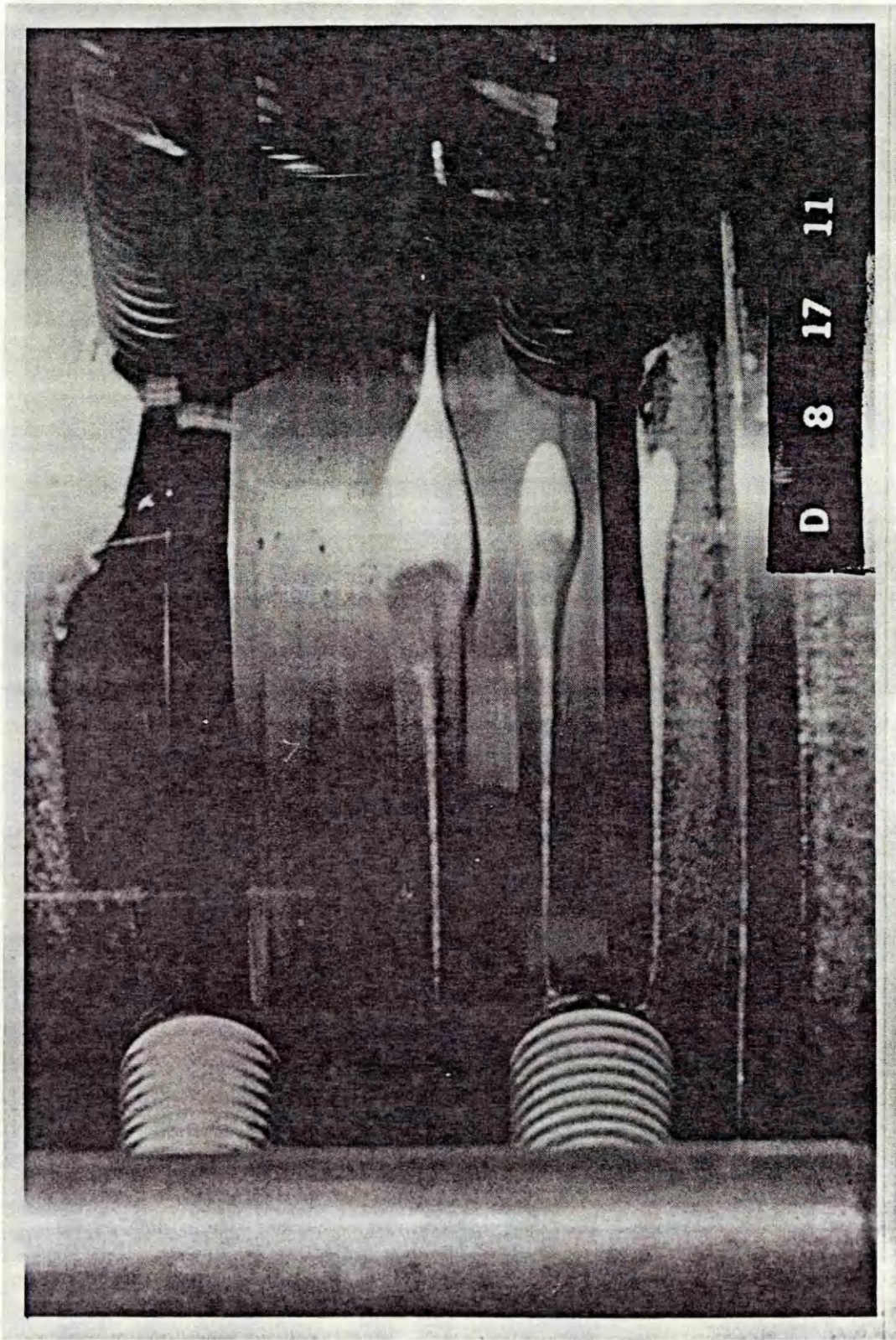


Figure 4.34 Flow visualisation using hollow glass spheres,  $Ta = 15450$

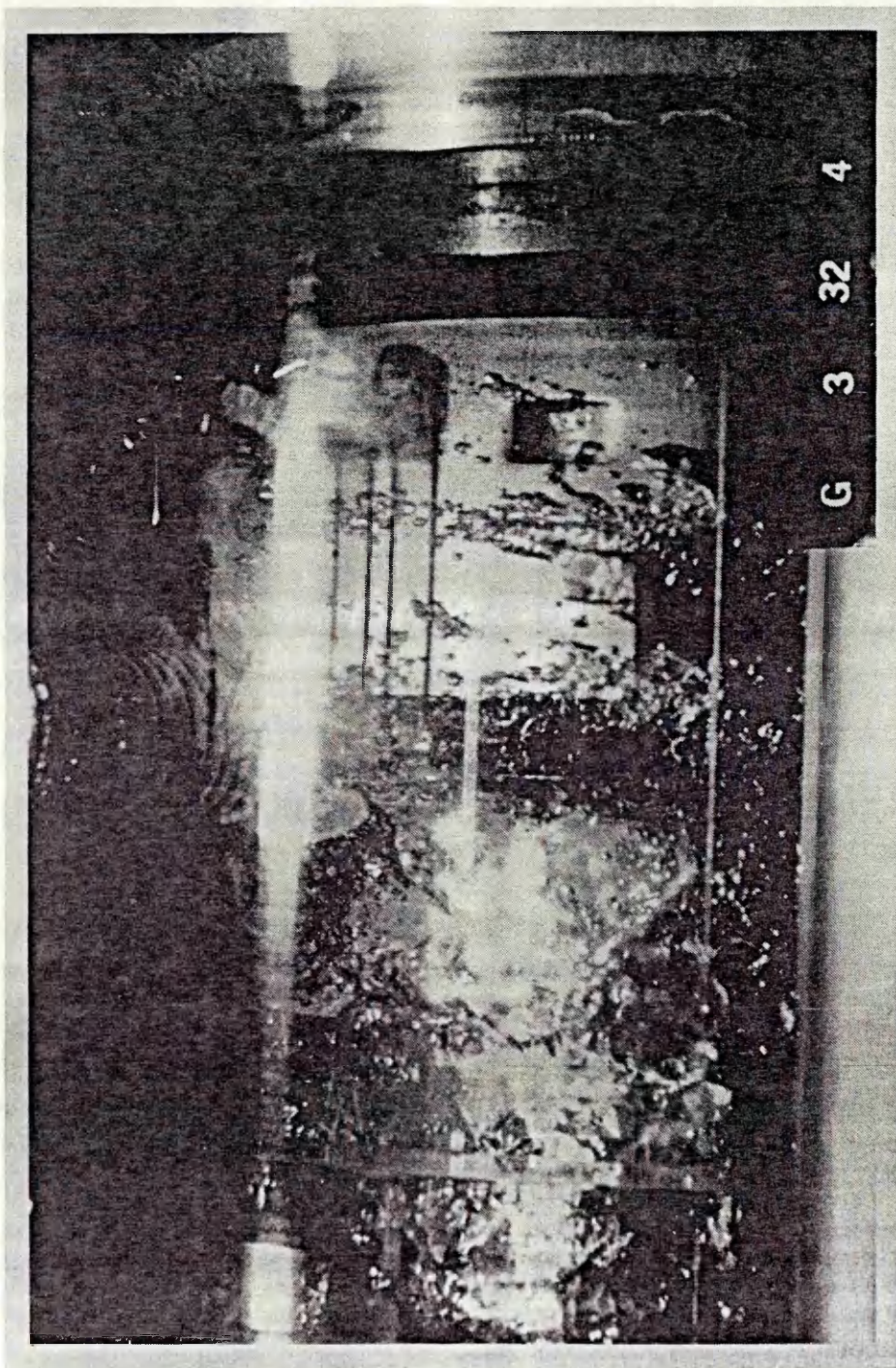


Figure 4.35 Flow visualisation using high-speed flash photography

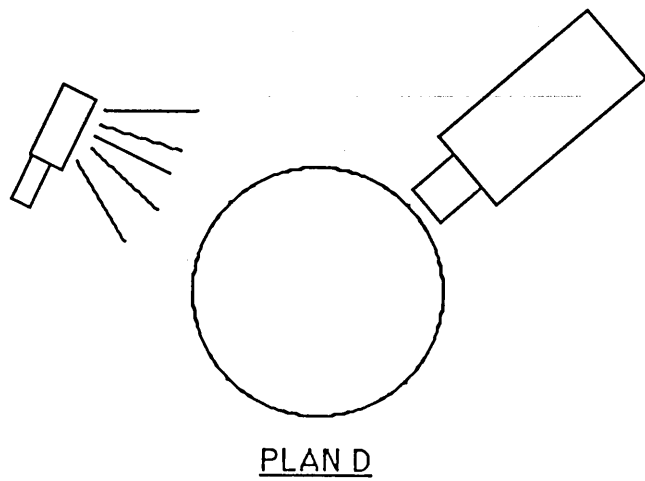
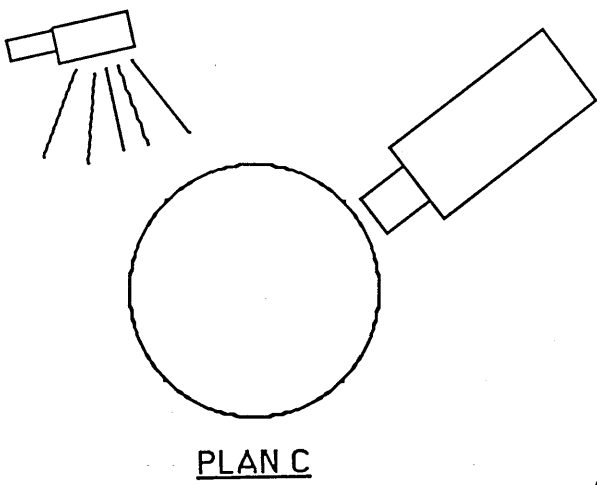
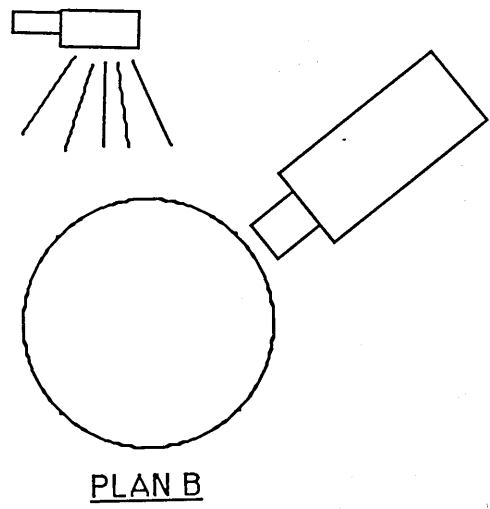
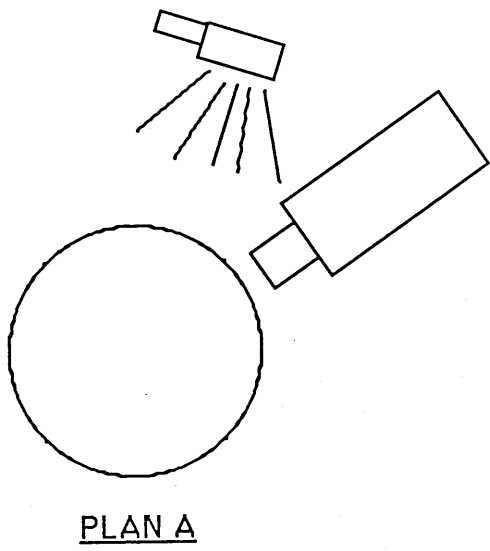


Figure 4.36 Alternative flash/camera positions

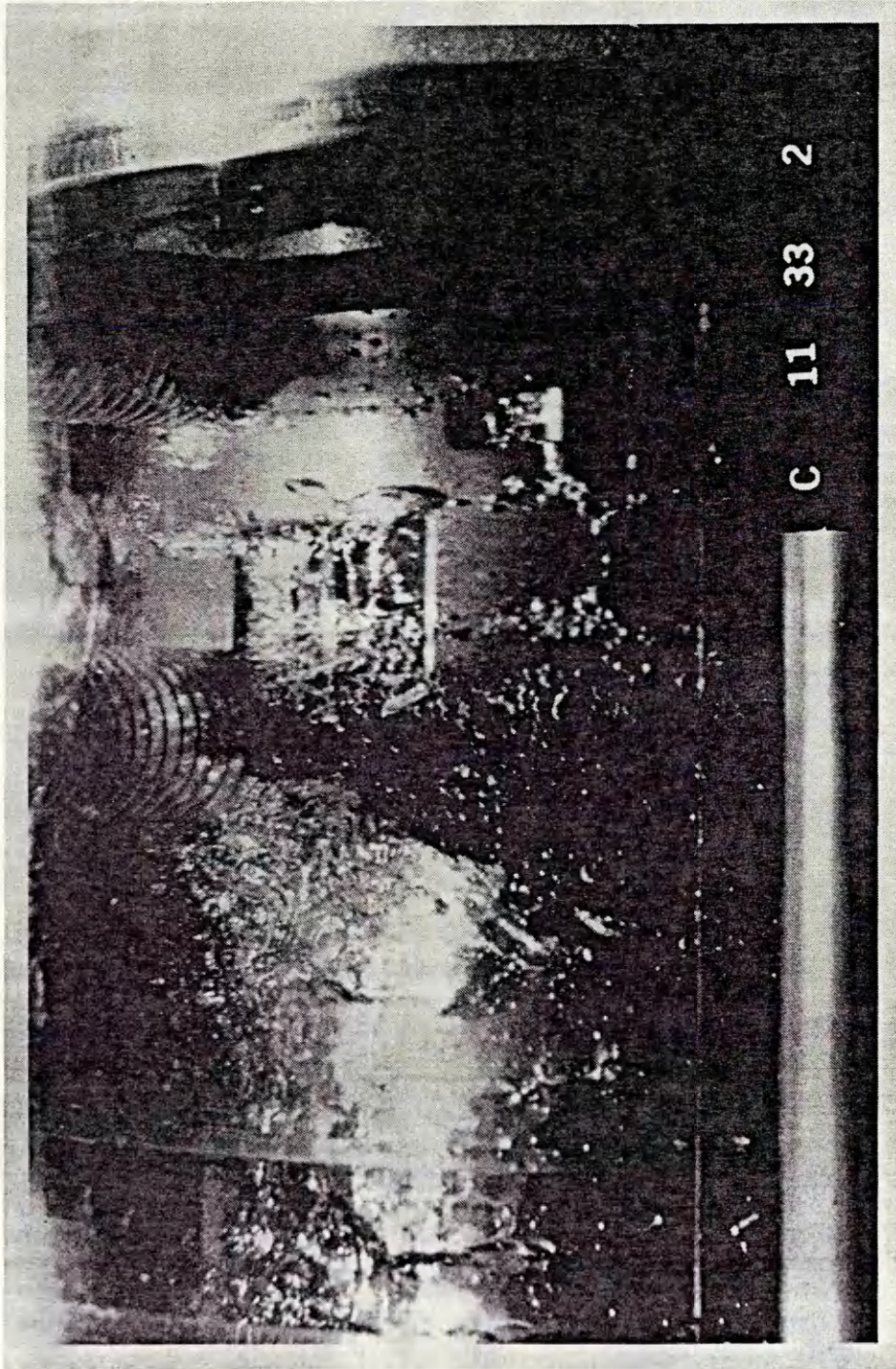
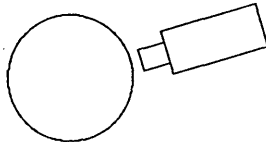
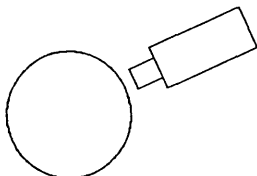


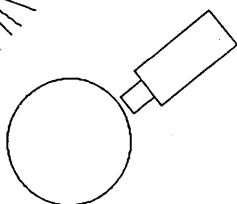
Figure 4.37 Flow picture taken from position A & B



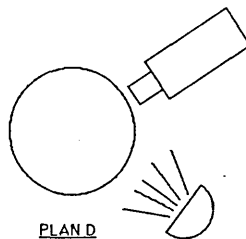
PLAN A



PLAN B

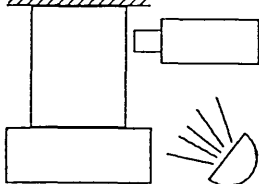


PLAN C



PLAN D

Plan View



PLANE

Figure 4.38 Alternative lighting/camera positions

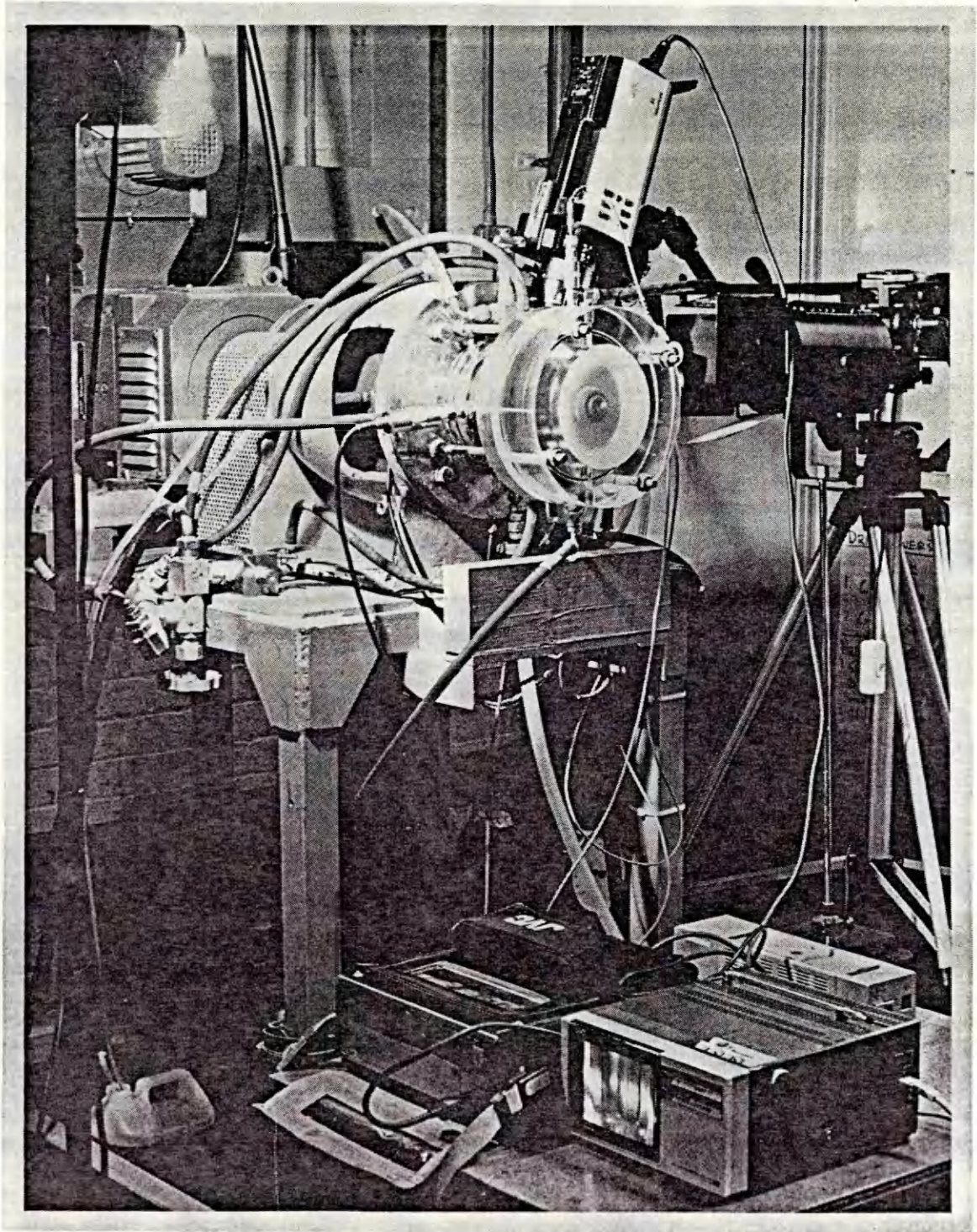


Figure 4.39 Favoured lighting/camera arrangement

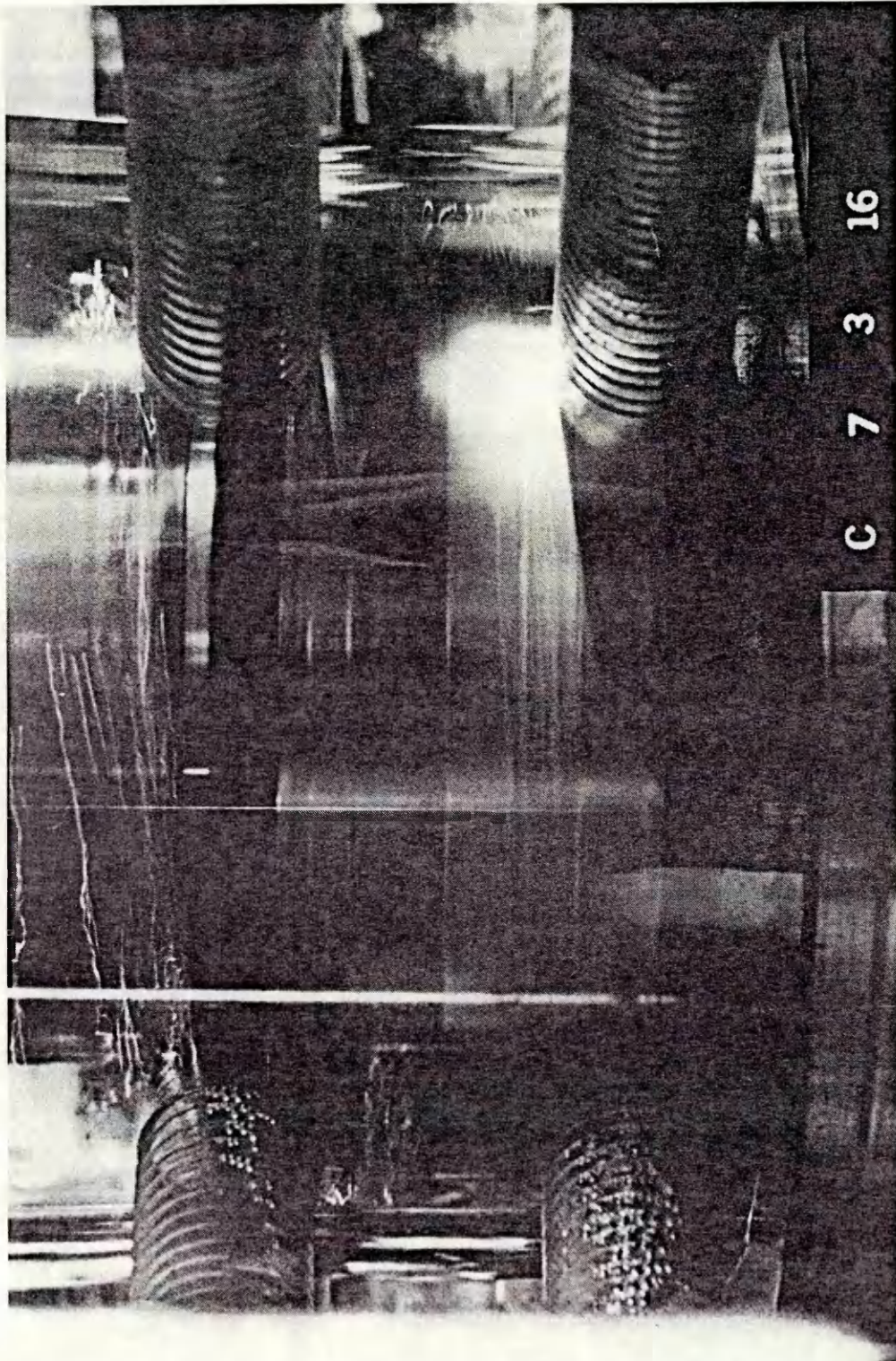


Figure 4.40 Typical flow picture obtained using arrangement in Fig 4.39

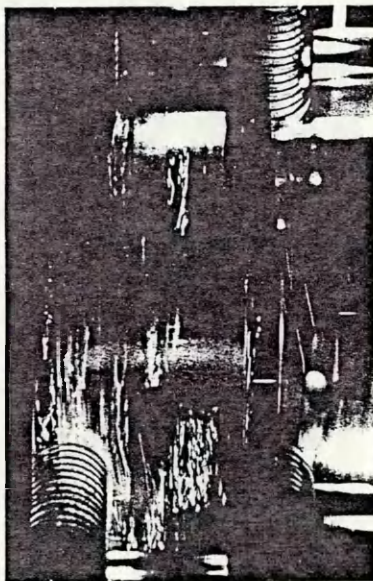
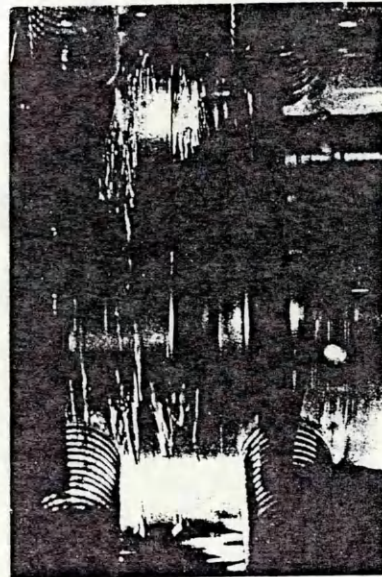
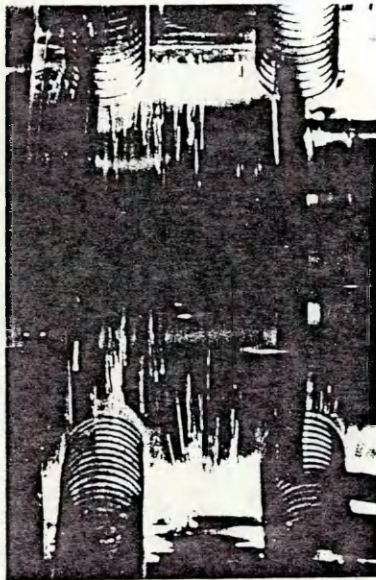


Figure 4.41 Long exposure photographs showing bubble vectors.



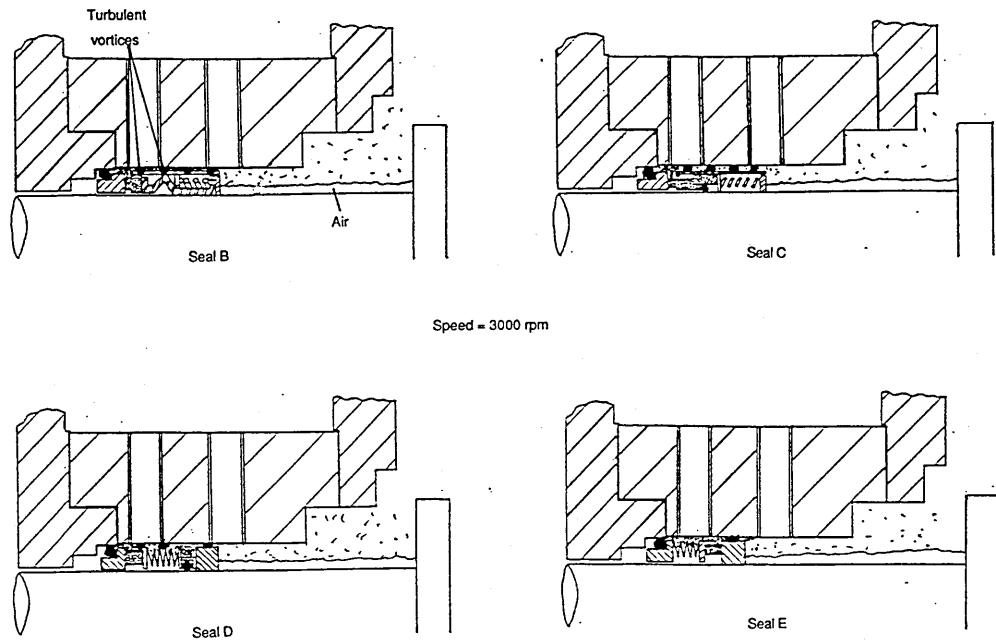


Figure 6.1 Narrow radial clearance housing - Seal B/Plan A/Water

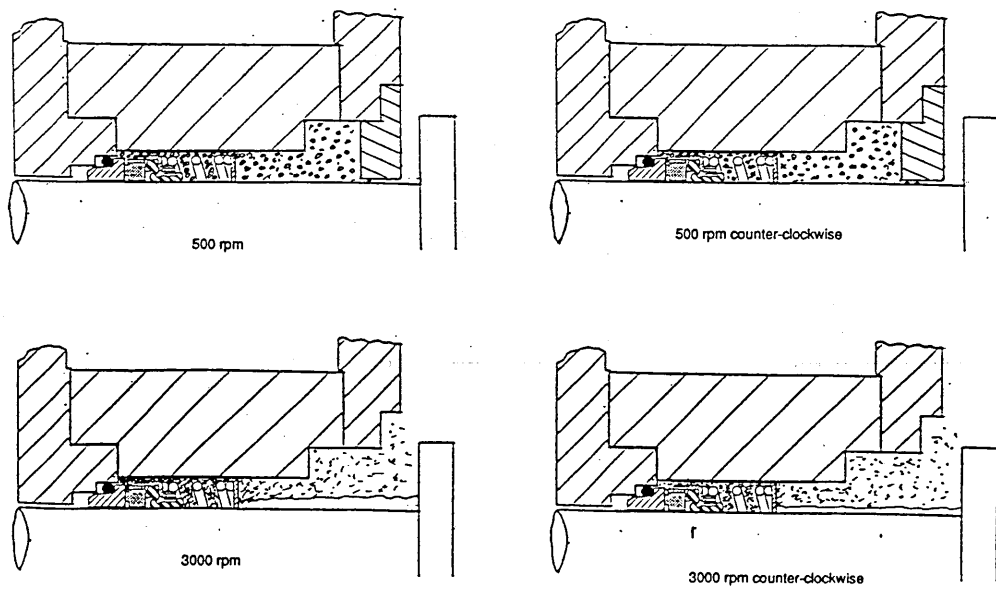


Figure 6.2 Narrow radial clearance housing - Seal A/Plan A/Water

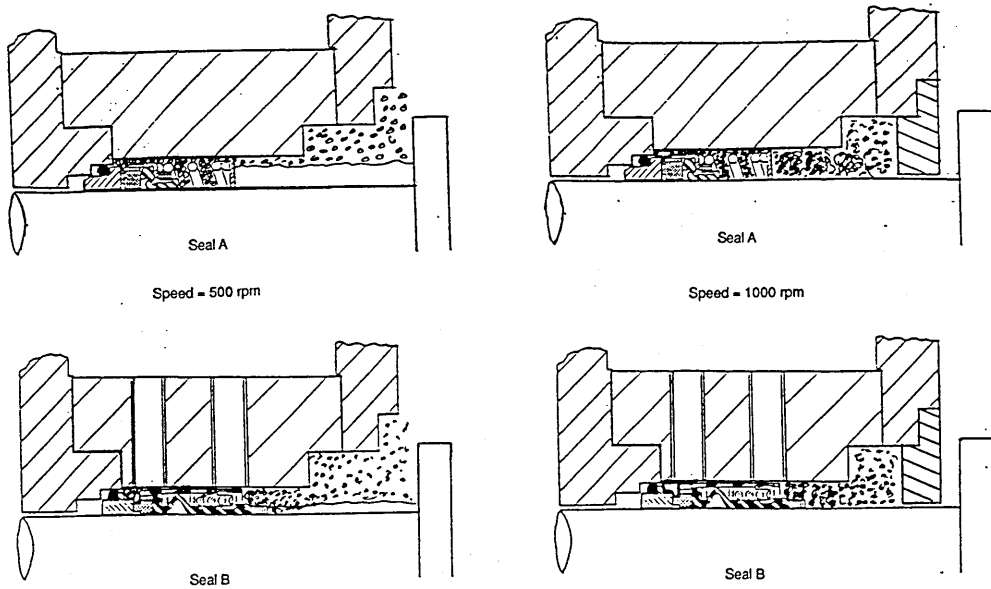


Figure 6.3 Narrow radial clearance housing - Plan A/Glycerol solution

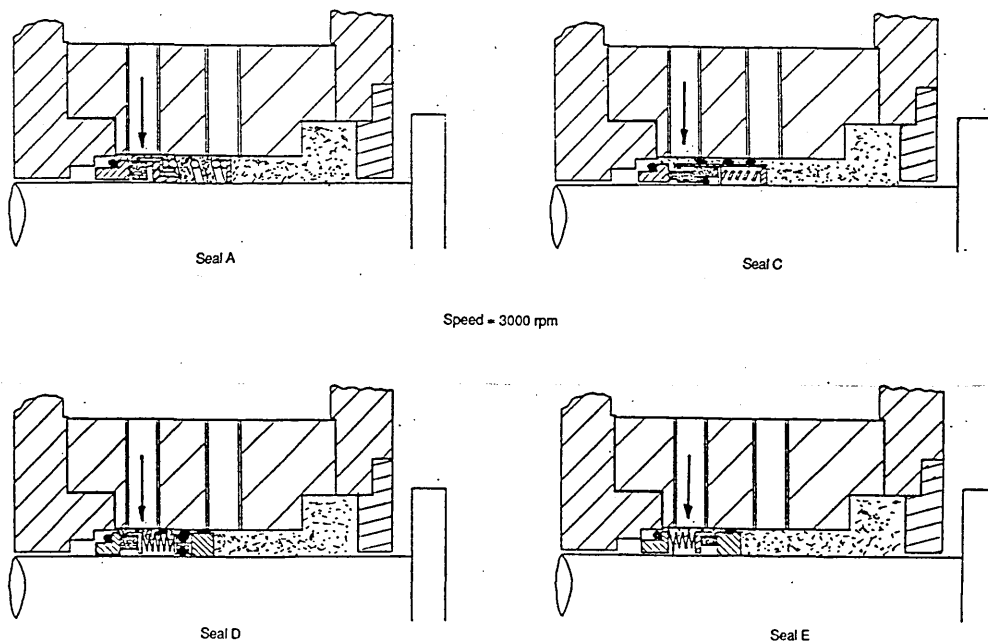


Figure 6.4 Narrow radial clearance housing - Plan B/Water

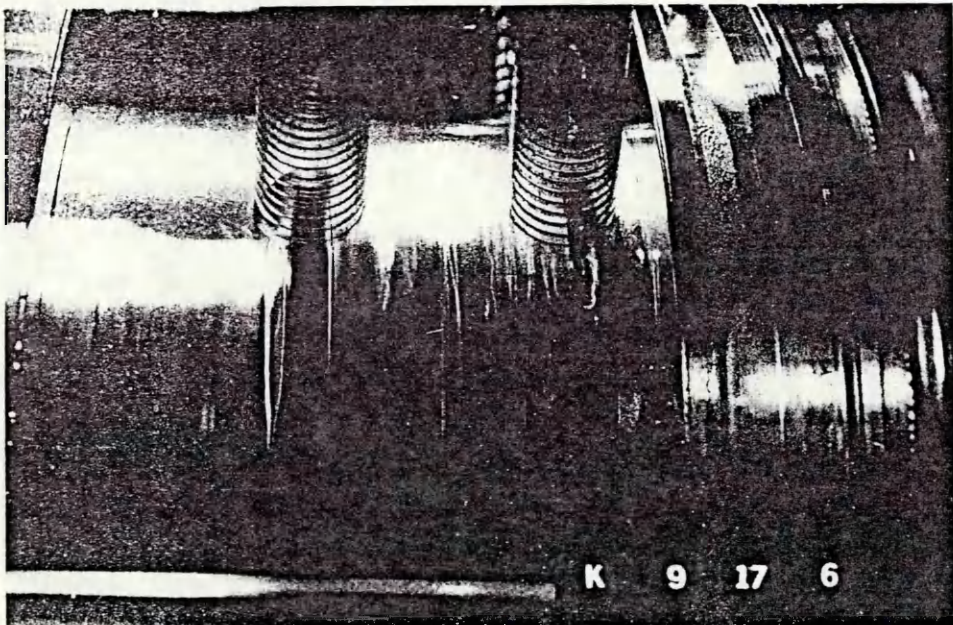
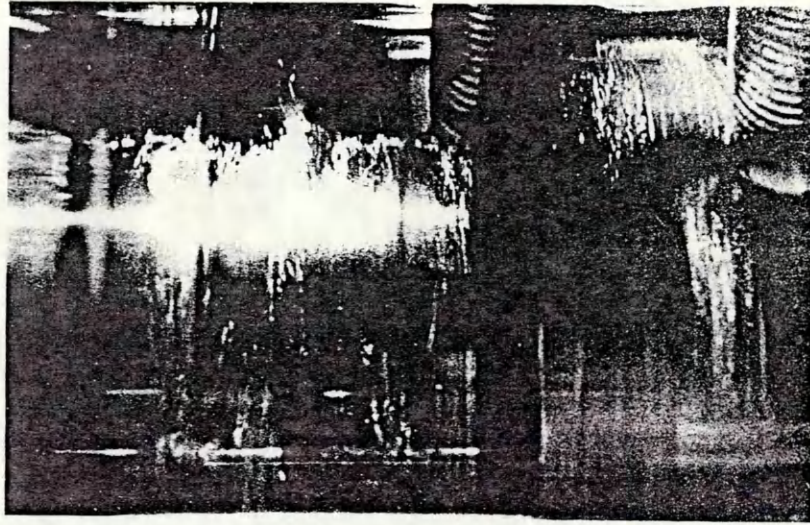


Figure 6.5 Narrow radial clearance housing - Plan B/Water

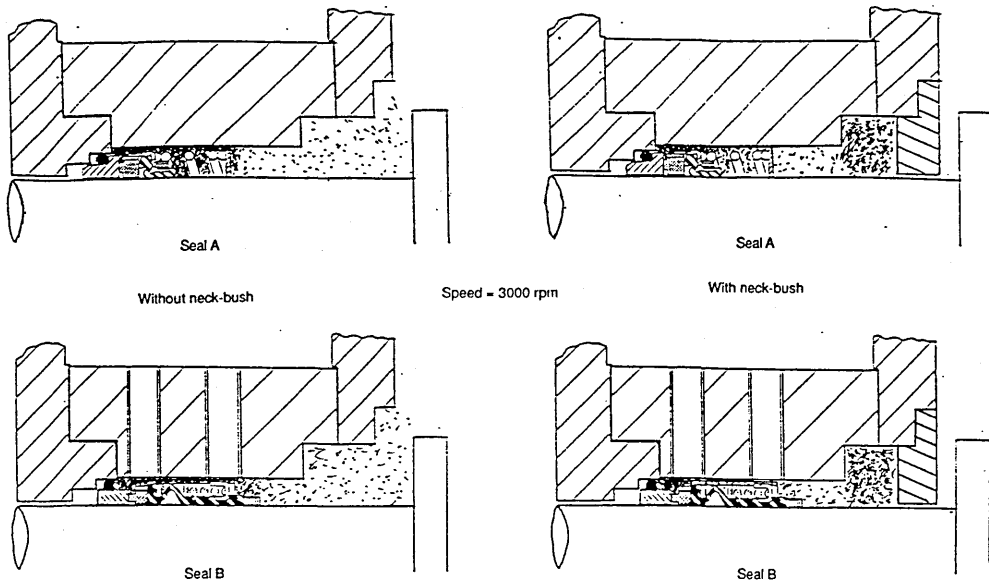


Figure 6.6 Narrow radial clearance housing - Plan A/Solids in suspension

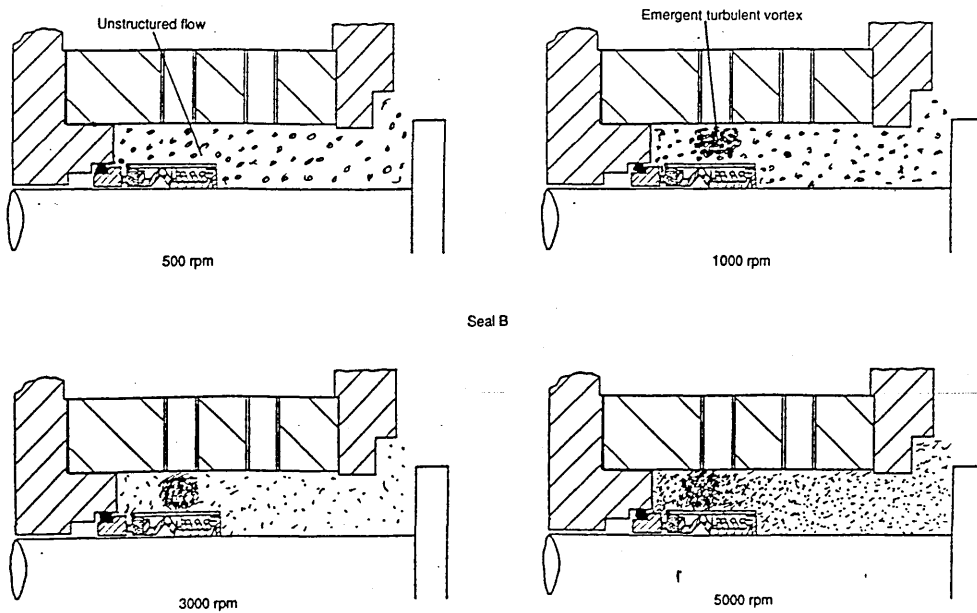
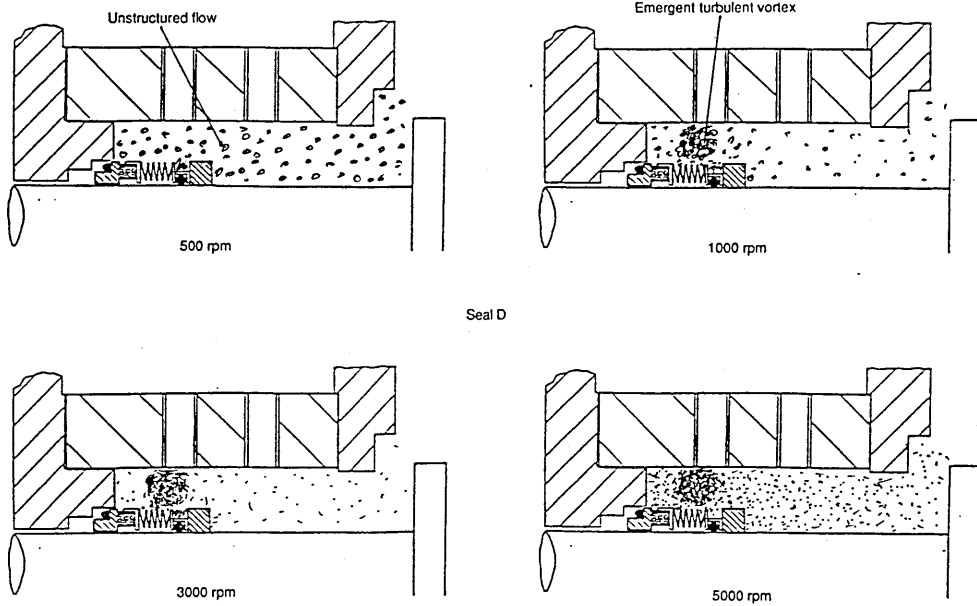
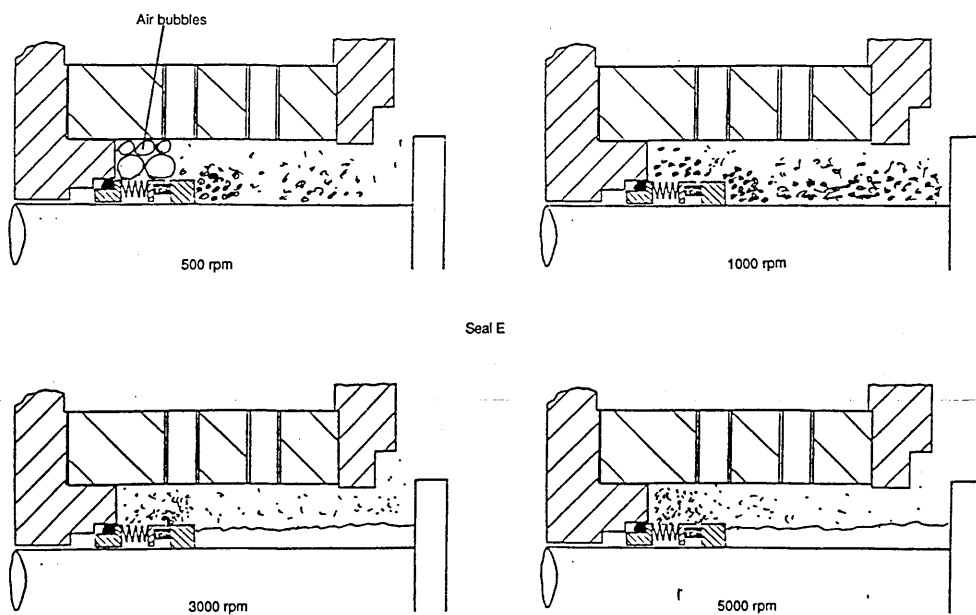


Figure 6.7 Wide radial clearance housing - Plan A - formation of vortex



**Figure 6.8** Wide radial clearance housing - Plan A - high Taylor number flows



**Figure 6.9** Wide radial clearance housing - Plan A - high Taylor number flows

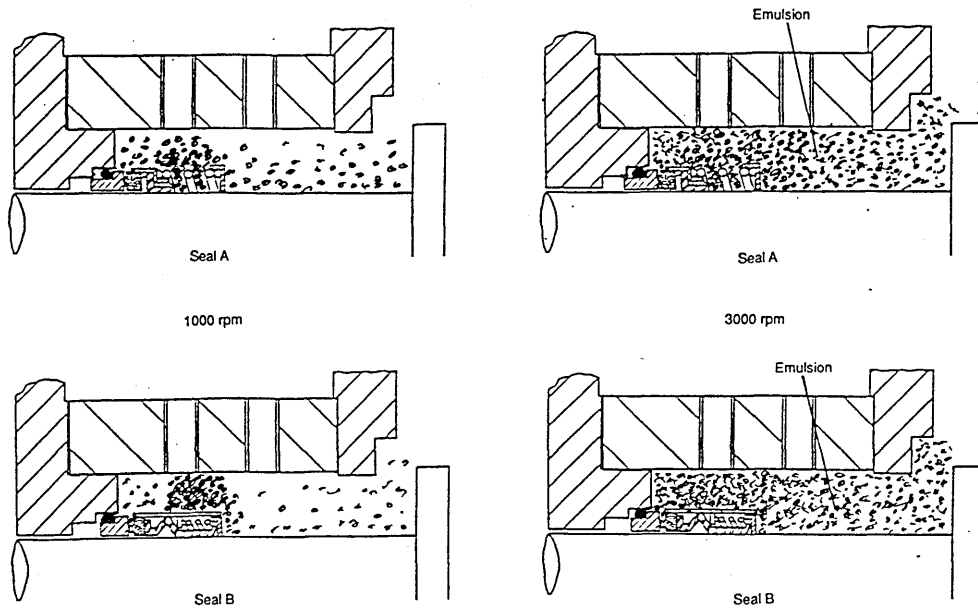


Figure 6.10 Wide radial clearance housing - Plan A/Glycerol solution

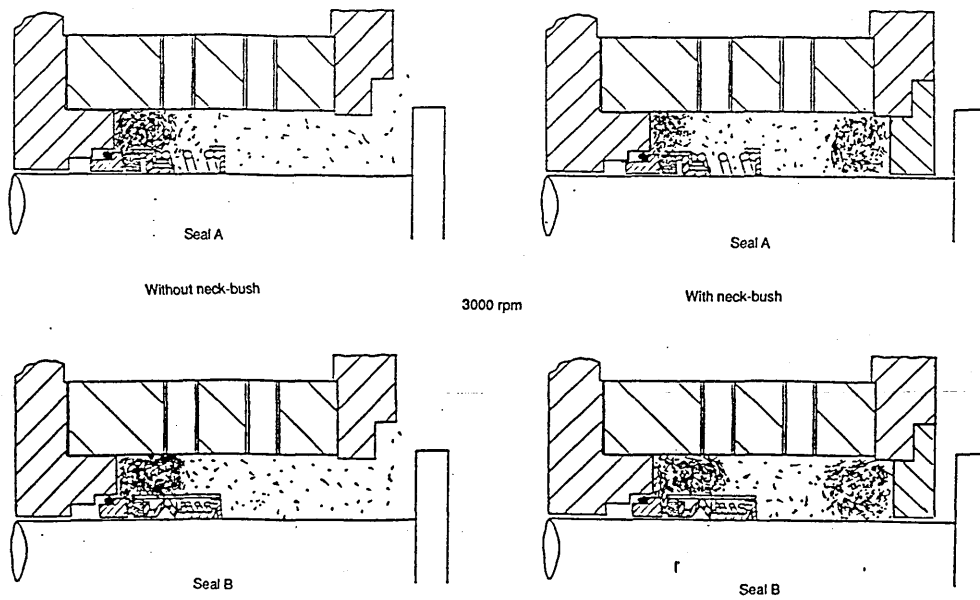


Figure 6.11 Wide radial clearance housing - Plan A/Solids in suspension

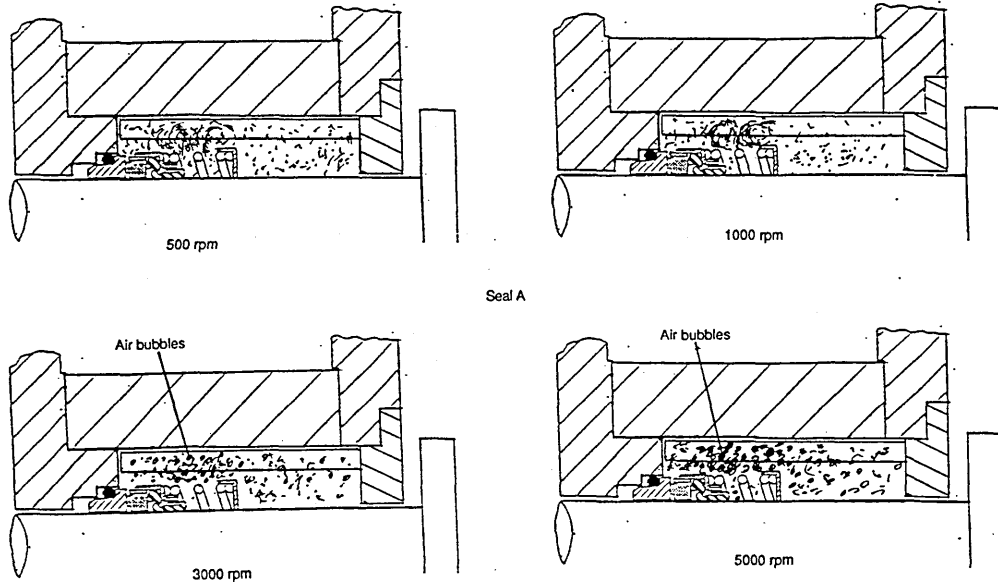


Figure 6.12 Wide radial clearance housing - Plan A/Axial strakes

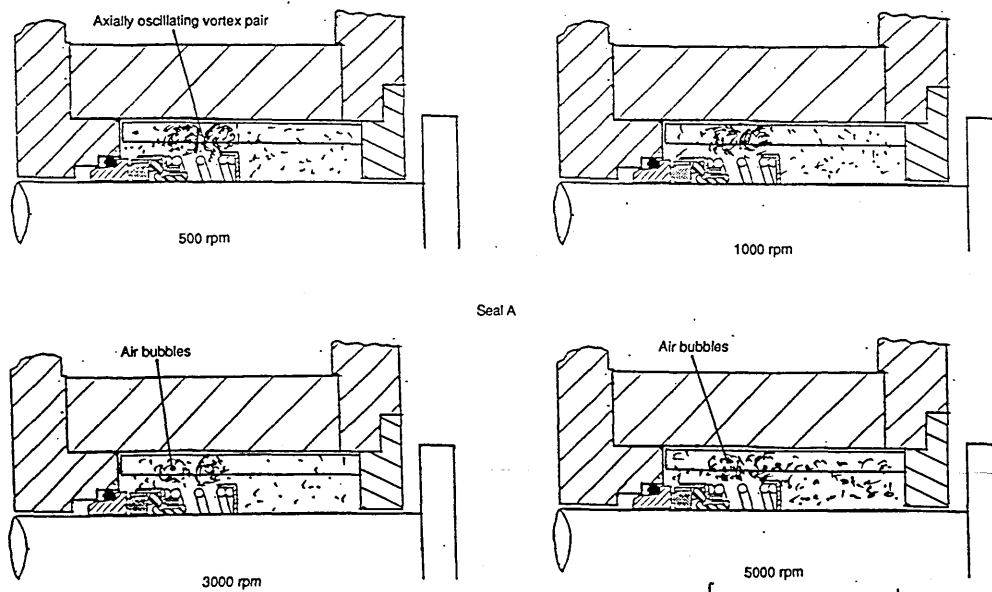


Figure 6.13 Wide radial clearance housing - Plan A/Helical strakes

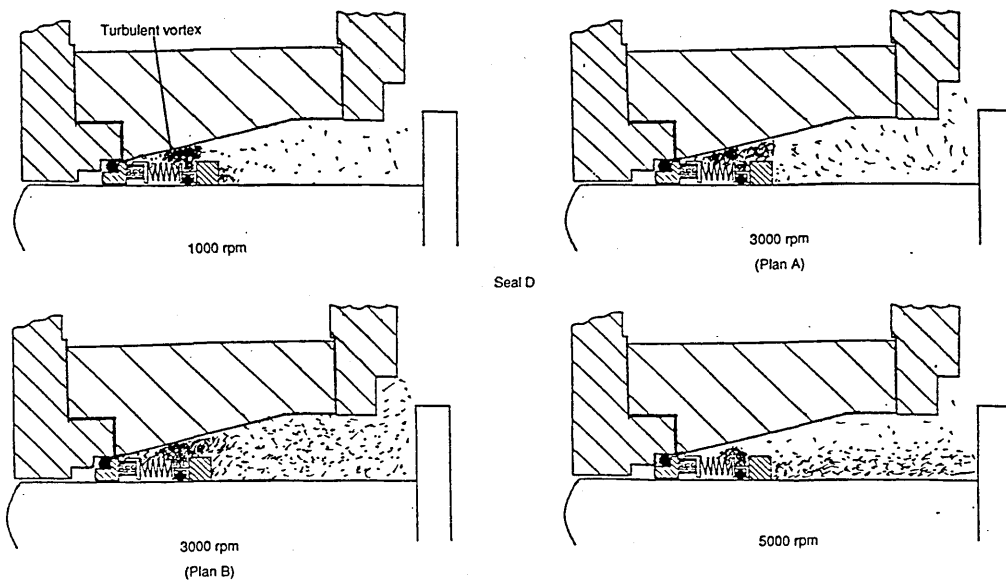


Figure 6.14 12° positively flared housing - Plan A/Water

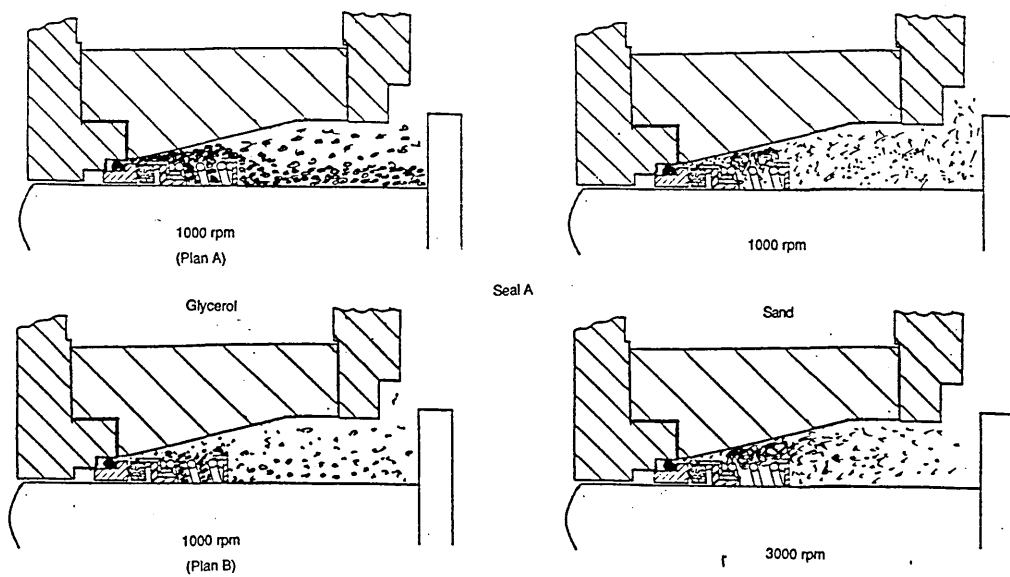


Figure 6.15 12° positively flared housing - Plan A/Solids



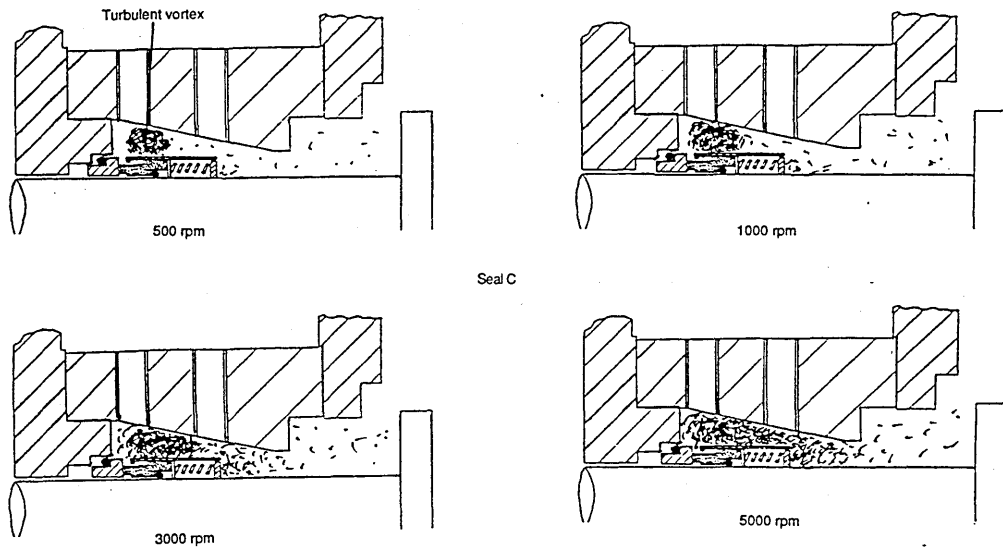


Figure 6.16 12° negatively flared housing - Plan A/Water

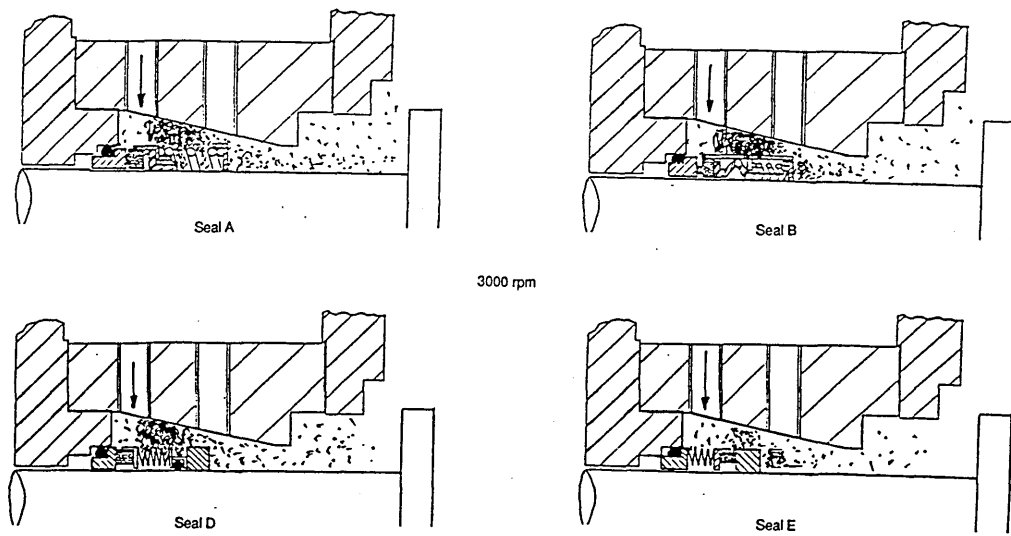


Figure 6.17 12° negatively flared housing - Plan B/Water

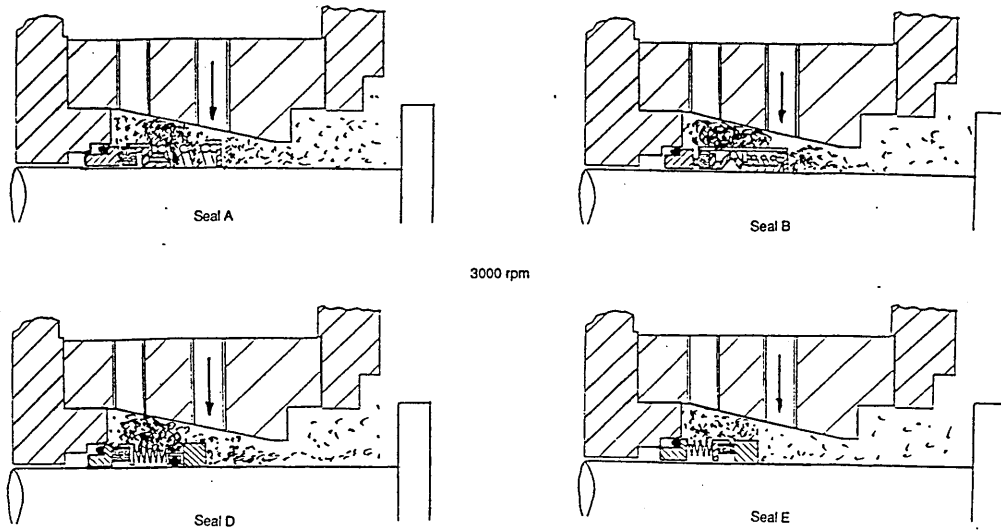


Figure 6.18 12° negatively flared housing - Plan D/Water

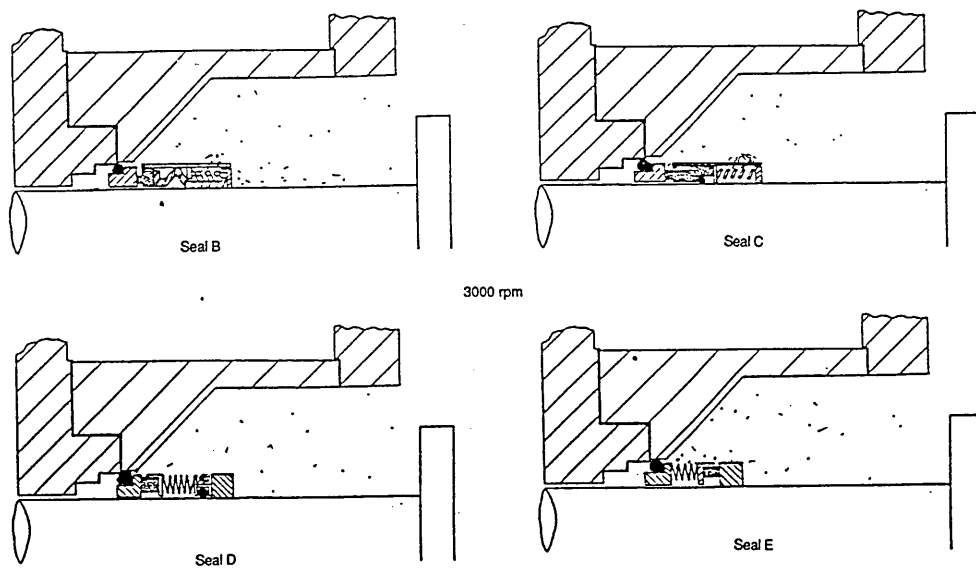


Figure 6.19 45° positively flared housing - Plan A/Water

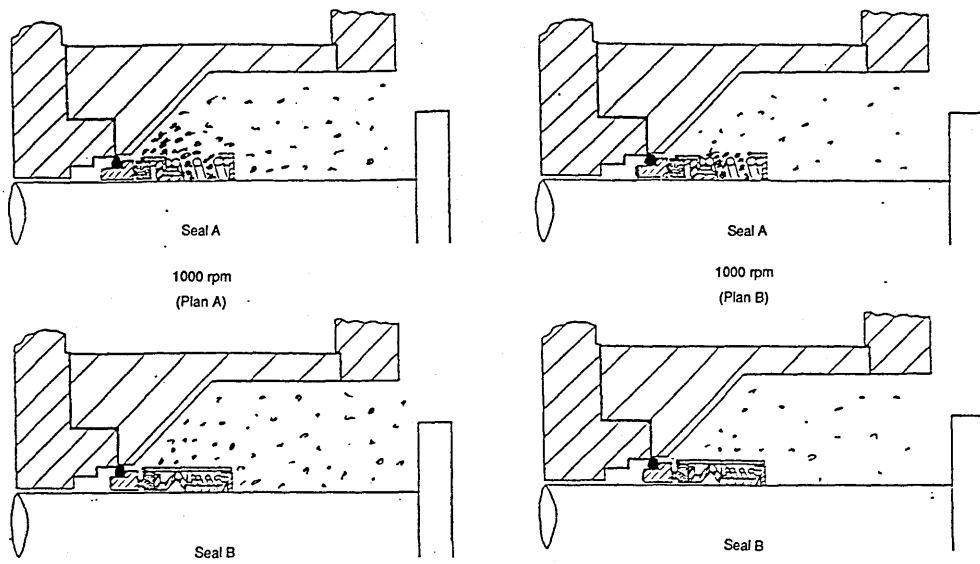


Figure 6.20 45° positively flared housing - Plan A/Glycerol solution

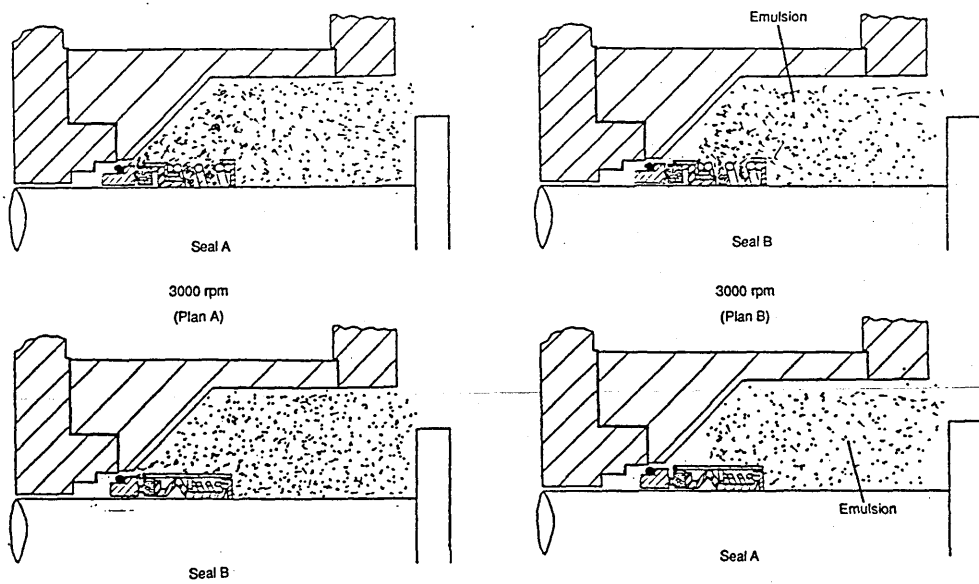


Figure 6.21 45° positively flared housing - Plan A - emulsification with glycerol

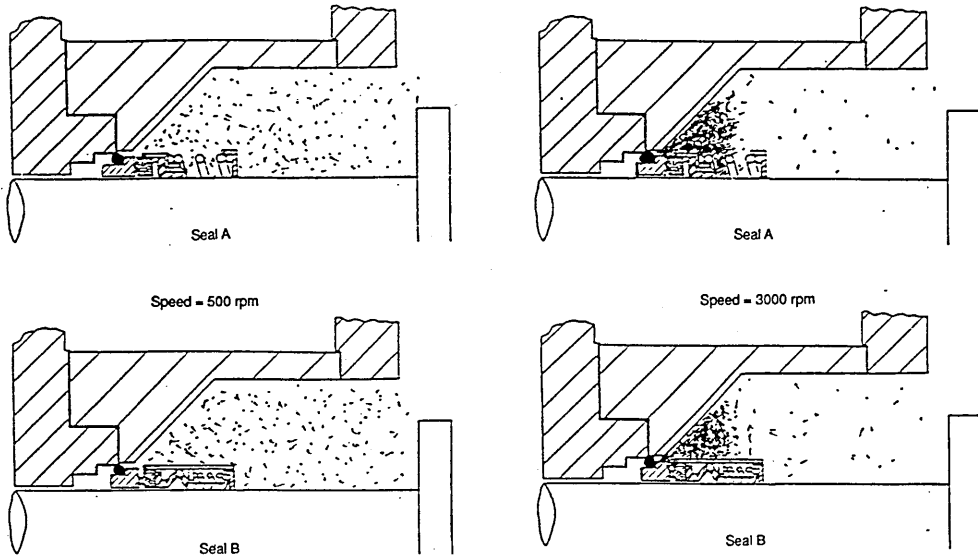


Figure 6.22 45° positively flared housing - Plan A/Solids

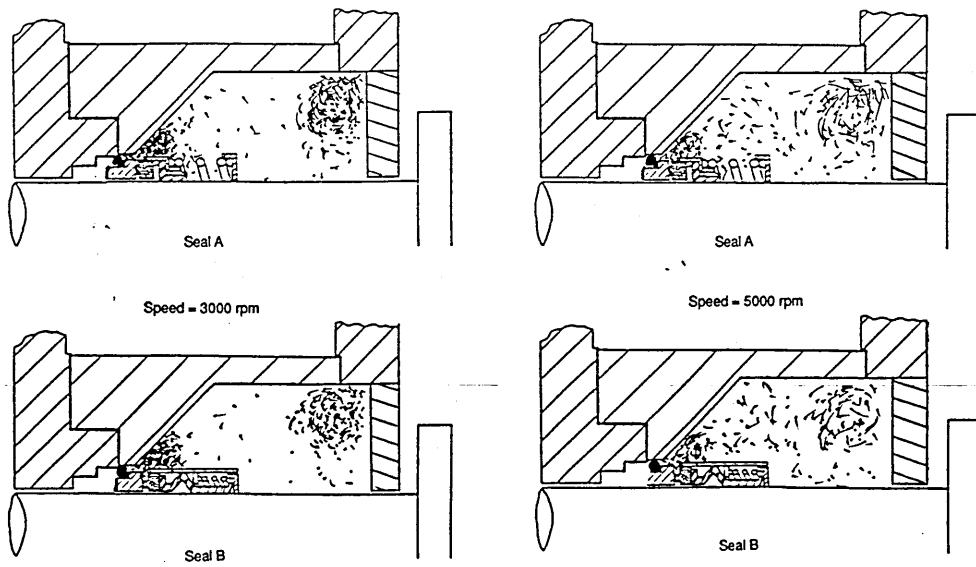


Figure 6.23 45° positively flared housing - Plan A/Neck-bush/Solids

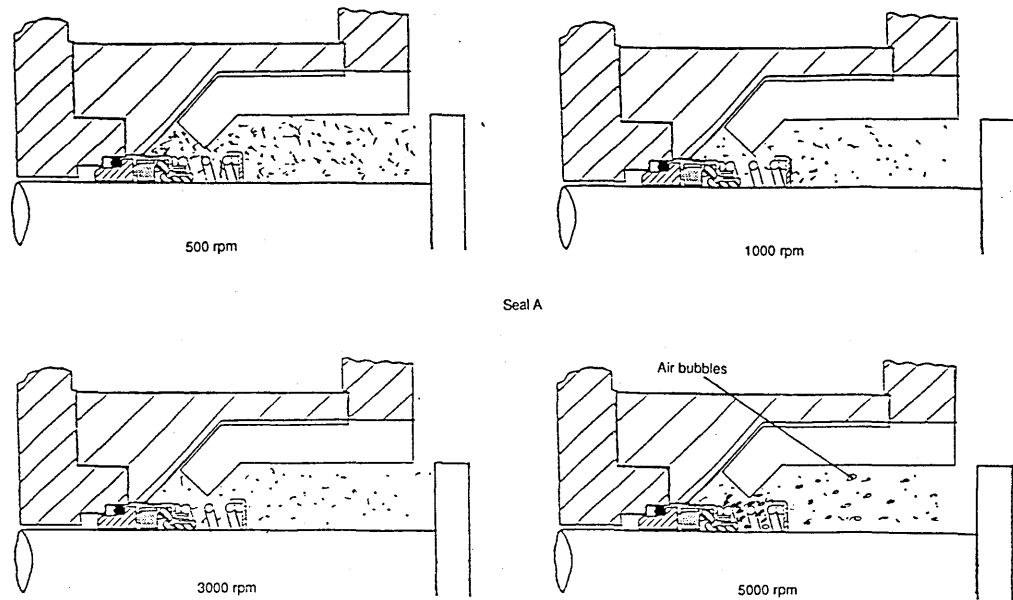


Figure 6.24 45° positively flared housing - Plan A/Axial strakes

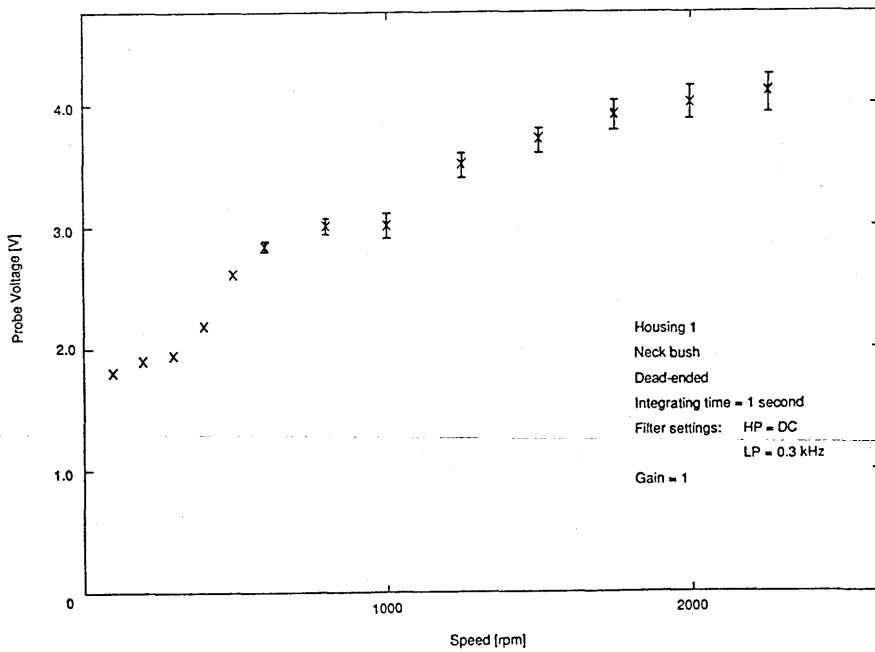


Figure 6.25 Heat transfer data from Seal B

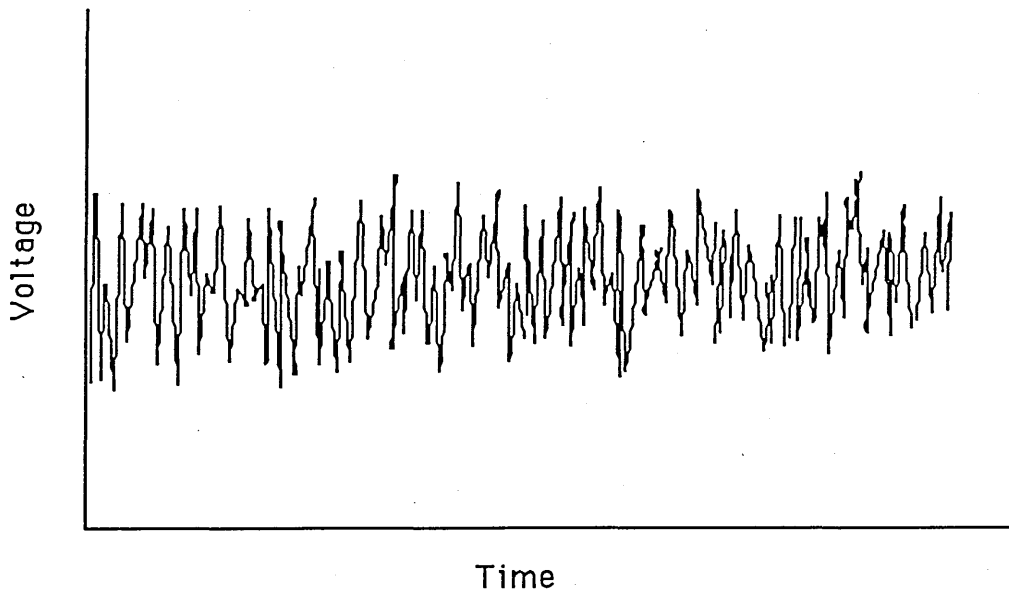


Figure 6.26 Wave form from hot-film probe, speed  $< 600\text{rpm}$

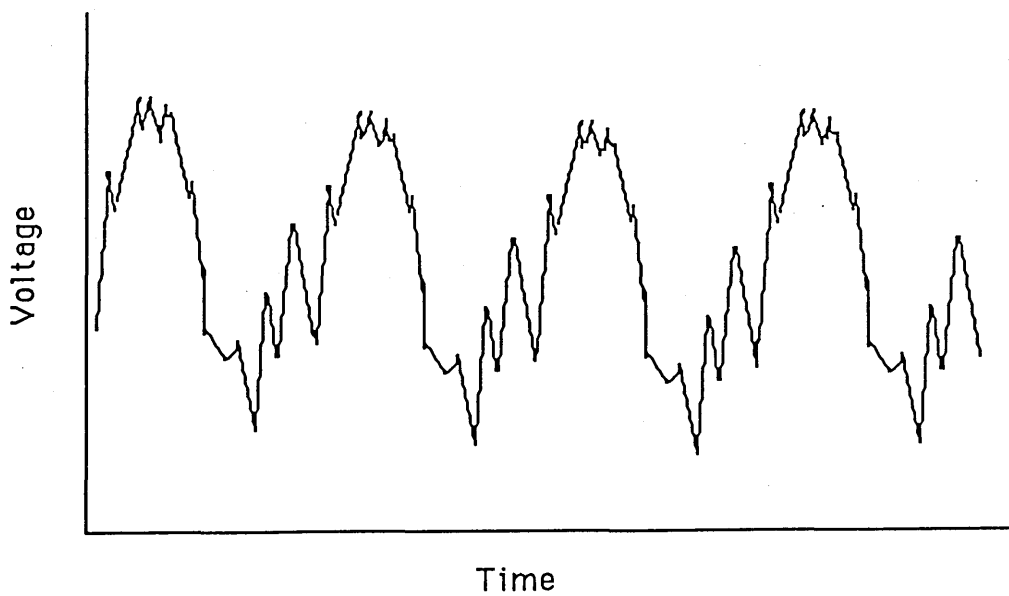


Figure 6.27 Wave form from hot-film probe, speed  $> 650\text{rpm}$

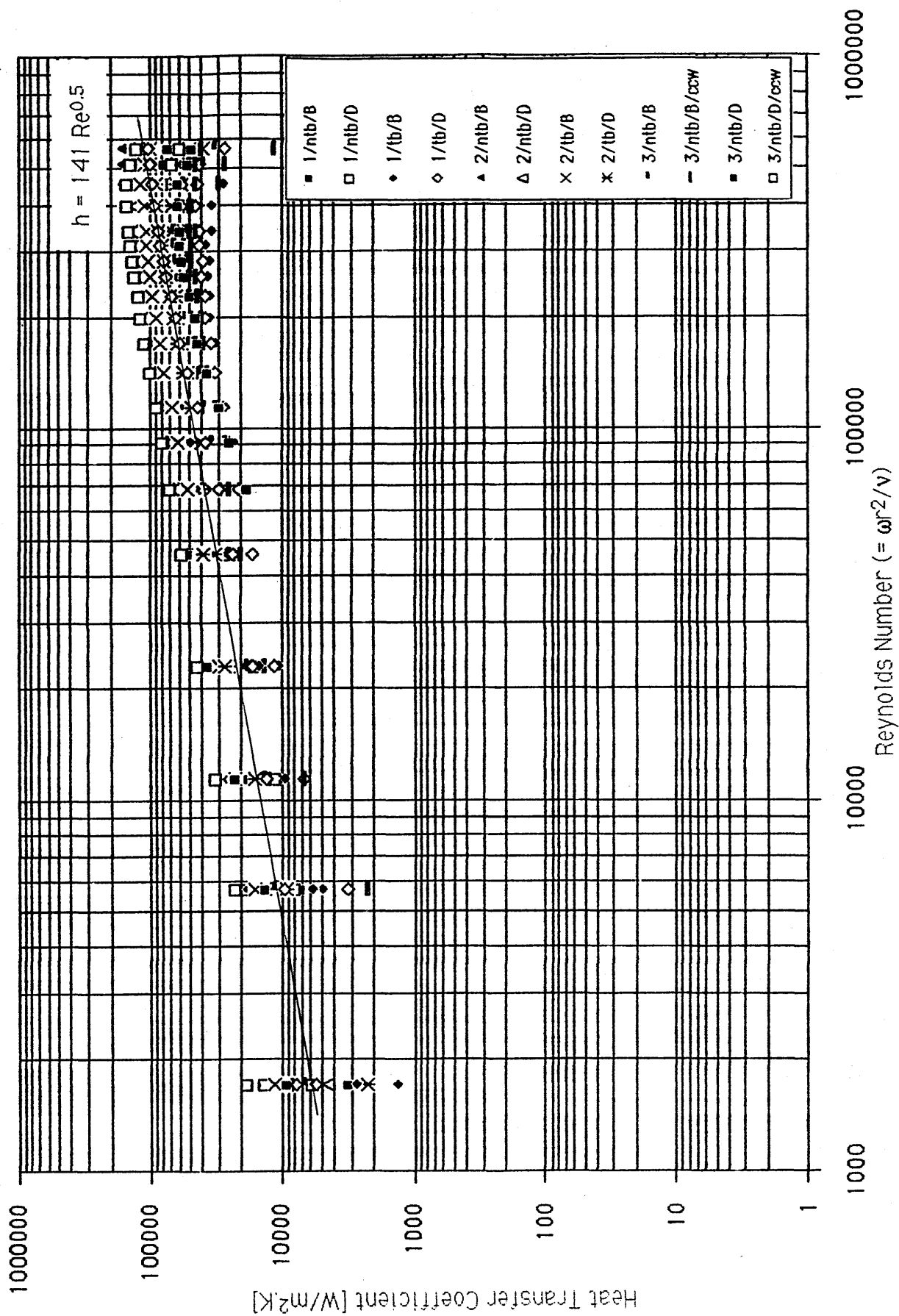


Figure 6.28 Heat Transfer Data (from Table 6.1)

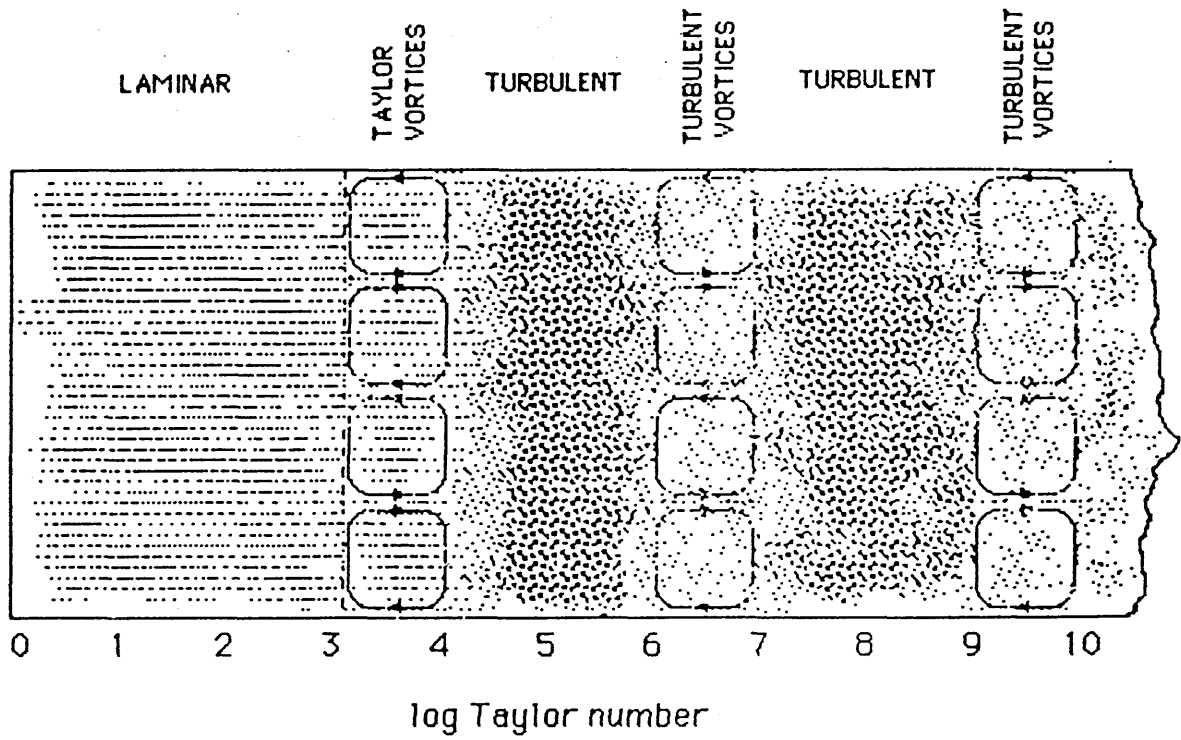


Figure 7.1 Flow Regime as a function of Taylor number

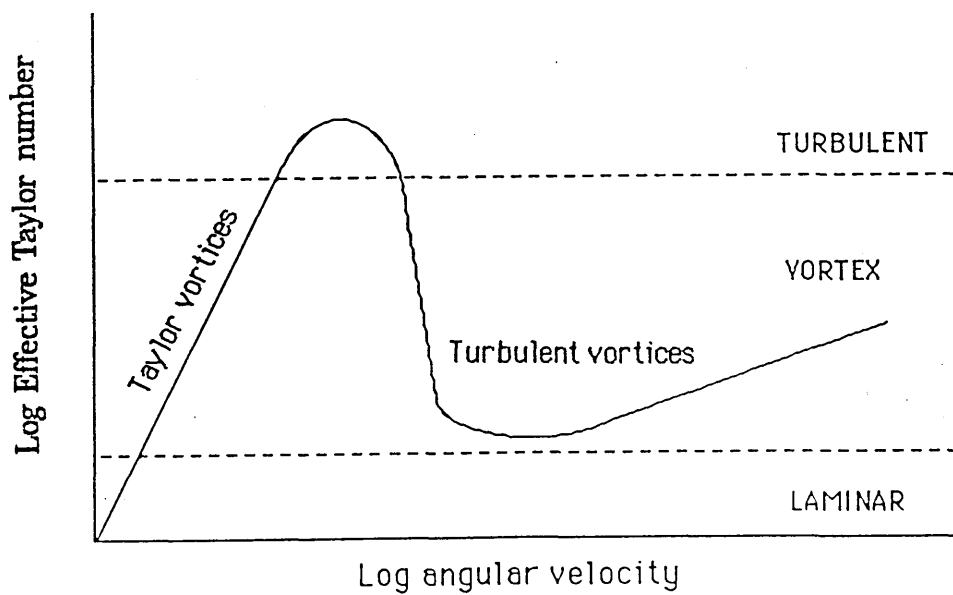


Figure 7.2 Effective Taylor number versus angular velocity



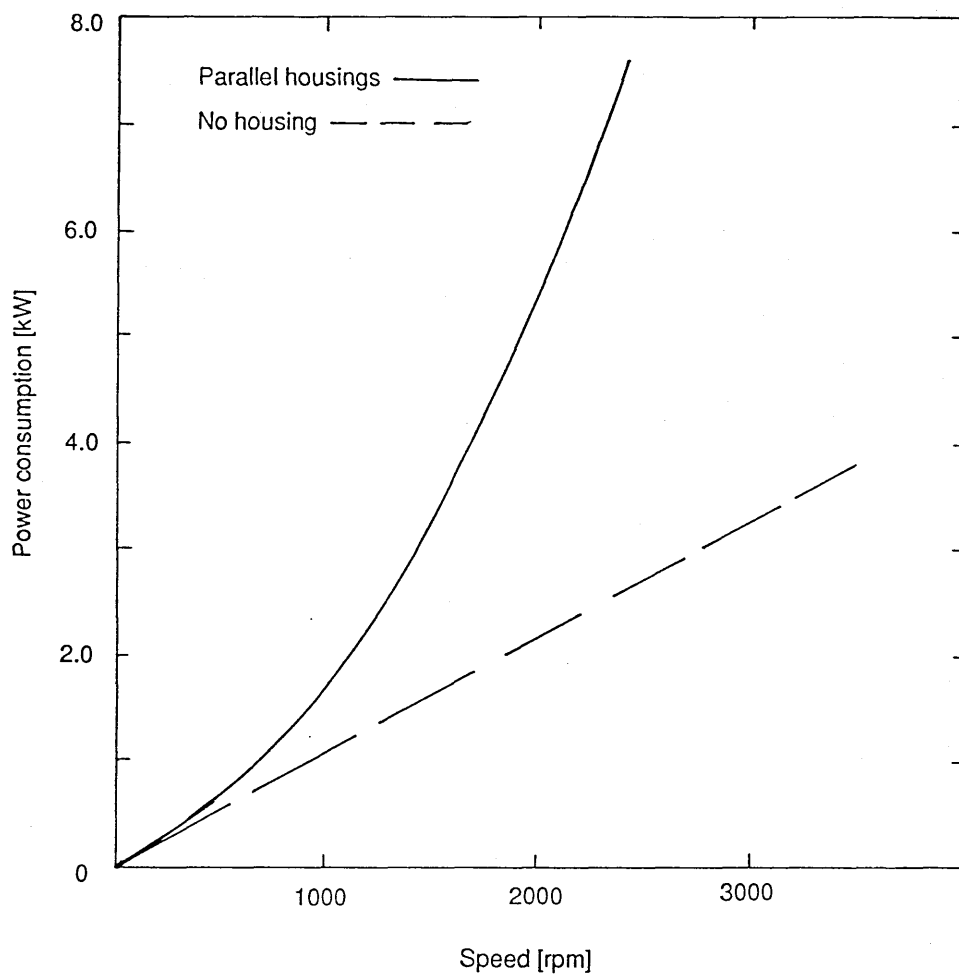


Figure 7.3 Experimental results of seal and bearing measurements

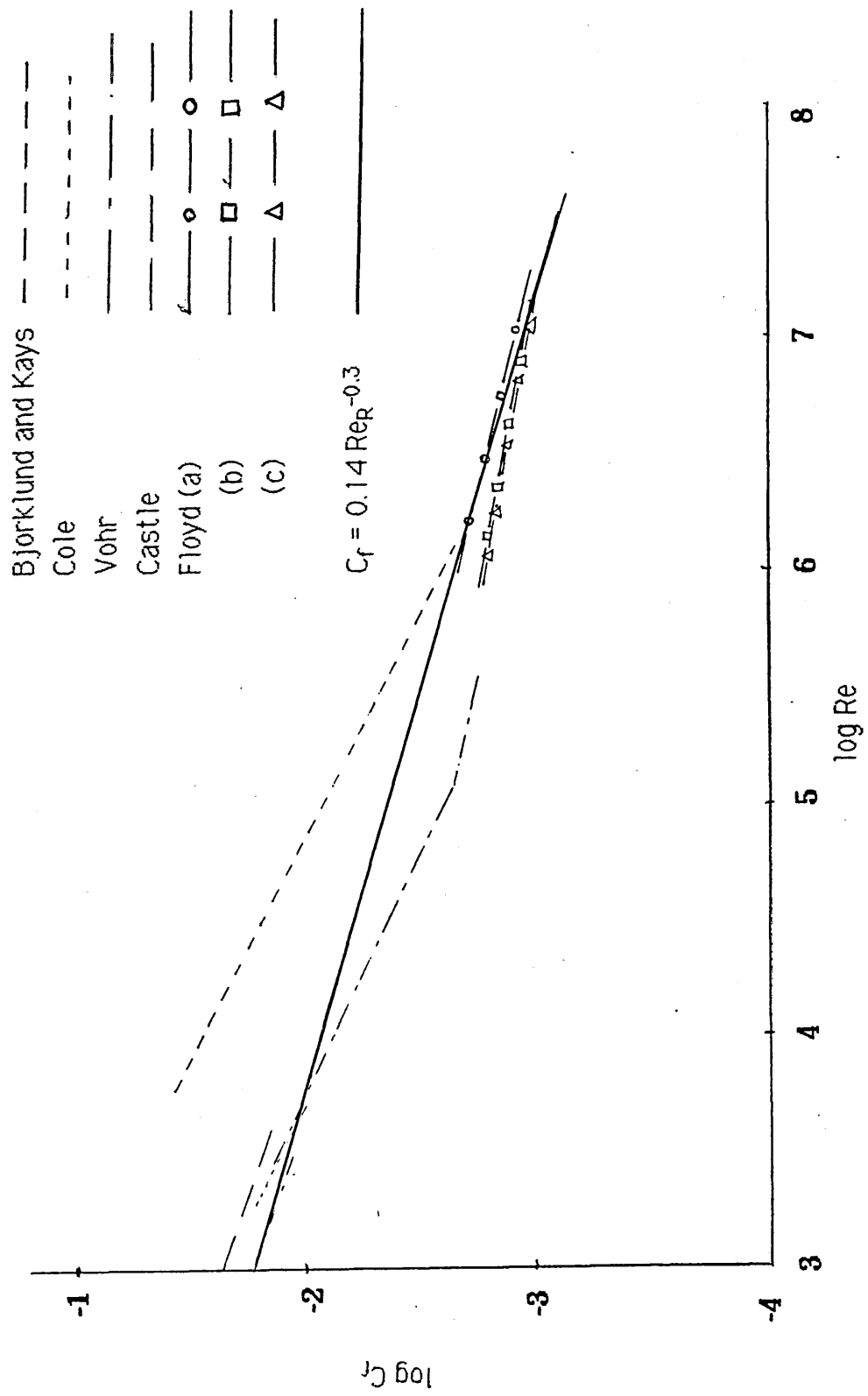
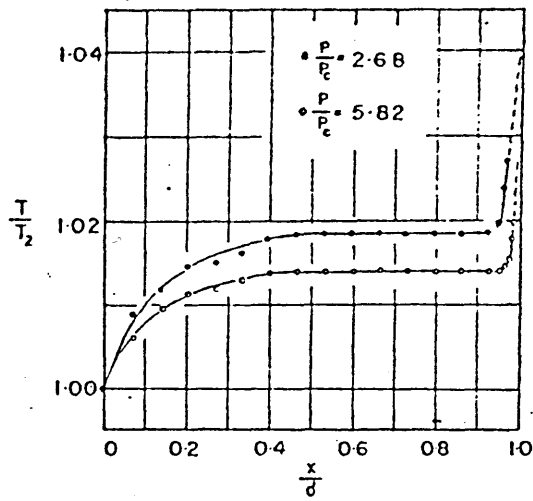
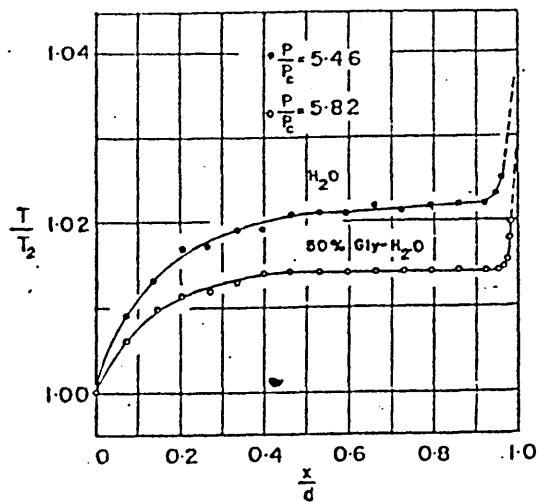


Figure 7.4 Comparison of reported friction coefficient equation

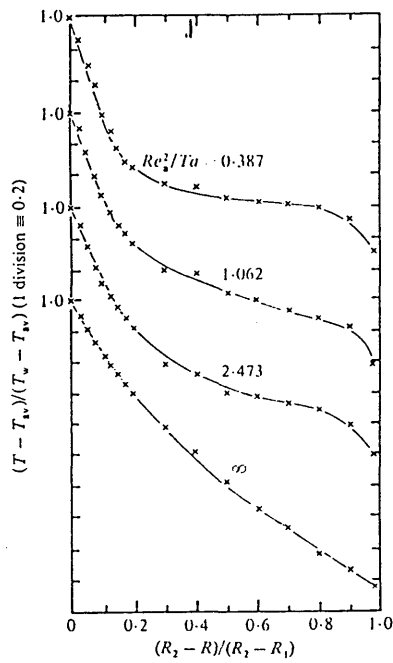


Radial temperature profiles for 50% glycerine-water solution.

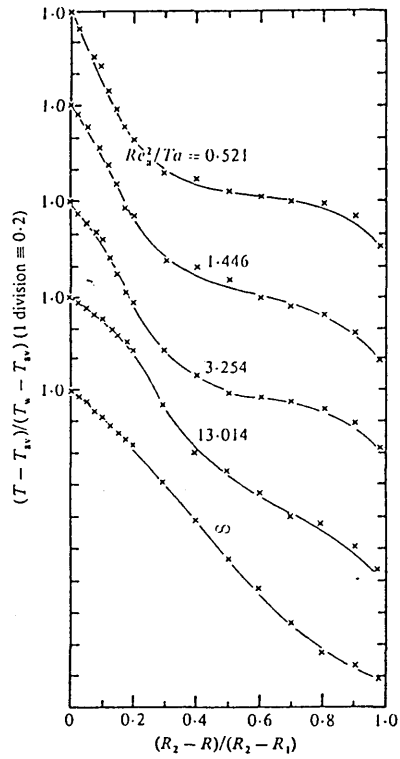


Radial temperature profiles for water and a 50% water-glycerine solution.

Figure 7.5 Measured velocity profiles (Ho et al, 1964)

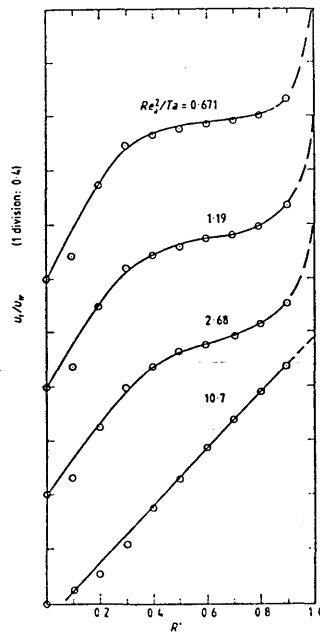


Radial temperature profiles at station D7, 0.106 m from the entrance ( $N = 0.8, Re_n = 1200$ )



Radial temperature profiles ( $N = 0.8, Re_n = 1200$ )

Figure 7.6 Measured velocity profiles (Simmers & Coney, 1979 (b))



Adiabatic tangential velocity profiles:  $N = 0.955, Re_n = 400$

Figure 7.7 Measured velocity profiles (Simmers & Coney, 1979(c))

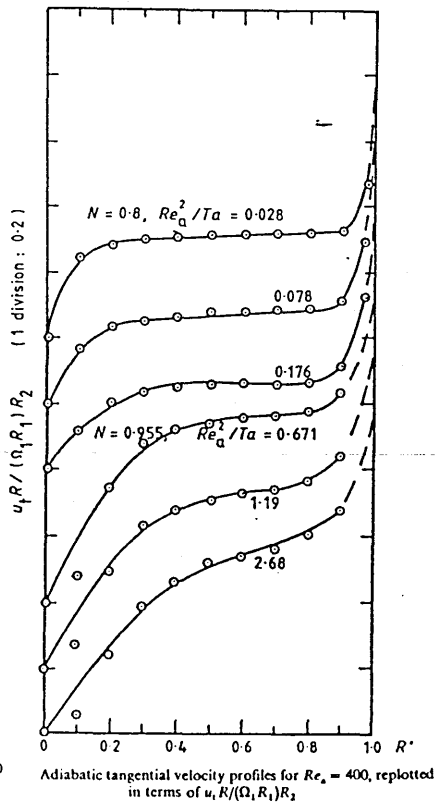
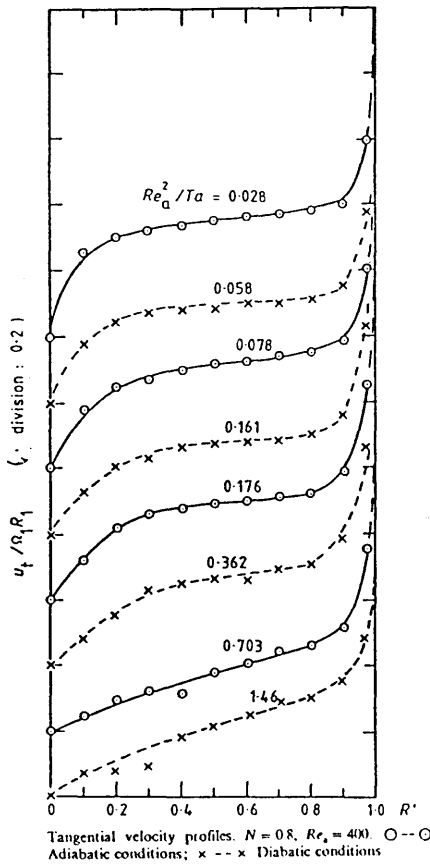
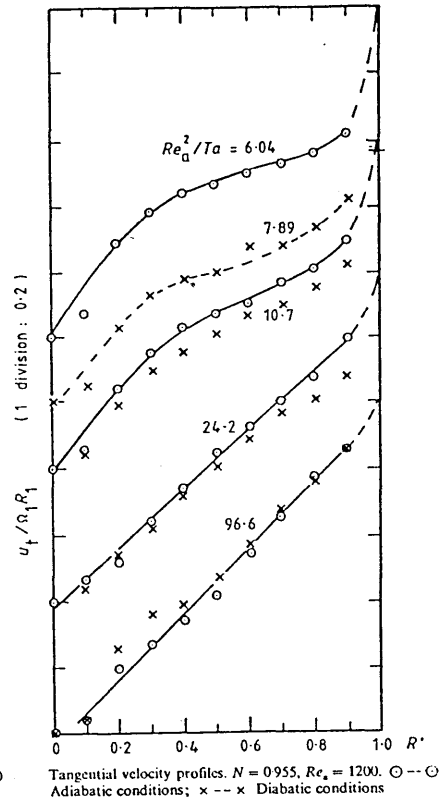
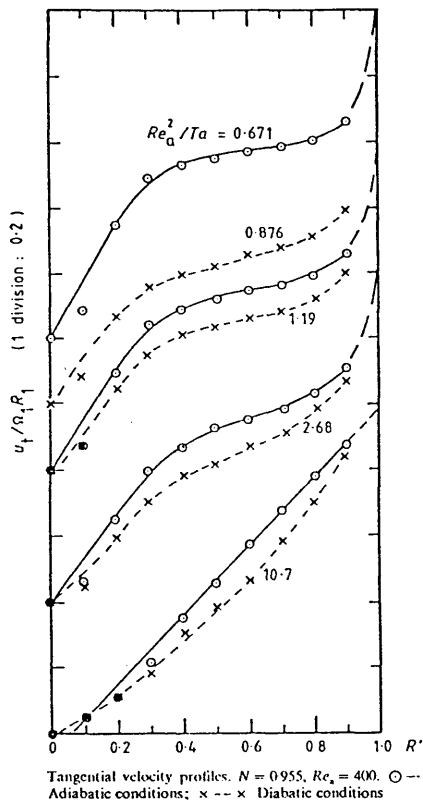
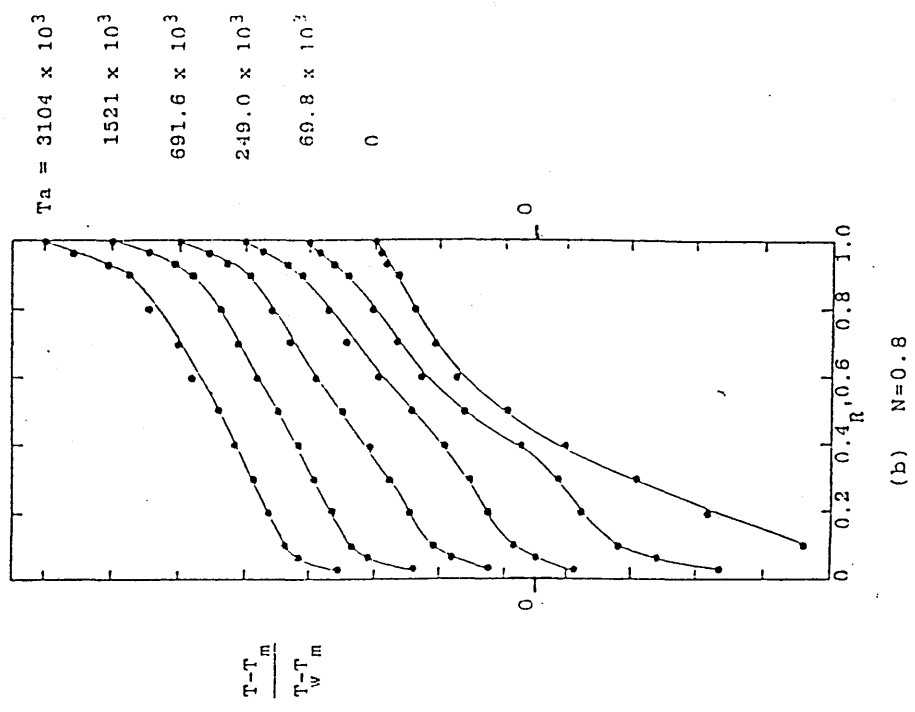
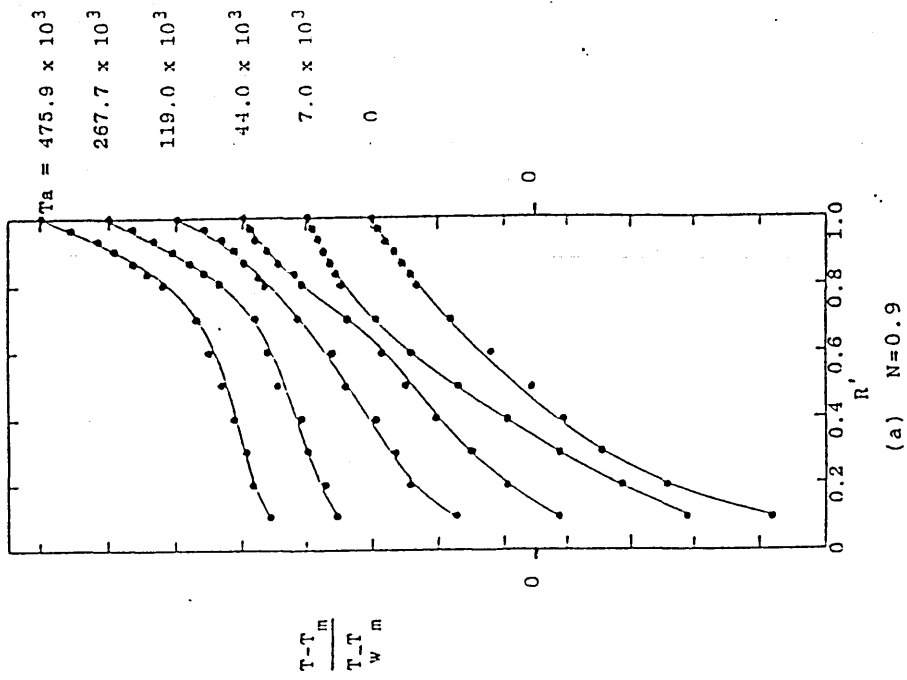


Figure 7.8 Measured velocity profiles (Simmers & Coney, 1980)



Radial Temperature Profiles (Downflow)

( Uncertainty in  $(T-T_m)/(T_w-T_m) = \pm 0.05$ , in  $R' = 0.003$  )

(  $(T-T_m)/(T_w-T_m)$  axes: 1 division=0.2. The zero relates to the lowest value of  $T_a$  )

Figure 7.9 Measured velocity profiles (Abdallah and Coney, 1988)

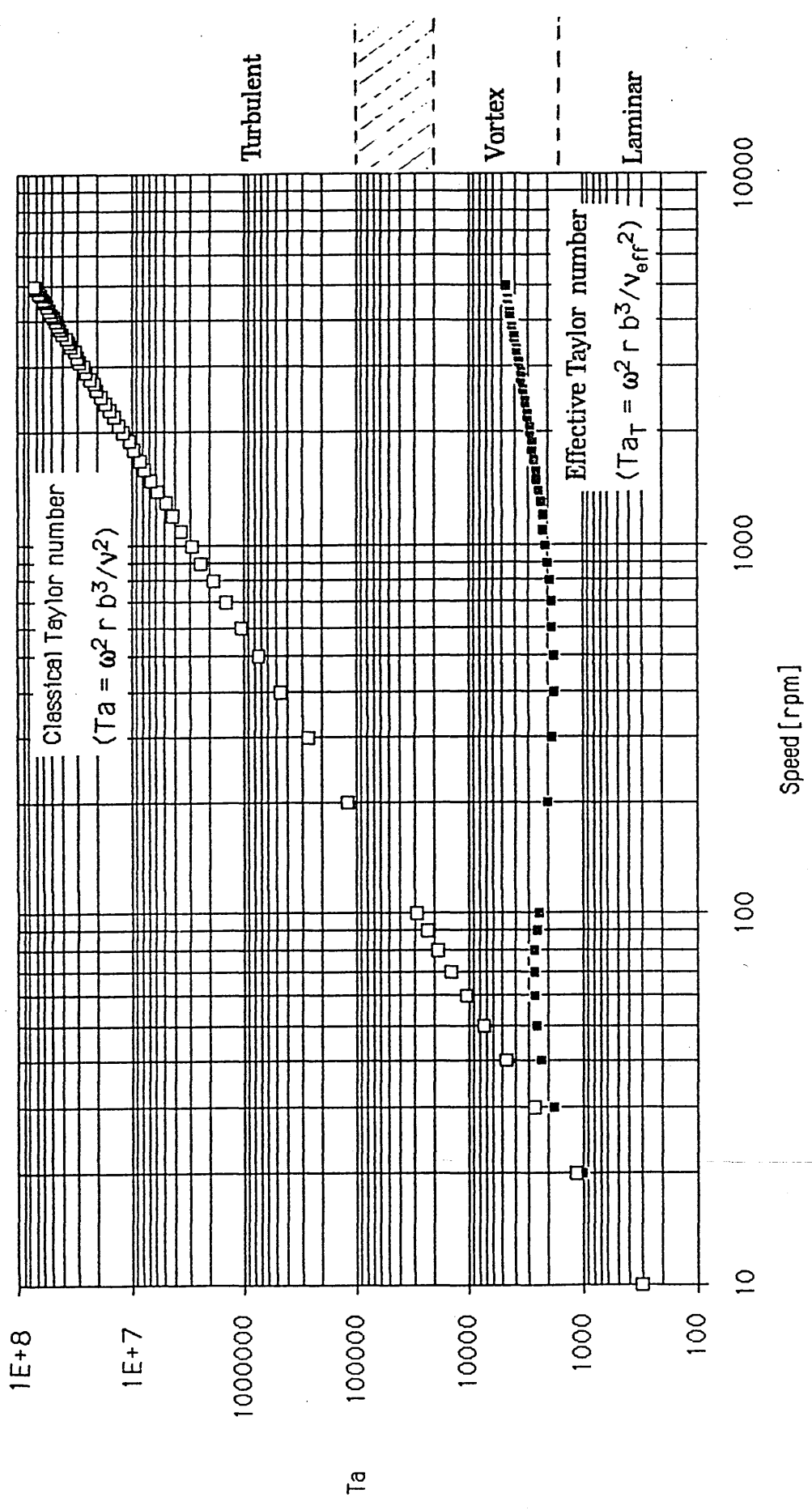


Figure 7.10 Housing 1, Water

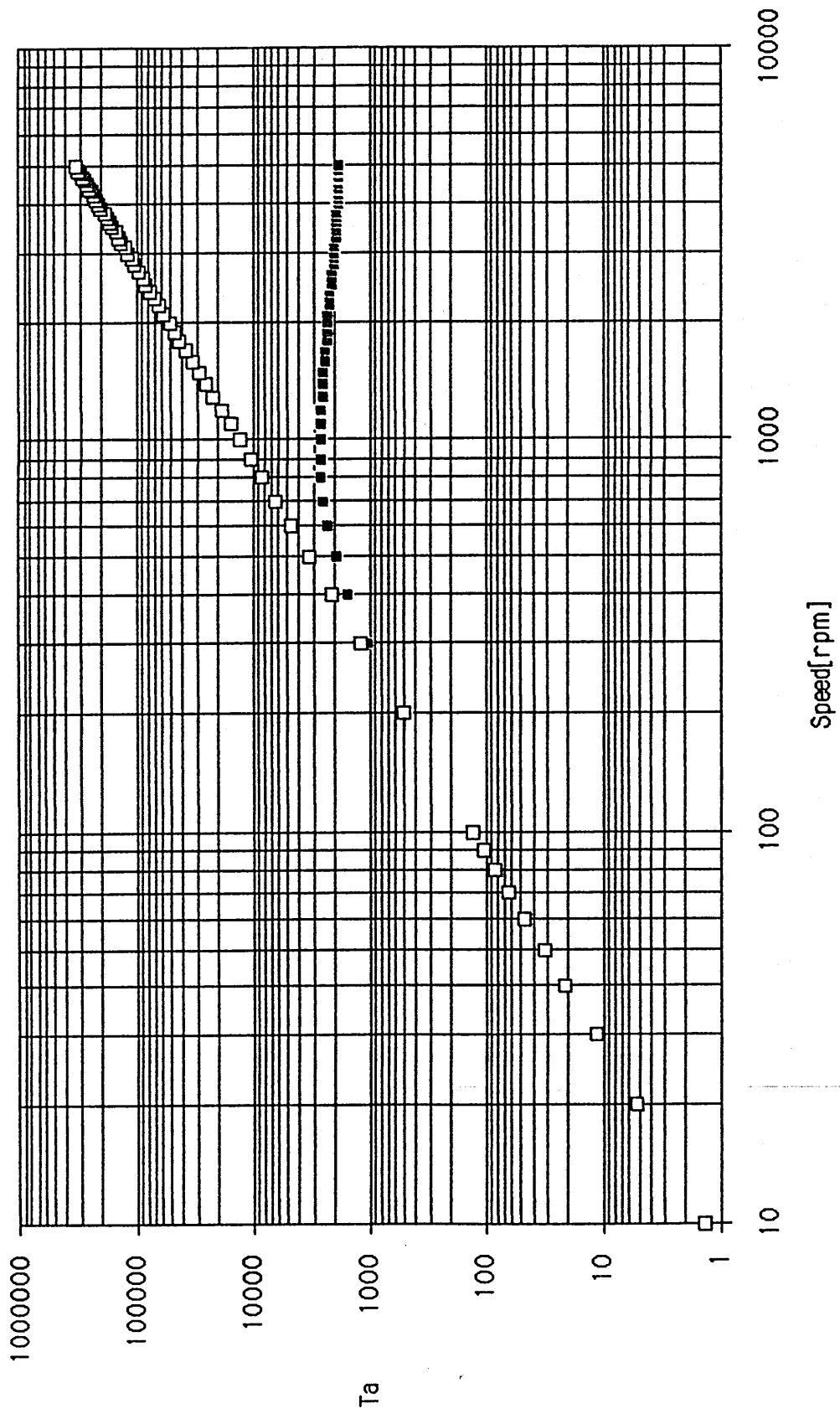


Figure 7.11 Housing 1,  $\nu = 15 \text{ mm}^2/\text{s}$



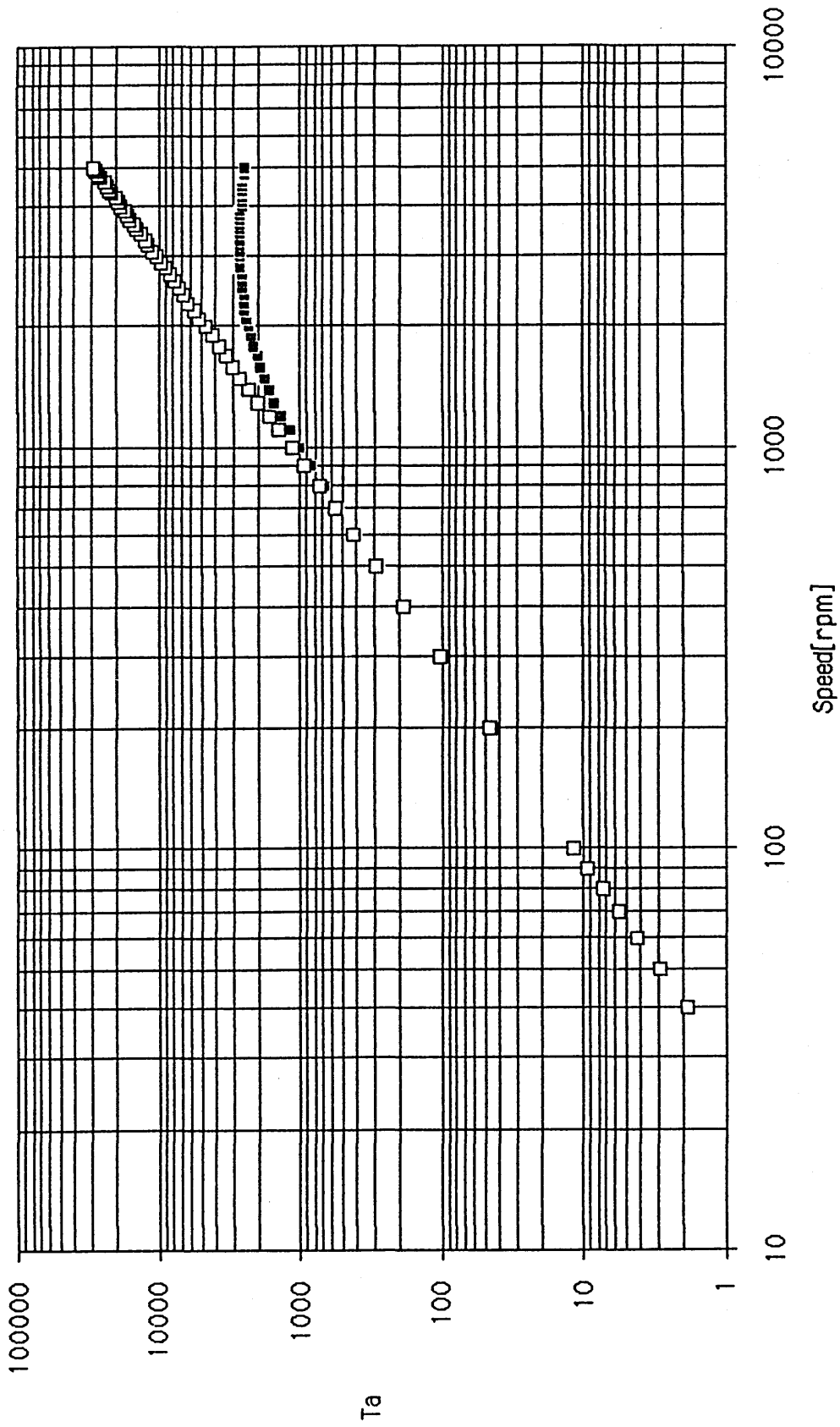


Figure 7.12 Housing 1,  $\nu = 50 \text{ mm}^2/\text{s}$

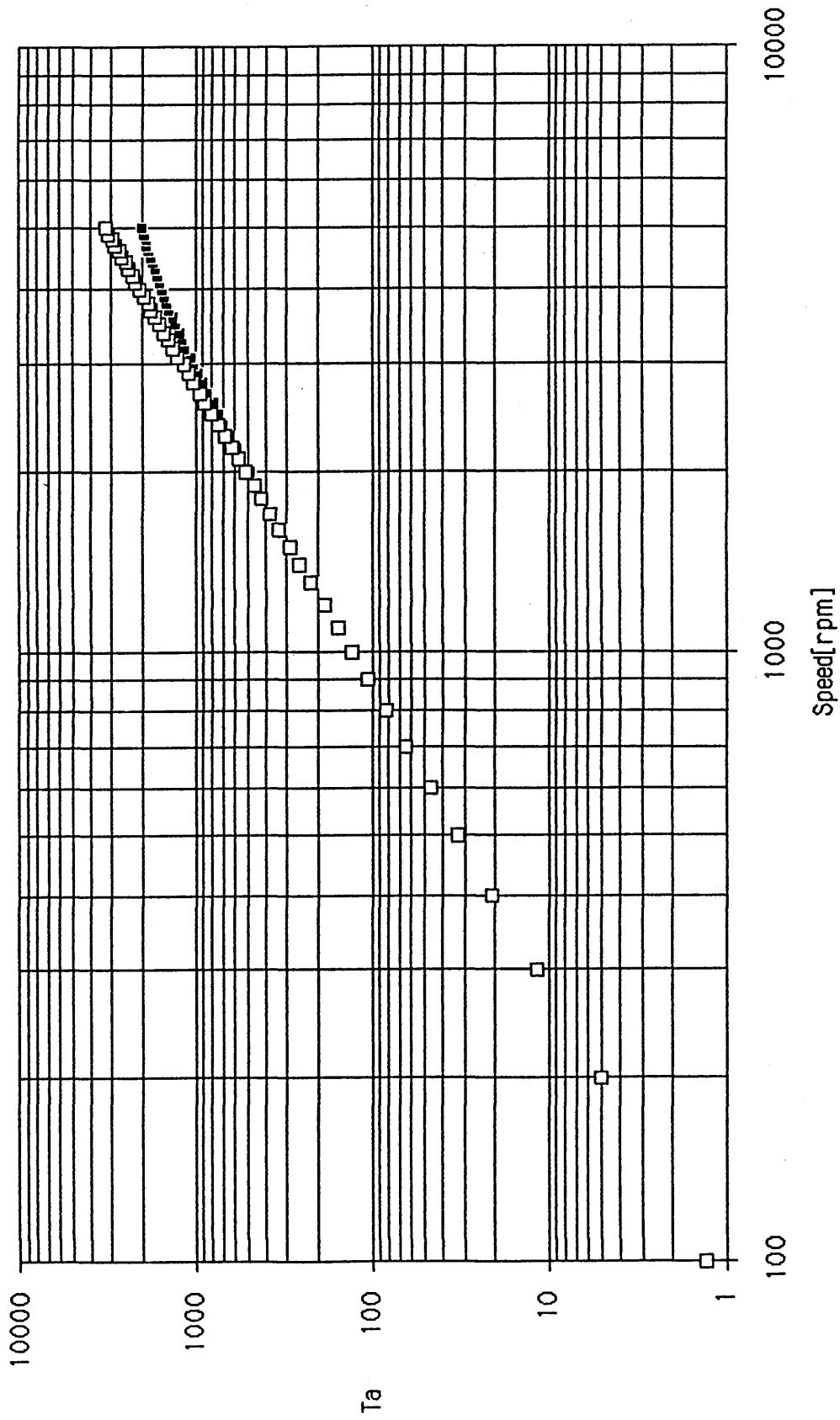


Figure 7.13 Housing 1,  $\nu = 150 \text{ mm}^2/\text{s}$

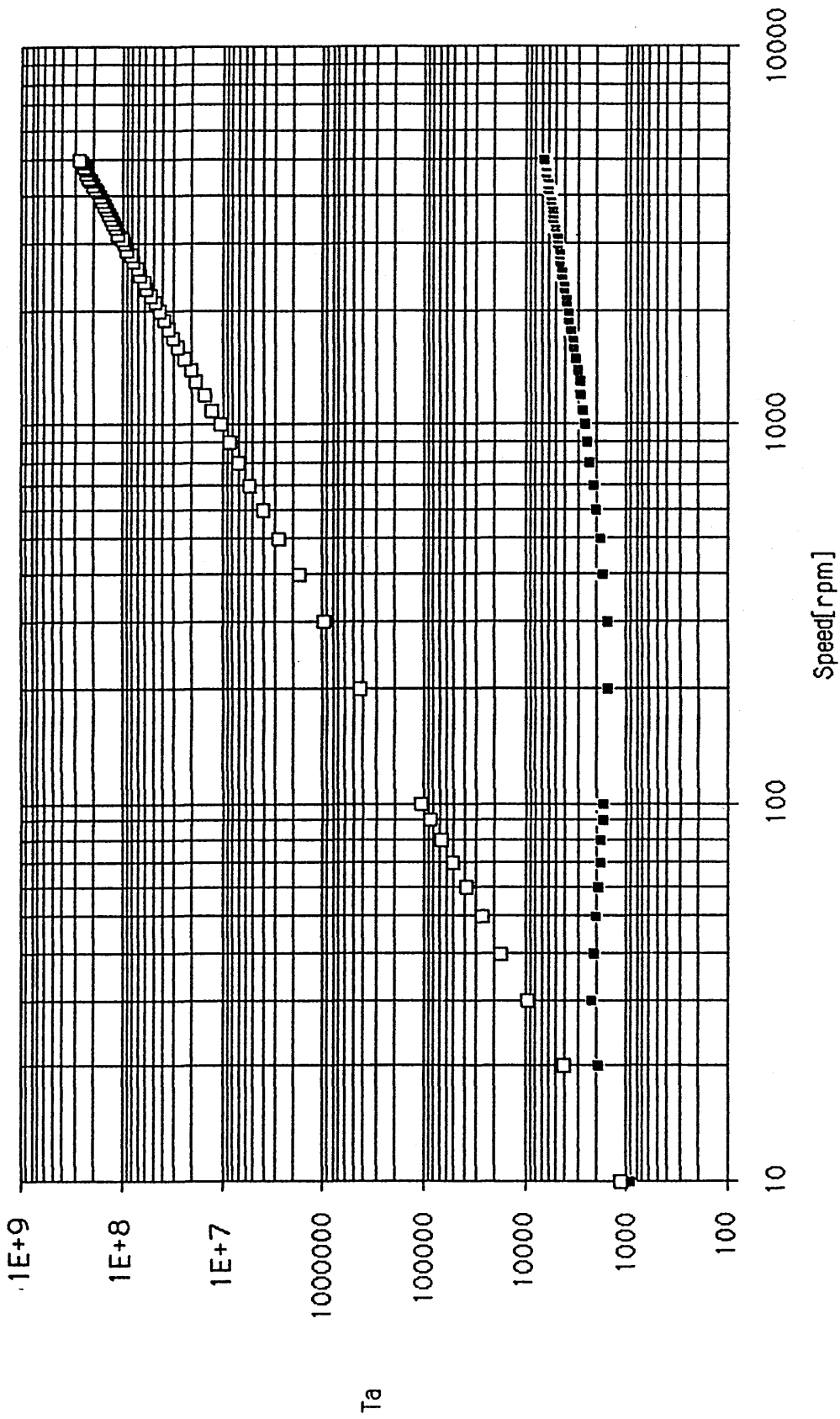


Figure 7.14 Housing 100-1, Water

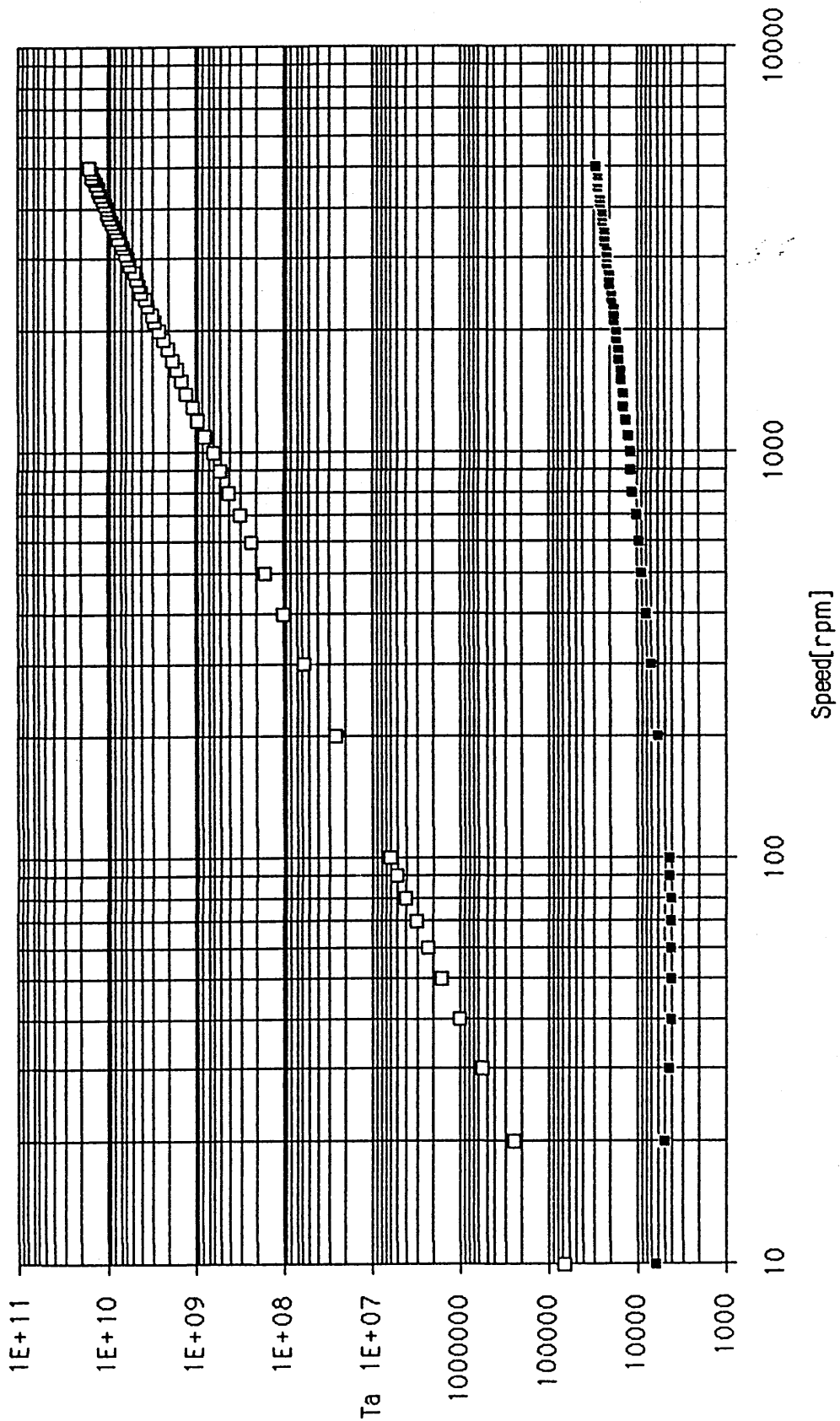


Figure 7.15 Housing 2, Water

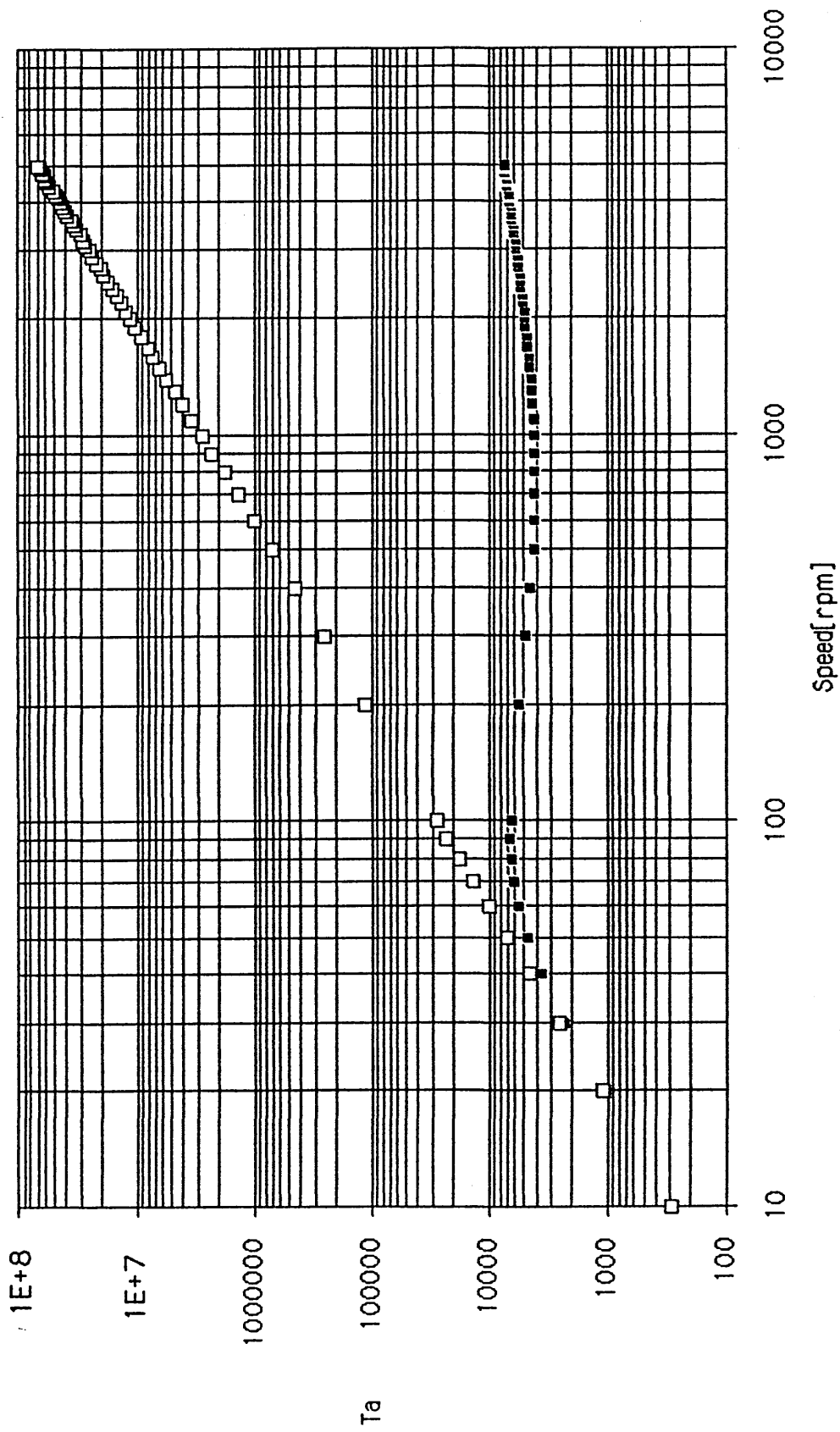


Figure 7.16 Housing 2,  $v = 15 \text{ mm}^2/\text{s}$

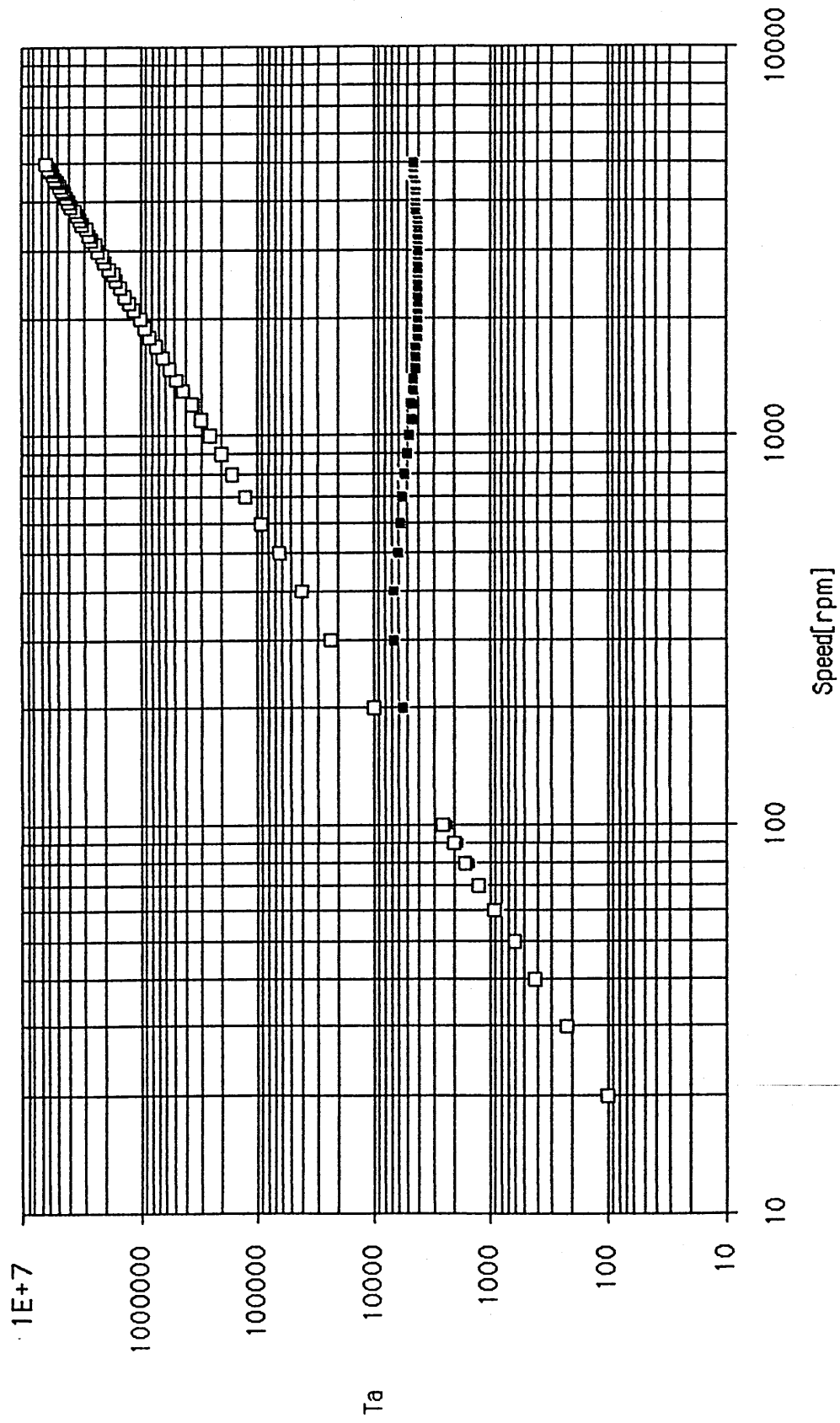


Figure 7.17 Housing 2,  $\nu = 50 \text{ mm}^2/\text{s}$

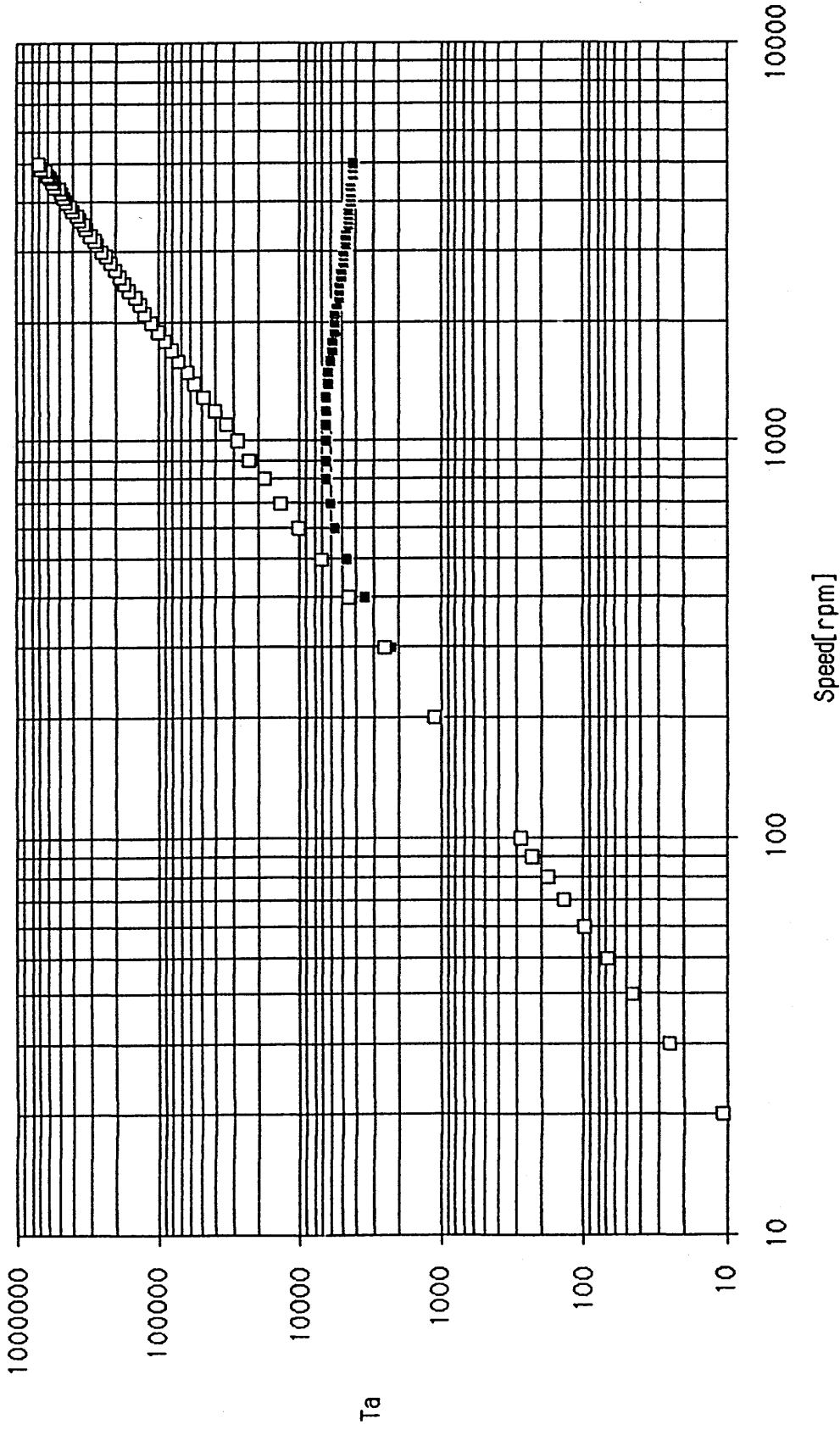


Figure 7.18 Housing 2,  $\nu = 150 \text{ mm}^2/\text{s}$

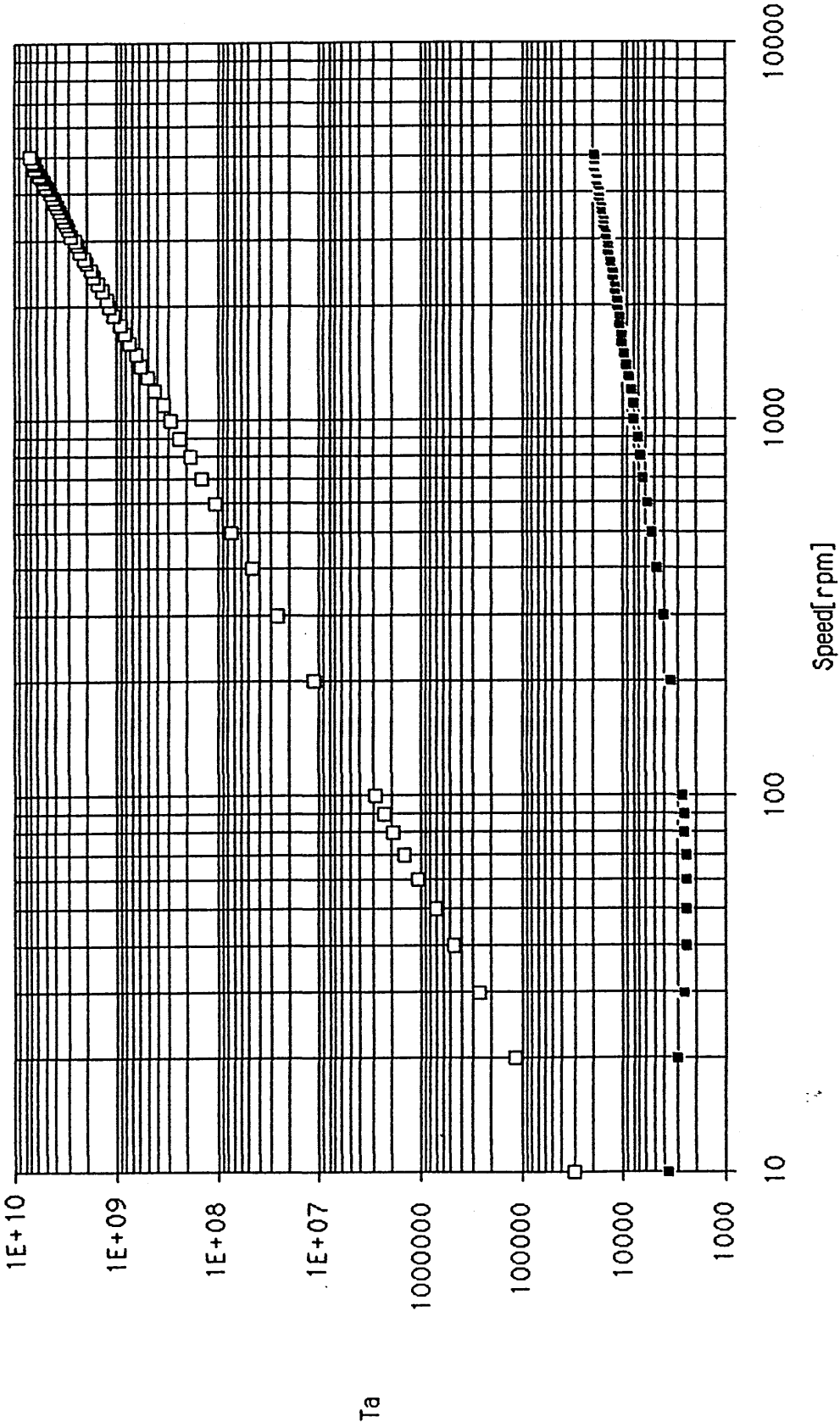


Figure 7.19 Housing 100-2, Water



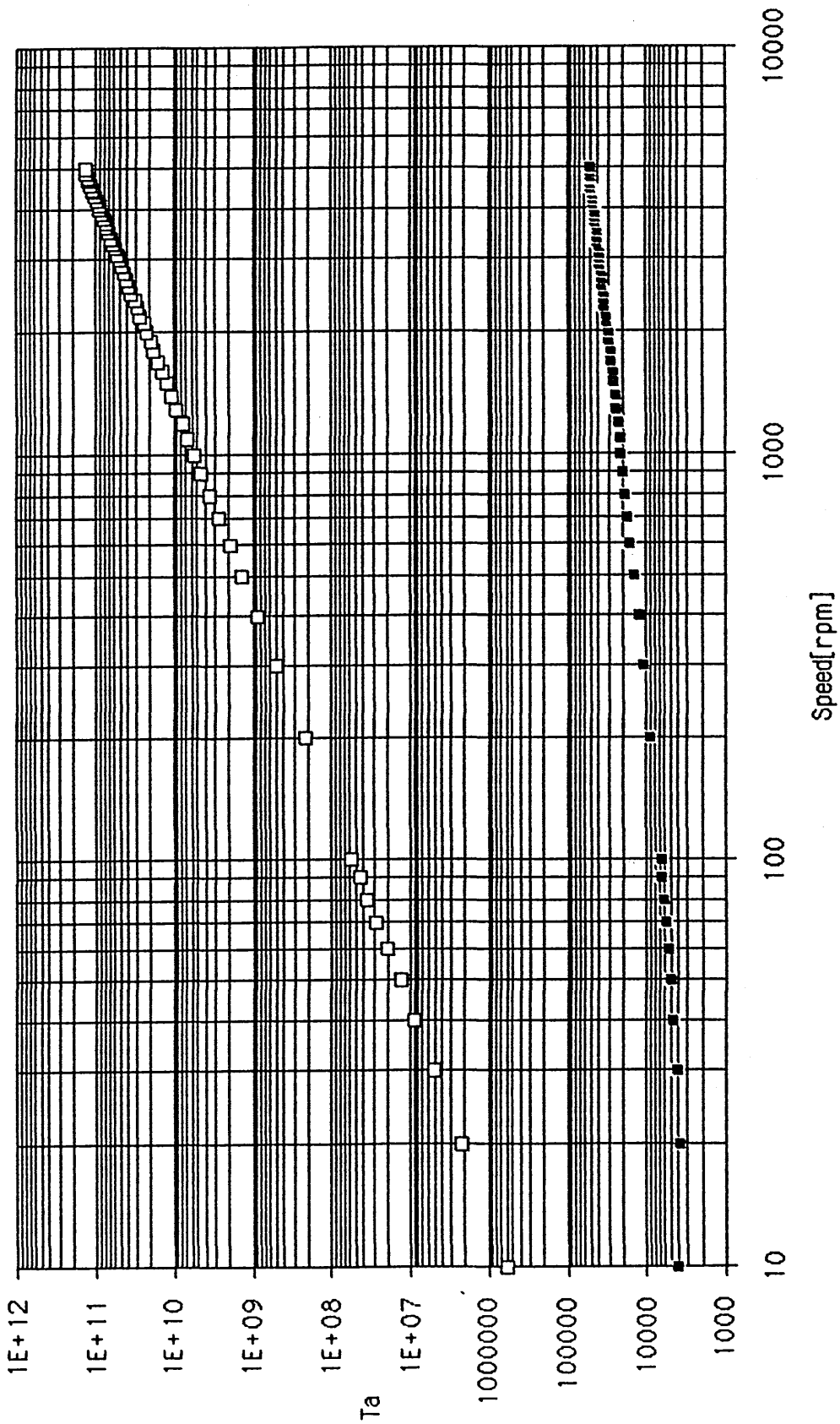


Figure 7.20 Housing 100-3, Water

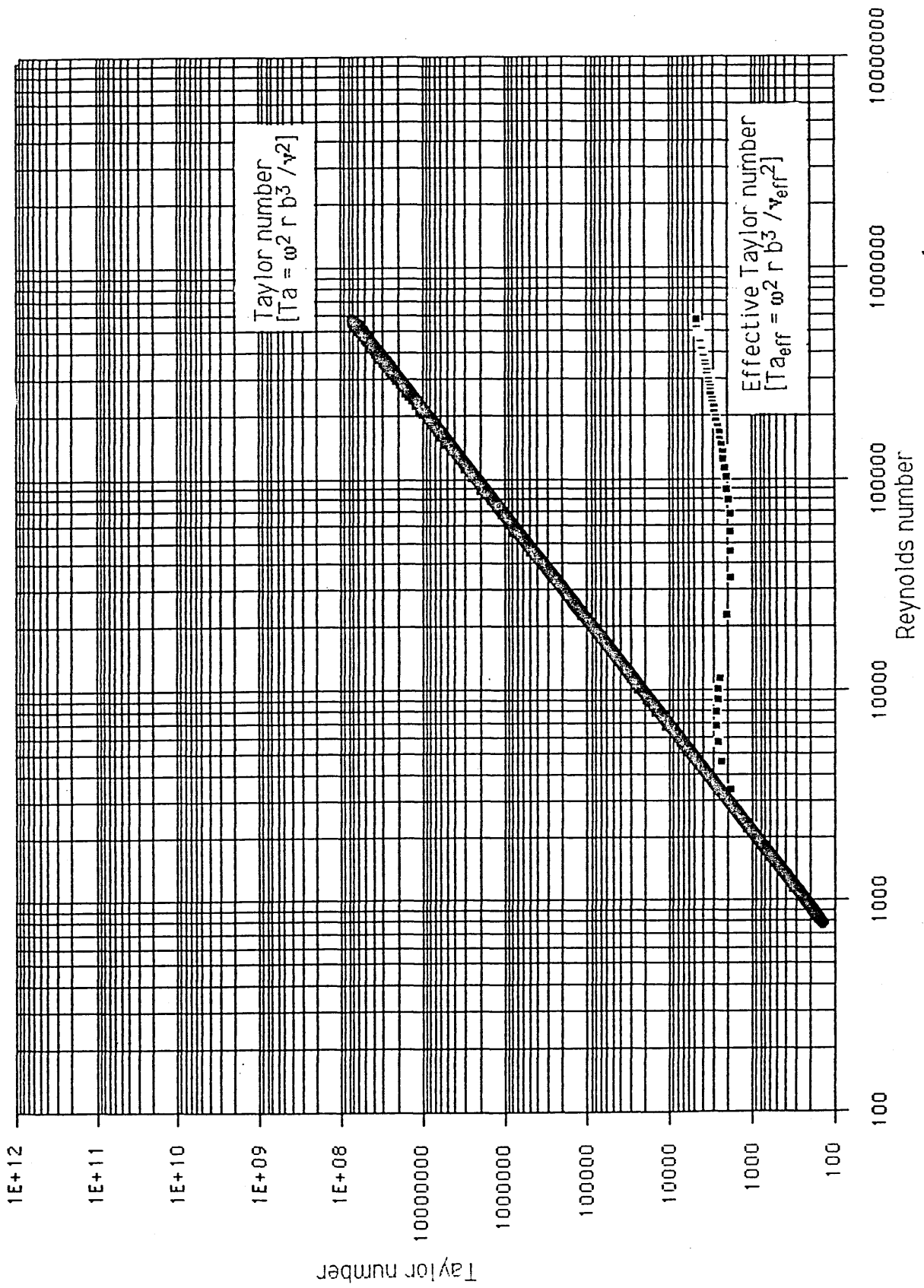


Figure 7.21 Taylor number versus Reynolds number - Housing 1

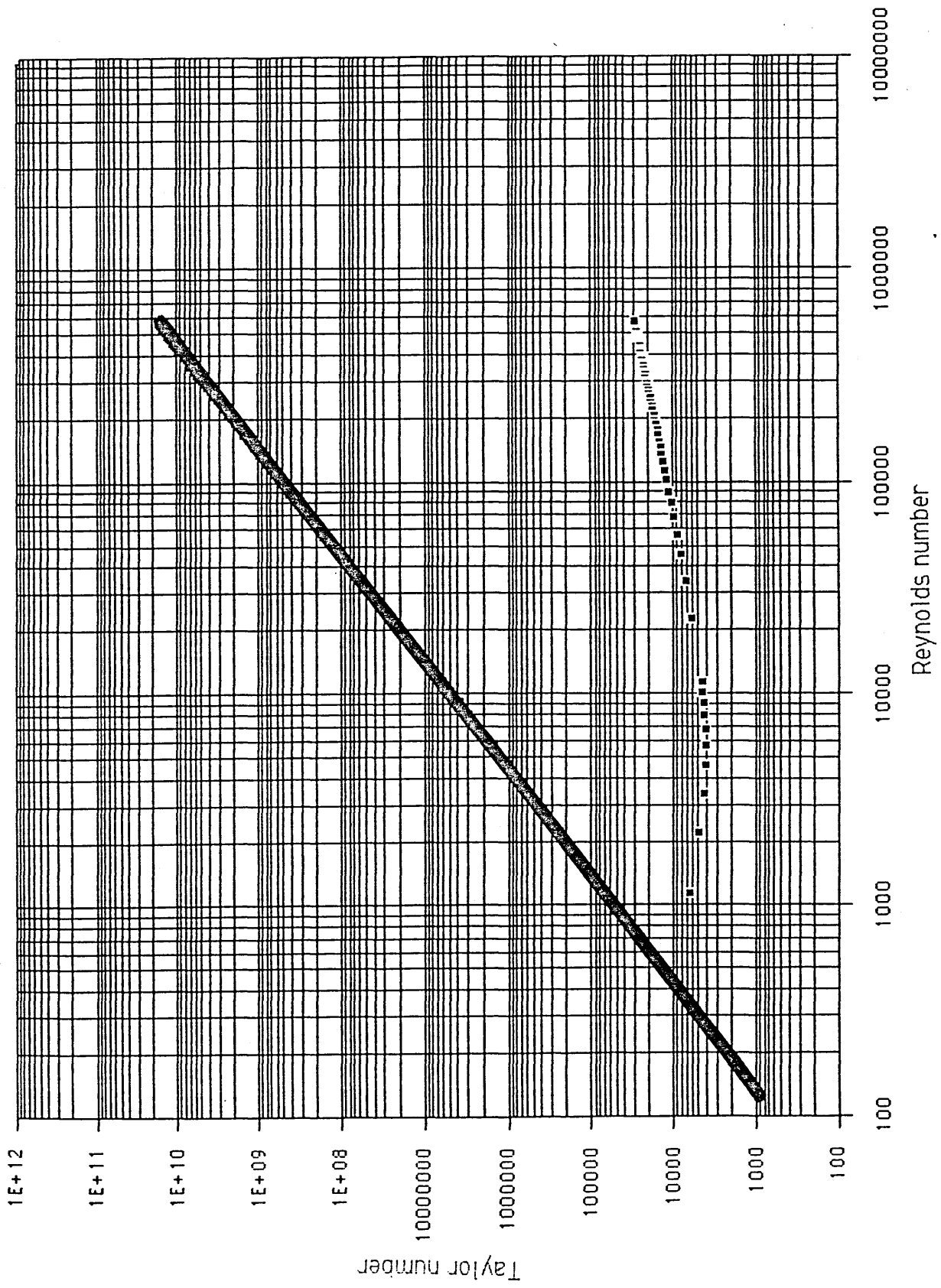


Figure 7.22 Taylor number versus Reynolds number - Housing 2

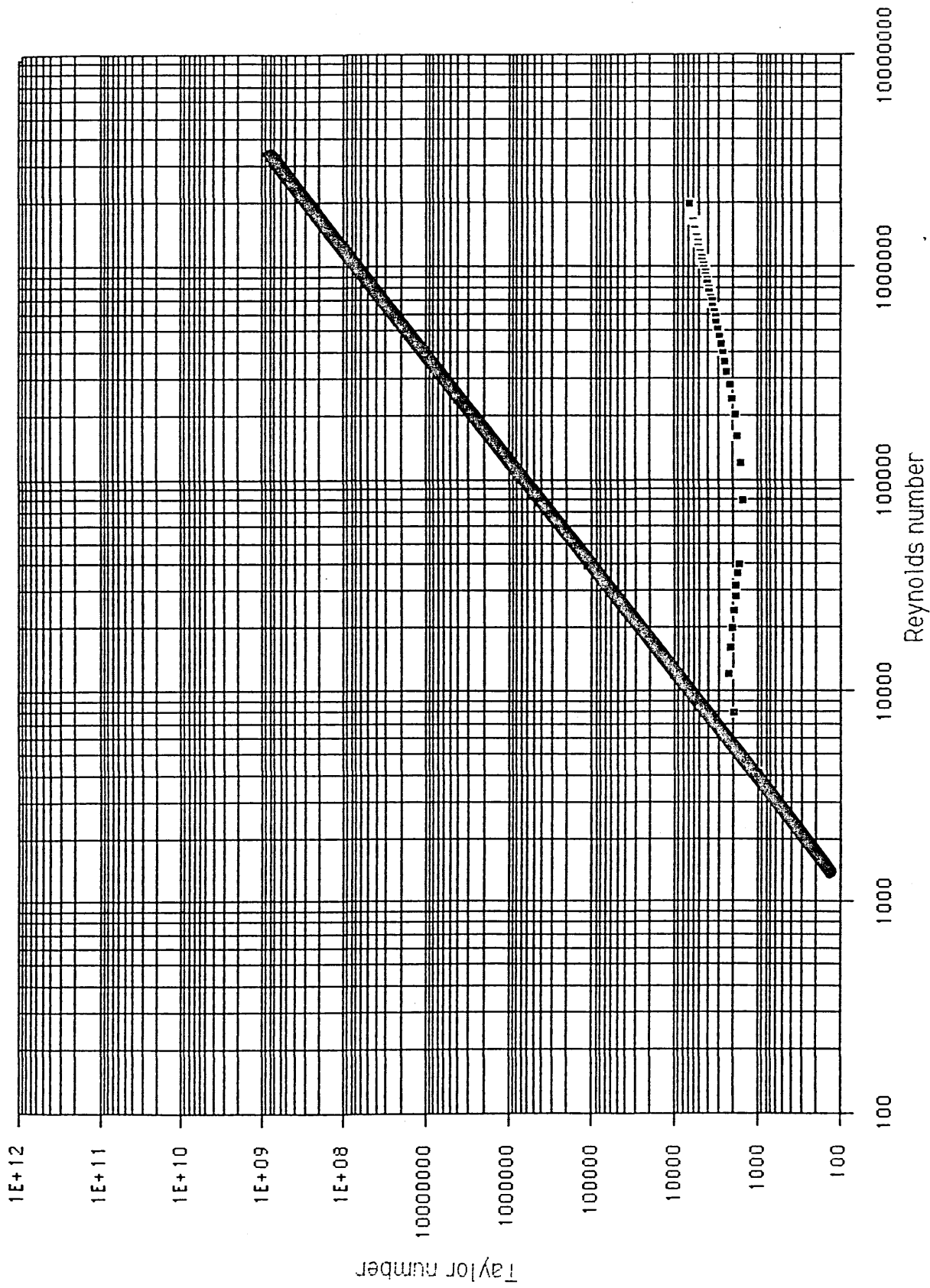


Figure 7.23 Taylor number versus Reynolds number - Housing 100-1

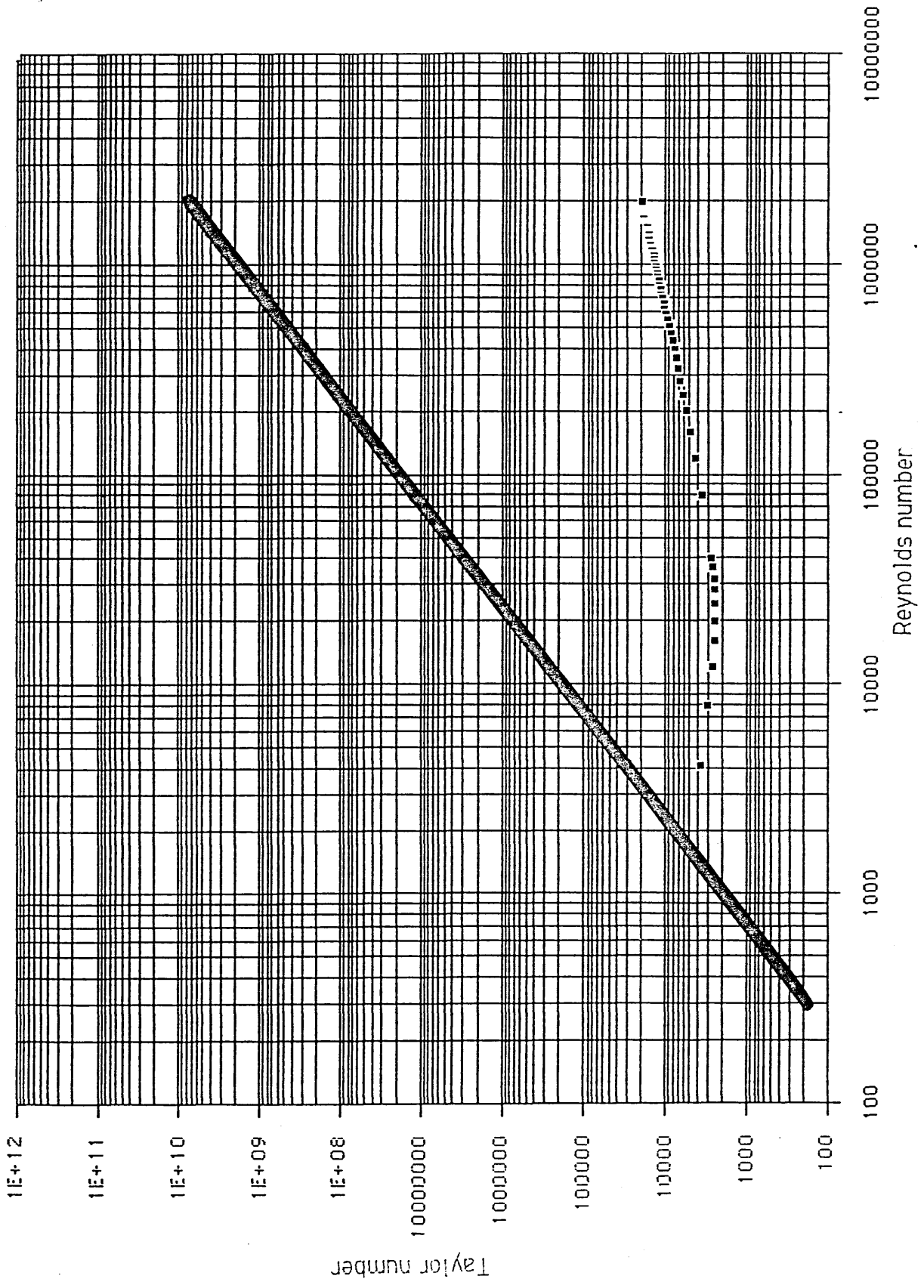


Figure 7.24 Taylor number versus Reynolds number - Housing 100-2

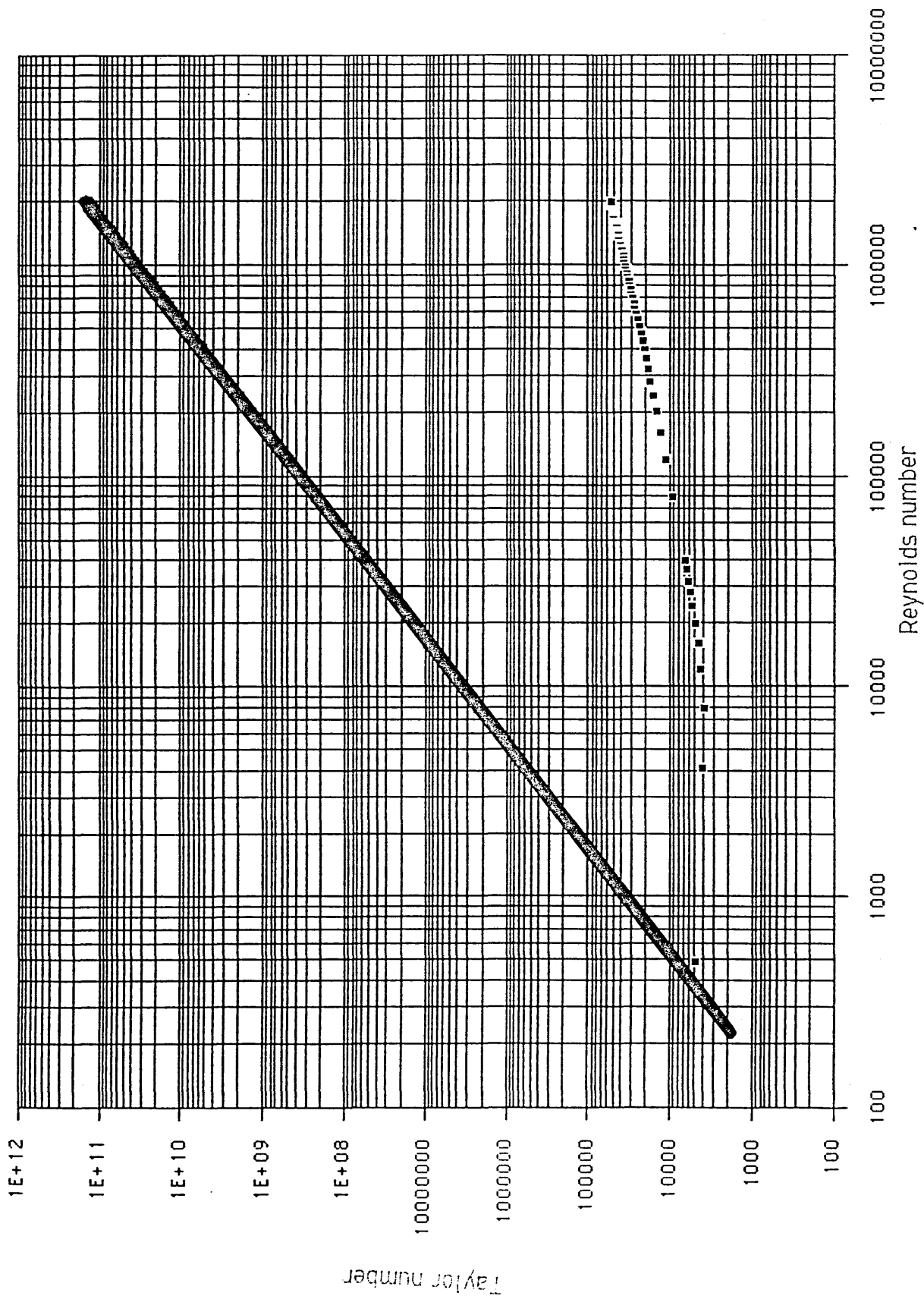
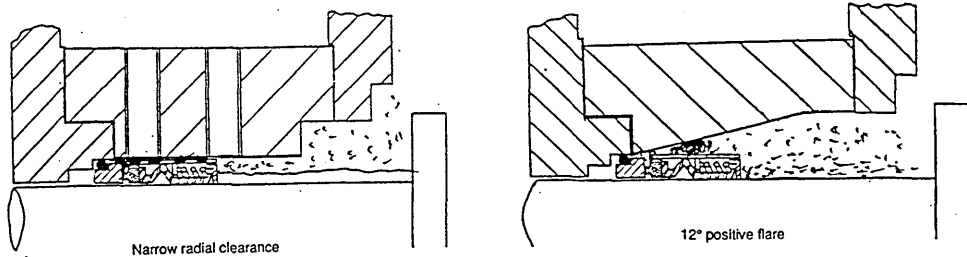
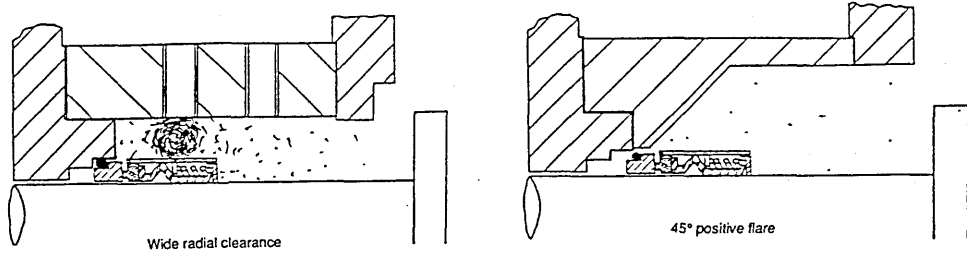


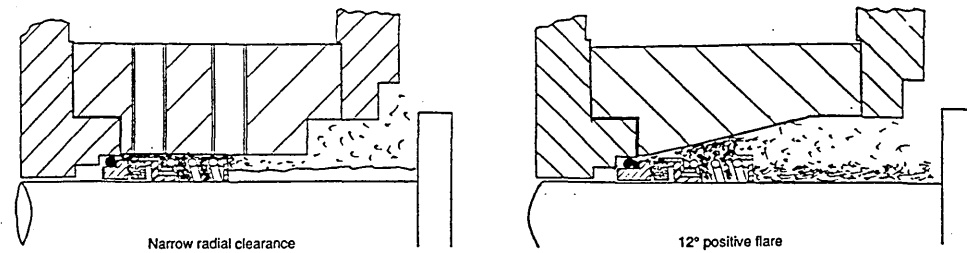
Figure 7.25 Taylor number versus Reynolds number - Housing 100-3



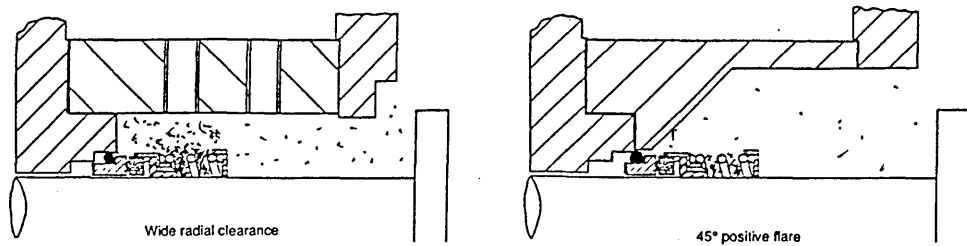
3000 rpm



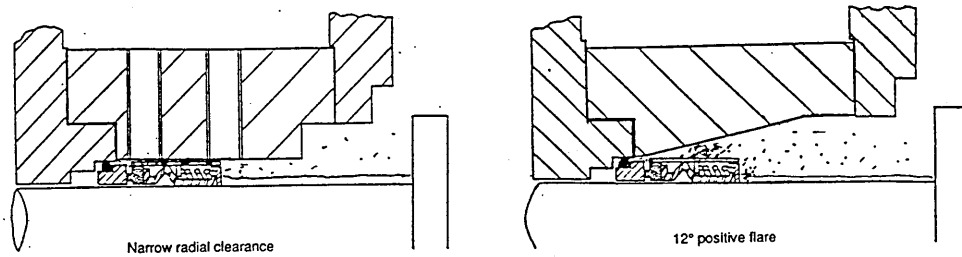
**Figure 8.1 Comparison of housings - water/Plan A/Seal B**



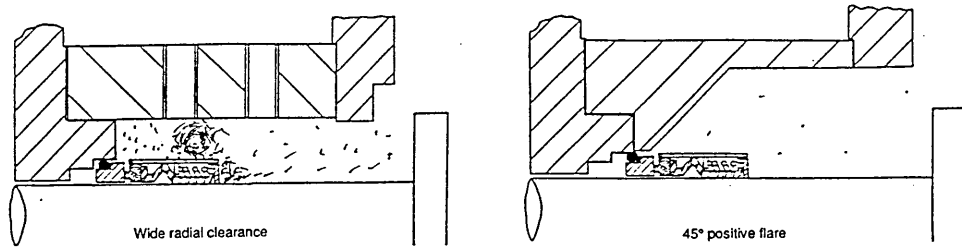
3000 rpm



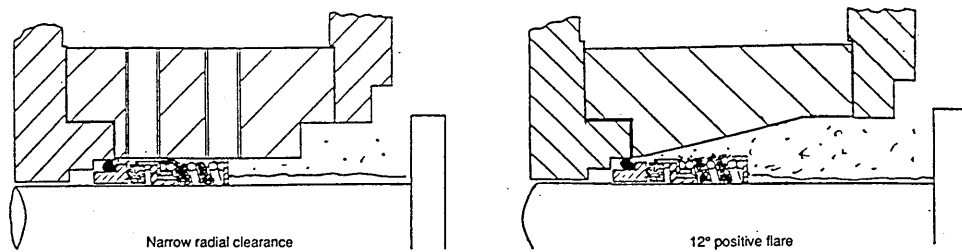
**Figure 8.2 Comparison of housings - water/Plan A/Seal A**



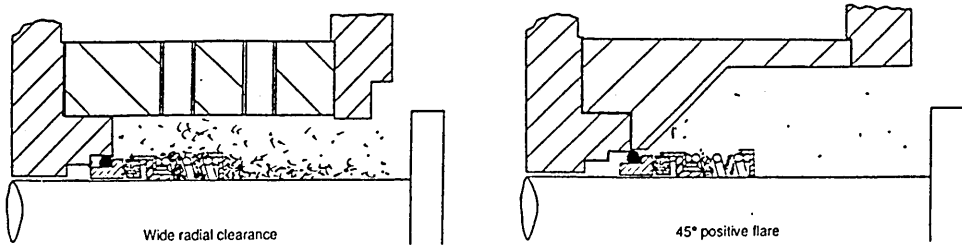
3000 rpm



**Figure 8.3 Comparison of housings - water/Plan B/Seal B**



3000 rpm



**Figure 8.4 Comparison of housings - water/Plan B/Seal A**



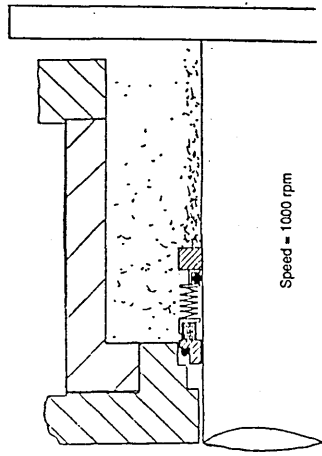
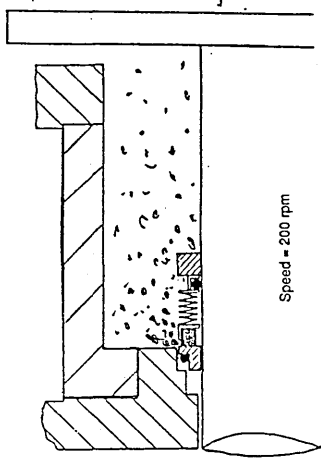


Figure 8.6 Housing 100-3 - effect of speed

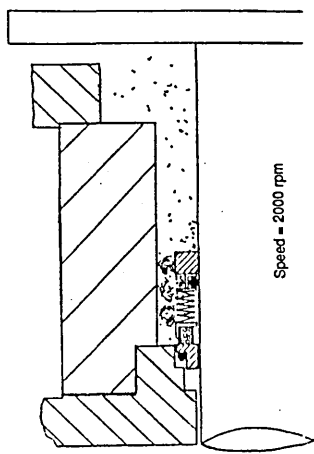
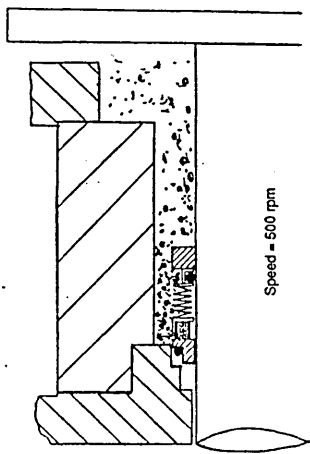


Figure 8.5 Housing 100-2 - effect of speed

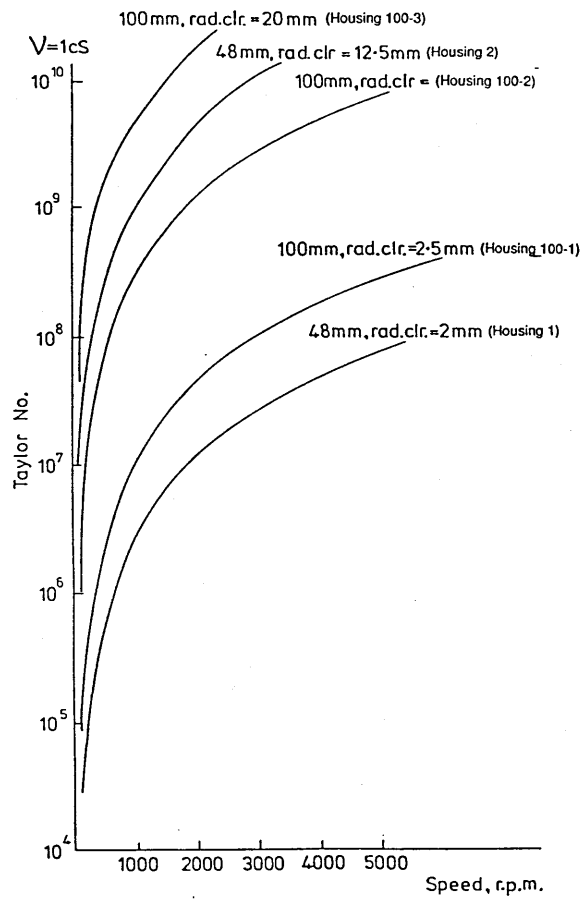


Figure 8.7 Taylor number as a function of speed - parallel housings

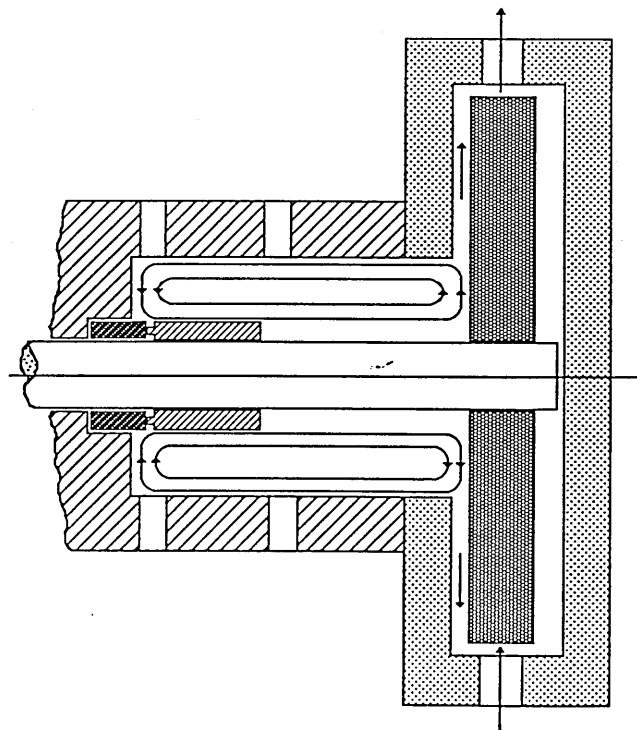


Figure 8.8 Effects of the impeller

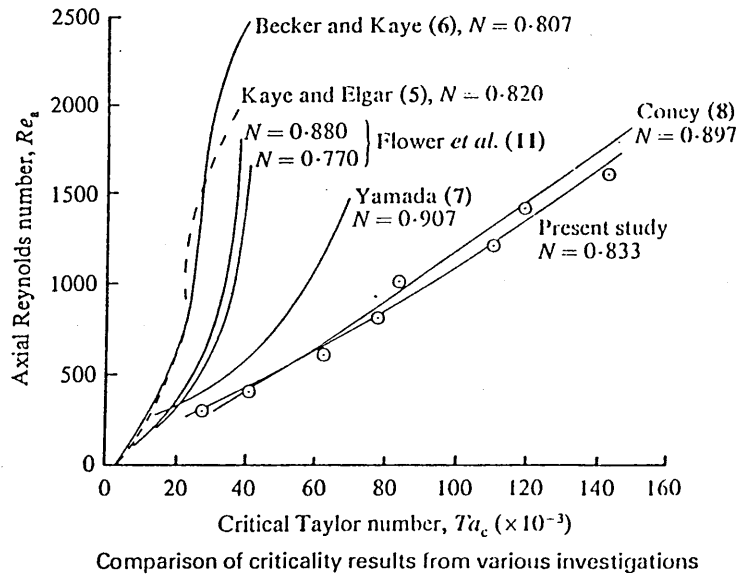


Figure 8.9 Effect of axial flow on critical Taylor number (Coney & Simmers 1979 (a))

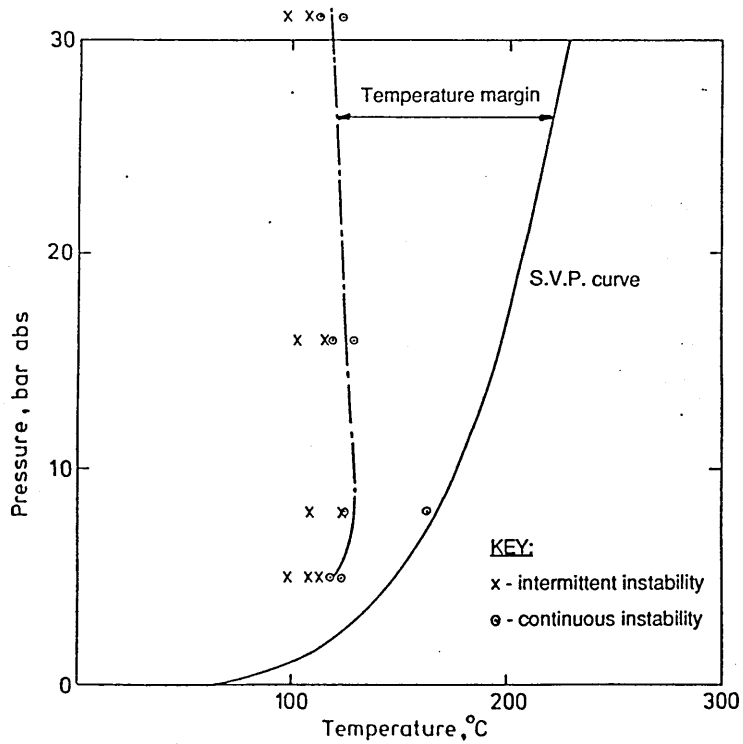


Figure 9.1 Typical seal instability curve

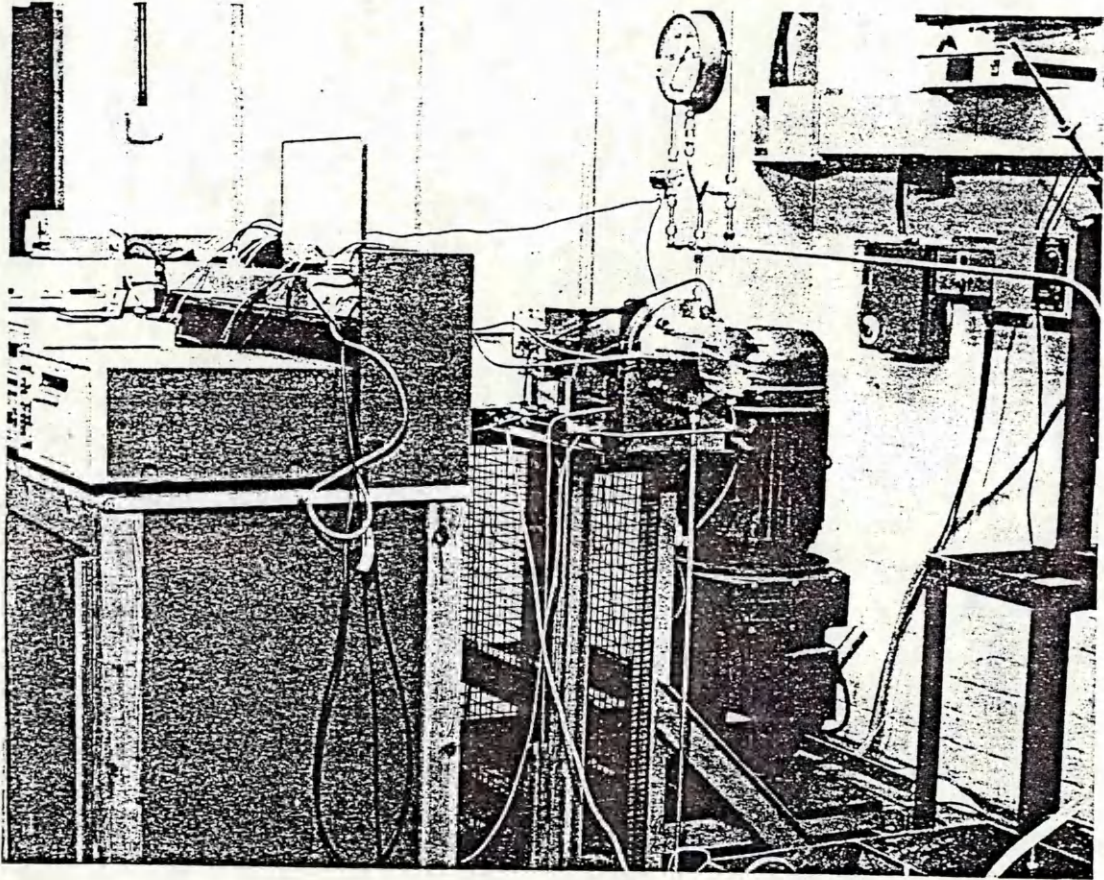


Figure 9.2 General view of instability rig

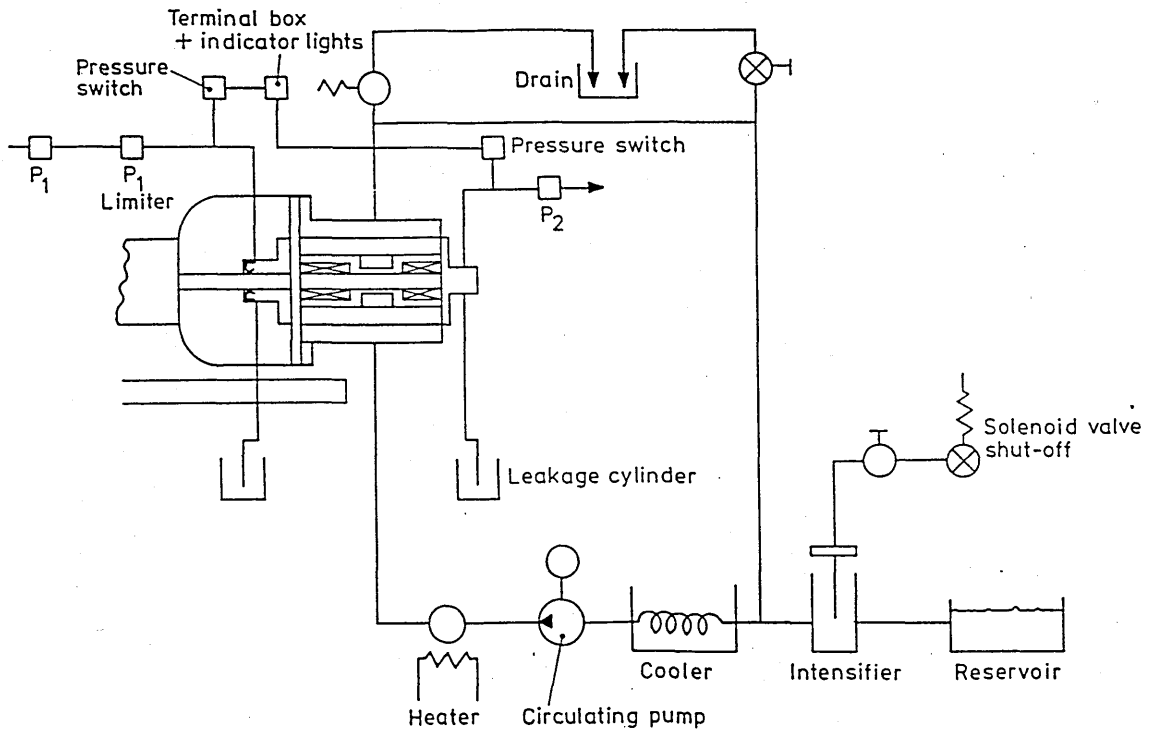


Figure 9.3 Test circuit

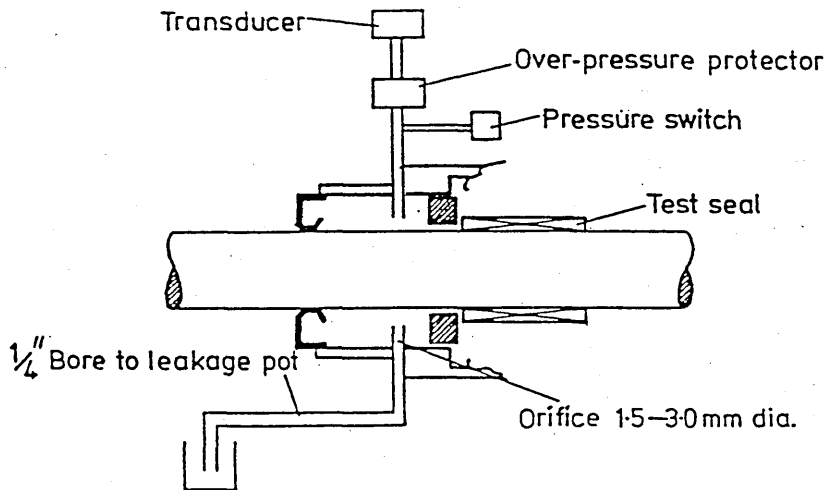
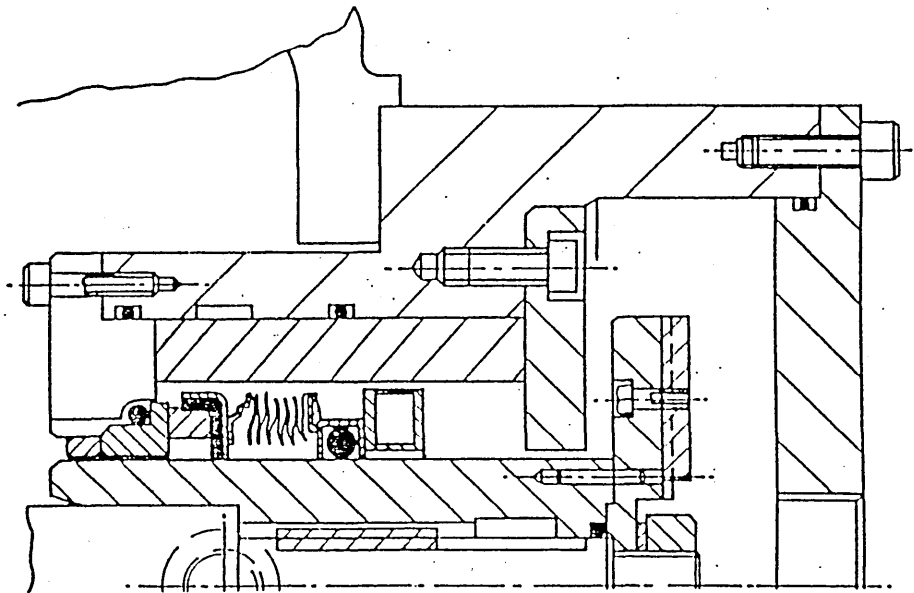
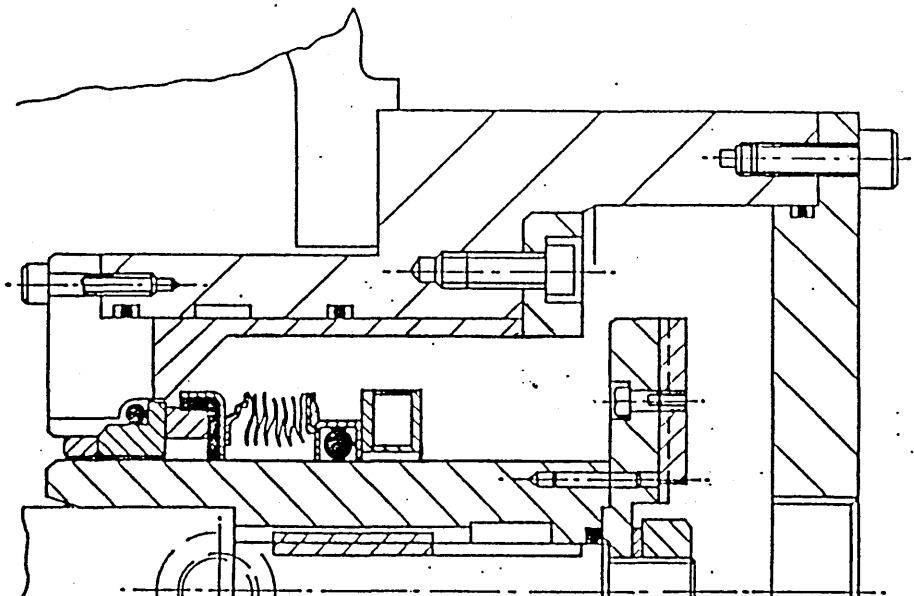


Figure 9.4 Leakage measuring system



ISO/DIN HOUSING WITH NECK BUSH



45° FLARE WITH NO NECK BUSH

Figure 9.5 General arrangement of test chamber

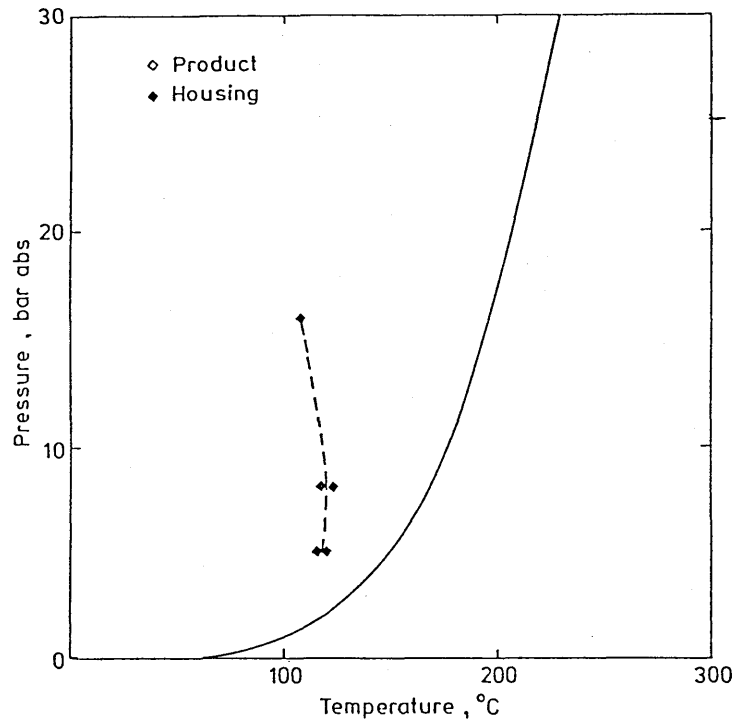


Figure 9.6 Instability curve - "good" housing

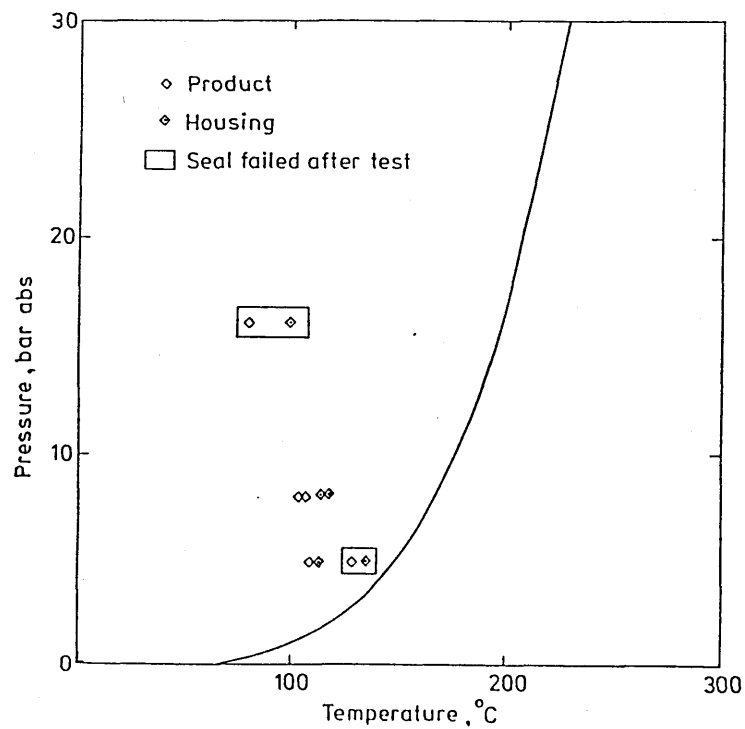


Figure 9.7 Instability curve - "poor" housing

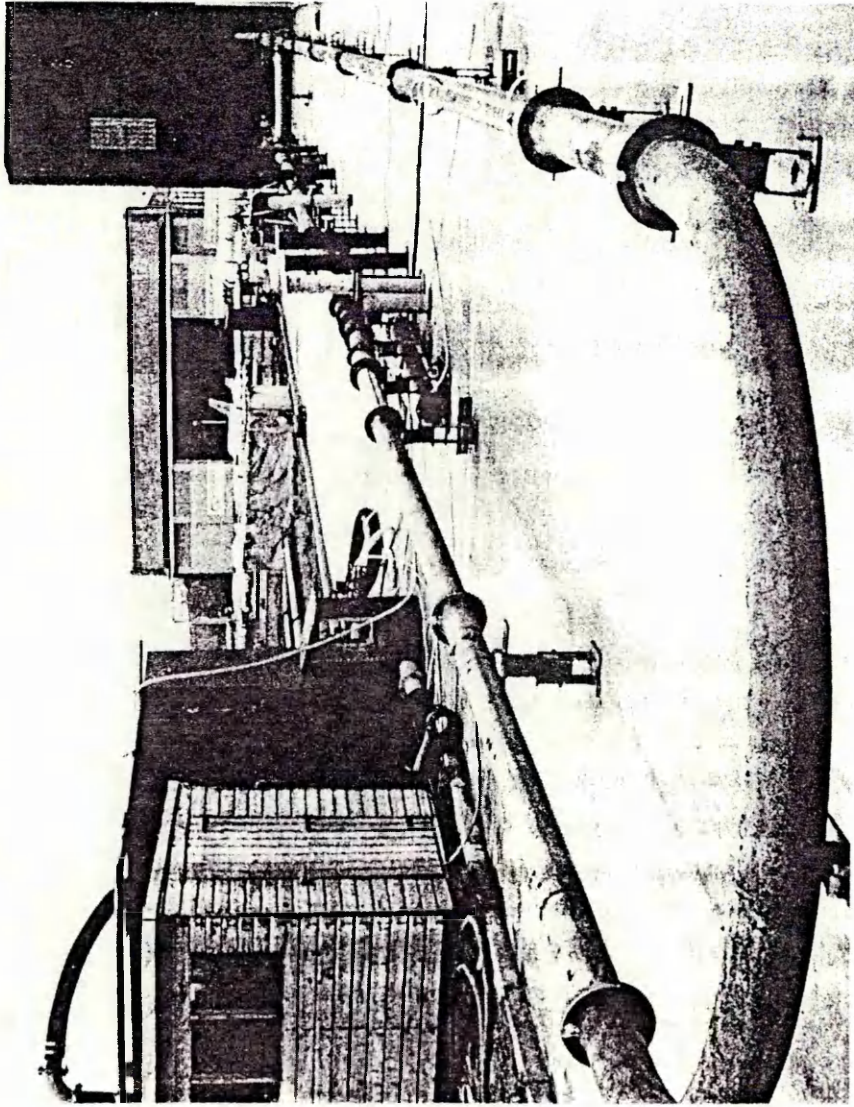


Figure 10.1 BHRA Large Slurry Pipe facility



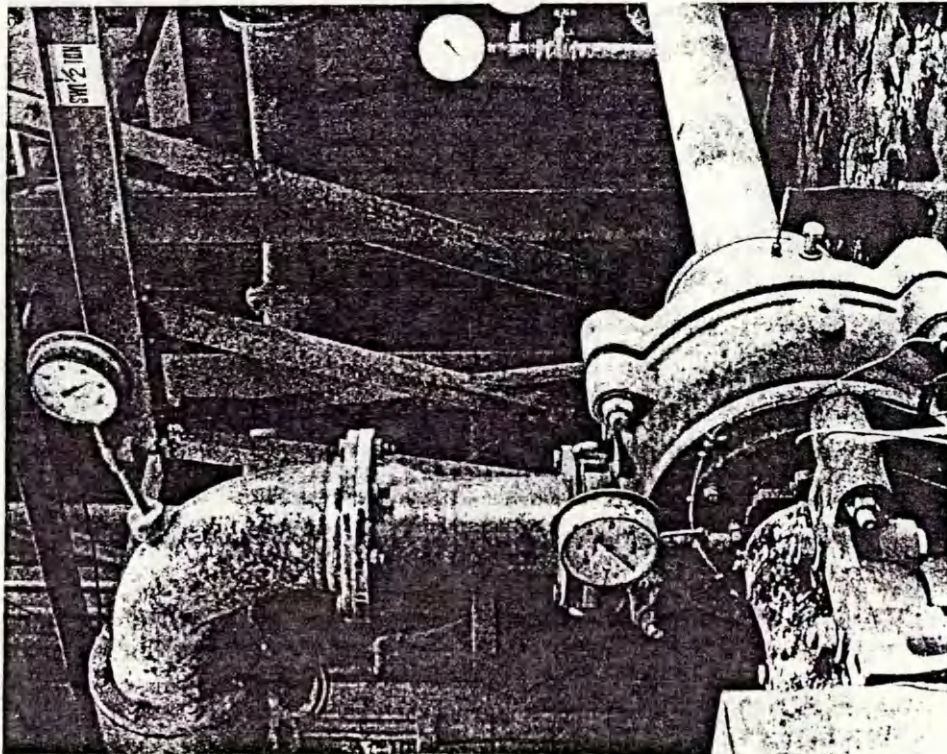
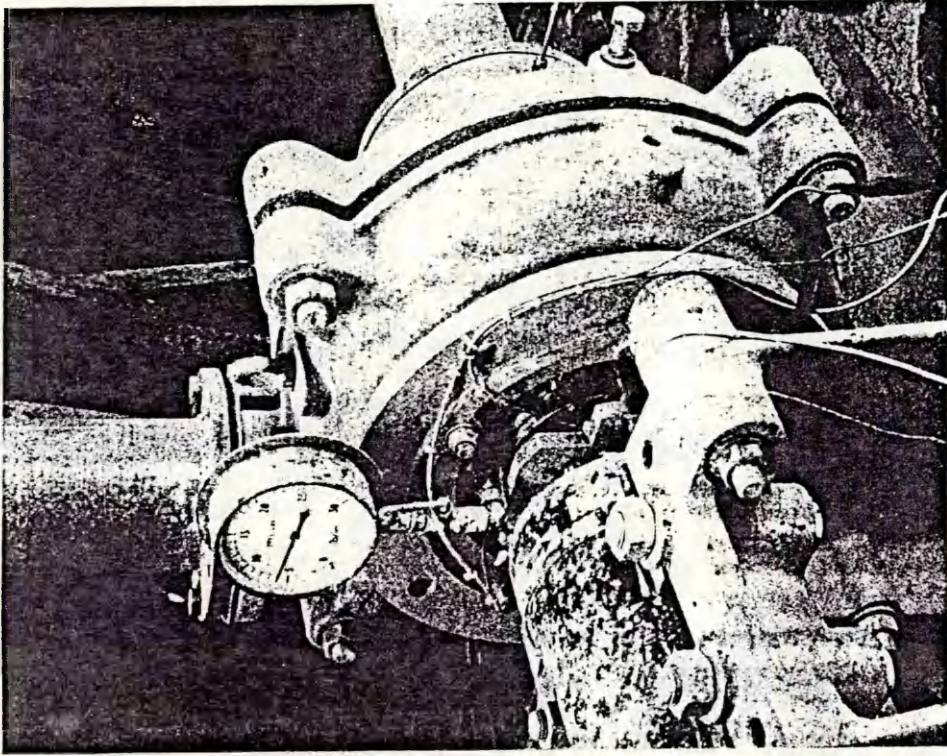


Figure 10.2 Instrumented pump

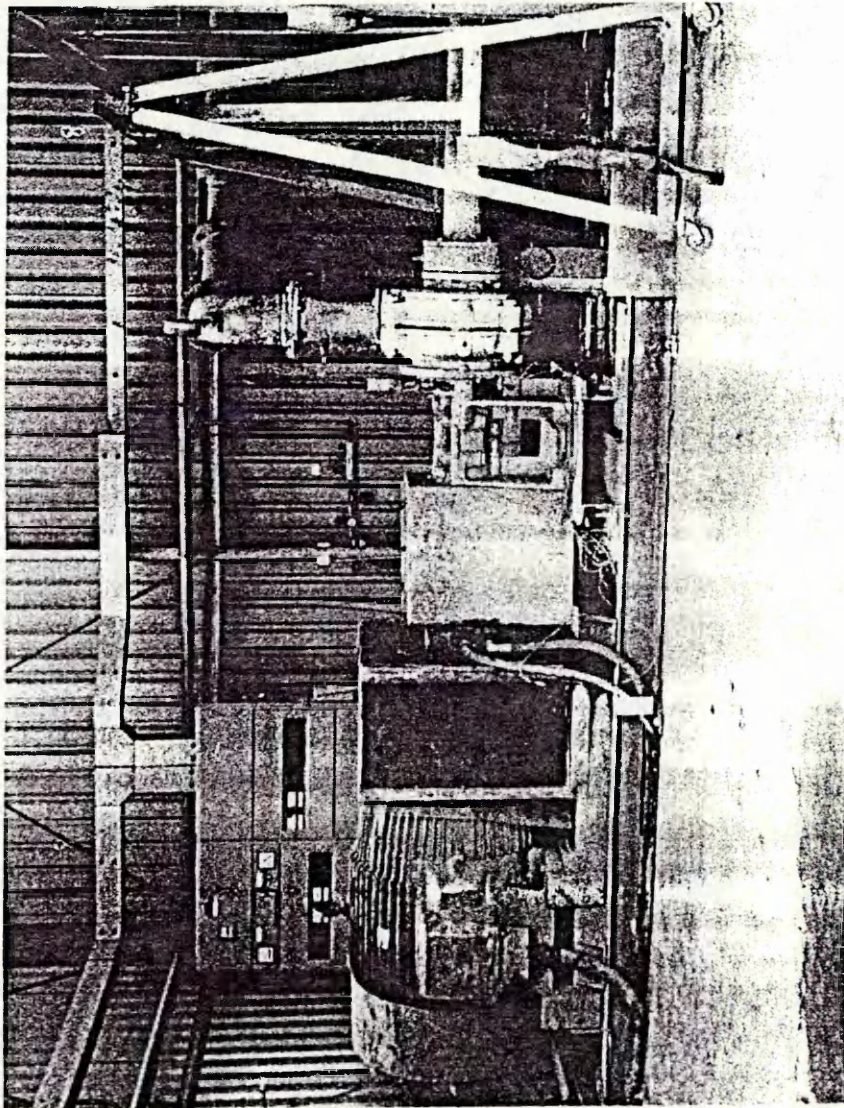


Figure 10.3 View of pumpset

Thermocouple

Seal face

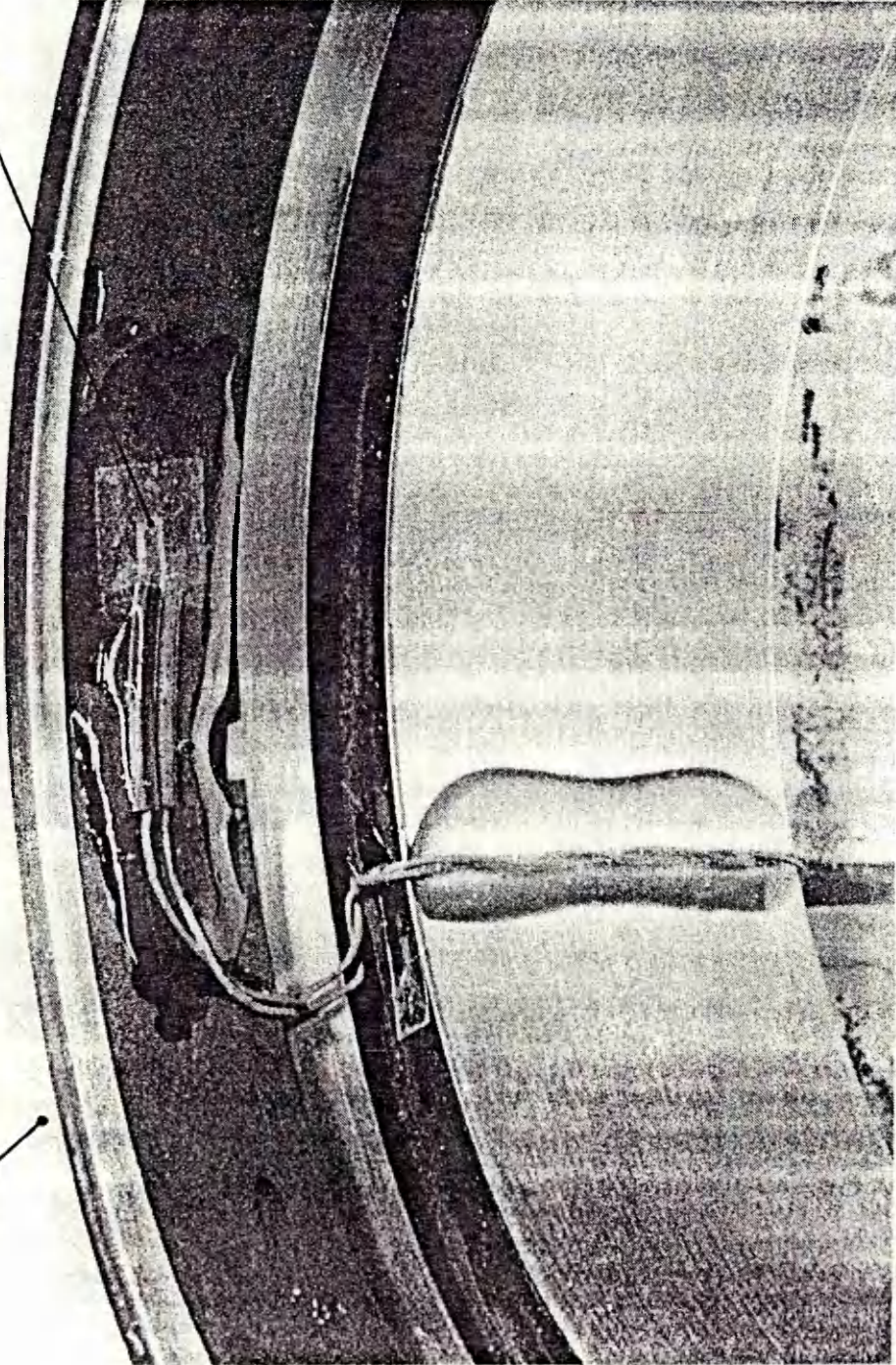


Figure 10.4 Slurry seal fitted with face thermo-couples

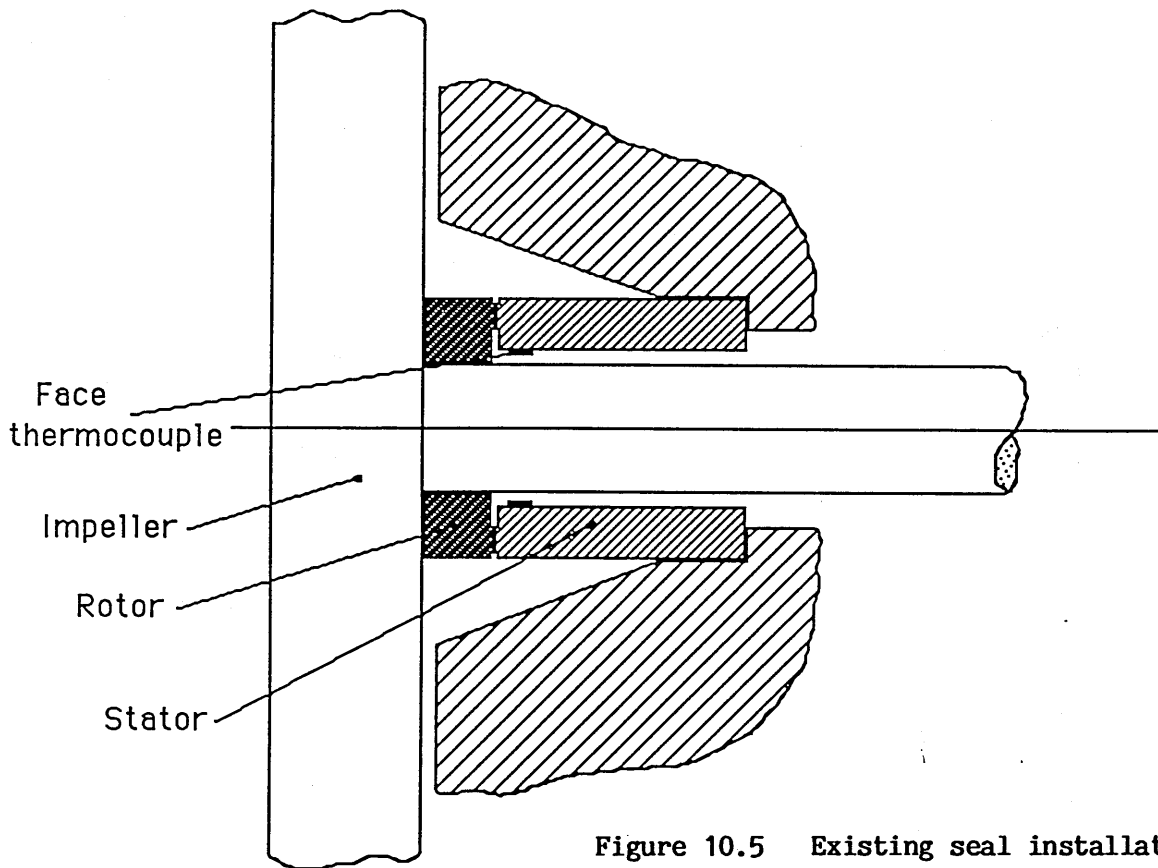


Figure 10.5 Existing seal installation

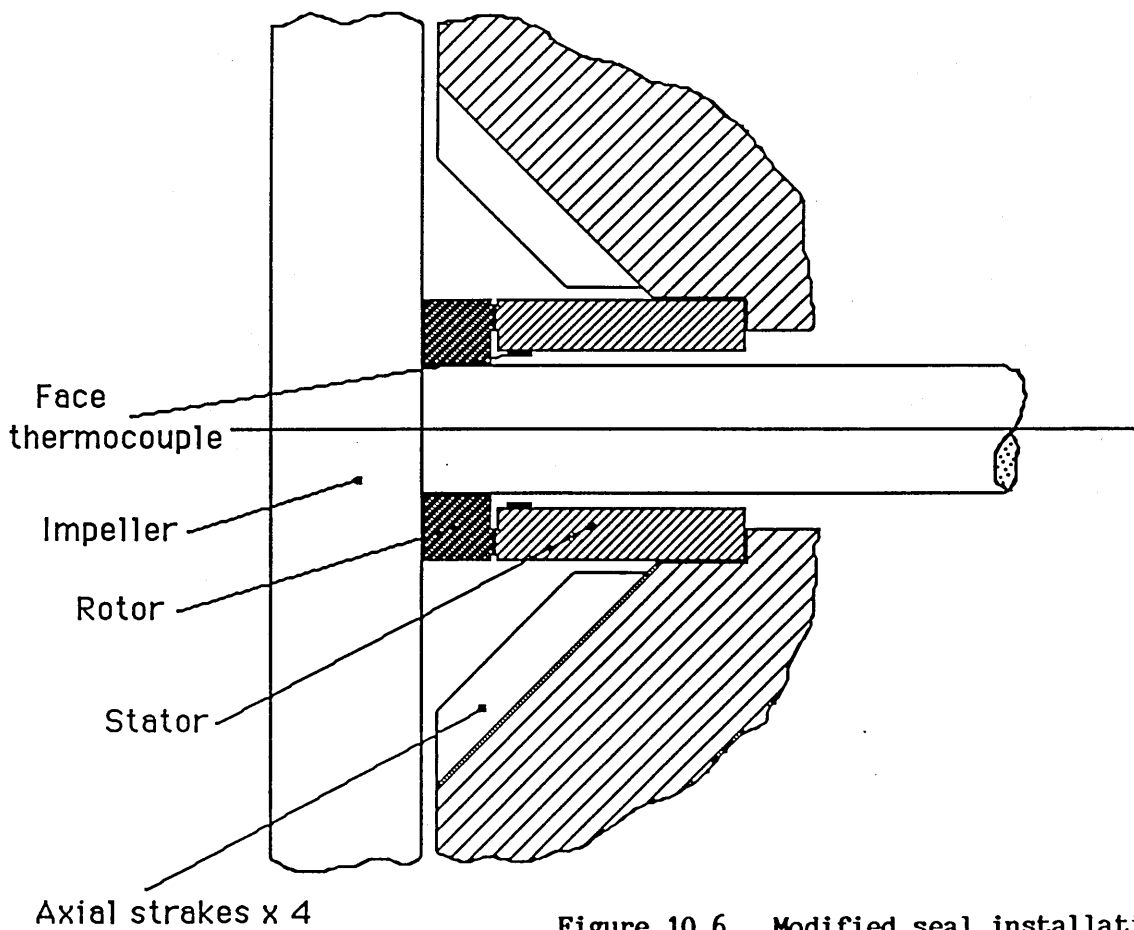
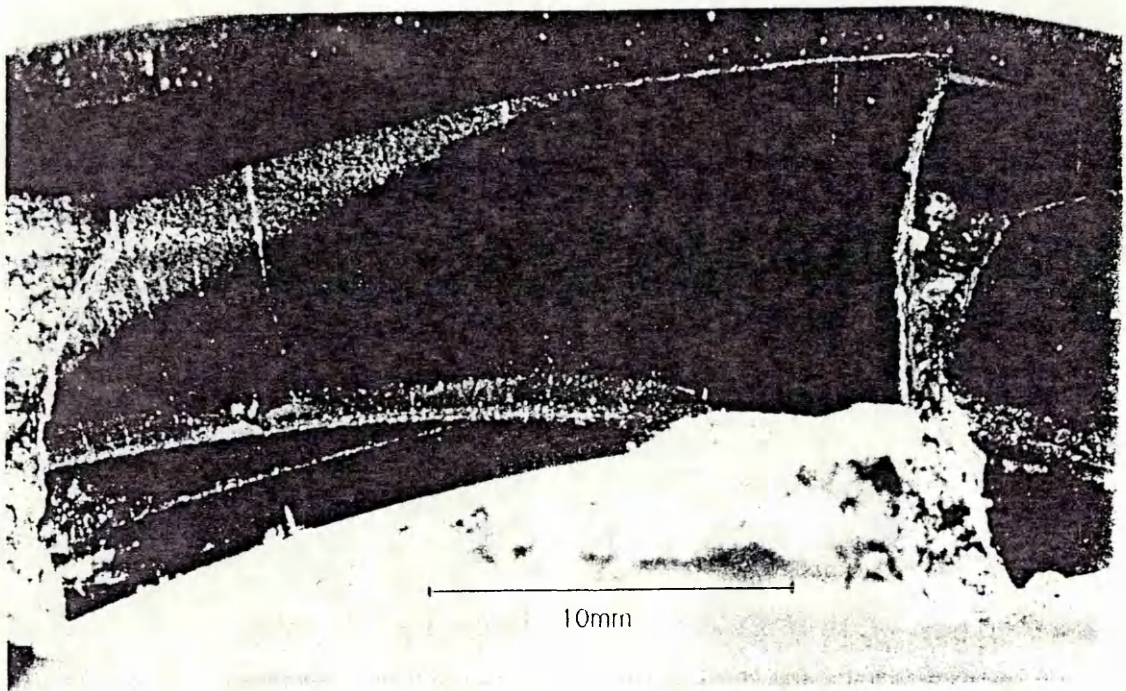
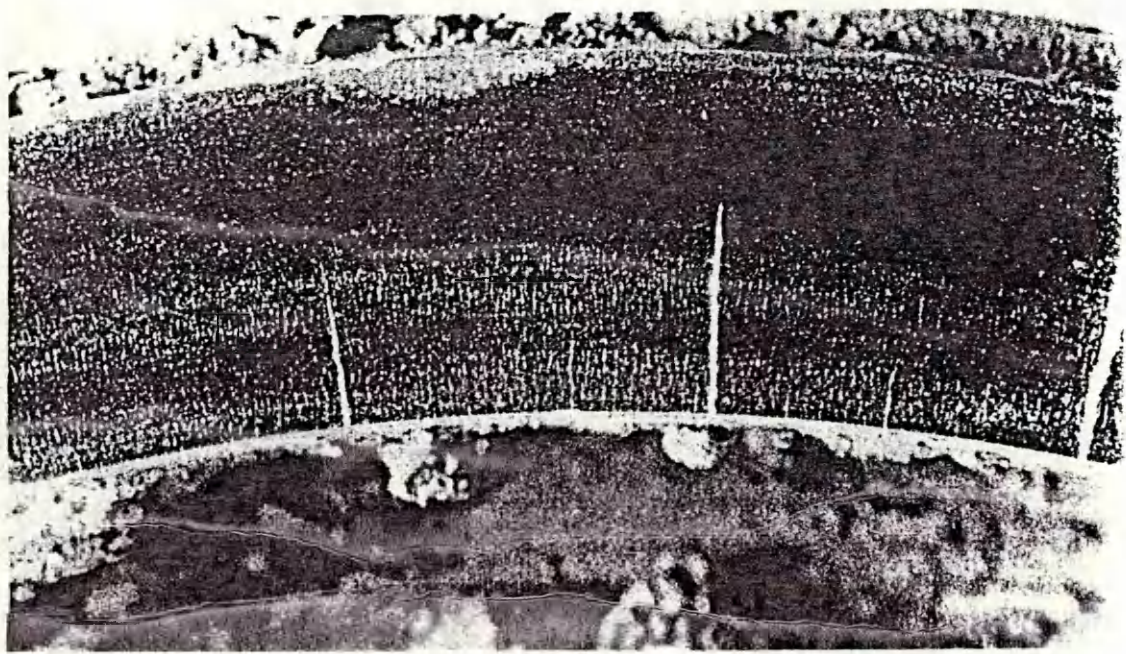


Figure 10.6 Modified seal installation



Stator



Rotor

Figure 10.7 Seal 1

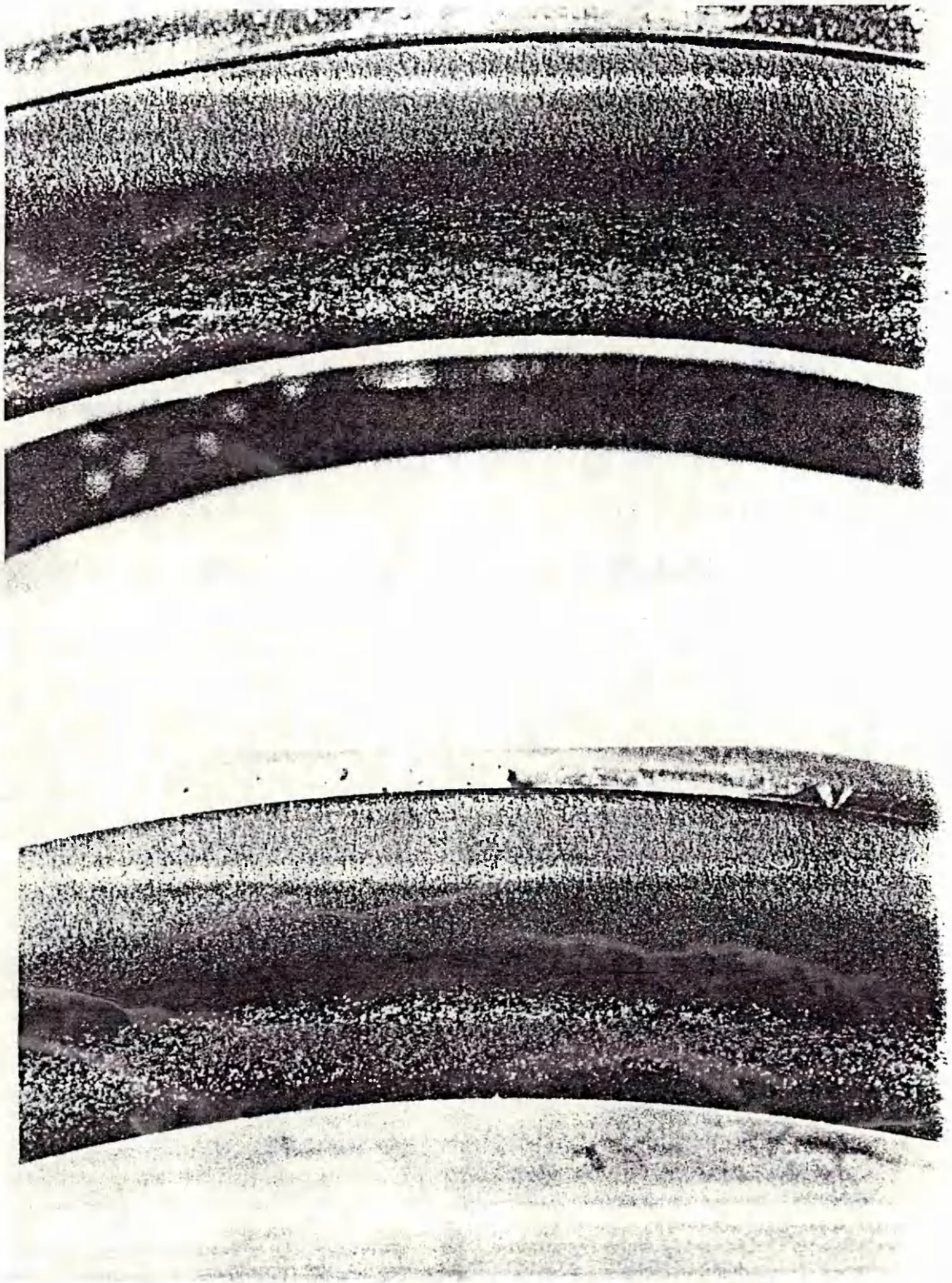


Figure 10.8 Seal 2

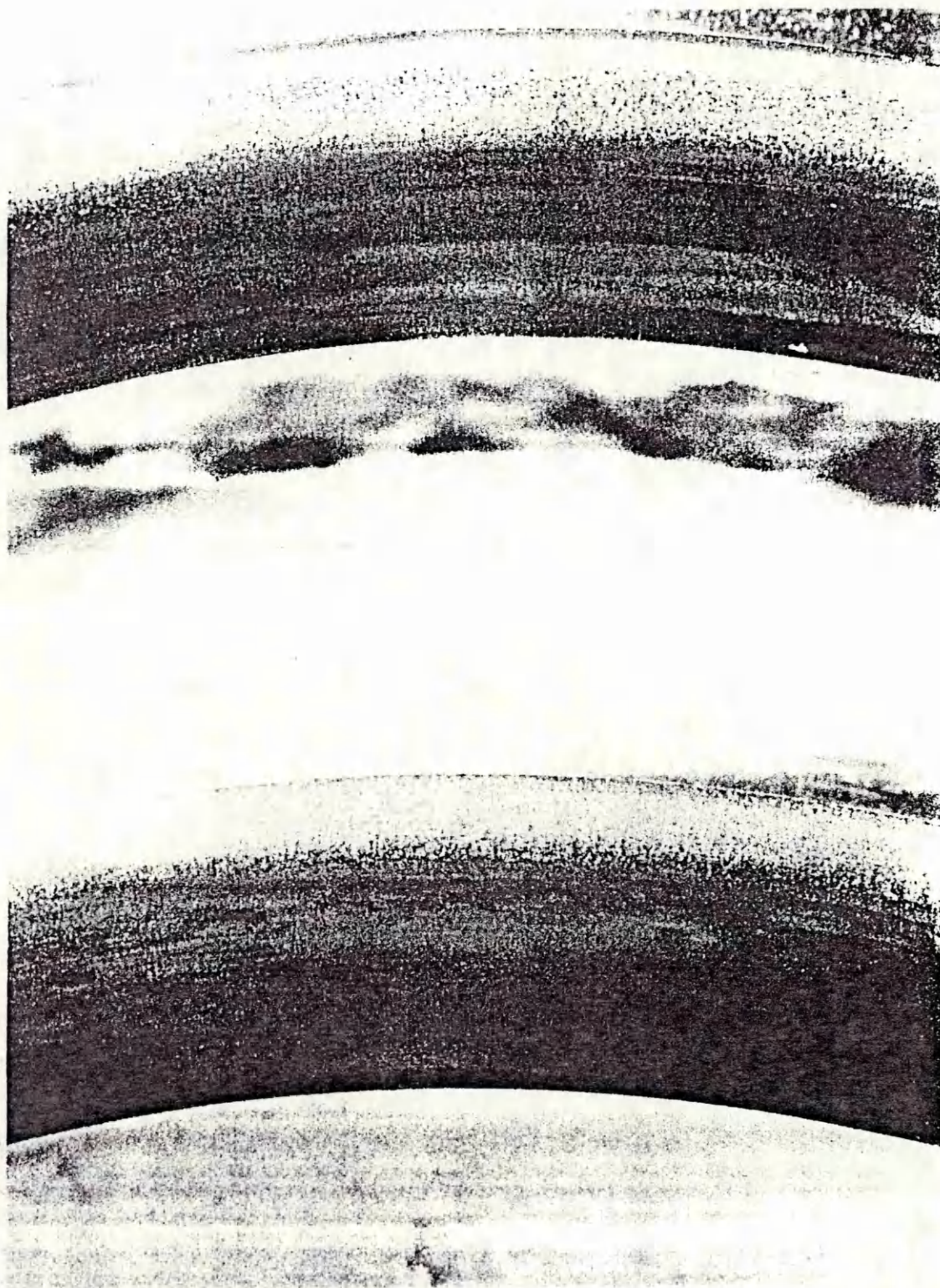


Figure 10.9 Seal 3

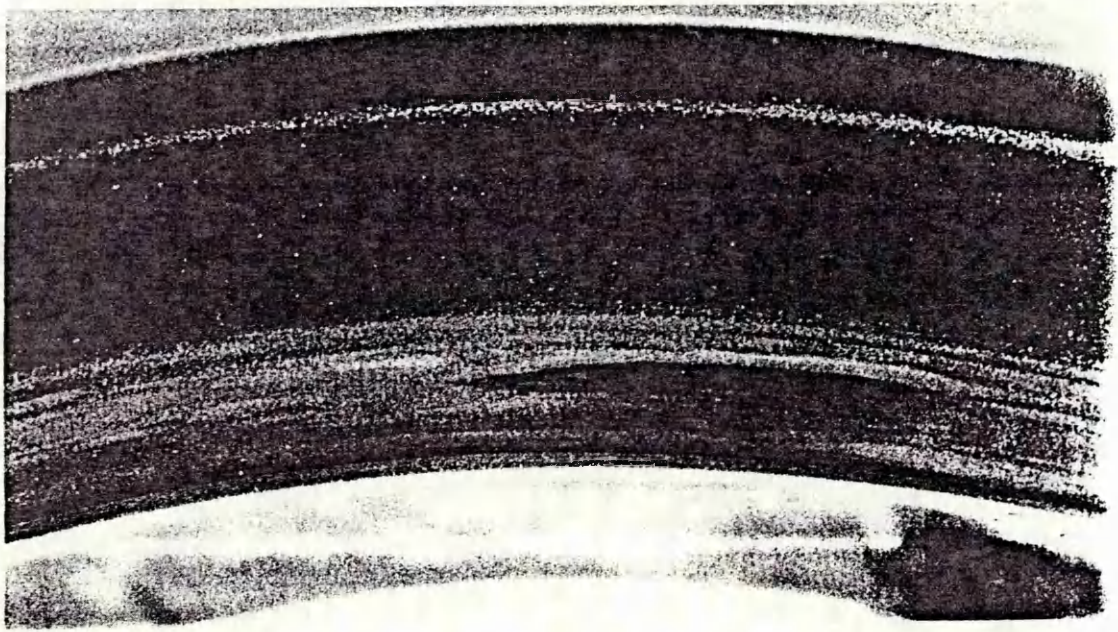


Figure 10.10 Seal 4



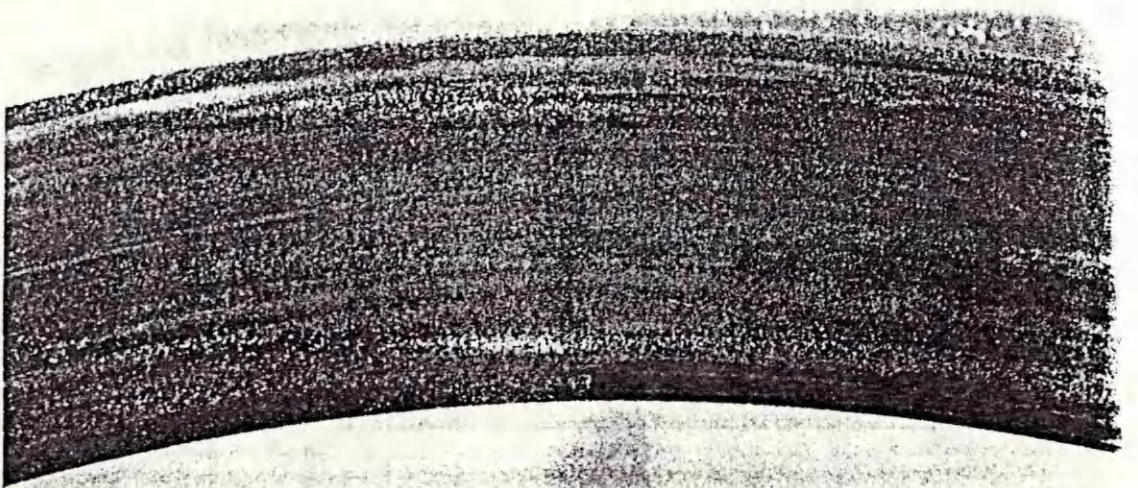


Figure 10.11 Seal 5

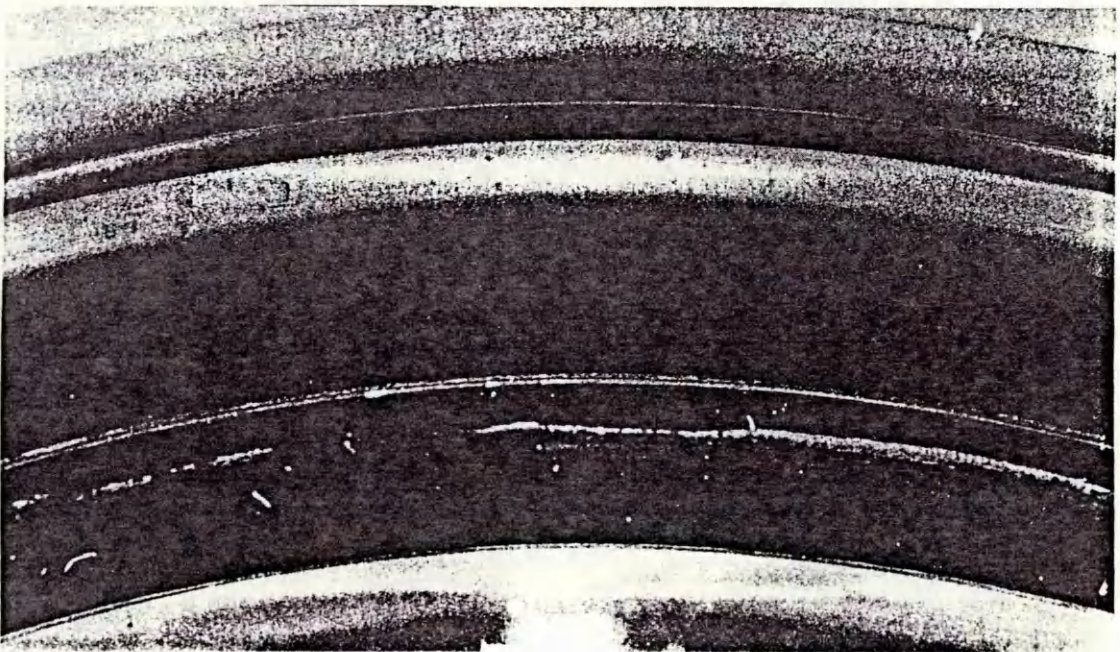
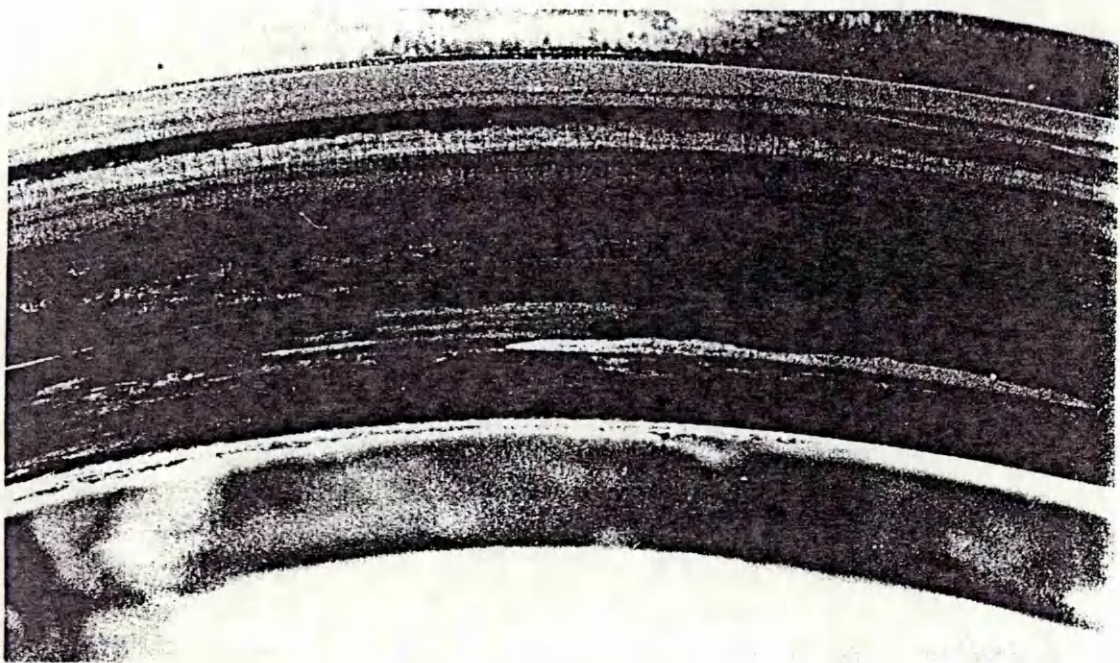


Figure 10.12 Seal 6

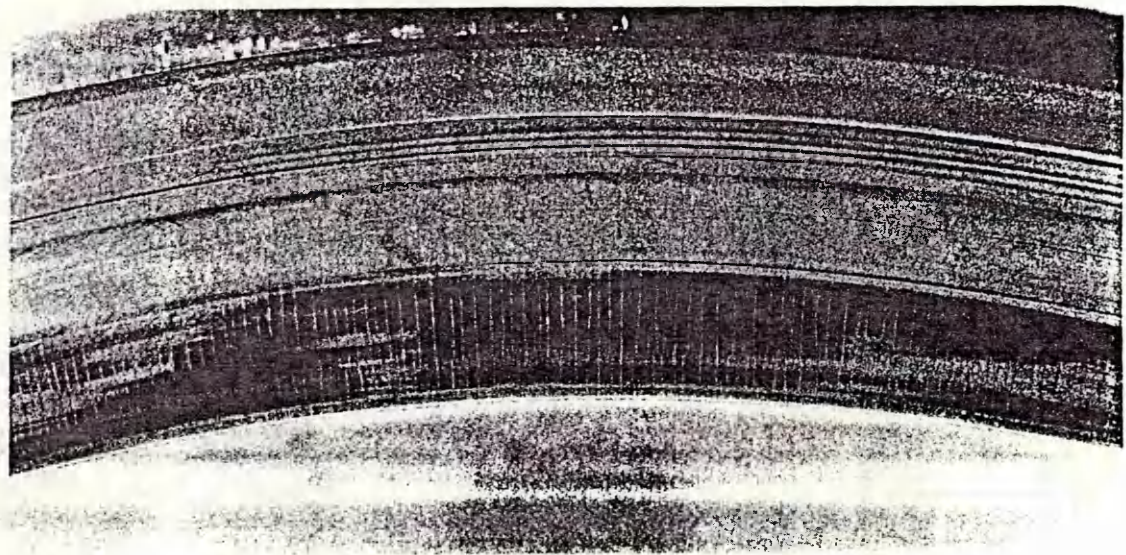


Figure 10.13 Seal 7

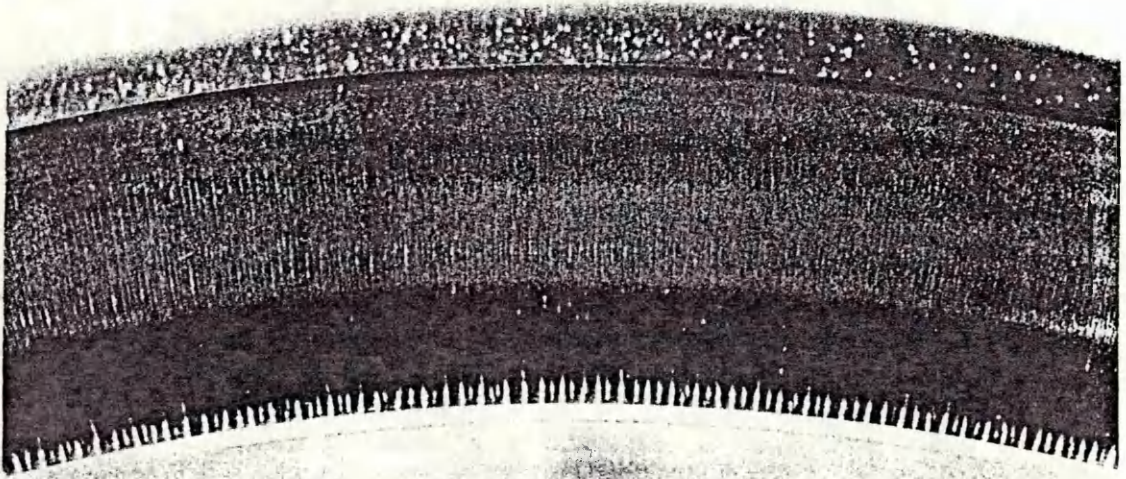
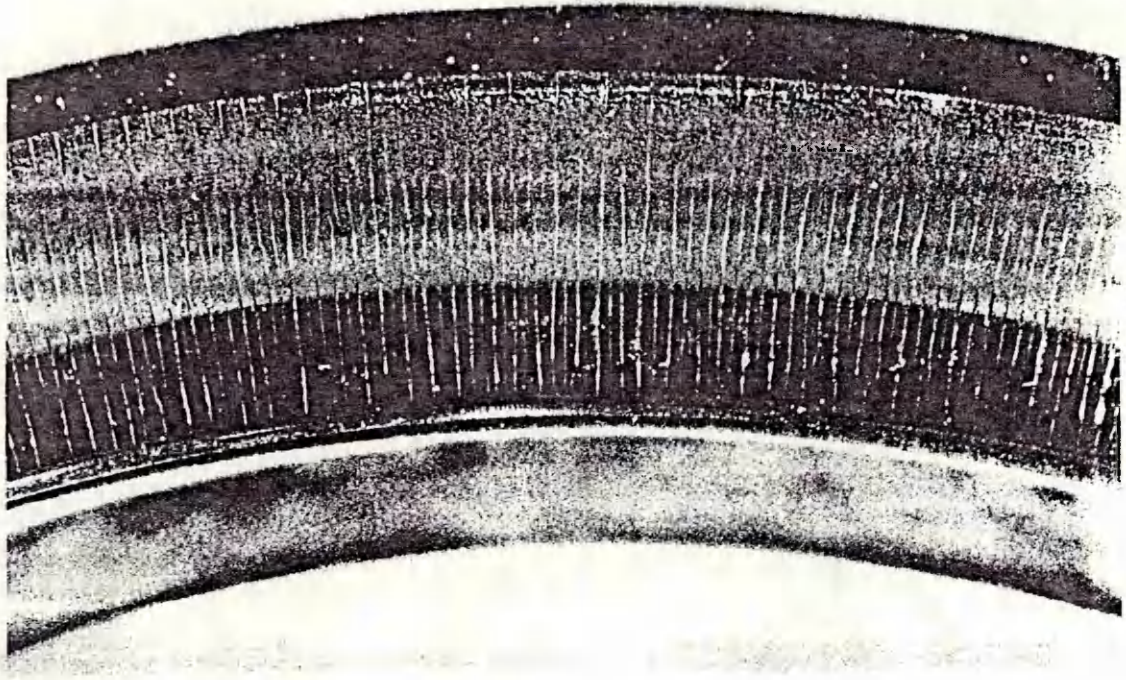


Figure 10.14 Seal 8

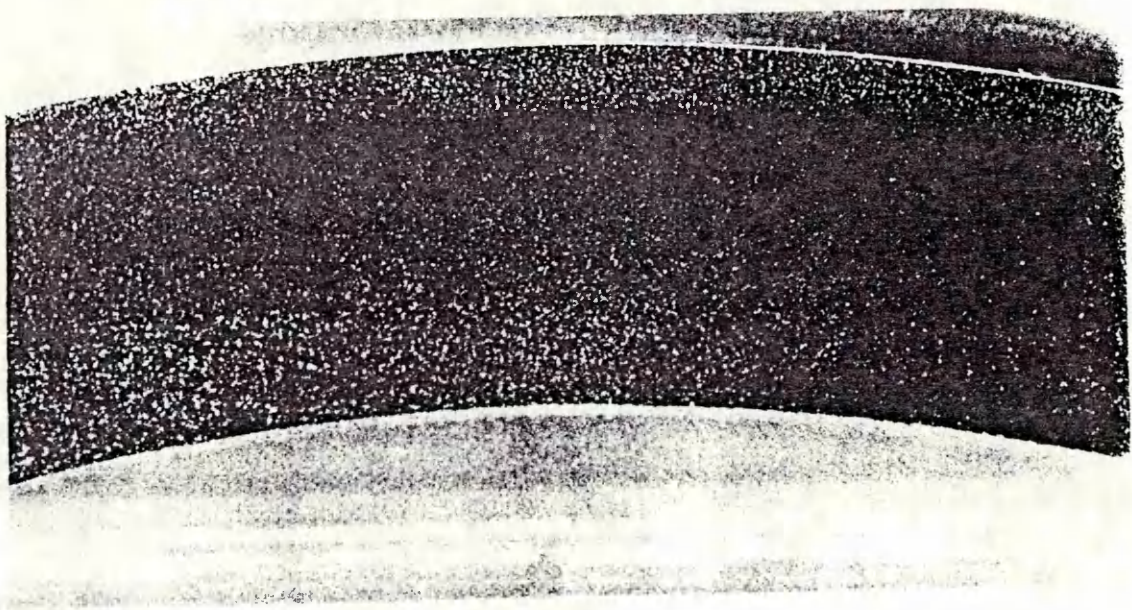


Figure 10.15 Seal 9



Figure 10.16 Seal 10

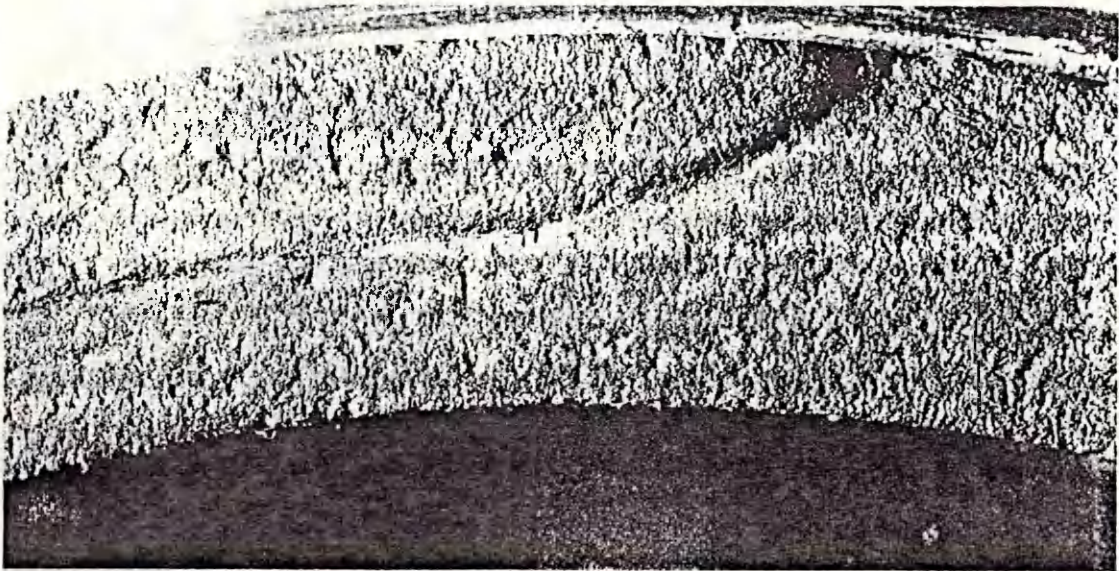
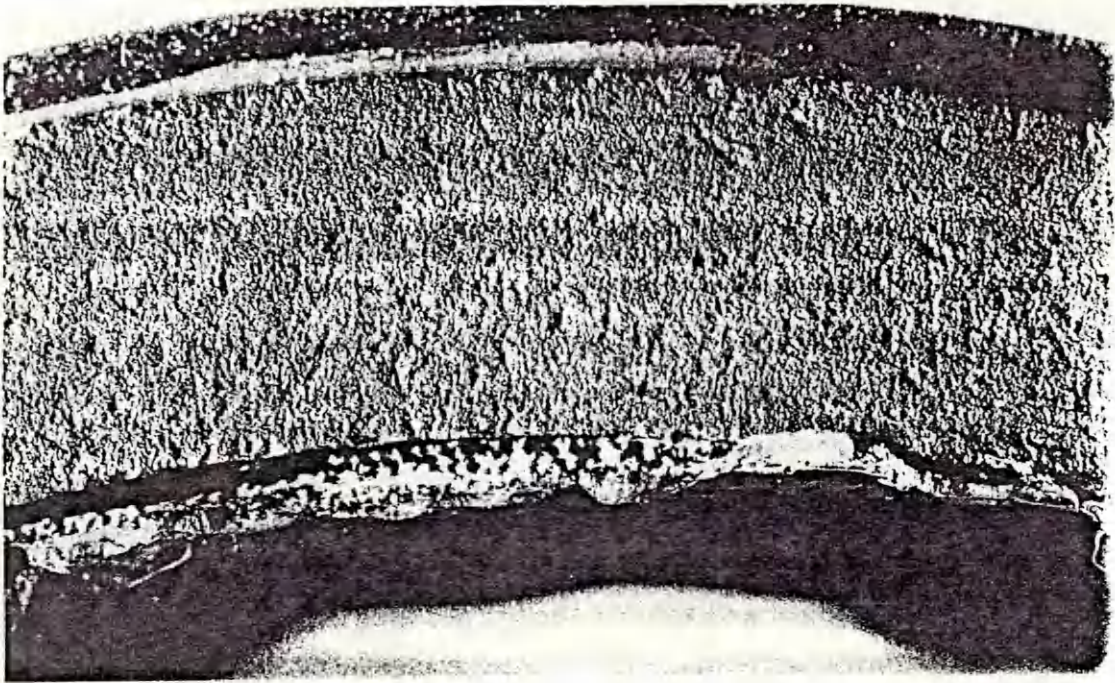


Figure 10.17 Seal 11

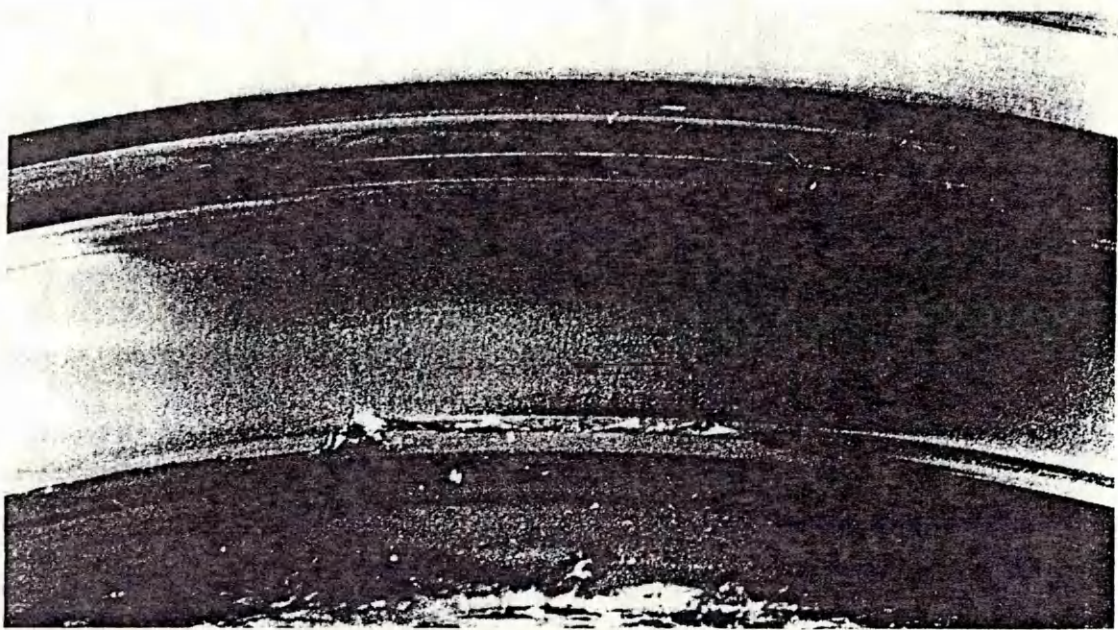


Figure 10.18 Seal 12 - mid-test inspection



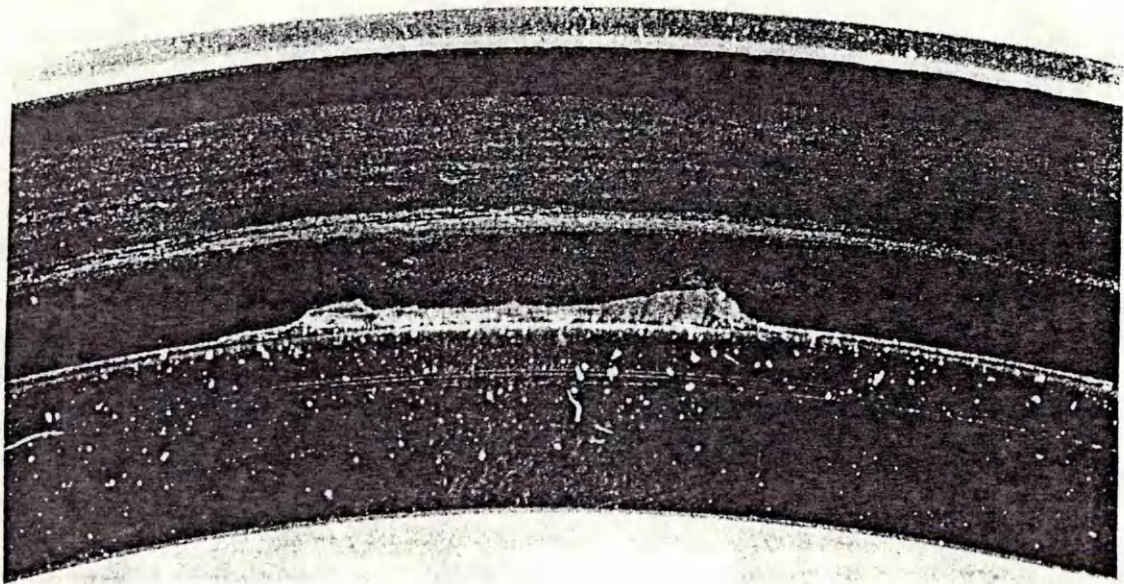
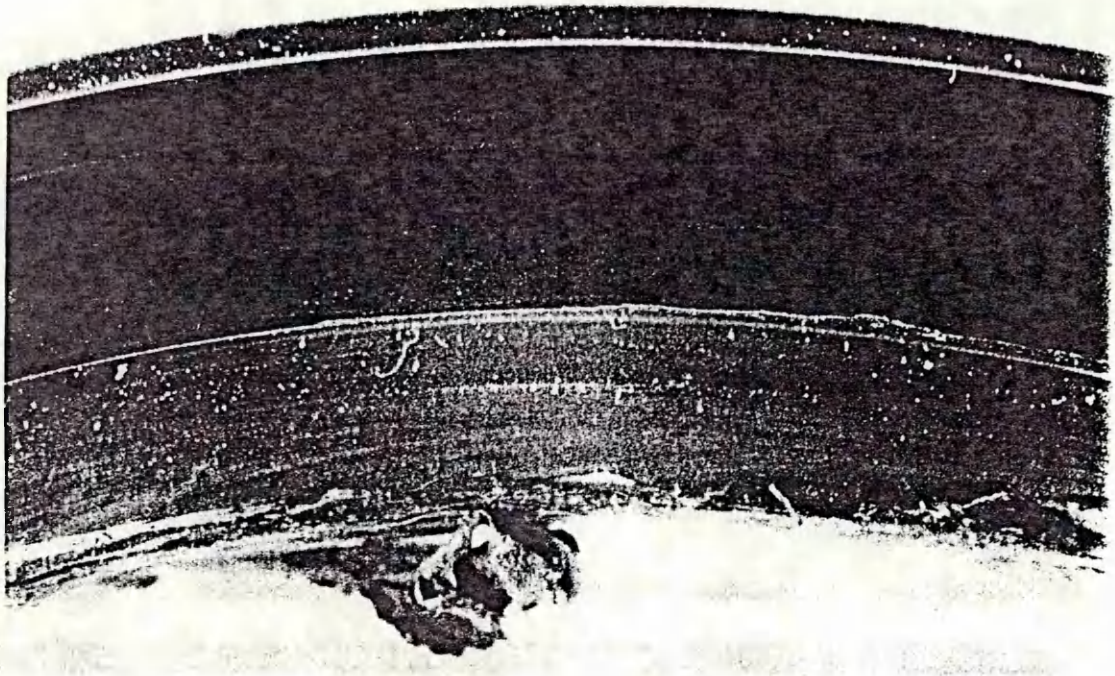


Figure 10.19 Seal 12 - final inspection

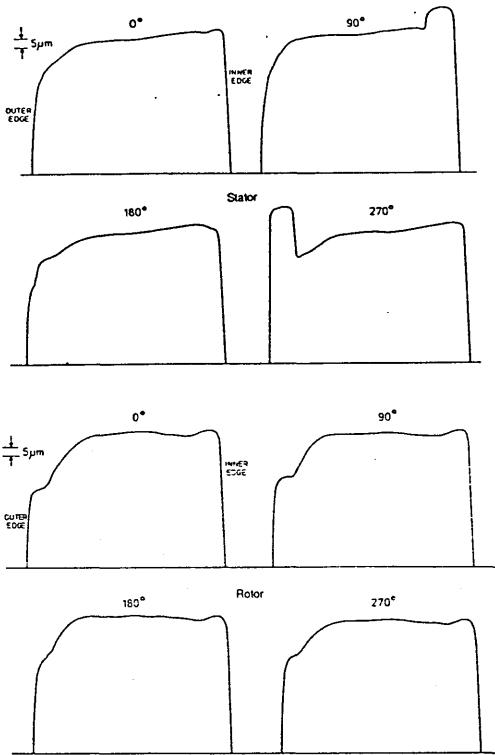


Figure 10.20 Wear profile - Seal 2

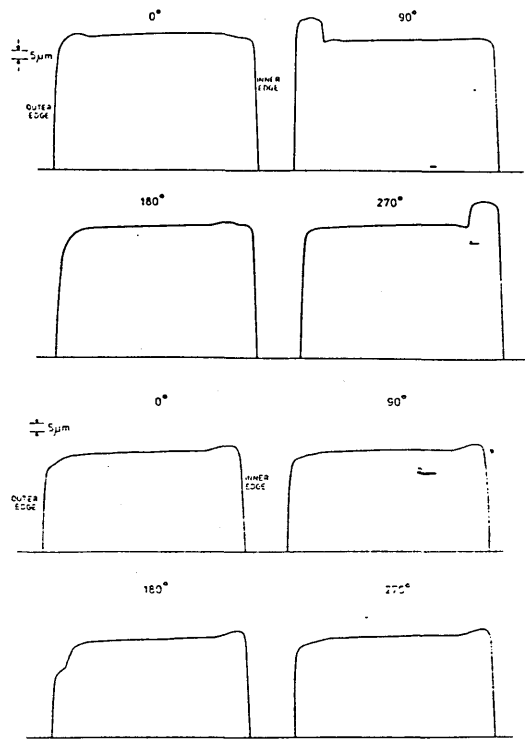


Figure 10.21 Wear profile - Seal 3

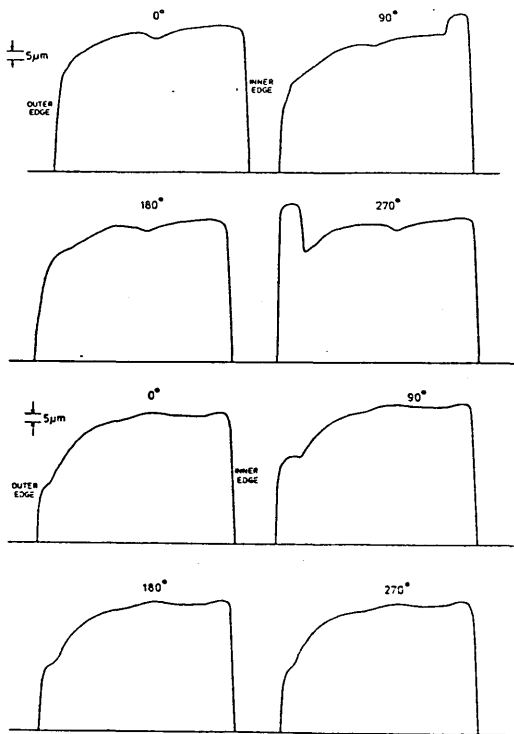


Figure 10.22 Wear profile - Seal 4

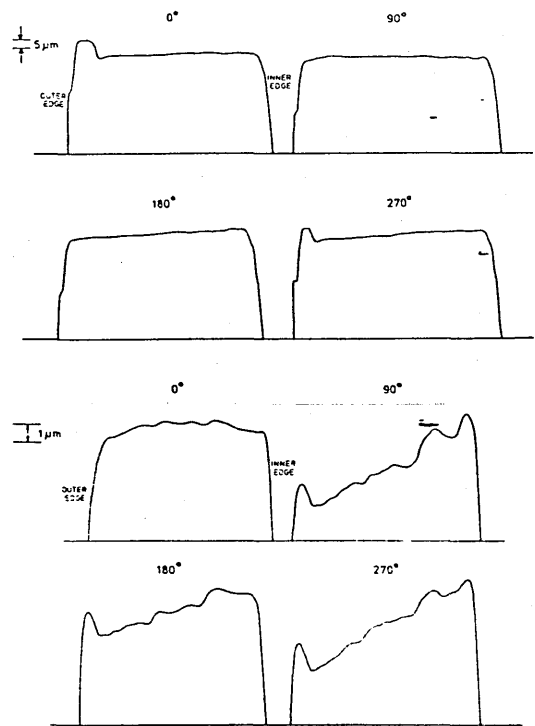


Figure 10.23 Wear profile - Seal 5

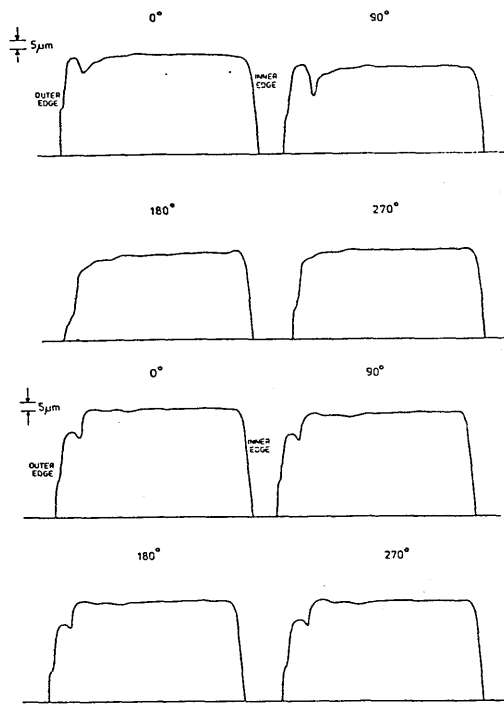


Figure 10.24 Wear profile - Seal 6

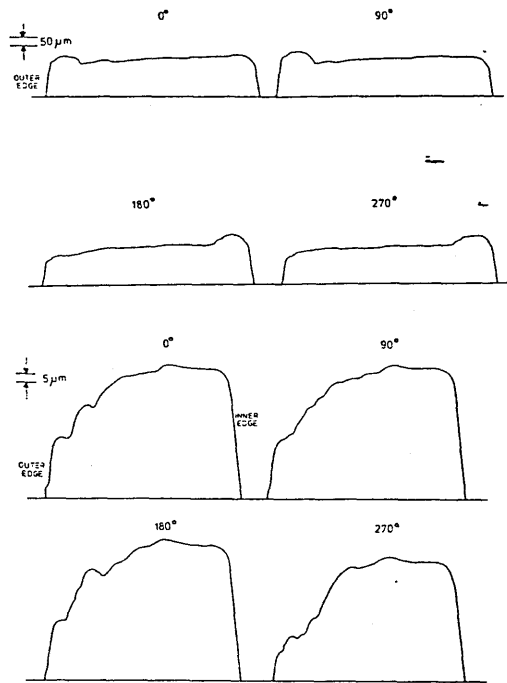


Figure 10.25 Wear profile - Seal 7

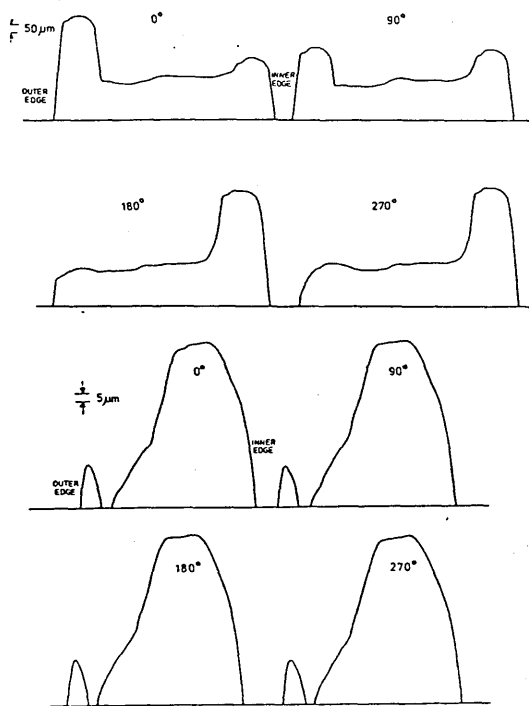


Figure 10.26 Wear profile - Seal 8

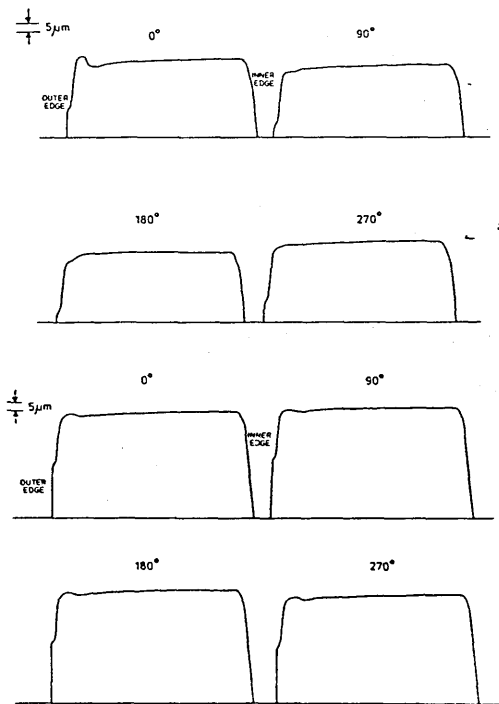


Figure 10.27 Wear profile - Seal 9

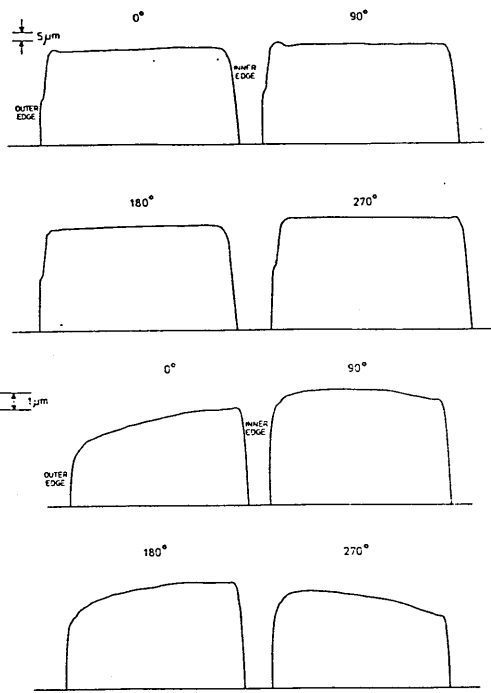


Figure 10.28 Wear profile - Seal 10

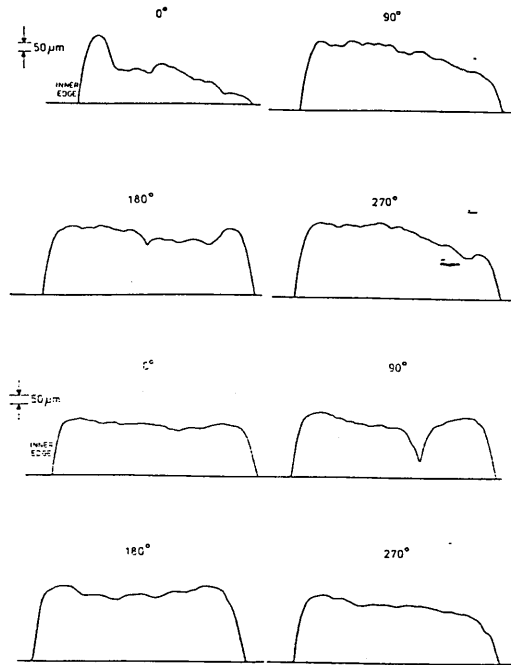


Figure 10.29 Wear profile - Seal 11

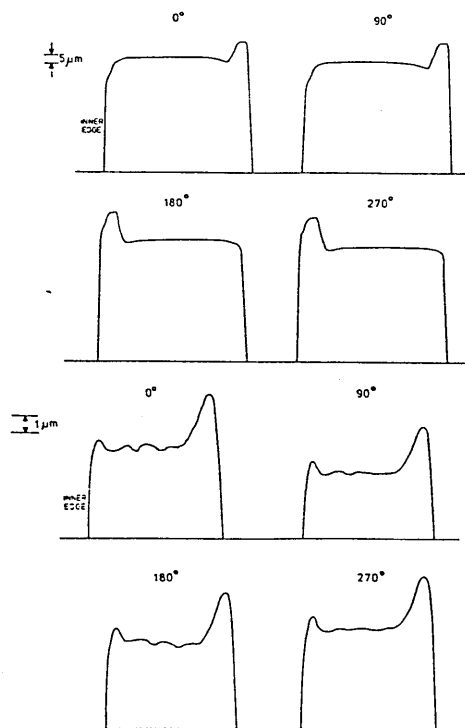


Figure 10.30 Wear profile - Seal 12

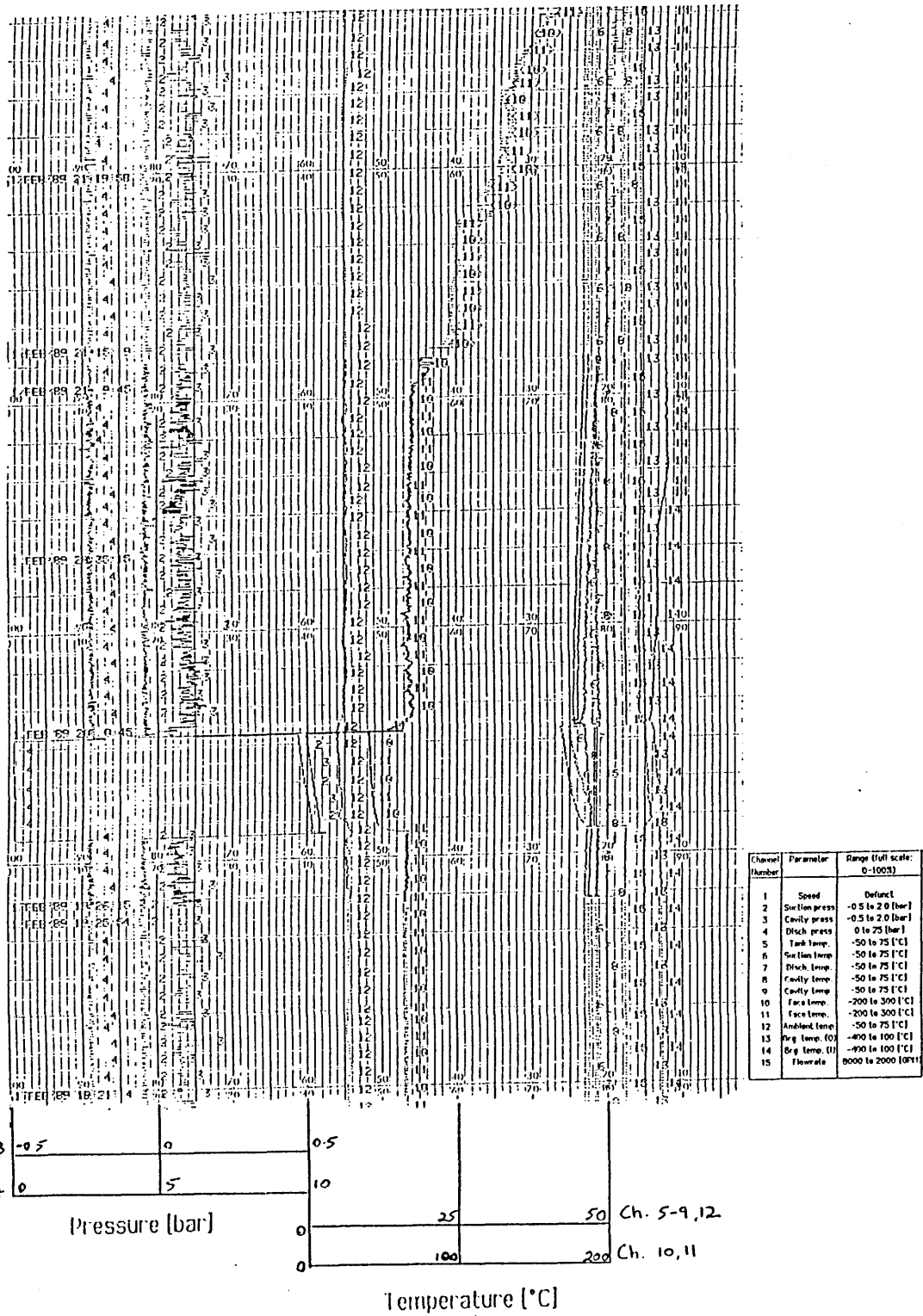
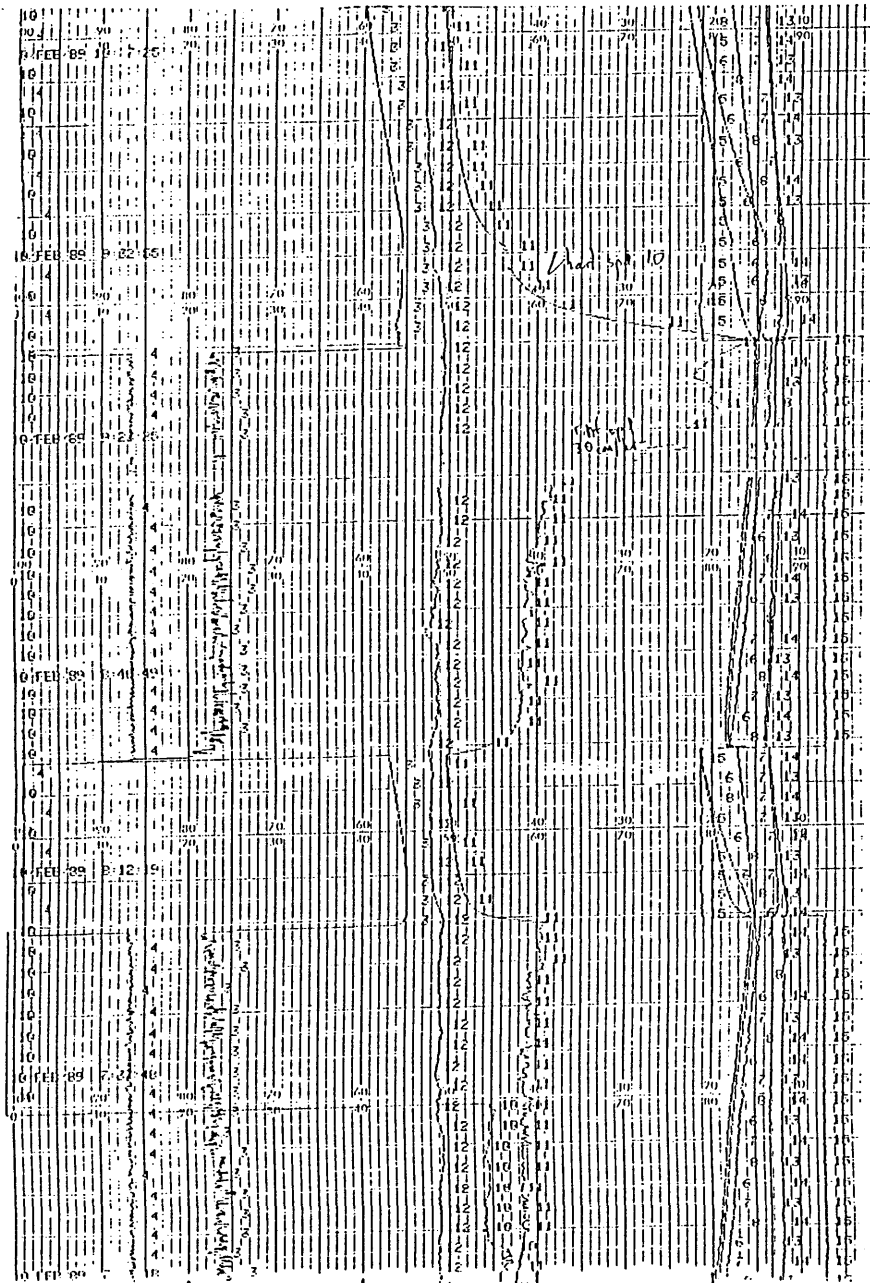


Figure 10.31 Chart trace - Seal 1



Channel Number	Parameter	Range (full scale: 0-100%)
3	Cavity press	-0.5 to 2.0 [bar]
4	Disch press	0 to 75 [bar]
5	Ink temp.	-50 to 75 [°C]
6	Suction temp	-50 to 75 [°C]
7	Disch. temp.	-50 to 75 [°C]
8	Cavity temp	-50 to 75 [°C]
9	Cavity temp.	-50 to 75 [°C]
10	Face temp.	-200 to 300 [°C]
11	Face temp.	-200 to 300 [°C]
12	Ambient temp.	-50 to 75 [°C]
13	Dry. temp. (I)	-400 to 100 [°C]
14	Dry. temp. (II)	-400 to 100 [°C]
15	Flowrate	0000 to 2000 [GPM]

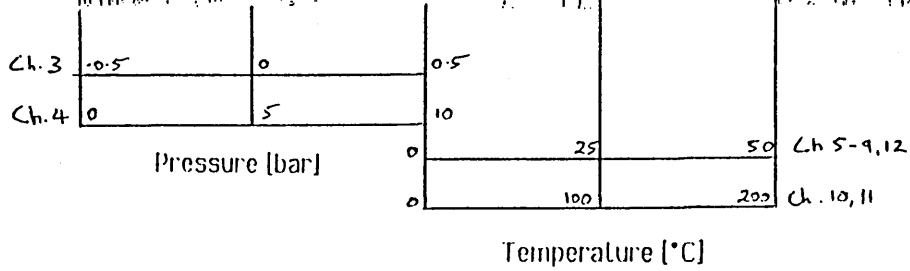
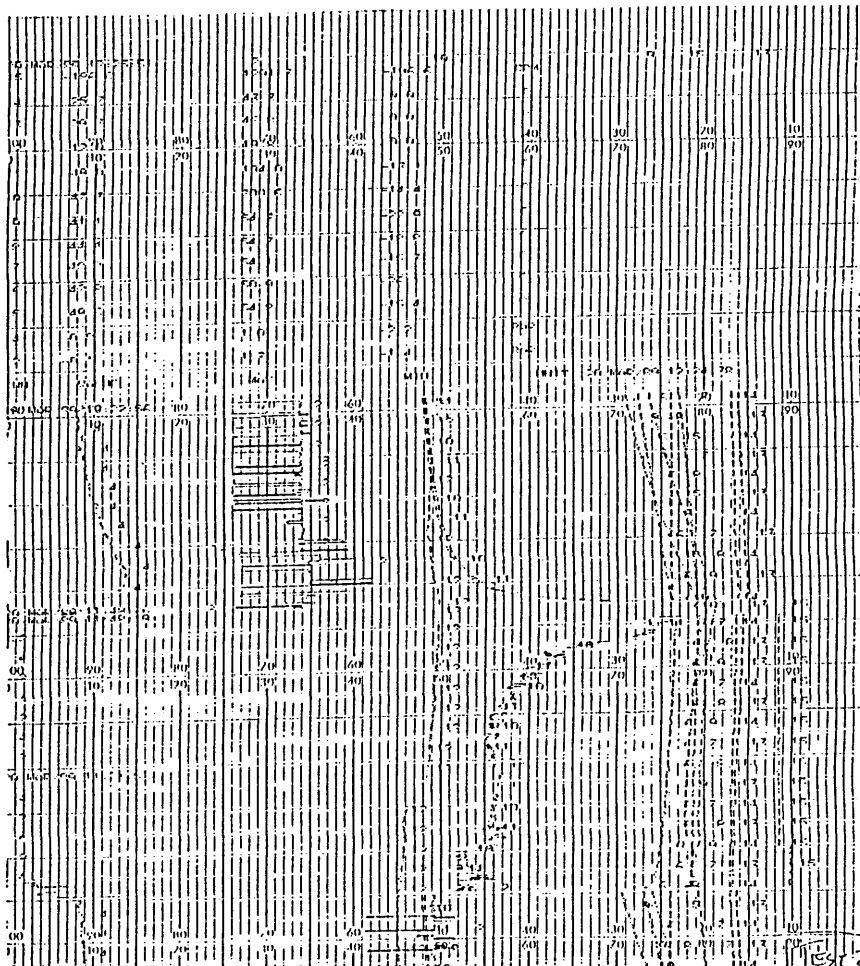


Figure 10.32 Chart trace - Seal 2



Channel Number	Parameter	Range (full scale: 0-100%)
2	Cavity press	-0.5 to 2.0 (bar)
4	Cavity press	-0.5 to 2.0 (bar)
6	Suction temp	-50 to 75 (°C)
7	Disch. temp.	-50 to 75 (°C)
8	Cavity temp.	-50 to 75 (°C)
9	Cavity temp.	-50 to 75 (°C)
10	Face temp.	-200 to 300 (°C)
11	Face temp.	-200 to 300 (°C)
12	Ambient temp.	-50 to 75 (°C)
13	Dis. temp. (I)	-400 to 100 (°C)
14	Dis. temp. (II)	-400 to 100 (°C)
15	Flowrate	0000 to 2000 (g/min)

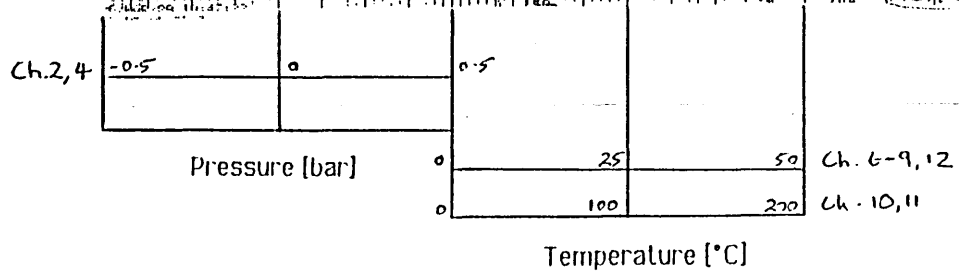


Figure 10.33 Chart trace - Seal 6

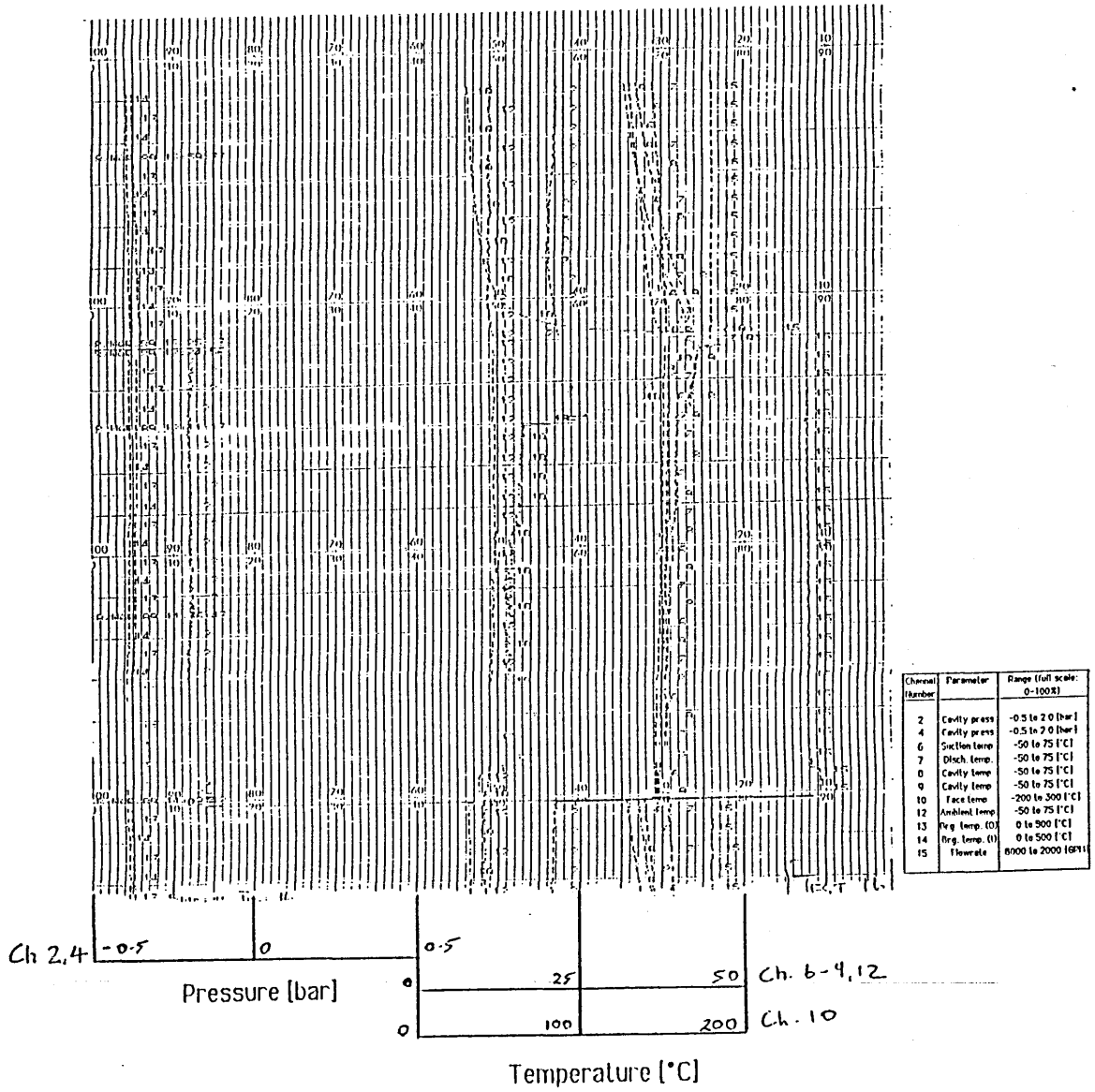


Figure 10.34 Chart trace - Seal 5



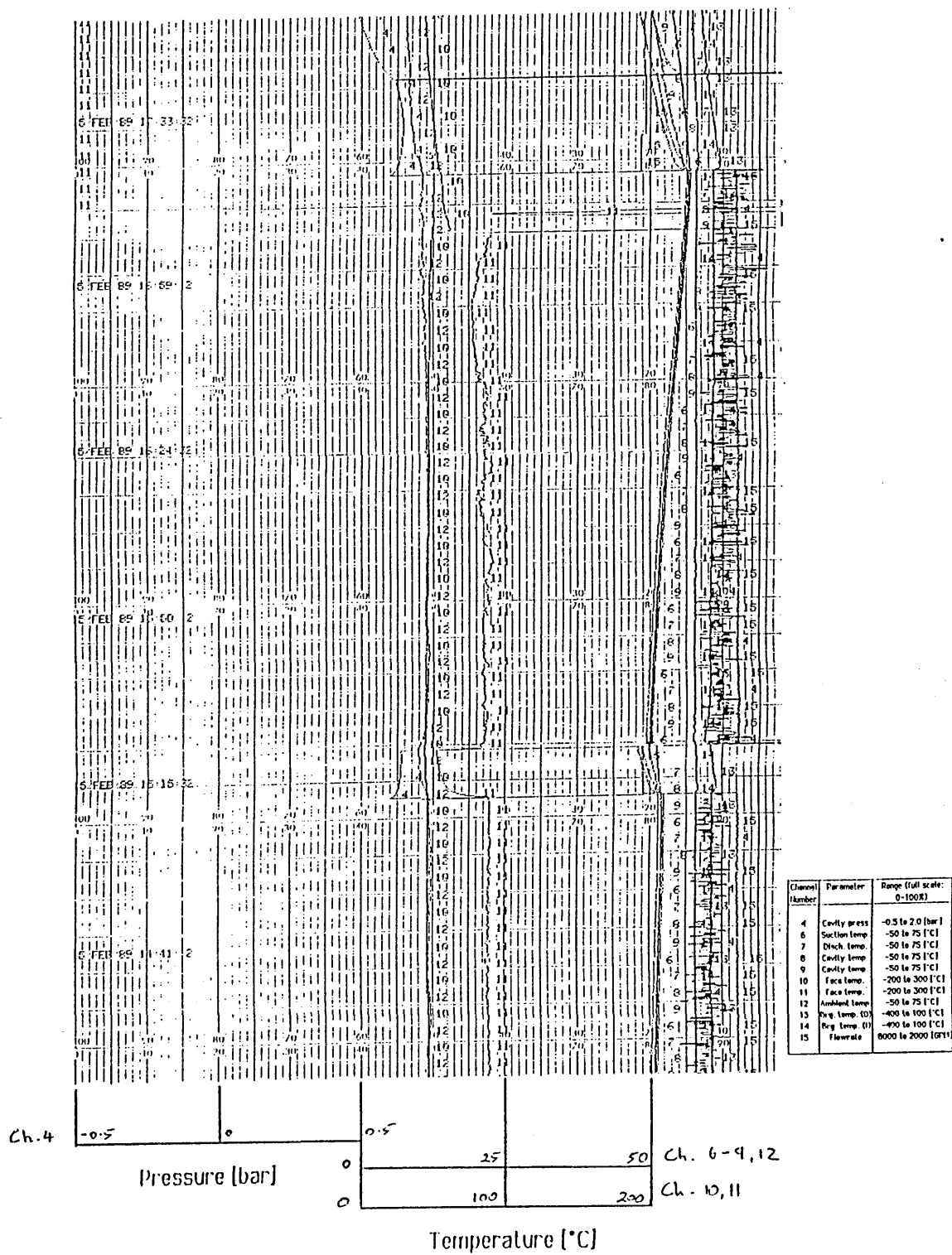


Figure 10.35 Chart trace - Seal 3

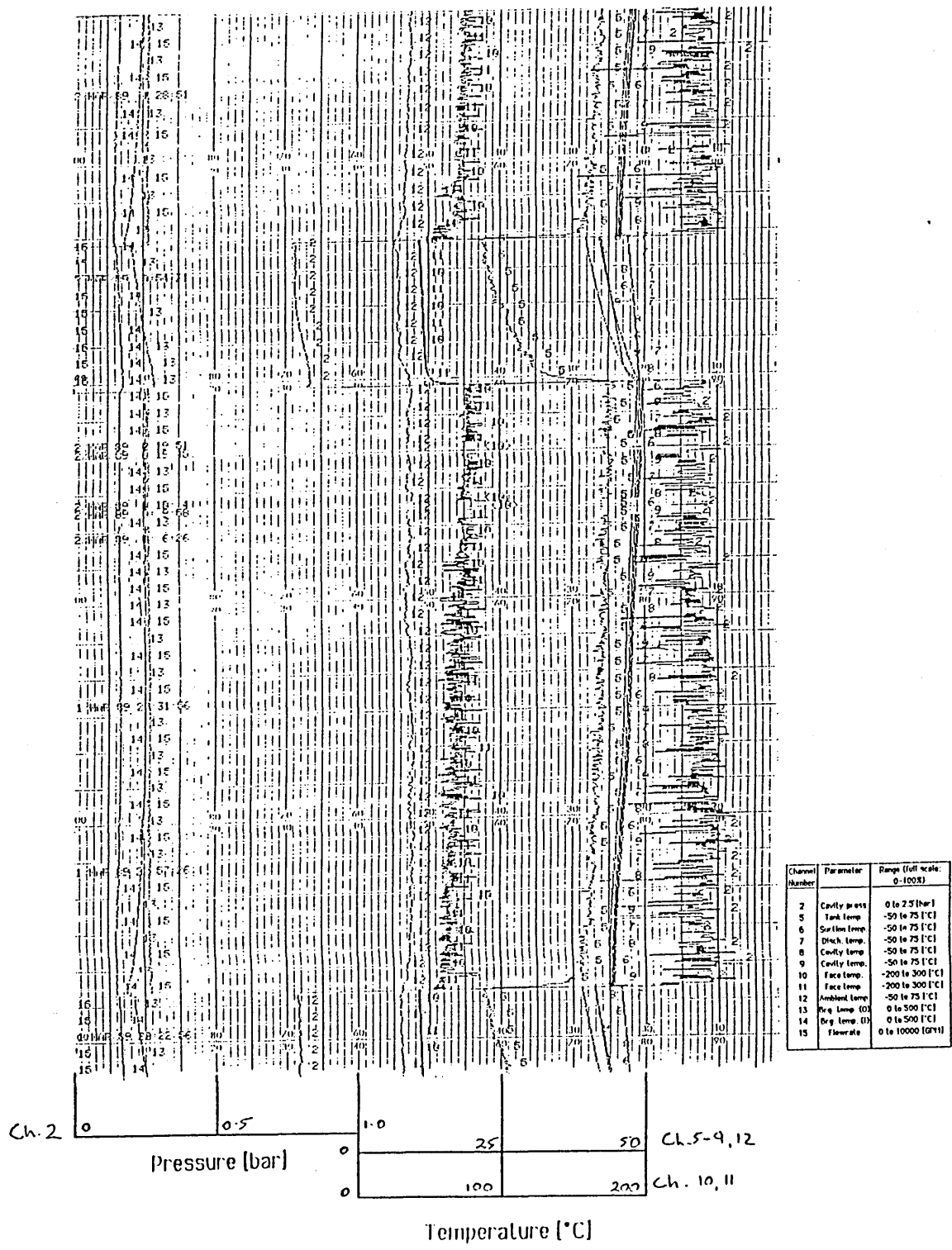


Figure 10.36 Chart trace - Seal 4

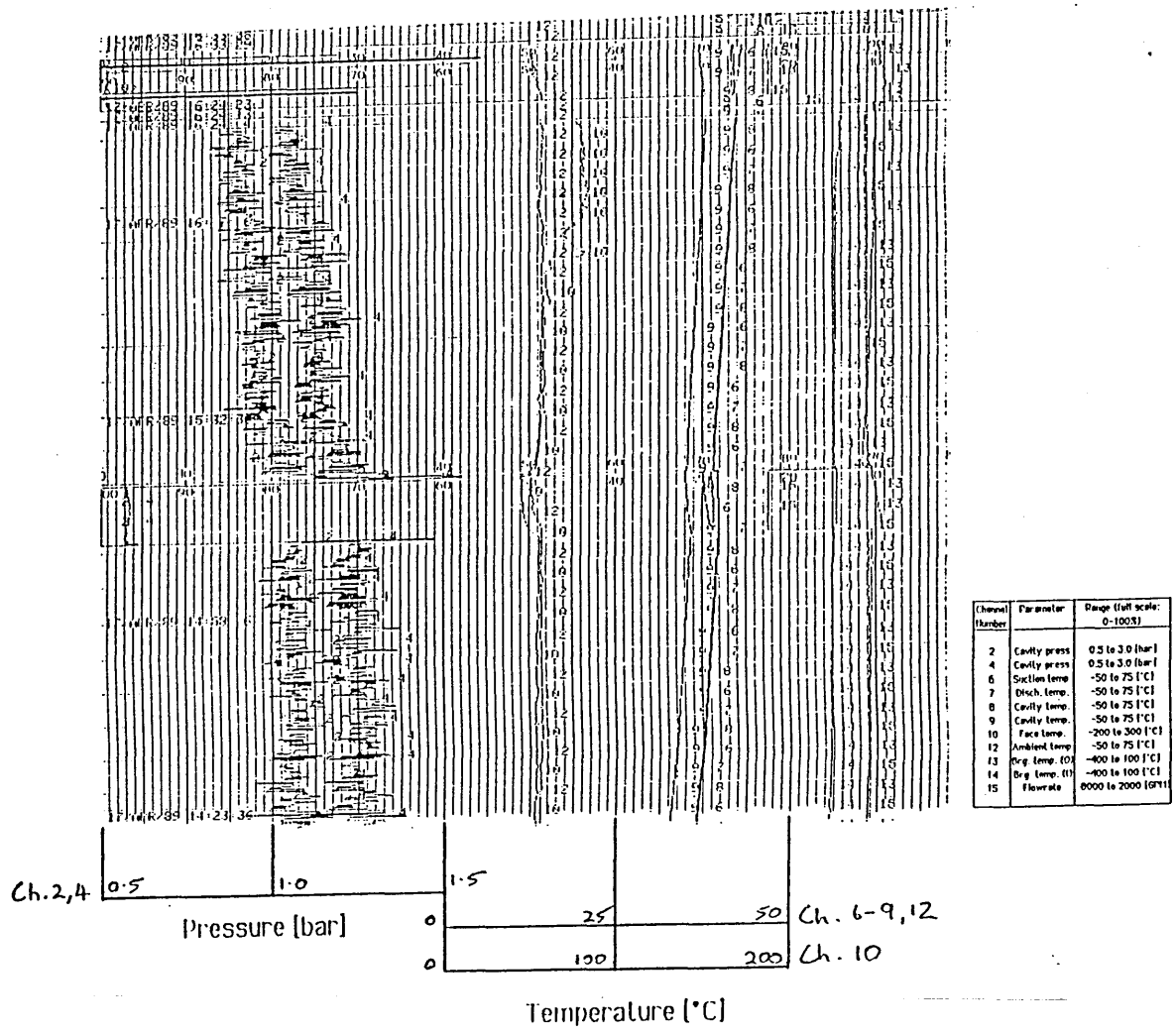


Figure 10.37 Chart trace - Seal 7

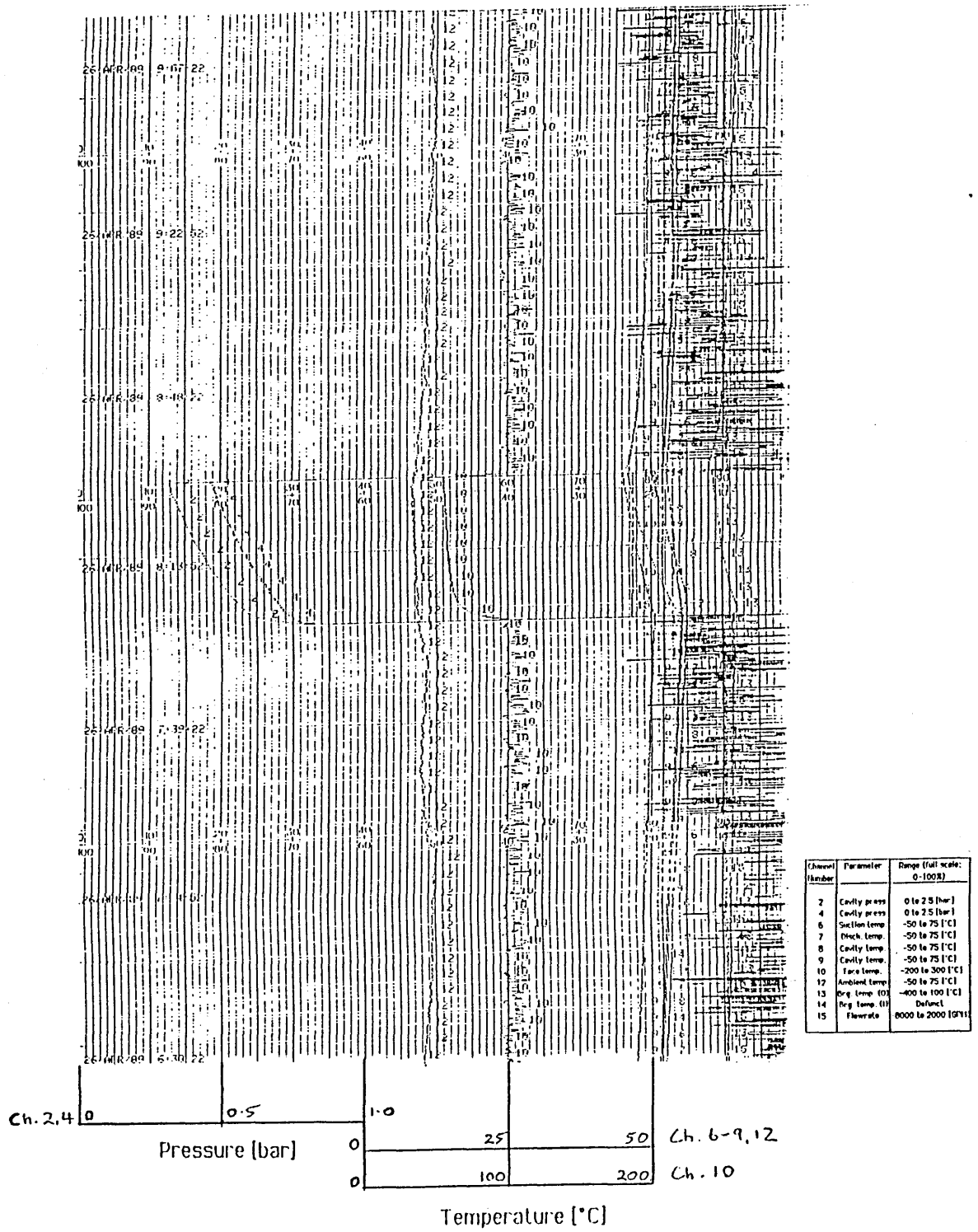


Figure 10.38 Chart trace - Seal 8

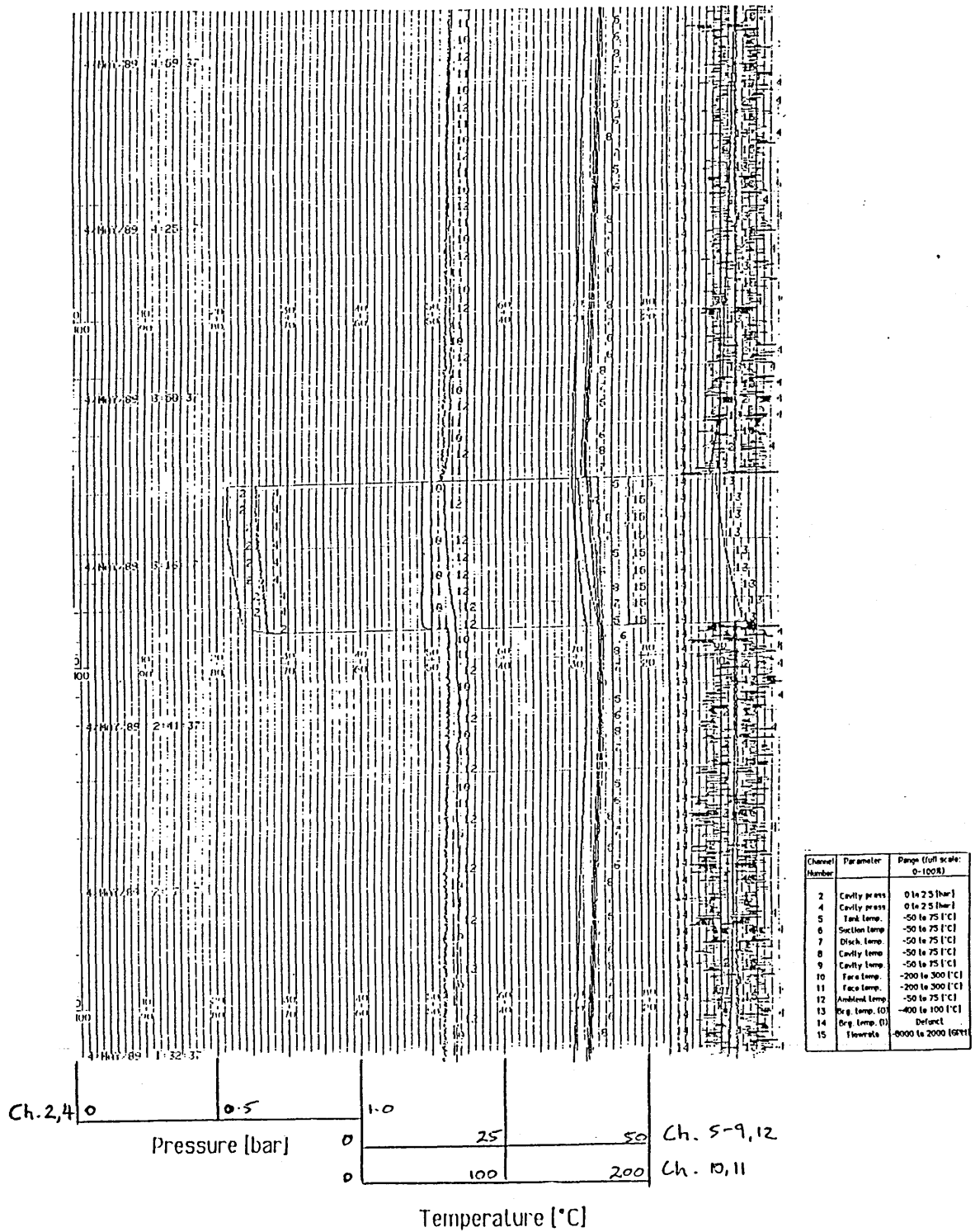


Figure 10.39 Chart trace - Seal 9

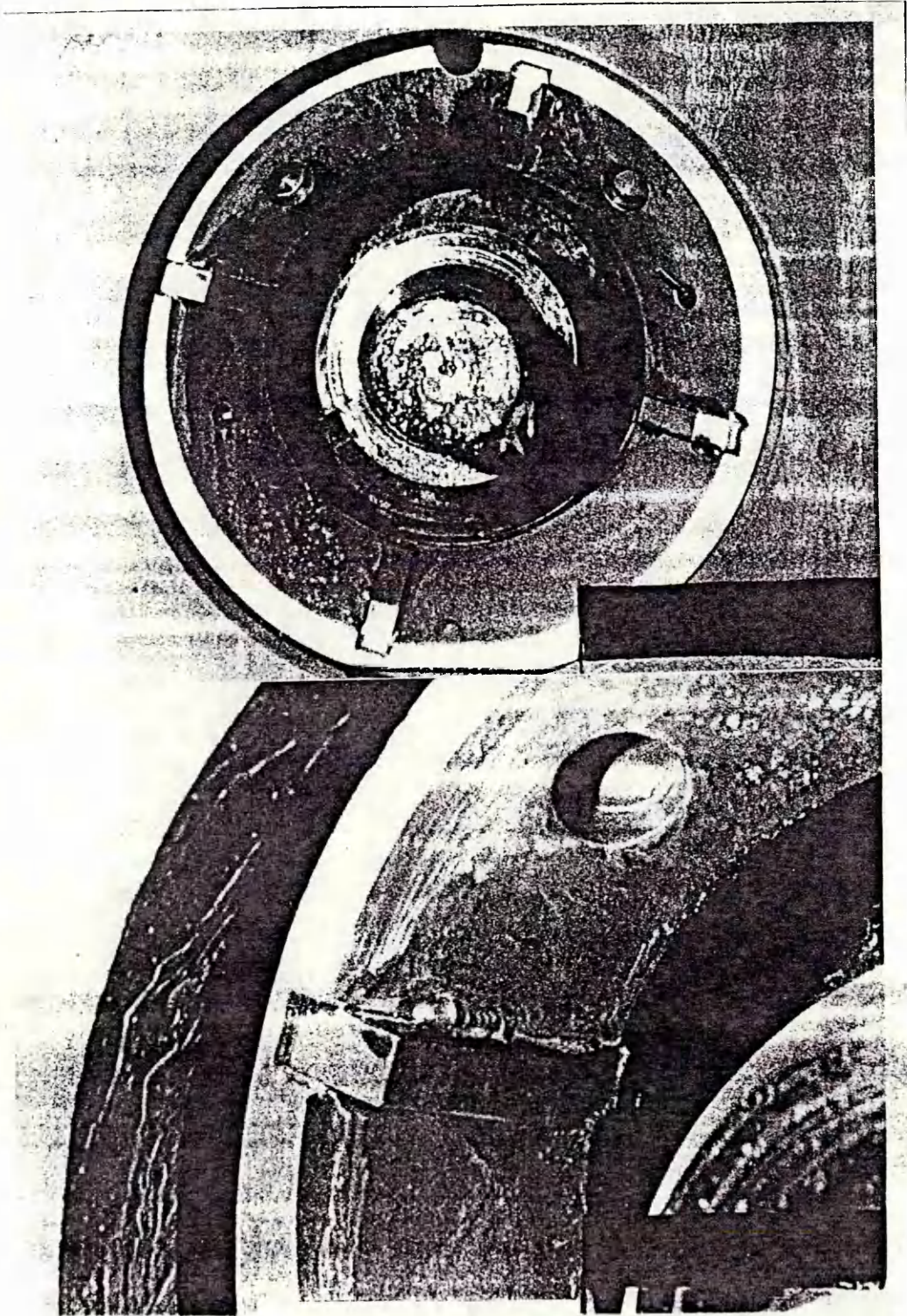


Figure 10.40 Seal cover erosion

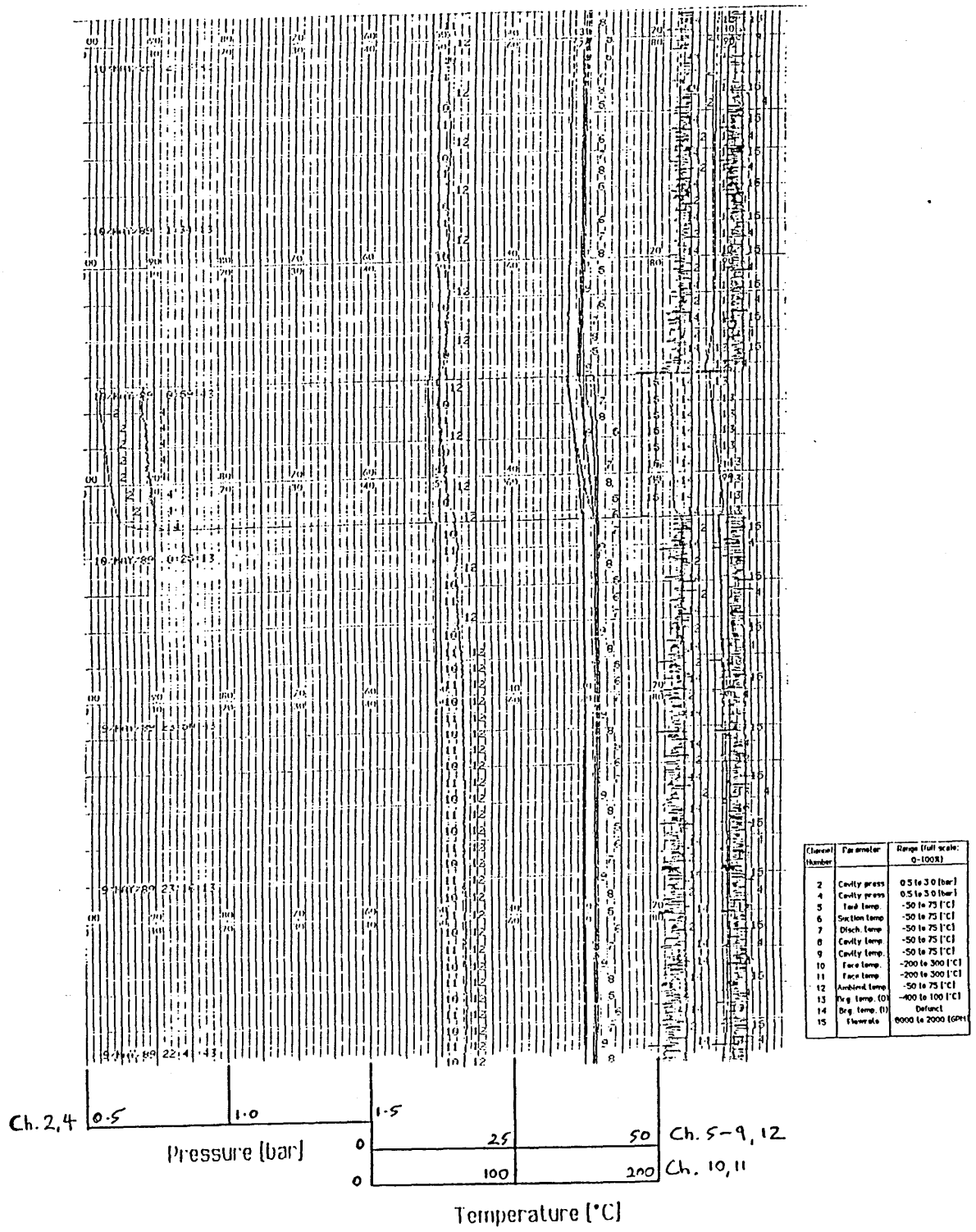
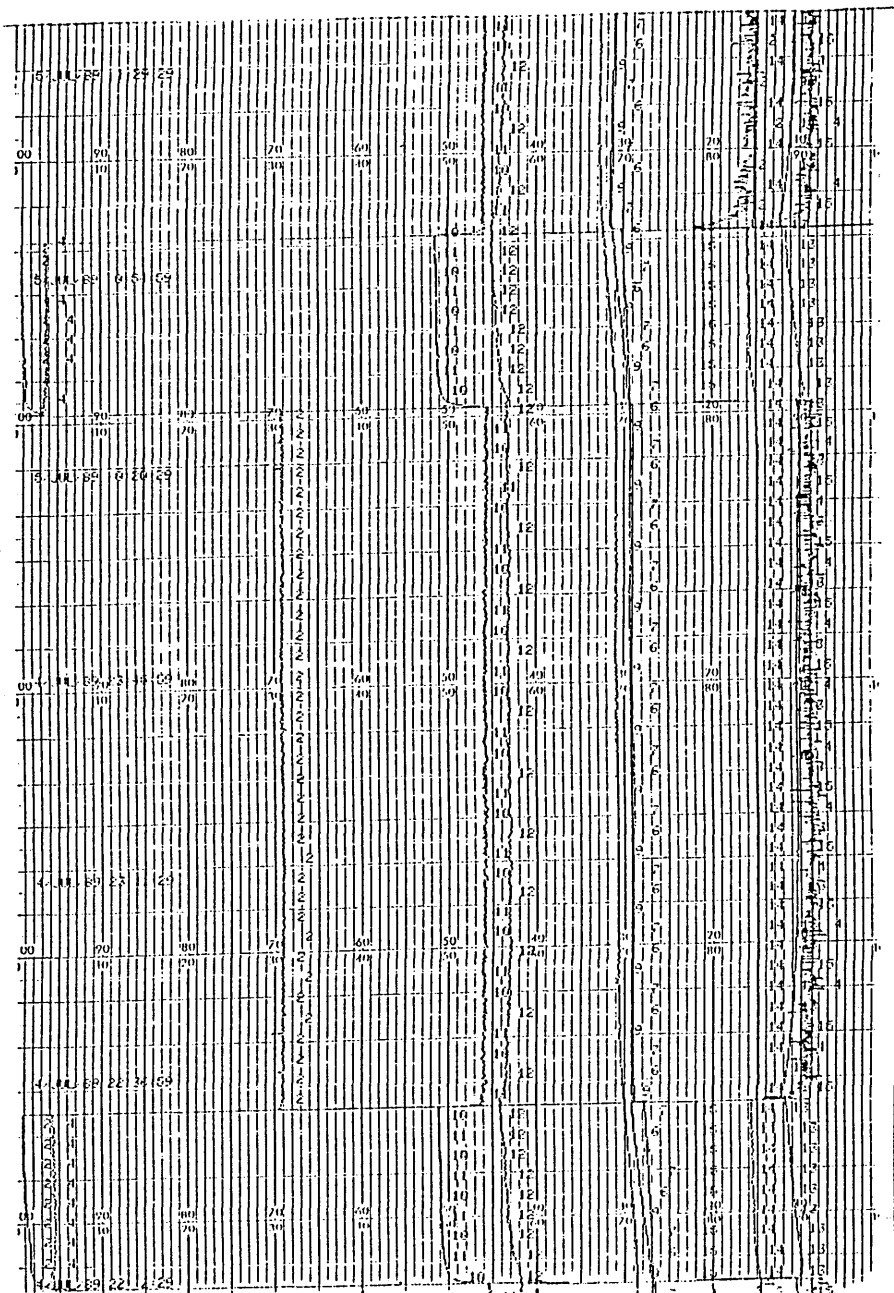


Figure 10.41 Chart trace - Seal 10



Channel Number	Parameter	Range (full scale: 0-100%)
2	Cavity press	Offset error
4	Cavity press	0.5 to 3.0 (bar)
6	Surface temp	-50 to 75 (°C)
7	Truck temp	-50 to 75 (°C)
8	Cavity temp	-50 to 75 (°C)
9	Cavity temp	-50 to 75 (°C)
10	Face temp	-200 to 300 (°C)
11	Face temp	-200 to 300 (°C)
12	Ambient temp	-50 to 75 (°C)
13	Org temp. (I)	-400 to 100 (°C)
14	Org temp. (II)	Default
15	Flowrate	0000 to 2000 (g/min)

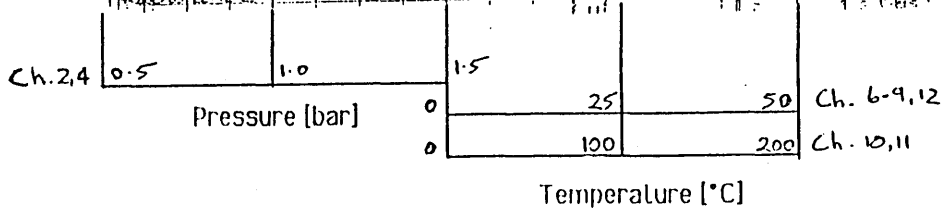


Figure 10.42 Chart trace - Seal 12



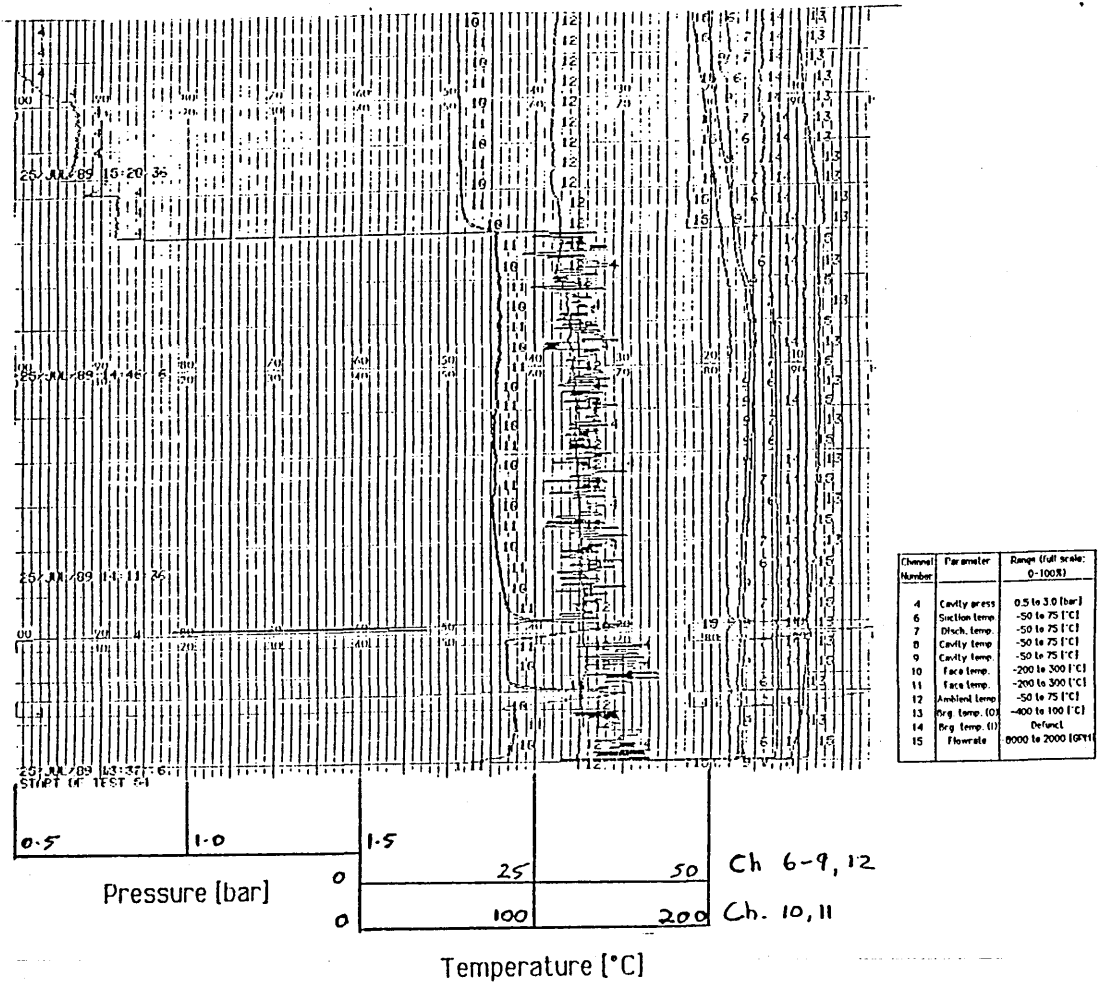


Figure 10.43 Chart trace - Seal 12  
starved suction test

POWER-DISSIPATION RESULTS, ALL SEALS

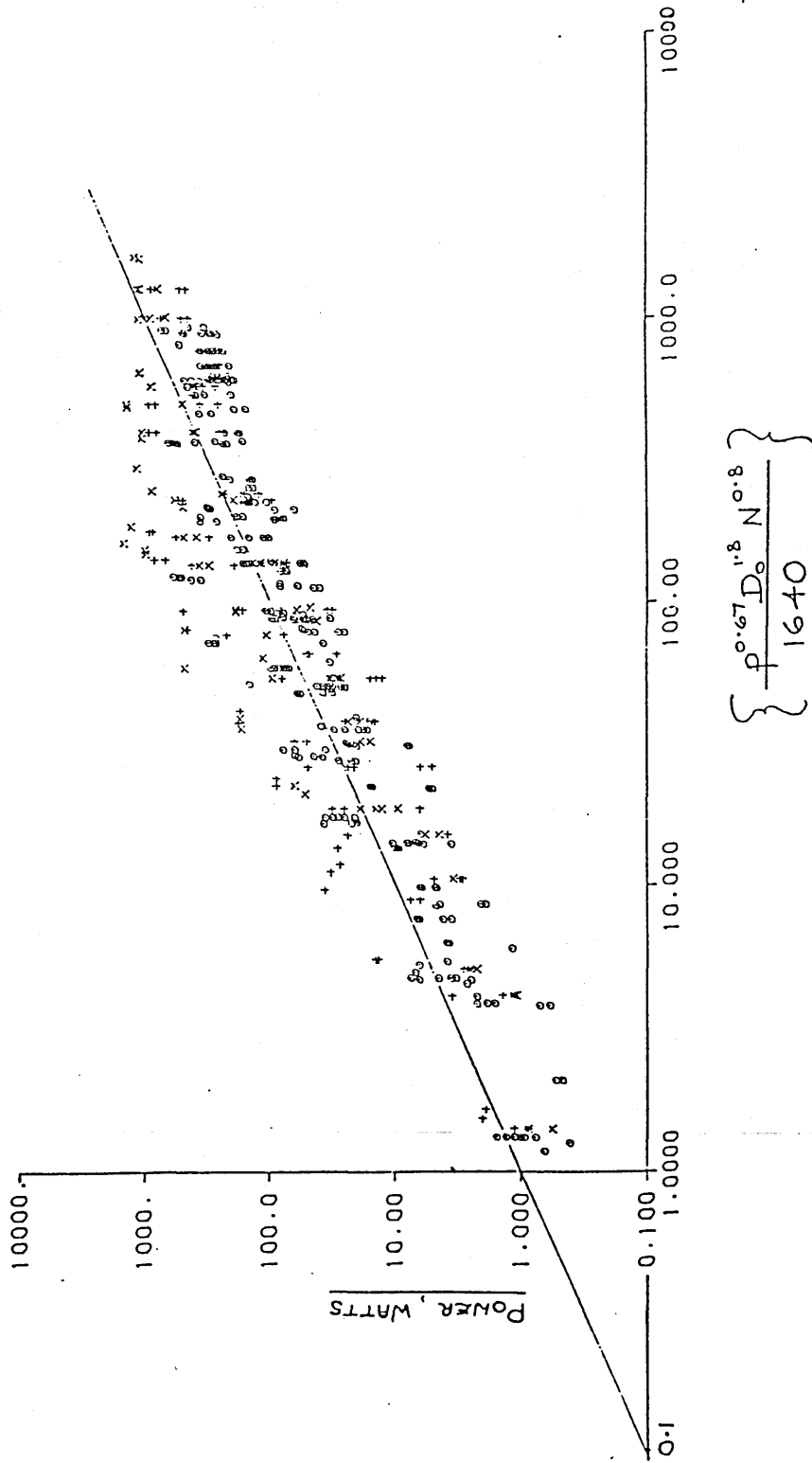


Figure 13.1 Power dissipation results (Nau, 1987)

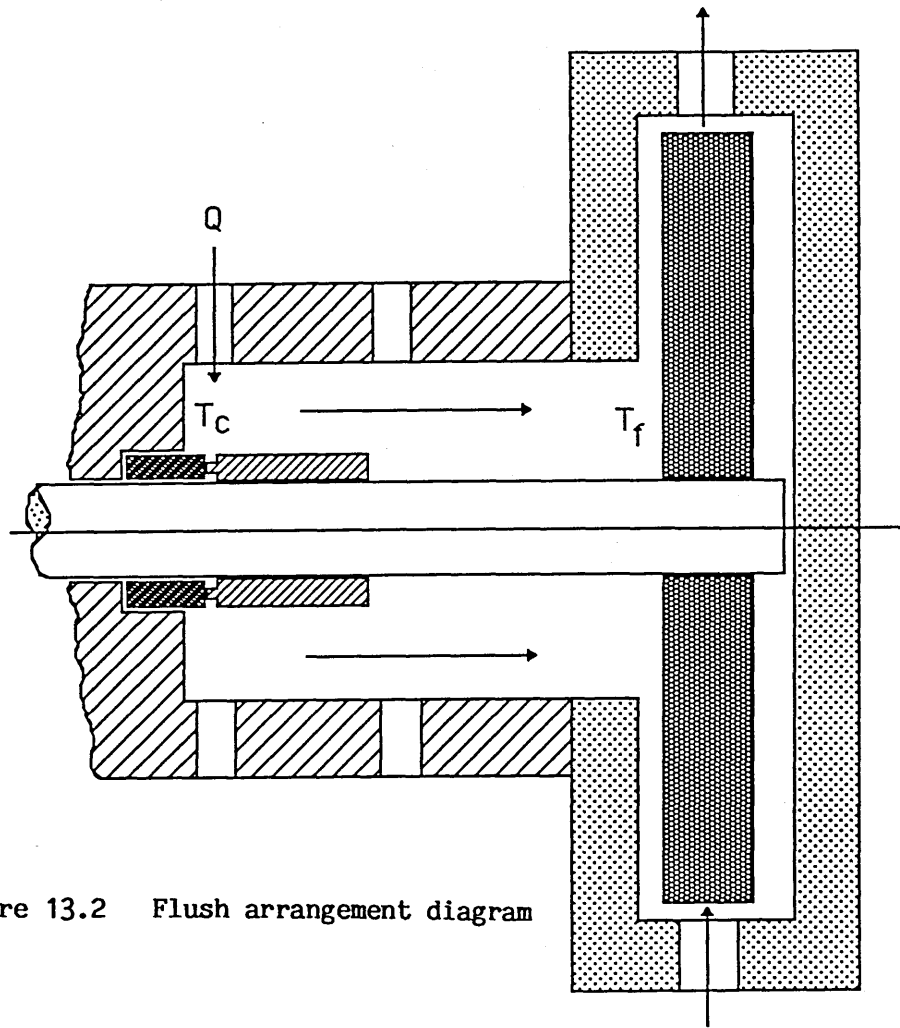


Figure 13.2 Flush arrangement diagram

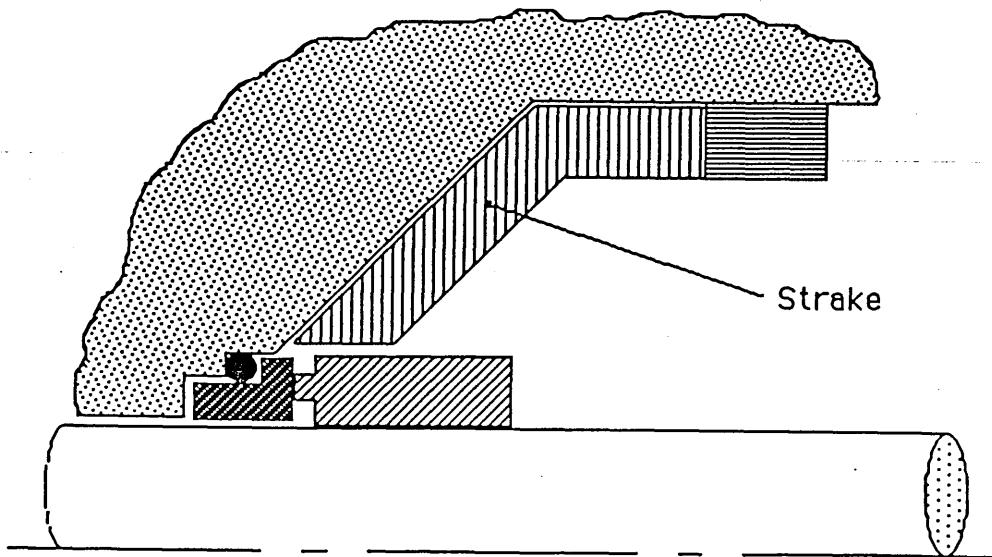


Figure 13.3 Axial strakes for the 45° flared housing

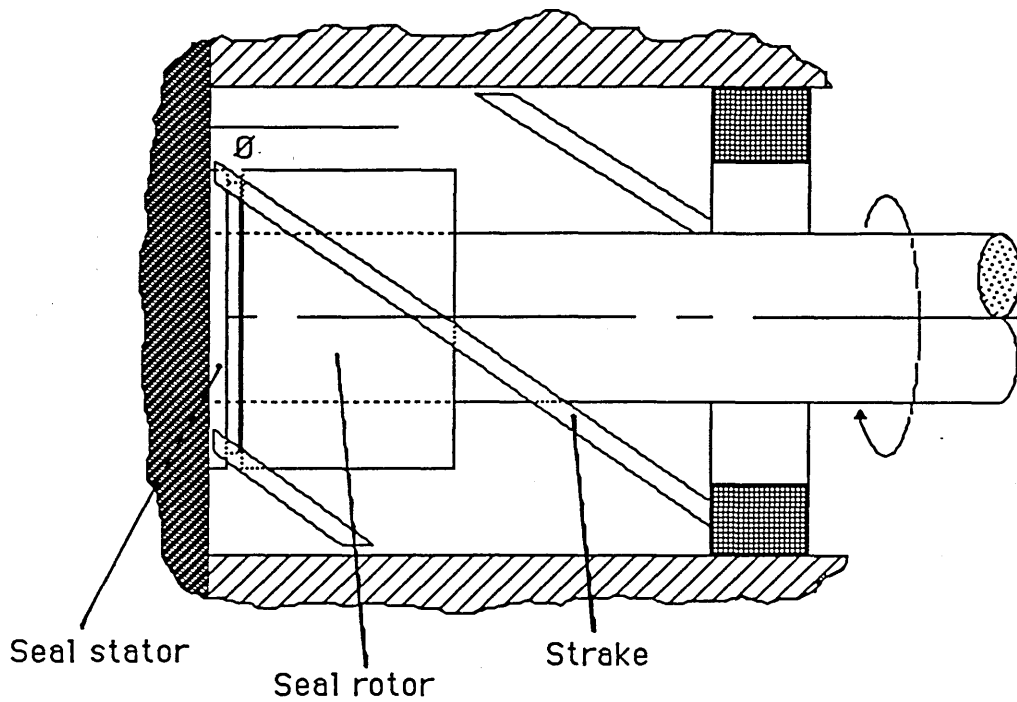


Figure 13.4 Helical strake arrangement

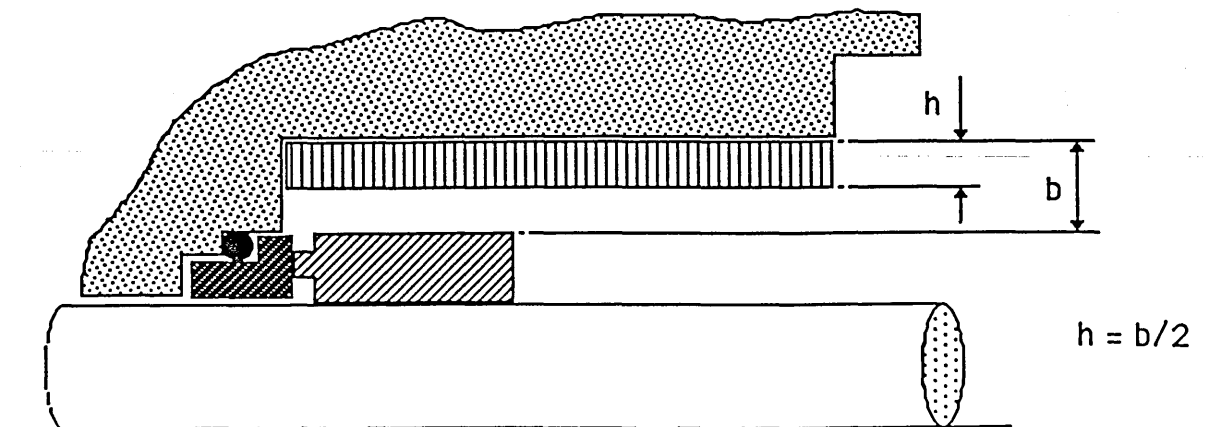


Figure 13.5 Axial strakes for a wide radial clearance housing